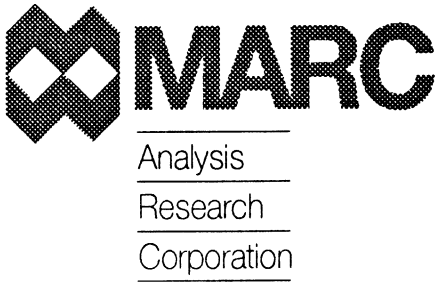

VOLUME E DEMONSTRATION PROBLEMS

Part IV

- *Contact*
- *Advanced Topics*

Disclaimer of Warranties and Limitation of Liabilities

The authors have taken due care in preparing this manual and the examples in it, including the research, development, and testing to ascertain their effectiveness. In no event shall MARC Analysis Research Corporation be liable for incidental or consequential damages in connection with or arising out of the furnishing, performance, or use of any of the examples.

MARC Analysis Research Corporation:

North America

Corporate Headquarters
MARC Analysis Research Corporation
260 Sheridan Avenue, Suite 309
Palo Alto, CA 94306, USA
Telephone: (415) 329-6800
FAX: (415) 323-5892

National Sales Office
MARC Analysis Research Corporation
#6 Venture, Suite 202
Irvine, CA 92718, USA
Telephone: (714) 453-0840
FAX: (714) 453-0141

Europe

European Headquarters
MARC-Europe
Bredewater 26
2715 CA Zoetermeer, The Netherlands
Telephone: 31-79-510411
FAX: 31-79-517560

German Office
MARC Software Deutschland GmbH
Ismaninger Strasse 9
85609 Aschheim, Germany
Telephone: 49-89-904-5033
FAX: 49-89-903-0676

Italian Office
Espri-MARC
Piazza Rossetti 5/16A
16129 Genova, Italy
Telephone: 39-10-585949
FAX: 39-10-585949

Pacific Rim

Far East Headquarters
Nippon MARC Co., Ltd.
P.O. Box 5056
Shinjuku Daiichi Seimei Bldg.
2-7-1 Nishi-Shinjuku
Shinjuku-ku, Tokyo 163, Japan
Telephone: 81-3-3345-0181
FAX: 81-3-3345-1529

Osaka Office
Nippon MARC Co., Ltd.
Dai 2 Kimi Bldg., 4F
2-11 Toyotsu-cho
Suita-city, Osaka 564, Japan
Telephone: 81-6-385-1101
FAX: 81-6-385-4343

Contents Volume E Demonstration Problems

PART IV

VOLUME E
DEMONSTRATION PROBLEMS

Chapter 7
Contact

Contents Chapter 7 Contact

Figures Chapter 7 Contact

Chapter 7 Contact

SPECIAL ANALYSIS CAPABILITIES IN MARC

In addition to the various analysis capabilities discussed in previous chapters concerned with problems of linear elasticity, plasticity and creep, large displacement, heat transfer as well as dynamics, this chapter contains demonstration problems for the illustration of additional analysis capabilities in the MARC problem. Detailed discussions of these capabilities can be found in Volume A and a summary of the various capabilities illustrated is given below.

- Steady, creeping flow of rigid, perfectly plastic material (R-P Flow).
- The use of gap-friction element (Element Type 12).
- Analysis of concrete (CRACKING) structures.
- Analysis of rubber structures (MOONEY and OGDEN).
- Simulation of composite material (COMPOSITE).
- Simulation of viscoelastic material.
- Axisymmetric structure under nonsymmetric loading (FOURIER Analysis).
- Study of mesh refinement (QUALIFY).
- Analysis of hydrodynamic bearings.
- Use of the rezoning technique for large deformation analysis.

Compiled in this chapter are a number of solved problems. Table E 7.0-1 shows MARC elements and options used in these demonstration problems.

Table E 7.0-1 Special Topics Demonstration Problems

Problem Number (E)	Element Type	Parameter Options	Model Definition	Load Incrementation	User Subroutines	Problem Description
7.1	32	ELSTO R-P FLOW	CONTROL	AUTO LOAD	—	Steady, creeping flow of rigid, perfectly plastic material (R-P Flow).
7.2	10 12	—	OPTIMIZE CONTROL ISOTROPIC GAP DATA	POINT LOADS DIST LOADS AUTO LOAD	—	The use of gap-friction element in the analysis of a man-hole cover in a pressure vessel.
7.3	75	SHELL SECT	UFXORD CONTROL CRACK DATA ISOTROPIC	AUTO INCREMENT	UFXORD	Analysis of a concrete barrel vault shell subjected to self-weight.
7.4	12 32	LARGE DISP	RESTART CONTROL MOONEY GAP DATA	PROPORTIONAL AUTO LOAD	—	Side pressing of a hollow rubber cylinder.
7.5	33 82 119	LARGE DISP FOLLOW FOR	NODE FILL CONTROL MOONEY	DIST LOADS	—	Analysis of a thick rubber cylinder.
7.6	75	SHELL SECT	DEFINE COMPOSITE ORIENTATION ORTHOTROPIC PRINT ELEM	—	—	Elastic analysis of a multi-layered square plate under uniform pressure (composite material).
7.7	75	SHELL SECT	DEFINE COMPOSITE ORTHOTROPIC PRINT ELEM ORIENTATION INITIAL STATE CHANGE STATE	—	—	Elastic analysis of a multi-layered square plate subjected to uniform pressure and thermal loading (composite material).

Table E 7.0-1 Special Topics Demonstration Problems (Continued)

Problem Number (E)	Element Type	Parameter Options	Model Definition	Load Incrementation	User Subroutines	Problem Description
7.8	62	FOURIER	CONTROL FOURIER RESTART	—	UFOUR	Fourier analysis of a cylinder under external pressure.
7.9	62	FOURIER	CONTROL FOURIER RESTART CASE COMBIN	—	UFOUR	Fourier analysis of a cylinder in plane strain subjected to a line load.
7.10	27	MESH PLOT QUALIFY	POST	—	—	Use of the QUALIFY option for the study of mesh refinement.
7.11	3 9	—	CONTROL CRACK DATA ISOTROPIC RESTART	POINT LOAD	—	Analysis of a simply supported concrete beam subjected to concentrated loads.
7.12	27	—	TYING PRINT CHOICE ISOTROPIC VISCELPROP	AUTO LOAD TIME STEP	—	Analysis of a simply supported concrete beam subjected to concentrated loads.
7.13	14 17	SCALE ELSTO	TYING	AUTO LOAD PROPORTIONAL INC	—	Analysis of pipeline structure using element type 14 and 17, and the pipeline mesh generator MARCPIPE.
7.14	28	—	ISOTROPIC VISCELPROP PRINT CHOICE	AUTO LOAD TIME STEP	—	Internal pressurization of an externally reinforced long, thick walled, viscoelastic cylinder.
7.15	37	BEARING	THICKNESS VELOCITY TYING	—	UFXORD UFCONN UTHICK UVELOC UGROOV	Calculation of the pressure distribution in a spiral groove thrust bearing including grooves.

Table E 7.0-1 Special Topics Demonstration Problems (Continued)

Problem Number (E)	Element Type	Parameter Options	Model Definition	Load Incrementation	User Subroutines	Problem Description
7.16	39	BEARING	CONN GENER NODE FILL THICKNESS VELOCITY	DAMPING COMPONENTS STIFFNESS COMPONENTS THICKNESS CHANGE	UTHICK UBEAR	Analysis of a journal bearing. Determine the load carrying capacity of the bearing.
7.17	10	UPDATE FINITE LARGE DISP REZONE	FORCDT WORK HARD	AUTO LOAD COORDINATE CHANGE REZONE	FORCDT	Analysis of a thick-walled cylinder under internal pressure. Demonstration of rezoning capability.
7.18	32 12	LARGE DISP	MOONEY GAP DATA VISCELMOONEY	AUTO LOAD TIME STEP	—	Side pressing of a hollow viscoelastic rubber cylinder.
7.19	26	—	MOONEY TYING	AUTO LOAD	—	Plane stress stretching of a rubber sheet with a hole.
7.20	82	FOLLOW FOR PRINT, 5	DEFINE CONTACT CONTROL OGDEN	MOTION CHANGE AUTO LOAD DIST LOADS TIME STEP	—	Compression of an O-ring.
7.21	26	—	OGDEN	DISP CHANGE AUTO LOAD		Plane stress stretching of a rubber sheet with a hole.
7.22	75	LARGE DISP SHELL SECT	OGDEN DIST LOADS DAMAGE VISCELOGDEN	AUTO LOAD DIST LOADS TIME STEP	—	Loading of a rubber plate including damage and rate effects.

E 7.1 Rigid Perfectly Plastic Extrusion

This example illustrates the use of the R-P FLOW option in a classic plastic flow problem – the extrusion of metal in-plane strain through a 50% reduction, frictionless die. The problem is shown in Figure E 7.1-1; a uniform velocity is applied at the left-hand side. The required solution is the velocity field and extrusion force. The slip-line solution to this problem is well known [1,2].

The rigid-plastic flow option uses Herrmann incompressible elements to solve for the velocity field. The material is modeled as a non-Newtonian fluid and the program iterates for the viscosity, which is $\frac{2}{3}\frac{\bar{\sigma}}{\dot{\bar{\varepsilon}}}$, where σ is the yield stress and $\dot{\bar{\varepsilon}}$ is the equivalent plastic strain rate.

Element

In this example the plane strain Herrmann element (element 32) is used. This element is second-order distorted quadrilateral (plane-strain). There are 32 elements and a total of 121 nodes.

Material Properties

The equivalent von Mises yield stress is entered as 30×10^3 psi in this option. The property is specified for elements 1 through 32.

Geometry

No geometry is specified.

Loading

No loading is specified.

Boundary Conditions

The material entering the die is assigned a velocity of 1 in/sec. in the x-direction. The material velocities normal to the die walls are fixed as zero.

Control

A 10% tolerance on the relative residual force was chosen to determine if convergence was achieved. In a rigid plastic analysis, the computational time would have been reduced if the convergence based upon velocities was requested.

Results

The solution for the 50% reduction case chosen here is a centered fan – outside the fan the material moves as a rigid body or is stationary. The mesh is confined to the neighborhood of the fan region (Figure E 7.1-2).

Note a special consideration for the fully incompressible Herrmann formulation: since the system is semi-definite, it is only possible to solve by Gauss elimination if the first active degree of freedom is a stiffness degree of freedom and not a pressure variable (Lagrange multiplier). Thus, node 1 must have at least one unconstrained velocity component. In this case, 1 and 2 are swapped to achieve this by adding additional CONNECTIVITY and COORDINATES set by hand. The value of the input velocity is arbitrary in this case, since the yield is assumed to be rate independent. The accuracy of the solution is determined by the convergency requirements. In this analysis, nine iterations were required.

Extrusion force in 50% reduction, frictionless die. (Normalized by the tensile yield stress and input width).

Calculated at input stream	1.347
Calculated from reaction on die face	1.393
Exact (slip line) solution, $.5(1 + \pi/2)$	1.285

The predicted flow field is illustrated in Figure E 7.1-3. Velocity vectors are shown in this figure. The slip-line fan has been superimposed on this picture. The 'dead' region in the corner of the die is well predicted by the finite element model, before it reaches the fan. The downstream solution also shows a little rotation of the velocity field just below the corner of the die. This is more accurate than the upstream solution. The strain gradients on entry to the fan are very high. At this point, the slip solution shows a discontinuity in tangential velocity. A finer mesh in this region would improve this part of the solution.

References

1. Hill, R., *Mathematical Theory of Plasticity*, Chapter 4, (Oxford University Press, 1950.)
2. Prager, W., and Hodge, P. G., *Theory of Perfectly Plastic Solids*, Section 298 (John Wiley, 1951).

Summary of Options Used

Listed below are the options used in example e7x1.dat:

Parameter Options

ELEMENT
ELSTO
END
R-P FLOW
SIZING
TITLE

Model Definition Options

CONNECTIVITY
CONTROL
COORDINATE
END OPTION
FIXED DISP
ISOTROPIC

Load Incrementation Options

AUTO LOAD
CONTINUE

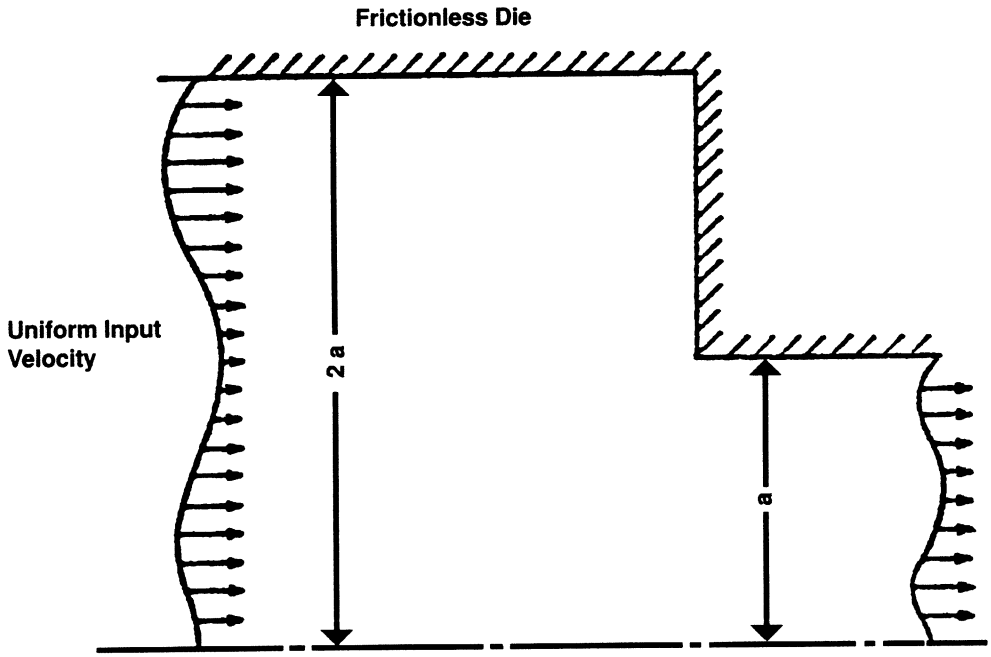

Figure E 7.1-1 50% Reduction Die Problem

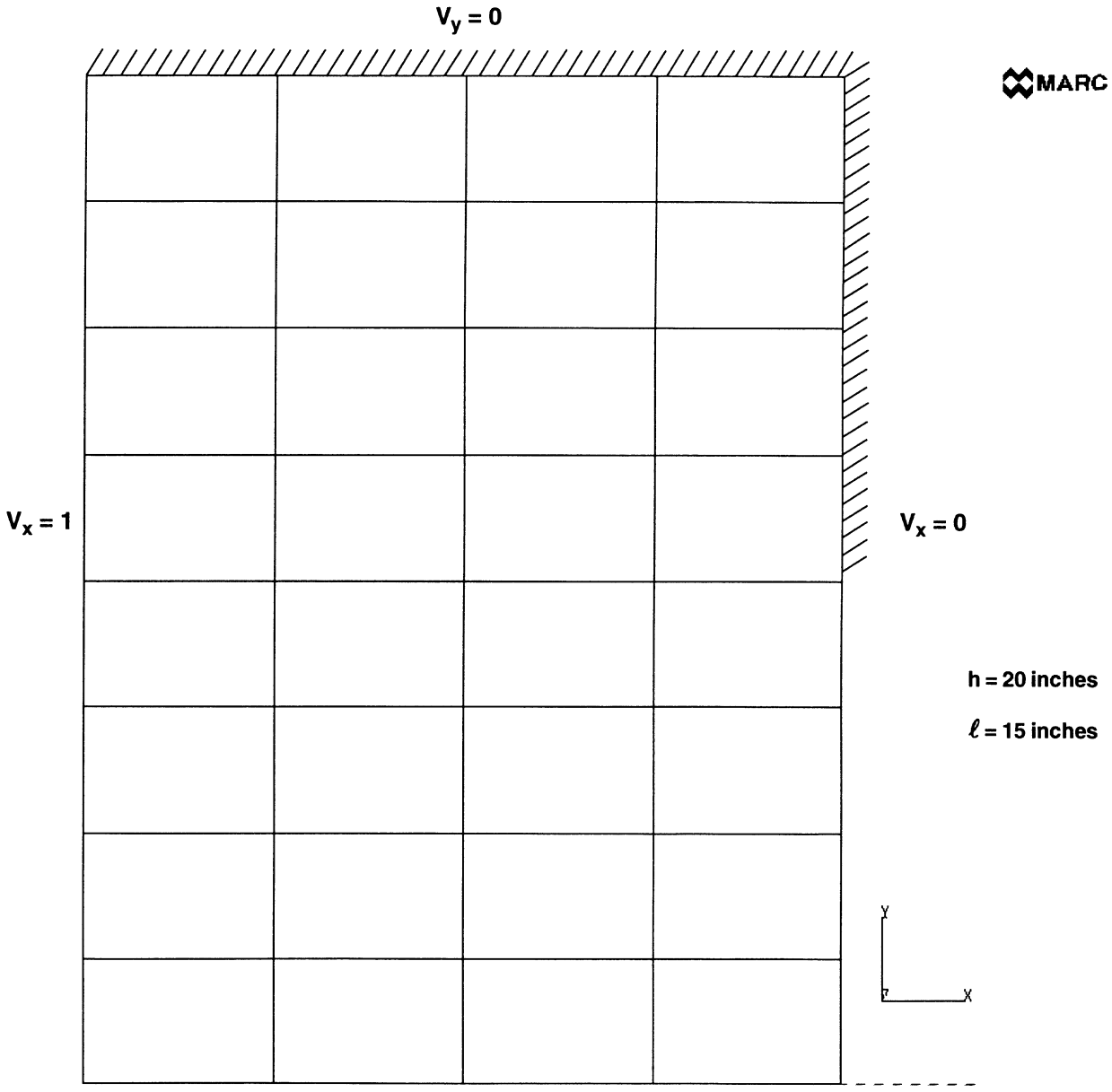

Figure E 7.1-2 Mesh and Boundary Conditions for 50% Reduction Example

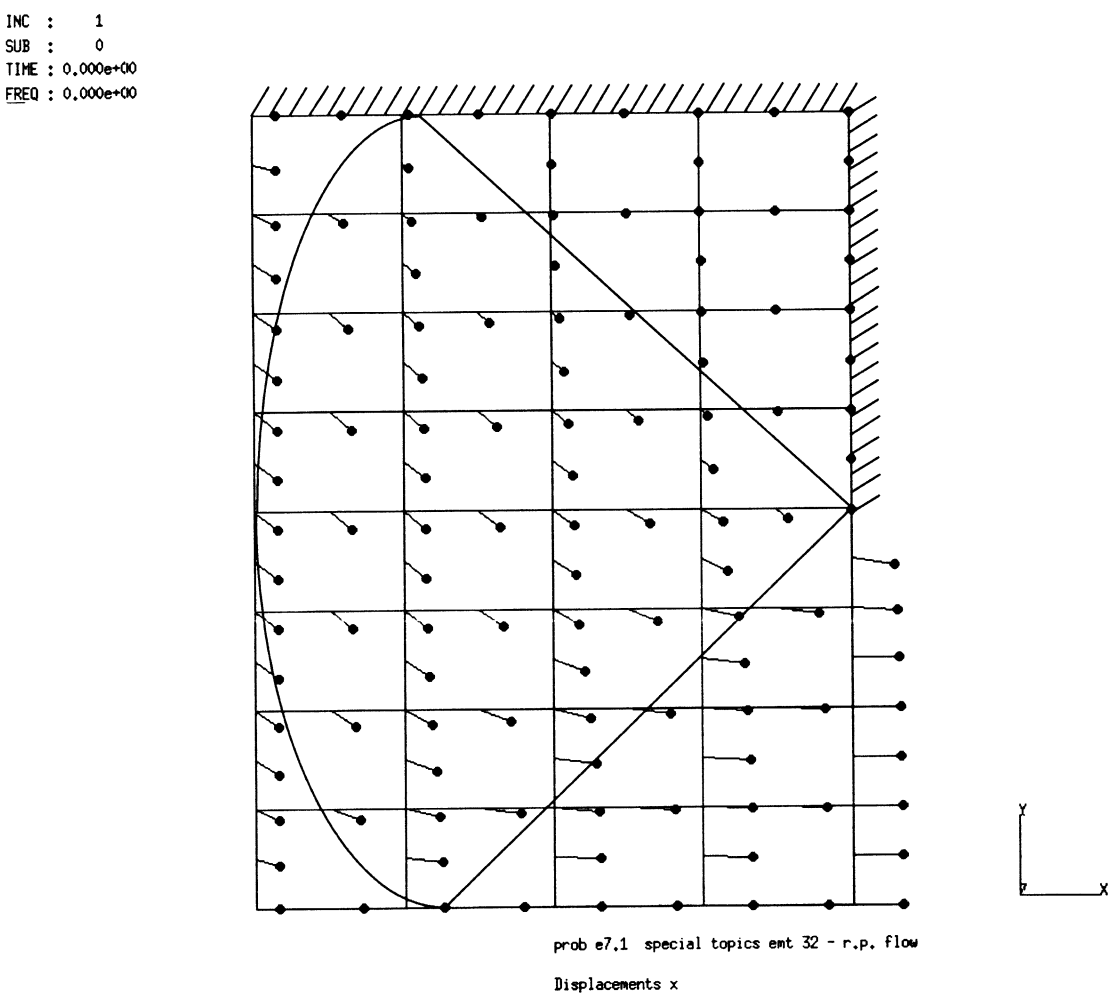

Figure E 7.1-3 50% Reduction Extrusion Velocity Field

E 7.2 End-Plate-Aperture Breakaway

This example illustrates the use of the gap and friction link, element type 12. This element allows surface friction effects to be modeled. This example is a simple model of a man-hole cover in a pressure vessel. The axisymmetric mesh is shown in Figure E 7.2-1. The object of this analysis is to establish the response of the bolted joint between the man-hole cover (elements 1-12) and the vessel (elements 13-27). The bolts are first tightened, and then the main vessel expands radially (as might occur due to thermal or internal pressure effects). The user should be aware that this problem is presented only as a demonstration. The mesh is too coarse for accurate results.

Elements

Element 12 is a friction and gap element. It is based on the imposition of a gap closure constraint and/or a frictional constraint via Lagrange multipliers. The element has four nodes: nodes 1 and 4 are the end nodes of the link and each has two degrees of freedom (u, v,) in the global coordinate direction; node 2 gives the gap direction cosines (n_x, n_y) and has λ_n, the force in the gap direction, as its one degree of freedom; node 3 gives the friction direction cosines (t_{1_x}, t_{1_y}) and has γ_1, the frictional shear forces, and p, the net frictional slip, as its two degrees of freedom.

Model

Twenty-seven type 10 elements are used for the two discrete structures, the end cap and the aperture. These are then joined by four type 12 elements. There are 54 nodes and a total of 108 degrees of freedom in the mesh.

Loading

The load history consists of applying bolt loads (i.e., tightening down the bolts), then pulling out the outer perimeter of the main vessel model. Bolt loads are modeled here as point loads applied in opposite directions (self-equilibrating) on node pairs 4 and 32, 5 and 33. Since there is a possibility of gaps developing between the facing surfaces of the cover and vessel, the bolt load is initially applied as a small magnitude, then incremented up to the total value of 2000 lb per bolt ring. This usually requires two runs of the problem: an initial run with a "small" load to see the pattern developing, from which some judgement can be made about the load steps which can be used to apply the total bolt force. In this case, it was determined by this method that no surface separation will occur, so that, in the actual run, the full bolt loads are applied in one increment.

The radial expansion of the main vessel is modeled as a uniform negative pressure on the outer surfaces of the outer elements (15, 21, 27). (Note this is given as load type 8 to apply it to the correct face of the elements.) Again, the purpose of the analysis is to watch the development of slippage between the main vessel and the cover plate, and the analyst cannot easily estimate the appropriate load increments to apply to model this nonlinearity. For this purpose, the RESTART option may be used effectively. A restart is written at the point where full bolt load is applied, and then a trial increment of pull-out force is applied. Based on the response to this (in the

friction links), a reasonable size for the sequence of loading increments can be determined. This procedure is frequently necessary in such problems. For brevity, this example shows only the final load sequence obtained as a result of such trials.

Boundary Conditions

The nodes on the axis of symmetry are constrained radially, and the rigid body mode in the axial direction is removed at node 46.

Isotropic

The ISOTROPIC option is used to enter the mechanical properties of the man-hole cover.

Gap Data

In this example, a small negative closure distance of -0.001 is given for the gaps. This indicates that the gaps are initially closed and solve for an interference fit in increment 0. The coefficient of friction μ is 0.8.

Results

The results of the analysis are shown in Figure E 7.2-2 through Figure E 7.2-4. First of all, it is observed in Figure E 7.2-2 that the force at node 53, associated with gap element 31 goes to zero, indicating that the gap has opened. The interested user can investigate here possible model changes and their effect – for example, the effect of inaccurate bolt tightening, so that the two bolt rings have different loadings.

In this case, the initial bolt load is carried quite uniformly (A in Figure E 7.2-2), but as the pull-out increases, the inner two links take more of the stress and the outer link (element 31) sheds stress. The shear stress development is followed in Figure E 7.2-3 – initially (bold load only), all shear stresses are essentially zero. The two outer links slip first, but then the additional forces required to resist the pull develops in the inner two elements until the shear stress pattern follows the normal stress pattern, when the shear in the pair of links also slip ($\tau = \mu\sigma$). Figure E 7.2-4 shows a plot of radial displacement of the outer perimeter against pull-out force. Notice the small loss of stiffness caused by slip developing as the vessel model has to resist the extra force along without any further force transfer to the cover.

Summary of Options Used

Listed below are the options used in example e7x2.dat:

Parameter Options

DIST LOADS
ELEMENT
END
SIZING
TITLE

Model Definition Options

CONNECTIVITY
CONTROL
COORDINATE
END OPTION

FIXED DISP
GAP DATA
ISOTROPIC
OPTIMIZE
POINT LOAD

Load Incrementation Options

AUTO LOAD
CONTINUE
DIST LOADS
POINT LOAD

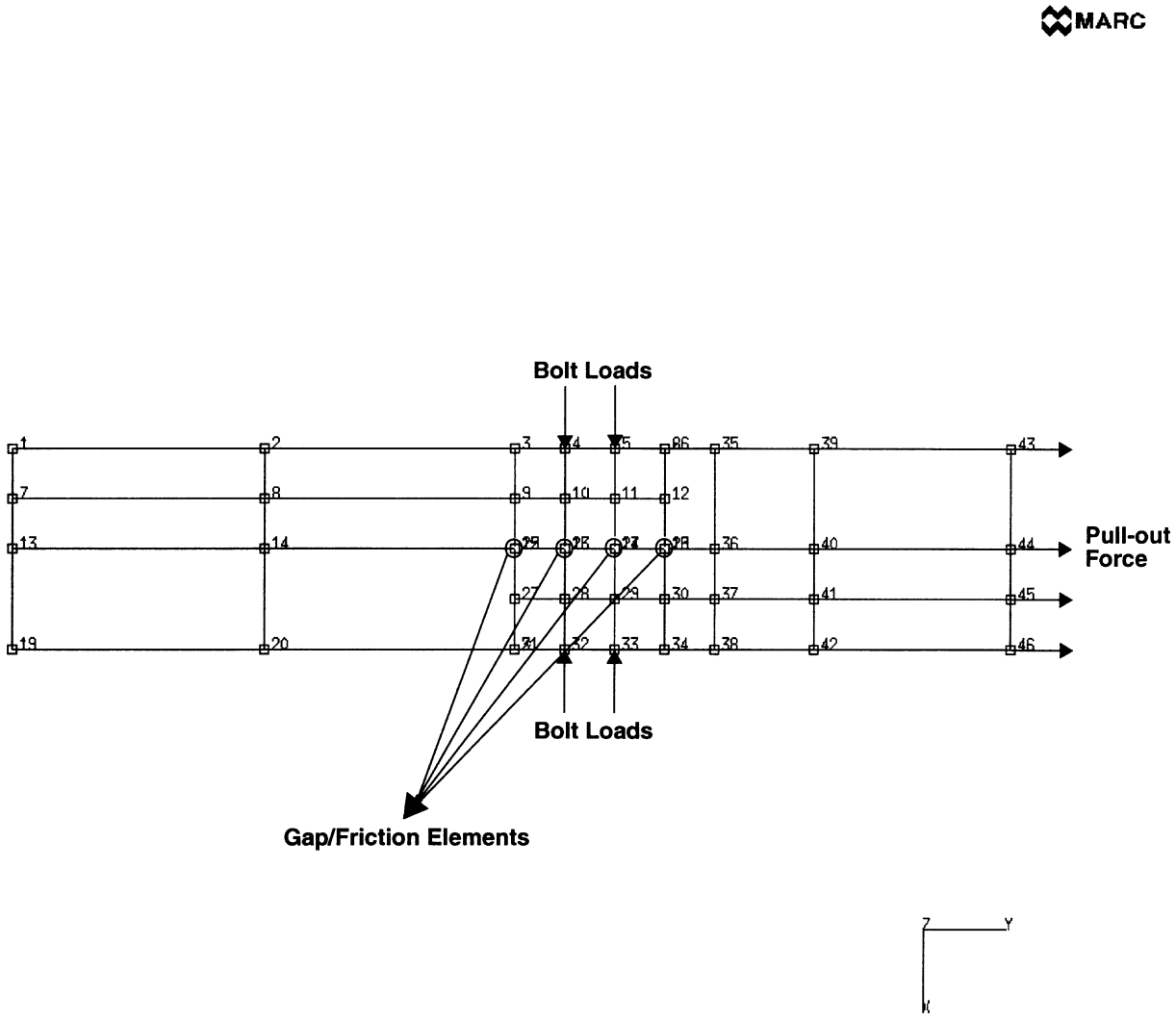

Figure E 7.2-1 Geometry and Mesh of End Plate-Aperture

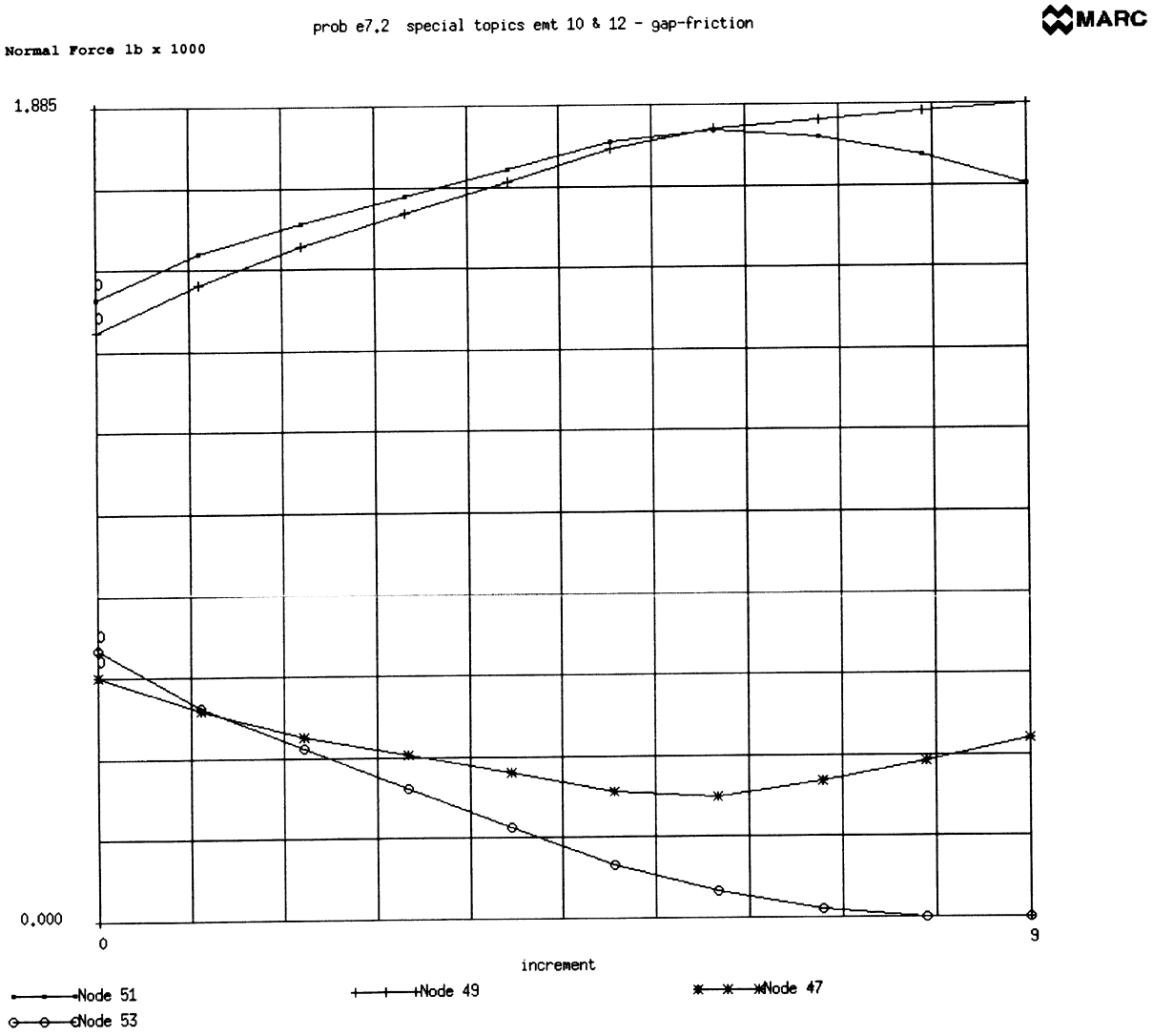

Figure E 7.2-2 Transient Normal Forces in Bolts

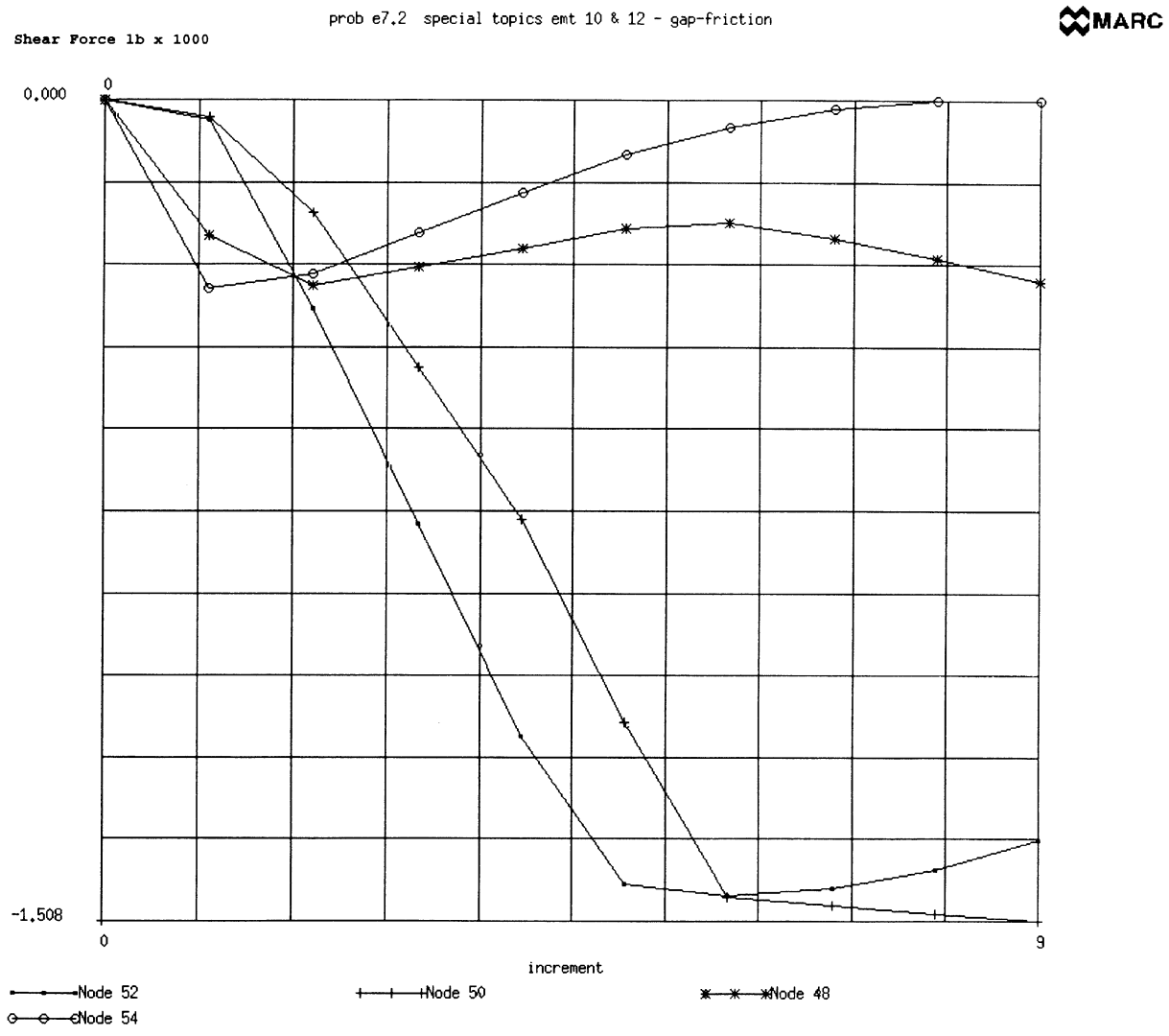

Figure E 7.2-3 Transient Shear Force in Bolts

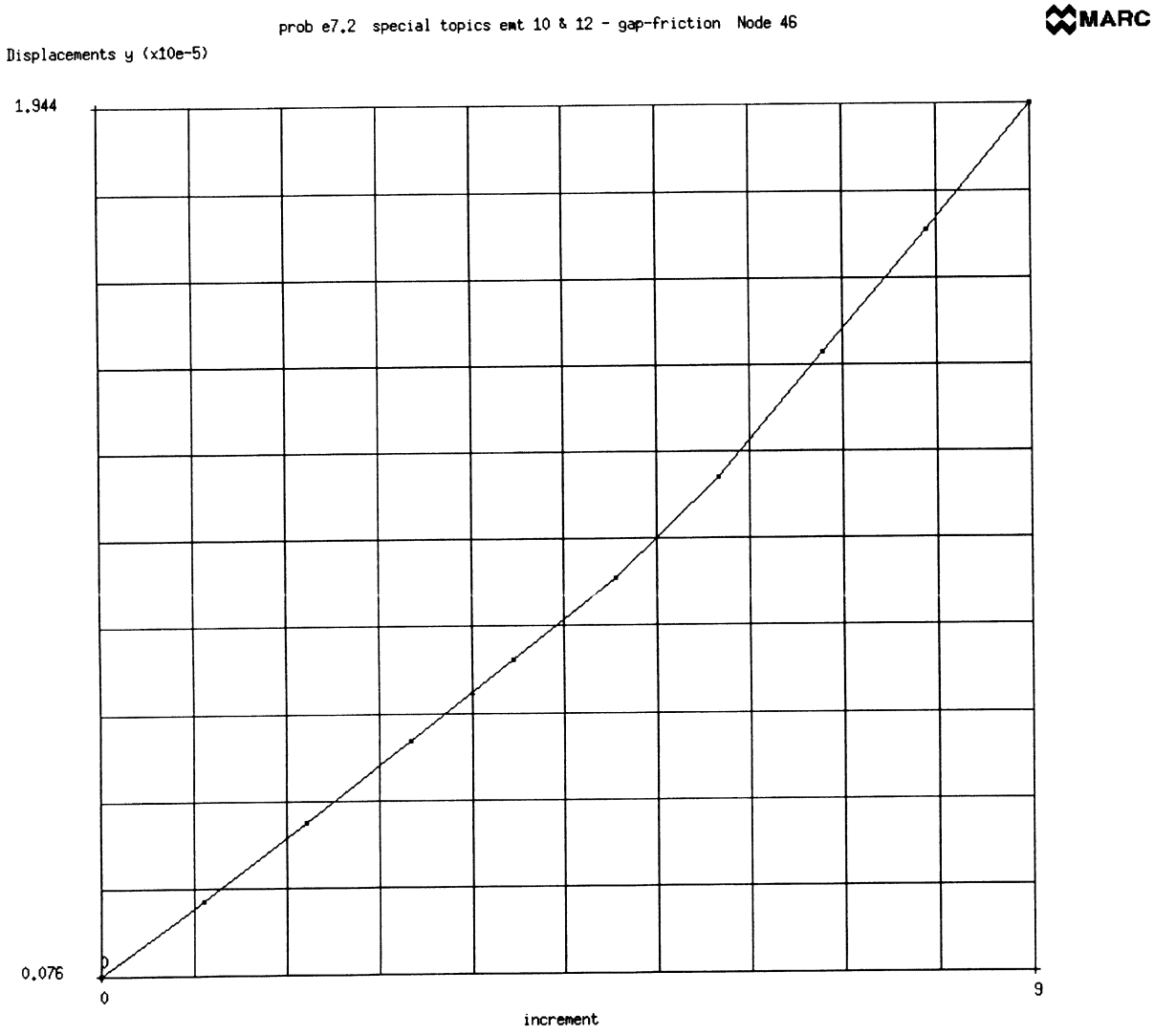

Figure E 7.2-4 Radial Displacement at Outside Top (Node 46)

E 7.3 Barrel Vault Shell Under Self-Weight (Shell Cracking)

A concrete barrel vault shell is loaded under increasing snow load until cracking is developed. This is the same problem as E 3.23 with the addition of nonlinear behavior.

Element

Element type 75, a 4 node thick shell element, is used. The cylinder has a half length of 100 inches and a constant thickness of 3 inches. The radius is 300 inches.

Model

Thirty-six elements are used to model one-quarter of the shell taking advantage of symmetry. The model has 49 nodes. The mesh is shown in Figure E 7.3-1. Subroutine UFXORD is used to generate the full set of coordinates.

Material Properties

The Young's modulus is 3×10^6 psi, the ultimate compressive strain is 0.002 in/in. Failure in tension is assumed to occur at 1000 psi. The material is given a strain softening modulus of 3×10^5 psi. A shear retention coefficient of 0.5 is used for the concrete. The ISOTROPIC option is used to indicate that cracking is to be used.

Loading

An initial uniformly distributed load of 0.625 psi is applied, and these loads are then increased in 0.25-psi increments.

Boundary Conditions

The ends of the structure are supported by diaphragms. There are two free edges.

Results

The first cracks occur at the bottom layers of element numbers 24 and 36 during increment 5. Subsequent loading results in formation of new cracks. Increasing loads propagate the cracks through the thickness of the shell.

The load deflection results for the midpoint of the edge of the shell (node 3), as shown in Figure E 7.3-2. The effect of cracking is highly pronounced. This results in significant nonlinearity and leads to a reduction in the effective stiffness of the structure. The concrete's failure in tension dominates the response of this structure. In addition, a few points also fail due to crushing.

A rather large tolerance was necessary to obtain convergence in this analysis. This is not unusual for problems involving cracking.

Summary of Options Used

Listed below are the options used in example e7x3.dat:

Parameter Options

ELEMENT
END
SHELL SECT
SIZING
TITLE

Model Definition Options

CONNECTIVITY
CONTROL
COORDINATE
CRACK DATA
DIST LOADS
END OPTION
FIXED DISP
GEOMETRY
ISOTROPIC
POST
PRINT CHOICE
RESTART
UFXORD

Load Incrementation Options

AUTO INCREMENT
CONTINUE
DIST LOADS

Listed below is the user subroutine found in u7x3.f:

UFXORD

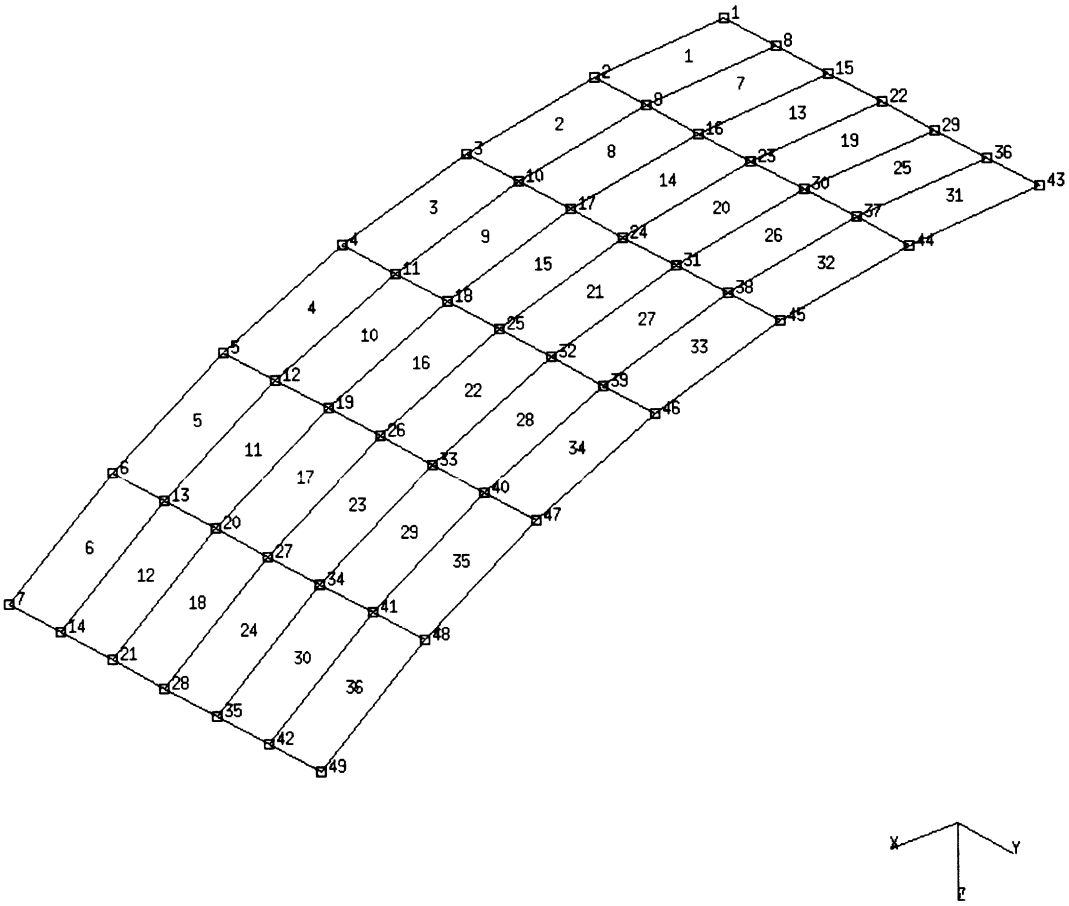

Figure E 7.3-1 Mesh for the Shell Roof

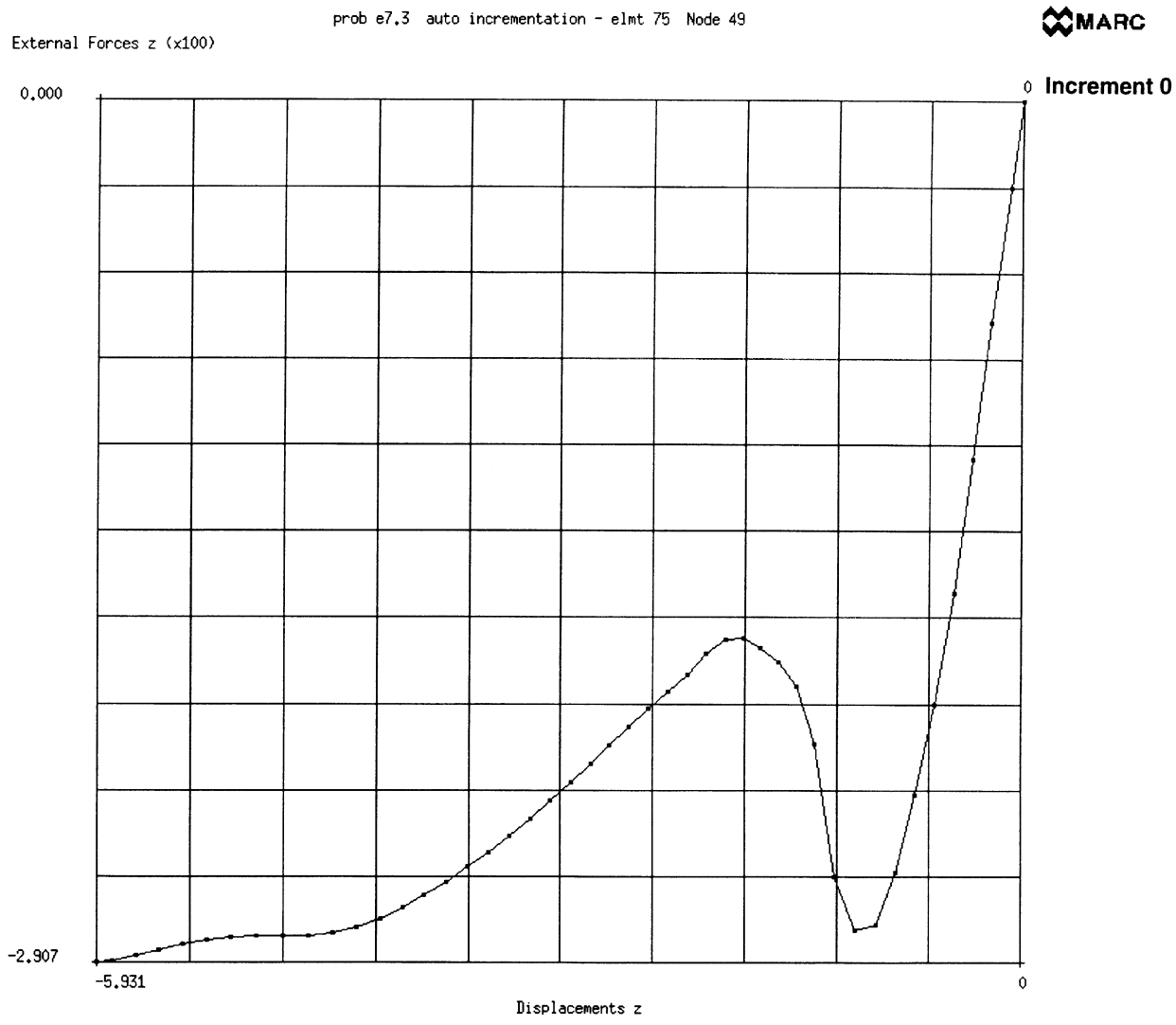

Figure E 7.3-2 Load-Vertical Deflection Curve at Node 3

E 7.4 Side Pressing Of A Hollow Rubber Cylinder (Mooney Material)

The behavior of a thick hollow rubber cylinder, compressed between two rigid plates, is analyzed. The cylinder is long; hence, a condition of plane strain in the cross section will be assumed. For reasons of symmetry, only one-quarter of the cylinder needs to be modeled. No friction will be assumed between cylinder and plates. A MOONEY material behavior is used to represent the rubber. The LARGE DISPLACEMENT option is used.

Element

The quarter cylinder is modeled by using 8-node hybrid plane strain elements (MARC element type 32). This element may be used in conjunction with Mooney material.

Model

Twelve elements are used for the mesh, with two elements specified over the thickness. The geometry of the cylinder and a mesh are shown in Figure E 7.4-1.

MOONEY

The MOONEY option is used to specify the rubber properties. The rubber material may be modeled as a Mooney-Rivlin material with $C_{10} = 8$ N/mm^2, $C_{01} = 2$ N/mm^2.

GAP DATA

The gap closure distance is defined as the initial nodal distance between the cylinder and the plate and is entered via the GAP DATA option.

Loading

The AUTO LOAD option is used to apply five displacement increments to the plate. The increment is equal to the one applied in the increment 0. After load application, one iteration is carried out by using PROPORTIONAL INCREMENT option with zero load increment to insure that the solution is in equilibrium. This is not necessary if the tolerance specified on the CONTROL option is sufficiently small.

Boundary Conditions

This option is used twice: one to read the data of the mesh of the cylinder; second to read GAP data.

Tying

TYING establishes the connections between the nodal degrees of freedom of the cylinder and that of the gaps. This is necessary because the degrees of freedom of these two elements are not the same.

Results

The cylinder diameter is reduced from 6 in. to 4 in. in five increments. The cylinder is in contact with the plate at four nodes (four gaps have been closed). The incremental displacements have become very small and that the equilibrium is satisfied with high accuracy. The incremental full Newton-Raphson method was used to solve the nonlinear system. The total force on the plate may either be calculated by summing up the gap forces, or may be directly obtained from the reaction force on node 75. In both cases, this leads to a total force F = 1.91 N. A plot of the deformed cylinder is shown in Figure E 7.4-2.

Summary of Options Used

Listed below are the options used in example e7x4.dat:

Parameter Options

ELEMENT
END
LARGE DISP
SIZING
TITLE

Model Definition Options

CONNECTIVITY
CONTROL
COORDINATE
END OPTION
FIXED DISP
GAP DATA
MOONEY
RESTART
TYING

Load Incrementation Options

AUTO LOAD
CONTINUE
PROPORTIONAL INCREMENT

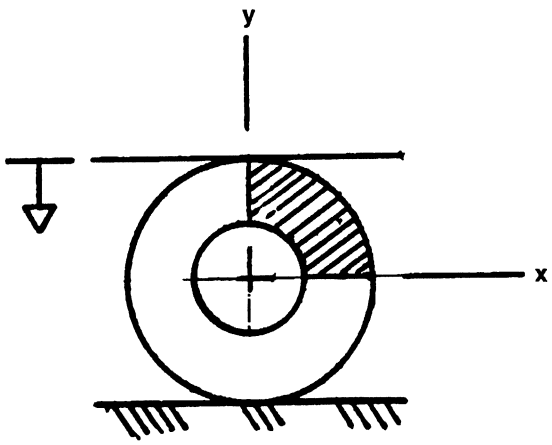

$C_1 = 8$
$C_2 = 2$
$r_i = 2$
$r_o = 3$

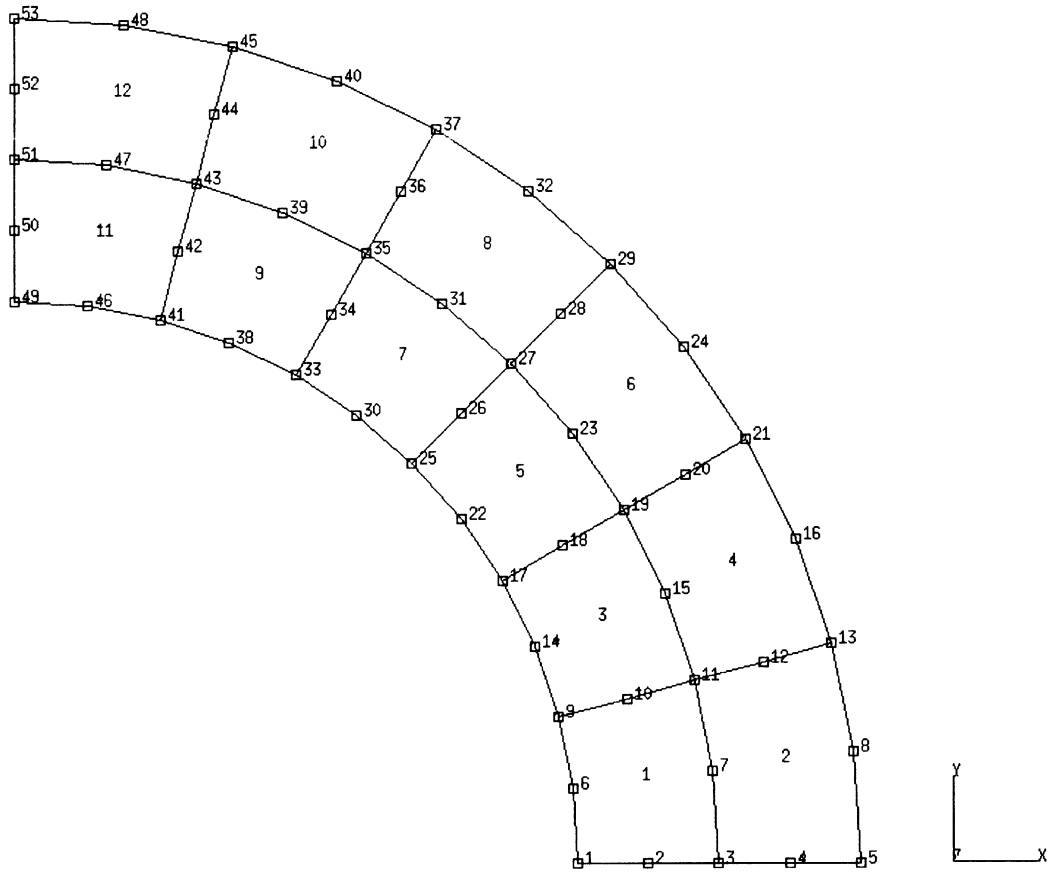

Figure E 7.4-1 Rubber Cylinder and Mesh

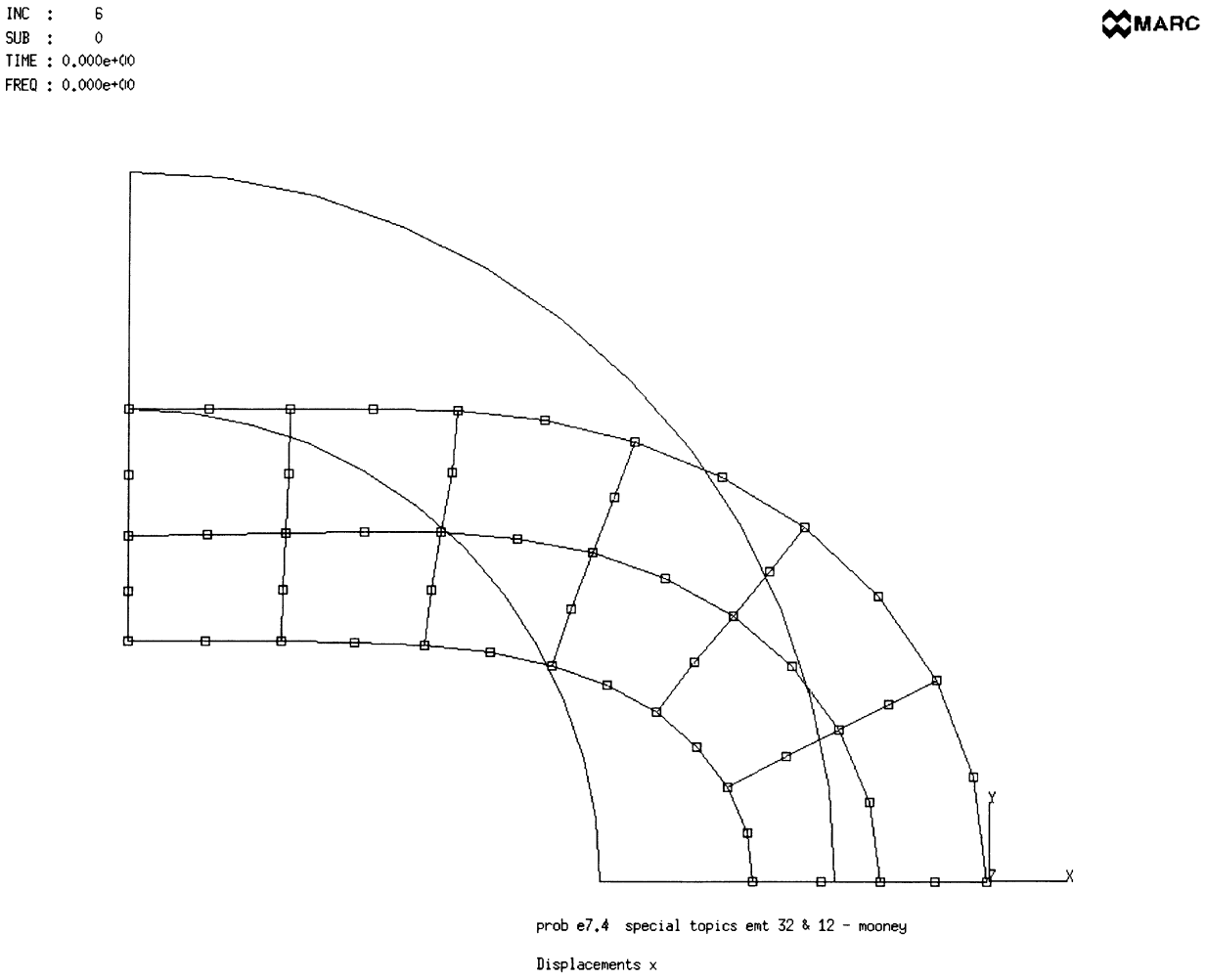

Figure E 7.4-2 Deformed Mesh Plot

E 7.5 Analysis Of A Thick Rubber Cylinder Under Internal Pressure

This problem illustrates the use of MARC elements types 33, 82, and 120 (8- and 4-node incompressible, axisymmetric elements) and options, LARGE DISP, FOLLOW FOR, and MOONEY for an elastic, large strain analysis of a rubber cylinder subjected to a uniformly distributed internal pressure. The pressure load is applied in a single step, and the Newton-Raphson iteration procedure is used to obtain an equilibrium state.

Model

The dimensions of the rubber cylinder and finite element meshes are shown in Figure E 7.5-1. The 8-node model consists of four elements of type 33 and 23 nodes, and the 4-node model consists of four elements of type 82 or type 120, and 14 nodes.

Material Properties

The material of the rubber cylinder is assumed to be MOONEY material with material constants:

$C_{10} = 8$ N/mm^2
$C_{01} = 2$ N/mm^2

Loading

Uniformly distributed internal pressure = 11.5 N/mm^2 is applied on element number 1. This load is applied in increment zero. In MARC, increment zero is treated as linear so an additional increment, with no additional load, is used to bring the solution to the correct nonlinear state.

Boundary Conditions

u = 0 on the planes z = 0 and z = 1.0 to simulate a plane strain condition.

Note

LARGE DISP is included to obtain the geometric nonlinear effects; the full Newton-Raphson technique is used.

FOLLOW FOR indicates that pressures will be applied on the current geometry of the cylinder.

CONTROL block is used to specify the number of increments in the analysis. In this analysis two increments are specified with a maximum of 15 Newton-Raphson iterations to obtain equilibrium.

Newton-Raphson iterations are obtained with PROPORTIONAL INCREMENT. This indicates that the previous load increment has to be multiplied by a certain user specified factor and has to be added to the current loads. The loads may be pressures, nodal loads, or non-zero kinematic boundary conditions. If the multiplication factor is set to be zero (0), then no load will be added. Iterations will be performed until the maximum residual force is less than 10% of the maximum reaction force.

Results

A. 8-Node Model (Element Type 33)

After the linear elastic step (increment 0), the radial displacements of the inside nodes (nodes 1, 10 and 15) are:

Node	Radial Displacement (mm) (MARC)
1	0.38351
10	0.38351
15	0.38350

They are in good agreement with analytical solution which predicts a radial displacement of 0.38333.

After ten iterations, the radial displacement at the inside node is 1.0026 and the corresponding pressure can be computed from the following expression:

$$P = (C_1 + C_2)\left[\log\left(\frac{B^2a^2}{A^2(B^2 - A^2 + a^2)}\right) + \frac{(a^2 - A^2)(B^2 - A^2)}{a^2(B^2 - A^2 + a^2)}\right]$$

where A and B are the inner and outer radius of the cylinder in the undeformed state, and "a" is the inner radius in the deformed state, and C_1 and C_2 are material constants.

The computed pressure (11.49) is in very good agreement with the prescribed value of 11.5.

B. 4-Node Model (Element Type 82, 120)

After the linear elastic step (increment 0), the radial displacements of the inside nodes (nodes 1 and 6) are:

Node	Radial Displacement (MARC) type 82	Radial Displacement (MARC) type 120
1	0.38174	0.38335
6	0.38174	0.38335

Agreement with analytical solution of 0.38333 is good. After ten iterations, the radial displacement at inside node is 1.0061, and the corresponding pressure is 10.35 for element 82. For element 120, the displacement at the inside node is 1.0063 and the corresponding pressure is 11.5. Agreement with prescribed value or 11.5 is excellent.

Summary of Options Used

Listed below are the options used in example e7x5.dat:

Parameter Options

ELEMENT
END
FOLLOW FORCE
LARGE DISP
SIZING

Model Definition Options

CONNECTIVITY
CONTROL
COORDINATE
DIST LOADS
END OPTION
FIXED DISP
MOONEY
NODE FILL
POST

Load Incrementation Options

CONTINUE
CONTROL
DIST LOADS

Listed below are the options used in example e7x5b.dat or e7x5c.dat:

Parameter Options

ELEMENT
END
FOLLOW FORCE
LARGE DISP
SIZING
TITLE

Model Definition Options

CONNECTIVITY
CONTROL
COORDINATE
DIST LOADS
END OPTION
FIXED DISP
MOONEY
POST

Load Incrementation Options

CONTINUE
CONTROL
DIST LOADS

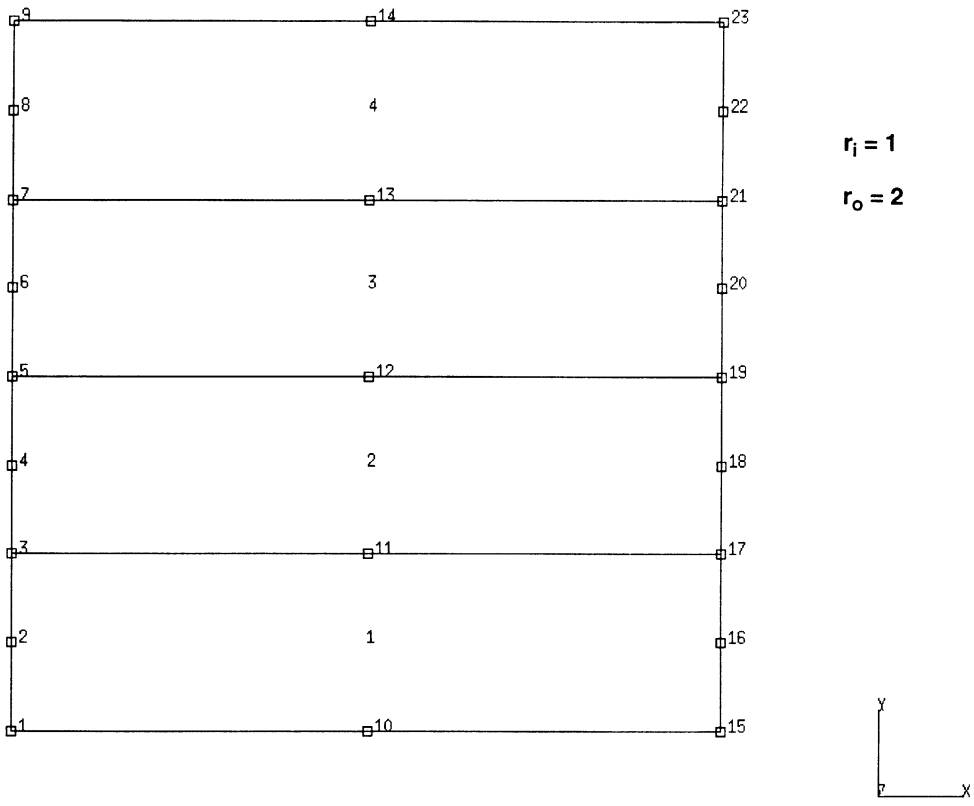

Figure E 7.5-1 Cylinder Mesh (8-Node Model)

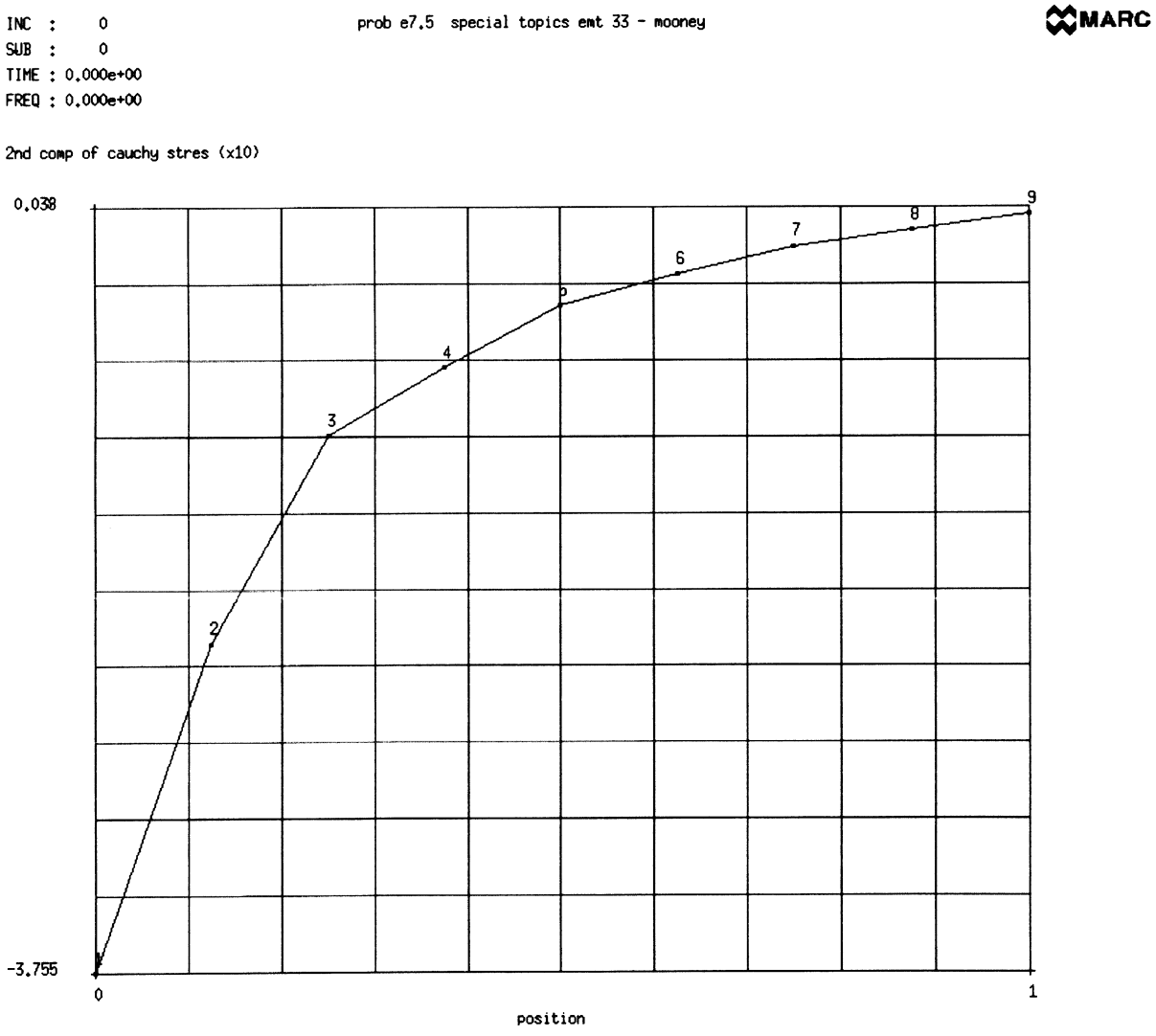

Figure E 7.5-2 Radial Stress Through Radius

E 7.6 Biaxial Stress In A Composite Plate

This problem illustrates the analysis of a plate made of layered composite material as shown in Figure E 7.6-1. A biaxial stress field is applied and the results are compared with a textbook solution (Reference 1).

Element

Shell element 75 is used to model the plate. It is a four node bilinear thick shell element capable of modeling the behavior of layered composite materials.

Model

A 4 x 4 mesh of shells is used for a total of 16 elements, 25 nodes and 150 degrees-of-freedom. (See Figure E 7.6-2.)

Material Properties

The plate consists of three layers of an orthotropic material. The top layer is 3 mm thick and is offset 45° from the middle layer. The middle layer is 4 mm thick. The bottom layer is also 3 mm thick and is offset 45° from the middle layer. This data is entered in the COMPOSITE option.

The orthotropic material properties are entered in the ORTHOTROPIC option. The data entered here are the engineering constants E_{11}, E_{22}, E_{33}, ν_{12}, ν_{23}, ν_{31}, G_{12}, G_{22}, and G_{33} with respect to the three planes of elastic symmetry. The ply angle for the various layers is given in the COMPOSITE option.

Loading

The biaxial stresses applied to the plate are $\sigma_x = 1. \times 10^6$ N/m^2, $\sigma_y = 2. \times 10^5$ N/m^2 and $\tau_{xy} = 0$. These distributed loads are specified in the DIST LOADS option (the units in this problem are m-kg-s). The applied load magnitudes are negative so that the applied loading is directed out of the element.

Boundary Conditions

In order to fully restrain the rigid body modes without introducing any elastic constraints, a special set of boundary conditions is used. Degrees-of-freedom 1 to 5 are suppressed at node 1 and degree-of-freedom 1 is suppressed along the entire left hand edge. Since the layup is symmetric, only in-plane deformations are expected. The specification of additional rotational constraints at the left hand edge is irrelevant.

Print Control

The use of the sub-option PREF under PRINT ELEM allows the user to obtain print out of the layer stresses in the preferred (ply) coordinate system. The generalized shell resultant quantities are always expressed in the local shell $\tilde{v}^1$, $\tilde{v}^2$ system. Here, these coordinates are parallel to global X and Y, respectively.

Results

Results for this problem are given in the reference, p. 169. They are summarized below:

		Reference	MARC
ε_x^o		.00685	.006875
ε_y^o		.00332	.003324
ε_{xy}^o		-.00784	-.007845
	σ_1	29.6	29.85
Layers 1,3	σ_2	18.8	18.87
x 10^6N/m^2	σ_{12}	-2.5	-2.49
	σ_1	139.3	139.8
Layer 2	σ_2	11.4	11.46
x 10^6N/m^2	σ_{12}	-5.5	-5.49

Figure E 7.6-3 shows the deformed shape of the structure. The displacements are all planar, and there is no coupling between bending and axial extension due to the symmetry of the layup. There is, however, coupling between axial extension and in-plane shear.

Reference

Agarwal, B.D., Broutman, L., *Analysis and Performance of Fiber Composites*, Wiley, 1980.

Summary of Options Used

Listed below are the options used in example e7x6.dat:

Parameter Options

ELEMENT
END
SHELL SECT
SIZING
TITLE

Model Definition Options

COMPOSITE
CONNECTIVITY
COORDINATE
DEFINE
DIST LOADS
END OPTION
FIXED DISP
ORIENTATION
ORTHOTROPIC
POST
PRINT ELEM

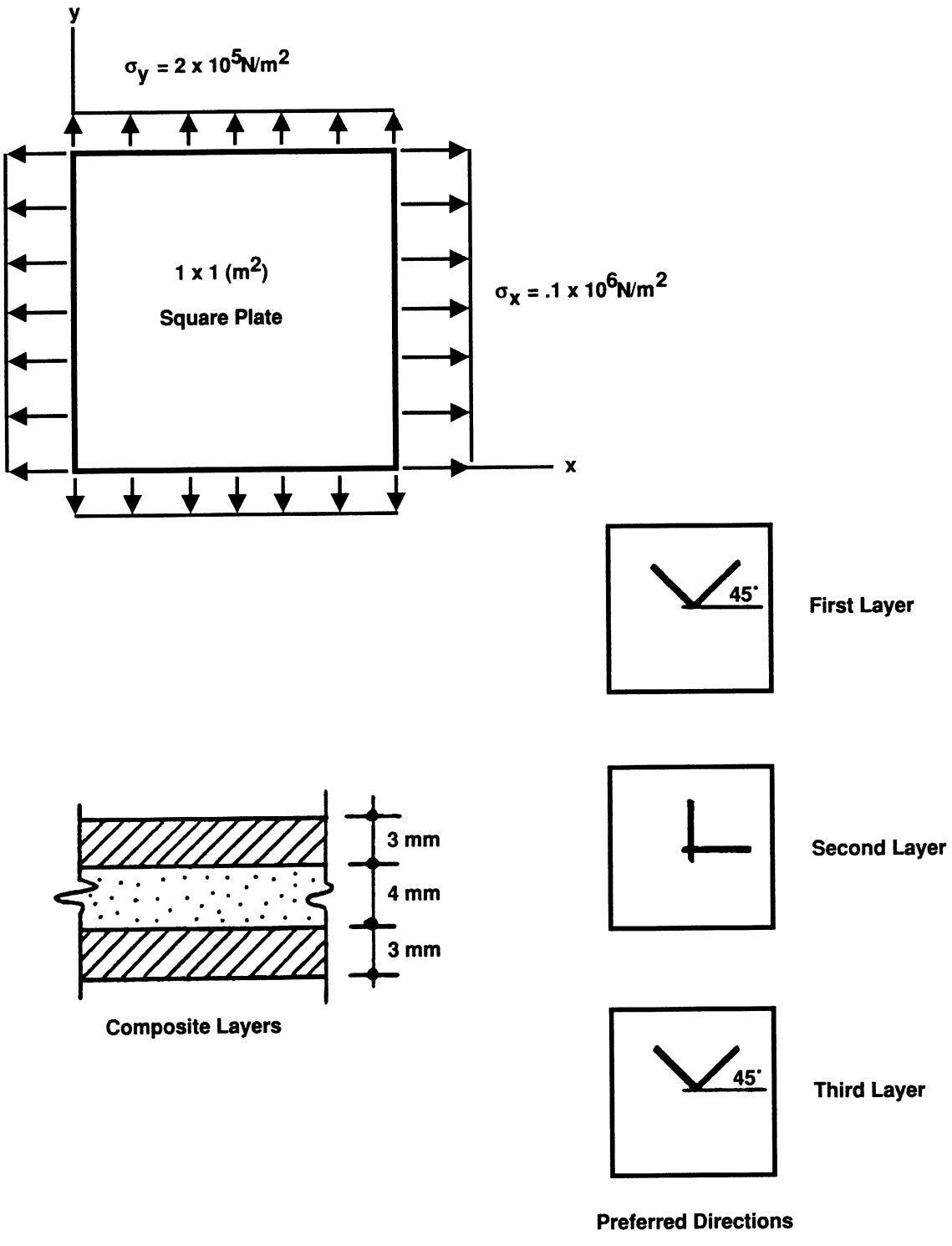

Figure E 7.6-1 Composite Plate

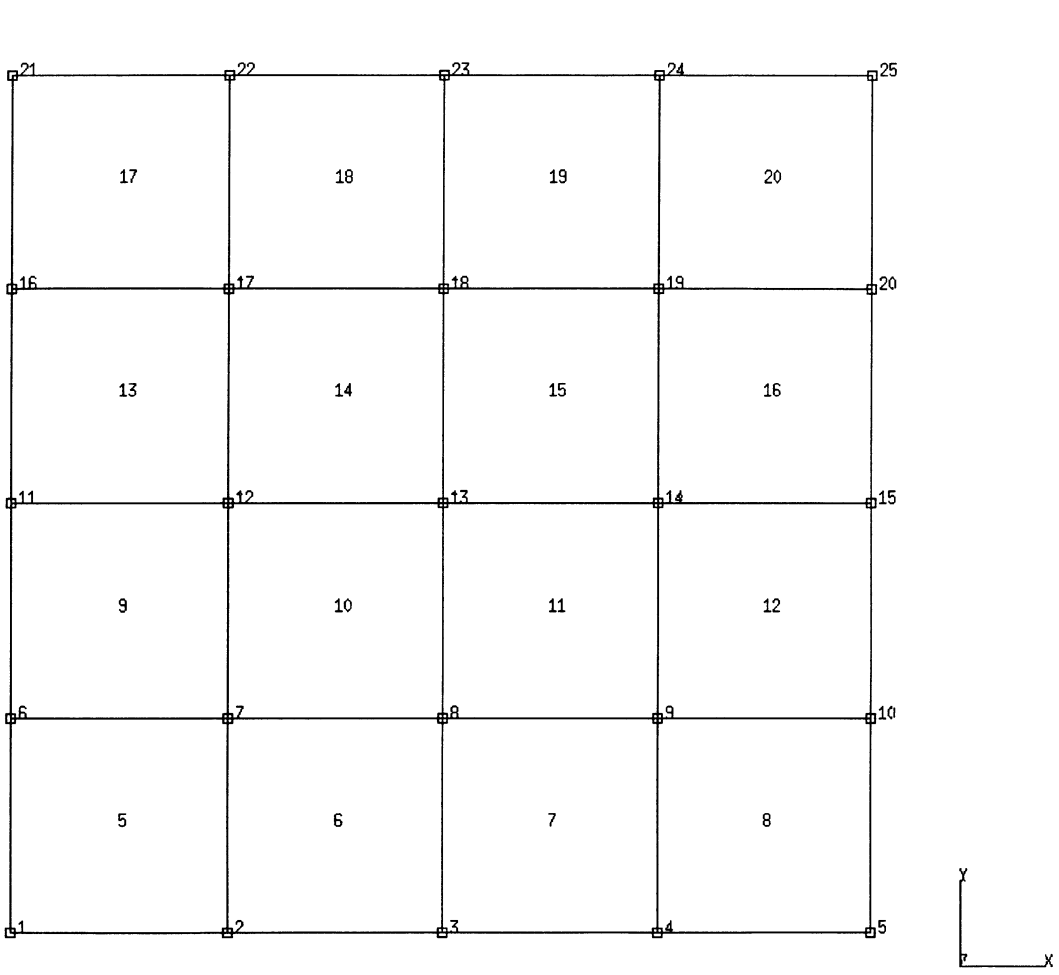

Figure E 7.6-2 Finite Element Mesh

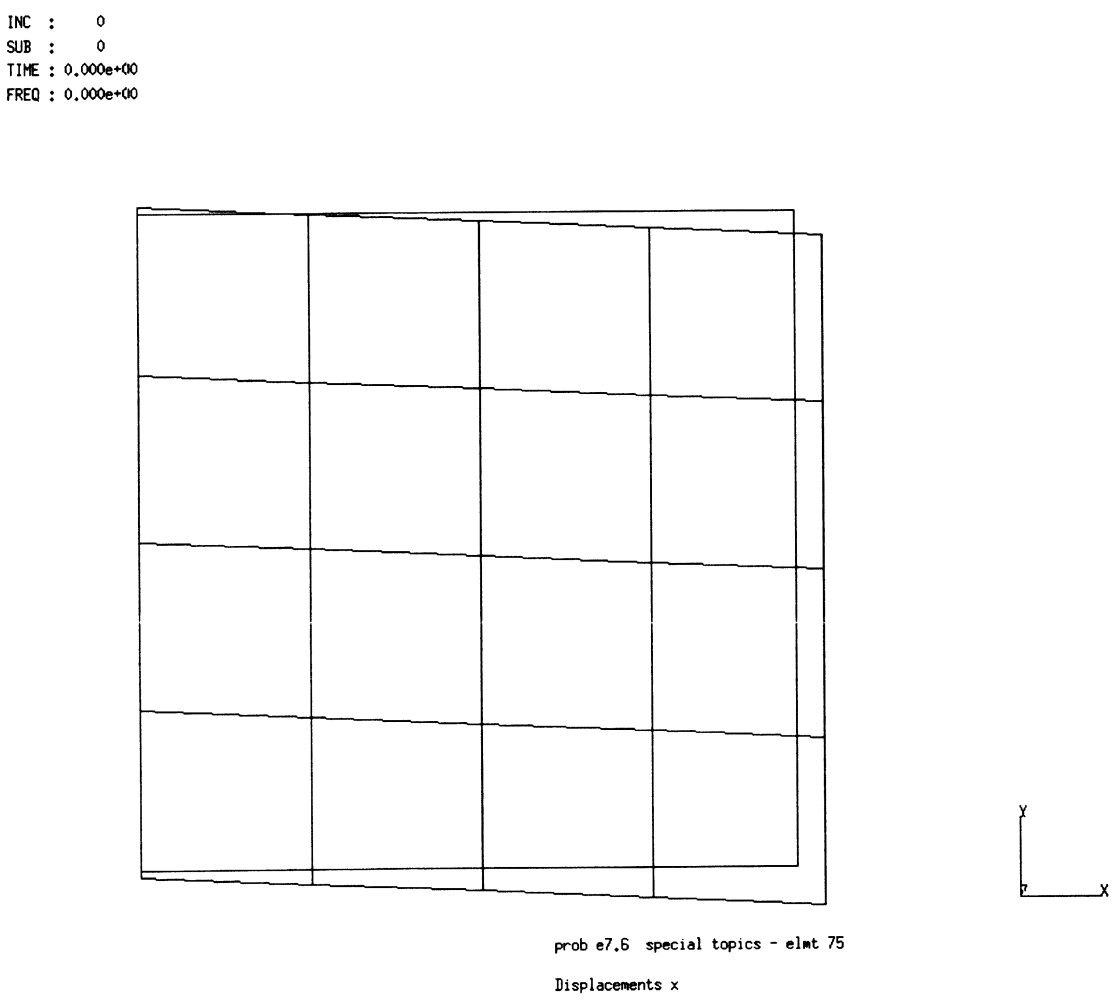

Figure E 7.6-3 Deformed Mesh Plot

E 7.7 Composite Plate Subjected To Thermal Load

A composite plate is subjected to a uniform thermal load.

Element

Element 75, the four-node bilinear thick shell element, is used. In this analysis, three layers will be used through the thickness.

Model

The square plate of 1 inch length has been divided into 16 elements with 25 nodes as shown in Figure E 5.7-1. To demonstrate that the element numbers do not need to begin with 1, they are given id's of 5 to 20.

Geometry

No geometry specification is used. The plate thickness on a layer-by-layer basis is specified with the COMPOSITE option. There the thickness of layers 1 to 3 are 0.003, 0.0025, 0.0025 respectively, giving a total thickness of 0.008 inch.

Loading

The initial temperature for all the layers is 125°F, and the plate is cooled to 25°F in increment 0. All elements, integration points and layers are given the same temperature. The INITIAL STATE and CHANGE STATE options are used to define this data.

Boundary Conditions

The edge x = 0, with nodes 1, 6, 11, 16, 21 are prescribed to have no x-displacement. Additionally, node 11 is constrained such that $u_y = u_z = \phi_x = \phi_y = 0$. This eliminates any rigid body motion. Note that if the material was isotropic, there would be free thermal expansion given these boundary conditions, and the stresses would be zero.

Material Properties

The plate is made of a single orthotropic material which is oriented differently between layers 1 and 2 and 3. First the ORTHOTROPIC option is used to define the material properties:

$E_{11} = 19.8 \times 10^9$	$\upsilon_{12} = .35$	$G_{12} = 70 \times 10^7$	$\alpha_{11} = .7 \times 10^{-5}$ in/in°F
$E_{22} = 19.8 \times 10^8$	$\upsilon_{23} = 0.0$	$G_{13} = 70 \times 10^7$	$\alpha_{22} = .23 \times 10^{-5}$ in/in°F
$E_{33} = 0$	$\upsilon_{31} = 0.0$	$G_{31} = 70 \times 10^7$	$\alpha_{33} = 0.0$

As element 75 has only two direct components of stress (NDI = 2), it is not necessary to define E_{33} and α_{33}. Since the element has three components of shear (in-plane and transverse), all values of G were entered. As $\upsilon_{23} = \upsilon_{31} = 0$, this is an odd material.

The base material orientation is given in the ORIENTATION block as being at 0° with respect to the 1-2 edge which will place it along the x-axis. The actual orientation is given in the COMPOSITE option as ply angles with respect to this base orientation.

The base material orientation is given in the ORIENTATION block as being at 0° with respect to the 1-2 edge which will place it along the x-axis. The actual orientation is given in the COMPOSITE option as ply angles with respect to this base orientation.

The COMPOSITE option is used to define three layers, each of the same material but with thickness of 0.003, 0.0025 and 0.0025 inch. The stacking sequence is +45./0./0.

There are no temperature dependent effects in this example. If necessary, the ORTHO TEMP option would be used to enter this data.

Controls

The PRINT ELEM option is used to request that the stresses are output in both the conventional elements system and the local preferred system.

Results

The results indicate that the non-isotropic nature of the composite plate results in a generation of out-of-plane displacements as large as 0.05 inch and equivalent stresses as high as 1 x 10^6 psi.

Summary of Options Used

Listed below are the options used in example e7x7.dat:

Parameter Options

ELEMENT
END
SHELL SECT
SIZING
TITLE

Model Definition Options

CHANGE STATE
COMPOSITE
CONNECTIVITY
COORDINATE
DEFINE
END OPTION
FIXED DISP
INITIAL STATE
ORIENTATION
ORTHOTROPIC
POST
PRINT ELEM

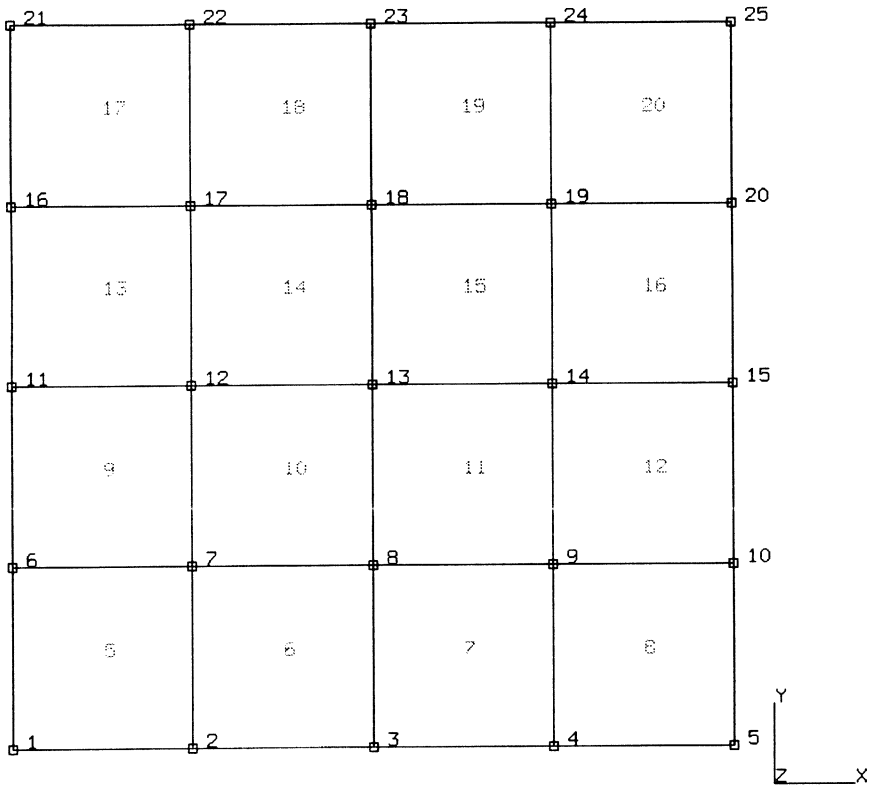

Figure E 7.7-1 Plate Geometry and Mesh

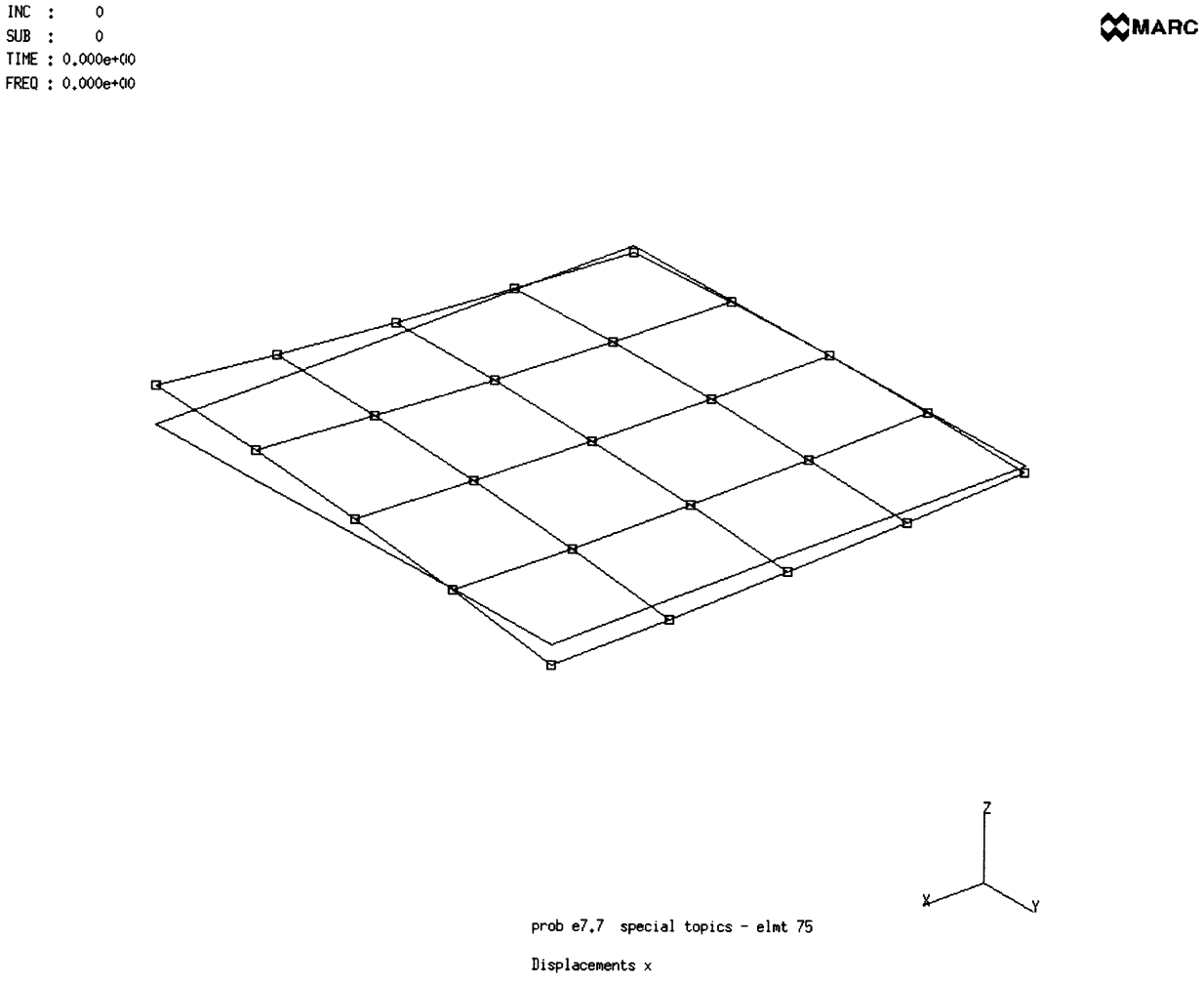

Figure E 7.7-2 Displaced Mesh

E 7.8 Cylinder Under External Pressure (Fourier Analysis)

A solid cylinder in plane strain with radius (a) and external pressure (p_o) is elastically analyzed. Love [1] gives the solutions to the first and second modes of this problem as follows:

$$\sigma_{rr} = p_o\, r \cos\theta$$
$$\sigma_{\theta\theta} = 3p_o\, r \cos\theta$$
$$\sigma_{r\theta} = p_o\, r \sin\theta$$

for the first mode, and

$$\sigma_{rr} = p_o \cos 2\theta$$

$$\sigma_{\theta\theta} = p_o\left(\frac{2r^2 - a^2}{a^2}\right)\cos 2\theta$$

$$\sigma_{r\theta} = p_o\left(\frac{r^2 - a^2}{a^2}\right)\sin 2\theta$$

for the second mode. It should be noted that for the first mode, the condition $\sigma_{rr}(a) = p_o \cos\theta$ requires that $\sigma_{r\theta}(a) = p_0 \sin\theta$, where "a" is 1 inch. Two FOURIER series are used for expansion of the 100 psi pressure loading. One series is for the cosine terms and the other for the sine terms. Three different methods, as shown in Problems e7-8a, e7.8b and e7.8c are demonstrated in describing the series. Comparison of the results with Love's [1] exact solution is presented.

Element (Ref. B62.1)

Element type 62, the axisymmetric quadrilateral element for arbitrary loading, is used here. Details on this element are found in Volume B.

Model

The geometry and mesh used are shown in Figure E 7.8-1. The solid cylinder has a height of 0.1 in. and a radius of 1.0 in. The mesh has 10 elements and 53 nodes.

Geometry

This option is not required for this problem.

Material Properties

The elastic material data assumed for this example is Young's modulus (E) is 30. x 10^6 psi and Poisson's ratio (v) is 0.25.

Loading

The 100 psi external pressure is specified as a distributed load (IBODY=0) and associated with FOURIER series number 1. The -100 psi shear is specified as a uniform load in the circumferential direction (IBODY=14) and associated with FOURIER series number 2. Only element 10 is specified with the above loads using the DIST LOAD option.

Boundary Conditions

All nodes on the plane Z = 0. and Z = 0.1 are constrained in the axial direction such that only radial motion is permitted. Nodes 1, 2 and 3 on the plane R = 0 are also constrained in the radial direction due to symmetry.

FOURIER

Three different ways are used to describe the series:

1. Specify the first two non-zero terms for series number 1 by evaluating the following integral:

$$a_n = \frac{1}{\pi}\int_0^{2\pi} \begin{pmatrix} \cos\theta \\ \cos 2\theta \end{pmatrix} \cos\ n\theta\ d\theta = \begin{cases} 0, \text{ all n except} \\ 1, \text{ n = 1, and 2} \end{cases}$$

   and the first non-zero term for series number 2 by evaluating the following integral:

$$b_n = \frac{1}{\pi}\int_0^{2\pi} \sin\ \theta\ \sin\ n\theta\ d\theta = \begin{cases} 0, \text{ all n except} \\ 1, \text{ n = 1} \end{cases}$$

2. Describe the function F(θ) which is to be expanded into a FOURIER series by an arbitrary number (say 5) of [θ, F(θ)] pairs of data.

3. Use user subroutine UFOUR to generate an arbitrary number of [θ,F(θ)] pairs and let the program calculate the FOURIER series coefficients. Five pairs of [θ,F(θ)] are defined in this example.

It should be pointed out that five pairs of [θ,F(θ)] have been chosen for demonstration only. It is easy to add more by changing the number 5 in the user subroutine UFOUR. An increased number of [θ,F(θ)] pairs would yield better results in comparison with the exact coefficient evaluations.

Results

The results for the radial and circumferential stresses of Problem e7.8a and Love's exact solution are plotted in Figure E 7.8-2 and Figure E 7.8-3. They indicate that the finite element solutions are in good agreement with the exact solutions.

Reference

Love, A.E.H., *A Treatise on the Mathematical Theory of Elasticity*, Dover, New York.

Summary of Options Used

Listed below are the options used in example e7x8a.dat:

Parameter Options

ELEMENT
END
FOURIER
SIZING
TITLE

Model Definition Options

CONNECTIVITY
CONTROL
COORDINATE
DIST LOADS
END OPTION
FIXED DISP
FOURIER
ISOTROPIC
RESTART

Listed below are the options used in example e7x8b.dat:

Parameter Options

ELEMENT
END
FOURIER
SIZING
TITLE

Model Definition Options

CONNECTIVITY
CONTROL
COORDINATE
DIST LOADS
END OPTION
FIXED DISP
FOURIER
ISOTROPIC
RESTART

Listed below are the options used in example e7x8c.dat:

Parameter Options

ELEMENT
END
FOURIER
SIZING
TITLE

Model Definition Options

CONNECTIVITY
CONTROL
COORDINATE
DIST LOADS
END OPTION
FIXED DISP
FOURIER
ISOTROPIC
RESTART

Listed below is the user subroutine found in u7x8c.f:

UFOUR

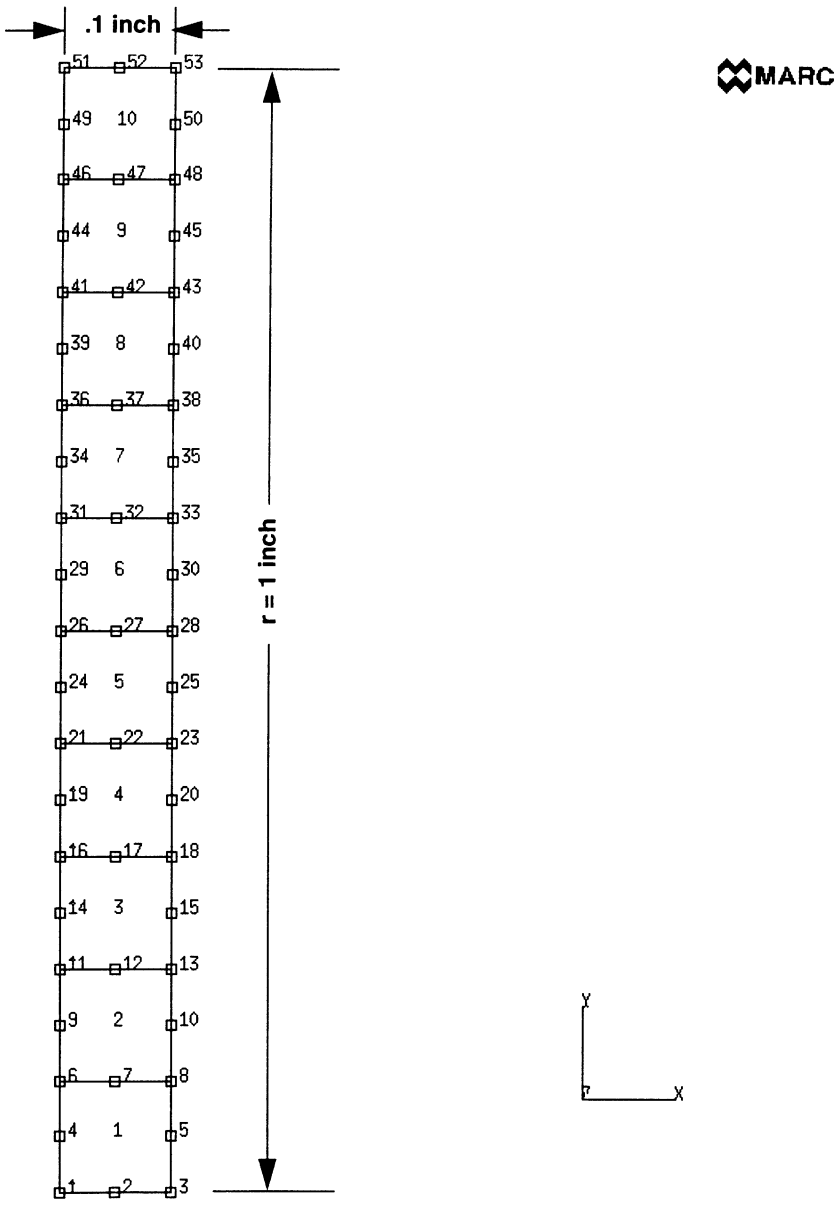

Figure E 7.8-1 Cylinder and Mesh

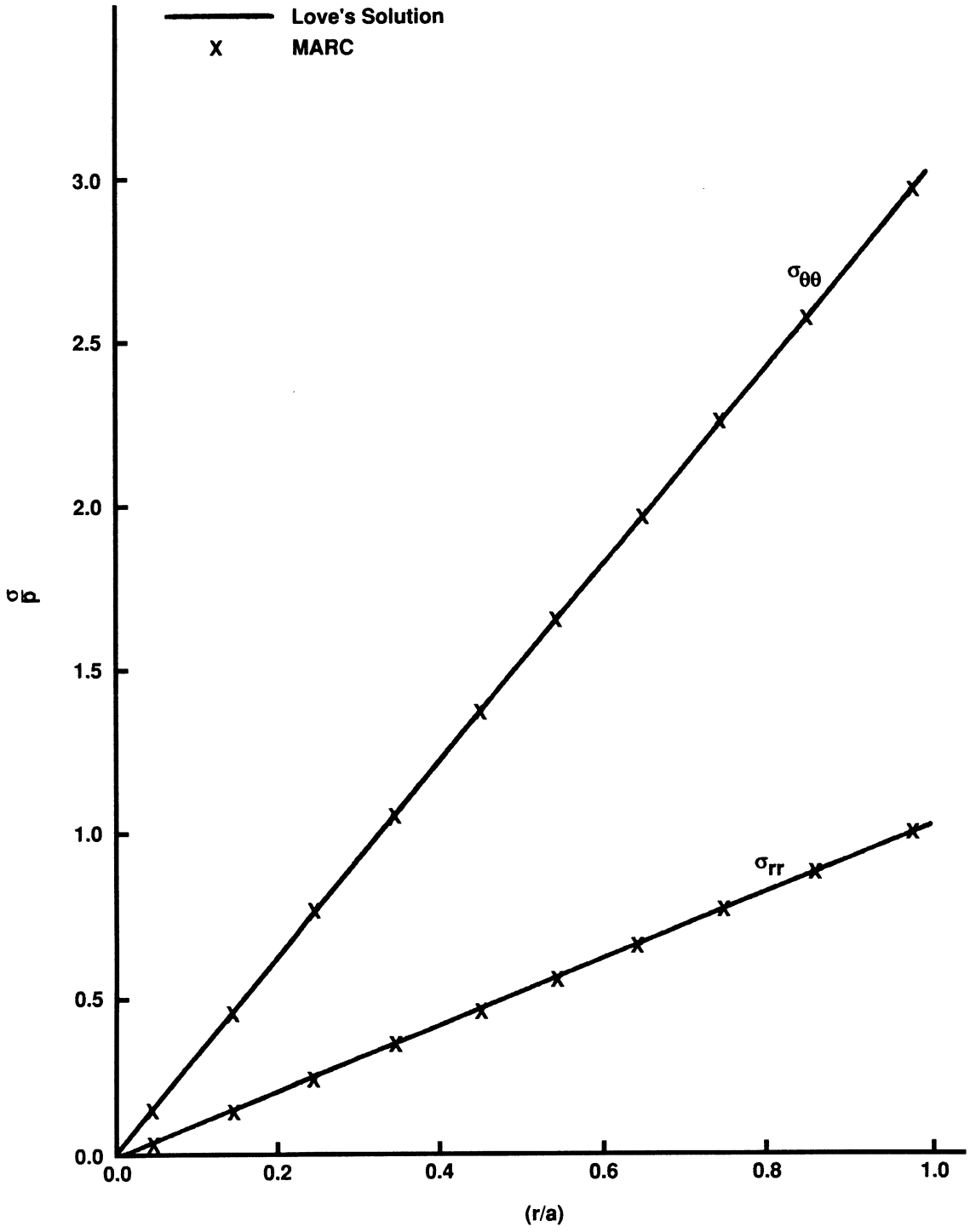

Figure E 7.8-2 First Mode Solid Cylinder Plane Strain

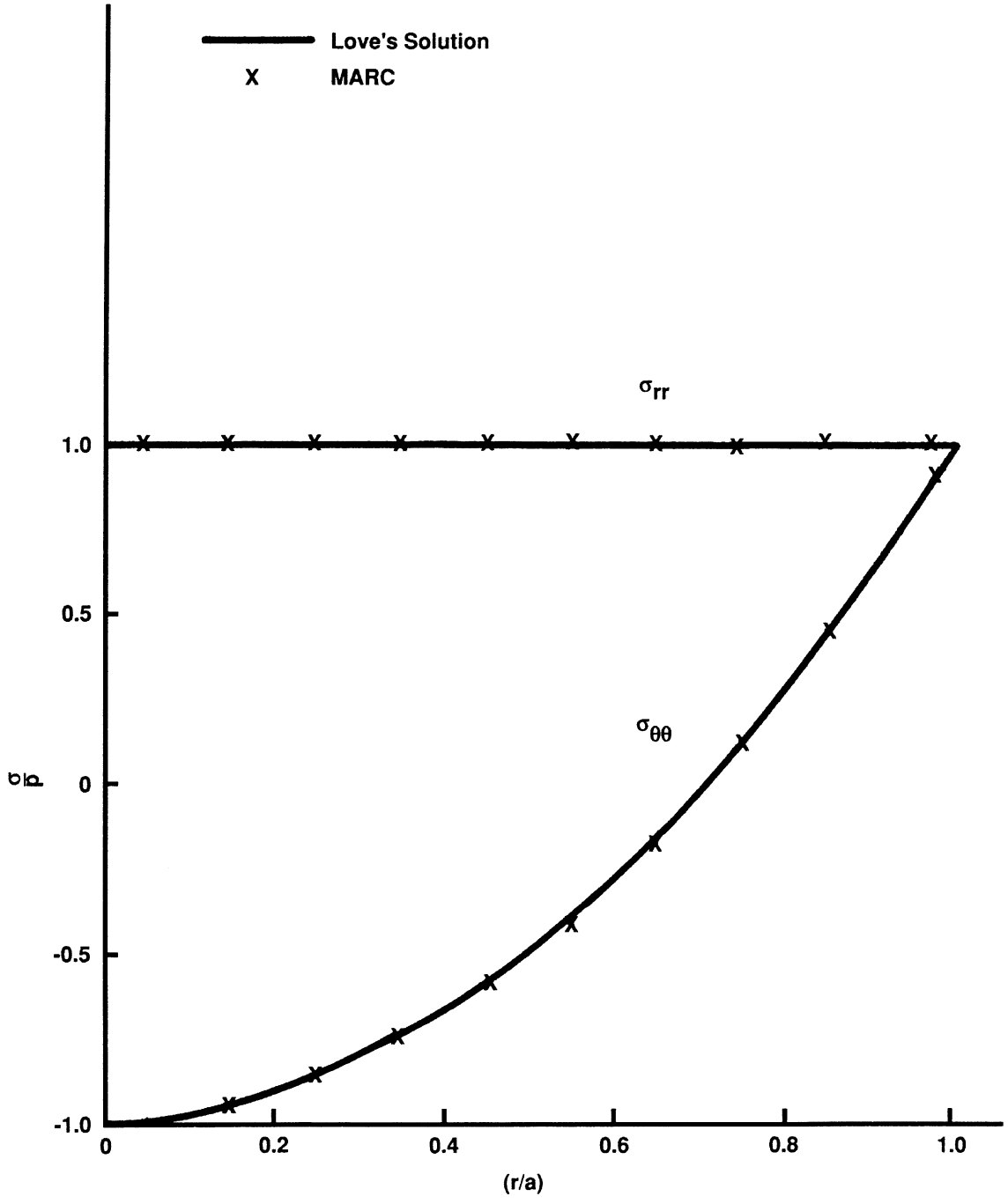

Figure E 7.8-3 Second Mode Solid Cylinder Plane Strain

E 7.9 Cylinder Under Line Load (Fourier Analysis)

A solid cylinder in plane strain with a concentrated line load acting across the diameter is elastically analyzed. One FOURIER series with only symmetric terms is used to characterize the circumferential variation of the loading. Two different methods are demonstrated in describing the FOURIER series (problems e7.9a and e7.9b). The CASE COMBIN option is used to obtain the final results by superposition at four equally spaced stations around the circumference in problem e7.9c.

Element

Element 62, the axisymmetric quadrilateral for arbitrary loading, is used here. Details on this element are found in Volume B.

Model

The geometry and mesh are shown in Figure E 7.9-1. The solid cylinder has a height of 0.1 in. and a radius of 1.0 in. The mesh consists of 10 elements and 53 nodes.

Geometry

This option is not required for this problem.

Material Properties

The elastic material data assumed for this example is Young's modulus (E) of 30. x 10^6 psi and Poisson's ratio (v) of 0.25.

Loading

The 100 lb. line load acting across the diameter is specified as a distributed load (IBODY=0) on element 10 and associated with FOURIER series number 1. The force magnitude given in the DIST LOAD block is equal to $100/\pi$.

Boundary Conditions

All nodes on the planes Z = 0. and Z = 0.1 are constrained in the axial direction such that only radial motion is permitted. Nodes 1, 2 and 3 on the plane R = 0 are also constrained in the radial direction due to symmetry.

FOURIER

Two different methods are used to describe the series:

1. Specifying the first 8 non-zero terms to approximate the infinite series representing the actual loading:

$$a_o = \frac{1}{2\pi}\int_0^{2\pi} P(\theta)\, d\theta = \frac{1}{\pi}$$

$$a_n = \frac{1}{\pi}\int_o^{2\pi} P(\theta) \cos\, n\theta\, d\theta = \begin{cases} 0, \text{ n-odd} \\ \frac{2}{\pi}, \text{ n-even} \end{cases}$$

2. Using user subroutine UFOUR generates an arbitrary number (say 361) of [θ,F(θ)] pairs and the program calculates the series coefficients. The results should compare closely with the above exact calculations. In this example six function pairs are generated by the subroutine.

Results

Figure E 7.9-2 gives a comparison of the radial displacements at $\theta = 0^\circ$ predicted by this analysis with the exact solution of Muskhelishvili. For $\theta = 0^\circ$, $a = 1.0$ and $\nu = 0.25$, the solution is:

$$u_r(\theta=0^\circ) = \frac{1}{2\pi}\left[3\, \ln\frac{(1+\frac{r}{a})}{(1-\frac{r}{a})} - \frac{r}{a}\right]\frac{P(1+\nu)}{E}$$

The comparison is very good except at r ' a. Here, the finite element solution cannot capture the singular behavior of the problem and falls below the unbounded exact solution.

Reference

Muskhelishvili, N. I., *Some Basic Problems of the Mathematical Theory of Elasticity*, translated by J.R.M. Radok, Erven P. Noordhoff, The Netherlands, 1963.

Summary of Options Used

Listed below are the options used in example e7x9a.dat:

Parameter Options

ELEMENT
END
FOURIER
SIZING
TITLE

Model Definition Options

CONNECTIVITY

CONTROL
COORDINATE
DIST LOADS
END OPTION
FIXED DISP
FOURIER
ISOTROPIC
RESTART

Listed below are the options used in example e7x9b.dat:

Parameter Options

ELEMENT
END
FOURIER
SIZING
TITLE

Model Definition Options

CONNECTIVITY
CONTROL
COORDINATE
DIST LOADS
END OPTION
FIXED DISP
FOURIER
ISOTROPIC
RESTART

Listed below is the user subroutine found in u7x9b.f:

UFOUR

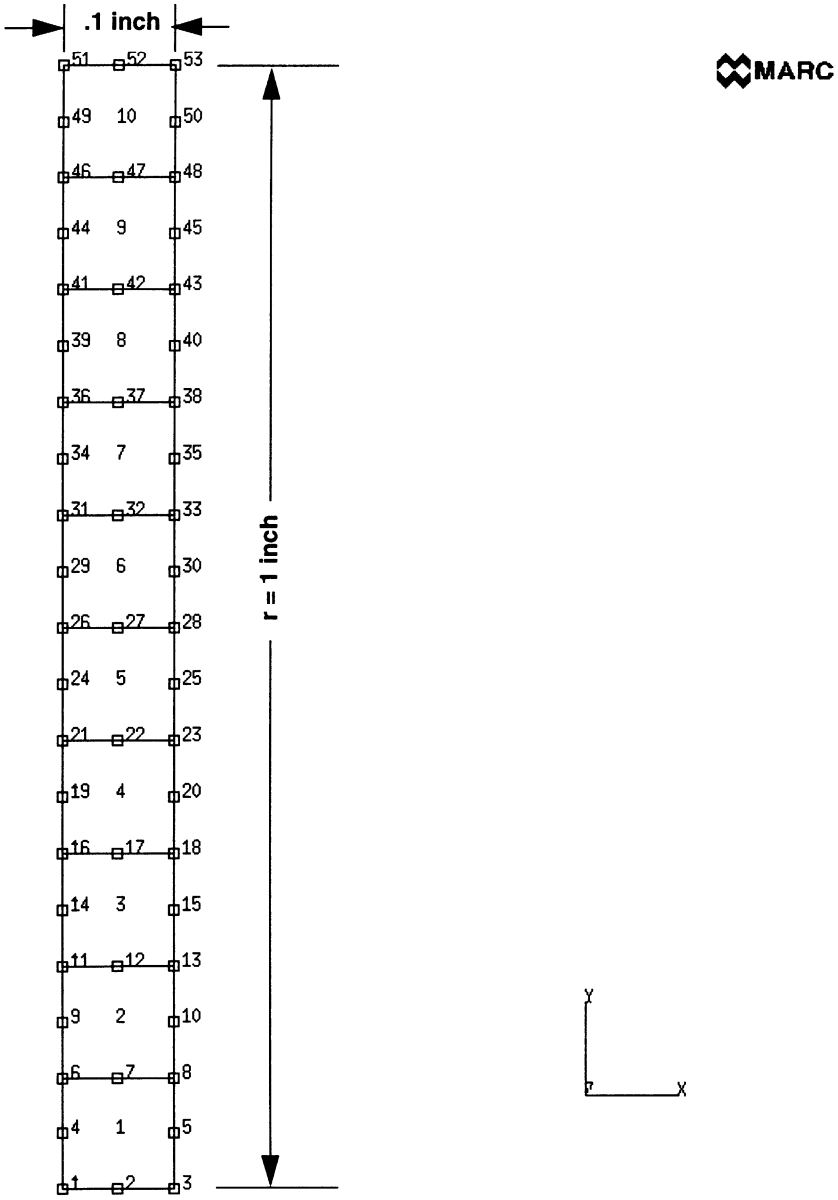

Figure F 7.9-1 Cylinder and Mesh

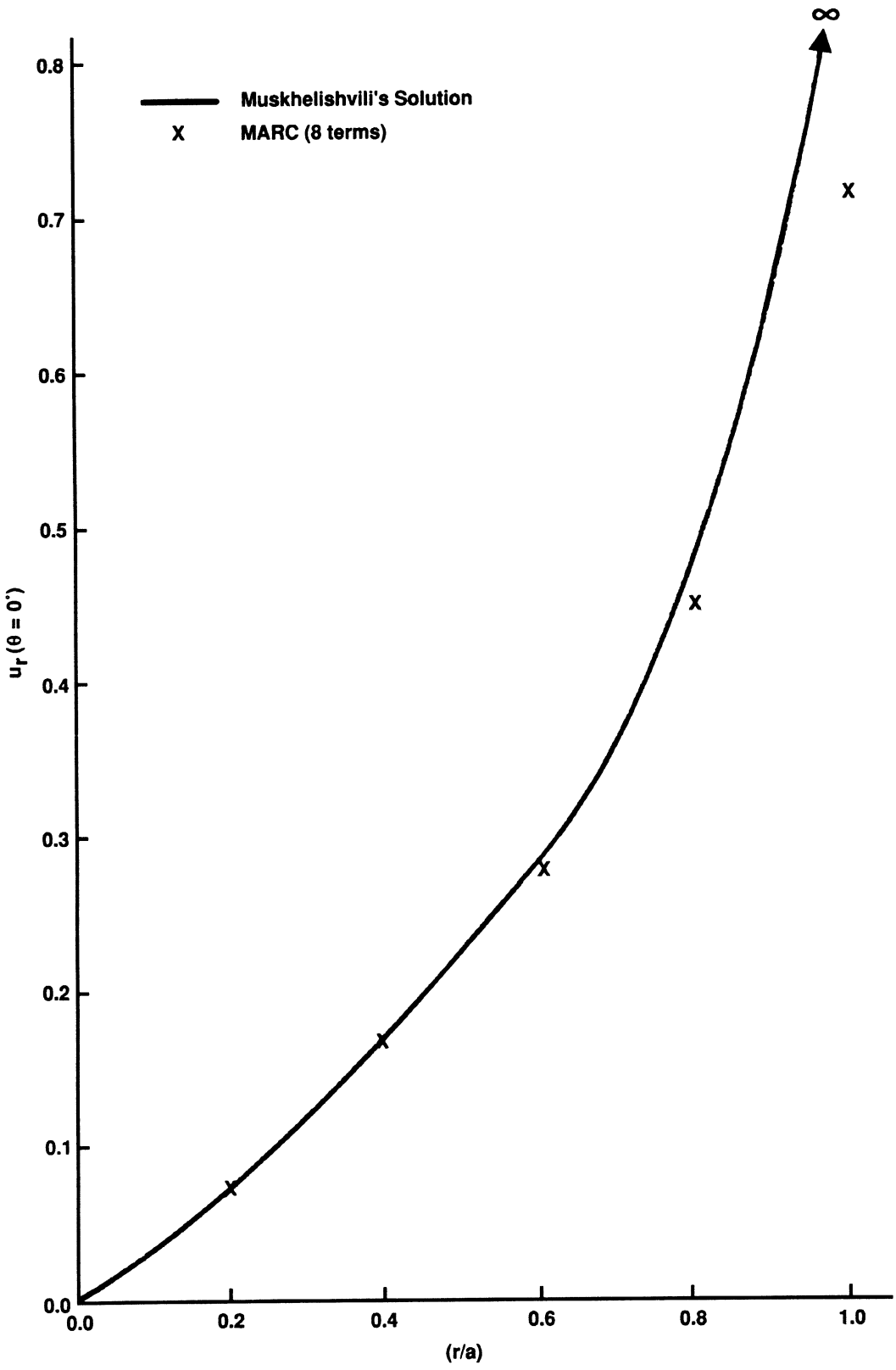

Figure E 7.9-2 Concentrated Load on a Solid Cylinder

E 7.10 Mesh Qualification

This problem uses the QUALIFY option for mesh refinement studies. This option is invoked by adding the QUALIFY parameter. It is only applicable for the higher order isoparametric elements. The model and input data of the problem follow.

Model

A quarter of a square membrane structure is modeled using four 8-node quadrilateral elements type 27, 8-node plane-strain element). Dimensions of the model and a finite element mesh are shown in Figure E 7.10-1.

Material Properties

The Young's modulus and Poisson's ratio of the membrane are assumed to be 10E6 psi and 0.3, respectively.

Loading

Two concentrated forces of equal magnitude are applied at the corner of the membrane (node 21). The forces are $F_x = F_y = 7.07$ pounds.

Boundary Conditions

Displacement at lines of symmetry are constrained ($u = 0$ at $x = 0$ and $v = 0$ at $y = 0$).

Geometry

The membrane thickness is 0.1 inch.

Results

Strain Energy Difference (SED) contours are shown in Figure E 7.10-2. The large value in the corner implies that for this loading condition the mesh refinement should take place in the corner region of element number 4.

Summary of Options Used

Listed below are the options used in example e7x10.dat:

Parameter Options

ELEMENT
END
MESH PLOT
QUALIFY
SIZING
TITLE

Model Definition Options

CONNECTIVITY
COORDINATE
END OPTION
FIXED DISP
GEOMETRY
ISOTROPIC
POINT LOAD

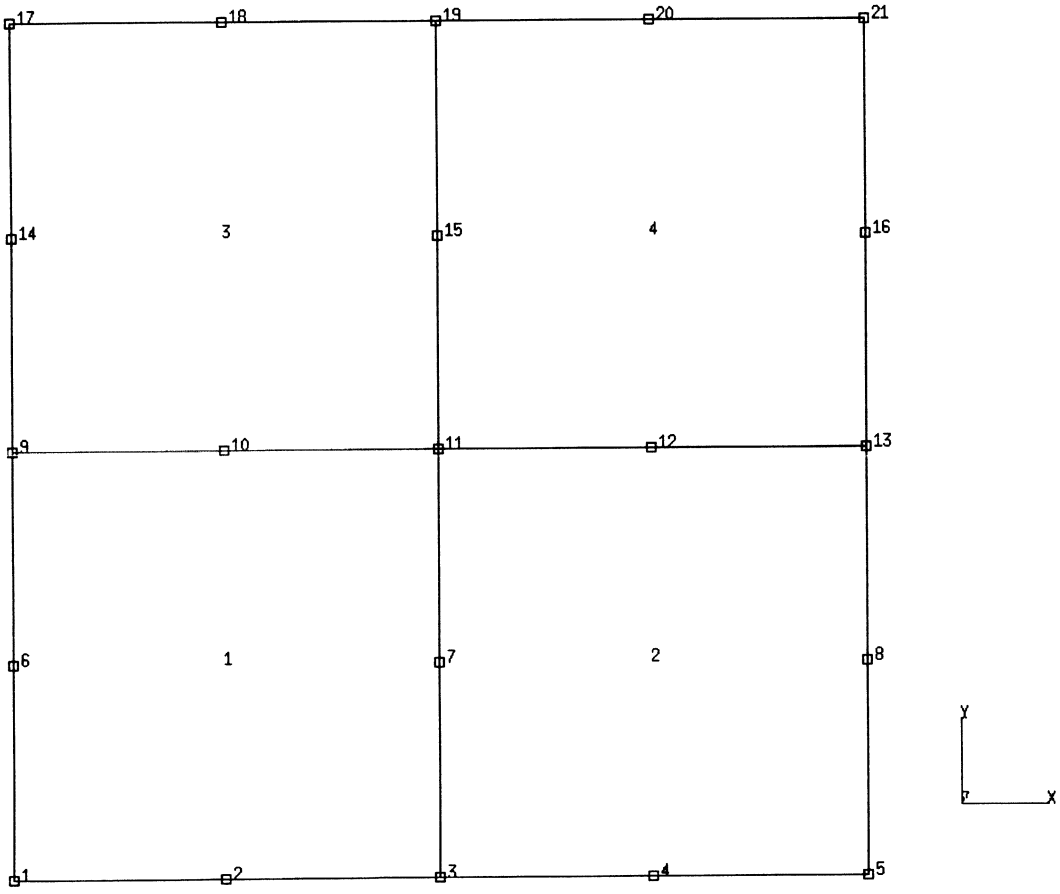

Figure E 7.10-1 Membrane and Mesh

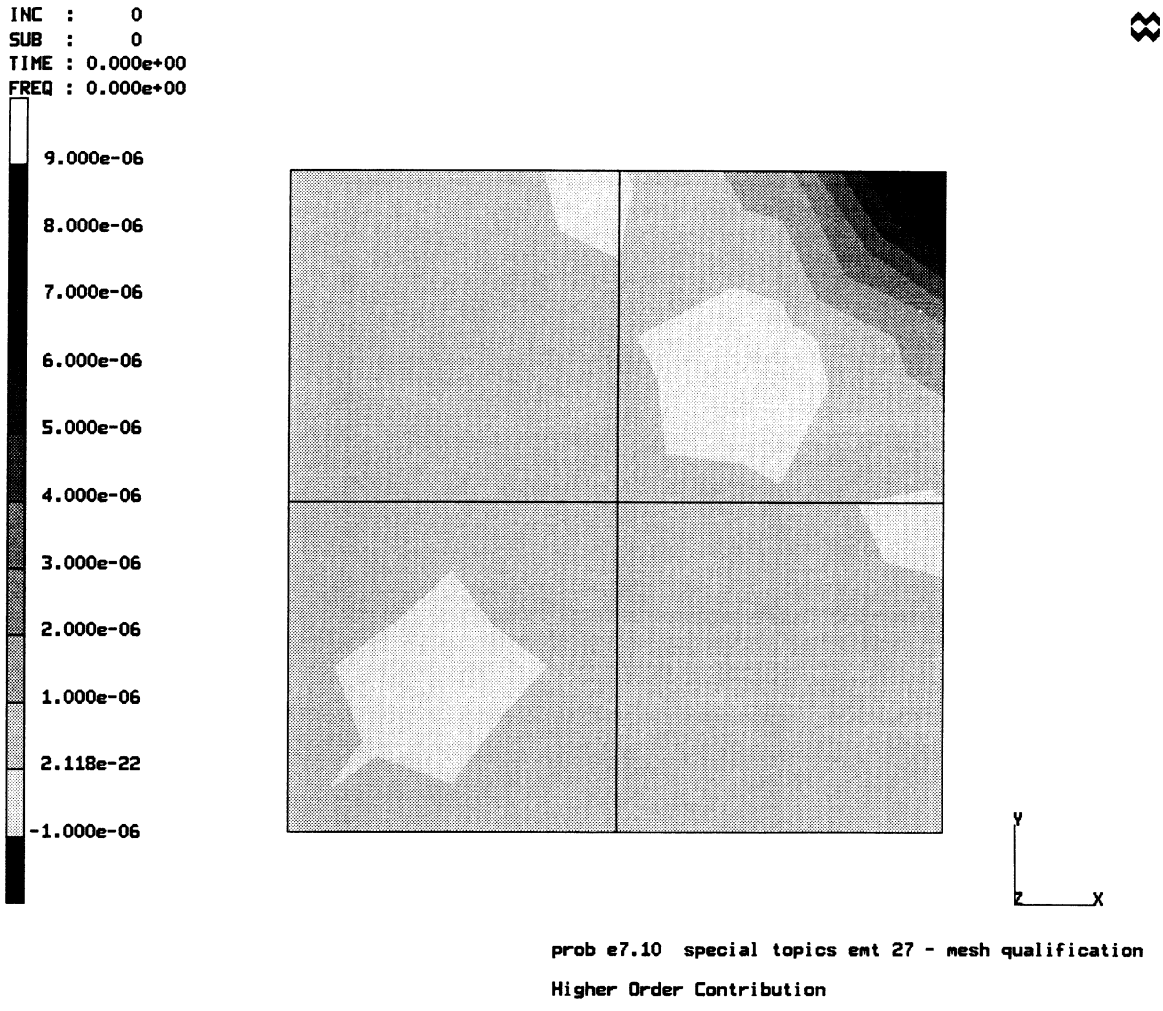

Figure E 7.10-2 Strain Energy Difference

E 7.11 Concrete Beam Under Point Loads

A simply supported concrete beam is subjected to two concentrated loads. The beam is analyzed using the concrete cracking option in the MARC program. Plane stress element (element type 3) is used for modeling the concrete and truss element (element type 9) is chosen for the simulation of steel reinforcement. The cracking option allows cracks to initiate in the concrete elements. The model and input data of the problem follow.

Model

The dimensions of the beam and the finite element mesh are shown in Figure E 7.11-1. The model consists of 80 elements representing the concrete and 10 elements representing the steel.

Material Properties

The elastic-plastic material data is given through the ISOTROPIC option.

For concrete (Elements 1-80), material id of 1

E_c = 3.E6 psi
ν_c = 0.15
σ_{yc} = 1250 psi

For steel reinforcement (Elements 81-90), material id of 2

E_s = 3.E7 psi
ν_s = 0.3
σ_{ys} = 40,000 psi

For both the concrete and the rebars, an isotropic plasticity model is used. For the concrete elements the cracking flag is initiated.

Crack Data

The concrete (material id of 1) has an ultimate tensile stress of 700 psi. The shear retention factor is 0.5. The strain softening modulus is 365 psi.

Geometry

Thickness of the concrete beam 1.0 inch; area of the steel reinforcement = 0.1 square inch.

Loading

Two concentrated loads are symmetrically placed near the centerline of the beam. A total of 1175 lb. (2 x 587.5 lb.) is applied to the beam in 10 increments. Variable load increments, through the use of options POINT LOAD, PROPORTIONAL INCREMENT, and AUTO LOADS are:

Inc. No.	Load Increment
0	2 x 250
1	2 x 62.5
2	2 x 62.5
3	2 x 62.5
4	0.
5	2 x 50.
6	0.
7	2 x 50.
8	0.
9	2 x 50.

Boundary Conditions

Out-of-plane degrees of freedom are constrained for all nodal points (w = 0 for all nodes). Symmetry conditions are imposed along line x = 68 (u = 0 for nodes 29, 31, 33, 89, 91, 93, 95, 97 and 99). Simply-supported conditions are placed at node 1 (v = 0).

Results

A deformed mesh plot is shown in Figure E 7.11-2. Cracking begins in increment 4 and the program begins to iterate. By increment 9, seven elements have developed cracks and the largest crack strain is about 0.034%. Figure E 7.11-3 shows the final cracked region consisting of 14 elements near the bottom center portion of the beam.

Summary of Options Used

Listed below are the options used in example e7x11.dat:

Parameter Options

ELEMENT
END
SIZING
TITLE

Model Definition Options

CONNECTIVITY
CONTROL
COORDINATE
CRACK DATA
END OPTION
FIXED DISP
GEOMETRY
ISOTROPIC
POINT LOAD
PRINT CHOICE

Load Incrementation Options

AUTO LOAD
CONTINUE
POINT LOAD
PROPORTIONAL INCREMENT

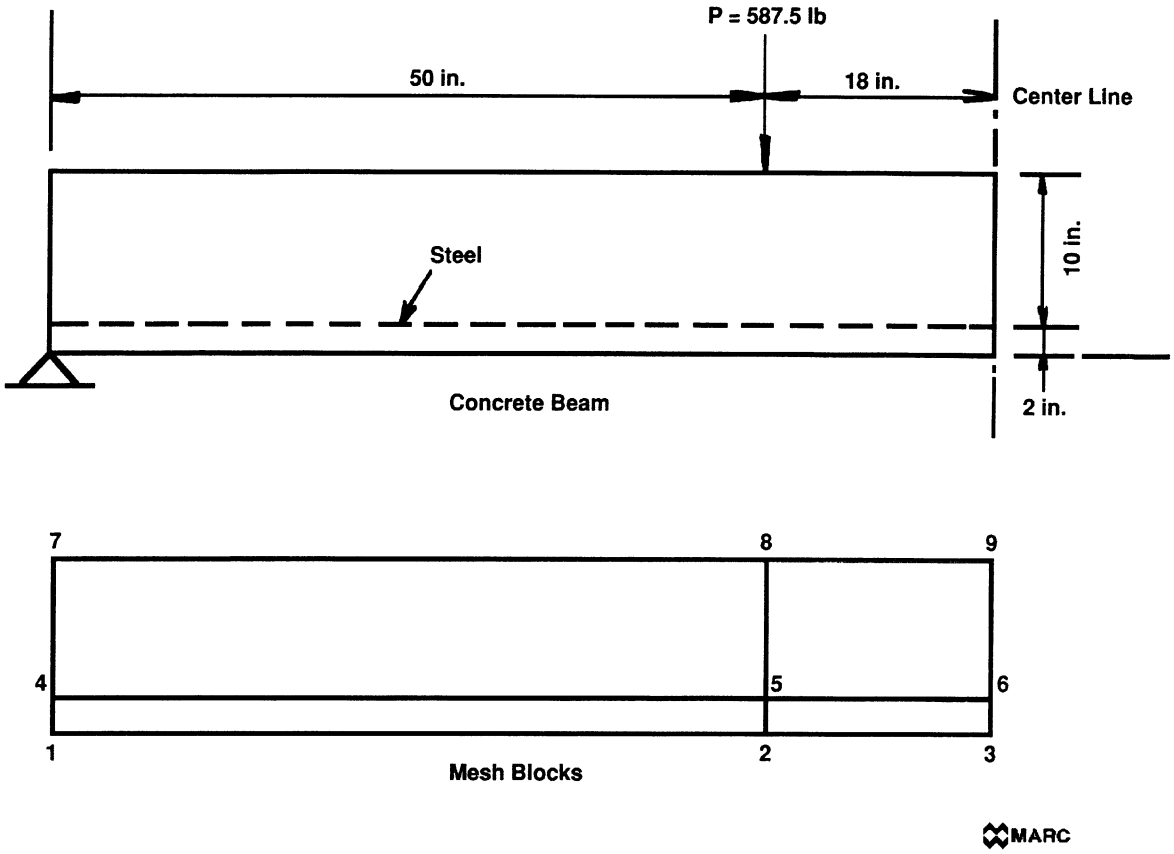

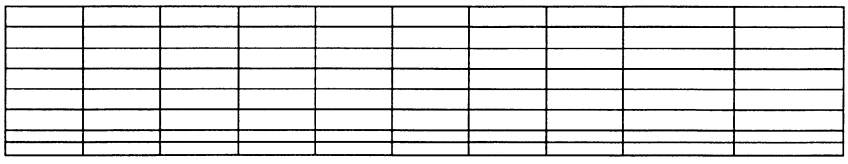

Figure E 7.11-1 Concrete Beam and Mesh

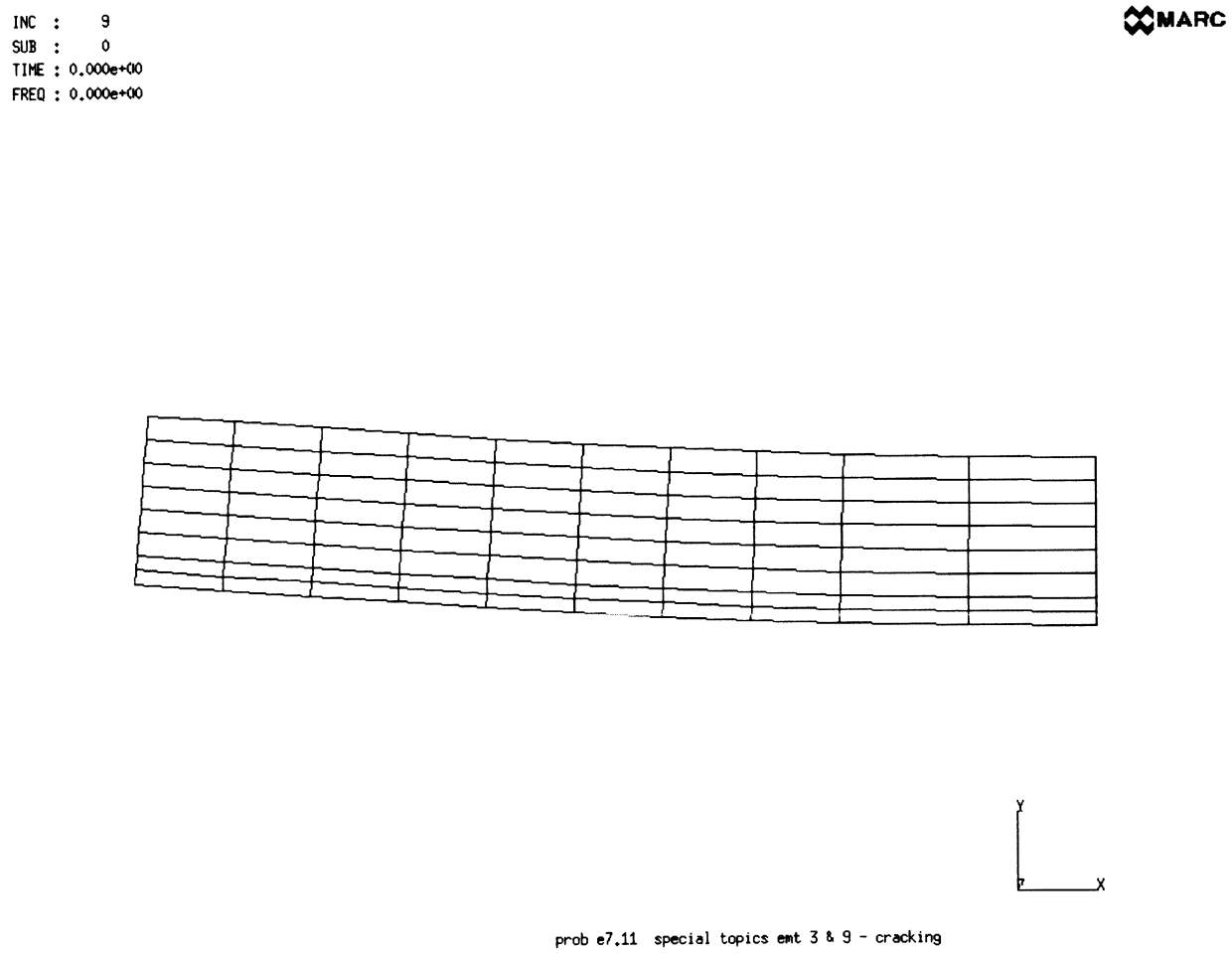

Figure E 7.11-2 Deformed Mesh Plot

61	62	63	64	65	66	67	68	79	80
53	54	55	56	57	58	59	60	77	78
45	46	47	48	49	50	51	52	75	76
37	38	39	40	41	42	43	44	73	74
29	30	31	32	33	34	35	36	71	72
21	22	23	24	25	26	27	28	69	70
9	10	11	12	13	14	15	16	19	20
1	2	3	4	5	6	7	8	17	18

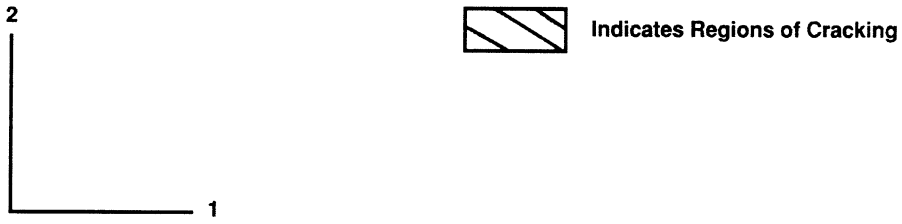

Figure E 7.11-3 Regions of Cracking

E 7.12 Constant Uniaxial Stress Applied To Plate In Plane Strain (Viscoelasticity)

A viscoelastic rectangular plate (Figure E 7.12-1) is subjected to a constant and uniform tensile stress of 10 psi in the x-direction. The deformation conforms to the plane strain idealization. The material is isotropic and strictly elastic in dilatational response. The bulk modulus is 20,000 psi. The time-dependent shear relaxation modulus is given as:

$$G(t) = 100 + 9900\, e^{-2.3979t} \quad \text{(psi)}$$

where the units of time are seconds. The displacements u_i (x_i,t) are required as well as the out-of-plane stress, $\sigma_{zz}(t)$. The numerical results will be compared to the closed form solution.

By converting the stress relaxation function defined above to a creep function, we obtain the creep function for isotropic shear behavior is obtained. The corresponding stress relaxation is:

$$J(t) = \left(1 \times 10^{-4}\right) + 9.9 \times 10^{-3}\,[1\text{-}\exp(-t/41.703)] \quad \text{sq.in/lb.}$$

The constant elastic dilatational response (bulk modulus, K) is now expressed in reciprocal form compatible with the creep function formulation.

This is:

$$B = \frac{1}{K} = 0.5 \times 10^{-4} \quad \text{sq.in/lb.}$$

Element

Element type 27 is used. This is an isoparametric distorted quadrilateral element for plane strain. There are two degrees of freedom at each node and four nodes per element.

Model

There are four elements and a total of 23 nodes as shown in Figure E 7.12-2.

Geometry

The thickness is specified in EGEOM1 as 0.2 inch.

ISOTROPIC/VISCELPROP

The details of any viscoelastic material model are given in the Model Definition section. For an isotropic material, strictly elastic in dilatational response, the material characteristics can be completely represented by the Model Definition options ISOTROPIC and VISCELPROP.

Both the Young's modulus (E) and Poisson's Ratio (ν) are entered through the ISOTROPIC option. Recall that the expressions of shear modulus (G) and the bulk modulus (K) are:

$$G = \frac{E}{2(1+\nu)} \quad ; \quad K = \frac{E}{3(1-2\nu)}$$

By eliminating E, we obtain the expression of ν in terms of G and K as:

$$3\,(1-2\nu)\,K = 2\,(1+\nu)\,G$$

In the current problem, the bulk modulus K is equal to 20,000. The shear modulus G is equal to 10,000 [G(0) = 100 + 9900]. So, we obtain the values of $\nu = 0.2857$ and E = 25714.

Rewrite the expression of time dependent shear relaxation modulus as:

$$G(t) = 100 + 9900\, e^{-(t/0.4170316)}$$
$$= G_0 + G_1 * e^{-(t/\tau_1)}$$

We have $G_1 = 9900$ and $\tau_1 = 0.4170316$ that are entered through the VISCELPROP option.

Loading

The execution of this analysis consisted of three parts. The application of the tensile 10 psi load was accomplished with the DIST LOADS block. The instantaneous elastic response was then determined in increment 0. This load was held constant for the duration of the analysis using a second DIST LOADS block after END OPTION with zero incremental load.

Subsequent to this, two creep stages were applied by means of the TIME STEP and AUTO LOAD load incrementation cards. Knowledge of the closed form solution shows that most of the deformation and stress relaxation occurs in the first five seconds. Consequently, the suggested time step in the first TIME STEP block was specified as 0.1 sec. for a time span of 5.0 sec. The number of increments was set at 50 and the time step was to remain fixed for all increments at the suggested value.

In the second TIME STEP load incrementation block, the constant time step size was increased to 4.0 sec. and 50 increments were requested to cover a span of 200 sec.

It will be noted that the step size in the second creep stage is approximately one-tenth of the retardation time. This is more typical of the appropriate size which should be used in an analysis where no other characteristic times are present. Such other factors that might influence the choice of a time step are (1) diffusional times for transient thermal analysis, (2) characteristic times associated with the application of external loads, or (3) the existence of a significant shift factor in the analysis of materials classified as being thermo-rheologically simple. A series of different time step sizes might be used for different stages of an analysis where materials exhibit several characteristic relaxation or retardation times.

It was predetermined, with consideration of the closed form solution, that 100 increments would be sufficient to reach approximately to the steady state condition. A maximum value of 200 was entered in the CONTROL block. Tolerances and control limits for the analysis assume default values.

FIXED DISP

The unloaded face of the plate (x = 0) is fixed against displacement in the x-direction. The plane strain assumptions limit all displacements of the plate to the x-y plane.

Results

The exact solution for displacement of the end face, u_x (2,t), is plotted in Figure E 7.12-3. The out-of-plane stress, $\sigma_{zz}(t)$, is shown in Figure E 7.12-4. The corresponding numerical results, obtained with the MARC Program, are also plotted in these figures. The numerical results were found to be identical to the exact solution even at the point in the numerical analysis where the time step was changed from 0.1 seconds to 4.0 sec.

Summary of Options Used

Listed below are the options used in example e7x12.dat:

Parameter Options

ELEMENT
END
SIZING
TITLE

Model Definition Options

CONNECTIVITY
CONTROL
COORDINATE
DIST LOADS
END OPTION
FIXED DISP
GEOMETRY
ISOTROPIC
PRINT CHOICE
TYING
VISCELPROP

Load Incrementation Options

AUTO LOAD
CONTINUE
DIST LOADS
TIME STEP

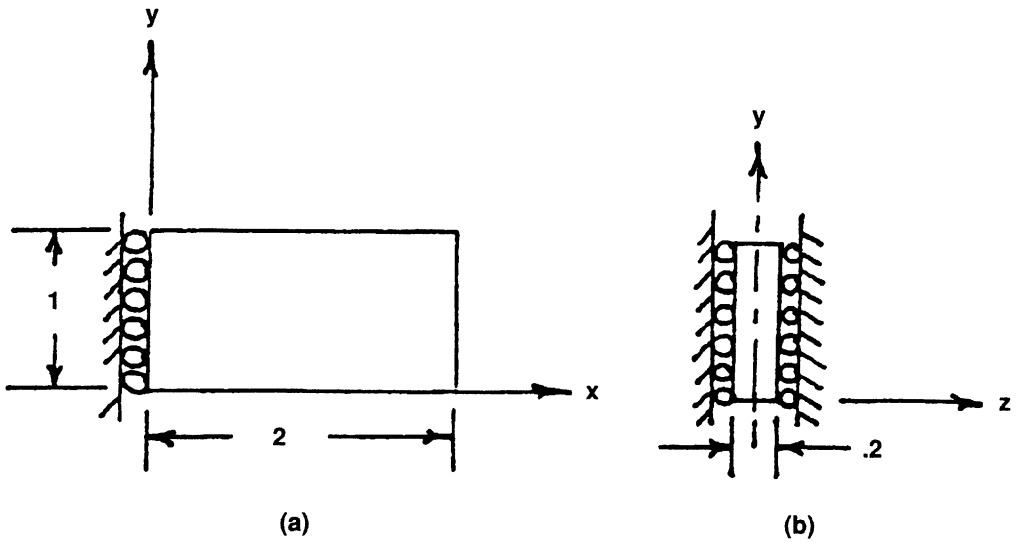

Figure E 7.12-1 Geometry

MARC

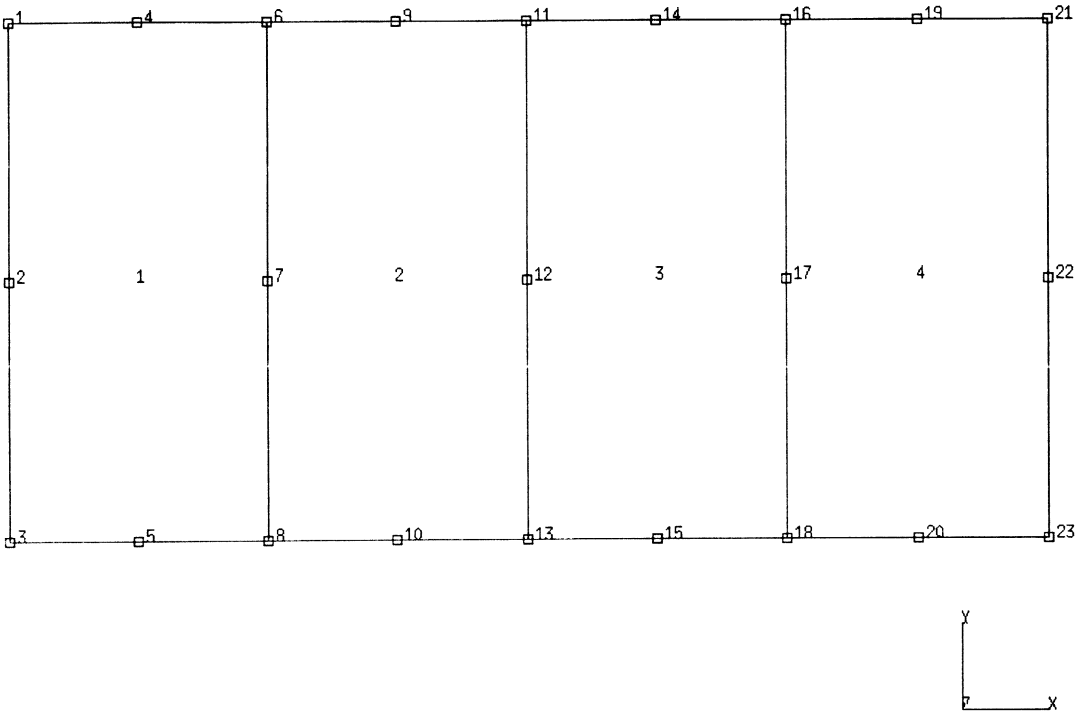

Figure E 7.12-2 Finite Element Model

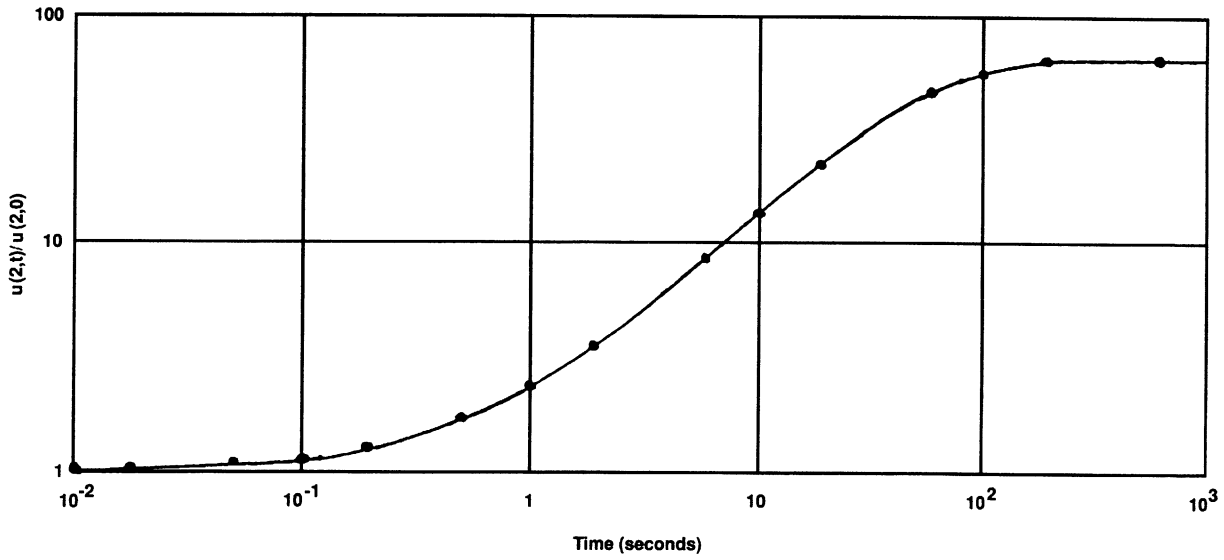

Figure E 7.12-3 Normalized Displacement vs. Time

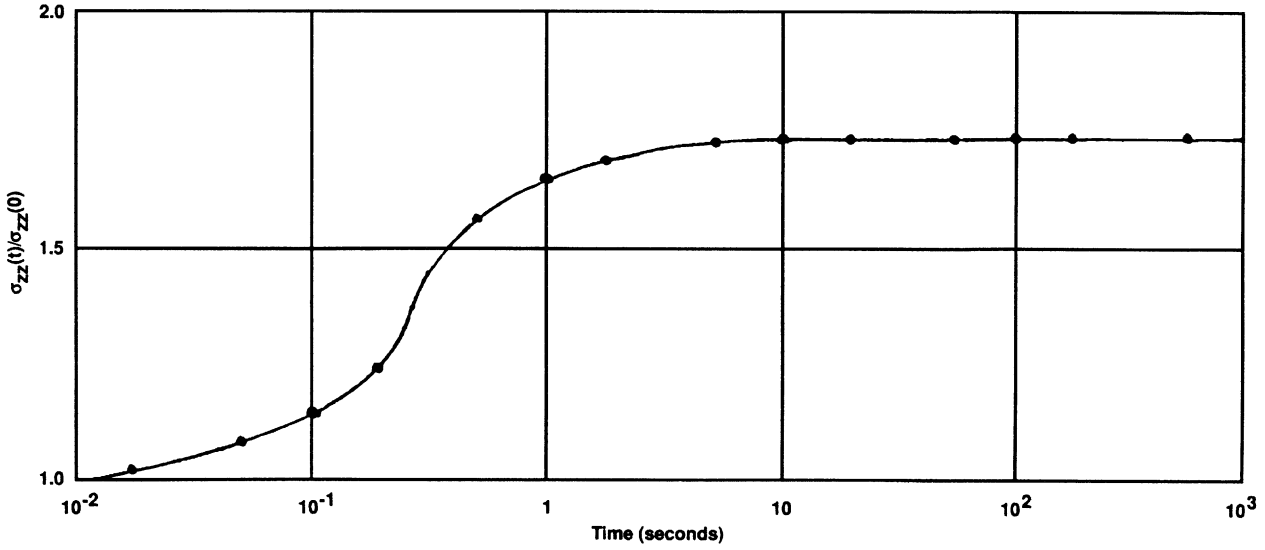

Figure E 7.12-4 Normalized Out-of-Plane Stress, σ_{zz} vs. Time

E 7.13 Analysis Of Pipeline Structure

MARC beam element type 14 and pipe-bend element type 17 are utilized for the elastic analysis of a pipeline structure subjected to either in-plane or out-of-plane bending. The structure is loaded until the limit load is reached. The pipeline mesh generation program MARC-PIPE is used for the generation of CONNECTIVITY and COORDINATES data blocks as well as the tying data required for the use of element types 14 and 17.

Model

There are a total of 20 elements in the model, of which 6 are type 14 and 14 are type 17. A total of 26 nodes are used. The dimension of the pipeline structure and a finite element mesh are shown in Figure E 7.13-1. The program MARC-PIPE is used for the mesh generation and the tying information.

Material Properties

The Young's modulus and Poisson's ratio of the pipeline material are 155.53×10^3 (ksi) and 0.3, respectively.

Tractions

An out-of-plane moment of 2.06×10^7 (in-kips) is applied at node 1 in the first analysis. As shown in Figure E 7.13-1, the applied load is a moment about the y-axis (the fifth degree of freedom of node 1). The load is increased to a final load of 3.71×10^7 (in-kips) by increment 8. In the second analysis an in-plane moment of 1.37×10^7 (in-kips) is applied at node 1. The applied load is about the z-axis (the sixth degree of freedom of node 1). The load is increased to a final load of 2.87×10^7 (in-kips) by increment 11.

Boundary Conditions

All degrees of freedom of node 26 are constrained for the fixed-end condition.

Geometry

The wall thickness and mean radius of the beam elements (element type 14) are:

For Elements 1, 2, 19 and 20:

Wall Thickness = 8.8 inches
Mean Radius = 275 inches

For Elements 3 and 18:

Wall Thickness = 10.4 inches
Mean Radius = 274.5 inches

For the pipe-bend elements (element type 17) the geometry data are:

Pipe thickness, t = 10.4 inches
The angular extent of the pipe-bend section, $\phi = 90^\circ$
The radius to the center of the pipe in the r-z plane, R= 838.2 inches

MARC-PIPE

As shown in Figure E 7.13-1 and in the MARC-PIPE input listing, the pipeline structure is subdivided into two straight and one curved segments for mesh generation. As a result, the number of joints and the number of sections on first card series are 4 and 3, respectively. Next, the two straight sections identified by nodal points 1-2 and 3-4, are further divided into three finite elements each, along the pipe direction. The input data for these two straight sections are:

Section No.	Section No.	Node Number	Subdivision Along the Pipe Direction
1	0	1 2	3
3	0	3 4	3

The curved portion of the pipeline structure, identified by nodes 2-3, is subdivided into 14 elements around the pipe cross section. There is no further subdivision along the pipe direction.

Section No.	Section No.	Node Numbers	Subdivision Pipe Direction	Subdivision Around Pipe Cross Section
2	1	2 3	1	14

Coordinates of Center of Curvature of the Curved Portion x	y	z	Pipe Radius
1500.0	838.2	0	274.2

Finally, the coordinates of the four joints are given below:

Joint No.	x	y	z
1	0	0	0
2	1500	0	0
3	2338.2	838.2	0
4	2338.2	2338.2	0

Connectivity, Coordinates and Tying Type

Since all three blocks of data are generated from the MARC-PIPE program, only the key word and the file number on which the data have been stored are required for the input.

Results

In both analyses, the load is scaled such that incipient yield occurs at increment 1. The loading was increased until the limit load was reached. This was due to an inability to obtain a convergent solution. At the limit load, plasticity had occurred through all 11 layers through the thickness of the elbow section. Figure E 7.13-2 shows the load-displacement results of this analysis. The special pipe bend element (type 17) allows the analyst to examine the ovalization of the cross section of the pipe. Using the SECTIONING option in the plot description section, we can examine this effect. Figure E 7.13-3 shows the ovalization due to the two types of loading conditions.

Summary of Options Used

The data file used for MARC-PLOT is e7x13a.dat:

Listed below are the options used in example e7x13b.dat:

Parameter Options

ELEMENT
ELSTO
END
SCALE
SIZING
TITLE

Model Definition Options

CONNECTIVITY
CONTROL
COORDINATE
END OPTION
FIXED DISP
GEOMETRY
ISOTROPIC
POINT LOAD
RESTART
TYING

Load Incrementation Options

AUTO LOAD
CONTINUE
PROPORTIONAL INCREMENT

Listed below are the options used in example e7x13c.dat:

Parameter Options

ELEMENT
ELSTO
END
SCALE
SIZING
TITLE

Model Definition Options

CONNECTIVITY
CONTROL
COORDINATE
END OPTION
FIXED DISP
GEOMETRY
ISOTROPIC
POINT LOAD
RESTART
TYING

Load Incrementation Options

AUTO LOAD
CONTINUE
PROPORTIONAL INCREMENT

Listed below are the options used in example e7x13d.dat:

Parameter Options

ELEMENT
ELSTO
END
MESH PLOT
SCALE
SIZING
TITLE

Model Definition Options

BOUNDARY COUNDITIONS
CONTROL
END OPTION
GEOMETRY
ISOTROPIC
POINT LOAD
RESTART

Load Incrementation Options

CONTINUE

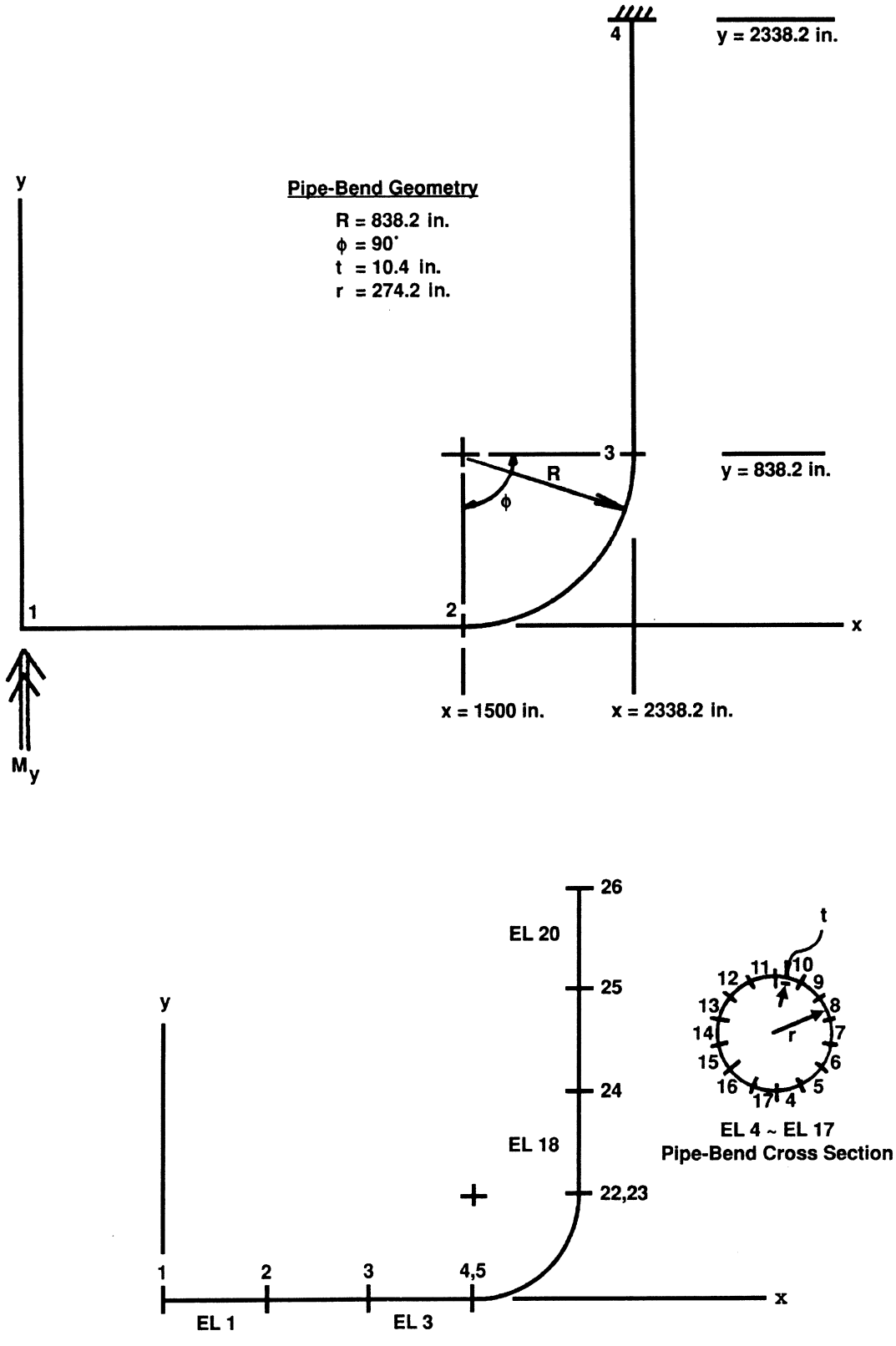

Figure E 7.13-1 Pipe Line Geometry and Model

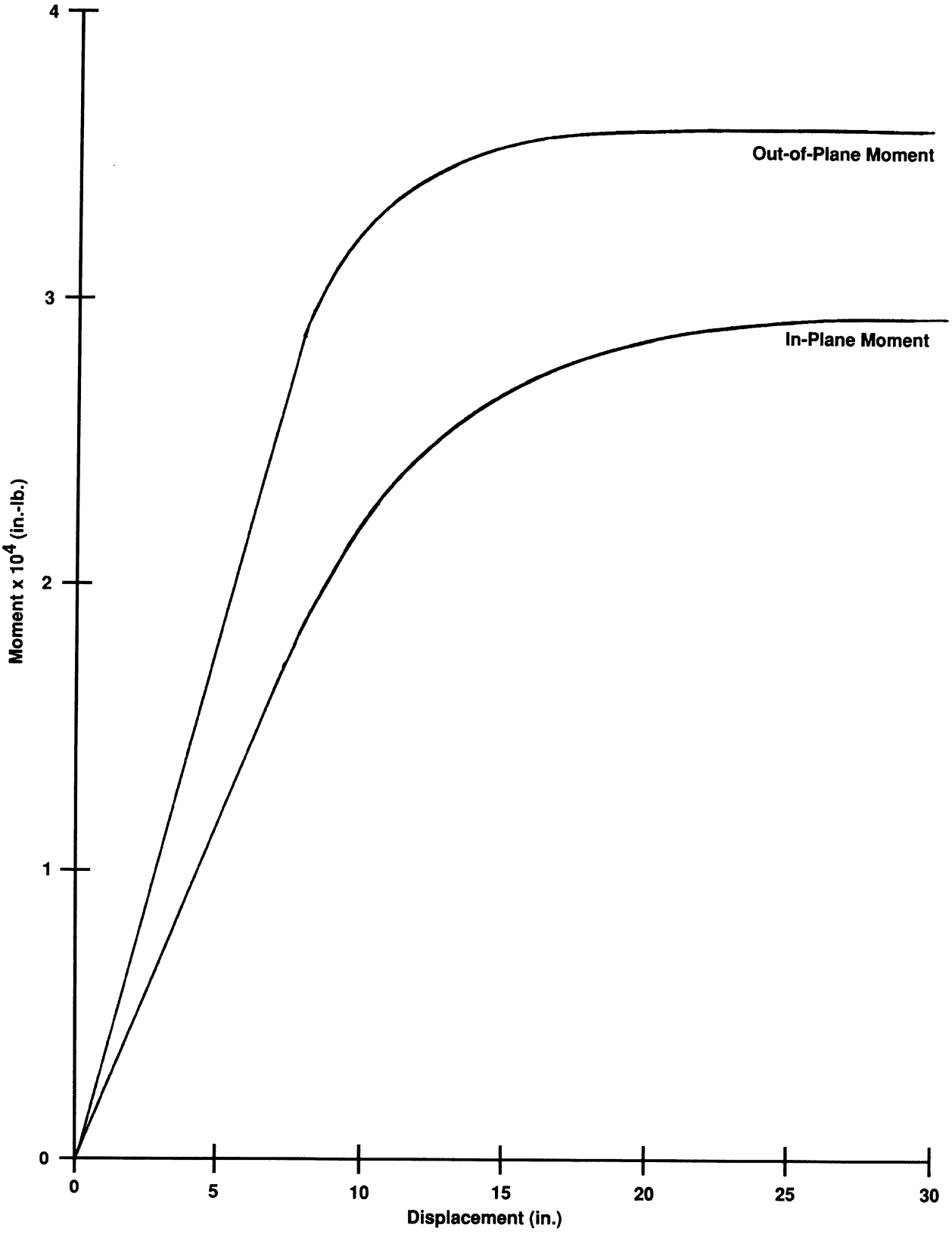

Figure E 7.13-2 Load vs. Displacement

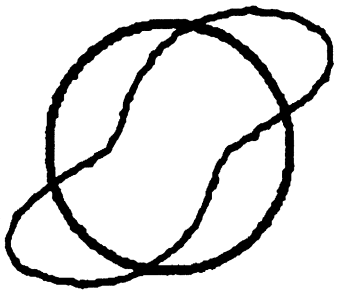

(a) Due to Out-of-Plane Moment

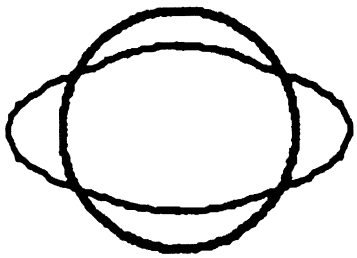

(b) Due to In-Plane Moment

Figure E 7.13-3 Ovalization Behavior Due to Out-of-Plane and In-Plane Moments

E 7.14 Viscoelastic Analysis Of An Externally Reinforced Thick-Walled Cylinder Under Internal Pressure

A very long thick-walled cylinder (Figure E 7.14-1) with an internal radius of 2 in. and an external radius of 4 in. is subjected to an internal pressure of 10 psi. The material is assumed to be isotropic and to be strictly elastic in dilatational response, having a constant bulk modulus of 10^5 psi. The time-dependent viscoelastic shear response is assumed to be represented by a simple Maxwell rheological model. A schematic diagram of such a model is shown in Figure E 7.14-2. The constitutive representation in differential equation form may be expressed as:

$$A\frac{\partial S_{ij}}{\partial t} + BS_{ij} = \frac{\partial e_{ij}}{\partial t}$$

where S_{ij} is the deviatoric or shear component of stress and e_{ij} is the tensor component of the deviatoric or shear strain (i.e., the engineering strain $\gamma_{ij} = 2\ e_{ij}$). The values of the coefficients A and B, which appear in the above expression, are those which were used by Lee et al. [1] and Zienkiewicz et al. [2] in their analyses of the same problem (i.e., $A = B = \frac{4}{3} \times 10^{-5}$).

A thin steel cylinder with an inner radius of 4 in. and thickness of 0.1212 in. is rigidly bonded to the outer surface of the viscoelastic cylinder. The Young's modulus for the steel casing is 30.0 x 10^6 and the Poisson's ratio is 0.3015. It is assumed that both cylinders are sufficiently long so that the deformation is considered to conform to the plane strain idealization with no axial motion.

We are interested in the time varying stresses within the inner viscoelastic cylinder. The numerical results will then be compared to the closed form solution, which is readily obtained for this test case and developed in the following.

Constitutive Representation

The differential equation, which describes the shear response, may be re-expressed in the following form:

$$\frac{\partial s_{ij}}{\partial t}(\underline{x}, t) + \frac{1}{\tau_1} S_{ij}(\underline{x}, t) = G_1 \frac{\partial \gamma_{ij}}{\partial t}(\underline{x}, t)$$

where the characteristic relaxation time, in this instance, is given by:

$$\tau_1 = \frac{A}{B} = 1$$

and the shear modulus amplitude is found to be:

$$G_1 = \frac{1}{2A} = 0.375 \times 10^5 \text{ psi}$$

In general, the expected form of the isotropic stress relaxation function in shear for the viscoelastic formulation is:

$$G(t) = G_\infty + \sum_{i=1}^{n} G_i \exp(-t/\tau_i)$$

where G_∞ is the final or steady state value of the shear modulus. For the simple Maxwell model under consideration, $G_\infty = 0$ and n = 1. Hence, $G(t) = G_1 \exp(-t/\tau_1) = 0.375 \times 10^5 \exp(-t)$.

Element (Ref. B28.1)

Element type 28 is an axisymmetric distorted quadrilateral element with six nodes and two degrees of freedom per node.

Model

Ten axisymmetric elements were used to represent the viscoelastic cylinder and one to represent the casing. The geometry of the cylinder and the obtained mesh are shown in Figure E 7.14-3.

Geometry

No geometry input is necessary for this element.

ISOTROPIC/VISCELPROP

In this problem, the steel properties ($E = 30.0 \times 10^6$, $\nu = 0.3015$) are entered through the ISOTROPIC model definition option and the viscoelastic material properties are represented by the model definition options ISOTROPIC and VISCELPROP.

Both the Young's modulus (E) and the Poisson's ratio (ν) of the viscoelastic material are entered through the ISOTROPIC option. Recall that the expressions of shear modulus (G) and the bulk modulus (K) are:

$$G = \frac{E}{2(1+\nu)} \quad ; \quad K = \frac{E}{3(1-2\nu)}$$

By eliminating E, we obtain the expression of ν in terms of G and K as:

$$3(1-2\nu)K = 2(1+\nu)G$$

In the current problem, the bulk modulus K is equal to 10 and the shear modulus G is equal to $G(0) = 0.375 \times 10^5$. Thus, we obtain the values of $\nu = 0.333$ and $E = 1.0 \times 10^5$.

Rewrite the expression of time dependent shear relaxation modulus as:

$$G(t) = 0.375\, e^{-(t/1.0)}$$
$$= G_1 * e^{-(t/t_1)}$$

We have $G = 0.375$ and $\tau_1 = 1.0$ that are entered through the VISCELPROP option.

DIST LOADS

A 10 psi internal pressure is entered through DIST LOADS Model Definition option. An incremental load of 0.0 psi is entered after the END OPTION for ensuring a constant pressure during transient analysis.

TIME STEP/AUTO LOAD

A multi-step viscoelastic analysis is accomplished by including the TIME STEP/AUTO LOAD load incrementation block. In this analysis, a time step of 0.1 sec. is sufficiently small (i.e. one-tenth of the relaxation time) to accurately determine the transient response. In addition, a total time span or period of 10.0 sec. (100 increments in AUTO LOAD option) is sufficient to reach approximately to the steady state condition. This analysis is performed with a constant time step. This is done for comparison of the numerical results with the closed form solution.

Results

Exact solutions of radially dependent stress distributions are plotted in Figure E 7.14-4 and Figure E 7.14-5. The numerical results are also shown in these figures. The agreement is excellent.

Figure E 7.14-4 shows the radial compression stress at the outside (r = b), increasing gradually from about half the internal pressure to the full internal pressure for long durations of loading (compared with the relaxation time of the material in shear). This is associated with the relaxation of the shear strength of the cylinder material according to its Maxwell behavior (Figure E 7.14-2), while constrained by the reinforcement. The shear strength relaxes to zero. In the limit, the viscoelastic material behaves as a liquid under uniform hydrostatic pressure ($\sigma_{rr} = \sigma_{\theta\theta} = \sigma_{zz}$) of magnitude 10 psi, the internally applied value. The full internal pressure is finally transmitted to the reinforcement.

An analytical calculation of the circumferential stress in the casing accurately reflects the fact that this tension is directly proportional to the external radial compressive stress in the cylinder, i.e.,

$$\sigma^{c}_{\theta\theta} = \frac{-b}{t}\sigma_{rr}$$

Figure E 7.14-5 shows that initial hoop tension occurs adjacent to the bore of the viscoelastic cylinder. The magnitude and sign of this stress depends on the stiffness of the reinforcement and the radius ratio, b/a. This circumferential tension changes to compression as the pressure is maintained, and the limit of uniform hydrostatic compression is reached when the shear strength has relaxed to zero.

It will be noted from the printout for this analysis that assembly of the overall stiffness matrix occurs only for the first three increments. Thereafter, only back-substitution is required to attain each incremental solution for this linear viscoelastic case. The effective incremental stress-strain matrix, $[G_{eff}]$, which is used to develop the overall stiffness matrix for the third and subsequent increments, was found to be:

$$[G_{eff}] = \left[[G_{\infty}] + \sum_{i=1}^{n} \frac{2\ \tau_i \beta_i (h_{\varepsilon})\ [G_i]}{h} \right]$$

This form reflects the assumption of a linearly varying strain rate over each increment. However, the associated numerical procedure requires that the strain rates at the previous step are known. In the first viscoelastic step, this is not the case. In this increment, the assumption is made that the strain rate is constant. It can then be shown that the incremental stress for this first step is given by:

$$\Delta\sigma \Big|_{t = \Delta t} = \left[[G_\infty] + \sum_{i=1}^{n} \tau_1 [1 - \alpha_i (h_\varepsilon)] [G_i] \right] \Delta\varepsilon \Big|_{t = \Delta t} =$$

$$= -\sum_{i=1}^{n} [1-\alpha_1 (h_\varepsilon)] \sigma_i \Big|_{t = 0^+}$$

where σ_i is the value of the state variable or stress supported by the i^{th} viscoelastic element in the generalized Maxwell model at the end of the instantaneous initial elastic step. It is given as:

$$(\sigma_i = G_\infty + G_i \cdot \varepsilon) \Big|_{t = 0^+}$$

The increment in this variable for the first viscoelastic step is given as:

$$\Delta\sigma_i \Big|_{t = \Delta t} = - [1 - \alpha_i (h_\varepsilon)] \sigma_i \Big|_{t = 0^+} + [1 - \alpha_i (h_\varepsilon)] G_i \frac{\Delta\varepsilon}{h} \Big|_{t = \Delta t}$$

In situations where there is a sudden and local sharp change in stress (e.g., to an abrupt change in temperature in a thermo-rheologically simple solid), a few very small starting steps may be required. This will minimize the effect that any starting approximation error might have on the evaluation of the transient response and on the residual or steady state. For example, without such precautions, this type of error has been found to arise in the analysis of the tempering of thermo-rheologically simple glass sheets [3].

References

1. Lee, E. H., Radok, J. R. M., and Woodward, W. B., "Stress Analysis for Linear Viscoelastic Materials", *Trans. of the Society of Rheology*, Volume III, pp. 41-59 (1959).
2. Zienkiewicz, O. C., Watson, M. and King, I. P., "A Numerical Method of Visco-Elastic Stress Analysis", *Int. J. Mech. Sci.*, Vol. 10, pp. 807-827 (1968).
3. Narayanaswamy, O. S. and Gardon, R., "Calculation of Residual Stresses in Glass", *Journal of the American Ceramic Society*, Volume 52, No. 10, pp. 554-558 (1969).

Summary of Options Used

Listed below are the options used in example e7x14.dat:

Parameter Options

ELEMENT
END
SIZING
TITLE

Model Definition Options

CONNECTIVITY
CONTROL
COORDINATE
DIST LOADS
END OPTION
FIXED DISP
ISOTROPIC
PRINT CHOICE
VISCELPROP

Load Incrementation Options

AUTO LOAD
CONTINUE
DIST LOADS
TIME STEP

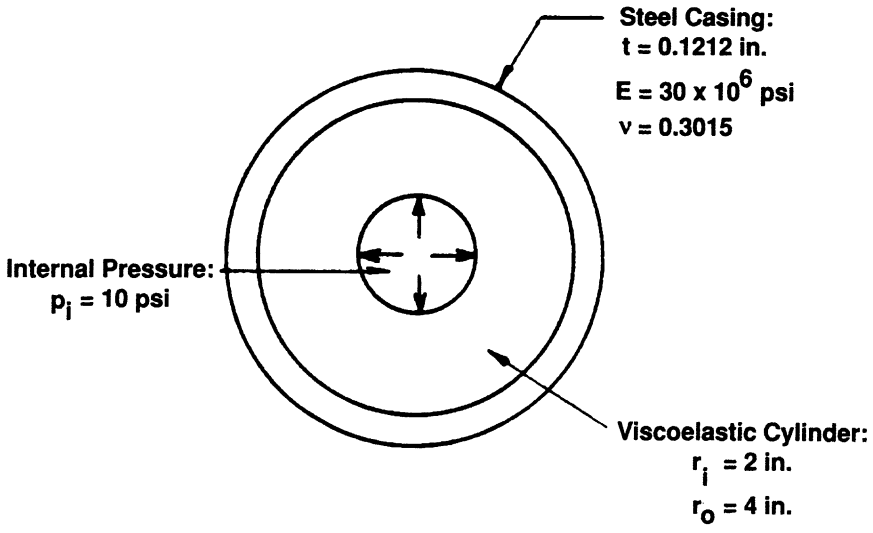

Figure E 7.14-1 Long Thick-Walled Cylinder

Figure E 7.14-2 Simple Maxwell Model

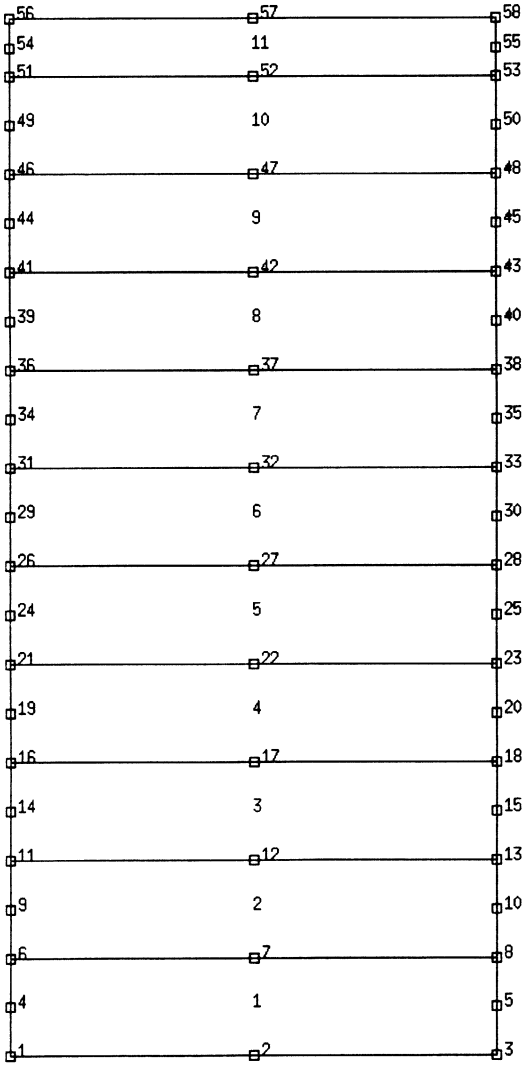

MARC

r_i = 2 inches

r_o = 4 inches

p = 10 psi

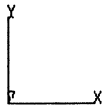

Figure E 7.14-3 Finite Element Model

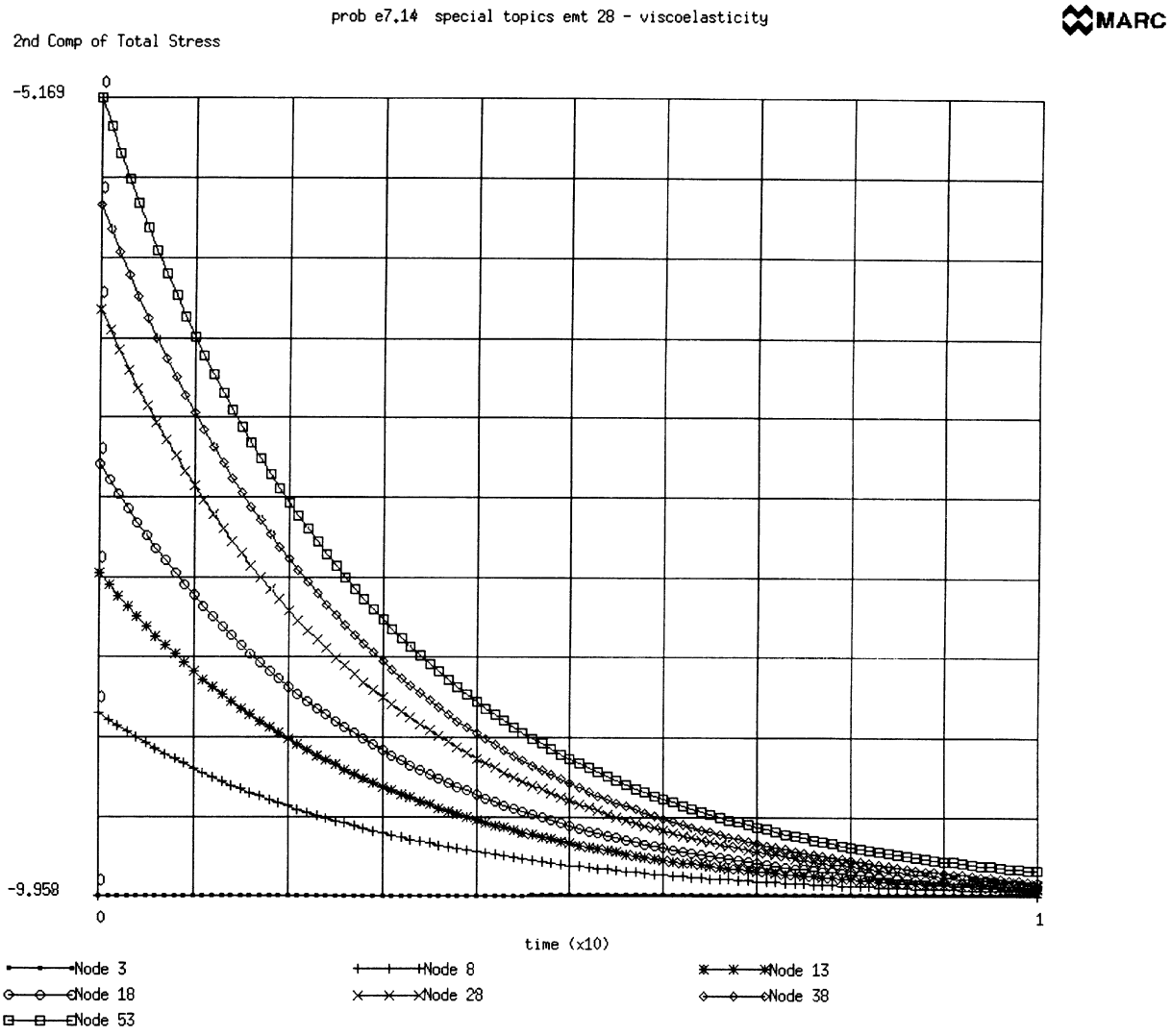

Figure E 7.14-4 Radial Stress vs. Time

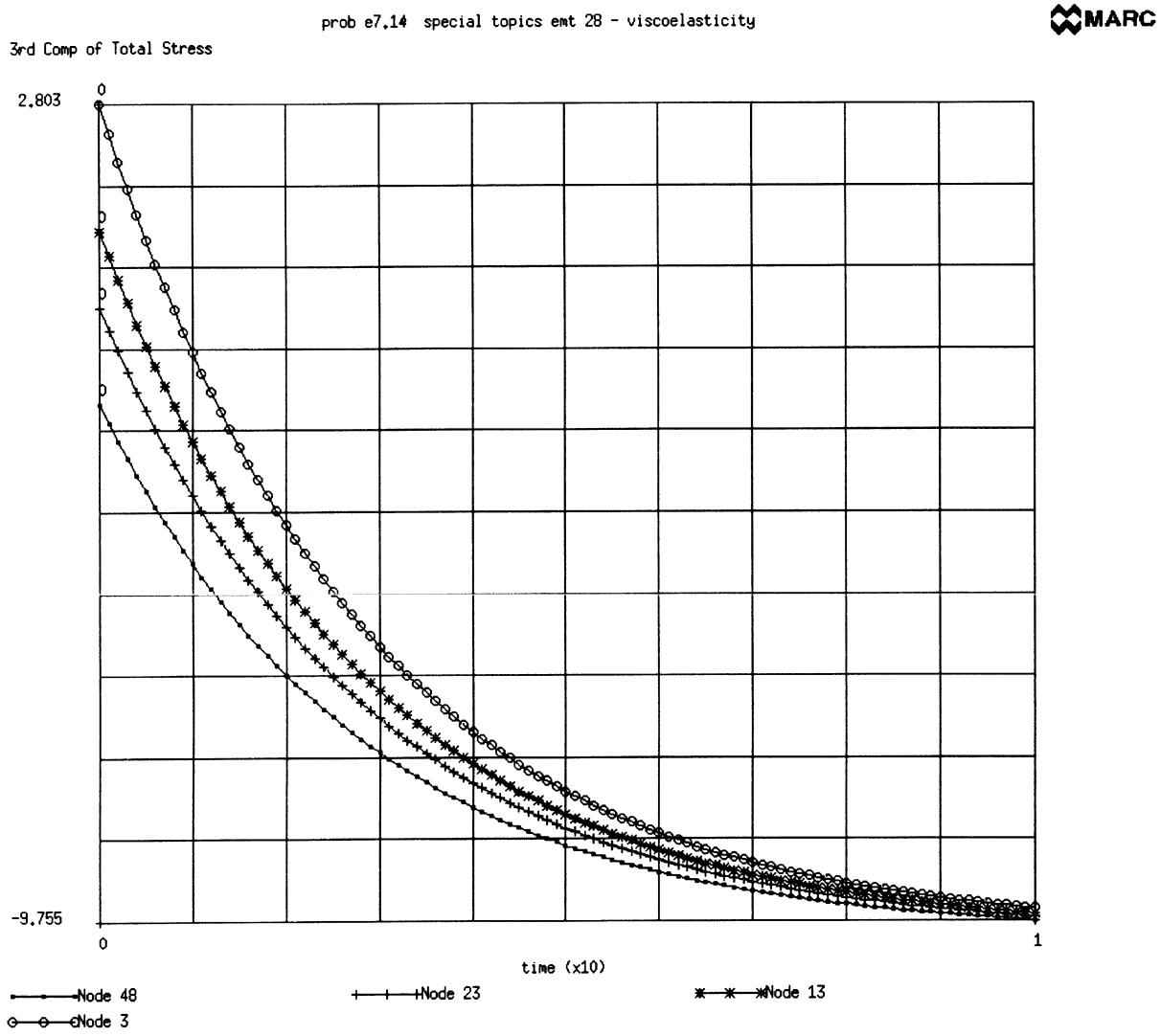

Figure E 7.14-5 Hoop Stress vs. Time

E 7.15 Spiral Groove Thrust Bearing With Tilt

A spiral groove thrust bearing with tilt is analyzed to demonstrate the treatment of discontinuous film profiles as a result of the presence of grooves.

Element

Element type 37, an arbitrary planar 3-noded triangular element, is chosen to model the lubricant.

Model

Problem details and the element mesh are shown in Figure E 7.15-1. The dotted areas represent the lubricant grooves. The geometric specifications are as follows:

$h_2 = 30 \times 10^{-6}$ m
$h_3 = 15 \times 10^{-6}$ m
$h_0 = 96.774 \times 10^{-6}$ m
$r_1 = 75 \times 10^{-3}$ m
$r_2 = 150 \times 10^{-3}$ m

Due to the tilt of the longitudinal axis, the position with the smallest film thickness occurs on the axis X = 0 at the maximum Y-value. A total number of five spiral grooves has to be modeled. The required element mesh is generated by specifying a subset of nodal coordinates and elemental connectivities which subsequently are being used in user subroutines UFXORD and UFCONN to generate the complete mesh.

Thickness Field

The circumferential variation of the lubricant profile is specified per node in user subroutine UTHICK based on the nodal coordinates. In addition, user subroutine UGROOV is used to specify the contribution from the grooves to the total lubricant thickness.

Velocity Field

The relative velocity of the lubricant at the rotor surface, with respect to the grooved stationary part, is specified in user subroutine UVELOC. The angular velocity equals 100 rpm.

Material Properties

Viscosity of 0.020 N-sec/m^2 and density of 800 kg/m^3 are assumed.

Boundary Conditions

Atmospheric pressure is applied at the outer radius. It is assumed that a constant pressure occurs at the internal oil chamber. For this reason, all nodes on the inner radius are tied.

Results

Pressure distribution is calculated in increment 0. In addition, the resulting load-carrying capacity is determined by integrating the pressure distribution over the grooved surface. This results in a bearing force of:

$F_x = 0$ N
$F_y = 0$ N
$F_z = 23.714 \times 10^3$ N

The calculated bearing moment components with respect to the center of the thrust bearing are:

$M_x = 129.3$ Nm
$M_y = -70.6$ Nm
$M_z = 0.0$ Nm

Based on these results, the position of the resulting bearing force can be determined. If the coordinates of this point are denoted by (X_0,Y_0), it follows that:

$$X_0 = -\frac{M_y}{F_z} = 2.997 \times 10^{-3}\text{m}$$

$$Y_0 = \frac{M_x}{F_z} = 5.4521 \times 10^{-3}\text{m}$$

The so-called attitude angle, which is the angle between the point (X_0,Y_0) and the Y-axis equals:

$$\arctan\frac{X_0}{Y_0} = \arctan\frac{M_y}{M_x} = 28.6 \text{ degrees}$$

Since the integration of the pressure distribution was only performed over the grooved surface, the contribution from the oil chamber has to be added. In addition, the contribution from the atmospheric pressure has to be subtracted.

A vector plot of the mass fluxes is shown in Figure E 7.15-2. This yields for the actual vertical bearing force component:

$$F^*_z = F_z + \overline{Y}\,(r_1^2 P_{ch} - r_2^2 P_{at}) = 25.83\ 10^{-3}\ \text{N}$$

where $P_{ch} = \text{N/m}^2$.

Summary of Options Used

Listed below are the options used in example e7x15.dat:

Parameter Options

ELEMENT
END
SIZING
TITLE

Model Definition Options

CONNECTIVITY
CONTROL
COORDINATE
DIST LOADS
END OPTION
FIXED DISP
ISOTROPIC
PRINT CHOICE
VISCELPROP

Load Incrementation Options

AUTO LOAD
CONTINUE
DIST LOADS
TIME STEP

Listed below are the user subroutines found in u7x15.f:

UFXORD
UFCONN
UTHICK
UVELOC
UGROOV

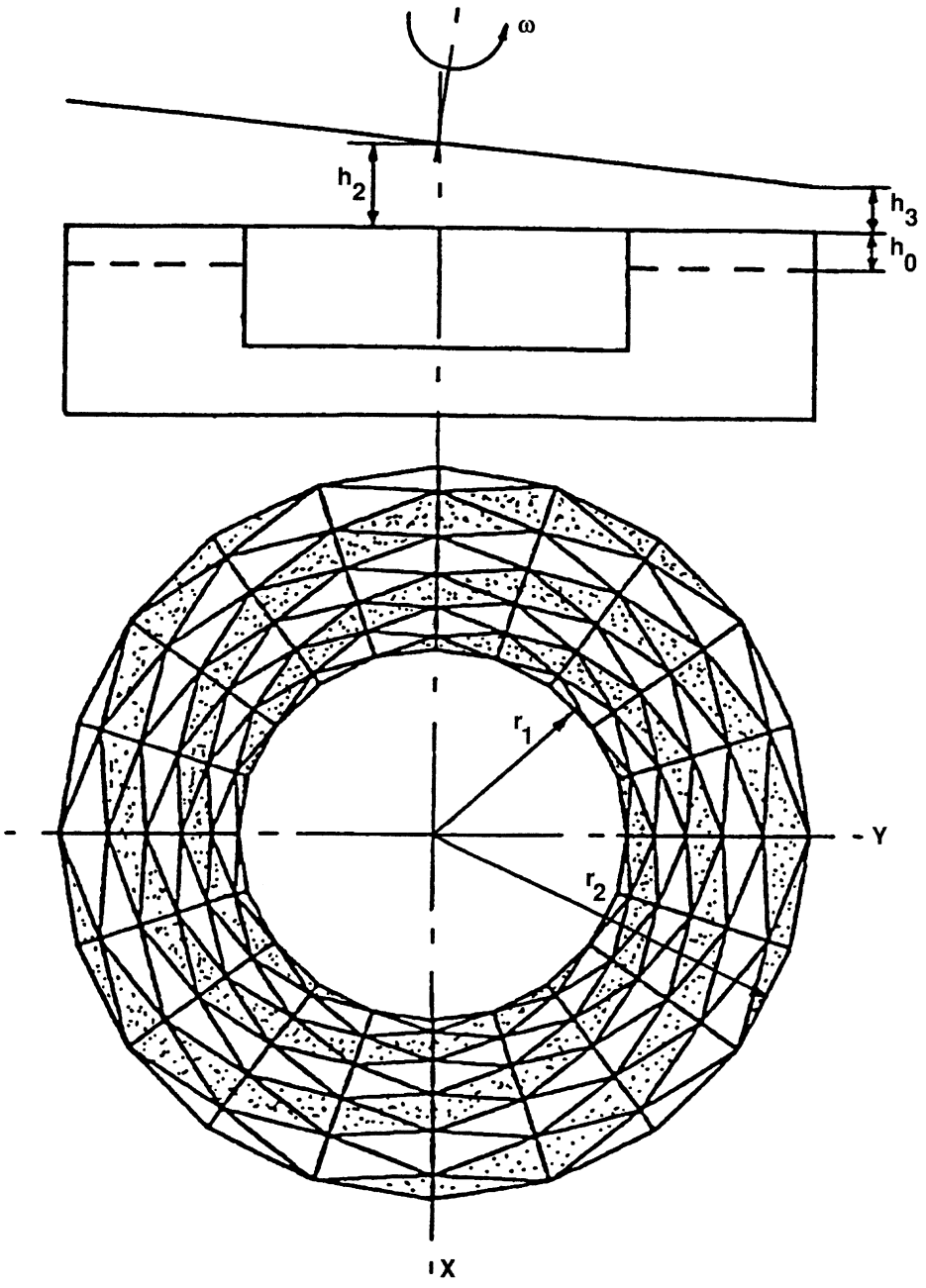

Figure E 7.15-1 Spiral Groove Thrust Bearing with Tilt

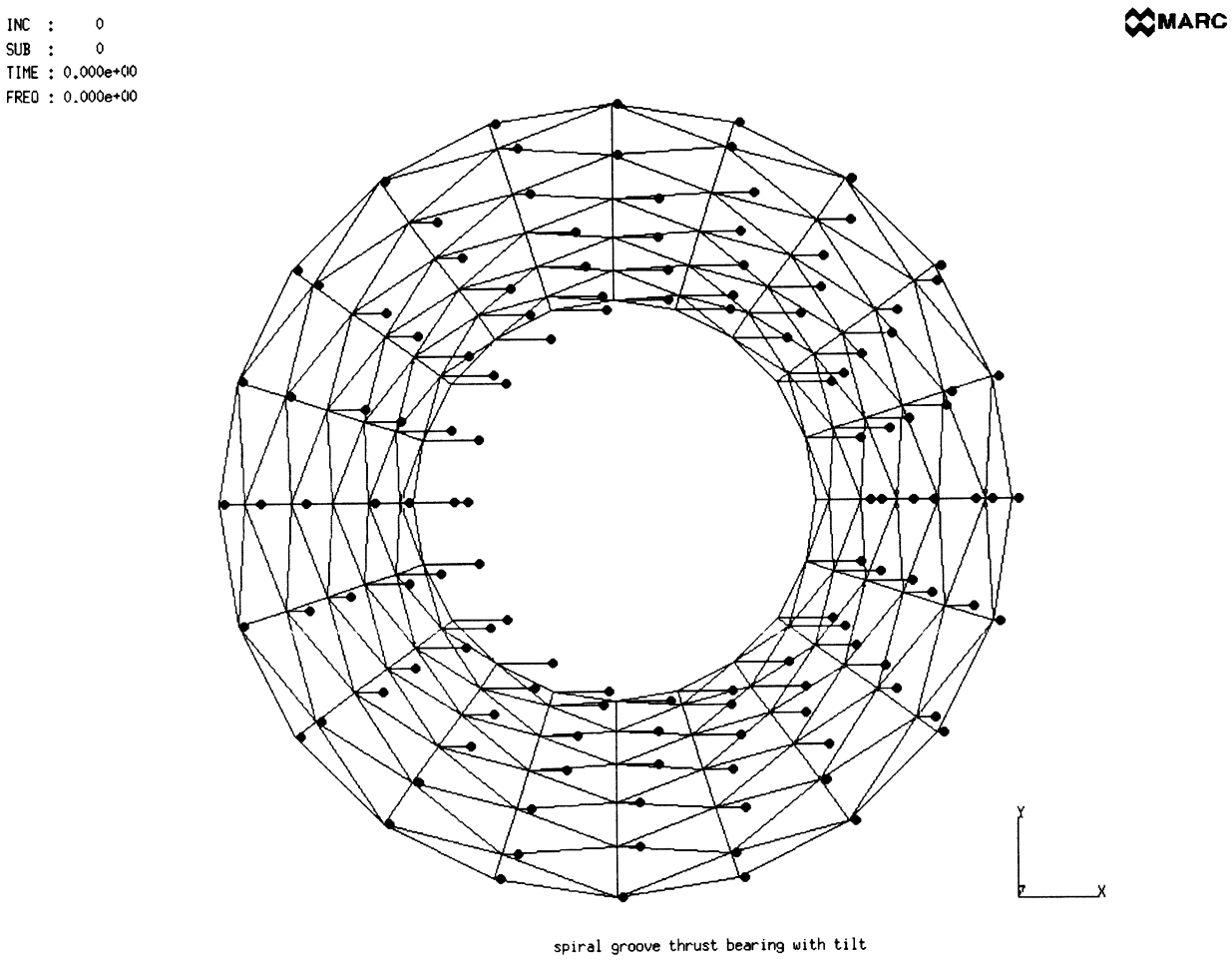

Figure E 7.15-2 Vector Plot of Mass Flow

E 7.16 Hydrodynamic Journal Bearing Of Finite Width

In this example, a journal bearing of finite width is analyzed. The load-carrying capacity as well as stiffness and damping properties are determined for a stationary bearing system. In addition, the procedure to be followed when analyzing the dynamic behavior of a nondeformable bearing system due to a change in the applied load vector is demonstrated.

Element

Element type 39, which is an arbitrary 4-node isoparametric quadrilateral element with bilinear pressure interpolation, is used to model the lubricant.

Model

The details of the journal bearing problem are given in Figure E 7.16-1. In bearing analyses the lubricant is modeled by means of planar finite elements. This is possible because it is assumed that the pressure does not vary over the lubricant thickness. Due to symmetry conditions, only half the bearing width needs to be modeled. The incremental mesh generators CONN GENER and NODE FILL are used to generate the element mesh.

Boundary Conditions

It is assumed that atmospheric pressure is acting on the end faces of the bearing system. The BC FILL option is used to generate these boundary conditions.

Tying

Tying was applied to the nodal pressures at both sides of the mesh to simulate the continuous pressure distribution in the circumferential direction.

Thickness Field

The variation of the lubricant thickness over the mesh due to the eccentric position of the rotor is specified in user subroutine UTHICK. This subroutine will determine the nodal thickness values using the following expression:

$$h(\theta) = (20 - 10 \cos \theta)\ 10^{-6}\ m$$

Velocity Field

The relative velocity of the lubricant at the rotor surface, with respect to the stationary surface, is specified in the VELOCITY block. The angular velocity is 1250 rad/sec.

Material Properties

All elements will have lubricant properties as follows: viscosity of .015 N-sec/m^2 and density of 800 kg/m^3.

Load-Carrying Capacity

The pressure distribution for the given bearing system will be calculated in increment 0. Because no external mass flux is prescribed, FLUXES need to be specified. The resulting pressure distribution will be integrated to calculate the actual bearing force components. User subroutine UBEAR is included to specify at each node the physical orientation of the lubricant film. The following expressions are used:

$X = r \sin \theta \qquad n_X = -\cos \theta$
$Y = r \cos \theta \qquad n_Y = -\sin \theta$
$Z = -y \qquad n_Z = 0$

In addition, the resulting bearing moment components with respect to the origin of the global coordinate X, Y, Z system are calculated. Figure E 7.16-2 shows a path plot of the calculated pressure distribution along the circumference.

The resulting bearing force yields:

$W_X = -1046$ N
$W_Y = -1814$ N
$W_Z = 0$

The resulting bearing moment yields:

$M_X = -6.846$ Nm
$M_Y = 3.938$ Nm
$M_Z = 0$

Because half of the structure was modeled, the components M_X and M_Y are not zero.

Damping and Stiffness Properties

The calculation of bearing characteristics (i.e., damping and stiffness properties) will be performed in subincrements based on a specified change in lubricant film thickness or thickness rate. This is achieved by activating the DAMPING COMPONENTS and the STIFFNS COMPONENTS options. The variation of the film thickness is again specified in user subroutine UTHICK. In total, four subincrements are specified. A displacement of the rotor center of 1.0×10^{-7}m in each global direction is given for both damping and stiffness properties.

The calculated properties are as follows:

Specified Thickness Rate	Damping Components	
$\dot{h} = -1 \times 10^{-7} * \cos \theta$ m/s	$B_{XX} = -543 \times 10^{-3}$ N-sec/m	$B_{YX} = -224 \times 10^{-3}$ N-sec/m
$\dot{h} = -1 \times 10^{-7} * \sin \theta$ m/s	$B_{XY} = -168 \times 10^{3}$ N-sec/m	$B_{YY} = -284 \times 10^{3}$ N-sec/m

Stiffness

Specified Thickness Rate	Stiffness Components	
$\Delta h = -1 \times 10^{-7} * \cos \theta$ m/s	$K_{XX} = -626 \times 10^{6}$ N/m	$K_{YX} = -841 \times 10^{6}$ N/m
$\Delta h = -1 \times 10^{-7} * \sin \theta$ m/s	$K_{XY} = 1198 \times 10^{6}$ N/m	$K_{YY} = 314 \times 10^{6}$ N/m

Load-Carrying Capacity at New Rotor Position

Assume that the actual loading of the bearing system increases to the force F = (1408, 1390, 0). Since the resultant load-carrying capacity is not in equilibrium with this force, the rotor will move to a new position. Based on the calculated damping and stiffness properties, a new rotor position, which implies an incremental thickness change in a particular time period, may be estimated. This is done by investigating the mechanical equilibrium of the total system.

The force equilibrium conditions for a nondeformable bearing requires that:

$$F + W + \Delta W = 0.$$

From this equation, the required correction for the load-carrying capacity can be calculated. This yields:

$$\Delta W = (-1362, 424, 0)$$

Any incremental change in position of the rotor center will cause a change in the load-carrying capacity according to the following relation:

$$[B]\ \Delta\dot{u} + [K]\ \Delta u = \Delta W$$

where u is the incremental movement of the rotor center.

After substituting the previously calculated stiffness and damping properties, the above equation may be solved, which yields:

$$\Delta u = (-.450, -1.832, 0)\ 10^{-6}\ m$$

where a time increment of 10^{-3} seconds is assumed.

From the difference in magnitude of the damping and stiffness properties, it can be concluded that the initial response is dominated by the damping effects.

The above procedure is applied in increment 1. The incremental thickness change is defined in user subroutine UTHICK, based on the previous calculated bearing properties at the original rotor position. This change in film thickness is automatically added to the previous thickness field if the calculation of damping and/or stiffness properties is not activated.

According to the calculated pressure distribution for increment 1, this results in a bearing force of:

$W_X = -1296$ N
$W_Y = -1513$ N
$W_Z = 0.0$ N

Summary of Options Used

Listed below are the options used in example e7x16.dat:

Parameter Options

BEARING
ELEMENT
END
SIZING
TITLE

Model Definition Options

BC FILL
CONN GENER
CONNECTIVITY
CONTROL
COORDINATE
END OPTION
FIXED PRESSURE
ISOTROPIC
NODE FILL
THICKNESS
TYING
VELOCITY

Load Incrementation Options

CONTINUE
DAMPING COMPONENTS
STIFFNS COMPONENTS
THICKNS CHANGE

Listed below are the user subroutines found in u7x16.f:

UTHICK
UBEAR

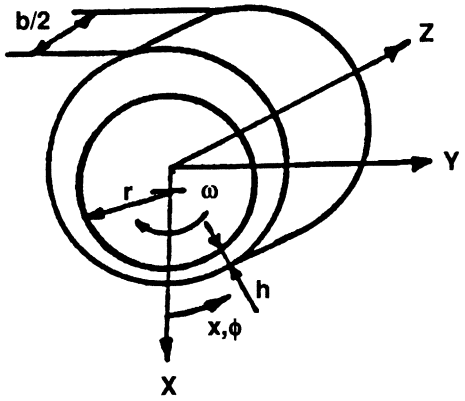

r = 20 mm

b = 10 mm

η = 0.015 N-sec/m^2

h = (20 – 10cosθ) 10^{-6} m

ω = 1250 rad/sec

MARC

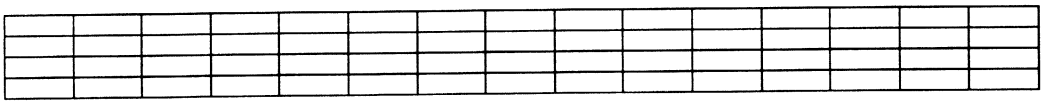

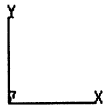

Figure E 7.16-1 Journal Bearing of Finite Width

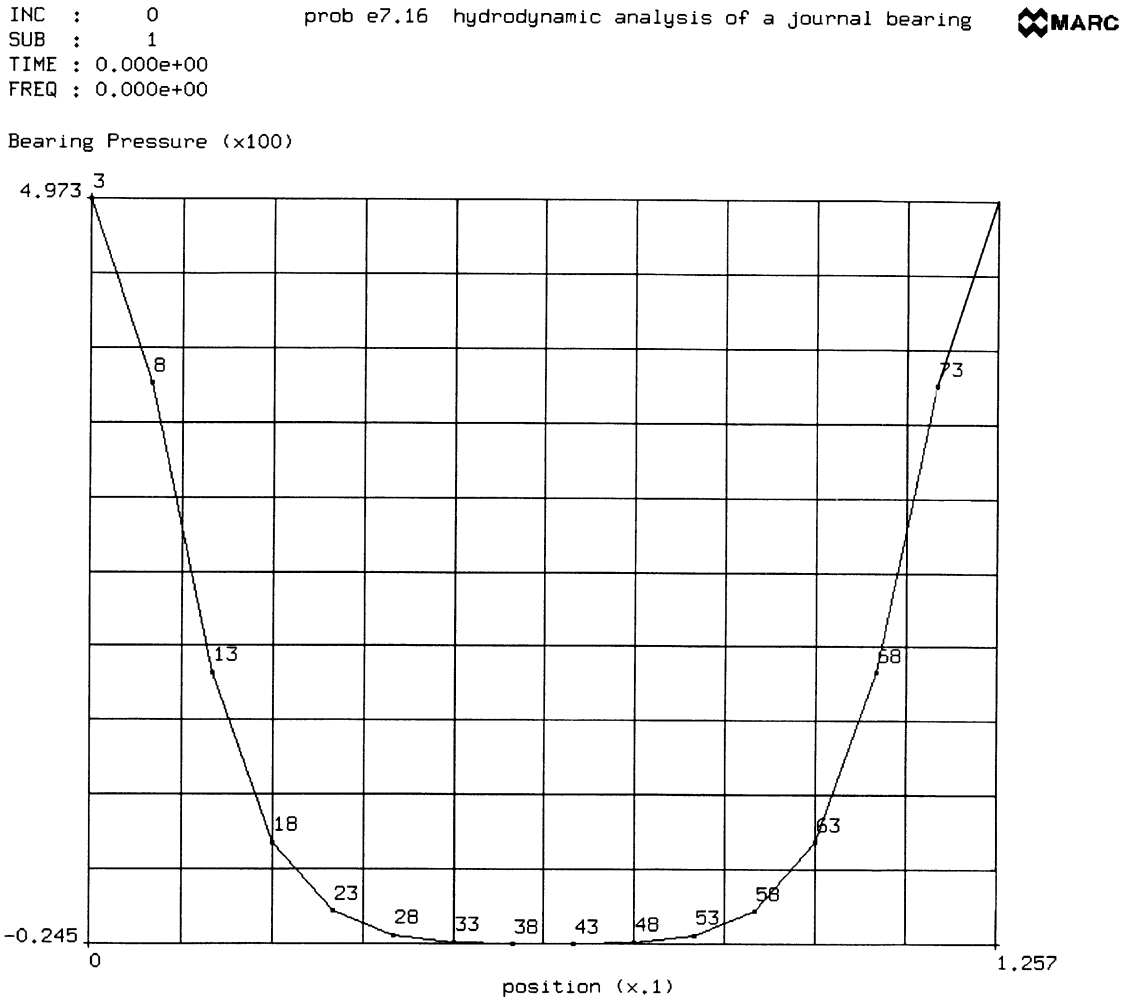

Figure E 7.16-2 Path Plot of Pressure Distribution

E 7.17 Elastic-Plastic Finite Deformation Of A Thick-Walled Cylinder

This problem demonstrates the rezoning technique for the elastic-plastic finite deformation of a thick cylinder. The cylinder is subjected to internal pressure which results in large elastic-plastic deformation, after which the load is removed leaving the structure in its permanent plastically deformed shape. Because of the amount of plastic deformation, the FINITE STRAIN option is used in conjunction with the UPDATED LAGRANGE option. Often, in this type of analysis, the mesh becomes seriously distorted, resulting in a low quality solution. This problem demonstrates the REZONING option to resolve this difficulty.

Model

The model consists of five axisymmetric type 10 elements and 12 nodes. The initial inner and outer radii are 1 and 2 m, respectively. The mesh is shown in Figure E 7.17-1.

Material Properties

The elastic properties of the material are Young's modulus of 1000 N/m^2 and Poisson's ratio of 0.3. The material has an initial yield stress of 1 N/m^2 and strain hardens at a rate of 3 N/m^2.

Geometry

No thickness is associated with an axisymmetric element. The constant dilatation method is used for this element by indicating a 1. in the second field of this option.

Boundary Conditions

The thick cylinder is constrained to be under plane-strain conditions ($e_{zz} = 0$).

Loading

An incremental nodal load will be prescribed to the nodes on the inner radius (nodes 1 and 2) through the FORCDT option. To determine the current applied pressure, this force will need to be divided by $2\pi R_{current}$. The prescribed load and resulting pressures are shown in Figure E 7.17-2.

Controls

All calculations are saved on the RESTART tape for every increment. The maximum number of increments allowed is 50. The maximum number of recycles was put to 10. This is because very large increments were chosen, and after a rezoning occurs the calculations will not be in equilibrium. The PRINT CHOICE option is used to restrict the output to element 1.

Procedure

Using the first input, the analysis is completely carried out in 42 increments. The second input demonstrates the use of the REZONING option. The first analysis is restarted at the end of increment 10. The REAUTO option is used to prematurely discontinue the AUTO LOAD sequence that was defined previously in the first analysis.

The data after the END OPTION, beginning with REZONE and finishing with END REZONE, form one rezoning increment. In this analysis, the coordinates are redefined such that the new inner and outer radii are the same as the deformed radii at increment 10 of the previous analysis. The other points are located such that the new mesh would be regular.

At the conclusion of the rezoning increment, the analysis is continued to the same level of loading.

Results

Figure E 7.17-3 shows the deformed mesh during different stages of the analysis. Clearly, the boundary of the deformed cylinder is virtually identical for both analyses.The pressure versus internal radius diagram is shown in Figure E 7.17-4, together with the analytical solution for an equivalent rigid work-hardening material. Excellent agreement is obtained, both between theory and finite element calculation and between the two analyses.

It should be commented that although rezoning was not necessary in this problem, it is extremely useful in many practical applications in the metal working area.

Summary of Options Used

Listed below are the options used in example e7x17a.dat:

Parameter Options

ALL POINTS
ELEMENT
END
FINITE
LARGE DISP
REZONE
SIZING
TITLE
UPDATE

Model Definition Options

CONNECTIVITY
CONTROL
COORDINATE
END OPTION
FIXED DISP
FORCDT
GEOMETRY
ISOTROPIC
POST
PRINT CHOICE
RESTART
WORK HARD

Load Incrementation Options

AUTO LOAD
CONTINUE

Listed below are the options used in example e7x17b.dat:

Parameter Options

ALL POINTS
ELEMENT
END
FINITE
LARGE DISP
REZONE
SIZING
TITLE
UPDATE

Model Definition Options

CONNECTIVITY
CONTROL
COORDINATE
END OPTION
FIXED DISP
FORCDT
GEOMETRY
ISOTROPIC
POST
PRINT CHOICE
REAUTO
RESTART
WORK HARD

Load Incrementation Options

AUTO LOAD
CONTINUE

Listed below is the user subroutine found in u7x17.f:

FORCDT

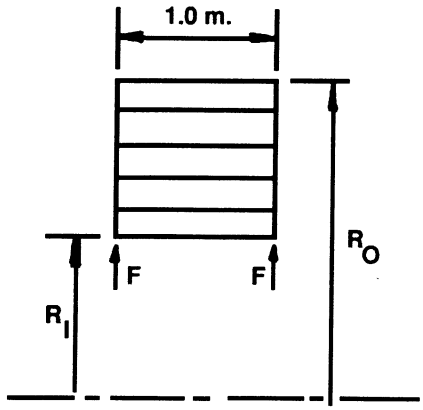

R_I = 1.0 m.

R_O = 2.0 m.

E = 1000 N/m^2

υ = 0.3

σ_y = 1.0 N/m^2

$\frac{\partial \bar{\sigma}_y}{\partial \varepsilon_p}$ = 3.0

Figure E 7.17-1 Thick-Walled Cylinder

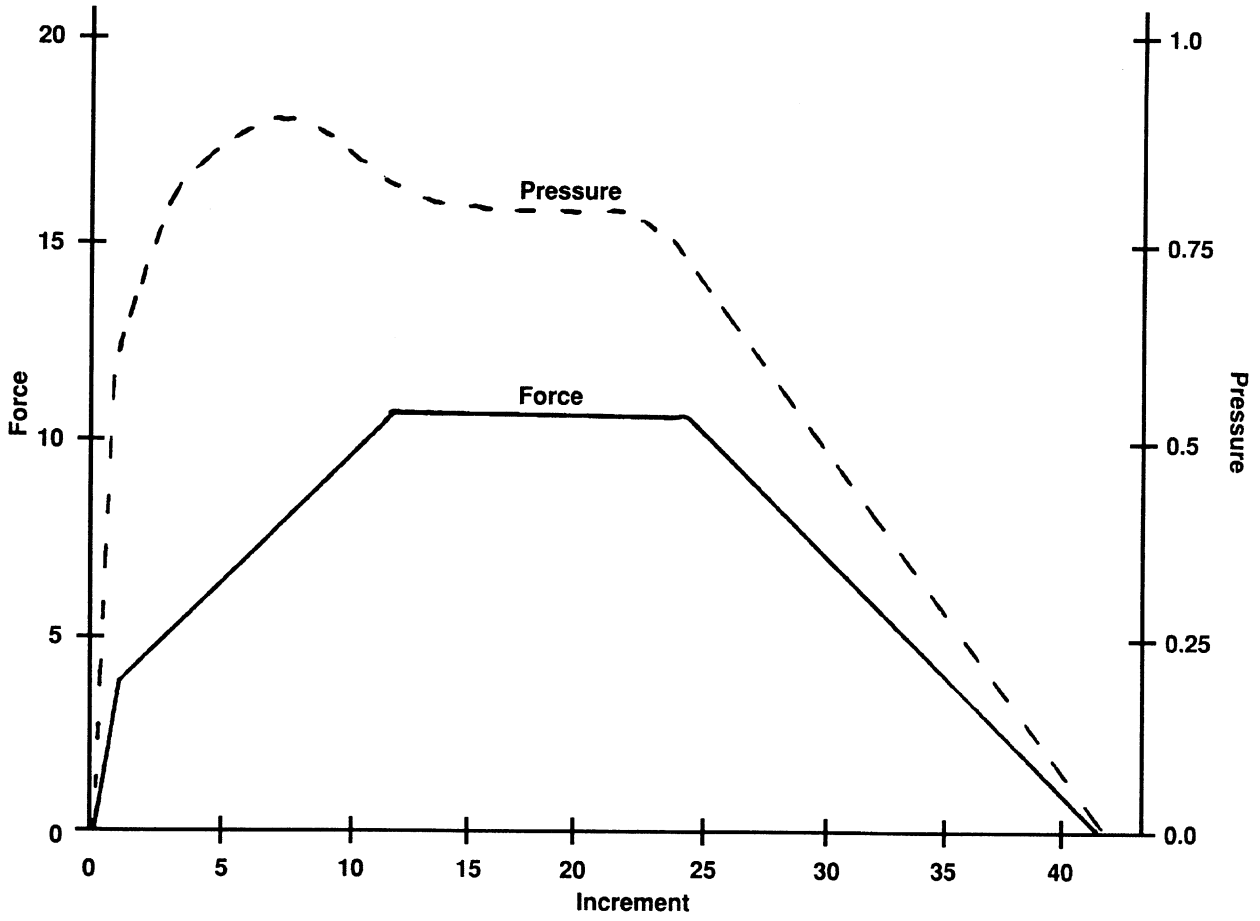

Figure E 7.17-2 Applied Load History

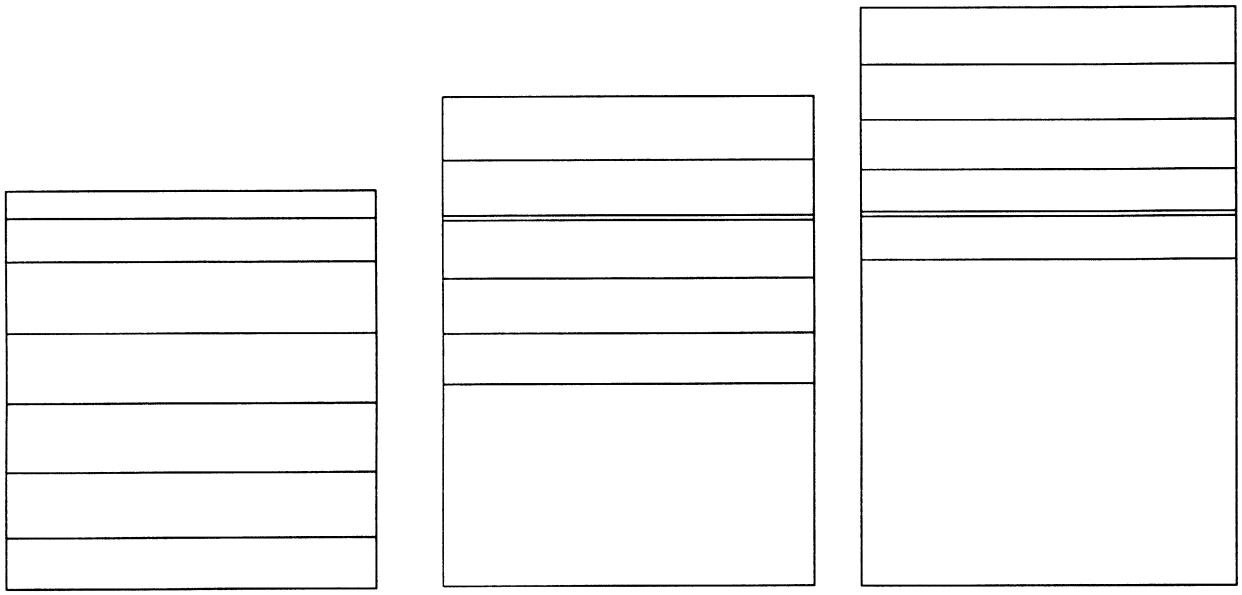

Figure E 7.17-3 Deformed Meshes at Increments 6, 10, and 20

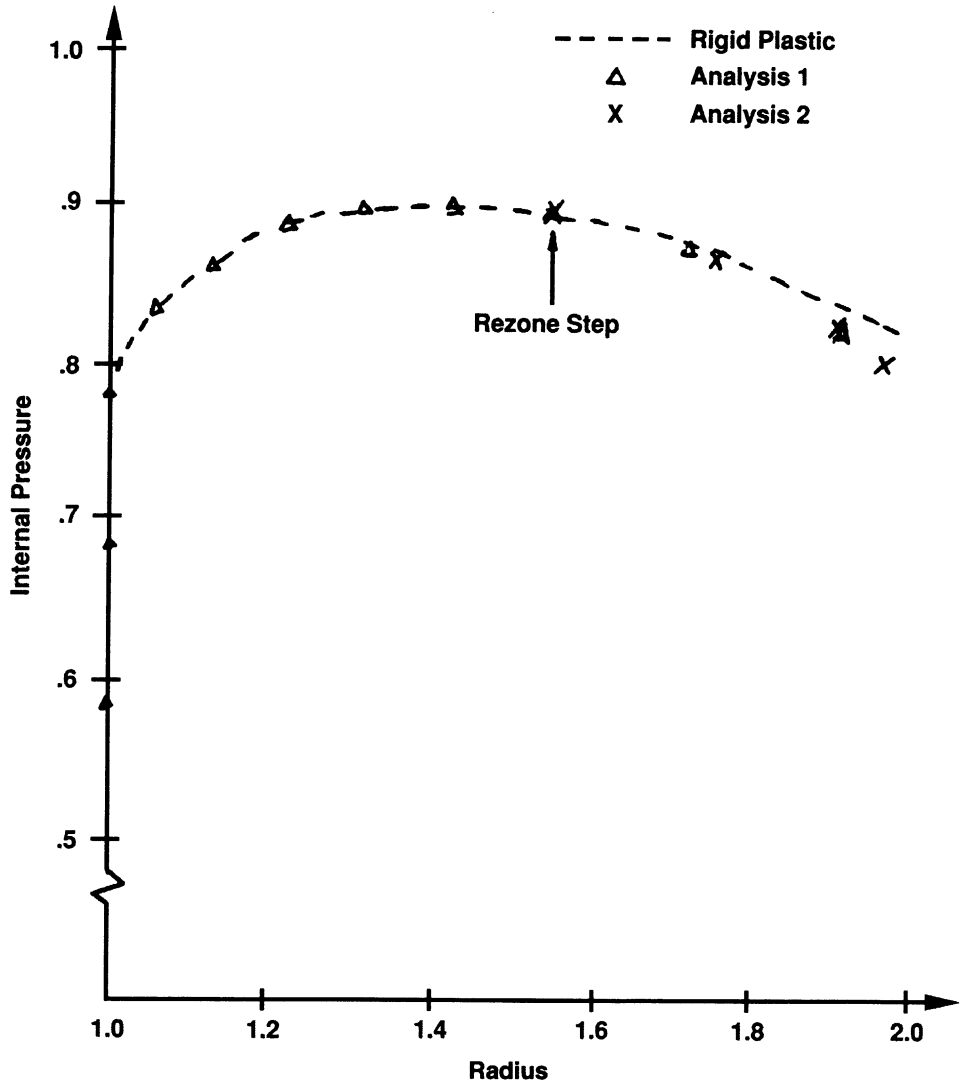

Figure E 7.17-4 Internal Pressure vs. Inner Radius

E 7.18 Side Pressing Of A Hollow Rubber Cylinder

The behavior of a thick hollow rubber cylinder, compressed between two rigid plates, is analyzed. The cylinder is long; hence, a condition of plane strain in the cross section will be assumed. For reasons of symmetry, only one-quarter of the cylinder needs to be modeled. No friction will be assumed between cylinder and plates. The VISCELMOONEY material behavior is used to represent the viscoelastic rubber. The LARGE DISPLACEMENT option is used.

Element

The quarter cylinder is modeled by using 8-node hybrid plane strain elements (MARC element type 32). This element may be used in conjunction with the Mooney material model. Element type 12 is used to model the contact conditions.

Model

Twelve elements are used for the mesh, with two elements specified over the thickness. The geometry of the cylinder and a mesh are shown in Figure E 7.18-1.

Material Properties

The MOONEY Model Definition option is used to specify the rubber properties; the GAP DATA option is used for the input of the gap data. The GAP closure distance is defined as the relative distance before contact occurs, which in this problem equals the initial nodal distance between cylinder and plate. The instantaneous response of the rubber material (MOONEY) may be modeled as a Mooney-Rivlin material with $C_{10} = 8$ N/mm^2, $C_{01} = 2$ N/mm^2. The time dependent response (VISCELMOONEY) is modeled by a single exponential decay function, with a decay factor of 0.5 at infinite time and a relaxation time of 0.3 seconds.

Loading

The AUTO LOAD option is used to apply five displacement increments to the plate at time t = 0. The increment is equal to the one applied in the increment 0. Subsequently, 15 time-steps (AUTO LOAD) of 0.1 seconds (TIME STEP) are applied with zero displacement increments (DISP CHANGE). The applied displacement is reversed and five steps are carried out without change in time, followed by a relaxation period of two seconds applied in 20 increments.

Boundary Conditions

Boundary conditions are along the line r = 0 and z = 0 due to symmetry and to apply the prescribed motion of the plate.

Tying

The TYING option establishes the connections between the nodal degrees of freedom of the cylinder and that of the gaps. This is necessary as the degrees of freedom of these two elements are not the same.

Results

The cylinder diameter is reduced from 6 mm to 4 mm in five increments. The cylinder is in contact with the plate at four nodes (four gaps have been closed). The incremental displacements have become very small, and the equilibrium is satisfied with high accuracy. The incremental full Newton-Raphson method was used to solve the nonlinear system. The total force on the plate may either be calculated by summing up the gap forces, or may be directly obtained from the reaction force on node 75. In both cases, this leads to a total force F = 1.9098 N. A plot of the deformed cylinder is shown in Figure E 7.18-2.

After relaxation for 1.5 seconds, the load is reduced by almost 50%, as predicted by the equation $F_t = F_0(1 - 0.5e^{-t/0.3})$. During that period, all properties are scaled down proportionally and the displacements do not change. The same is true for the second relaxation period.

Summary of Options Used

Listed below are the options used in example e7x18.dat:

Parameter Options

ELEMENT
END
LARGE DISP
SIZING
TITLE

Model Definition Options

CONNECTIVITY
CONTROL
COORDINATE
END OPTION
FIXED DISP
GAP DATA
MOONEY
POST
PRINT CHOICE
RESTART
TYING
VISCELMOON

Load Incrementation Options

AUTO LOAD
CONTINUE
DISP CHANGE
TIME STEP

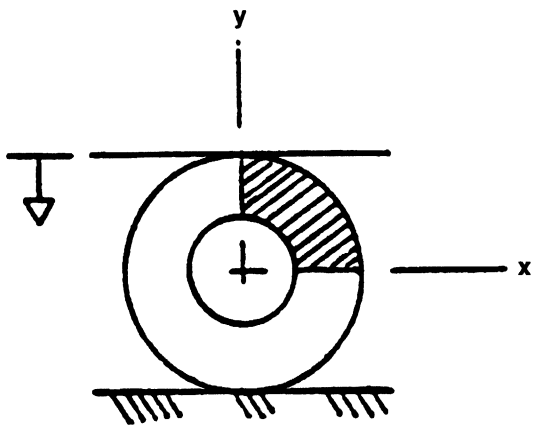

$C_{10} = 8\ N/mm^2$

$C_{01} = 2\ N/mm^2$

$r_i = 2\ mm$

$r_o = 3\ mm$

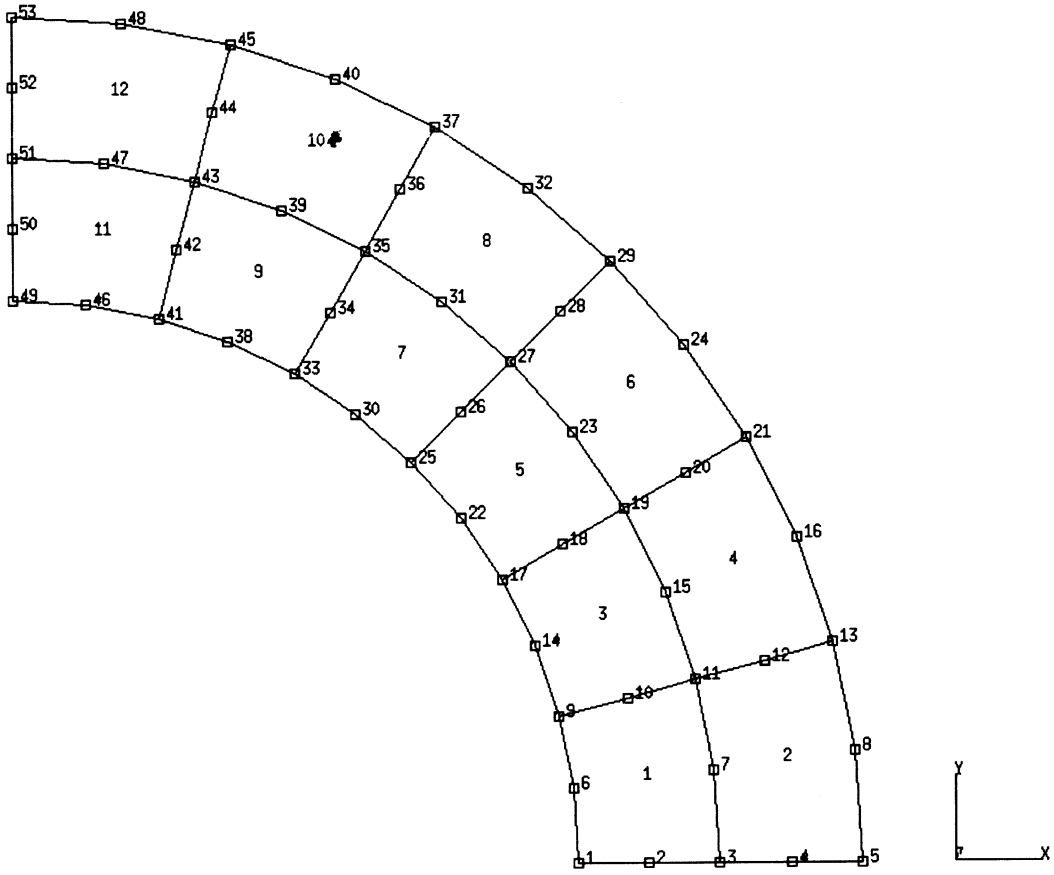

Figure E 7.18-1 Rubber Cylinder and Mesh

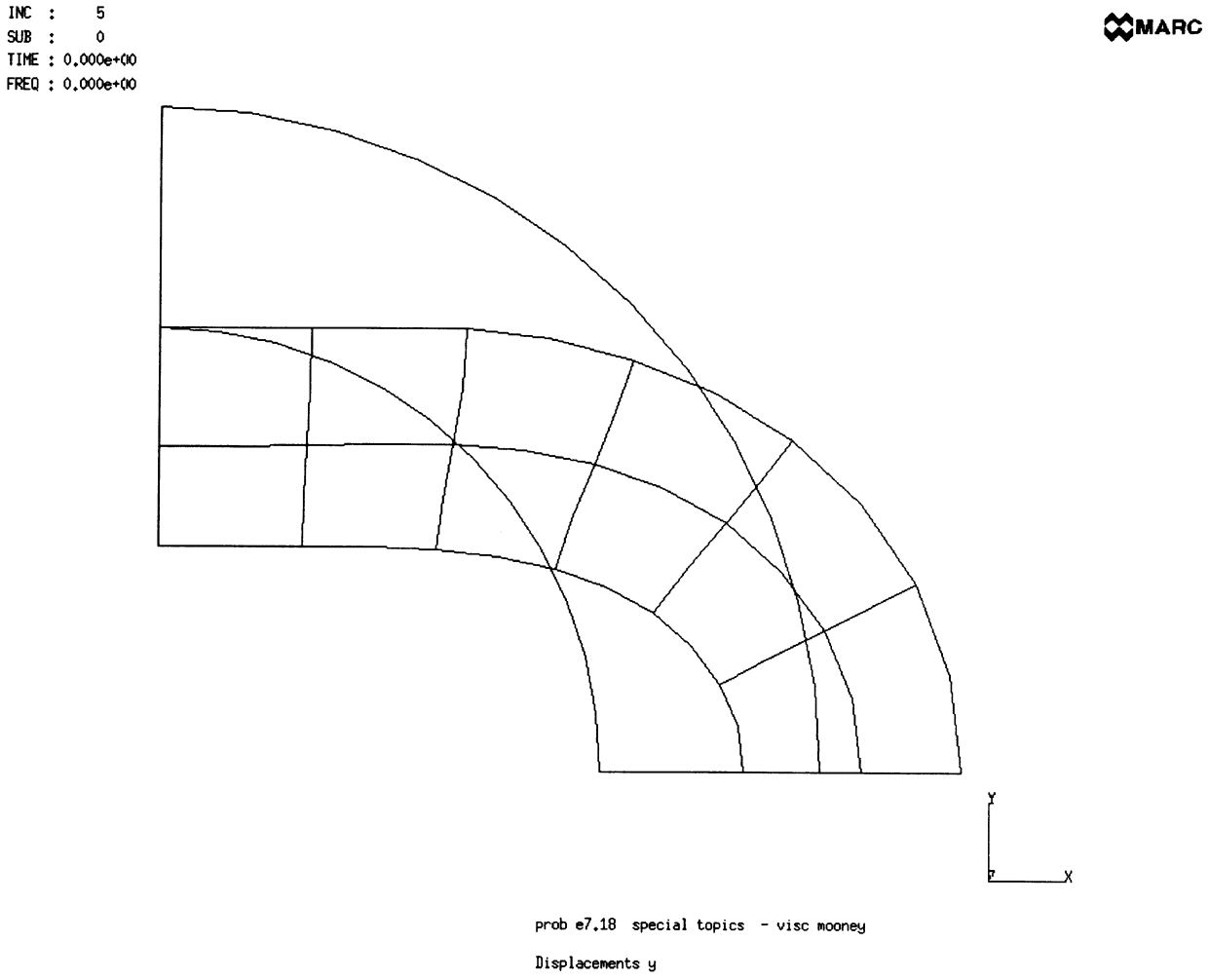

Figure E 7.18-2 Deformed Mesh Plot

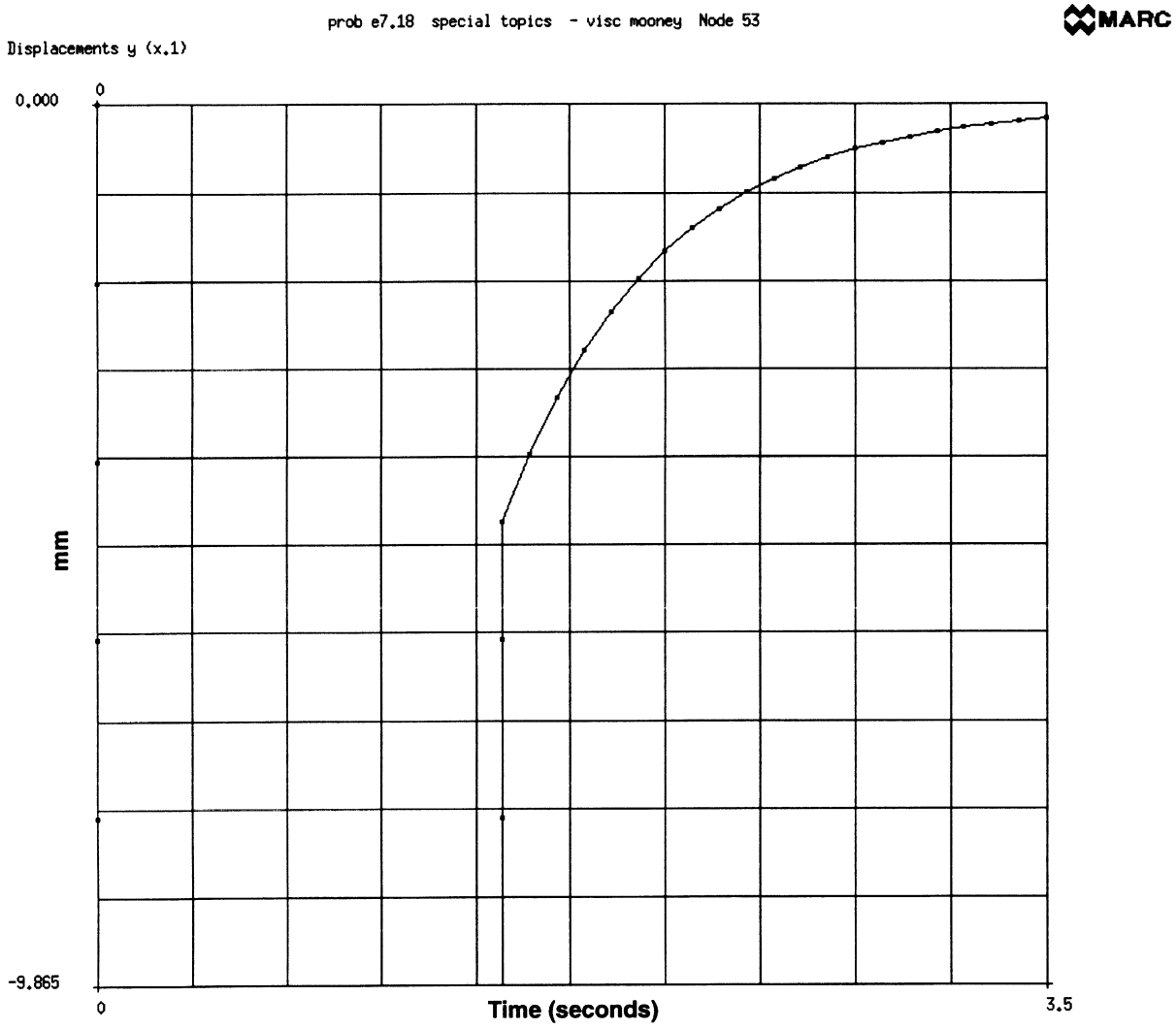

Figure E 7.18-3 Displacement History of Node 53

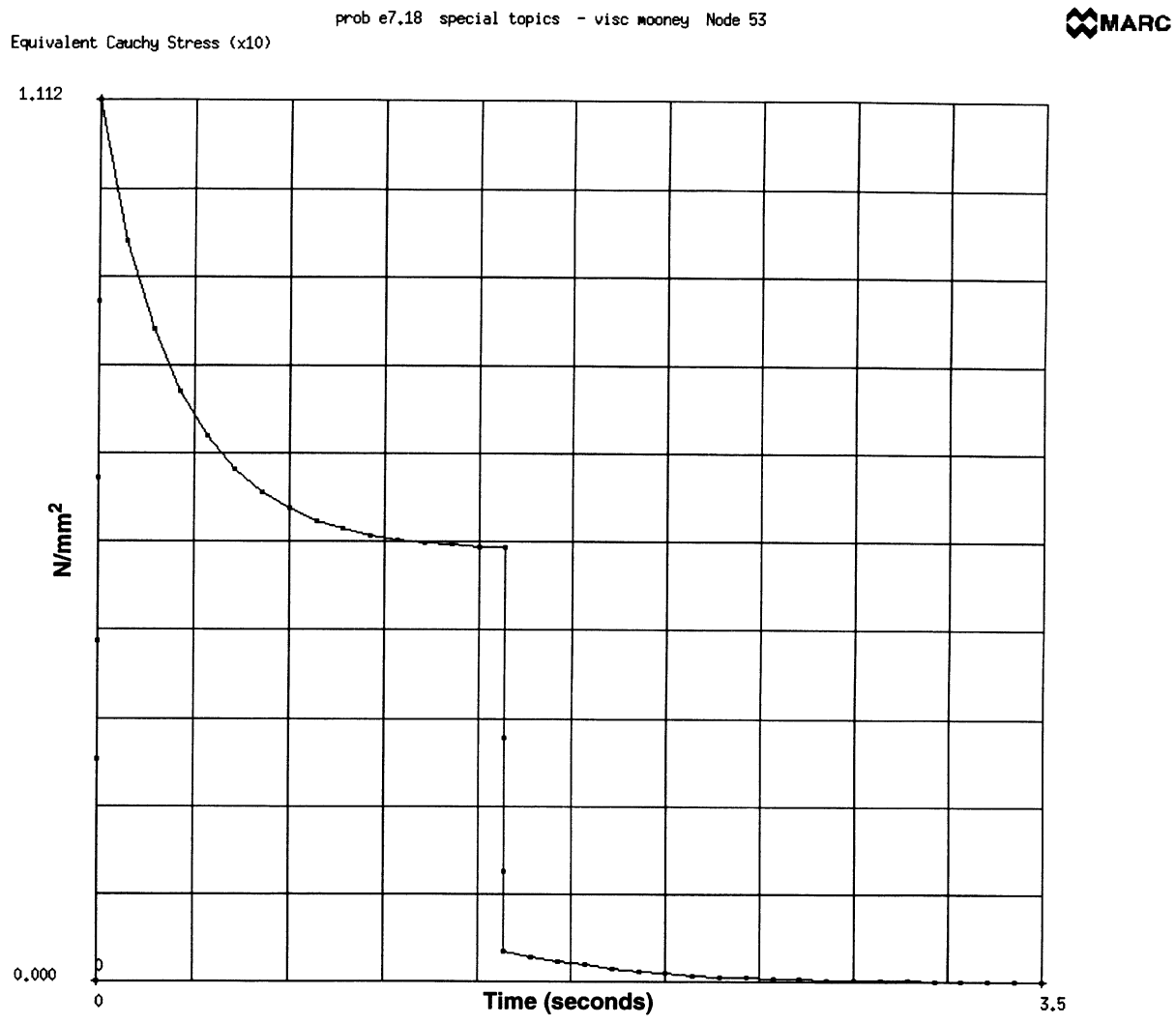

Figure E 7.18-4 Stress Relaxation

E 7.19 Stretching Of A Rubber Sheet With A Hole

This example demonstrates the Mooney-Rivlin material model for a this rubber sheet analysis with a hole.

Model

A square sheet of 6.5 cm x 6.5 cm with a hole of radius 0.25 cm is to be analyzed. One quarter of the model is represented due to symmetry. The mesh shown in Figure E 7.19-1 has 80 elements and 277 nodes. Element 26, the conventional displacement formulation 8 node quadrilateral, is used. Because this is a plane stress analysis, it is unnecessary to use Herrmann elements even through an incompressible material is being modeled. The thickness of the sheet is 0.079 which is entered through the GEOMETRY option.

Material Properties

The material is modeled using the general third-order deformation model with:

C_{10} = 20.300 N/cm^2
C_{01} = 5.810 N/cm^2
C_{11} = 0.000 N/cm^2
C_{20} = -0.720 N/cm^2
C_{30} = 0.046 N/cm^2

for all elements. This data is entered through the MOONEY option.

Boundary Conditions

The nodes along x = 0 (edge 1) are fixed in the x-direction. The nodes along y = 3.25 (edge 2) and along y = 0 (edge 4) are fixed in the y-direction. The nodes which are originally along x = 3.25 (edge 3) are all tied to node 277. This will allow us to keep this edge straight and easily calculate the total pulling force. The displacement of node 277 is first set to 0 in the x-direction and then changed through the DISP CHANGE option. The incremental displacement will be 0.325 cm/increment. A total of 10 increments are executed. Hence, the dimension in the x direction doubles.

Results

The deformed mesh is shown in Figure E 7.19-2. The load-deflection curve for node 277 is shown in Figure E 7.19-3.

Summary of Options Used

Listed below are the options used in the example e7x19.dat:

Parameter Options

ELEMENT
END
SIZING
TITLE

Model Definition Options

CONNECTIVITY
CONTROL
COORDINATES
END OPTION
DEFINE
FIXED DISP
GEOMETRY
MOONEY
POST
PRINT CHOICE
TYING

Load Incrementation Options

AUTO LOAD
CONTINUE
DIST CHANGE

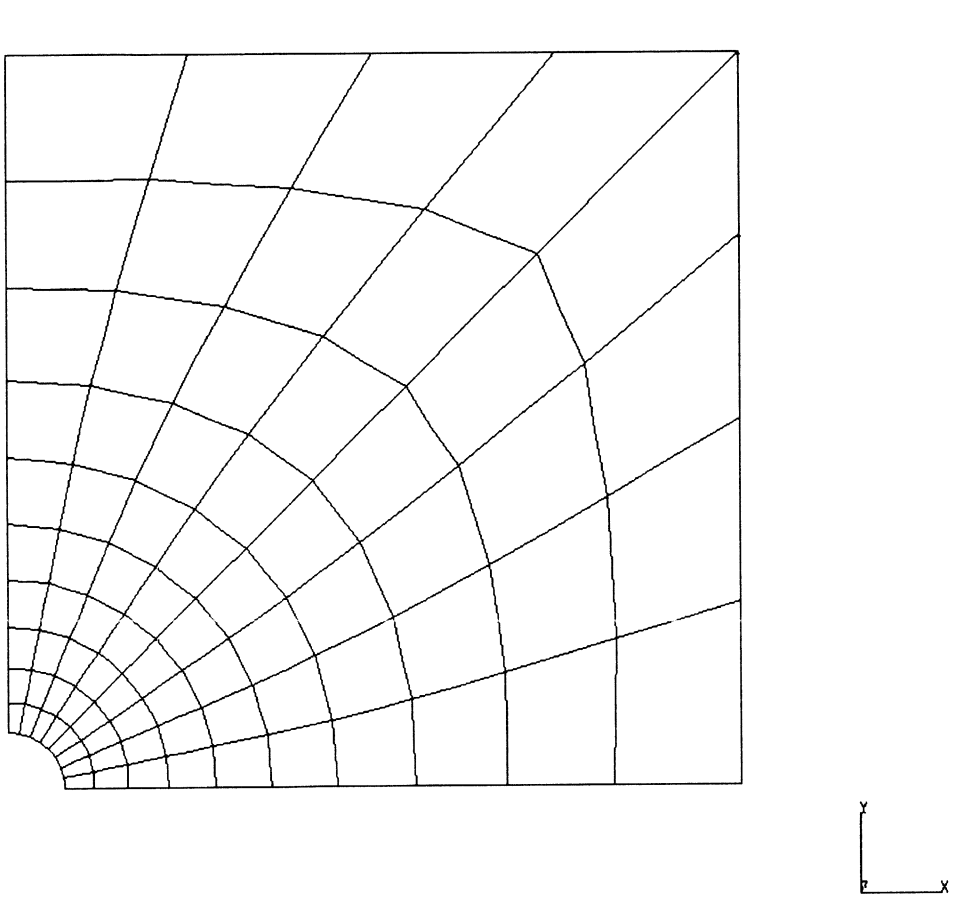

Figure E 7.19-1 Finite Element Mesh

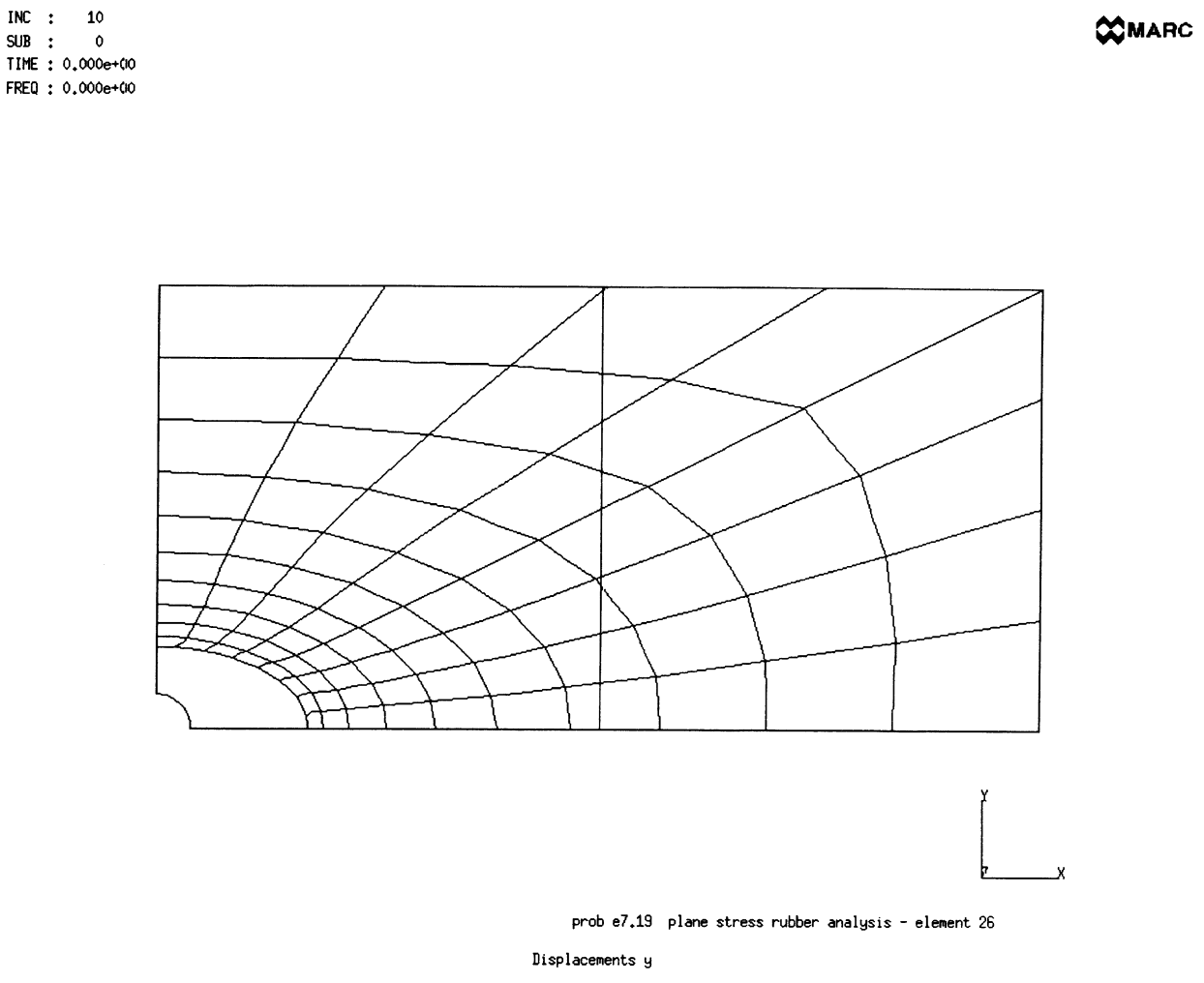

Figure E 7.19-2 Deformed Mesh

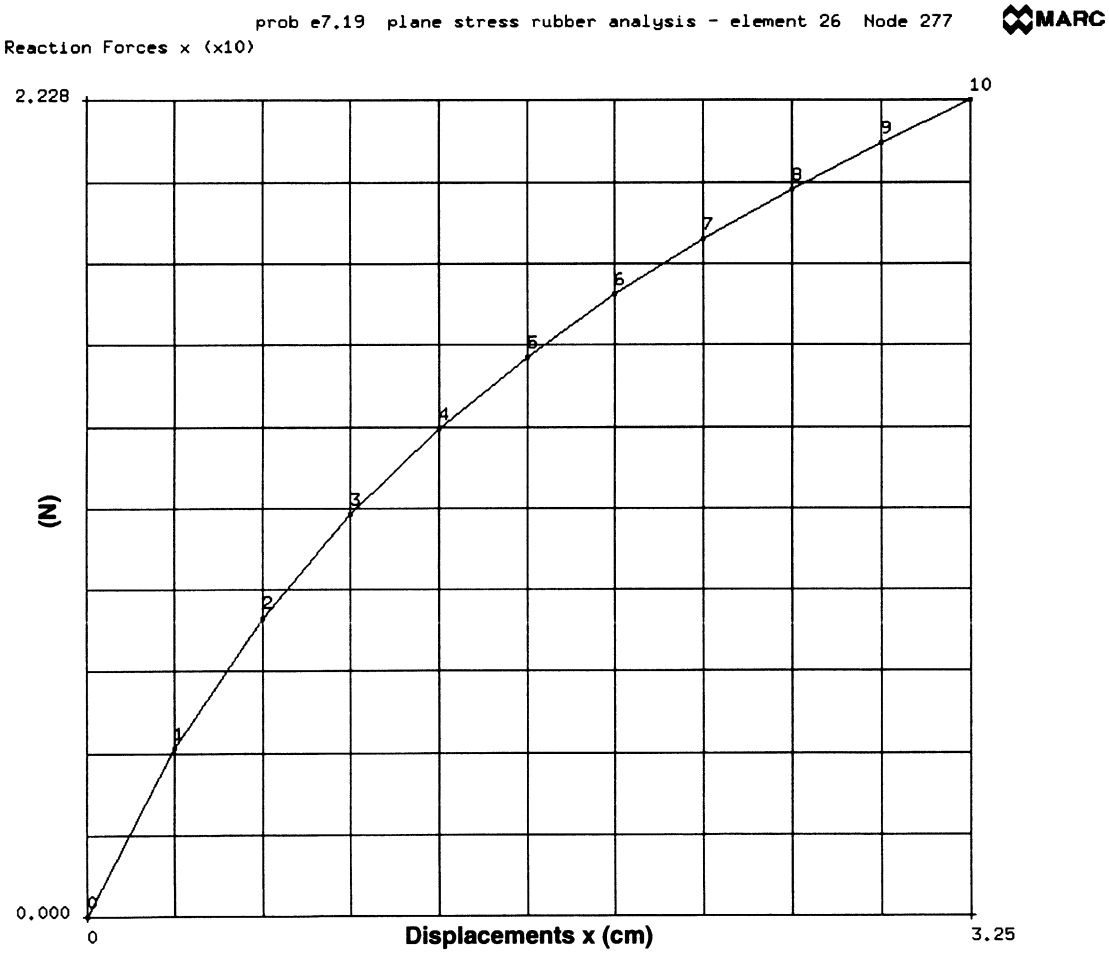

Figure E 7.19-3 Load Deflection Curve

E 7.20 Compression Of An O-Ring Using Ogden Model

This example demonstrates the use of the Ogden rubber model for the high compression of an O-ring. The ring is compressed into a rigid channel.

Element

Library element 82, a five-node axisymmetric element using the Herrmann formulation, is used for this analysis. There are 544 elements and 1149 nodes in the model, as shown in Figure E 7.20-1. Three rigid bodies are used to simulate the channel. The ring has a mean radius of 12 cm and the loading radius is 1.5 cm.

The rigid surface at the outside radius is first moved inwards a distance of 0.5 cm in a period of 50 seconds. The surface is then frozen and an external pressure of 18.8 N/cm^2 is applied onto the left face during 47 increments. The FOLLOW FOR option is used to insure that the load is applied on the deformed geometry.

Material Properties

The O-ring can be described using the Ogden material model using a three term series. The stress-strain curve for this model is shown in Figure E 7.20-2. The data was fit such that:

Term	μ (N/cm^2)	α
1	6.30	1.3
2	0.12	5.0
3	-0.10	-2.0

and the bulk modulus was 1.0E9 N/cm^2.

Contact/Boundary Conditions

All of the kinematic constraints are provided using rigid contact surfaces. Coulomb friction with a coefficient of friction of 0.1 is specified.

Controls

The full Newton-Raphson iterative method is used with a convergence tolerance of 10% on residuals requested. Because of the large compressive stresses that are generated, the solution of non-positive definite systems is forced. Additionally, a flag is set that tells the program to only use the deviatoric stresses in the initial stress stiffness matrix. While this may slow convergence, it tends to improve stability. The PRINT,5 option is used to obtain more information regarding the contact behavior. The NO PRINT option is used to suppress the printout.

Results

The deformed mesh at increments 10, 30, and 50 are shown in Figure E 7.20-3 through Figure E 7.20-5. One observes that at increment 50, the ring almost completely fills the corner regions. The mean second Piola-Kirchhoff stresses are shown in Figure E 7.20-6. One should note that in all these plots, the free surface to which the pressure is applied remains almost perfectly circular. Finally, the contact forces are shown in Figure E 7.20-7.

Summary of Options Used

Listed below are the options used in example e7x20.dat:

Parameter Options

ELEMENT
END
FOLLOW FOR
LARGE DISP
PRINT
SIZING
TITLE

Model Definition Options

CONNECTIVITY
CONTROL
COORDINATES CONTACT
DEFINE
DIST LOADS
END OPTION
OGDEN
OPTIMIZE
POST

Load Incrementation Options

AUTO LOAD
CONTINUE
DIST LOADS
MOTION CHANGE
TIME STEP

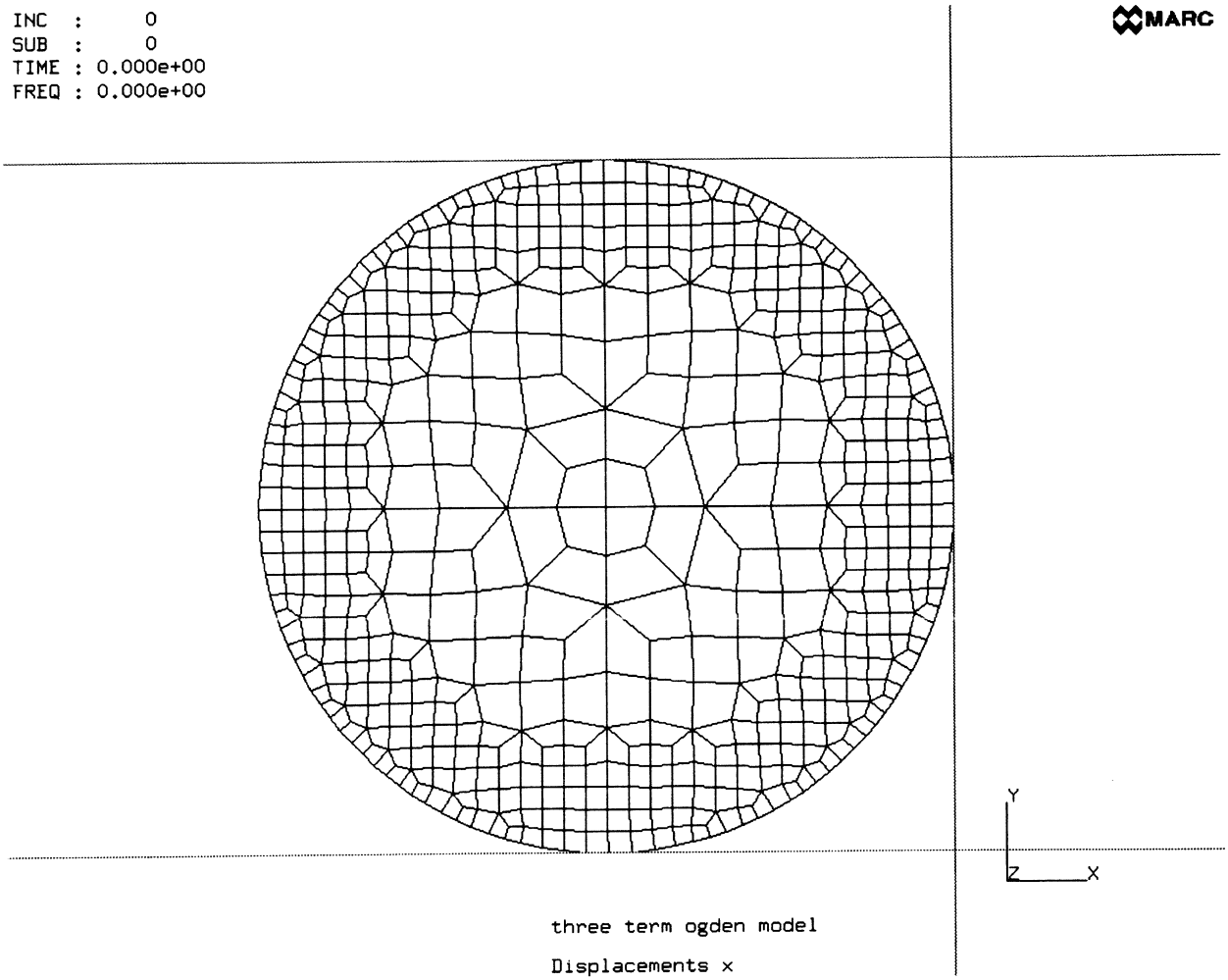

Figure E 7.20-1 O-ring Mesh

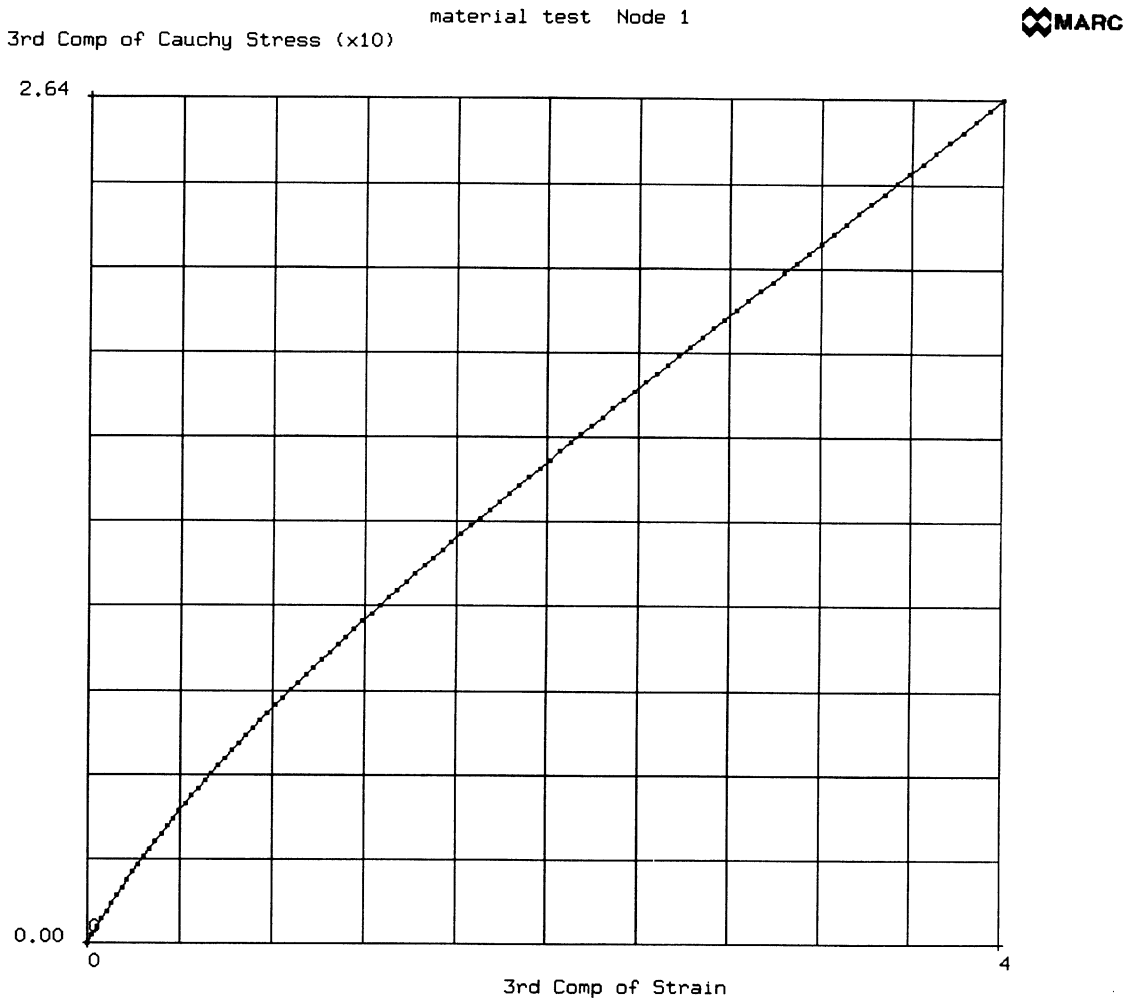

Figure E 7.20-2 Stress-Strain Curve

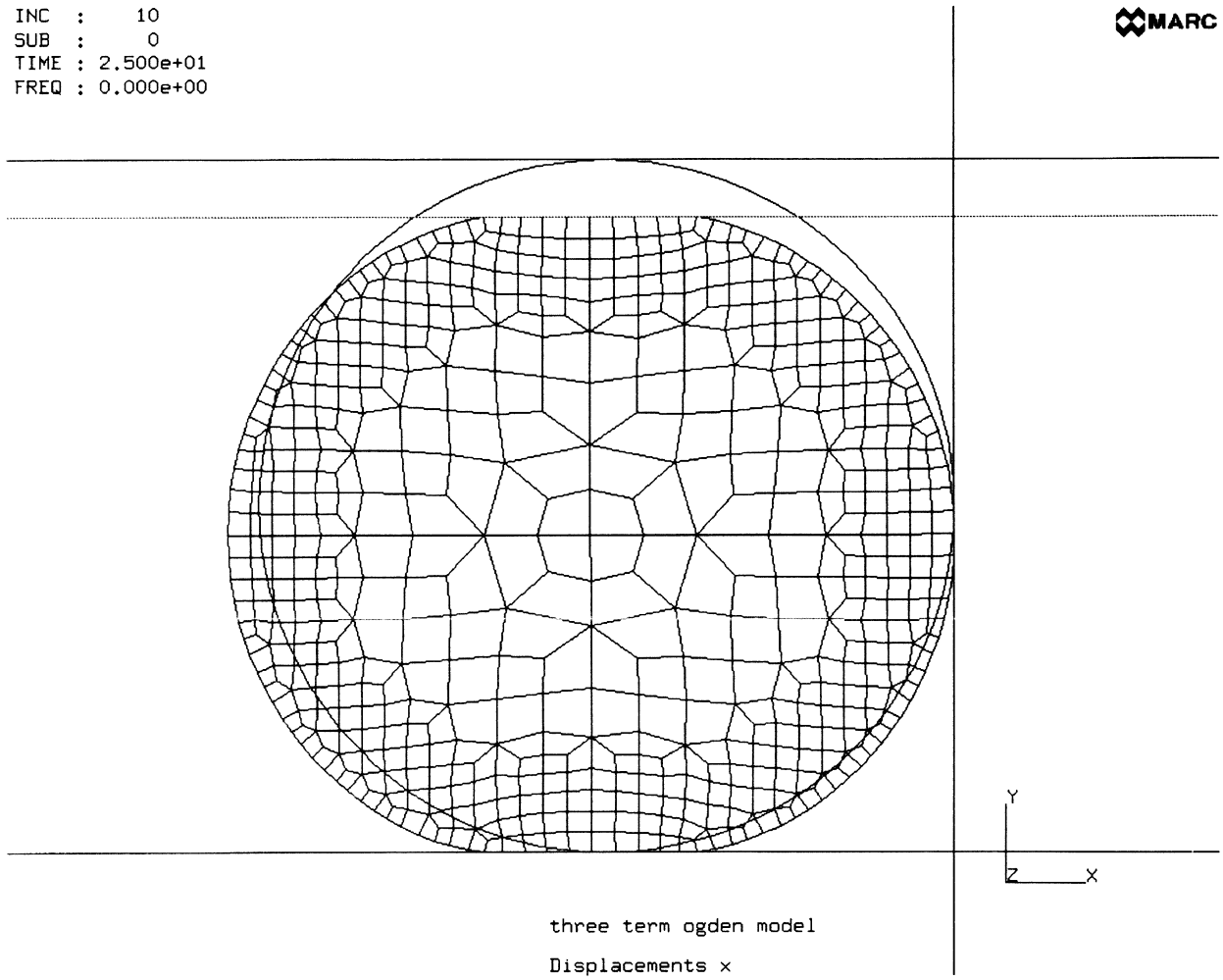

Figure E 7.20-3 Deformed Mesh, Increment 10

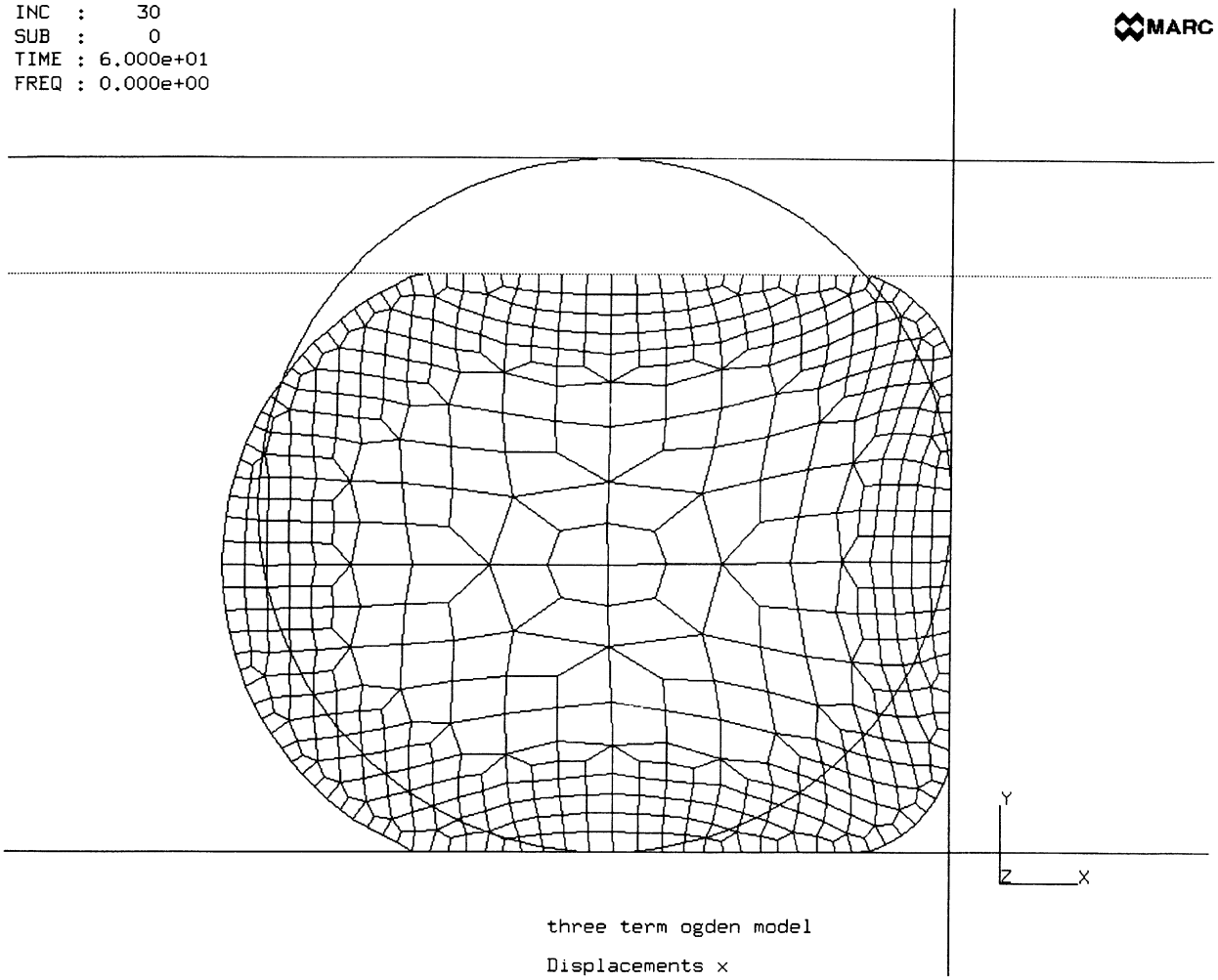

Figure E 7.20-4 Deformed Mesh, Increment 30

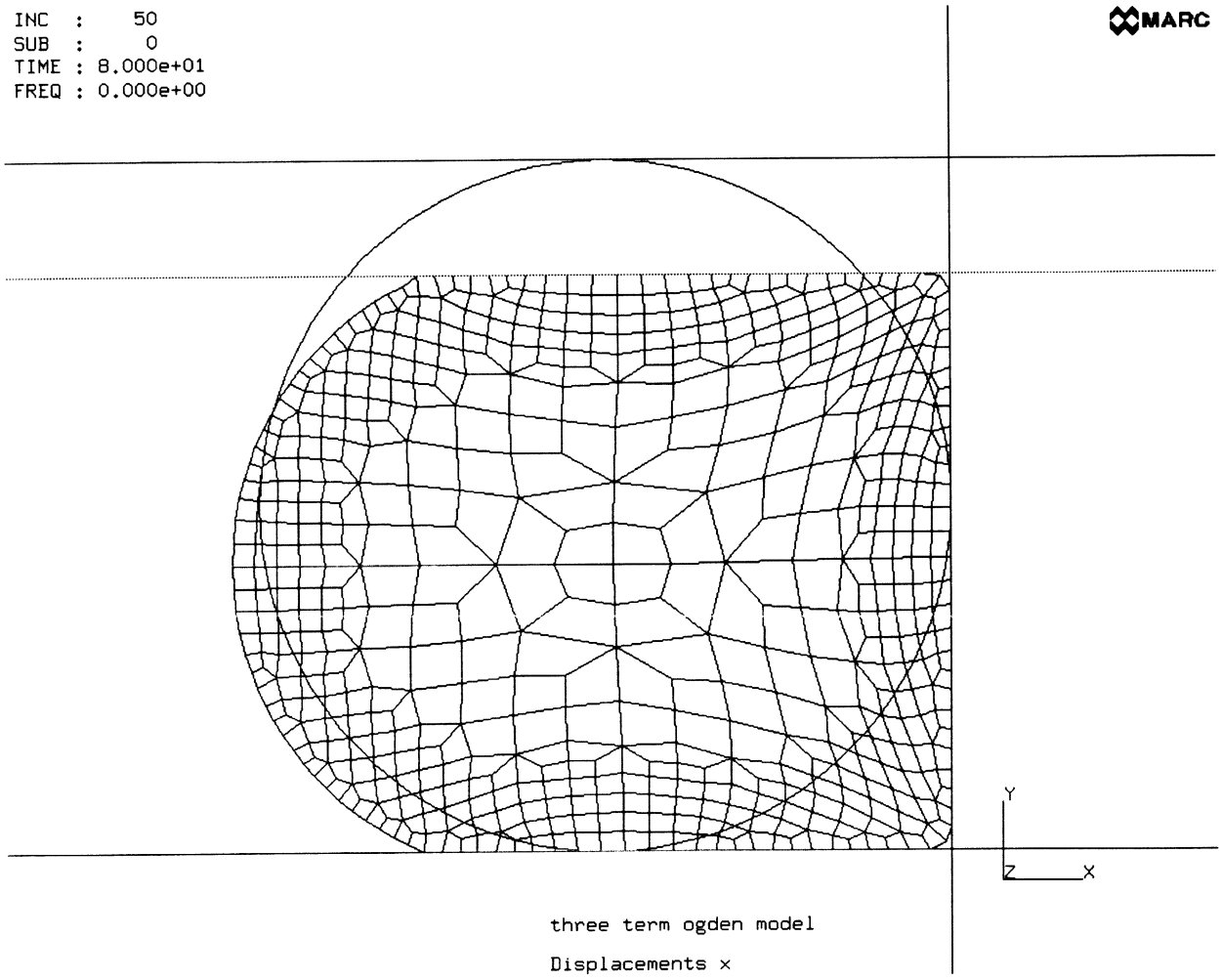

Figure E 7.20-5 Deformed Mesh, Increment 50

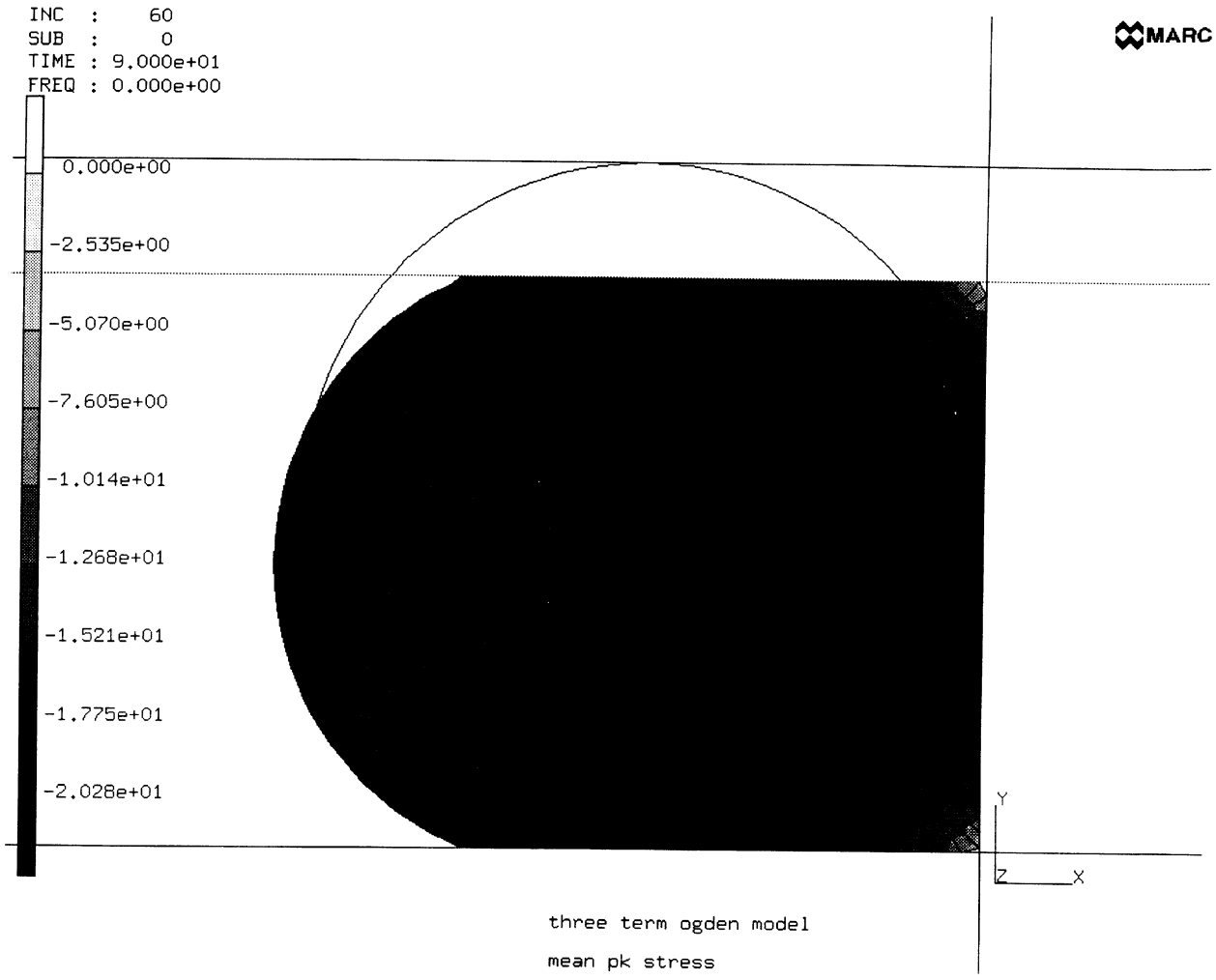

Figure E 7.20-6 Mean Stress Distribution

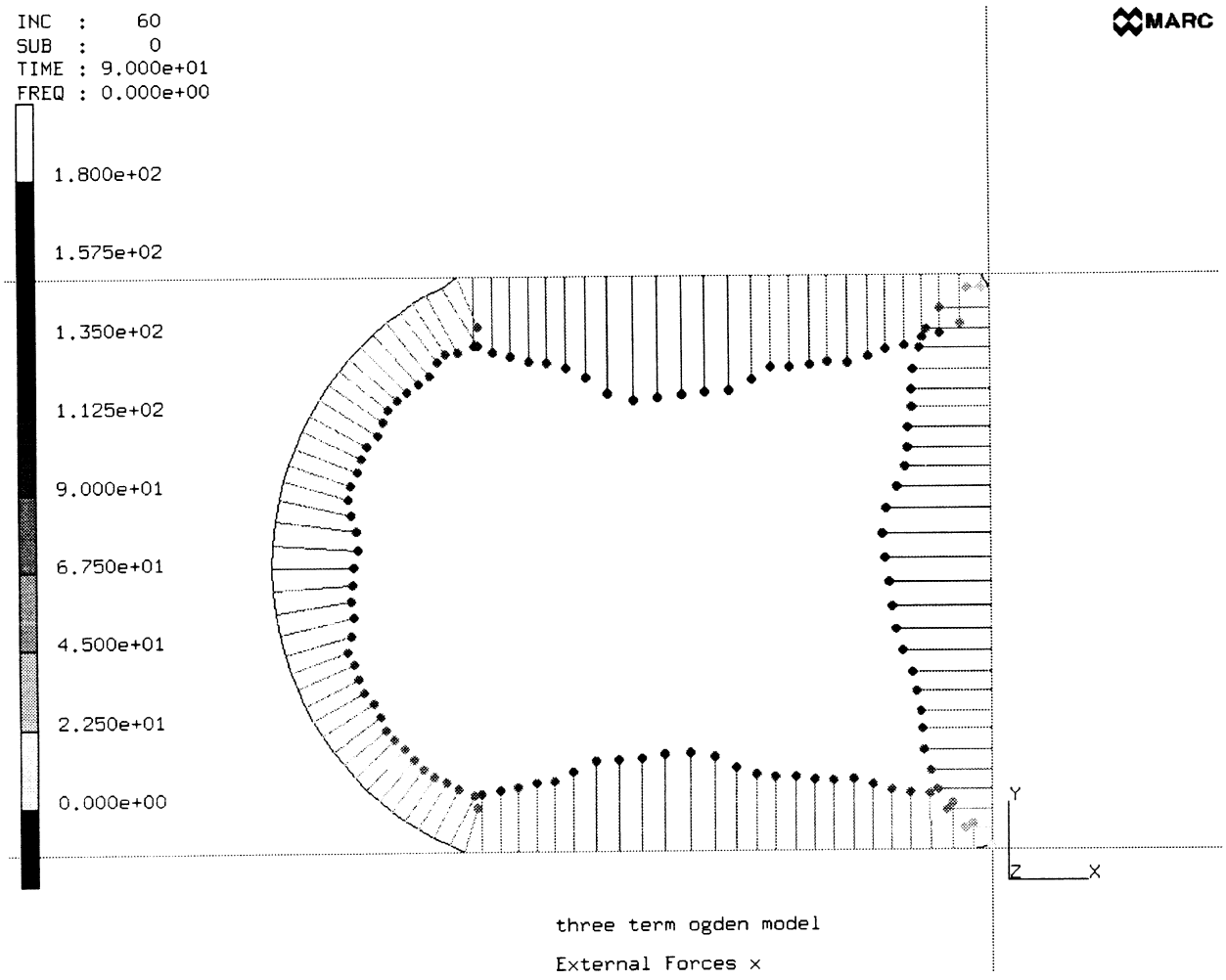

Figure E 7.20-7 Contact Forces

E 7.21 Stretching Of A Rubber Plate With Hole

This example demonstrates the use of the Ogden material model for a rubber sheet analysis.

Element

Element type 26, an eight-node plane stress element, is used. The plate is 10 cm x 10 cm and the hole has a radius of 1. Due to symmetry, only one quarter of the model is used. The mesh is shown in Figure E 7.21-1.

Loading

The x = 0 and y = 0 are symmetry planes. The line at x = 5 cm is being pulled with a uniform displacement of 2.5 cm over 5 increments through the DISP CHANGE and AUTO LOAD options.

Material Properties

The sheet is represented using the Ogden material model using a three-term series. The stress-strain curve for this model is shown in Figure E 7.21-2. The data was fit such that:

Term	μ (N/cm^2)	α
1	19.7	1.3
2	0.038	5.0
3	-0.32	-2.0

The bulk modulus is 1 x 10^8 N/cm^2.

Geometry

The plate thickness is 1.0.

Controls

The full Newton-Raphson procedure is used with a convergence tolerance of one percent of residuals. Typically, one iteration was required to achieve convergence.

Results

The final deformed mesh is shown in Figure E 7.21-3. The stress contours and the strain contours are shown in Figure E 7.21-4 and Figure E 7.21-5, respectively. One can observe that the strain was 250% in the vicinity of the hole.

Summary of Options Used

Listed below are the options used in example e7x21.dat:

Parameter Options

ELEMENT
END
LARGE DISP
SIZING
TITLE

Model Definition Options

CONNECTIVITY
CONTROL
COORDINATES
END OPTION
FIXED DISP
GEOMETRY
OGDEN
OPTIMIZE
POST

Load Incrementation Options

AUTO LOAD
CONTINUE
DISP CHANGE

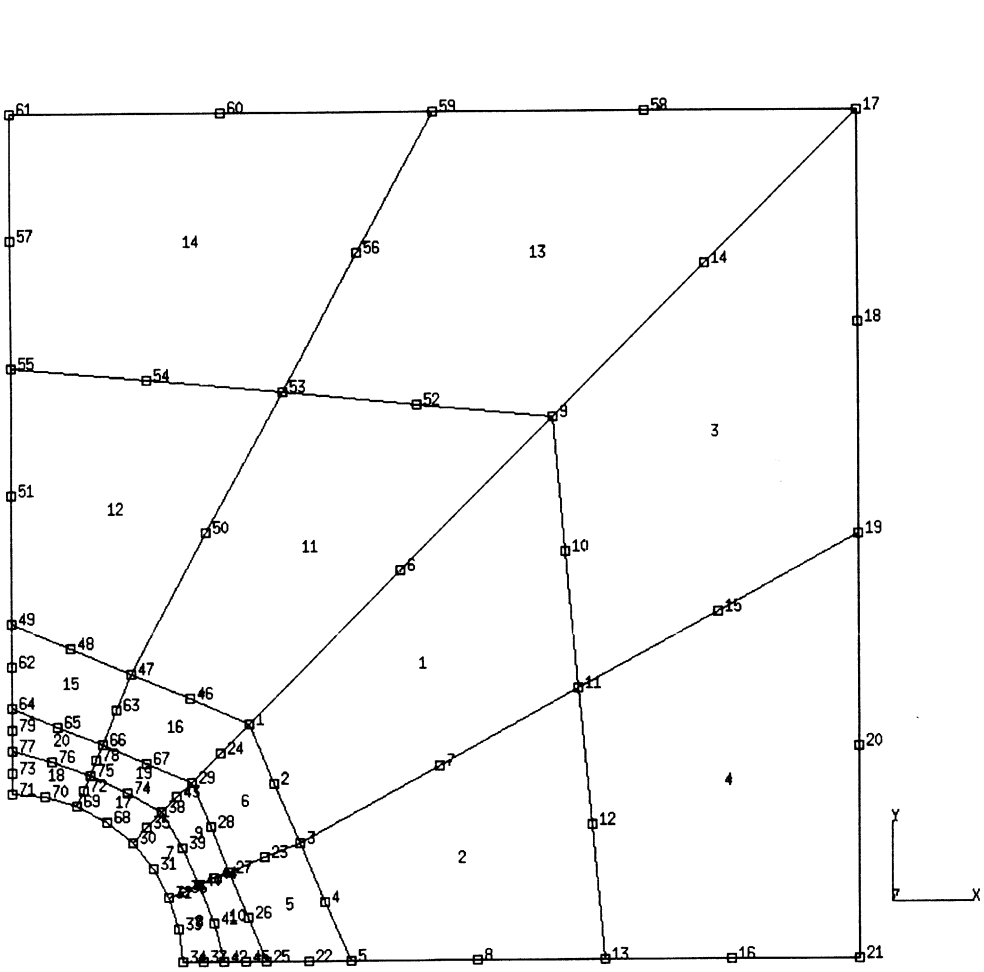

Figure E 7.21-1 Finite Element Mesh

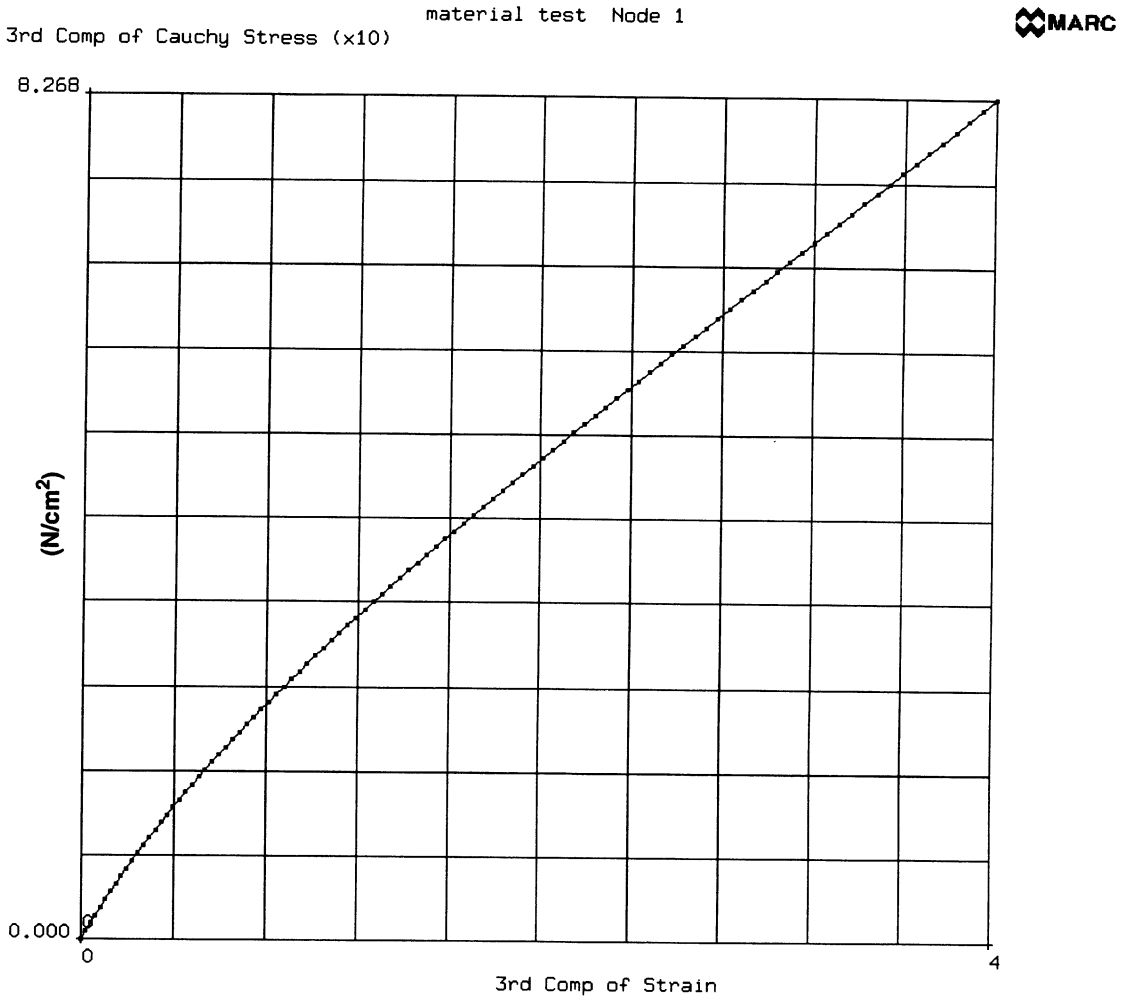

Figure E 7.21-2 Stress-Strain Curve

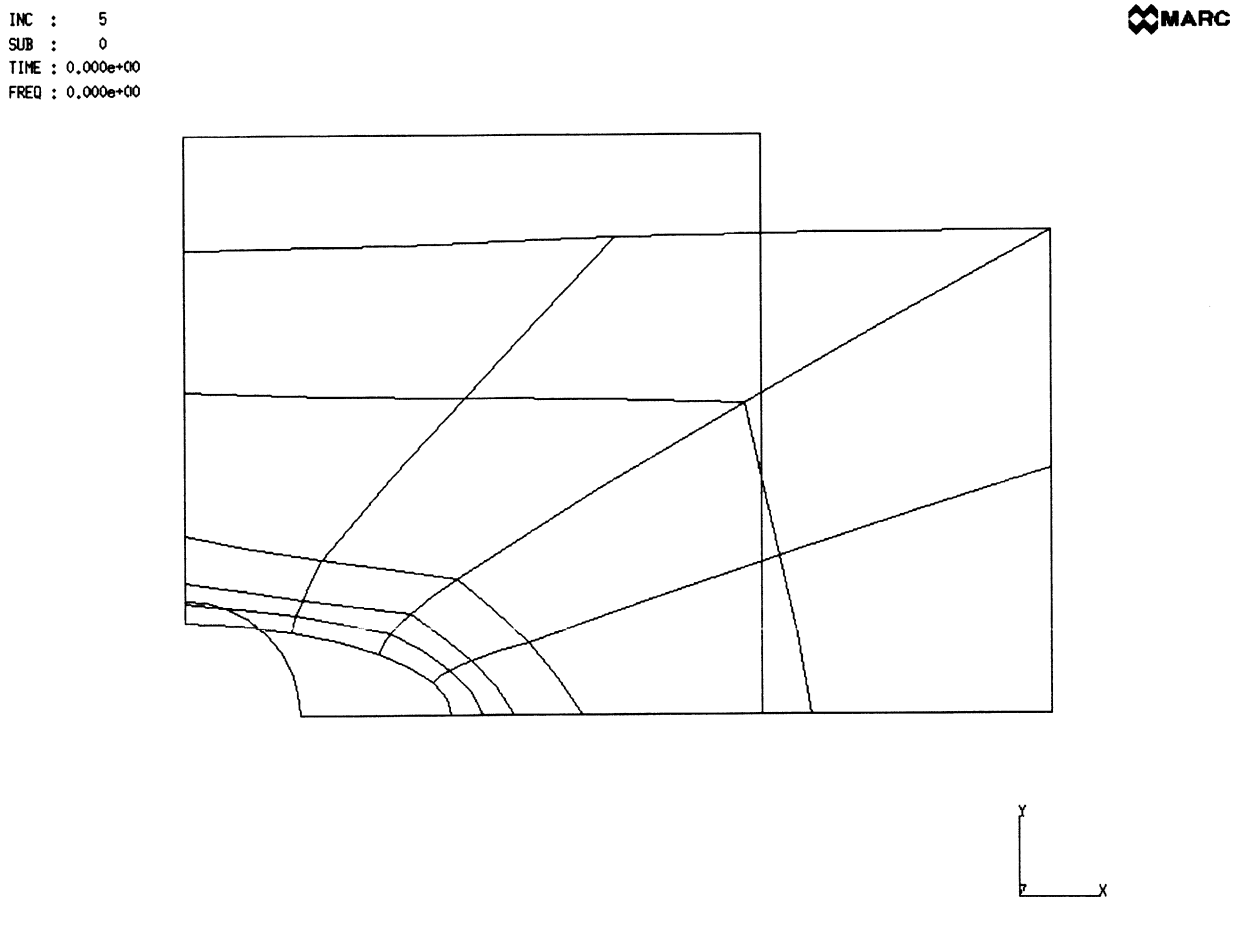

Figure E 7.21-3 Deformed Mesh

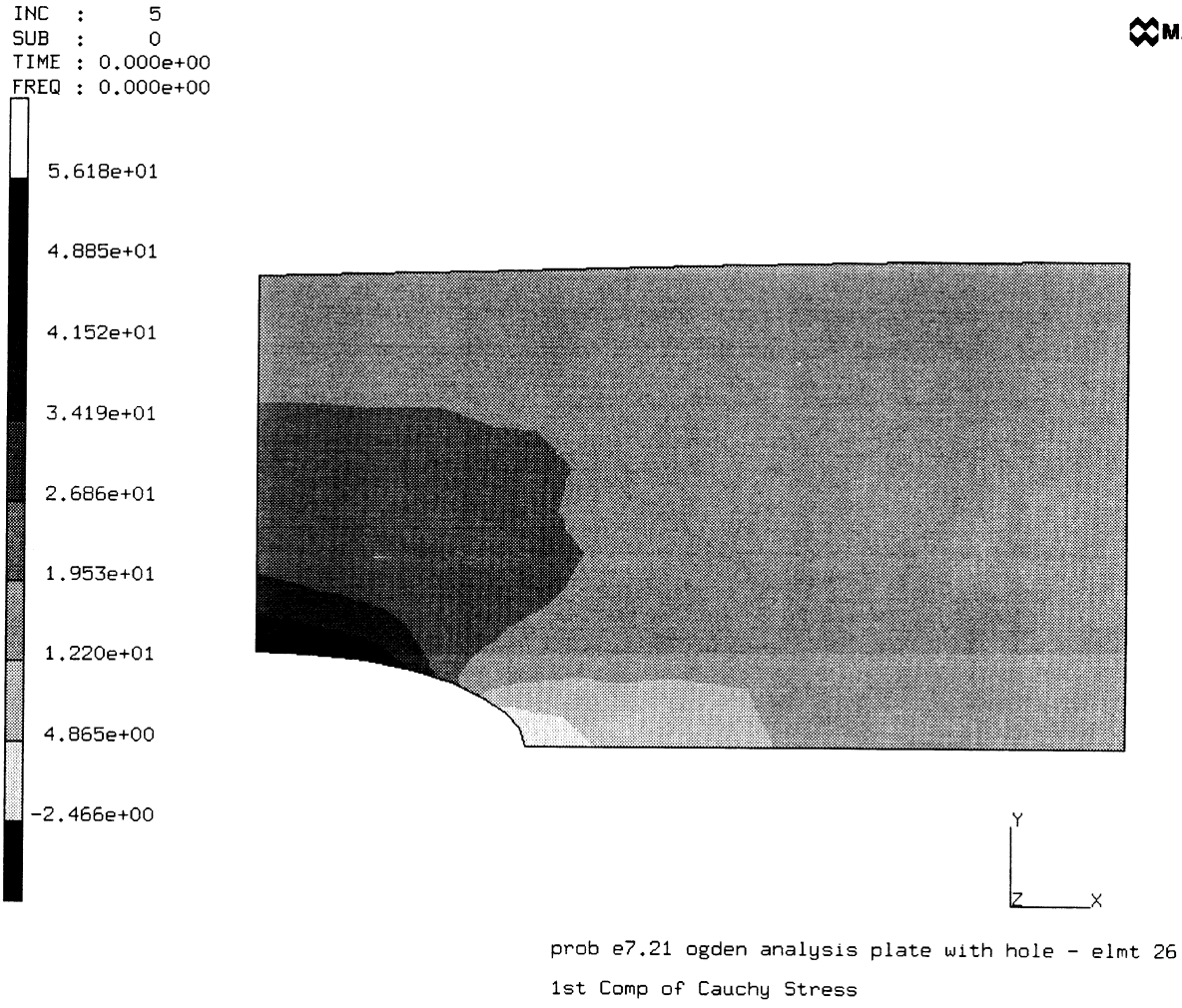

Figure E 7.21-4 Stress Distribution

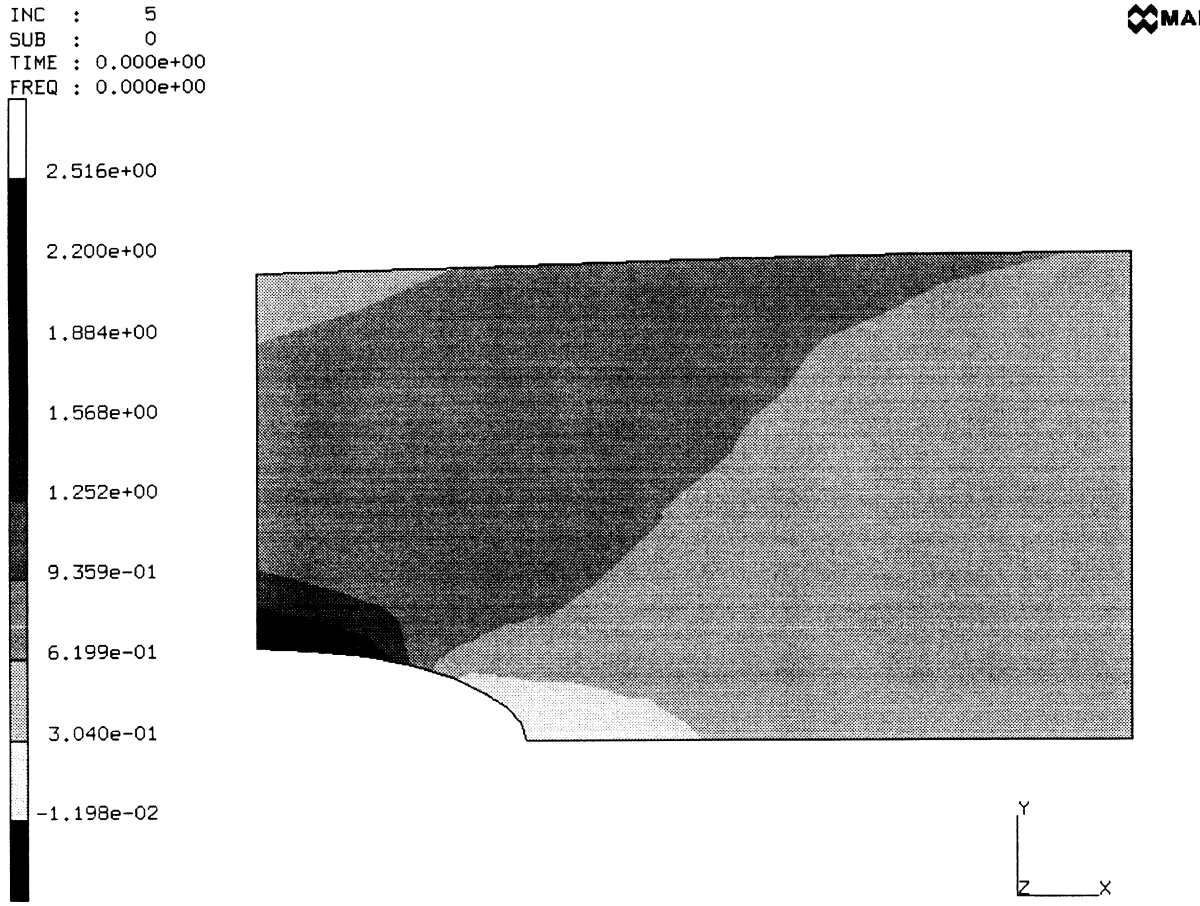

Figure E 7.21-5 Strain Distribution

E 7.22 Loading Of A Rubber Plate

This example illustrates the analysis of a rubber plate under cyclic loading. The analysis uses three different material models. The first analysis uses simply a three term Ogden series; the second model incorporates damage; the third and most complex model incorporates both damage and viscoelasticity.

Element

Element type 75, a four-node shell element, is used for this analysis. A 60 cm x 60 cm simply-supported plate is to be modeled. Because of symmetry, only one quarter of the plate is represented using 25 elements as shown in Figure E 7.22-1. The SHELL SECT option is used to prescribe three layers. This is adequate because it is a linear analysis. The thickness of 3 cm is specified in the GEOMETRY option.

Loading

The first and second models are rate insensitive. Two increments are taken to apply a distributed load of 0.004 on the complete plate followed by two increments to remove the load. In the third analysis, the initial load is also applied in two increments instantaneously; that is, the time step is zero. Hence, creep (viscoelasticity) will not occur. This is followed by a period of one second in which relaxation occurs in which no additional load is applied. Then, two increments follow during which the load is removed again and instantaneously followed by a final relaxation period of five seconds.

Material Properties

The rubber material is defined as a three-term Ogden series with a finite compressibility. The bulk modulus = 6000 N/cm^2 and the coefficients are:

Term	μ (N/cm^2)	a
1	6.300	1.3
2	0.012	5.0
3	-0.3100	-2.0

The stress-strain law is shown in Figure E 7.22-2.

The rubber damage model is used in the second and third analyses. Only deviatoric damage will be considered with the damage rate being 0.050 and the maximum damage factor = 0.90. This is specified through the DAMAGE option.

The third model includes viscoelastic deviatoric behavior. Two terms are included in the Prony series to express the strain energy relaxation function:

Series	Multiplier	Relaxation Time (Seconds)
1	0.6	1.0
2	0.1	10.0

Notice that the total time of the analysis falls within the relaxation times specified.

Boundary Conditions

Displacements are prescribed such that nodes 1 to 6 and 1 to 31 by 6 are clamped, and nodes 31 to 36 and 6 to 36 by 6 are symmetric boundary conditions.

Controls

The full Newton-Raphson method is used in this analysis. In those increments where the total applied load is nonzero, a five percent tolerance on residuals is required. When the applied load is zero, we would be attempting to measure residual/noise so the convergence is changed to displacement control. This is very important to insure efficient convergence to a meaningful accuracy.

Results

Figure E 7.22-3 shows the displacement of the center node (36) as a function of the increment number for the first model. One can observe that the material goes back to the original configuration when the load has been removed. Displacement is of the order 10^{-6}. In Figure E 7.22-4, one observes the displacement history when damage is included. Note that the maximum displacement is larger and the slope of the loading and unloading curve is substantially different. Upon unloading, there is a permanent deformation of the order 2.5×10^{-2}. Finally, Figure E 7.22-5 shows the displacement history when both damage and viscoelasticity occur. One observes that there are four different regions: loading, creep, unloading and creep. Figure E 7.22-6 is the same information but now plotted as a function of time.

Summary of Options Used

Listed below are the options used in example e7x22a:

Parameter Options

ELEMENT
END
LARGE DISP
SHELL SECT
SIZING
TITLE

Model Definition Options

CONNECTIVITY
CONTROL
COORDINATES
DIST LOADS
END OPTION
FIXED DISP
GEOMETRY
OGDEN
OPTIMIZE
POST

Load Incrementation Options

AUTO LOAD
CONTINUE
DIST LOADS

Listed below are the options used in example e7x22b:

Parameter Options

ELEMENT
END
LARGE DISP
SHELL SECT
SIZING
TITLE

Model Definition Options

CONNECTIVITY
CONTROL
COORDINATES
DAMAGE
DIST LOADS
END OPTION
FIXED DISP
GEOMETRY
OGDEN
OPTIMIZE
POST

Load Incrementation Options

AUTO LOAD
CONTINUE
DIST LOADS

Listed below are the options used in example e7x22c:

Parameter Options

ELEMENT
END
LARGE DISP
SHELL SECT
SIZING
TITLE

Model Definition Options

CONNECTIVITY
CONTROL
COORDINATES
DAMAGE
DIST LOADS
END OPTION
FIXED DISP
GEOMETRY
OGDEN
OPTIMIZE
POST
VISCELOGDEN

Load Incrementation Options

AUTO LOAD
CONTINUE
DIST LOADS

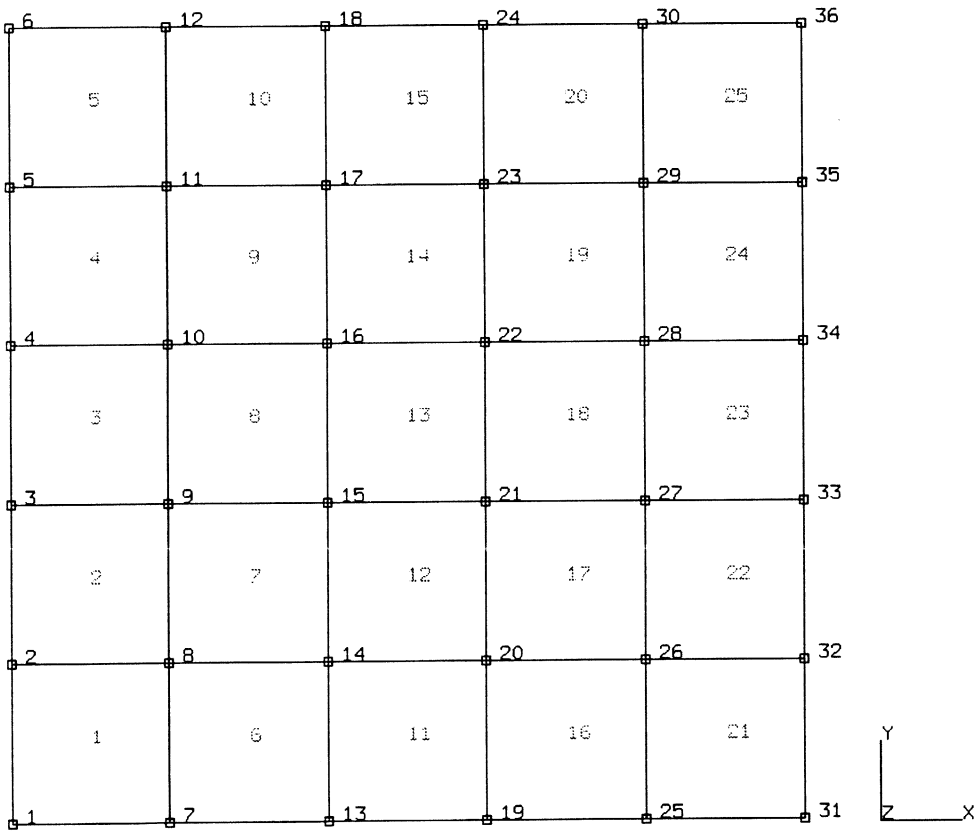

Figure E 7.22-1 Finite Element Mesh

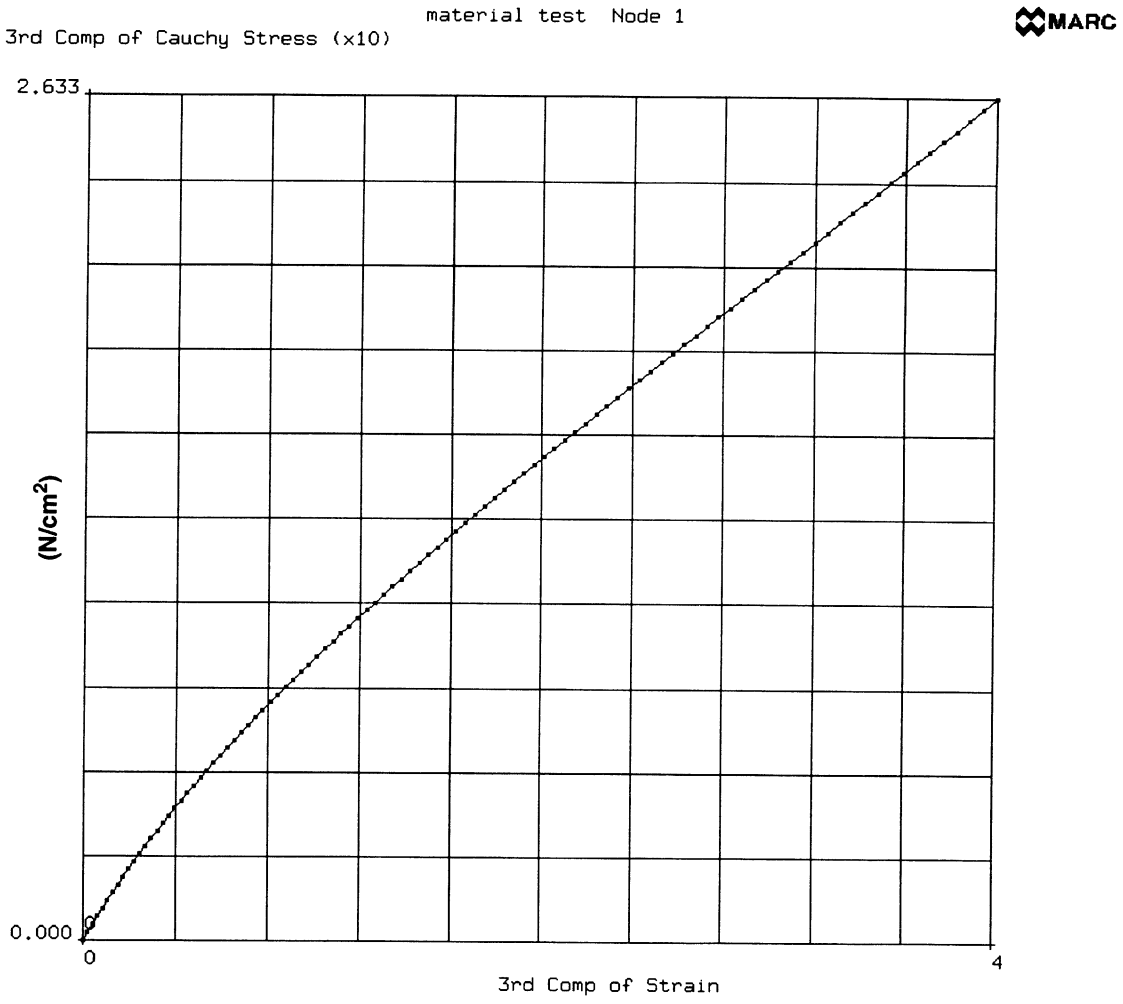

Figure E 7.22-2 Stress-Strain Curve

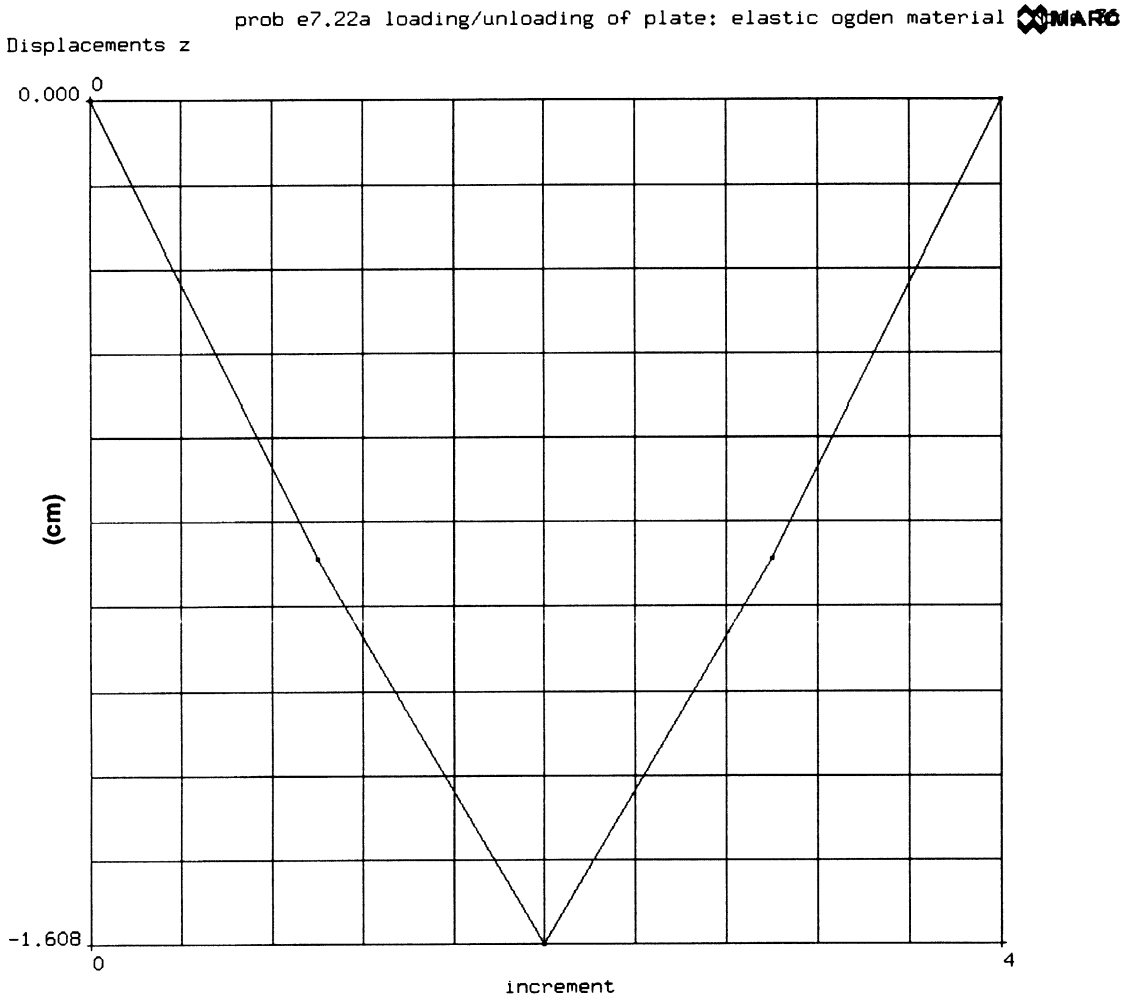

Figure E 7.22-3 Displacement History of Center Node – Elastic Effects Only

Contents Chapter 8 Advanced Topics

Figures Chapter 8 Advanced Topics

Tables Chapter 8 Advanced Topics

Chapter 8 Advanced Topics

This chapter demonstrates capabilities that have been added to MARC in the last few releases. These capabilities include substructures, cracking, composites, contact, electrostatics, magnetostatics, and acoustics capabilities among others. Discussions of these capabilities can be found in Volume A, and a summary of the various capabilities is given below:

Substructures

- Linear analysis
- Nonlinear analysis
- Cracking analysis

Thermal-mechanical coupled analysis

- Composite analysis
- Failure criteria

Progressive failure

Activate and deactivate

Contact analysis

- Two-dimensional
- Three-dimensional
- Springback
- Friction

Electrostatic analysis

Magnetostatic analysis

Acoustic analysis

Compiled in this chapter are a number of solved problems. Table E 8.0-1 shows the MARC elements and options used in these demonstration problems.

Table E 8.0-1 Recent Analysis Capabilities in MARC

Problem Number (E)	Element Type	Parameter Options	Model Definition	Load Incrementation	User Subroutines	Problem Description
8.1	26	ELASTIC SUBSTRUCT NEWDB SUPER	SUBSTRUCTURE DIST LOAD SUPERINPUT RESTART	BACK TO SUBS	SSTRAN	Hole in plate. Generate substructure (1-1) and 1-2). Combine substructures, perform analysis. Read RESTART tape, Go back to substructures to obtain results.
8.2	27	SUBSTRUCT NEWDB SUPER J-INT SCALE	SUBSTRUCTURE DIST LOADS SUPERINPUT J-INTEGRAL WORK HARD	AUTO LOAD PROPORTIONAL INC	WKSLP	Double-edge notch specimen using substructure. Elastic region away from the crack is treated as a substructure.
8.3	10 12	SUBSTRUCT NEWDB SUPER	SUBSTRUCTURE SUPERINPUT POINT LOADS GAP DATA	POINT LOADS AUTO LOAD BACK TO SUBS	—	End plate aperture breakaway problem. The rate is treated as a substructure leaving the contact elements to be at highest level.
8.4	26	—	ISOTROPIC CRACK DATA TYING	PROPORTIONAL INC AUTO LOAD	—	Collapse of a notched concrete beam.
8.5	75	PRINT	CONN GENER COMPOSITE ISOTROPIC ORTHOTROPIC	POINT LOADS AUTO INCREMENT	—	Cracking of a plate one-way reinforced using shell elements.
8.6	27 46	PRINT	CONN GENER NODE FILL CRACK DATA ISOTROPIC	POINT LOADS AUTO INCREMENT	REBAR	Cracking of a one-way reinforced plate using rebar elements.

Table E 8.0-1 Recent Analysis Capabilities in MARC (Continued)

Problem Number (E)	Element Type	Parameter Options	Model Definition	Load Incrementation	User Subroutines	Problem Description
8.7	11 12 39	FINITE UPDATE LARGE DISP COUPLE MESH PLOT	CONTROL FIXED DISP FIXED TEMP INITIAL TEMP ISOTROPIC GAP DATA CONVERT WORK HARD TEMP EFFECTS RESTART DIST FLUXES	TRANSIENT	—	Thermal-mechanically coupled analysis of the compression of a block.
8.8	21	—	ORTHOTROPIC DIST LOADS	—	HOOKLW ANELAS	Bending of a thick anisotropic plate.
8.9	3	—	DEFINE ORTHOTROPIC ORIENTATION FALL DATA PRINT ELEM	—	—	Failure criteria calculation of an orthotropic plate.
8.10	52	—	HYPOELASTIC	—	UBEAM	Nonlinear beam bending.
8.11	26	—	ERROR ESTIMATE	DEACTIVATE ACTIVATE	—	Example of Activate, Deactivate and error estimates.
8.12	10	PRINT,5 FINITE LARGE DISP UPDATE REZONING	WORK HARD CONTACT	AUTO LOAD TIME STEP REZONE CONTACT CHANGE ISOTROPIC CHANGE CONNECTIVITY CHANGE COORDINATE CHANGE END REZONE AUTO TIME	—	Forging of the head of a bolt.

Table E 8.0-1 Recent Analysis Capabilities in MARC (Continued)

Problem Number (E)	Element Type	Parameter Options	Model Definition	Load Incrementation	User Subroutines	Problem Description
8.13	10 116	PRINT,5 FINITE LARGE DISP UPDATE COUPLE	POST FIXED TEMP FIXED DISP TEMP EFFECTS WORK HARD DIST FLUXES CONTACT INITIAL TEMP CONVERT	TRANSIENT DISP CHANGE AUTO TIME	—	Coupled analysis of ring compression.
8.14	7	UPDATE FINITE LARGE DISP PRINT,5	—	AUTO LOAD TIME STEP	—	3D indentation problem demonstrating how rigid surfaces are defined.
8.15	11 27	UPDATE FINITE LARGE DISP PRINT,5	CONTACT CONTACT TABLE DEFINE RESTART LAST	AUTO LOAD TIME STEP	—	Double-sided contact between deformable bodies.
8.16	11	UPDATE FINITE LARGE DISP PRINT,5	SPRINGS CONTACT WORK HARD	AUTO LOAD TIME STEP RELEASE MOTION CHANGE	MOTION	Formation of a metal part and the examination of springback.
8.17	7	REZONING UPDATE FINITE LARGE DISP PRINT,8	CONTACT RESTART LAST	AUTO LOAD TIME STEP	—	Metal extrusion analysis using the CONTACT option. Coulomb friction.
8.18	75	SHELL SET,7 LARGE DISP UPDATE FINITE PRINT,8	CONTACT	AUTO LOAD TIME STEP MOTION CHANGE	WKSLP	Stretch forming of a circular sheet. Coulomb friction between sheet and punch.

Table E 8.0-1 Recent Analysis Capabilities in MARC (Continued)

Problem Number (E)	Element Type	Parameter Options	Model Definition	Load Incrementation	User Subroutines	Problem Description
8.19	7	UPDATE FINITE LARGE DISP PRINT,8 SIZING	CONTACT UMOTION	AUTO LOAD TIME STEP	MOTION	Three dimensional indentation rolling of elastic-perfectly plastic material.
8.20	39	SIZING ELECTRO	POINT CHARGE FIXED POTENTIAL	STEADY STATE	—	Point charge in a circular region.
8.21	43	SIZING ELECTRO	FIXED POTENTIAL POINT CHARGE	STEADY STATE	—	Point charge in a circular cylinder.
8.22	39	SIZING\ MAGNET	POINT CURRENT FIXED POTENTIAL	STEADY STATE	—	Point current in a circular region.
8.23	109	MAGNET	FIXED POTENTIAL POINT CURRENT	STEADY STATE	—	3D analysis of a magnetic field in a coil.
8.24	39	MAGNET	ISOTROPIC FIXED POTENTIAL POINT CURRENT B-H RELATION	STEADY STATE	—	2D nonlinear magnetostatic analysis.
8.25	39	ACOUSTIC PRINT,3	ISOTROPIC	DYNAMIC CHANGE	—	2D acoustic problem demonstrating the eigenvalue analysis in a circular cavity with barrier.
8.26	39	ACOUSTIC	ISOTROPIC FIXED PRESSURE	DYNAMIC CHANGE	FORCDT	2D acoustic problem demonstrating the eigenvalue analysis of a rectangular cavity.
8.27	26	INPUT TAPE	FIXED DISP ORTHOTROPIC	AUTO LOAD PROPORTIONAL CONTROL	—	Progressive failure of a plate with a hole.
8.28	41 103	ELECTRO	POINT CHARGE FIXED POTENTIAL	STEADY STATE	—	Linear distribution of dipoles.

Table E 8.0-1 Recent Analysis Capabilities in MARC (Continued)

Problem Number (E)	Element Type	Parameter Options	Model Definition	Load Incrementation	User Subroutines	Problem Description
8.29	41 103	MAGNET	POINT CHARGE FIXED POTENTIAL	STEADY STATE	—	Magnetic field around two wires carrying opposite currents.
8.30	111	EL-MA HARMONIC PRINT, 3	DIST CURRENT FIXED POTENTIAL	DIST CURRENT HARMONIC POINT CURRENT	—	Harmonic electromagnetic analysis of a waveguide.
8.31	112	EL-MA PRINT, 3	FIXED POTENTIAL	DYNAMIC CHANGE POTENTIAL CHANGE	—	Transient electromagnetic analysis around a conducting sphere.
8.32	113	EL-MA HARMONIC	FIXED POTENTIAL	DIST CURRENT HARMONIC	—	Calculate the resonance in a cavity.
8.33	111	EL-MA HARMONIC	FIXED POTENTIAL	POINT CURRENT CURRENT DYNAMIC CHANGE HARMONIC	—	Steady state analysis of an infinitely long wire using both harmonic and transient analysis.
8.34	28	PORE UPDATE ISTRESS	SOIL INITIAL PC INITIAL VOID INITIAL STRESS DIST LOADS	DIST LOADS TIME STEP DISP CHANGE AUTO LOAD	—	Drained triaxial test on normally consolidated clay.
8.35	32	PORE ISTRESS	SOIL SOLVER INITIAL PC INITIAL STRESS INITIAL VOID DIST LOADS DEFINE	DIST LOADS TIME STEP AUTO TIME CONTROL	—	Coupled pore-pressure calculation of stratified soil embankment.

Table E 8.0-1 Recent Analysis Capabilities in MARC (Continued)

Problem Number (E)	Element Type	Parameter Options	Model Definition	Load Incrementation	User Subroutines	Problem Description
8.36	116	PRINT, 5	SPRINGS CONTACT DEFINE	CONTACT TABLE AUTO LOAD TIME STEP	—	Interference fit of two cylinders.
8.37	11	PRINT, 8	CONTACT SPRINGS DEFINE	CONTACT TABLE AUTO LOAD TIME STEP	—	Interference fit between sectors of two cylinders. Demonstrates symmetry surfaces.

E 8.1 Plate With Circular Hole Using Substructures

In this problem, the substructuring capability is demonstrated to solve an elastic problem of a square plate with a circular hole (see Figure E 8.1-1). This example demonstrates the three aspects of using substructures:

1. Generate superelement
2. Combine superelements, obtaining results for external nodes
3. Obtain solution within the substructure.

Element

Element type 26, an 8-node plane stress quadrilateral is used.

Model

Due to symmetry, only one quarter of the specimen is modeled. Because of symmetry about a 45° line, this quarter plate is modeled using two identical substructures.

Geometry

A unit thickness is used.

Boundary Conditions

Boundary conditions are used to enforce symmetry about the x-axis. When the 1,1 superelement is mirrored about the 45° line, this boundary condition will effectively be about the y-axis.

Material Properties

The material is elastic. Values for Young's modulus, Poisson's ratio are 30×10^6 psi and 0.3, respectively.

DIST LOADS

A uniform pressure of 0 psi is applied to substructure 1,1. A uniform pressure of -1 psi is applied to substructure 1,2.

Substructure Procedure

In the first part of the first analysis, superelement level 1 number 1 is formed. On the SUBSTRUC parameter, it is requested that the substructure database be written to unit 31. Unit 16 is used to write the stiffness matrix. The NEWDB parameter option indicates that this is the first superelement created, and hence the data base should be initialized. The SUBSTRUCTURE model definition option indicates which nodes are the external nodes. There are 11 external nodes.

In the second part of the first analysis, substructure level 1 number 1 is copied to substructure level 1 number 2. This is performed using the SUBSTRUC parameter option. This new substructure is placed on unit 17. This substructure is given a different load factor than the previous one. When using substructures, the load may be modified using the AUTO LOAD option or the PROPORTIONAL increment option.

While forming substructures, multiple substructure formations may be performed during the same run. This is achieved by putting the MARC input "decks" back-to-back to create one large input.

In the second analysis, the two previous superelements are combined and the solution obtained for the external degrees-of-freedom. The SUPER parameter option is used to indicate that superelements will be used in this analysis. It also indicates the maximum number of nodes and degrees-of-freedom associated with a superelement. The SUPERINPUT model definition option is used to enter a correspondence table between previously defined external nodes and the nodes used in this analysis. In this problem, the externals lie along the 45° diagonal (see Figure E 8.1-2). As there are no normal elements, there are no stresses or strains calculated here. A restart tape is written. In addition, the calculated displacements are written back to the database.

User subroutine SSTRAN is used to reflect substructure level 1 number 2 by 90°. In the third analysis, the displacements calculated at the external nodes are used to calculate the internal degrees-of-freedom, the strains and the stresses. This is performed using the BACKTOSUBS option.

If desired, after the results are obtained in the subelement, plots could be obtained. In addition, if the post option was used, the results would have been written for both substructures.

Summary of Options Used

Listed below are the options used in example e8x1a.dat:

Parameter Options

ELASTIC
ELEMENT
END
MESH PLOT
NEWDB
SIZING
SUBSTRUCTURE
TITLE

Model Definition Options

CONNECTIVITY
COORDINATE
DIST LOADS
END OPTION
FIXED DISP
GEOMETRY
ISOTROPIC
SUBSTRUCTURE

Load Incrementation Options

CONTINUE
DIST LOADS

Listed below are the options used in example e8x1b.dat:

Parameter Options

END
PRINT
SIZING
SUPER ELEMENT
TITLE

Model Definition Options

END OPTION
RESTART
SUPERINPUT

Listed below is the user subroutine found in u8x1.f:

SSTRAN

Listed below are the options used in example e8x1c.dat:

Parameter Options

END
MESH PLOT
PRINT
SIZING
SUPER ELEMENT
TITLE

Model Definition Options

END OPTION
RESTART
SUPERINPUT

Load Incrementation Options

BACKTOSUBS
CONTINUE

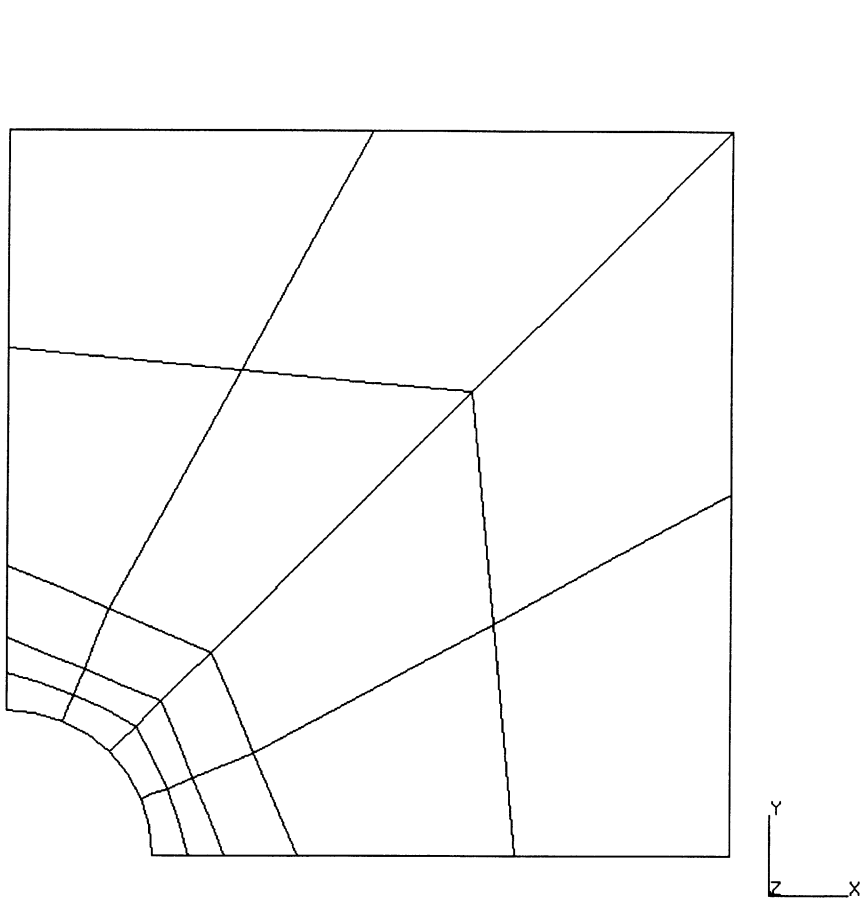

Figure E 8.1-1 Hole in Plate

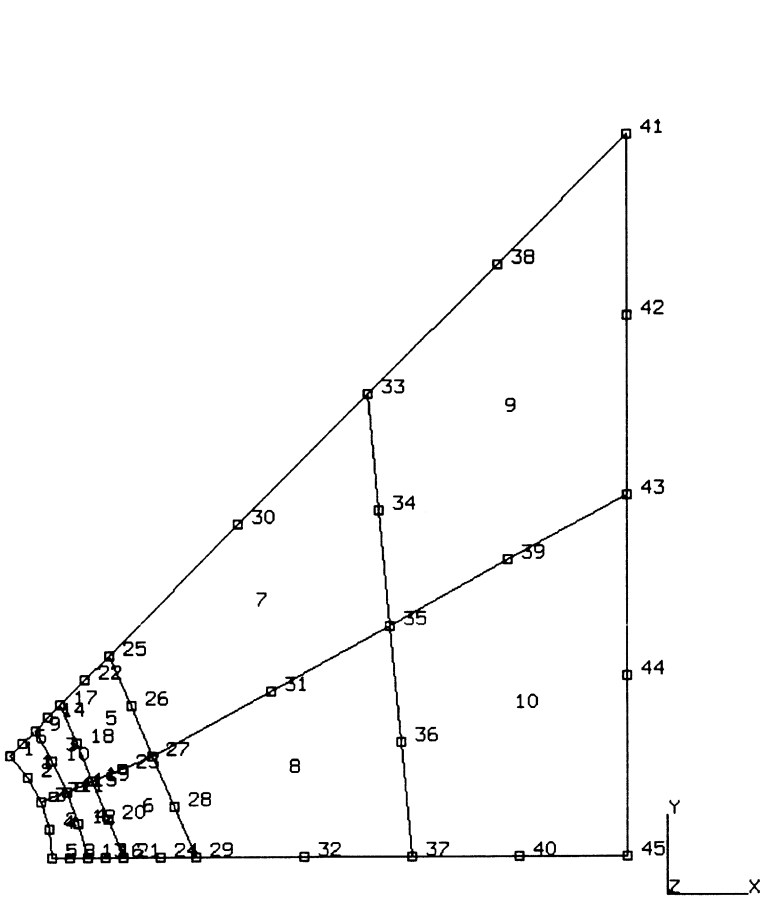

Figure E 8.1-2 Substructure 1,1

E 8.2 Double-Edge Notch Specimen Using Substructures

In this problem, the J-integral is evaluated for an elastic-plastic double-edge notch specimen under axial tension. The use of substructures for a nonlinear problem is demonstrated. Two different paths are used for the J-integral evaluation. The variation in the value of J between the two paths indicates the accuracy of the solution. This problem is identical to problem E 3.8 with the exception that substructures are used. Substructures may be used in a nonlinear analysis as long as the area that is in the superelement remains linear elastic.

Element

Element type 27, an eight-node plane strain quadrilateral is used.

Model

The full double-edge specimen with loading is shown in Figure E 8.2-1. Due to symmetry, only one-quarter on the specimen is modeled. Figure E 8.2-2 shows the mesh with 32 elements and 107 nodes.

Geometry

The option is not required for this element as a unit thickness will be considered.

Boundary Conditions

Boundary conditions are used to enforce symmetry about the x- and y-axes.

Material Properties

The material is elastic-plastic with strain hardening. Values for Young's modulus, Poisson's ratio and yield stress used here are 30×10^6 psi, 0.3, and 50×10^3 psi, respectively.

Work Hard

User subroutine WKSLP is used to input the work-hardening slope. The work-hardening curve is shown in Figure E 8.2-5.

$$\bar{\sigma}(\bar{\varepsilon}^p) = \sigma_o (1 + E\bar{\varepsilon}^p/\sigma_o)^{0.2}$$

$$\frac{\partial \bar{\sigma}}{\partial \bar{\varepsilon}^p} = 0.2 \times E (1 + E\bar{\varepsilon}^p/\sigma_o)^{-0.8}$$

J-Integral

The J-integral is evaluated numerically by moving nodes within a certain ring of elements around the crack tip and measuring the change in strain energy. (This node movement represents a differential crack advance.) This mesh has two obvious "rings" of elements around the crack tip, so that two evaluations of J are provided. A differential movement of 10^{-2} is used in all three evaluations. In problem E 3.8, three paths were used. Because of the use of substructures, only two paths are possible at the highest level.

Loading

An initial uniform pressure of 100 psi is applied using the DIST LOAD option. The SCALE parameter option is used to raise this pressure to a magnitude such that the highest stressed element (element 20 here) is at first yield. The pressure is scaled to 3,047 psi. The pressure is then incremented for five steps until the final pressure is 3,308 psi.

Substructure Technique

In performing a nonlinear analysis using substructures, it is important that the area included in the substructure remains elastic. In this analysis, that portion of Figure E 8.2-2 that is cross-hatched was considered one substructure. Figure E 8.2-2 and Figure E 8.2-4 show the elements in the substructure and the highest level, respectively. It is far enough removed from the crack tip that plasticity is unlikely to occur there.

In the first part of the analysis, the superelement is created. It is written to the direct access database on unit 31. In this problem, no auxiliary sequential file is used. The SUBSTRUCTURE model definition option lists those nodes which are external. There are 17 external nodes along the thick line as shown. The distributed load is applied to the superelement. This will be incremented in the second part. In the second part, the previously generated substructure is combined with the 16 elements nearest to the crack tip. The SUPER parameter option indicates that file 31 is to be used; the number of super elements is one and there are 17 externals with 2 degrees-of-freedom. The SUPERINPUT model definition gives a correspondence table between the external node numbers and the node numbers used in this analysis. In this analysis, they are the same. After the END option is the load incrementation data. AUTO LOAD and/or PROPORTIONAL INC options may be used to modify loads in the SUBSTRUCTURE.

Results

The program provides an output of the strain energy differences. This must be normalized by the crack opening area to obtain the value of J. Since this specimen is of unit thickness, the crack opening area is $\Omega 1$, where $\Omega 1$ is the differential crack motion. The mesh used symmetry about the crack line, so that the strain energy change in the actual specimen would be twice that printed out. These results are summarized in Table E 8.2-1. It is clear that these results do demonstrate the path independence for the J-integral evaluation. Because of the use of substructures, this analysis was executed in 66% the time of problem E 3.8. If the J-integrals were not evaluated, the run time would have been 50%. This shows the advantage of using substructures for locally nonlinear analysis.

Table E 8.2-1 J-Integral Evaluation Results

	Move Tip Only	Move First Ring of Elements
Strain Energy Change for increment 0 (Δu)	6.23×10^{-2}	6.212×10^{-2}
J-Integral $(\frac{2\Delta u}{\Delta l})$	12.46	12.424
Strain Energy Change for increment 1 (Δu)	6.869×10^{-2}	6.849×10^{-2}
J-Integral $(\frac{2\Delta u}{\Delta l})$	13.738	13.698
Strain Energy Change for increment 2 (Δu)	7.539×10^{-2}	7.517×10^{-2}
J-Integral $(\frac{2\Delta u}{\Delta l})$	15.078	15.034
Strain Energy Change for increment 3 (Δu)	8.241×10^{-2}	8.217×10^{-2}
J-Integral $(\frac{2\Delta u}{\Delta l})$	16.482	16.434
Strain Energy Change for increment 4 (Δu)	8.974×10^{-2}	8.948×10^{-2}
J-Integral $(\frac{2\Delta u}{\Delta l})$	17.948	17.896
Strain Energy Change for increment 5 (Δu)	9.738×10^{-2}	9.711×10^{-2}
J-Integral $(\frac{2\Delta u}{\Delta l})$	19.476	19.422

Summary of Options Used

Listed below are the options used in example e8x2.dat:

Parameter Options

ELEMENT
END
NEWDB
SIZING
SUBSTRUCTURE
TITLE

Model Definition Options

CONNECTIVITY
COORDINATE
DIST LOADS
END OPTION
FIXED DISP
ISOTROPIC
SUBSTRUCTURE

Load Incrementation Options

AUTO LOAD
BOUNDARY CHANGE
CONTINUE
PROPORTIONAL INCREMENT

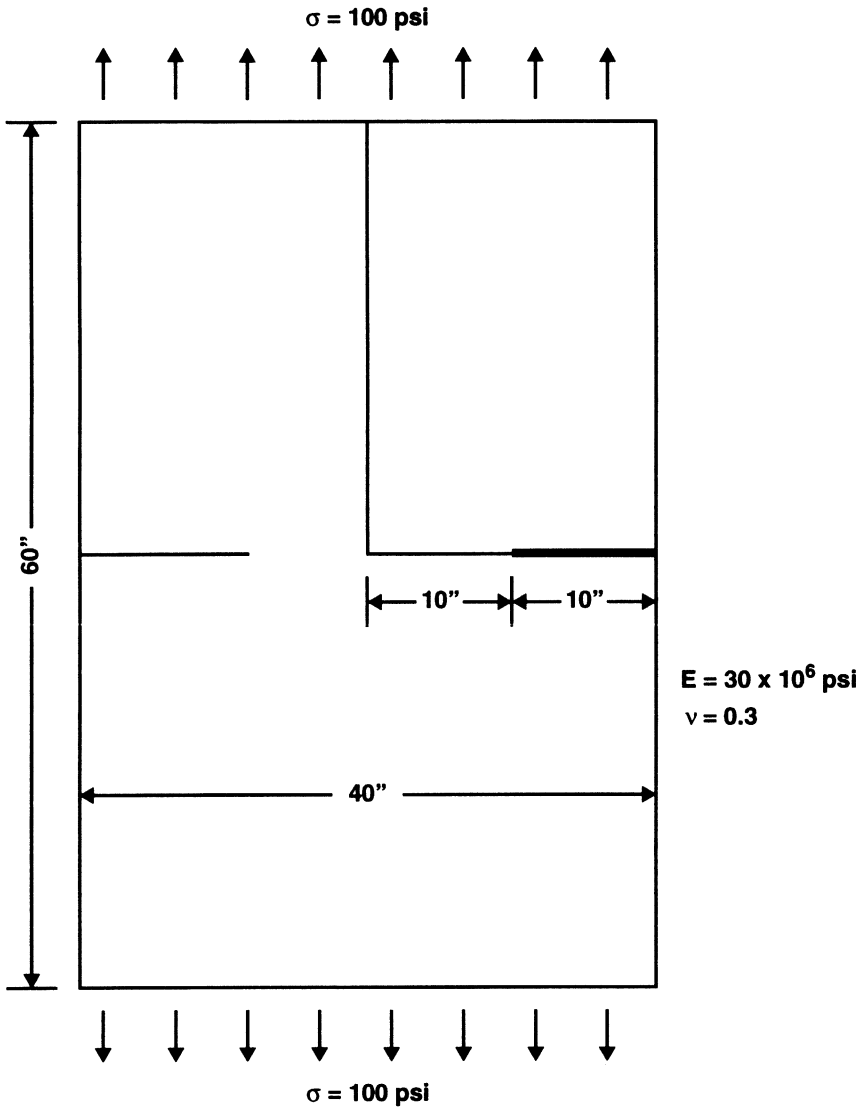

Figure E 8.2-1 Double-Edge Notch Specimen

MARC

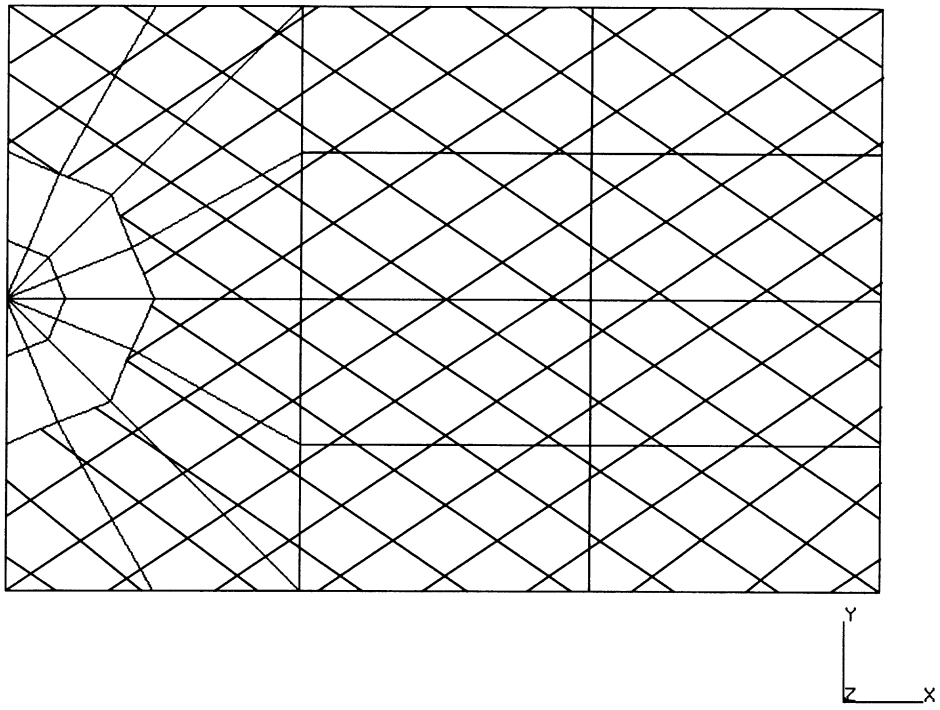

Figure E 8.2-2 Mesh for Double-Edge Notch Specimen
Cross-Hatched Area Indicates Substructures

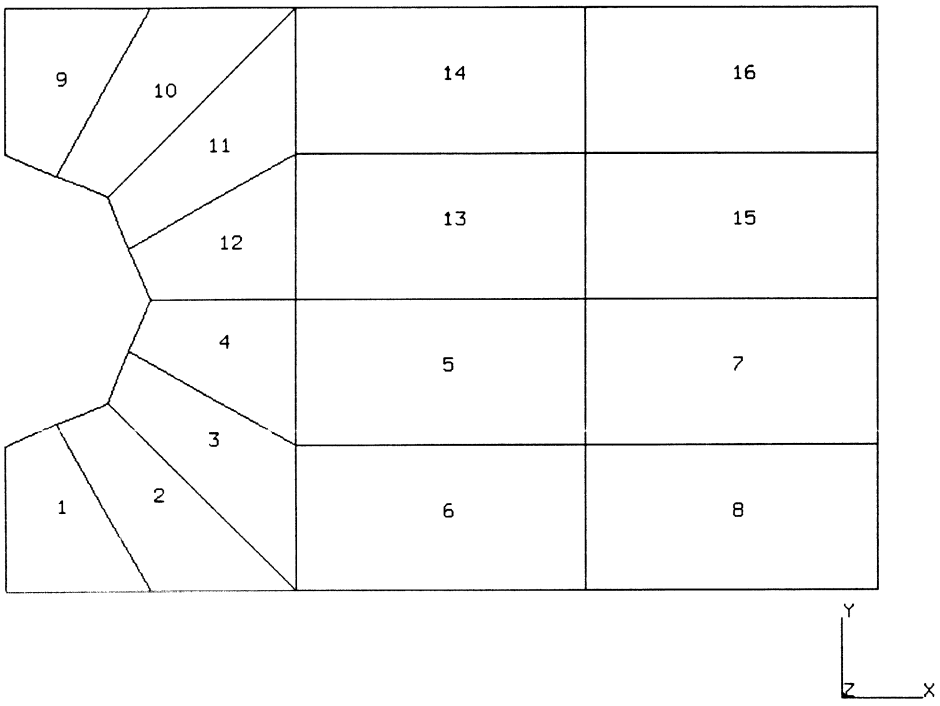

Figure E 8.2-3 (A) Elements in Substructure 1-1

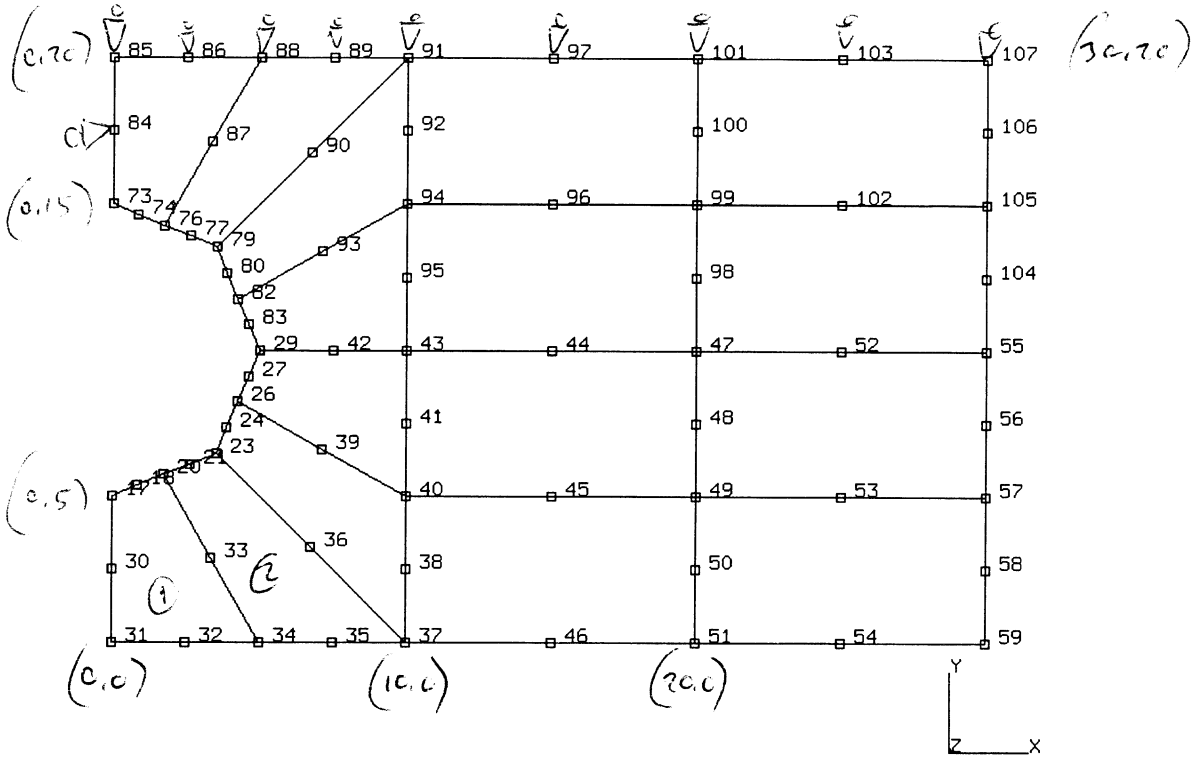

Figure E 8.2-3 (B) Nodes in Substructure 1-1

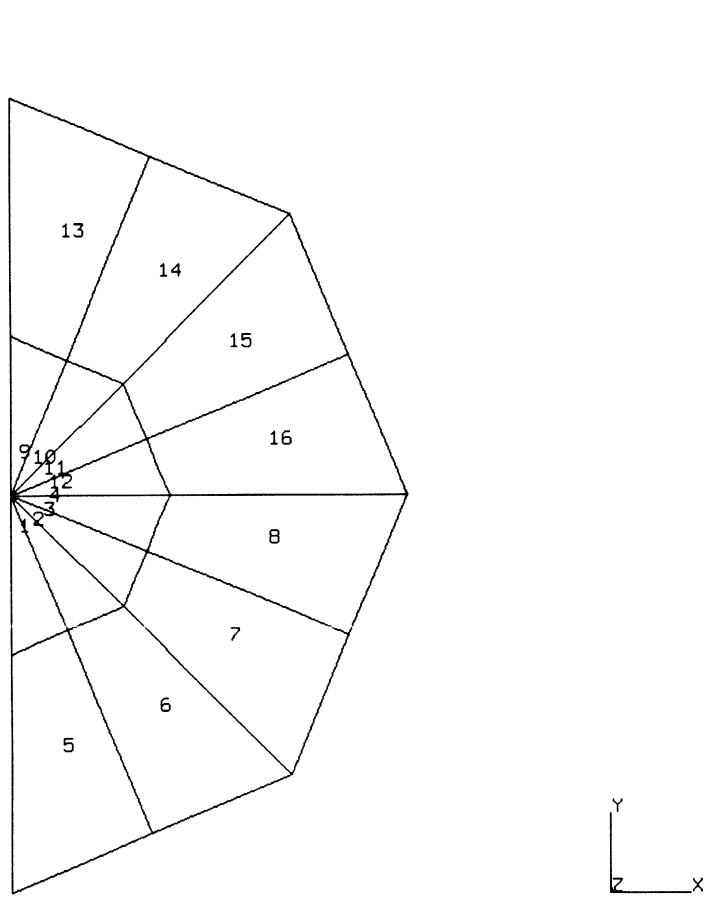

Figure E 8.2-4 (A) Elements at Highest Level

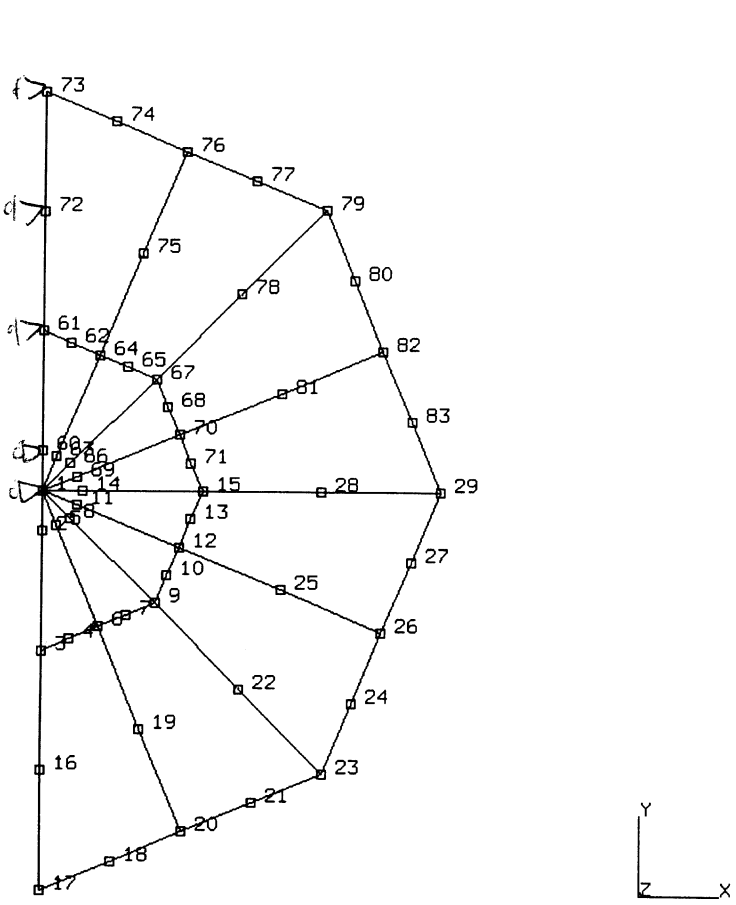

Figure E 8.2-4 (B) Nodes at Highest Level

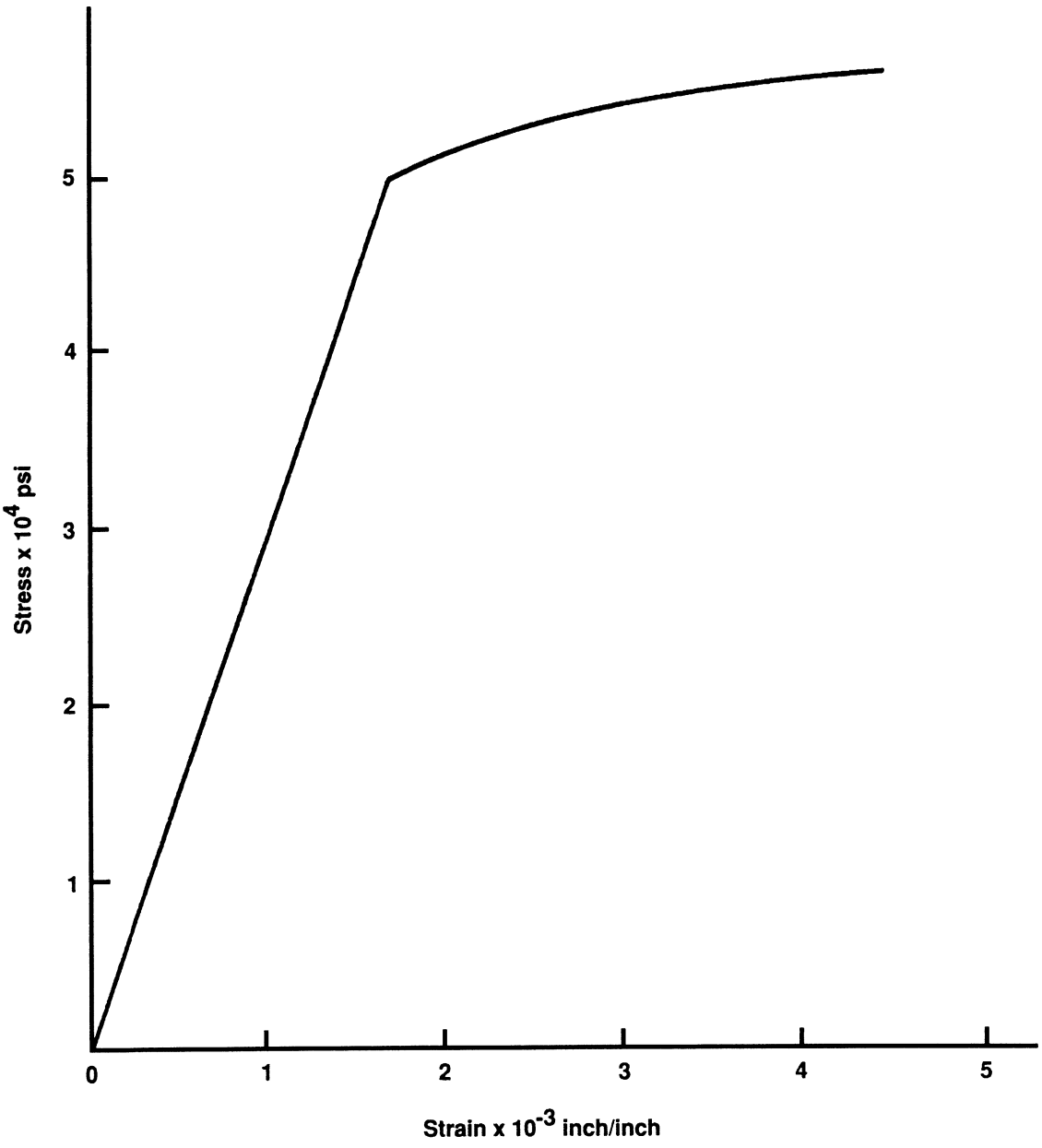

Figure E 8.2-5 Work-Hardening Slopes

E 8.3 End-Plate-Aperture Breakaway

This example illustrates the use of substructures in an elastic contact problem. All of the elastic region is combined into one substructure. The gap elements which are inherently nonlinear are included in the highest level. This problem is identical to E 7.2 with the exception that substructures are used.

This example illustrates the use of the gap and friction link, element type 12. This element allows surface friction effects to be modeled. This example is a simple model of a man-hole cover in a pressure vessel. The axisymmetric mesh is shown in Figure E 8.3-1. The objective of this analysis is to establish the response of the bolted joint between the man-hole cover (elements 1-12) and the vessel (elements 13-27). The elements are combined into substructure level 1,1. The first bolts are tightened, and then the main vessel expands radially (as might occur due to thermal or internal pressure effects). The user should be aware that this problem is presented only as a demonstration. The mesh is too coarse for accurate results.

Elements

Element 12 is a friction and gap element. It is based on the imposition of a gap closure constraint and/or a frictional constraint via Lagrange multipliers. The element has four nodes: nodes 1 and 4 are the end nodes of the link and each has two degrees of freedom (u, v,) in the global coordinate direction; node 2 gives the gap direction cosines (n_x, n_y) and has γ_n, the force in the gap direction, as its one degree of freedom; node 3 gives the friction direction cosines (t_{1_x}, t_{1_y}) and has γ_1, the frictional shear forces, and p, the net frictional slip, as its two degrees of freedom.

Model

Twenty-seven type 10 elements are used for the two discrete structures, the end cap and the aperture. These are then joined by four type 12 elements. There are 54 nodes.

Substructure Strategy

A substructure consisting of all of the axisymmetric elements is formed. The external nodes are those where the bolt load will be applied (4,5,32,32), where the gap interfaces with the end cap and aperture (15 to 18 and 22 to 25) and where the radial load is applied (43 to 46). This is performed in the first part of the analysis.

In the second part of the analysis, the previously generated superelement is combined with the four gap elements.

Loading

The load history consists of applying bolt loads (i.e., tightening down the bolts), then pulling out the outer perimeter of the main vessel model. Bolt loads are modeled here as point loads applied in opposite directions (self-equilibrating) on node pairs 4 and 32, 5 and 33. Since there is a possibility of gaps developing between the facing surfaces of the cover and vessel, the bolt load is initially applied as a small magnitude, then incremented up to the total value of 2000 lbs per bolt ring. This usually requires two runs of the problem: an initial run with a "small"

load to see the pattern developing, from which some judgment can be made about the load steps which can be used to apply the total bolt force. In this actual run, the full bolt loads are applied in one increment.

The radial expansion of the main vessel is modeled as point loads on the outside circumference nodes (43 to 46). As there are no elements when performing the analysis, point loads rather than distributed loads are applied. Again, the purpose of the analysis is to watch the development of slippage between the main vessel and the cover plate, and the analyst cannot easily estimate the appropriate load increments to apply to model this nonlinearity. For this purpose, the RESTART option may be used effectively. A restart is written at the point where full bolt load is applied, and then a trial increment of pull-out force is applied. Based on the response to this (in the friction links), a reasonable size for the sequence of loading increments can be determined. This procedure is frequently necessary in such problems. For brevity, this example shows only the final load sequence obtained as a result of such trials.

Boundary Conditions

The nodes on the axis of symmetry are constrained radially, and the rigid body mode in the axial direction is suppressed at node 46.

Gap Data

In this example, a small negative closure distance of -.001 is given for the gaps to indicate that the gaps are closed initially allowing an interference fit solution is to be obtained in increment 0. The coefficient of friction, μ, is input as 0.8.

Results

The results of the analysis are shown in Figure E 8.3-2 through Figure E 8.3-4. First of all, it is observed in Figure E 8.3-2 that the link elements never go into tension.

In this case, the initial bolt load is carried quite uniformly (A in Figure E 8.3-2), but as the pull-out increases, the inner two links take more of the stress and the outer link (element 31) sheds stress. The shear stress development is followed in Figure E 8.3-3 – initially (bolt load only) all shear stresses are essentially zero. The two outer links slip first, but then the additional forces required to resist the pull develops in the inner two elements until the shear stress pattern follows the normal stress pattern, when the shear in the pair of links also slip ($\tau = \mu\sigma$). Figure E 8.3-4 shows a plot of the radial displacement of the outer perimeter against the pull-out force – notice the small loss of stiffness caused by slip developing, as the vessel model has to resist the extra force along without any further force transfer to the cover.

Convergence

Because the only 'nodes' in this structure are external nodes during the analysis phase, a different convergence path is followed than in problem E 7.2. Displacement testing is automatically invoked by the program. The gap forces at any increment are within one percent of those calculated in E 7.2.

Computational Costs

Because of the use of substructures, this analysis was performed in 30% of the time of demo E 7.2, which is a considerable computational savings.

Summary of Options Used

Listed below are the options used in example e8x3.dat:

Parameter Options

ELEMENT
END
NEWDB
SIZING
SUBSTRUCTURE
TITLE

Model Definition Options

CONNECTIVITY
COORDINATE
END OPTION
FIXED DISP
ISOTROPIC
SUBSTRUCTURE

Load Incrementation Options

AUTO LOAD
BACKTOSUBS
CONTINUE
CONTROL
POINT LOAD

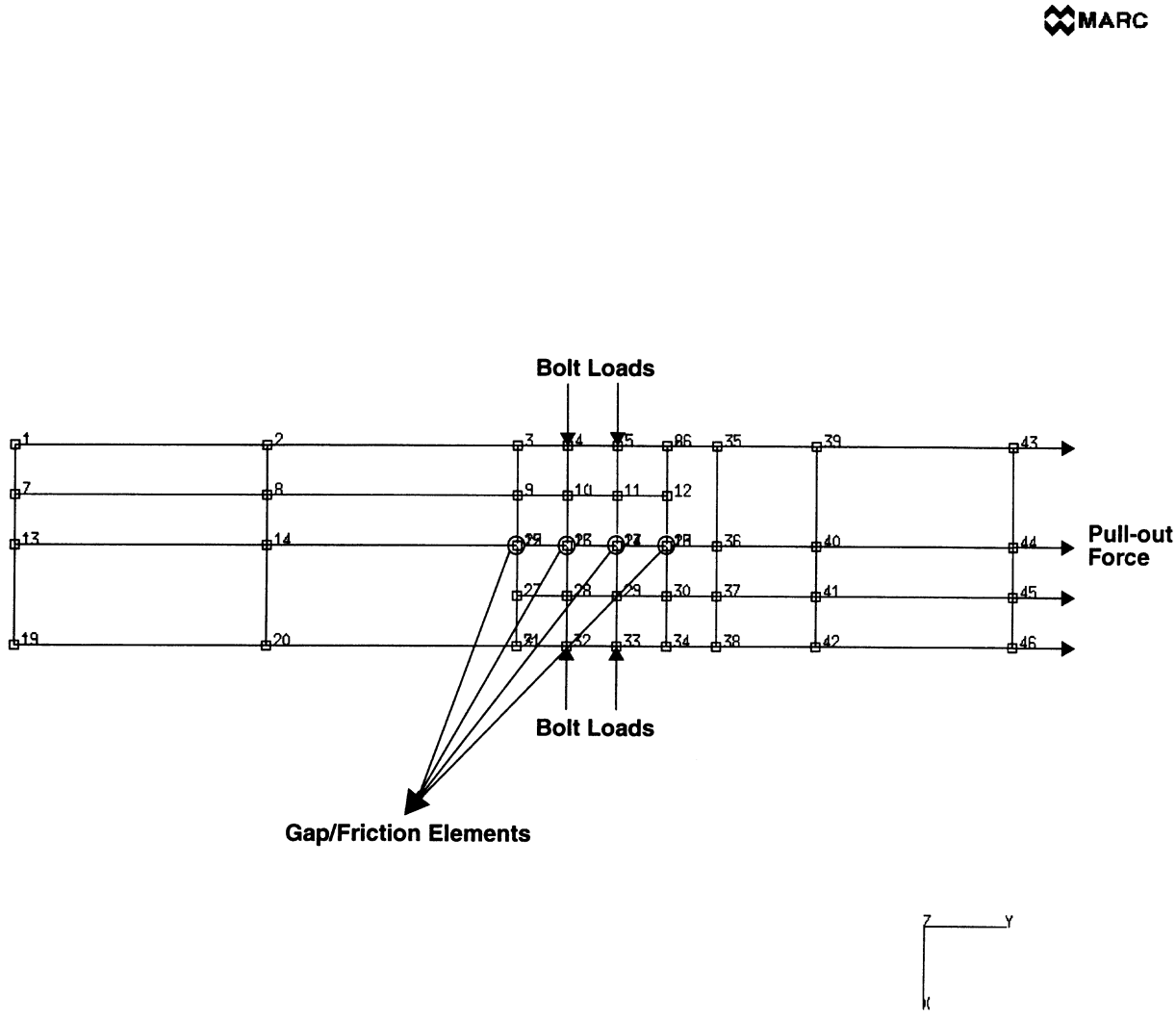

Figure E 8.3-1 Geometry and Mesh of End Plate-Aperture

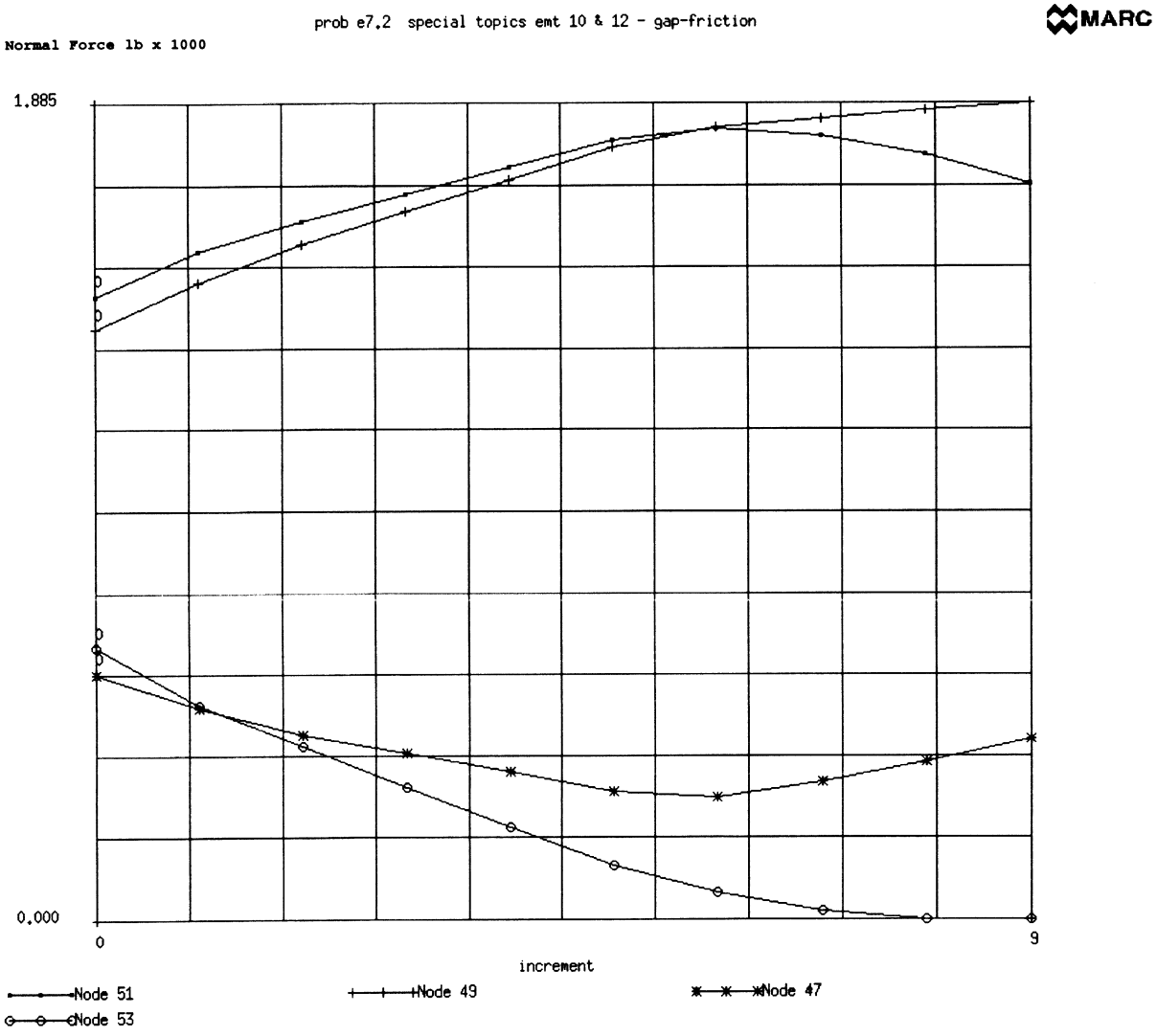

Figure E 8.3-2 Transient Normal Force in Bolts

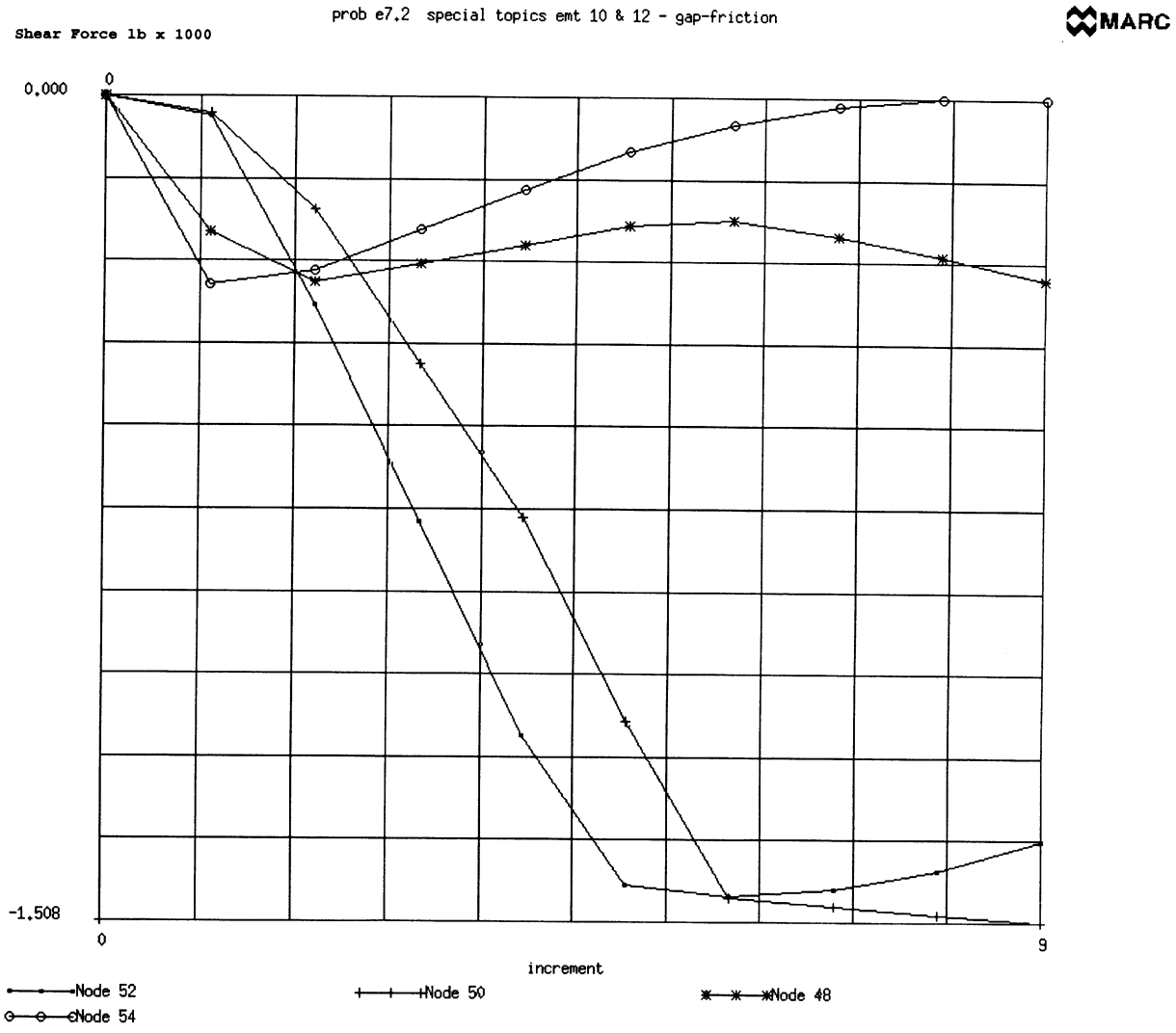

Figure E 8.3-3 Transient Shear Force in Bolt

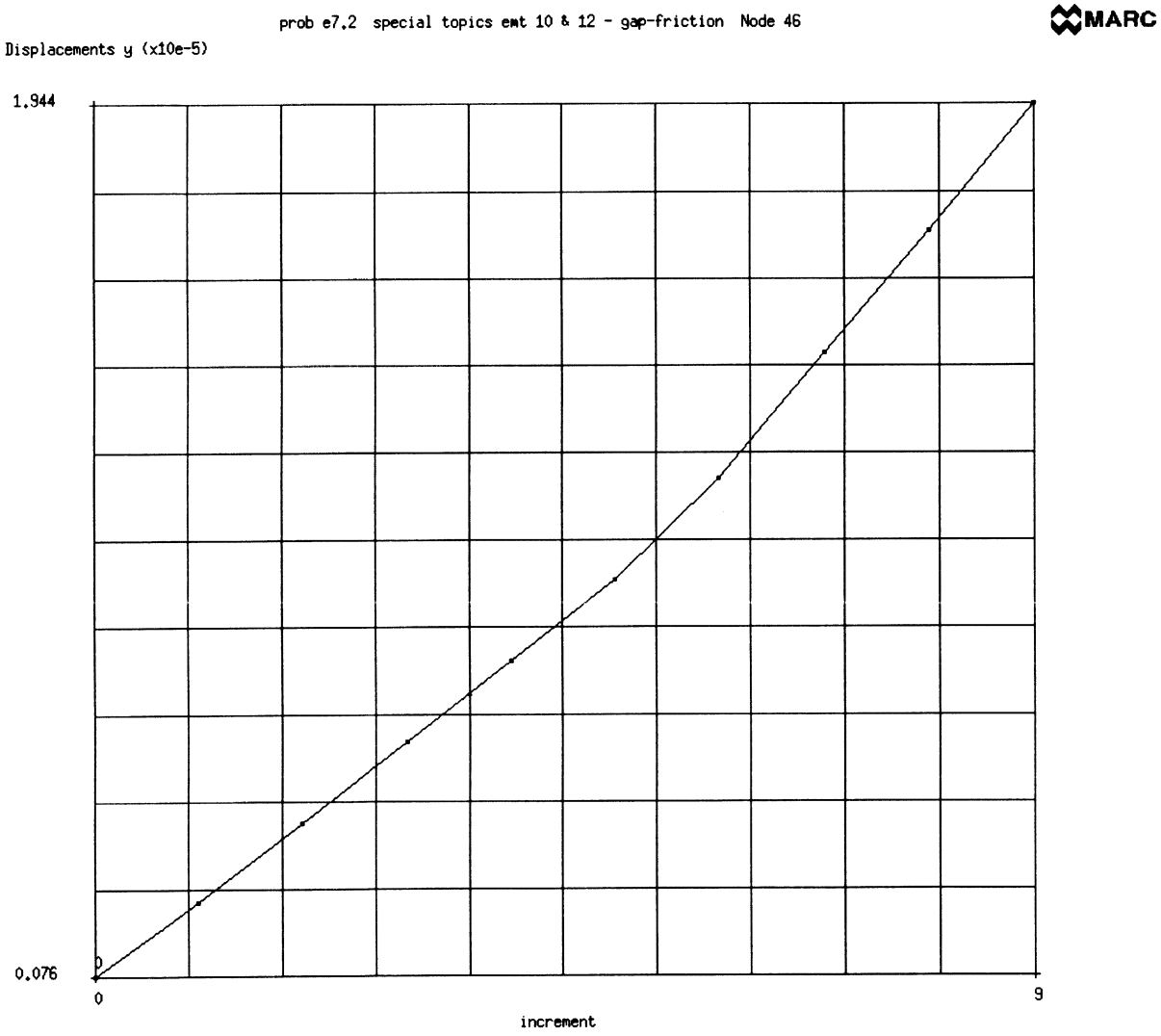

Figure E 8.3-4 Radial Displacement at Outside Top (Node 46)

E 8.4 Collapse Of A Notched Concrete Beam

A quasi static collapse analysis is carried out for a notched concrete beam. This analysis demonstrates the use of the cracking option for plane stress elements. An elastic tension softening material has been used in this analysis and the results obtained have been compared with experimental data (1).

Element

Element type 26, an eight-node quadrilateral plane stress element with a nine point integration scheme, is used.

Model

This notched beam (dimensions and element mesh in Figure E 8.4-3)has been divided in 26 elements with a refinement near the notch. The beam is supported at its ends and loaded by a force applied just above the notch.

Tying

Tying type 32 is used to ensure a consistent displacement behavior near the mesh refinement. With this tying, the interior nodes of the elements of the refined side are coupled to the three retained nodes of the element on the coarse side. Eight tying equations of this type are needed.

Tying type 2 is needed to ensure equal displacements in the y-direction of the three nodes of the element above the notch on which the loads have to be applied.

Boundary Conditions

Simply supported and sliding conditions have been prescribed at the left and right bottom corners, respectively. At the mid-node of the element above the notch, displacement increment in negative y-direction is prescribed. In the analysis, initially two displacement increments of -0.5 mm have been applied. With proportional increment, the displacement is scaled to 0.002 mm and 30 increments of this size have been applied.

Isotropic

An elastic isotropic material with Young's modulus E = 30000 N/mm^2 and a Poisson's ratio $\upsilon = 0.2$ has been specified through the ISOTROPIC option. In addition, the cracking flag is turned on for material id 1.

Crack Data

In this block, the cracking data needs to be specified for each material group. The critical cracking stress is set to 3.33 N/mm^2. A linear tension softening behavior has been specified with a softening modulus E_s = 1790 N/mm^2 and is assumed to be independent of the element size. The choice of a value of the tension softening modulus can be related to on the fracture energy G_f. Assuming that the micro-cracks are uniformly distributed over the specimen length ℓ_s, the fracture energy is related to $G_f = \ell_s \int \sigma d\varepsilon^{cr}$, which results for a linear tension softening

behavior in $G_f = \frac{1}{2}\ell_s\sigma_c\varepsilon_u$. For this particular analysis, it can be assumed that cracking only occurs in the elements just above the notch with a width h and in the energy expression, G_f can be expressed by $G_f = \frac{1}{2}h\sigma_c\varepsilon_u$. It is clear, that depending on the width of the notch, the value ε_u needs to be adapted and the tension softening modulus $E_s = \sigma_c/\varepsilon_u$ needs to be a function of the width of the notch.

The critical crushing strain is not set, and default a high value 10^{11} is used (crushing occurs at a critical value of the plastic strain and since no plasticity is allowed in the analysis, crushing will not occur). The shear retention factor is set to zero, hence no shear stiffness is present at an integration point once a crack occurs.

Control

A maximum number of 32 loadsteps have been specified. In each step, maximal 5 iterations are allowed. The default full Newton-Raphson iterative technique has been used with tolerance checking on the residual forces (10% of the maximum reaction force).

Results

In increment 1, the first cracks initiate in the element just above the notch. At this increment, three recycles are needed to reach convergence. In the subsequent increments, no new cracks initiate and no recycles are needed. In increment 7, new cracks initiate with recycling followed by a number of steps with only back substitution. In subsequent increments, new cracks occur in increment 14, 20, 27 and 29. Cracks occur only in the elements above the notch (width 40 mm). The assumption needed in the choice of the tension softening modulus was correct. The calculated load-deflection curve is shown in Figure E 8.4-5 and is compared with the experimental result (1). It is seen that the experimental result is overestimated. The reason for this overly stiff behavior can probably be found in the choice of the linear tension softening behavior.

Reference

1. Petersen, P. E., "Crack growth and development of fracture zones in plain concrete and similar materials," Report TVM-1006, Lund Institute of Technology, Lund, Sweden, 1981.

Summary of Options Used

Listed below are the options used in example e8x4.dat:

Parameter Options

ELEMENT
END
PRINT
SIZING
TITLE

Model Definition Options

CONNECTIVITY
CONTROL
COORDINATE
CRACK DATA
END OPTION
FIXED DISP
GEOMETRY
ISOTROPIC
POST
PRINT CHOICE
TYING

Load Incrementation Options

AUTO LOAD
CONTINUE
PROPORTIONAL INCREMENT

MARC

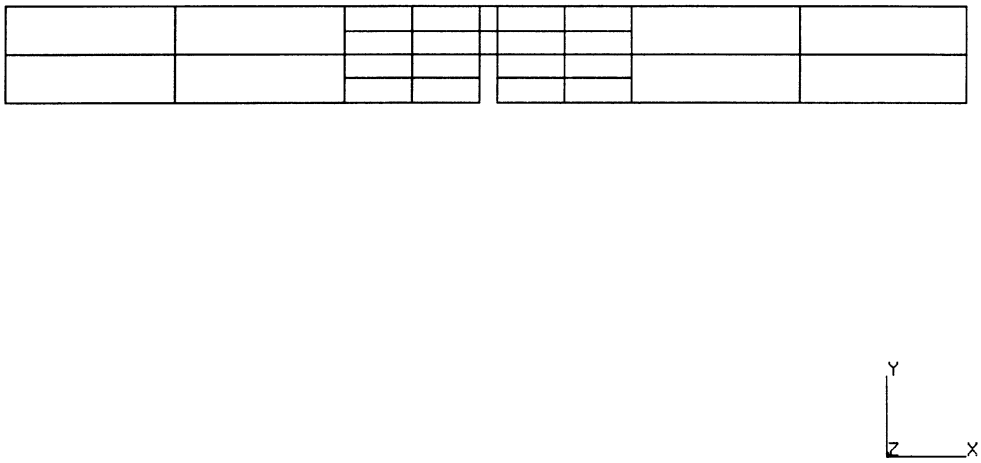

Figure E 8.4-1 Geometry and Element Mesh

MARC

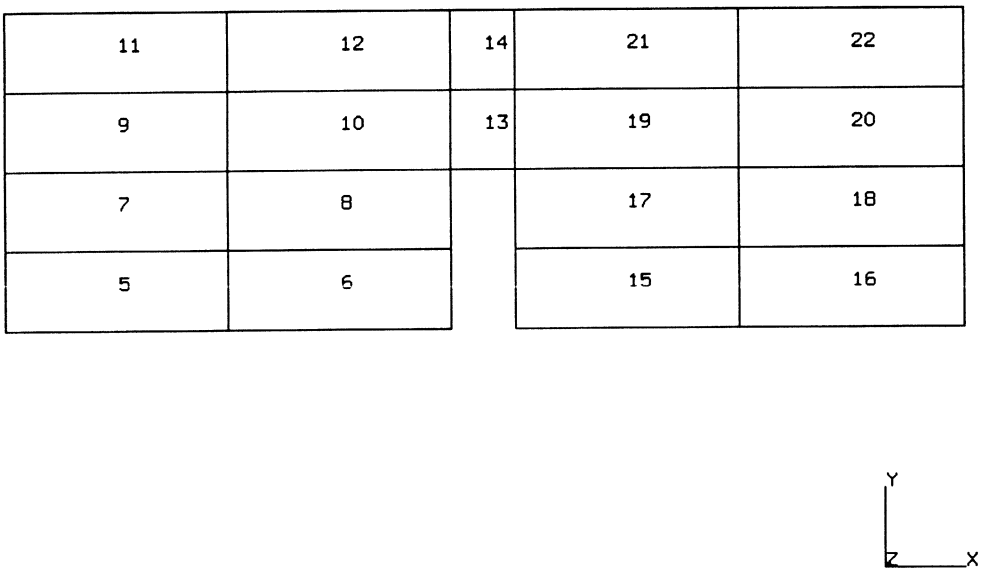

Figure E 8.4-2 Element Numbering Detail of Mesh

MARC

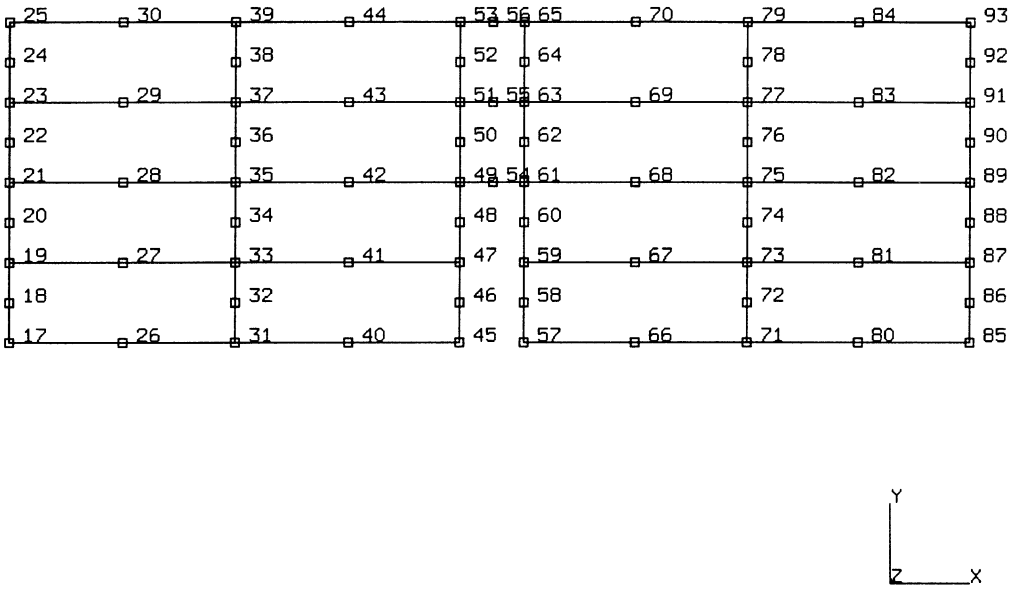

Figure E 8.4-3 Node Numbering Detail of Mesh

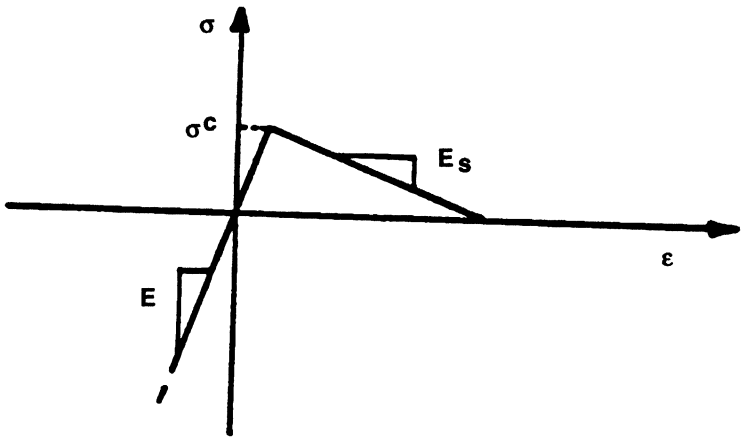

$E = 30.000\ N/mm^2$

$\upsilon = 0.2$

$\sigma^c = 3.33\ N/mm^2$

$E_s = 1790.0\ N/mm^2$

Figure E 8.4-4 Material Properties

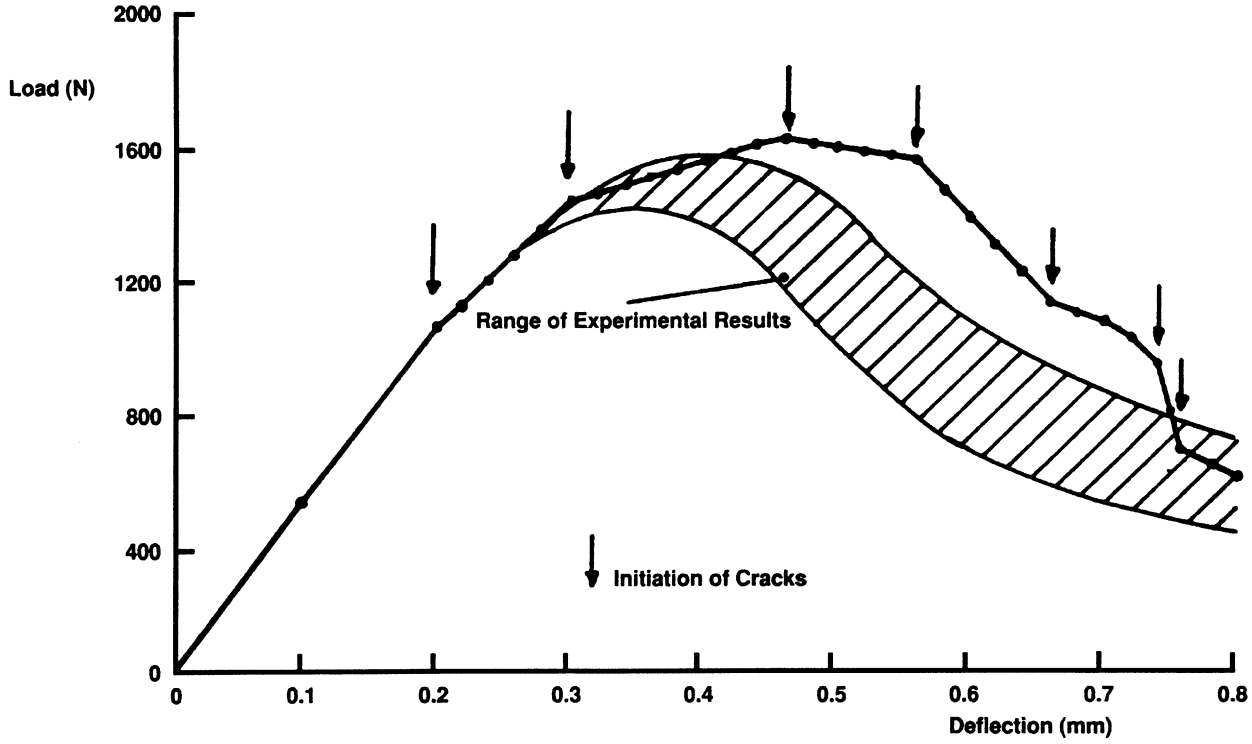

Figure E 8.4-5 Comparison of Calculated and Experimental Load Deflection Curve Notched Beam Test

E 8.5 Cracking Behavior Of A One-Way Reinforced Concrete Slab Using Shell Elements

This example demonstrates the analysis of a one-way reinforced concrete slab, which was tested by Jain and Kennedy [1] and material data for this problem can be found [2]. The slab is line supported at its ends (Figure E 8.5-1) and loaded by a line load. The elastic cracking behavior with tension softening of the concrete and the elastic-plastic behavior of the steel reinforcement is demonstrated.

Element (Ref. B75.1)

Element type 75, a 4-node thick shell element with 6 global degrees of freedom at each node, is used.

Model

The slab with dimensions shown in Figure E 8.5-1 has been divided in 6 shell elements. In these shell elements, integration of the material properties over the thickness has been performed using 9 layers; one layer represents the (smeared) steel reinforcement, while the other eight layers represent the concrete behavior. The mesh (Figure E 8.5-2) has been generated using the CONN GENER and NODE FILL option. Only one half of the plate has been modeled.

Material Properties

The concrete material is defined using the ISOTROPIC and the CRACK DATA options. First in the ISOTROPIC option, it is defined to have a material ID of 1, and the cracking option is flagged. The properties are Young's modulus of 28960 N/mm^2, Poisson's ratio of 0.2 and initial yield stress of 31.6 N/mm^2. The CRACK DATA option indicates that the concrete has a ultimate stress of 2N/mm^2 and a shear retention of 0.5. In the first analysis, no tension softening is specified. In the second analysis, a tension softening of 3620 N/mm^2 has been specified.

The steel reinforcement is modeled as a uniaxial material in a single layer of the shell element. This is done using the ORTHOTROPIC option, specifying an E_{xx} = 20,000 N/mm^2 and $E_{yy} = E_{zz}$ = 0.01 N/mm^2. The associated shear moduli were G_{xy} = 10,000 N/mm^2 and $G_{yz} = G_{zx} = G_{zx}$ = 0.005 N/mm^2. The steel has an initial yield stress of 221 N/mm^2.

COMPOSITE

The COMPOSITE option is used to indicate that there are 9 layers of materials. The first 6 are of equal thickness of 5.166 mm each and are composed of material 1 (concrete). The seventh layer is the very thin steel layer, thickness of 0.272 mm and material ID = 2. Finally, layers 8 and 9 are concrete with a thickness of 3.364 mm.

Boundary Conditions

Symmetry conditions have been specified on node 1 and 2 of the element mesh. On the line Y = 0, Z = 0 no translation in y-direction is allowed and at nodes 13 and 14 a sliding support (no displacement in z-direction) has been prescribed.

Control

On the control card a maximum of 25 load steps has specified with a maximum of 7 recycles per load increment. The default Newton-Raphson iterative procedure with testing on the relative residual forces (tolerance 10%) has been used. The solution of non-positive definite systems has forced by the PRINT,3 option.

Loading

On node 9 and 10, a point load with magnitude -1500 in z-direction has been applied. This is the estimated maximum value of the collapse load. Via the AUTO INCREMENT option, the automatic load stepping procedure using Riks algorithm starts with 10% of the total load and a desired number of 3 recycles (must be smaller than the maximum number specified on the CONTROL card). The maximum numbers of steps in this load incrementation set is set to 20 and the maximum step size is set to 10% of the load.

Results

The calculated load center-deflection response is shown in Figure E 8.5-4 for the run with and without tension softening. Without tension softening, an unstable behavior in the response is present caused by the loss of stiffness between reinforcement and concrete once a crack occurs. With tension softening, some artificial interaction is introduced and usually this results in a more stable solution procedure. In the run with tension softening, fewer recycles are needed to reach convergence. Compared with the experimental result [1], [2], the effect of tension softening is clearly indicated. Best agreement is obtained with tension softening.

References

1. Jain, S.C. and Kennedy, J.B., "Yield criterion for reinforced concrete slabs," *J. Struct. Div.*, Am. Soc. Civ. Engrs.,100,513, March 1974, pp. 631-644
2. Crisfield, M.A."Variable step lengths for non-linear structural analysis," Report 1049, Transport and Road Research Lab., Crowthorne, England, 1982.

Summary of Options Used

Listed below are the options used in example e8x5a.dat:

Parameter Options

ELEMENT
END
PRINT
SIZING
TITLE

Model Definition Options

COMPOSITE
CONN GENER
CONNECTIVITY
CONTROL
COORDINATE
CRACK DATA
END OPTION

FIXED DISP
ISOTROPIC
NODE FILL
ORIENTATION
ORTHOTROPIC
POST
PRINT CHOICE
RESTART

Load Incrementation Options

AUTO INCREMENT
CONTINUE
POINT LOAD

Listed below are the options used in example e8x5b.dat:

Parameter Options

ELEMENT
END
PRINT
SIZING
TITLE

Model Definition Options

COMPOSITE
CONN GENER
CONNECTIVITY
CONTROL
COORDINATE
CRACK DATA
END OPTION
FIXED DISP
ISOTROPIC
NODE FILL
ORIENTATION
ORTHOTROPIC
POST
PRINT CHOICE
RESTART

Load Incrementation Options

AUTO INCREMENT
CONTINUE
POINT LOAD

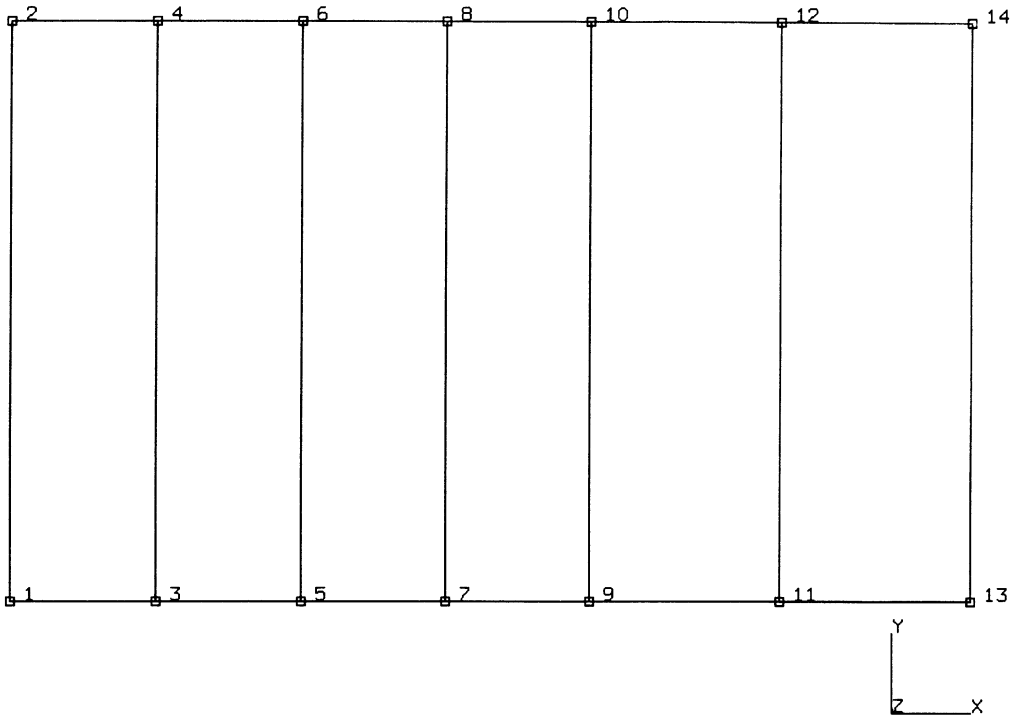

Figure E 8.5-1 Geometry of One-Way Reinforced Slab

MARC

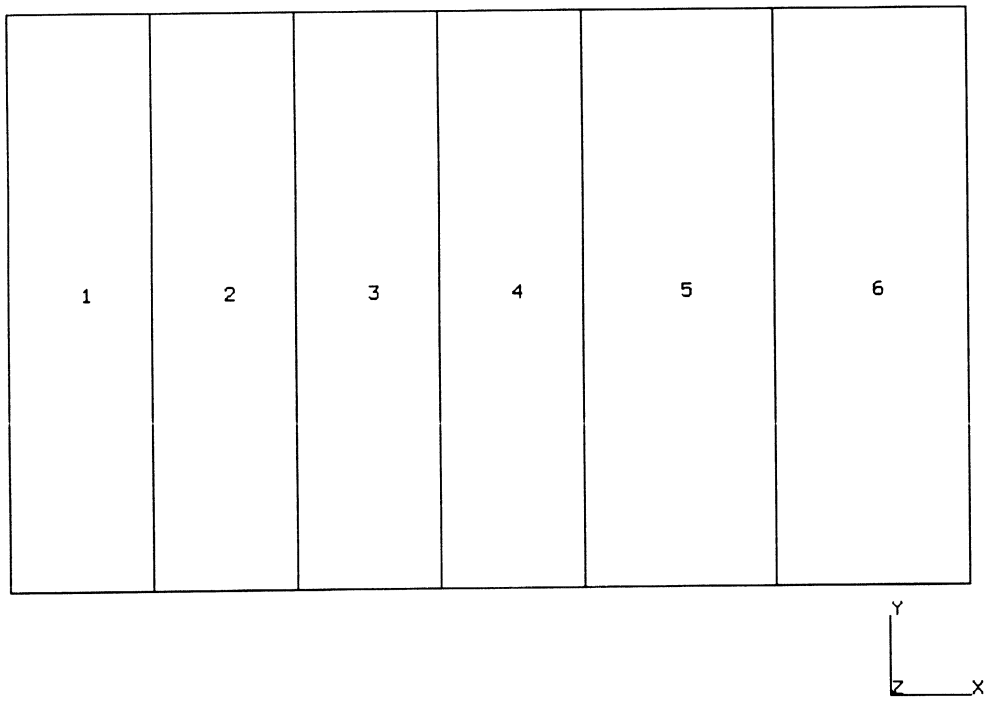

Figure E 8.5-2 Element Mesh with Node Numbering

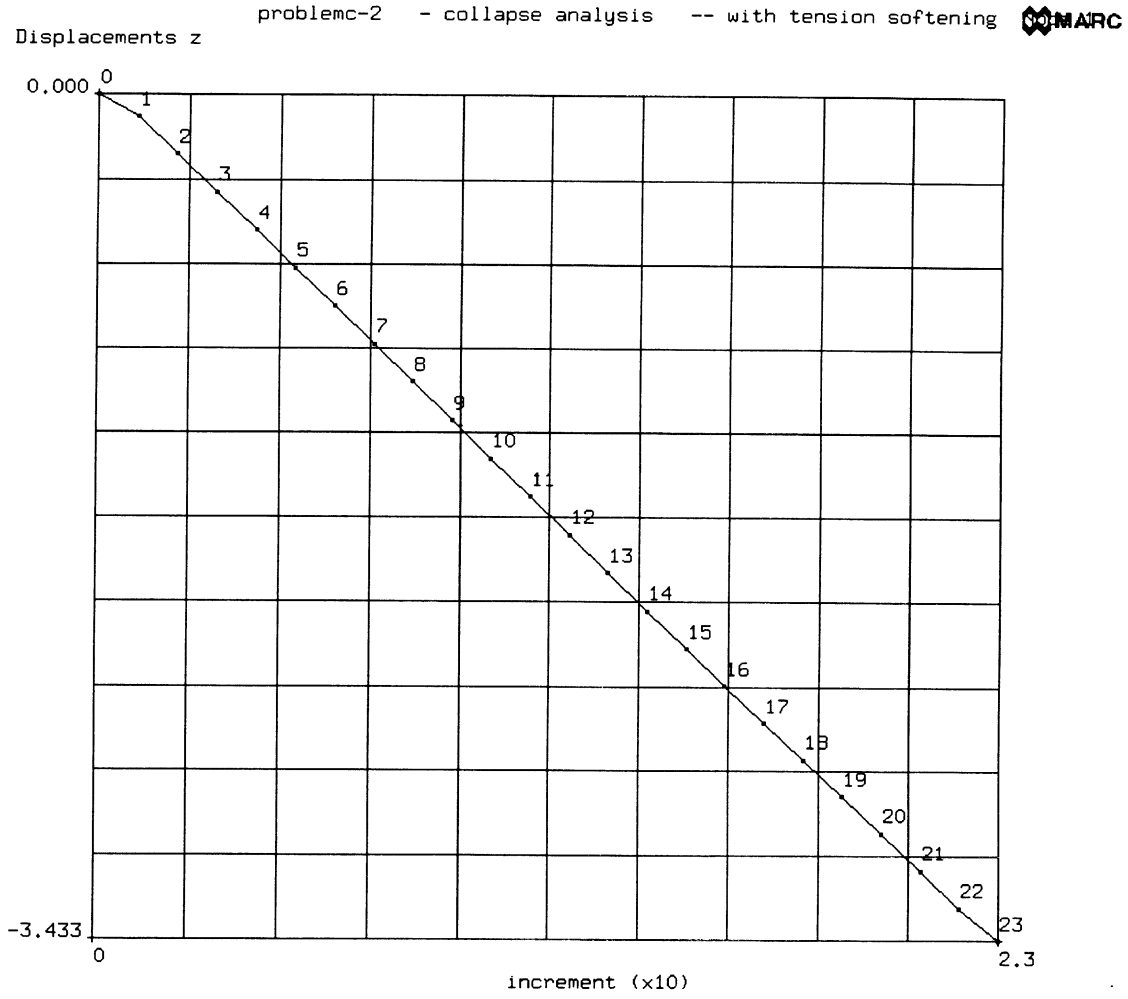

Figure E 8.5-3 Element Mesh with Element Numbering

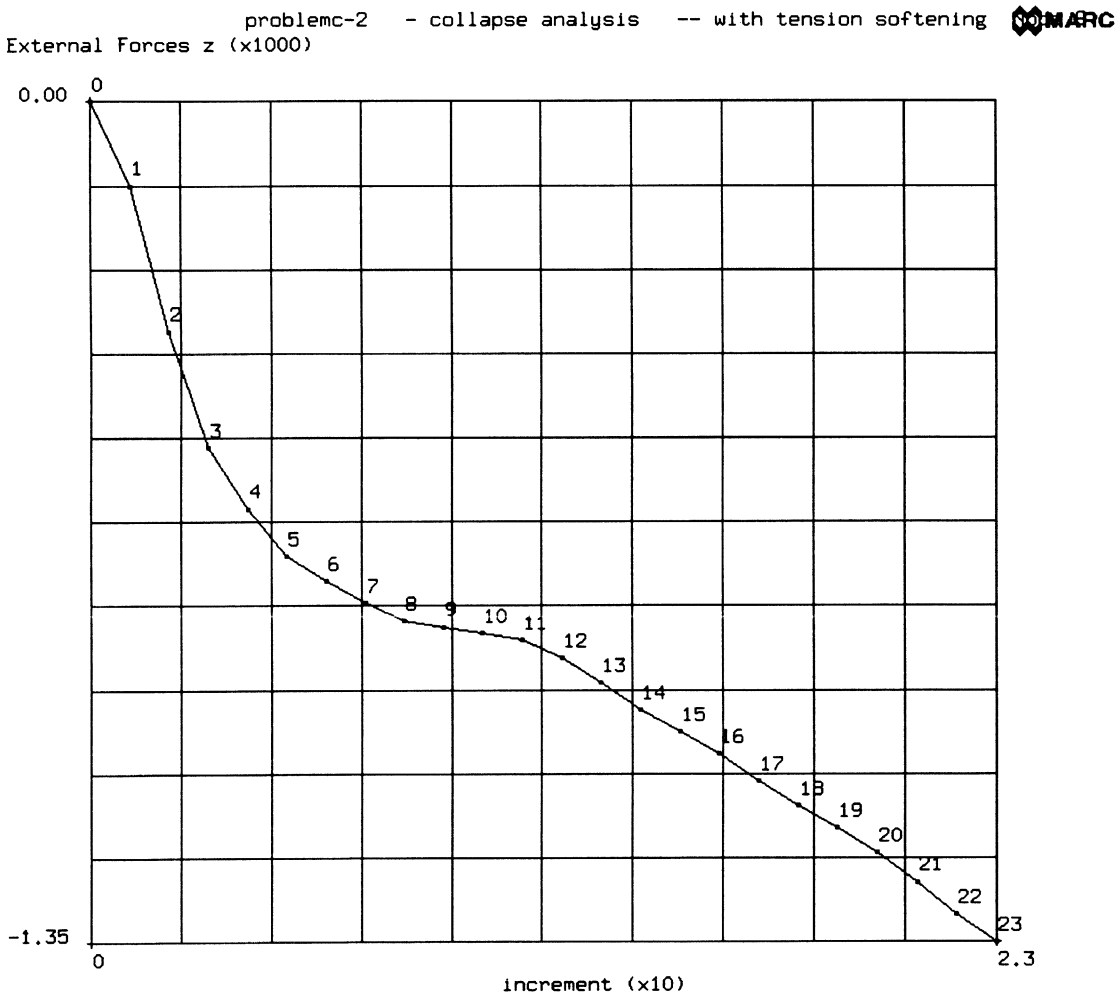

Figure E 8.5-4 Load-Deflection Relationship for One-Way Reinforced Slab

E 8.6 Cracking Behavior Of A One-Way Reinforced Concrete Slab Using Continuum Plane Strain And Rebar Elements

This example is the same type of analysis as described in problem E 8.5 (Figure E 8.6-1). Instead of shell elements, however, continuum plane strain elements and rebar elements have been used, which is allowed since the problem is essentially two-dimensional. For the concrete an elastic-cracking behavior with tension softening and shear retention is specified. In the rebar elements an elastic-plastic behavior is possible.

Element

Element type 27, an eight-node plane quadrilateral strain element with two degrees of freedom per node is used to model the concrete. This element is preferred over element 11 (four-node plane strain) since considerable shear is present in the beam. Element type 46, an eight-node plane strain rebar element compatible with element 27, is used to specify the reinforcement (Figure E 8.6-2).

Model

The concrete has been modeled with 10 plane strain elements (Figure E 8.6-3 and Figure E 8.6-4). At least two elements over the thickness are needed for accurate analysis of the bending of the beam. In each element, nine integration points are present, resulting in a six-point integration scheme over the thickness. Over the concrete elements below the neutral line (1 to 5), an overlay of rebar elements has been used (elements 11 to 15). The position, thickness and orientation of the reinforcement layers in this element, needs to be specified via user subroutine REBAR.

The mesh has been generated using the CONN GENER and NODE FILL option.

Material Properties

The elastic properties of the concrete (material identification number 1) have been taken as:

Young's modulus	$E = 28{,}960\ N/mm^2$
Poisson's ratio	$\nu = 0.3$

The cracking flag has been turned on for material number 1.

The following properties for the steel reinforcement (material identification number 2) have been taken:

Young's modulus	$E = 200{,}000\ N/mm^2$
Poisson's ratio	$\nu = 0.2$
Yield stress	$\sigma_y = 221\ N/mm^2$

Crack Data

Only one set of cracking data needs to be specified since cracking is only possible in the concrete elements (specified via the ISOTROPIC option). The following values have been taken:

Critical cracking stress	$\sigma_c = 2$ N/mm^2
Tension softening modulus	E = 3620 N/mm^2
Shear retention factor	0.5

Boundary Conditions

Symmetry conditions have been specified for nodes 1 to 5 and a sliding conditions for node 41.

Control

On the CONTROL option, a maximum of 25 load steps have been specified with a maximum of 7 recycles per load increment. The default Newton-Raphson iterative procedure with testing on the relative residual forces (tolerance 10%) has been used. The solution of non-positive definite systems has been forced by the PRINT,3 option.

Loading

On node 29, a point load with magnitude -1500 in y-direction has been applied. This is the estimated maximum value of the collapse load. Via the AUTO INCREMENT option, the automatic load stepping algorithm using the Riks algorithm starts with 10% of the total load and a desired number of 3 recycles (must be smaller than the maximum number specified on the CONTROL card). The maximum numbers of steps in this load incrementation set is set to 20 and the maximum step size is set to 10% of the load.

Results

The calculated load-deflection response is shown in Figure E 8.6-6 and compared with the experimental result. Compared with the results with tension softening using shell elements (Demo E8.5), a nearly identical load-deflection curve is obtained. In the run with shell elements, no shear retention factor was used but sufficient shear stiffness was present even if large scale cracking occurs. In the run with plane strain elements, the absence of shear retention (meaning there is no shear stiffness if a crack occurs) resulted in an unstable behavior and very poor convergence. With shear retention, a stable behavior is obtained. The shear retention factor can be specified as a function of the crack length via user subroutine UCRACK.

Summary of Options Used

Listed below are the options used in example e8x6.dat:

Parameter Options

ELEMENT
END
PRINT
TITLE

Model Definition Options

CONN GENER
CONNECTIVITY
COORDINATES
CONTROL
CRACK DATA
END OPTION
FIXED DISP
GEOMETRY
ISOTROPIC
NODE FILL
POST
RESTART

Load Incrementation Options

AUTO INCREMENT
CONTINUE
POINT LOAD

Listed below is the user subroutine found in u8x6.f:

REBAR

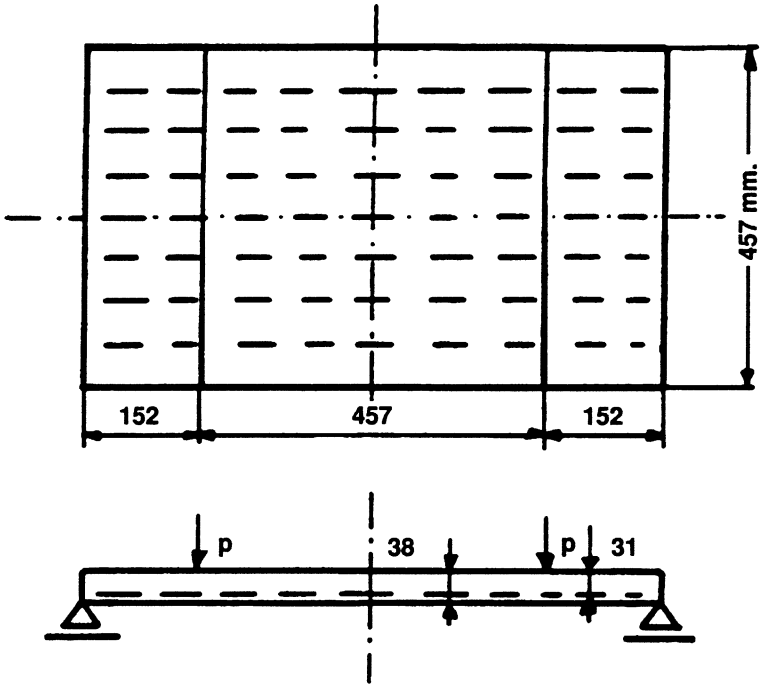

Figure E 8.6-1 One-Way Reinforced Slab

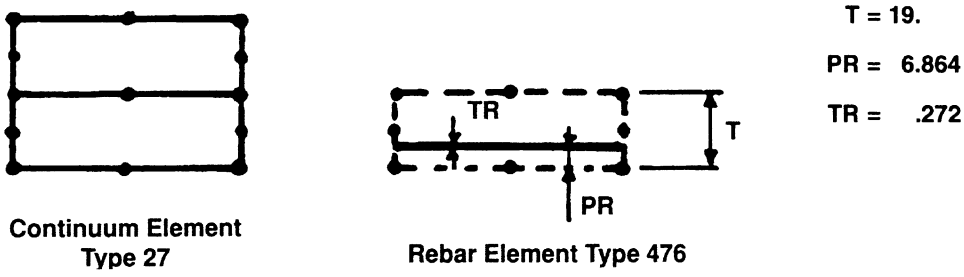

Figure E 8.6-2 Element Types used in Analysis

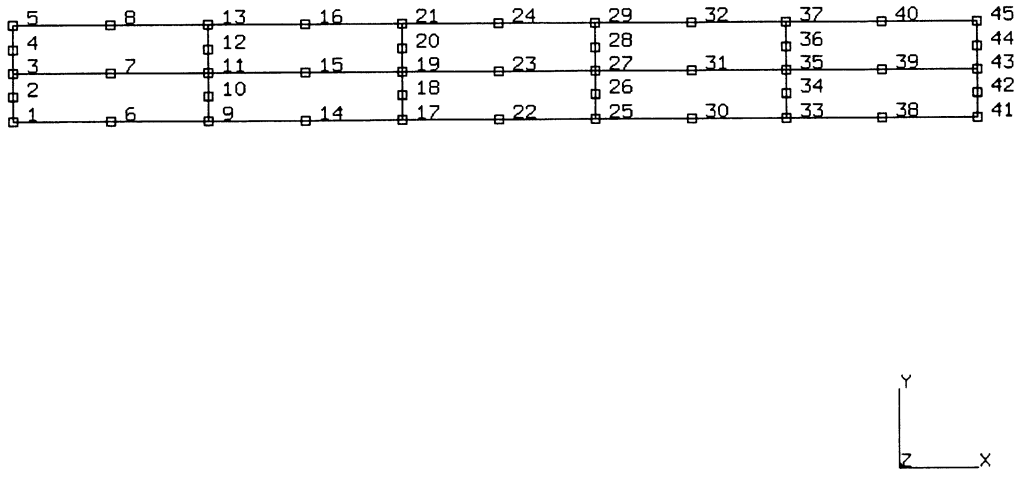

Figure E 8.6-3 Node Numbering

MARC

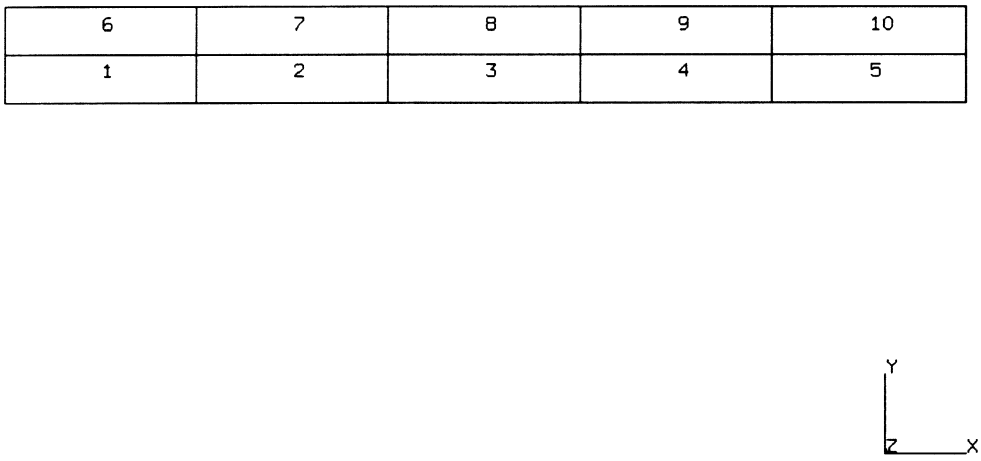

Figure E 8.6-4 Element Numbering Concrete Elements

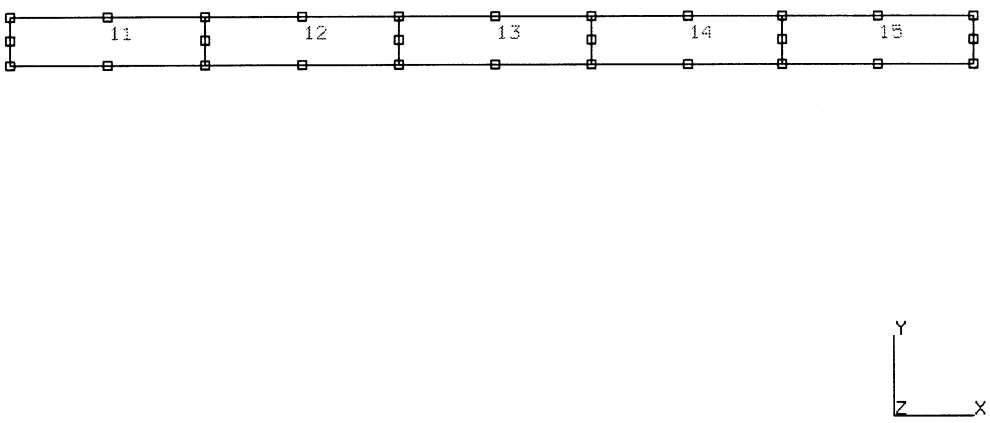

Figure E 8.6-5 Element Numbering Rebar Elements

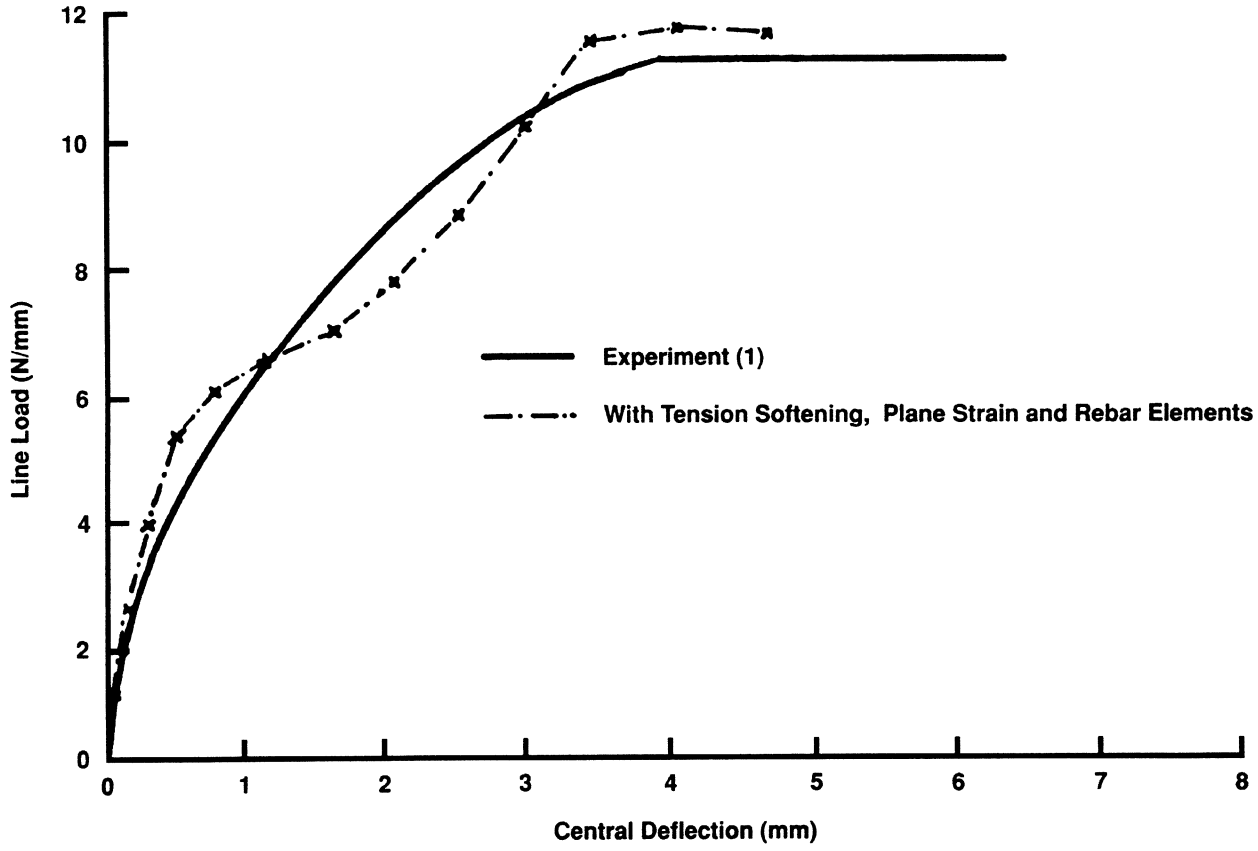

Figure E 8.6-6 Load/Deflection Relationship for One-Way Reinforced Slab

E 8.7 Compression Of A Block

This example demonstrates MARC's capability to perform a large deformation contact problem which incorporates thermal mechanical coupling. The block is considered an elastic-plastic deformable material, and both the deformations and temperatures are calculated. The platen is treated as a rigid region, and only temperatures are calculated. Gap elements are used to insure that the contact condition is properly accounted for.

Coupling

There are four sources of coupling in this analysis:

1. As the temperature changes, thermal strains are developed; this is due to non-zero coefficient of thermal expansion.
2. As the temperature changes, the mechanical properties change because of the temperature-dependent elasticity.
3. As the geometry changes, the heat transfer problem changes.
4. As plastic work is performed, internal heat is generated.

Parameters

The UPDATE, FINITE and LARGE DISP are included in the parameter section as this is a finite deformation analysis. The COUPLE option is used to indicate that a couple thermal-mechanical analysis is being performed.

Mesh Definition

Due to symmetry, only one quarter of the region is modeled. The mesh is shown in Figure E 8.7-1. The deformable block is modeled using Element type 11 (four-node quadrilateral), while the platen is modeled with Element type 39 (four-node quadrilateral). In a coupled analysis, if the element type is a displacement element, a coupled (displacement-temperature) formulation will be used. If the element type is a thermal element, only a heat transfer analysis will be performed in that region; i.e., rigid.

Two gap elements are used between the platen and the block. In a coupled analysis when the gap elements are open, there is no load transmitted across the gap and the gap acts as a perfect insulator. When the gap closes, load is transmitted and the gap acts as a perfect conductor.

Geometry

A unit thickness will be used. A one is placed in the second field which indicates that the constant dilatation formulation is used.

Boundary Conditions

Symmetry displacement boundary conditions are imposed on two surfaces. An applied displacement is used to model the plate. The intention is to compress the block to 60 percent of its original height. The displacement boundary conditions are entered via the FIXED

DISPLACEMENT option. On the outside surface of the platen, the temperature is constrained to 70°. This is done with the FIXED TEMPERATURE option. Because of an ambiguity in type, the BOUNDARY CONDITION option should not be used in a coupled analysis.

Initial Conditions

The block is given an initial temperature of 300° and the platen an initial temperature of 70°.

Material Properties

The block is treated as an elastic plastic material with a Young's modulus of 1. x 10^6 psi, Poisson's ratio of 0.3, mass density of 0.1 lb/in^3, coefficient of thermal expansion of 1.3 x 10^{-5} in/in°F and a yield stress of 50,000 psi. The material is given an initial work hardening slope of 10,000 psi which reduces to 1000 psi at an equivalent plastic strain of 0.01.

The thermal properties are a conductivity of 21.6 in-lb/in°F and the specific heat of 2147 in-lb/lb°F. In the platen, no mechanical properties are given as it is rigid. The thermal properties are the same as the block. In a coupled analysis, the mass density must be entered on the first property.

Gap Data

For the two gap elements, the only property necessary is the closure distance. This is the original distance between the gap nodes attached to the block and the platen.

Temperature Effects

The elastic modulus is assumed to be a linear function of temperature such that:

$$E(T) = 1 \times 10^7 - (T - T_o) \times 1 \times 10^4,$$

where the reference temperature T_o is 0°F.

Distributed Flux

This distributed flux block is used to indicate that internal heat is generated due to plastic deformation.

Convert

This option is used to give the conversion factor between the mechanical energy and the thermal energy.

The internal volumetric flux per unit volume becomes:

$$f = c \cdot W^p$$

where W^p is the plastic strain energy density.

Control Options

The Cuthill-McKee optimizer is used, to minimize the bandwidth. A formatted post tape containing only nodal variables is written every ten increments. In a coupled analysis, the nodal variables are the total displacements, applied forces, reaction forces, temperatures, and applied flux. The restart tape is written each increment. The PRINT CHOICE option is used to minimize the amount of output.

Two lines are used to enter the control tolerances. These are the default values.

Load Control

This problem was performed with a fixed time step, fixed increment size. This was specified with a time step of 1 sec., and a total of 80 sec was requested. As no proportional increment was used, each increment will impose a displacement of 0.2 inches.

In a coupled analysis, if an adaptive time-stepping is required, the AUTO TIME option should be invoked.

Results

Figure E 8.7-2 through Figure E 8.7-11 show the contour plots of the equivalent stress and the temperatures on the deformed body. The body folds over onto the platen at increment 45. The figures are shown until increment 70. At approximately increment 75 (depends on machine accuracy), the analysis stops because of very large distortion. A rezoning step should have been performed in increment 60.

The analysis shows in increment 30 that there is a small rigid region stress below yield under the platen, which remains for the entire analysis. The highest stress at increment 70 occurs where the material has folded over and is 10 percent above yield. This is an indication of the minimal amount of work hardening in the material. The final highest temperature of 340°F, an increment of 10°F above initial conditions is due to the plastic deformation.

The printed results for a coupled analysis give the stress, total strain, plastic strain and thermal strain and temperature for each integration point requested. In the platen (rigid region), only the temperatures are given. The nodal variables printed are the incremental and total displacements, temperatures, nodal forces and reaction forces.

Summary of Options Used

Listed below are the options used in example e8x7.dat:

Parameter Options

COUPLE
ELEMENT
END
FINITE
LARGE DISP
SIZING
TITLE
UPDATE

Model Definition Options

CONNECTIVITY
CONTROL
CONVERT
COORDINATE
DIST FLUXES
END OPTION
FIXED DISP
FIXED TEMPERATURE
GAP DATA
GEOMETRY
INITIAL TEMPERATURE
ISOTROPIC
POST
PRINT CHOICE
RESTART
TEMPERATURE EFFECTS
WORK HARD

Load Incrementation Options

CONTINUE
TRANSIENT

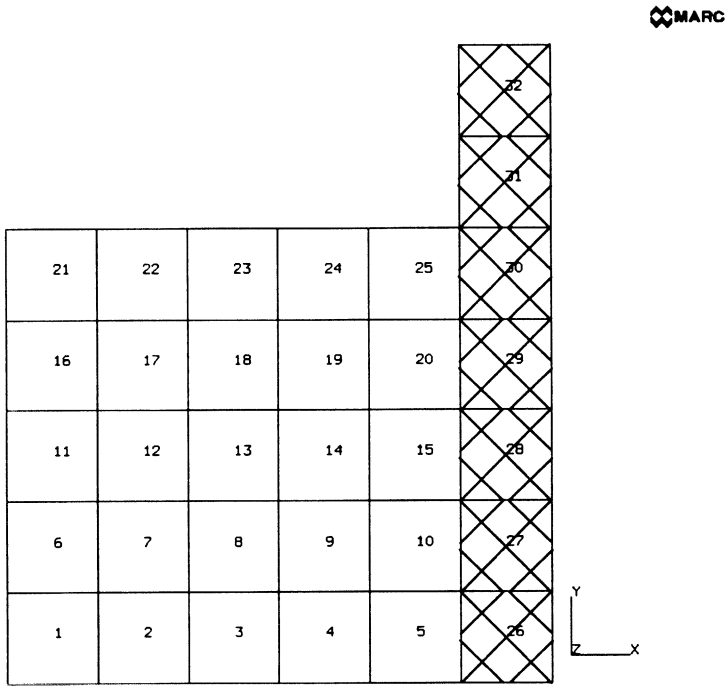

(a) Cross-Hatched Area Indicates Rigid Platen

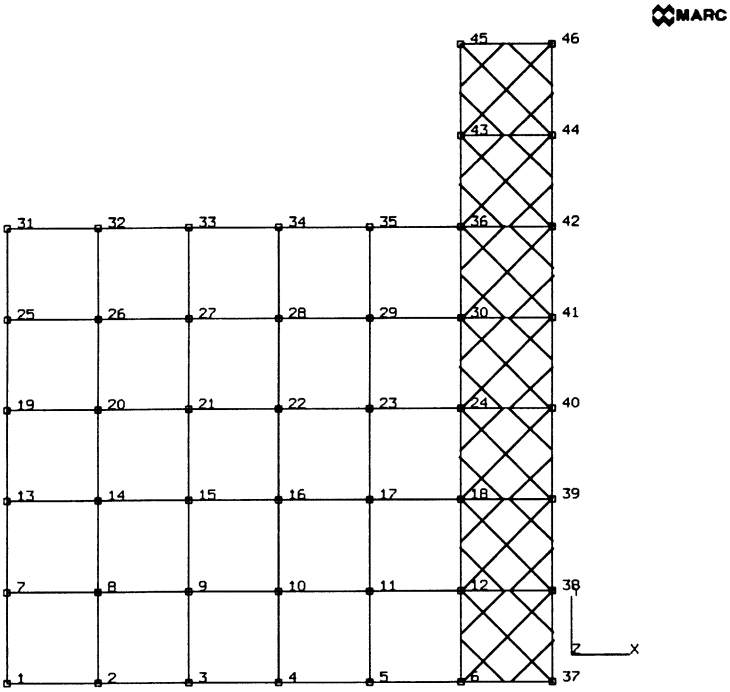

(b) Cross-Hatched Area Indicates Rigid Platen

Figure E 8.7-1 Mesh

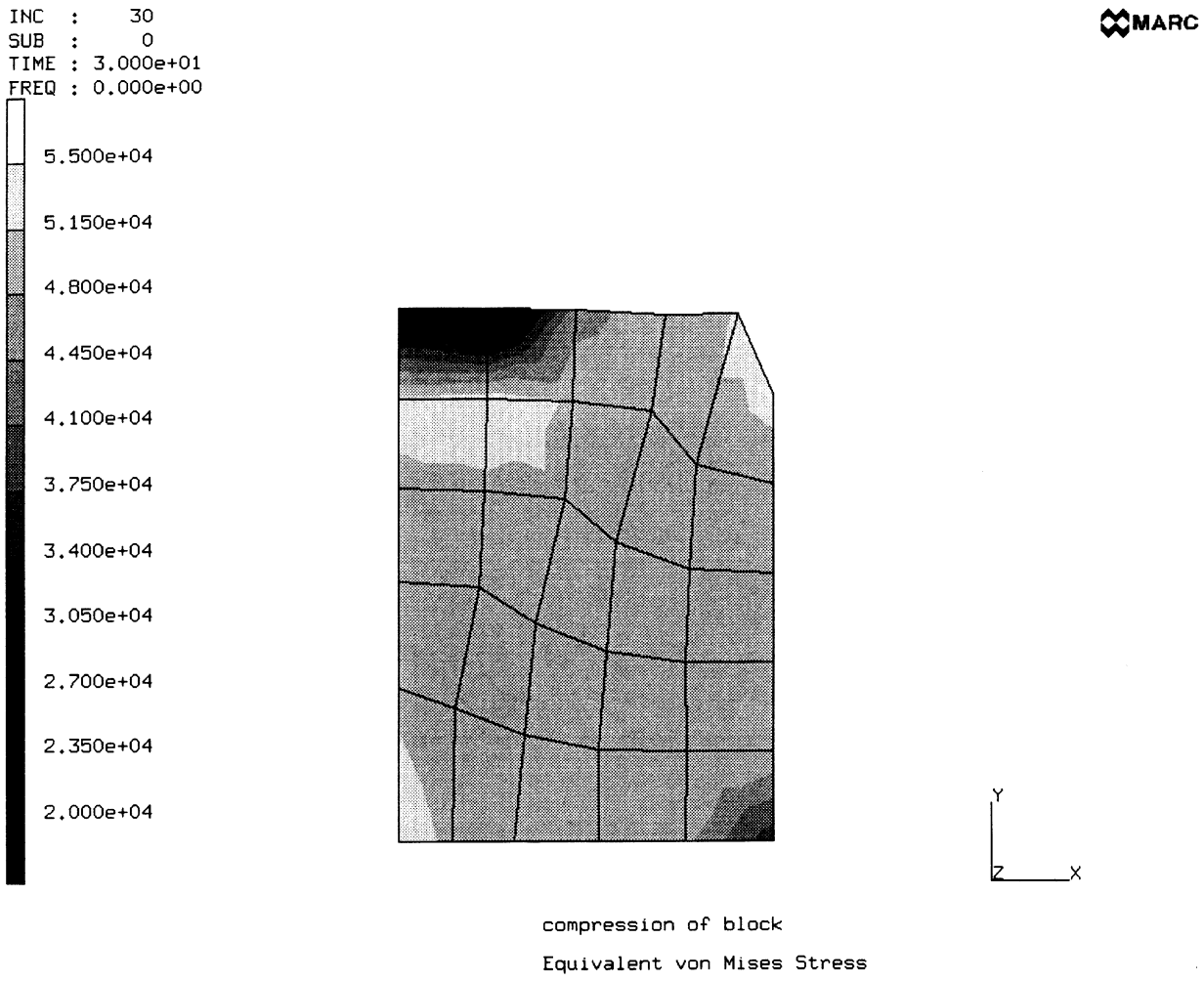

Figure E 8.7-2 Equivalent Stress, Increment 30

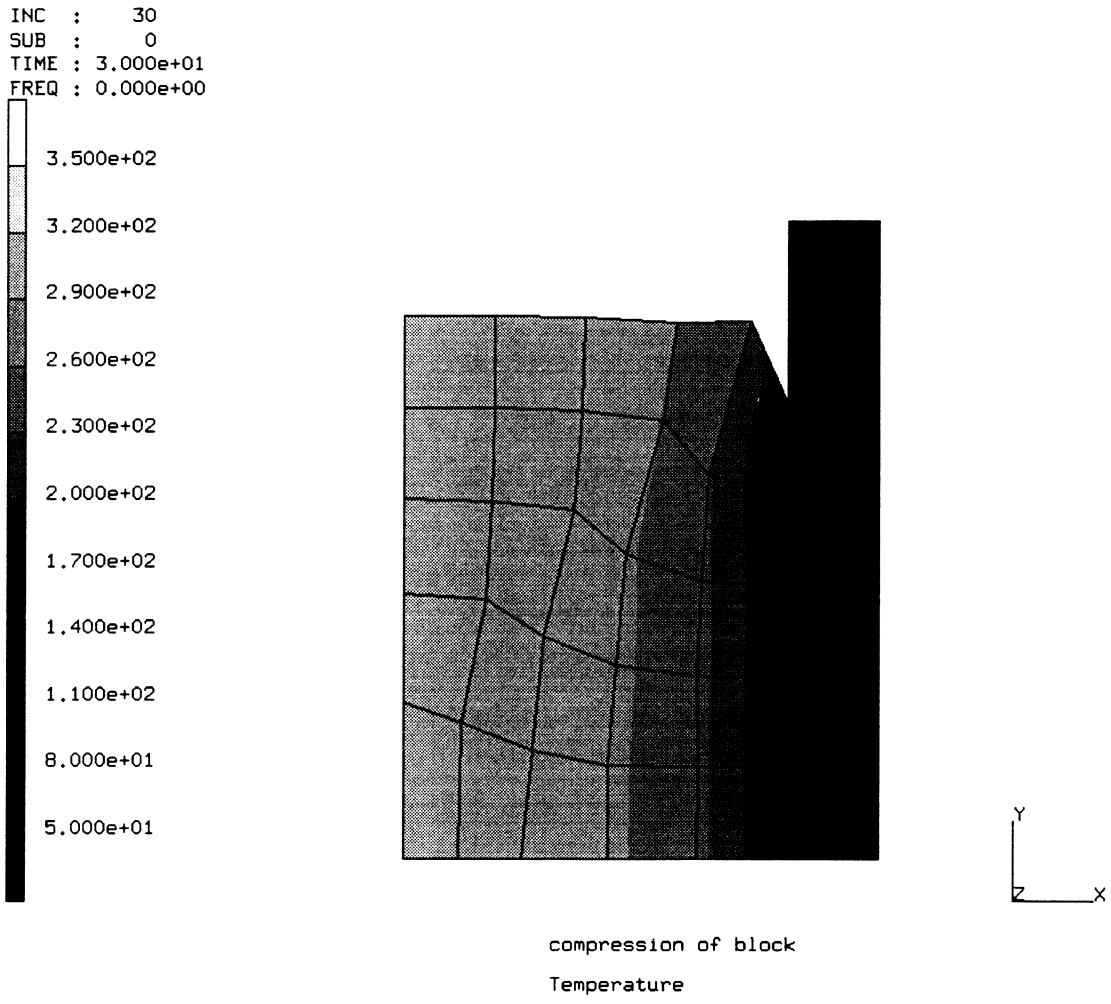

Figure E 8.7-3 Temperature, Increment 30

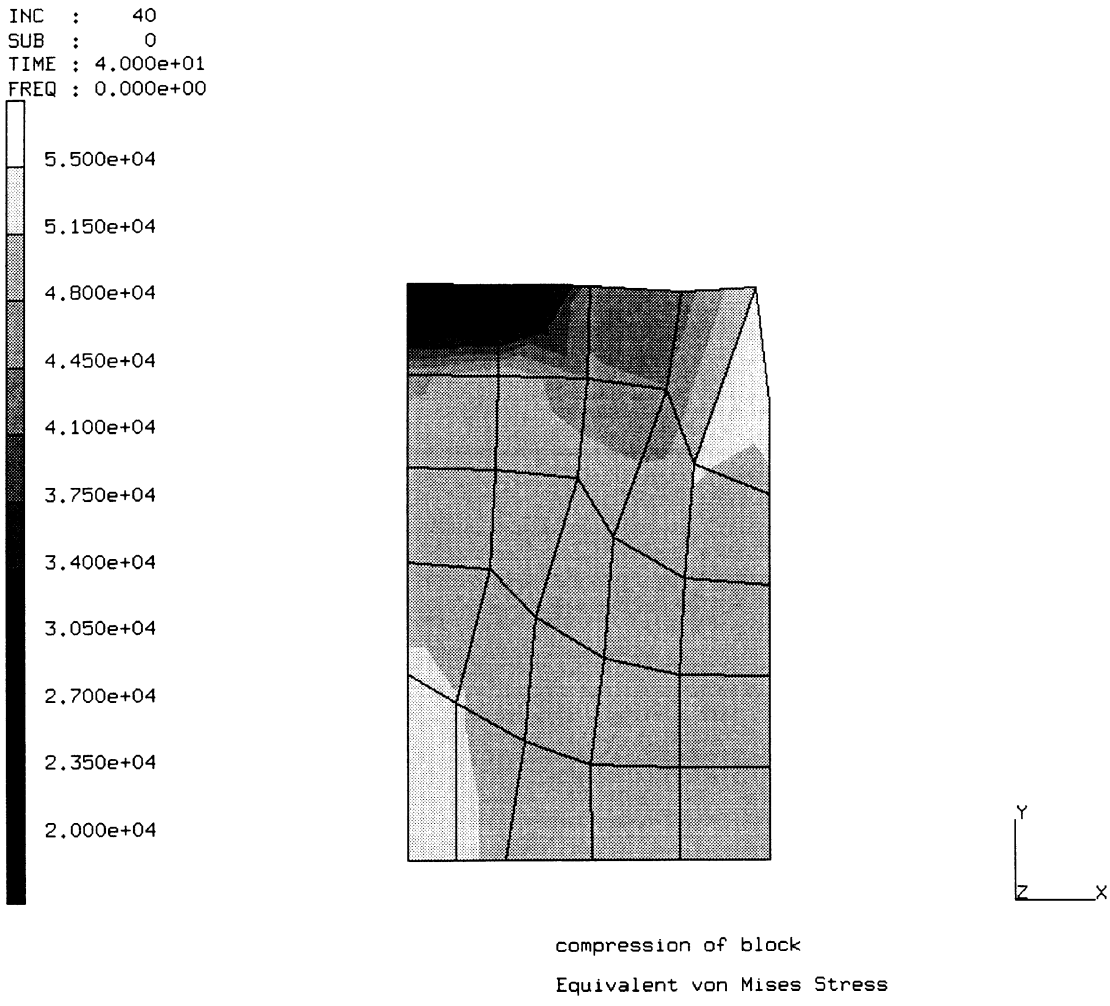

Figure E 8.7-4 Equivalent Stress, Increment 40

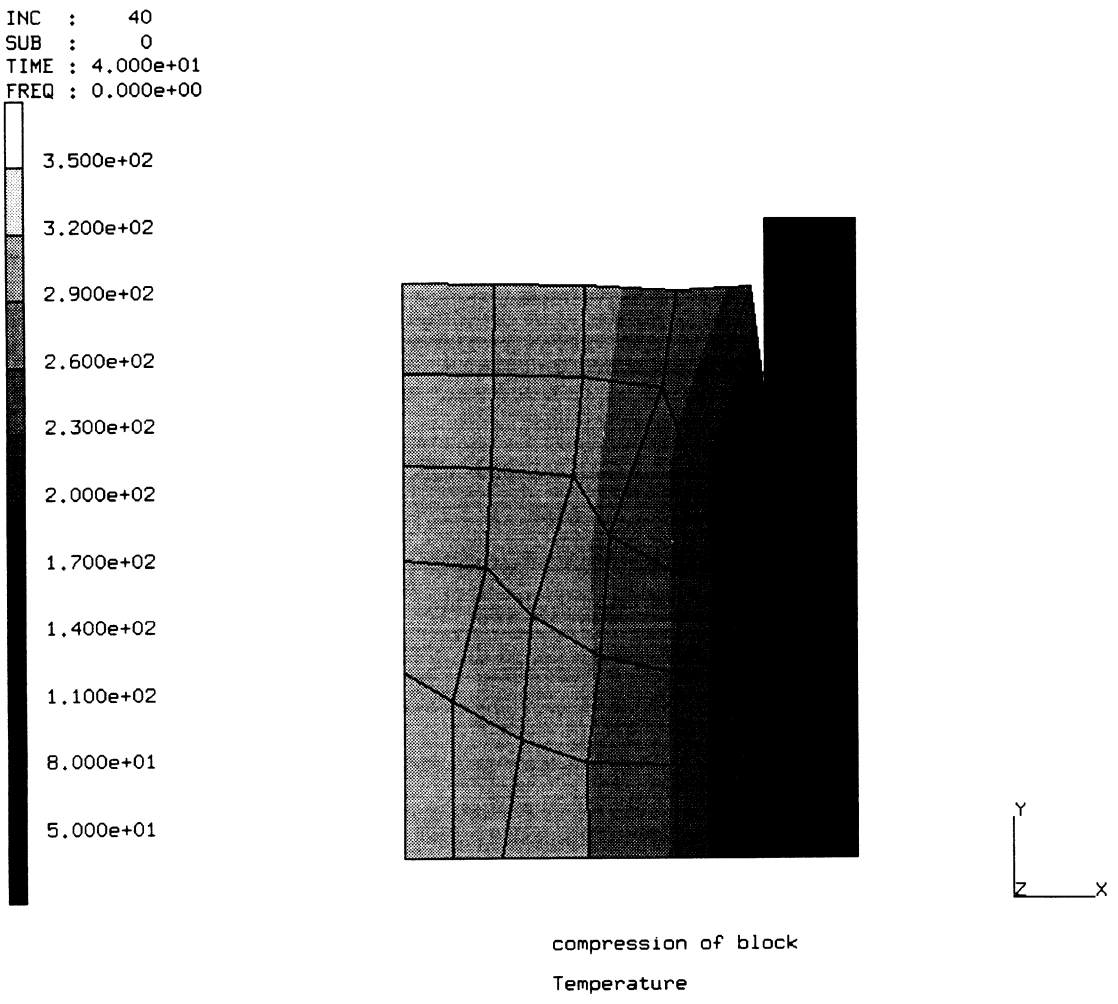

Figure E 8.7-5 Temperature, Increment 40

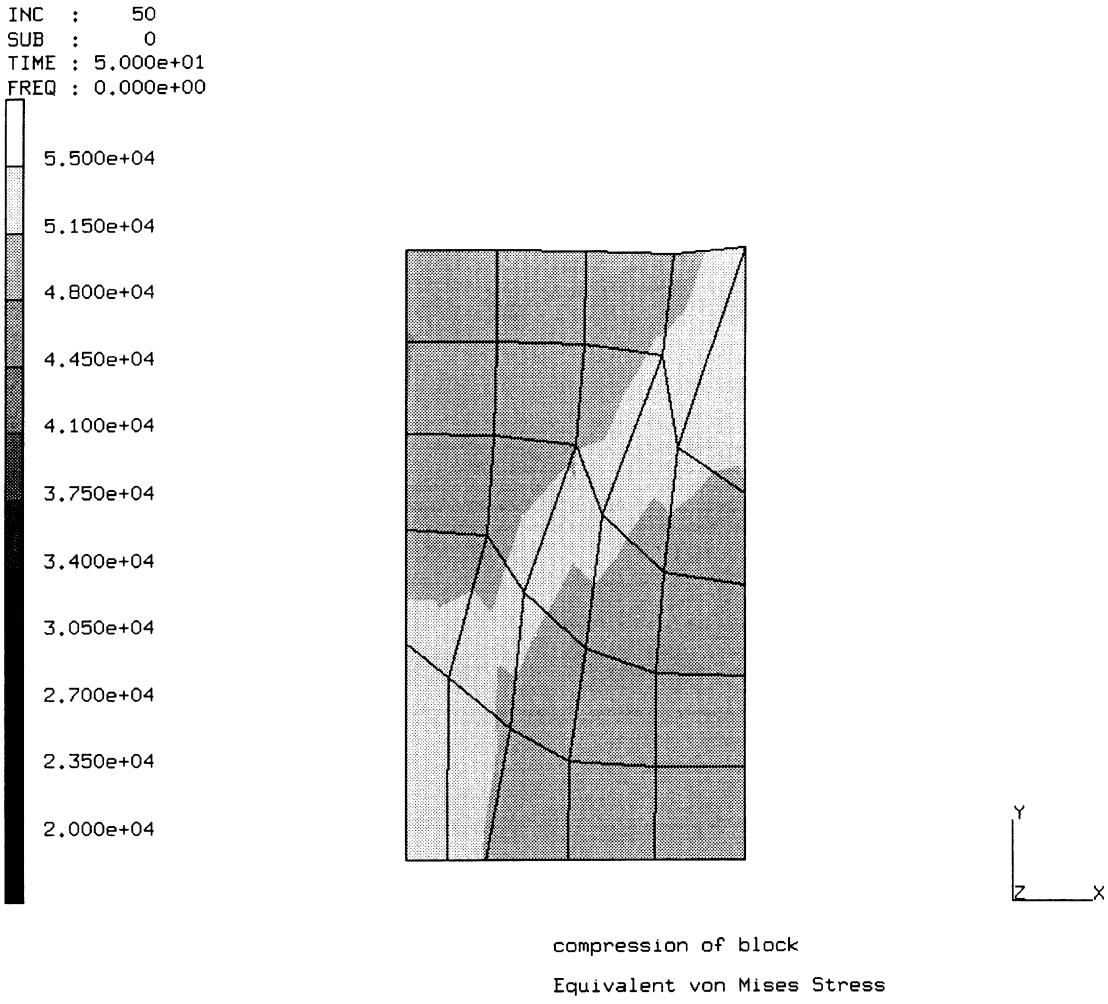

Figure E 8.7-6 Equivalent Stress, Increment 50

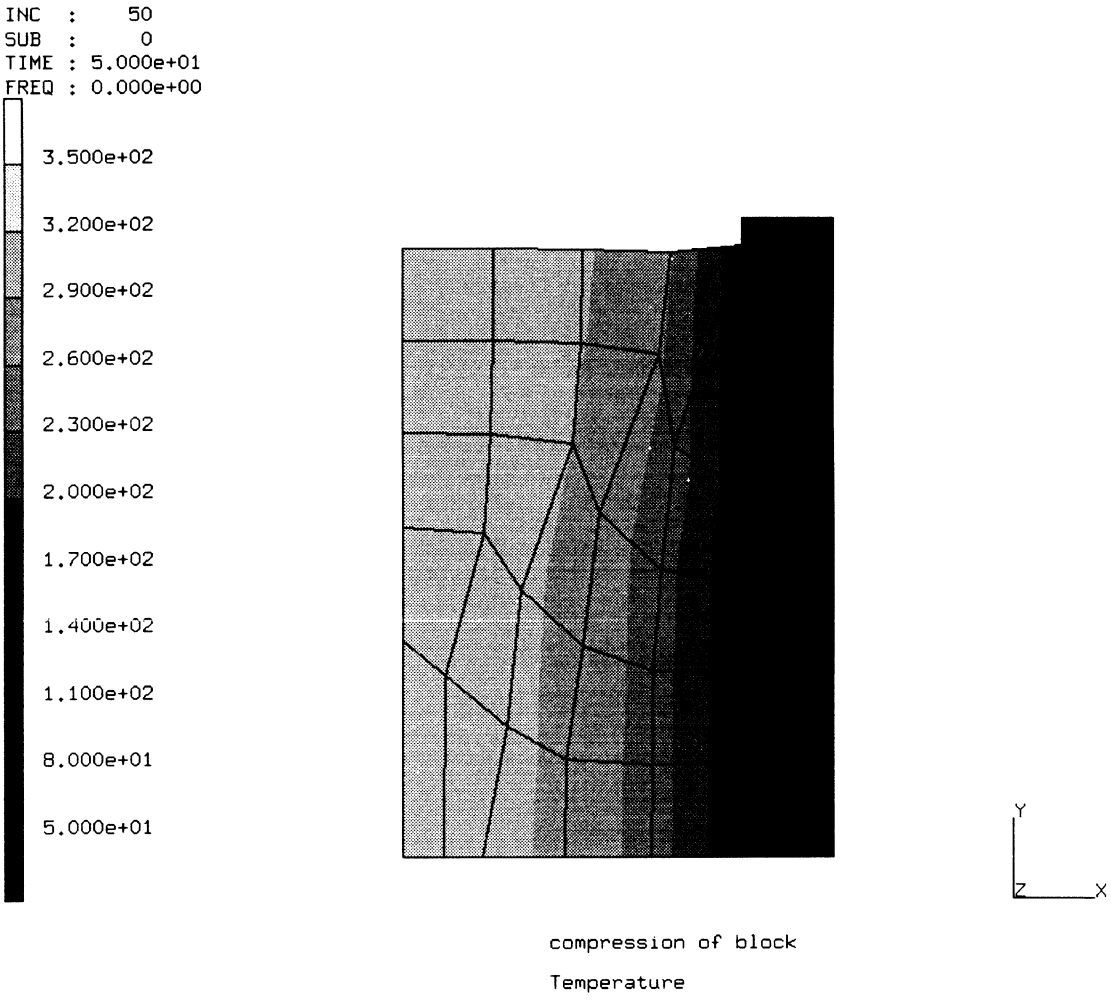

Figure E 8.7-7 Temperature, Increment 50

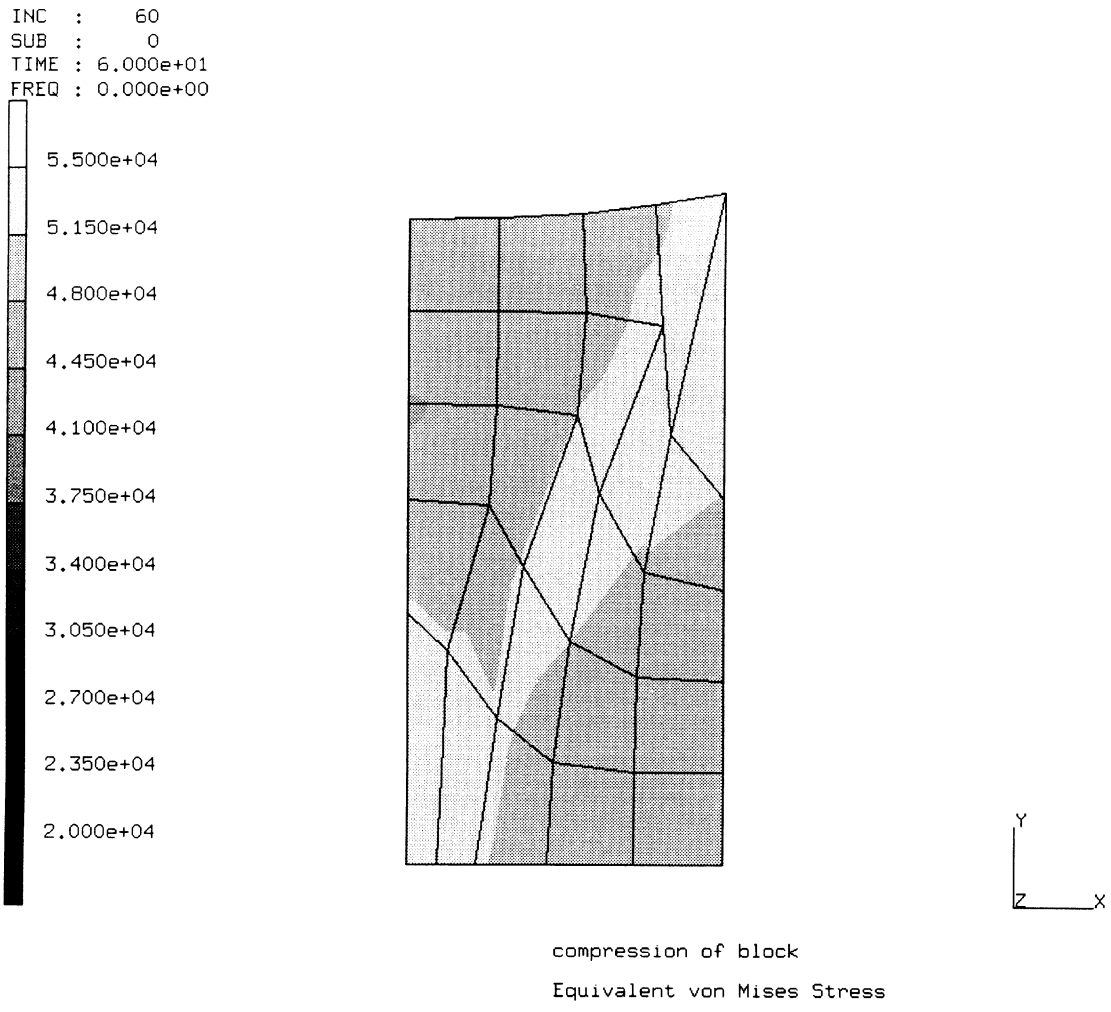

Figure E 8.7-8 Equivalent Stress, Increment 60

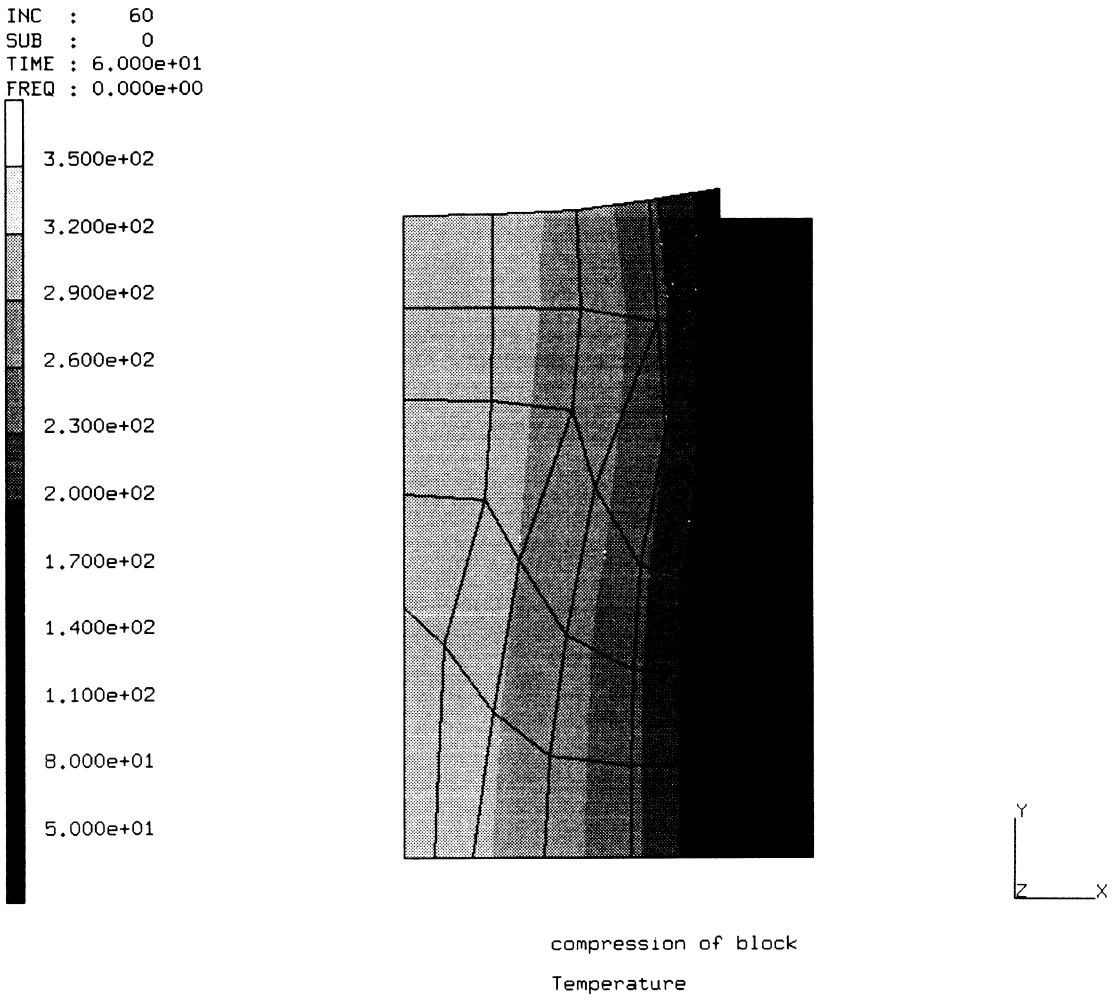

Figure E 8.7-9 Temperature, Increment 60

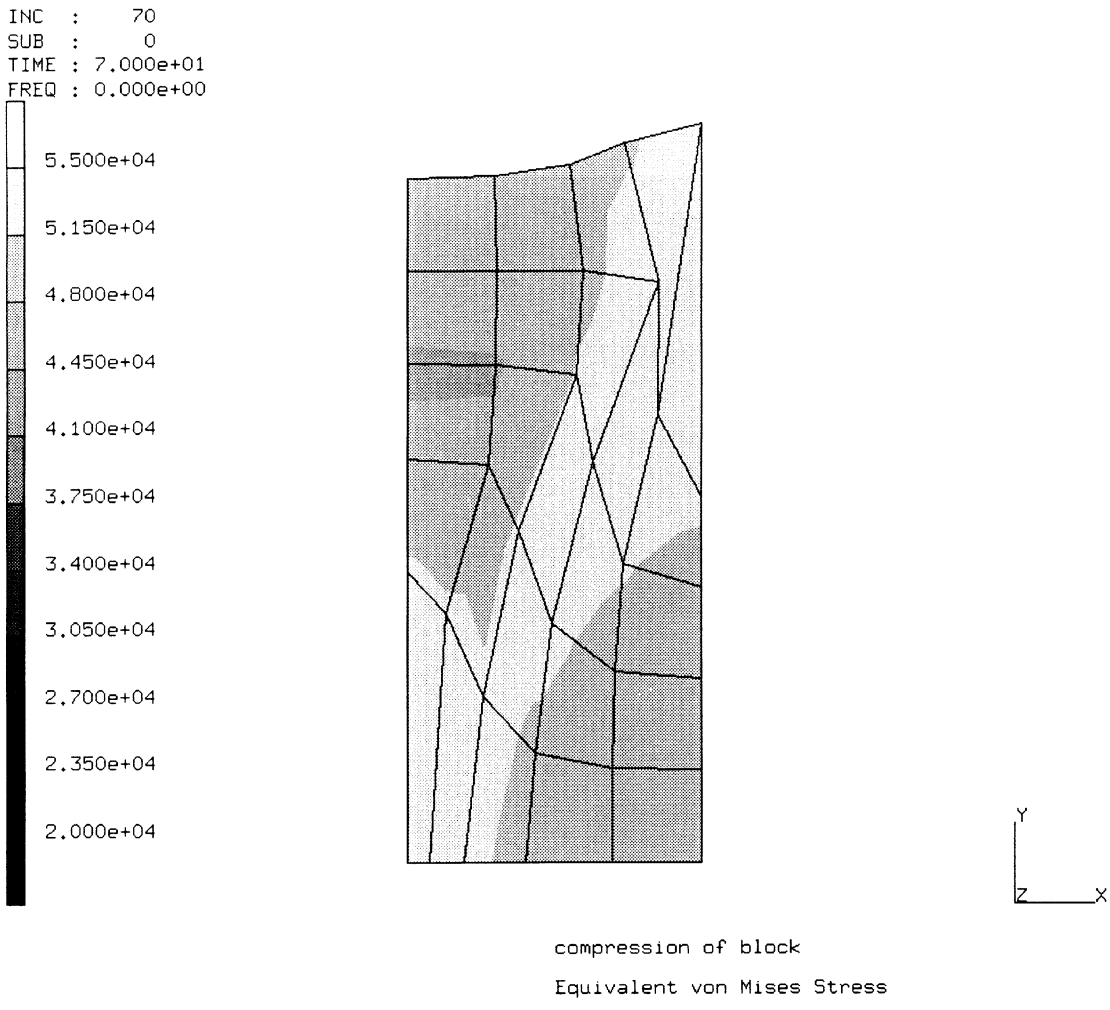

Figure E 8.7-10 Equivalent Stress, Increment 70

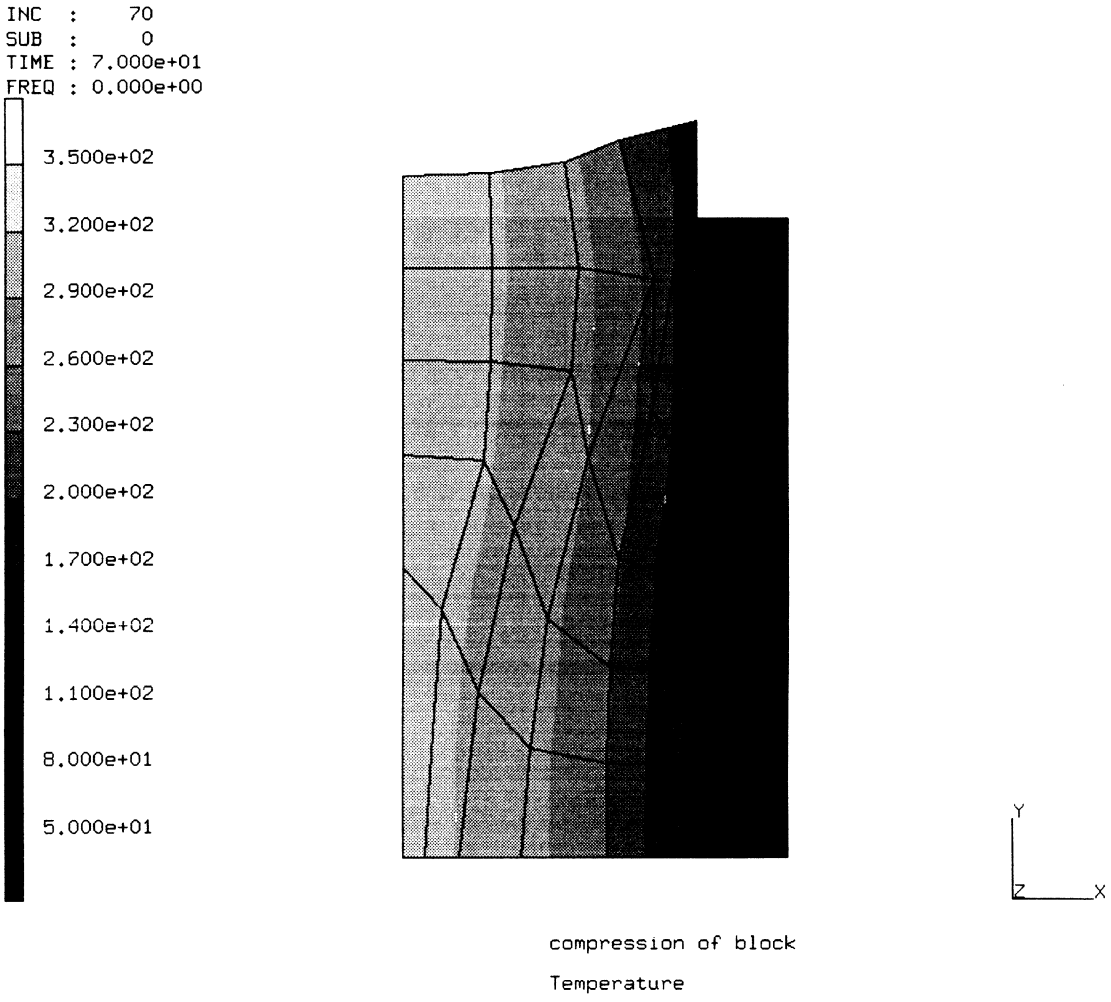

Figure E 8.7-11 Temperature, Increment 70

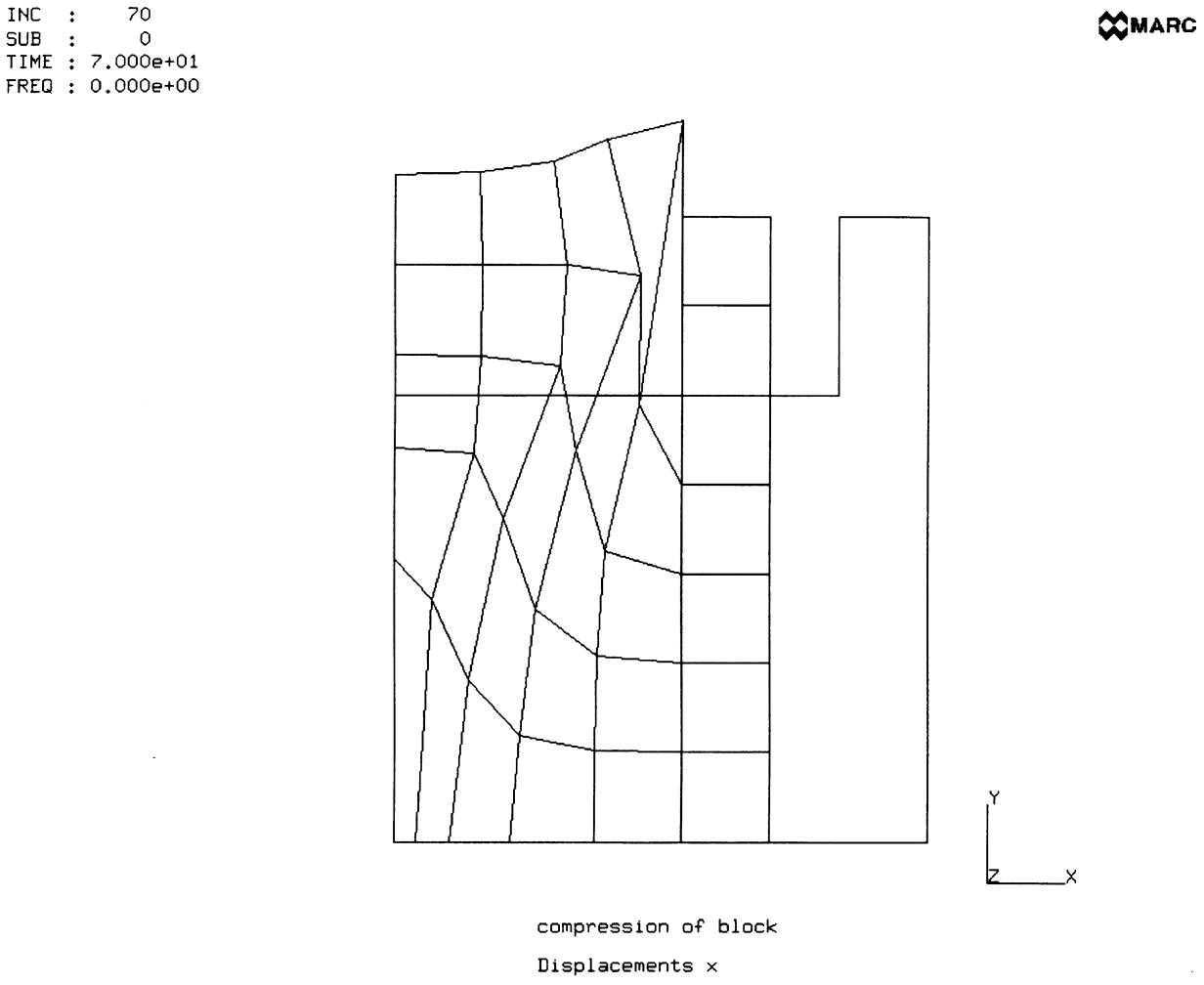

Figure E 8.7-12 Total Displacement, Increment 70

E 8.8 Simply-Supported Thick Plate Under Uniform Pressure With Anisotropic Properties

A thick plate, simply-supported around its perimeter, is analyzed with a pressure load normal to the plate surface. This problem demonstrates the use of various options for the input of anisotropic properties.

Element (Ref. B21.1)

Element type 21 is a 20-node isoparametric brick. There are three displaced degrees of freedom at each node; eight are corner nodes, 12 midside. Each edge of the brick may be parabolic; a curve is fitted through the midside node. Numerical integration is accomplished with 27 points using Gaussian quadrature. See Volume B for further details.

Model

Taking advantage of symmetry, only one-quarter of the plate is modeled. One element is used through the thickness, two in each direction in the plane of the plate. There are 51 nodes for a total of 153 degrees of freedom. See Figure E 8.8-1.

Anisotropic Properties

Material properties in this problem are assumed to be anisotropic. The Young's moduli, Poisson's ratios, and shear moduli are:

$$E_x = 30 \times 10^6 \quad , \quad E_y = 20 \times 10^6 \quad , \quad E_z = 10 \times 10^6$$
$$\nu_{xy} = 0.3 \quad , \quad \nu_{yz} = 0.25 \quad , \quad \nu_{zx} = 0.2$$
$$G_{xy} = 10 \times 10^6 \quad , \quad G_{yz} = 5 \times 10^6 \quad , \quad G_{zx} = 1 \times 10^6$$

The preferred directions of the material are aligned with the global x- ,y-, z-axes, which are also the basis for the continuum element. Three input options are demonstrated in this example for the input of anisotropic properties. These options are: model definition block ORTHOTROPIC, user subroutine HOOKLW and user subroutine ANELAS.

ORTHOTROPIC (Model Definition Block)

The anisotropic material properties can be directly entered through the model definition block ORTHOTROPIC. As shown in the input list E8.8A, this data block consists of seven lines. The keyword ORTHOTROPIC is on line series 1; the number of data sets is 1 on line series 2. On line series 3, the material identification number is entered as 1; on line series 4, 5, 6, the anisotropic properties (E_x, E_y, etc.) are sequentially entered. Finally, an element list (1 to 4) is entered on line series 7. In this example, the ORTHOTROPIC model definition block is used for entering the material data. The ORTHOTROPIC block can also be used for entering isotropic properties. In such a case, the material constants must be set to the same constant:

$E_x = E_y = E_z$; $\nu_{xy} = \nu_{yz} = \nu_{zx}$, etc.

HOOKLW (User Subroutine)

The user subroutine HOOKLW allows for the input of stress-strain relation [B] at each integration point of an element. For MARC element 21 (20-node brick) used in this problem, the strain-stress relation $[B]^{-1}$ is expressed as:

$$\begin{Bmatrix} \varepsilon_{xx} \\ \varepsilon_{yy} \\ \varepsilon_{zz} \\ \gamma_{xy} \\ \gamma_{yz} \\ \gamma_{zx} \end{Bmatrix} = \begin{bmatrix} 1/E_{xx} & -\nu_{yx}/E_{yy} & -\nu_{zx}/E_{zz} & 0 & 0 & 0 \\ -\nu_{xy}/E_{xx} & 1/E_{yy} & -\nu_{zy}/E_{zz} & 0 & 0 & 0 \\ -\nu_{xz}/E_{xx} & -\nu_{yz}/E_{yy} & 1/E_{zz} & 0 & 0 & 0 \\ 0 & 0 & 0 & 1/G_{xy} & 0 & 0 \\ 0 & 0 & 0 & 0 & 1/G_{yz} & 0 \\ 0 & 0 & 0 & 0 & 0 & 1/G_{zx} \end{bmatrix} \begin{Bmatrix} \sigma_{xx} \\ \sigma_{yy} \\ \sigma_{zz} \\ \sigma_{xy} \\ \sigma_{yz} \\ \sigma_{zx} \end{Bmatrix}$$

or $\{\varepsilon\} = [B]^{-1} \{\sigma\}$.

As shown in the subroutine list HOOKLW, the matrix $[B]^{-1}$ is first evaluated directly from the anisotropic material data (E_x, E_y, E_z, ν_{xy}, ν_{yz}, ν_{zx}, G_{xy}, G_{yz} and G_{zx}) and a MARC matrix inversion subroutine INVERT is called to invert the strain-stress matrix $[B]^{-1}$. The stress-strain matrix [B] is returned to the MARC program for the evaluation of element stiffness matrix. In order to activate the user subroutine HOOKLW, the model definition block ORTHOTROPIC must be used to indicate anisotropic material behavior as well as the use of HOOKLW user subroutine.

ANELAS (User Subroutine)

The user subroutine ANELAS allows for the input of anisotropy-to-isotropy ratios in the stress-strain relation at an integration point of an element. For MARC element 21 (20-node brick) used in this problem, the isotropic strain-stress relation is expressed as:

$$\begin{Bmatrix} \varepsilon_{xx} \\ \varepsilon_{yy} \\ \varepsilon_{zz} \\ \gamma_{xy} \\ \gamma_{yz} \\ \gamma_{zx} \end{Bmatrix} = \begin{bmatrix} 1/E & -\nu/E & -\nu/E & 0 & 0 & 0 \\ -\nu/E & 1/E & -\nu/E & 0 & 0 & 0 \\ -\nu/E & -\nu/E & 1/E & 0 & 0 & 0 \\ 0 & 0 & 0 & 1/G & 0 & 0 \\ 0 & 0 & 0 & 0 & 1/G & 0 \\ 0 & 0 & 0 & 0 & 0 & 1/G \end{bmatrix} \begin{Bmatrix} \sigma_{xx} \\ \sigma_{yy} \\ \sigma_{zz} \\ \sigma_{xy} \\ \sigma_{yz} \\ \sigma_{zx} \end{Bmatrix}$$

or $\{\varepsilon\} = [E]^{-1} \{\sigma\}$

and for anisotropic material as:

$$\begin{Bmatrix} \varepsilon_{xx} \\ \varepsilon_{yy} \\ \varepsilon_{zz} \\ \gamma_{xy} \\ \gamma_{yz} \\ \gamma_{zx} \end{Bmatrix} = \begin{bmatrix} 1/E_{xx} & -\nu_{yx}/E_{yy} & -\nu_{zx}/E_{zz} & 0 & 0 & 0 \\ -\nu_{xy}/E_{xx} & 1/E_{yy} & -\nu_{zy}/E_{zz} & 0 & 0 & 0 \\ -\nu_{xz}/E_{xx} & -\nu_{yz}/E_{yy} & 1/E_{zz} & 0 & 0 & 0 \\ 0 & 0 & 0 & 1/G_{xy} & 0 & 0 \\ 0 & 0 & 0 & 0 & 1/G_{yz} & 0 \\ 0 & 0 & 0 & 0 & 0 & 1/G_{zx} \end{bmatrix} \begin{Bmatrix} \sigma_{xx} \\ \sigma_{yy} \\ \sigma_{zz} \\ \sigma_{xy} \\ \sigma_{yz} \\ \sigma_{zx} \end{Bmatrix}$$

or $\{\varepsilon\} = [B]^{-1} \{\sigma\}$.

As shown in the subroutine list ANELAS, the matrices $[E]^{-1}$ and $[B]^{-1}$ are first evaluated from the isotropic material data (E and ν) and anisotropic material data (E_x, E_y, E_z, ν_{xy}, ν_{yz}, ν_{zx}, G_{xy}, G_{yz}, and G_{zx}). Then, the MARC matrix inversion subroutine INVERT is called to obtain the stress-strain relations [E] and [B] for isotropic and anisotropic properties, respectively. The anisotropy-to-isotropy ratios to be defined in the subroutine ANELAS are:

DRATS(I,J) = B(I,J)/E(I,J)
I,J = 1,...,3
DRATS(L,L) = B(L,L)/E(L,L)
L = 4,...,6

In order to activate the user subroutine ANELAS, the model definition block ORTHOTROPIC must be used to indicate anisotropic material behavior. In addition, the isotropic properties [$E_y = E_y = E_z = E$; $V_{xy} = V_{yz} = V_{zx} = \nu$; $G_{xy} = G_{zx} = G_{zx} = E/2(1+\nu)$] must also be entered through ORTHOTROPIC block.

Geometry

No geometry specification is used.

Loading

A uniform pressure of 1.00 psi is applied in the DIST LOADS block. Load type 4 is specified for uniform pressure on the 6-5-8-7 face of all four elements.

Boundary Conditions

On the symmetry planes, x = 30 and y = 30, in-plane movement is constrained. On the x = 30 plane, u = 0, and on the y = 30 plane, v = 0. On the plate edges, x = 0 and y = 0; the plate is simply supported, w = 0.

Results

A contour plot of the equivalent stress for all four elements is shown in Figure E 8.8-2. A comparison of the contours (Figure E 8.8-2) between isotropic and anisotropic behavior clearly shows the effect of anisotropy on stress distributions.

Summary of Options Used

Listed below are the options used in example e8x8a.dat:

Parameter Options

ELEMENT
END
SIZING
TITLE

Model Definition Options

CONNECTIVITY
COORDINATE
DIST LOADS
END OPTION
FIXED DISP
ORTHOTROPIC

Listed below are the options used in example e8x8b.dat:

Parameter Options

ELEMENT
END
SIZING
TITLE

Model Definition Options

CONNECTIVITY
COORDINATE
DIST LOADS
END OPTION
FIXED DISP
ORTHOTROPIC

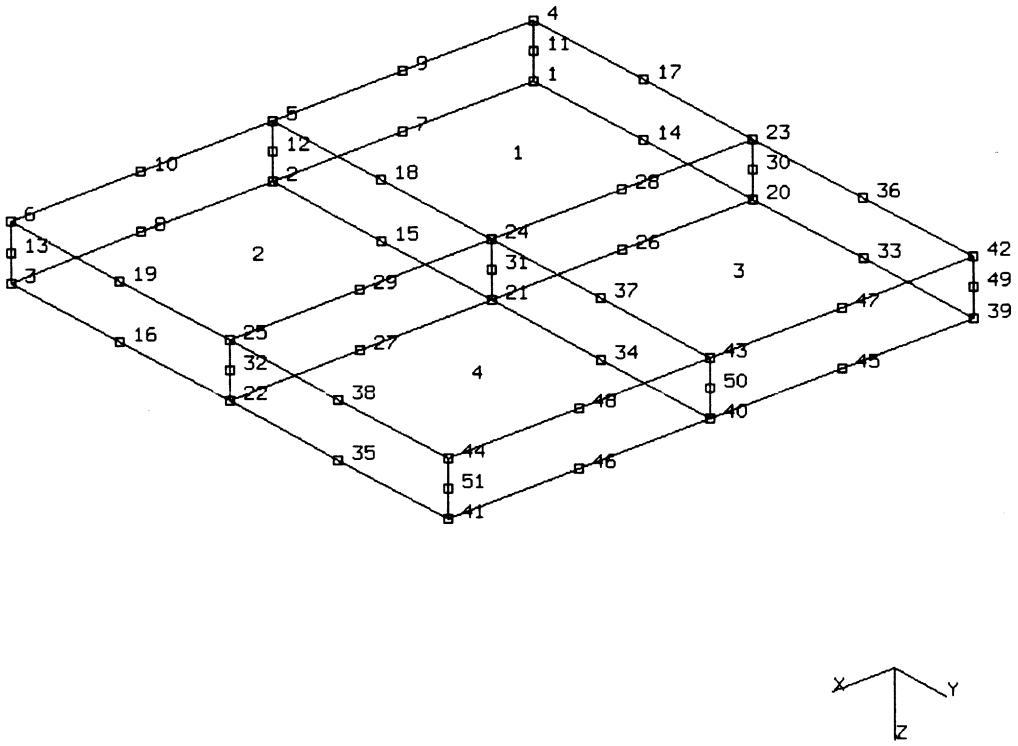

Figure E 8.8-1 Thick Plate Mesh

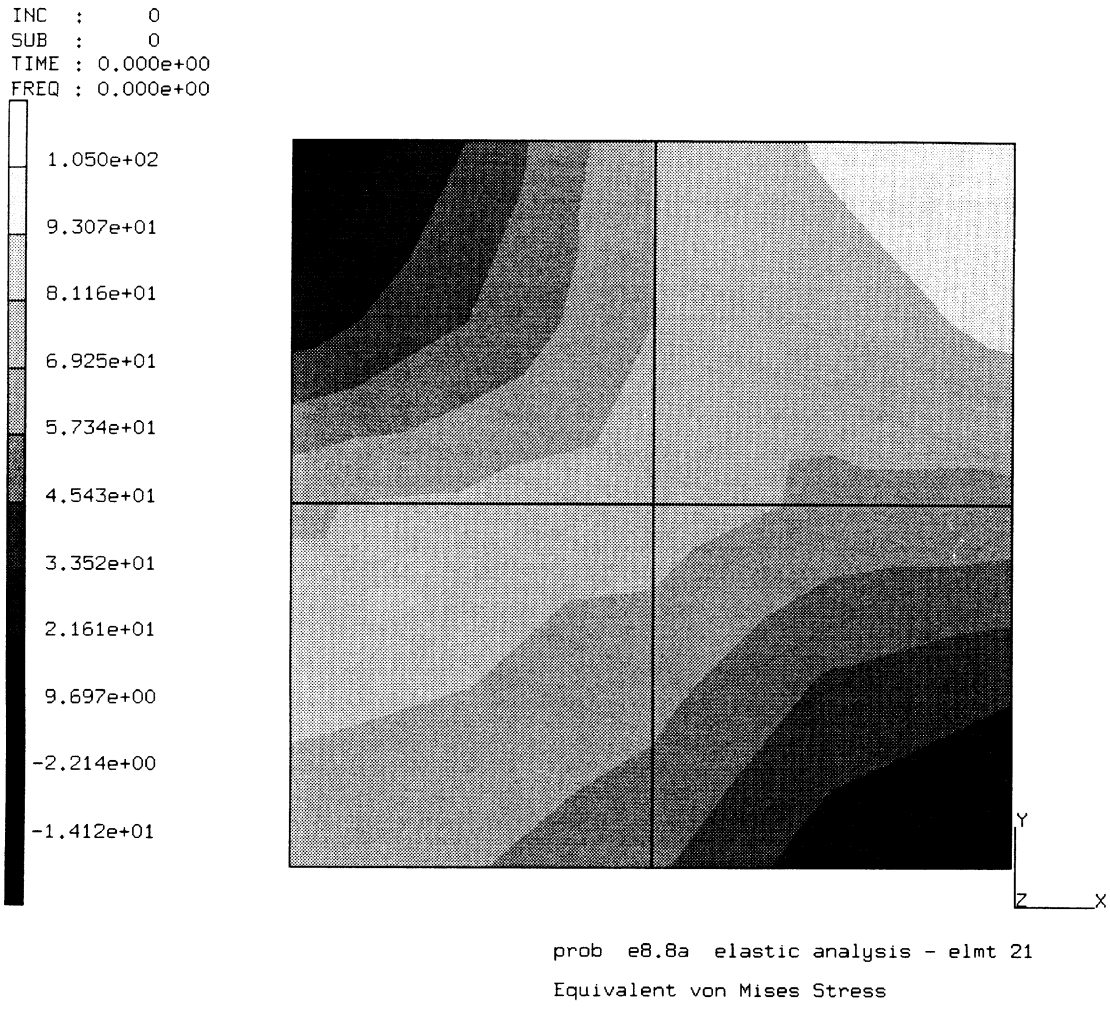

(a) Anisotropic Behavior

Figure E 8.8-2 Stress Contours

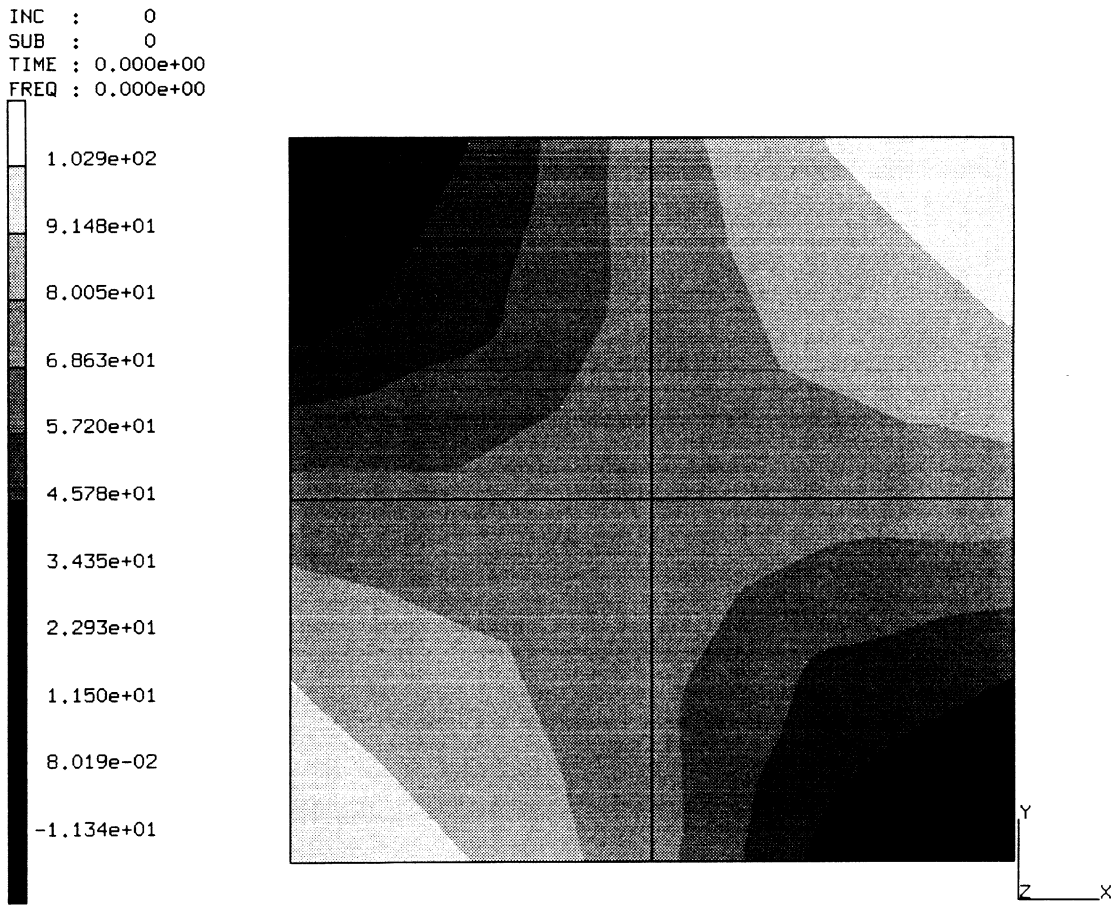

(b) Isotropic Behavior

Figure E 8.8-2 Stress Contours (Continued)

E 8.9 Failure Criteria Calculation For Plane Stress Orthotropic Sheet

This problem illustrates the use of the FAIL DATA model definition block to supply data used by MARC to calculate failure criteria based on the current state of stress in a material. In this problem, an ORTROTROPIC square plate is subjected to a biaxial state of stress. The resulting program calculated failure criteria is compared with a textbook solution of this problem.

Element

Element type 3, a two-dimensional plane stress quadrilateral is used to model the square plate. This element is a 4-node isoparametric arbitrary quadrilateral element with two translational (u,v) degrees-of-freedom at each node. See volume B for a detailed discussion of this element.

Model

As shown in Figure E 8.9-1, a square plate of 4 x 4 m^2 is subjected to a biaxial state of stress. The applied stresses are: $\sigma_x = -3.5 \times 10^6$ N/m^2; $\sigma_y = +7.0 \times 10^6$ N/m^2; and $\tau_{xy} = -1.4 \times 10^6$ N/m^2. The plate is assumed to be made of an orthotropic material with a preferred direction (LOCAL 1-DIRECTION) of 60 degrees from the global x-axis. Sixteen elements are used to model this plate. Both the element and the nodal numbers are purposely set to be nonconsecutive. For the purpose of preventing rigid body motion, roller and hinge supports are prescribed at one side of the plate. Set names are used for boundary nodes as well as elements in the mesh.

Orthotropic

The orthotropic material properties of the plate are:

$E_{11} = 14.0E9, \quad E_{22} = E_{33} = 3.5E9$
$\nu_{12} = 0.4 \quad \nu_{23} = \nu_{31} = 0.0$
$G_{12} = G_{23} = G_{31} = 4.2E9$

Orientation

The preferred material direction (LOCAL 1-DIRECTION) of 60 degrees from the global x-axis, is entered through the PGLOBAL X option.

Fail Data

Five program calculated failure criteria provided in MARC are as follows:

1. maximum stress
2. maximum strain
3. Hill
4. Tsai-Wu
5. Hoffman

A user-defined criterion is also available through user subroutine UFAIL. The five pre-programmed criteria are valid only for states of plane stress, while user subroutine UFAIL may be used for a general 3D state of stress using the FAIL DATA block.The user specifies on a material basis his failure data. Up to three failure criteria may be calculated per material.

Failure criterion output appears along with other element output. The failure data is given in the material principal coordinate system. These are the preferred coordinates in MARC and are specified by the ORIENTATION block.

Both the maximum stress (MX STRESS) and the Hill (HILL) failure criteria are requested in this analysis. The maximum stresses used for this criteria are:

MAX. X-TENSILE STRESS = 250.0E6
MAX. ABSOLUTE X-COMPRESSIVE STRESS = 0
MAX. Y-TENSILE STRESS = 0.5E6
MAX. ABSOLUTE Y-COMPRESSIVE STRESS = 10.0E6
MAX. ABSOLUTE SHEAR STRESS = 8.0E6

For Hill's criterion, a default failure index of 1.0 is used.

Fixed Disp

Roller supports (u = 0) are prescribed at nodes 2, 3, 4, 5 (LEFT EXCEPT 1); hinge (u = v = 0) support is prescribed at node 1, for the prevention of rigid body motion.

Point Load

Both the direct (σ_x,σ_y) and shear (τ_{xy}) stresses are represented by point loads acted at boundary nodal points. A distribution of the points loads is shown in Figure E 8.9-2.

Nodal Thickness

In this problem, the plate thickness is specified in the NODAL THICKNESS block. A thickness of 1.0 is assumed for all nodal points in the mesh.

Results

In the reference, a solution to this problem is given. These results along with MARC output is summarized in Table E 8.9-1. The comparison is favorable.

Table E 8.9-1 Comparison of Results

Criterion	Reference	MARC
Max σ_2	1.26%*	1.3%
Max σ_2	68.0%	67.5%
Max τ_{12}	65.6%	65.6%
Hill	89.0%	88.6%
* = 100% means failure occurs		

References

Argarwal, B.D., and Broutman, L.J., *Analysis and Performance of Fiber Composites*, Wiley, 1980.

Summary of Options Used

Listed below are the options used in example e8x9.dat:

Parameter Options

ELEMENT
END
SIZING
TITLE

Model Definition Options

CONNECTIVITY
COORDINATE
DEFINE
END OPTION
FAIL DATA
FIXED DISP
NODAL THICKNESS
ORIENTATION
ORTHOTROPIC
POINT LOAD
POST
PRINT ELEM

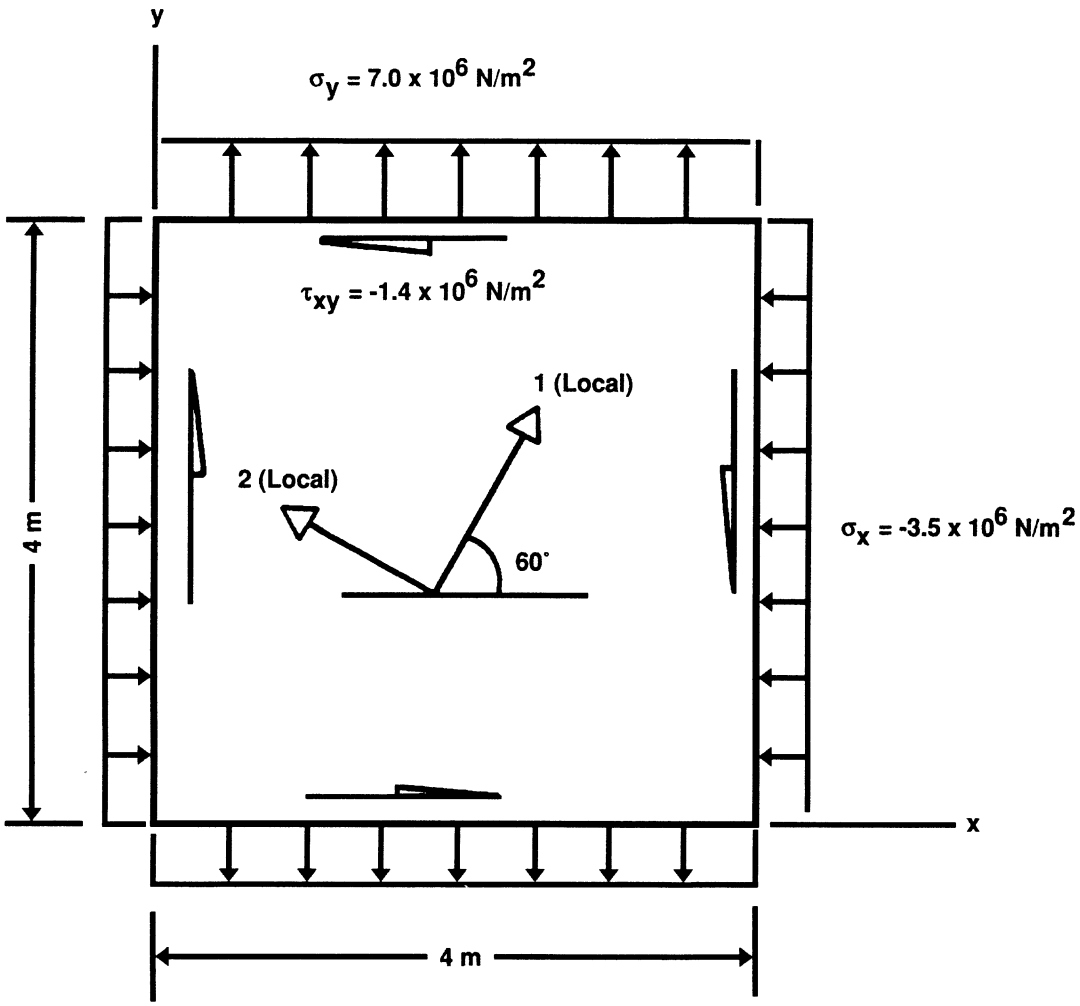

Figure E 8.9-1 Orthotropic Square Plate

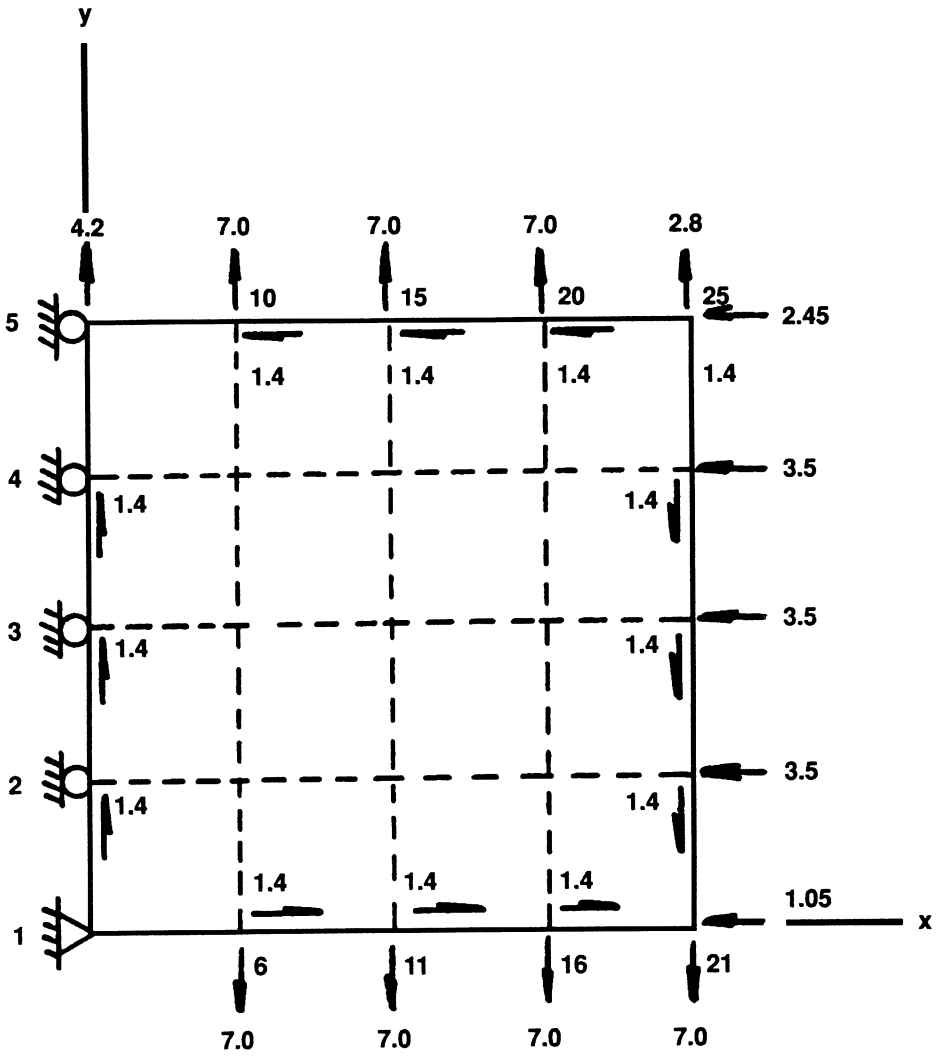

Figure E 8.9-2 Point Load (x 10^6) and Support

E 8.10 Beam Element 52 With Nonlinear Elastic Stress-Strain Relation

As described in Volume B, the beam element 52 may be used for nonlinear elastic material. This problem demonstrates the use of model definition card HYPOELASTIC and user subroutine UBEAM for the nonlinear elastic behavior of a cantilever beam, modeled by element type 52, subjected to prescribed tip displacements.

Element (Ref. B52.1)

Element type 52 is a straight, Euler-Bernoulli beam in space with three translations and three rotations as degrees-of-freedom at each node of the element. The element is defined by nodal coordinates in global coordinate system and by section properties such as area, bending stiffnesses, as well as torsional stiffness. See Volume B for further detail.

Model

As shown in Figure E 8.10-1, the cantilever beam is modeled by five beam elements with a fixed end at node 1, and prescribed displacements at node 6. The section and material properties are entered through GEOMETRY and HYPOELASTIC options; however, the user subroutine UBEAM is used for the description of nonlinear elastic stress-strain relation of the beam. The stress-strain relation is assumed to be dependent on strain quantities.

Geometry

A beam with a square cross section of length 0.2 inch is modeled. The area of the beam section is 0.04 $in.^2$ and moments of inertia are $I_x = I_y = 0.000133333$ $in.^4$.

HYPOELASTIC

The HYPOELASTIC model definition option is used to indicate that all of the elements use this formulation. User subroutine UBEAM defines the material behavior.

The initial Young's modulus is 1,000,000 psi and the Poisson's ratio is 0.2, which are given in the user subroutine.

FIXED DISP and DISP CHANGE

All degrees-of-freedom at node 1 are fixed for the simulation of a fixed-end condition. A 0.2 incremental displacement is prescribed at node 6, for degrees-of-freedom 1, 4, 5 and 6 (axial displacement and rotations). The same incremental displacements are repeated for increments 1 through 3, using DISP CHANGE load incrementation option.

Nonlinear Stress-Strain Relation (User Subroutine UBEAM)

The generalized stress-generalized strain relation for element 52 can be expressed as follows:

$$\begin{Bmatrix} F \\ M_x \\ M_y \\ T \end{Bmatrix} \begin{bmatrix} D_{11} & & & \\ & D_{22} & & \\ & & D_{33} & \\ & & & D_{44} \end{bmatrix} \begin{Bmatrix} \varepsilon \\ K_x \\ K_y \\ \theta \end{Bmatrix} \qquad \text{(EQ 1)}$$

where F, M_x, M_y and T are axial force, bending and twist moments (generalized stress components); ε, K_x, K_y and θ are axial stretch, curvatures and twist (generalized strain components), respectively.

For the purpose of demonstration, the terms D_{11}, D_{22}, D_{33} and D_{44} in the stress-strain matrix are assumed to have the following dependence on strains:

$$\begin{aligned} D_{11} &= (EA)\,EXP(-C|\varepsilon|) \\ D_{22} &= (EA)\,EXP(-C|K_x|) \\ D_{33} &= (EA)\,EXP(-C|K_y|) \\ D_{44} &= (EA)\,EXP(-C|\theta|) \end{aligned} \qquad \text{(EQ 2)}$$

In EQ 2, E is the Young's modulus, A is the area, I_x, I_y are moments of inertia; $G = E/2(1+\nu)$ and $J = (I_x + I_y)$. The constant C is assumed to be 13.8.

The incremental generalized stress-generalized strain relation D(I,I), the incremental generalized stress DF(I), and the total generalized stress at the end of increment GS(I), I = 1,..., 4, are respectively computed in the subroutine and returned to the MARC program for further computations.

Results

Table E 8.10-1 shows a comparison of MARC results with analytical solution computed from equations (EQ 1) and (EQ 2). The comparison is excellent.

Table E 8.10-1 Comparison of MARC Results vs. Analytical

Tip Displacements (in.)	F (lb.)		M_x (in-lb.)		M_y (in-lb.)		T (in-lb.)	
	MARC	Analytical	MARC	Analytical	MARC	Analytical	MARC	Analytical
0.2	9.21275E2	9.2127E2	3.07901E0	3.0709E0	3.07091E0	3.0709E0	2.55909E0	2.5591E0
0.4	1.06093E3	1.0609E2	3.53644E0	3.5364E0	3.53644E0	3.5364E0	2.94703E0	2.9470E0
0.6	9.16324E2	9.1632E2	3.05442E0	3.0544E0	3.05458E0	3.0544E0	2.54533E0	2.5453E0
0.8	7.03489E2	7.0349E2	2.34496E0	2.3450E0	2.34494E0	2.3450E0	1.95413E0	1.9541E0

Summary of Options Used

Listed below are the options used in example e8x10.dat:

Parameter Options

ELEMENT
END
SIZING
TITLE

Model Definition Options

CONNECTIVITY
CONTROL
COORDINATE
END OPTION
FIXED DISP
GEOMETRY
HYPOELASTIC

Load Incrementation Options

CONTINUE
DISP CHANGE

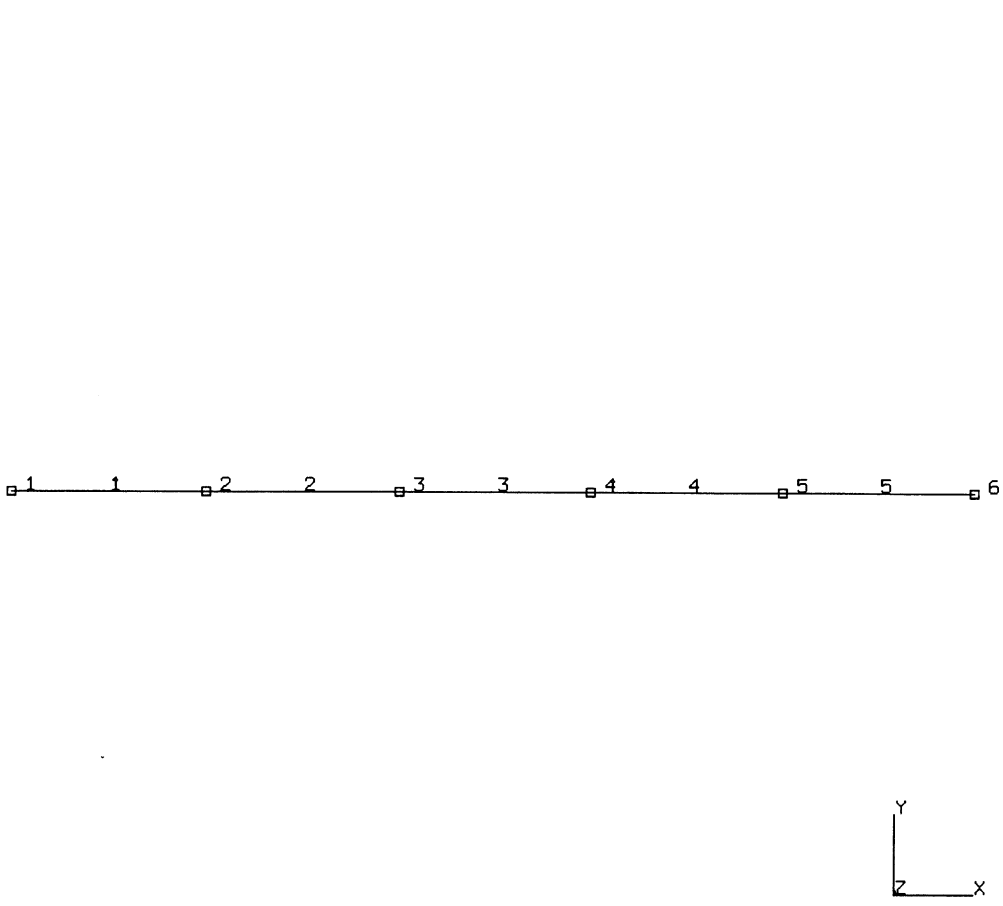

Figure E 8.10-1 Cantilever Beam with Prescribed Tip Displacement

E 8.11 Element Deactivation/Activation And Error Estimate In The Analysis Of A Plate With Hole

The problem of a plate with hole subjected to an in-plane tensile force (problem E 2.9) is analyzed with the options DEACTIVATE, ACTIVATE, and ERROR ESTIMATE. These options allow for the deactivation or activation of elements during the analysis, and the estimation of errors on stress continuity and geometric measures (aspect and skew ratios).

During analysis, after the elements are deactivated, they retain the stress state in effect at the time of deactivation. At a later stage in the analysis, the elements can again be activated with the ACTIVATE history definition option. Elements which were deactivated before analysis will have zero internal stress upon activation. Elements which were used earlier and deactivated during analysis will have an internal stress which is equal to the state when they were deactivated.

The ERROR ESTIMATE option provides information regarding the error associated with the finite element discretization. There are two measures. The first evaluates the stress discontinuity between elements. A large value implies that the stresses gradients are not accurately represented in the finite element mesh.

The second error measure examines geometric distortion in the model. It first examines the aspect ratios and warpage of the elements and in subsequent increments measures how much these ratios change. This measure can be used to indicate the adequacy of the original mesh.

Element

Element type 26 is a second-order, isoparametric two-dimensional element for plane stress. There are eight nodes with two degrees of freedom at each node.

Model

The example uses a coarse mesh for demonstration purposes only. The mesh generated by MARC is shown in Figure E 8.11-1.

Geometry

The plate thickness of one inch is entered in EGEOM1.

Property

Young's modulus is 30 x 10^6 psi, with Poisson's ratio as 0.3. These quantities are sufficient to define the material as isotropic linear-elastic.

Loading

To simulate a tension acting at infinity, a negative 1-psi load is applied to the top edge of the mesh.

FIXED DISP

The boundary conditions are determined by symmetry considerations. No displacement is permitted on the axis of symmetry perpendicular to the applied force direction. On the axis of symmetry parallel to the force direction, only parallel displacements are permitted.

Optimize

The Cuthill-McKee algorithm is chosen in this example. Ten iterations are sufficient to obtain a reasonably optimal bandwidth.

Error Estimates

Both the stress continuity and geometry measures are requested by inputting 1 , 1 , on the second card of this data block.

DEACTIVATE/ACTIVATE

After END OPTION, two DEACTIVATE increments and one ACTIVATE increment are provided for the deactivation of elements 7, 8, 17, 18 at the first increment; elements 9, 10, 19, 20 at the second increment; and the activation of all eight elements at the third increment.

Results

Table E 8.11-1 shows σ_{yy} at element 8, integration point 6 and element 10, integration point 6, at increments 0 through 3. The effects of deactivation/activation of elements are clearly demonstrated. In addition, the stress discontinuity and geometry measures at increment 0 (ERROR ESTIMATE option) are as follows:

WORST ORIGINAL ASPECT RATIO IS 3.343 AT ELEMENT 1
WORST ORIGINAL WARPAGE RATIO IS 1.957 AT ELEMENT 3

WORST CURRENT ASPECT RATIO IS 3.343 AT ELEMENT 1
WORST CURRENT WARPAGE RATIO IS 1.957 AT ELEMENT 3

LARGEST CHANGE IN ASPECT RATIO IS 1.000 AT ELEMENT 7
LARGEST CHANGE IN WARPAGE RATIO IS 1.000 AT ELEMENT 8

GENERALIZED STRESSES

LARGEST NORMALIZED STRESS JUMP IS:
0.11152E 02 AT NODE 17 COMPONENT 1 MEAN VALUE IS 0.28047E-02

LARGEST STRESS JUMP IS:
0.23227E 00 AT NODE 76 COMPONENT 2 MEAN VALUE IS 0.23237E 01

Table E 8.11-1 σ_{yy} vs. Load Increment (DEACTIVATE/ACTIVATE)

Inc. No.	EL 8, INT 6	EL 10, INT 6
0	2.62	1.89
1	2.62 (D)	6.24
2	2.62 (D)	6.24 (D)
3	2.88 (A)	5.68 (A)

(D) – element DEACTIVATED
(A) – element ACTIVATED

Summary of Options Used

Listed below are the options used in example e8x11.dat:

Parameter Options

ELEMENT
END
SIZING
TITLE

Model Definition Options

CONNECTIVITY
COORDINATE
DIST LOADS
END OPTION
ERROR ESTIMATES
FIXED DISP
GEOMETRY
ISOTROPIC
PRINT NODE

Load Incrementation Options

ACTIVATE
CONTINUE
DEACTIVATE

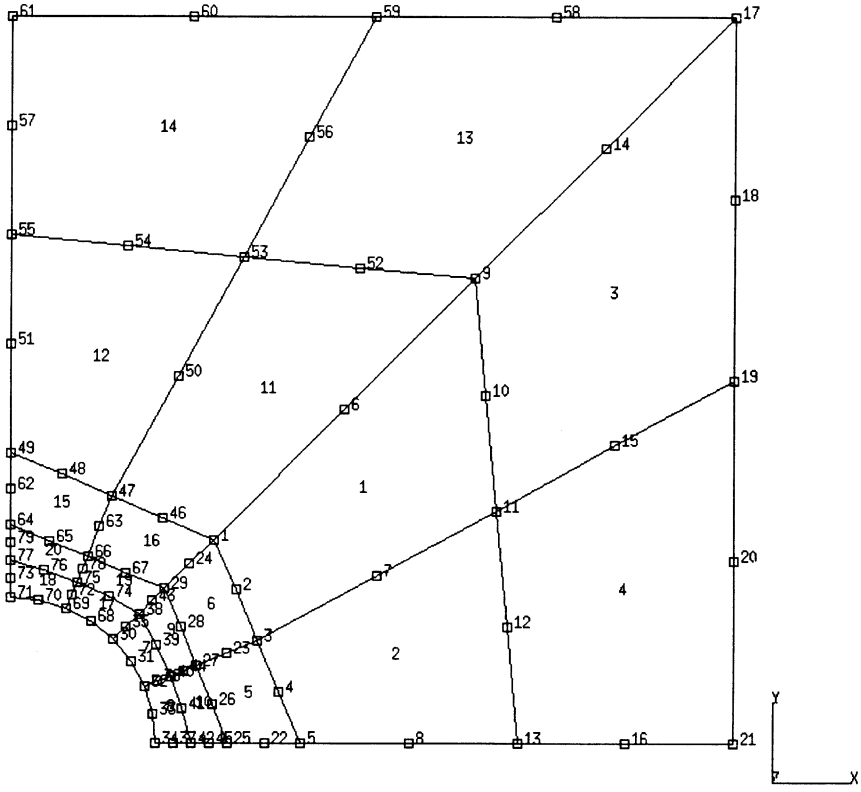

Figure E 8.11-1 Mesh Layout for Plate with Hole

E 8.12 Forging Of The Head Of A Bolt

This example demonstrates the CONTACT capability of the program, using rigid surfaces. An originally cylindrical block is sitting in a surface with the shape of a cavity, and is deformed by another rigid surface which has the shape of the bolt head and moves at constant speed (Figure E 8.12-2). The block is considered an elastic-plastic deformable material.

This problem also exemplifies the REZONING capabilities of the program.

Parameters

The UPDATE, FINITE, and LARGE DISP options are included to trigger a finite deformation analysis. The REZONING card indicates a rezoning step will be done during the analysis. Element 10, a 4-node bilinear axisymmetric element is used. The SIZING option reserves space for 120 elements, 150 nodes and 60 boundary conditions. These amounts are larger than the starting model, so that there is freedom to increase the size of the model upon rezoning. The PRINT,5 card requests printed information on change in contact status of boundary nodes.

Mesh Definition

CONNECTIVITIES and COORDINATES were brought from a pre-processor. The mesh depicted in Figure E 8.12-2 is quite regular over the rectangular block. Due to symmetry, only half of the cylinder needs to be modelled.

No gap elements are used in this problem.

Geometry

A '1' is placed in the second field to indicate that the constant dilatation formulation is used.

Boundary Conditions

Symmetry displacement boundary conditions are applied to all nodes on the axis.

Material Properties

The bolt is treated as an elastic plastic material with a Young's modulus of 17,225., Poisson's ratio of 0.35, mass density of 1., and initial yield stress of 34.45. The material work-hardens from the initial yield stress up to 150 at a strain of 400% according to the piece-wise linear curve entered in WORK HARD DATA.

Control Options

A formatted POST tape is requested every twenty increments, as well a RESTART tape. PRINT CHOICE is used to minimize the amount of output. Convergence CONTROL is done by relative residuals, with a tolerance of 10%.

Contact

This option defines three bodies with no friction between them. The code is expected to determine by itself a contact tolerance. (See Figure E 8.12-1.)

The first body is deformable and is made out of all the elements in the model.

The second body is the top rigid surface, defined by three sets of geometrical entities. It has a reference point along the axis, and is given a translational velocity of 1 parallel to the axis of symmetry. The first geometrical entity is a straight line, the second is a concave arc of a circle, and the third is another straight line. The last line was added so that the top node on the axis would not encounter the end of the rigid surface definition.

The third body is the bottom rigid surface, defined by one set of geometrical entities. It does not need a reference point and is not given any motion. The geometrical entities are three straight lines, defined by four points.

Note how the sequence of entering the geometrical data of the second and third bodies corresponds to following the profiles of such bodies in a counterclockwise direction.

Load Control

The first part of the analysis was performed with a fixed TIME STEP of 0.1 in a sequence of 100 increments.

As an alternative in the second input file, the AUTO TIME option was used to control the time step procedure. The initial time step was 0.1 second and a maximum of 150 steps were allowed to reach a total time of 10 seconds. Only 51 increments were necessary using this procedure.

Rezoning

The next increment performs a rezoning operation. A new mesh was created with a preprocessor, which covers the profile of the previously deformed mesh (Figure E 8.12-3). This mesh is defined by means of CONNECTIVITY CHANGE and COORDINATE CHANGE. Both the number of elements and the number of nodes was increased. The ISOTROPIC CHANGE option was also used to extend material properties to the new elements. Similarly, the CONTACT option was repeated to account for the new element definition of the deformable body; the contact tolerance was decreased because much thinner elements were created.

One increment of deformation, with a TIME STEP of 0.05, was executed then. At this point, it is necessary to include the DISPLACEMENT CHANGE to account for the new node numbers that are located along the axis of symmetry. An extra node at the convex corner of surface 3 was fixed. This was done to allow a very coarse mesh to represent a sharp corner without cutting it.

The rest of the deformation proceeded. Twenty increments with five steps of 0.04 were completed first, followed by seventy increments of time step 0.02. The reason for decreasing the time step is that as the deformation proceeds, the height of the bolt head becomes smaller and a constant movement of the second surface would produce larger and larger strains per increment.

Results

Figure E 8.12-4 through Figure E 8.12-6, show the contour plots of the equivalent plastic strain, the equivalent von Mises stress, and the average stress in the deformed configuration before rezoning. The block completely fills the bottom surface, and is folding into the top surface. The need to rezone stems from the fact that soon thereafter there will be too few nodes in the free surface that has to fit in the narrow gap between the two rigid bodies.

Virtually all the deformation takes place in the part of the block above the bottom surface.

Figure E 8.12-7 through Figure E 8.12-9 show the same contour plots in the final deformed configuration. At this stage, the full shape of the head of the bolt has been acquired by the original block and flash formed in the gap between surfaces. The strains are very concentrated in the part which folded on the bottom surface. The von Mises stress shows that the bottom cavity was elastic at the end of deformation.

The printed results of an analysis with the contact option include general information about rigid surfaces, such as the updated position of the reference point, the velocity of the surface, the loads on the surface, as well as the moment with respect to the reference point.

Summary of Options Used

Listed below are the options used in example e8x12.dat:

Parameter Options

END
FINITE
LARGE DISP
PRINT
REZONE
SIZING
TITLE
UPDATE

Model Definition Options

CONNECTIVITY
CONTACT
CONTROL
COORDINATE
END OPTION
FIXED DISP
GEOMETRY
ISOTROPIC
POST
PRINT CHOICE
RESTART

Load Incrementation Options

AUTO LOAD
DISPLACEMENT CHANGE
COMMENT
CONTINUE
TIME STEP

Listed below are the options used in example e8x12b.dat:

Parameter Options

END
FINITE
LARGE DISP
PRINT
REZONE
SIZING
TITLE
UPDATE

Model Definition Options

CONNECTIVITY
CONTACT
CONTROL
COORDINATE
END OPTION
FIXED DISP
GEOMETRY
ISOTROPIC
POST
PRINT CHOICE
RESTART

Load Incrementation Options

AUTO TIME
CONTINUE

Rezone Options

CONNECTIVITY CHANGE
CONTACT
CONTINUE
COORDINATE CHANGE
END REZONE
ISOTROPIC CHANGE
REZONE

Listed below are the options used in example e8x12r.dat:

Parameter Options

END
FINITE
LARGE DISP
PRINT
REZONE
SIZING
TITLE
UPDATE

Model Definition Options

CONNECTIVITY
CONTACT
CONTROL
COORDINATE
END OPTION
FIXED DISP
GEOMETRY
ISOTROPIC
POST
PRINT CHOICE
REAUTO
RESTART

Load Incrementation Options

AUTO LOAD
COMMENT
CONTINUE
DISP CHANGE
TIME STEP

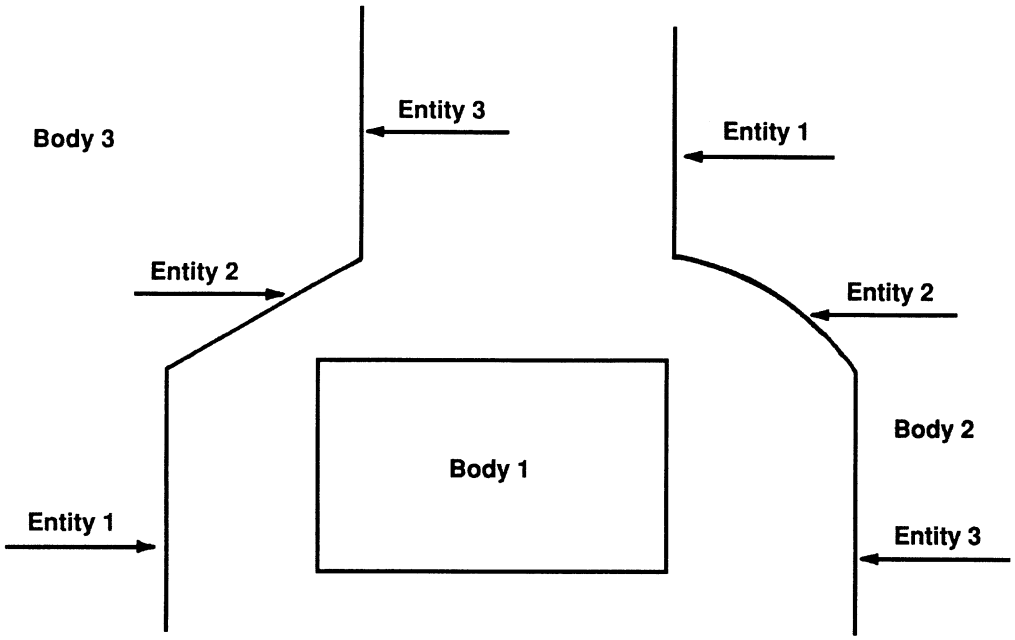

Figure E 8.12-1 Model

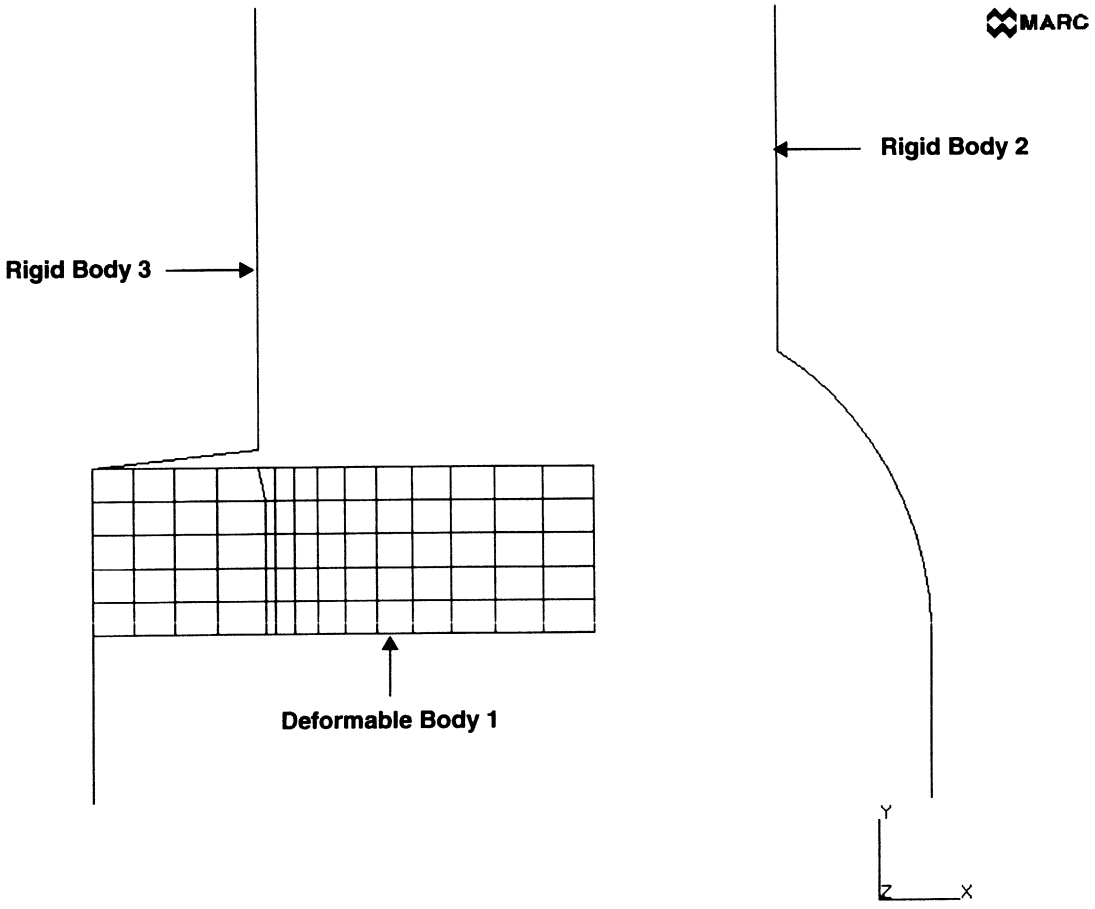

Figure E 8.12-2 Initial Mesh

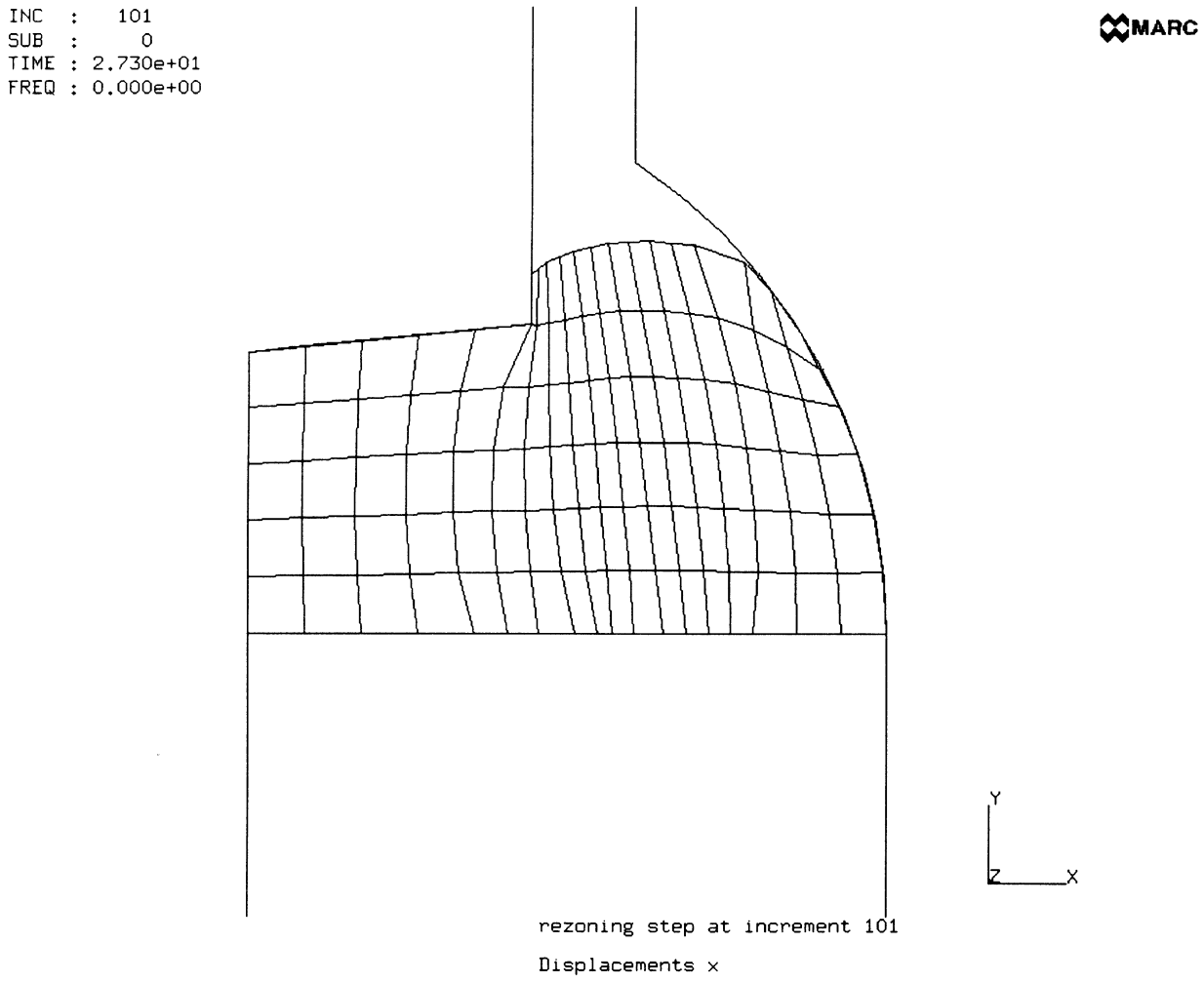

Figure E 8.12-3 Rezoning Mesh

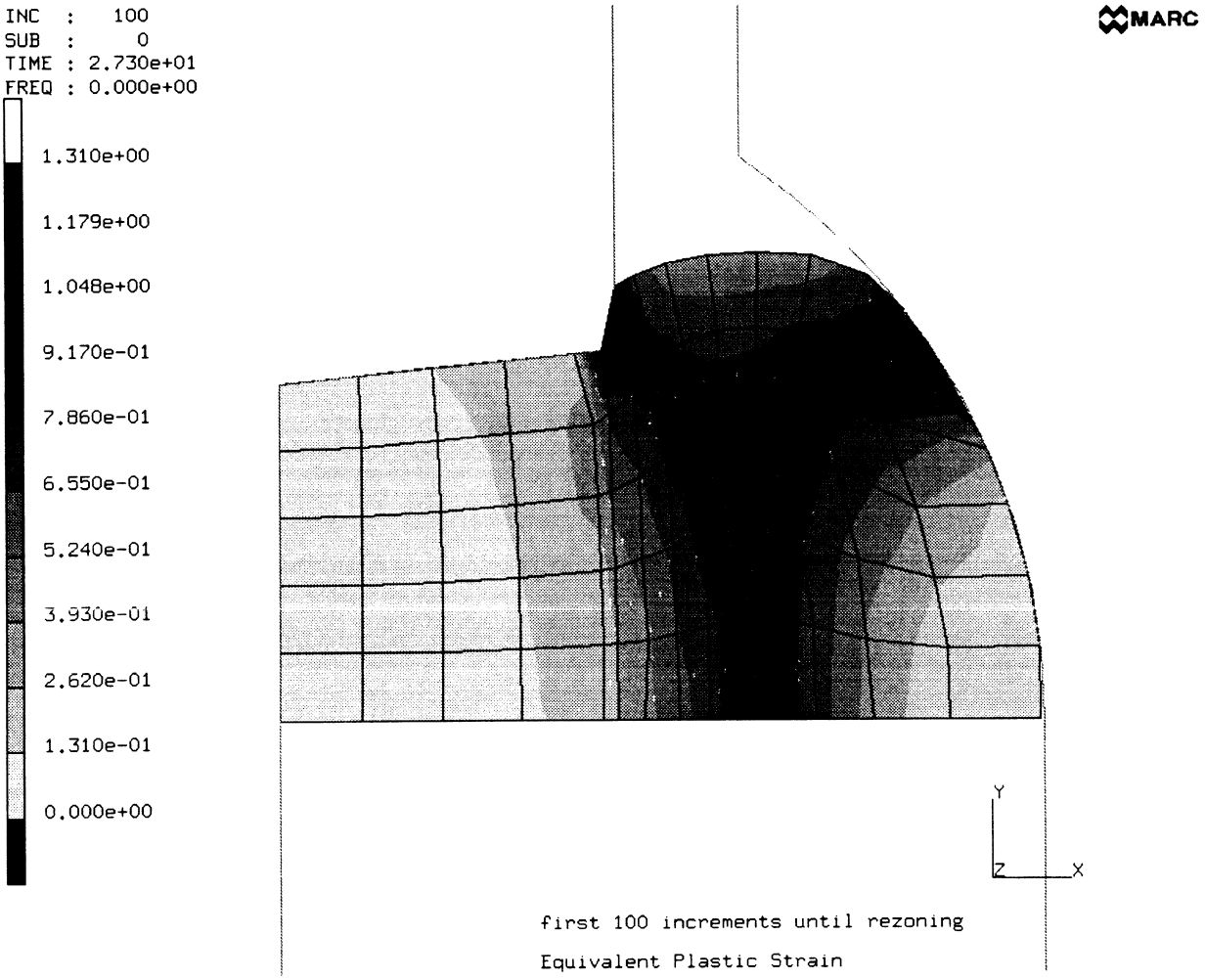

Figure E 8.12-4 Equivalent Plastic Strain until Rezoning

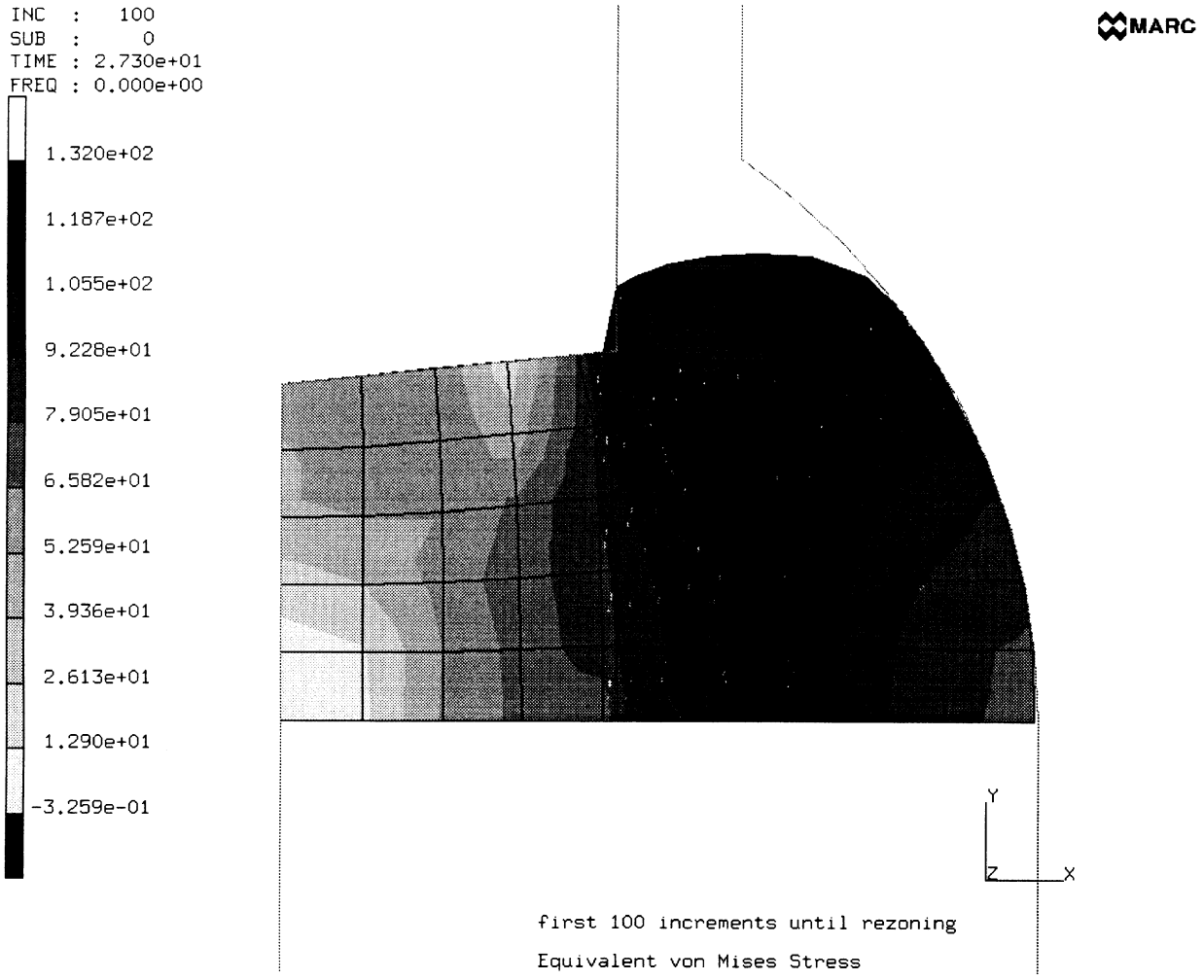

Figure E 8.12-5 Equivalent Mises Tensile Stress Until Rezoning

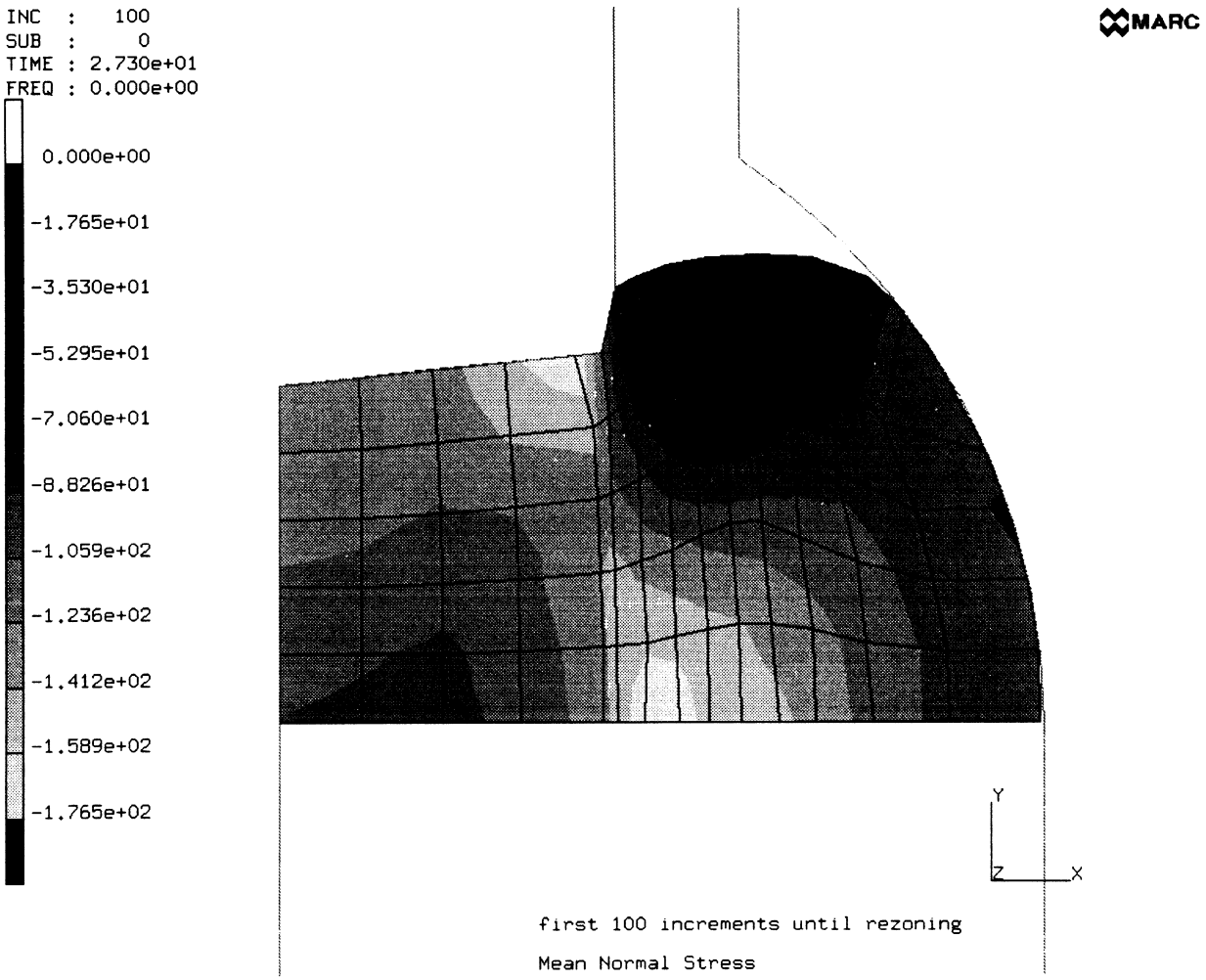

Figure E 8.12-6 Mean Normal Stress Until Rezoning

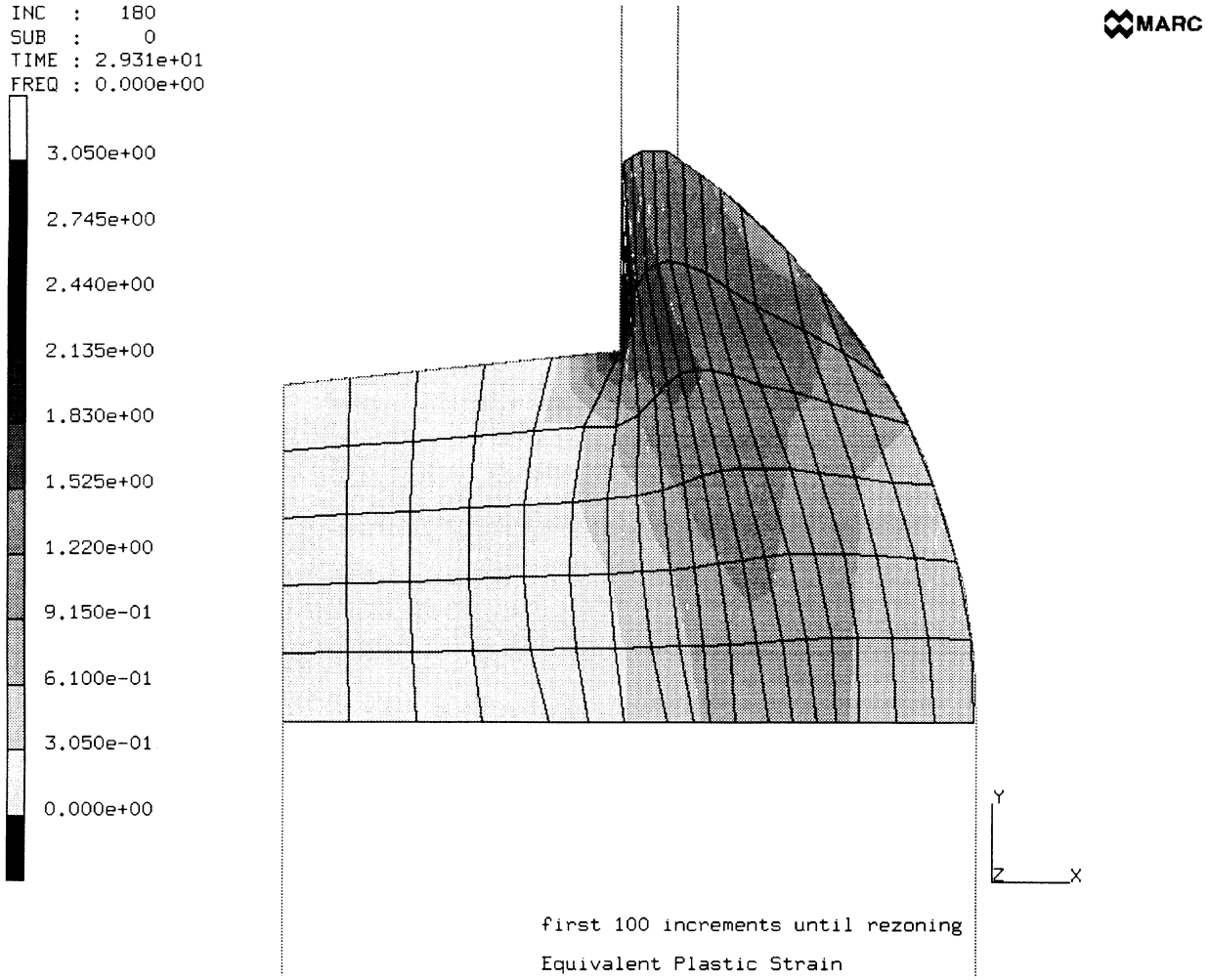

Figure E 8.12-7 Final Equivalent Plastic Strain

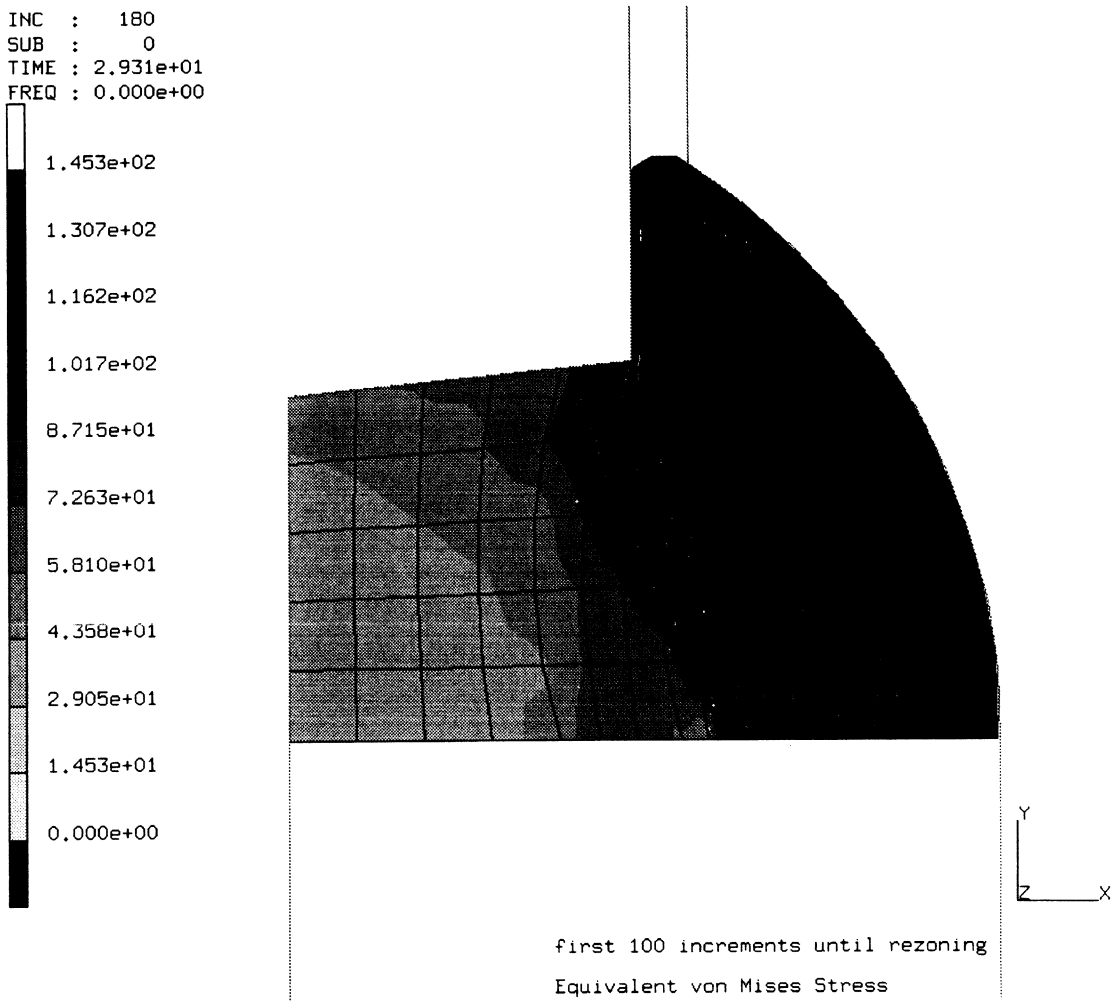

Figure E 8.12-8 Final Equivalent von Mises Tensile Stress

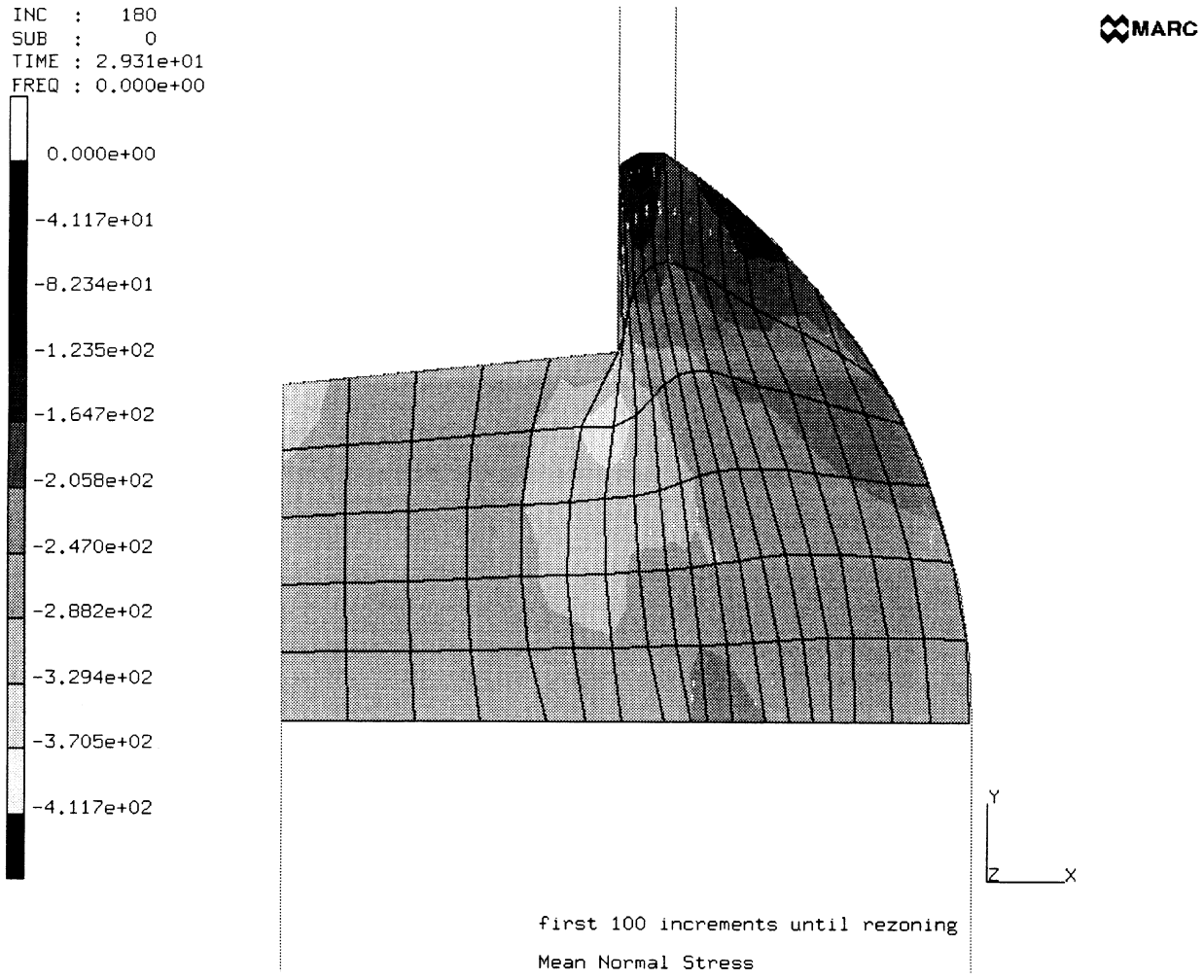

Figure E 8.12-9 Final Mean Normal Stress

E 8.13 Coupled Analysis Of Ring Compression

This example demonstrates the program's ability to perform a large deformation problem, incorporating thermal mechanical coupling and automated contact.

A ring of aluminum is deformed by a block of steel. Both have the capacity to deform, and possibly, slide between each other.

Coupling

There are several sources of coupling in this analysis.

1. As the temperature changes, thermal stresses are developed due to non-zero coefficient of thermal expansion.
2. As the temperature changes, the mechanical properties change. It happens in this case because of the temperature-dependent flow stress.
3. As the geometry changes, the heat transfer problem changes. This includes changes in the contacting interface.
4. As plastic work is performed, internal heat is generated.
5. As the bodies slide, friction generates heat.

Parameters

The UPDATE, FINITE and LARGE DISP options are included in the parameter section to indicate this is a finite deformation analysis.The COUPLE option is used to indicate that a coupled thermal-mechanical analysis is being performed. A four-node bilinear axisymmetric element is used. The PRINT,5 option requests additional information in the output regarding nodes acquiring or losing contact.

Mesh Definition

Mentat was used to determine the CONNECTIVITY and COORDINATES of the mesh. There are separate nodes along both sides of the contact interface so that sliding is possible. Due to symmetry, only one quarter of the region is modeled. The mesh is shown (with the units in mm) in Figure E 8.13-1. In a coupled analysis, a displacement element automatically produces the coupled (displacement-temperature) formulation to be used.

This analysis is performed using both element type 10 and element type 116. Both elements are four-node axisymmetric elements. Element type 116 uses a single integration point and an hourglass stiffness stabilization procedure.

No gap elements are used. Free surfaces may have convection heat transfer to the environment. As soon as contact is detected, a contact thermal barrier, defined by means of a film coefficient, starts operating.

Geometry

A "1" is placed in the second field to indicate that the constant dilatation formulation is used. This is not necessary for the analysis using element type 116.

Boundary Conditions

Symmetry displacement boundary conditions are imposed on the ring meridian plane and on the block axis. The block is moved down by application of displacement boundary conditions to the face opposite to the contact face. Space for such boundary conditions is reserved in the model definition section. The displacement boundary conditions are entered in the FIXED DISPLACEMENT option. On the outside surface of the block, the temperature is constrained to 20°C, to simulate a much larger size block. This is done with the FIXED TEMPERATURE option.

Control Options

A formatted POST tape containing stress components and effective plastic strain is written at the end of 50 increments. The NO PRINT option limits the amount of output to a minimum. Displacement control is used in the deformation part of the analysis, with a relative error of 15%. As far as the heat transfer part of the analysis is concerned, a 10°C maximum error in temperature estimate is entered. Even if thermal material properties are not temperature-dependent, this provides a means of forcing recycling when heat transfer between two bodies produces large variations of temperature per increment.

Initial Conditions

The ring is given an initial temperature of 427°C, and the block is given an initial temperature of 20°C.

Material Properties

The ring is treated as an elastic-plastic material with a Young's modulus of 1000 N/mm^2, a Poisson's ratio of 0.33, a mass density of 1.0g/mm^3, a coefficient of thermal expansion of 1.3 x 10^{-5} mm/mm°C, and an initial yield stress of 3.4 N/mm^2, corresponding to a reference temperature of 200°C. The material work-hardens from the initial yield stress to a yield stress of 5.78 N/mm^2 for strains above 70%, according to a piecewise linear function entered via WORK HARD DATA. The flow stress decreases with temperature increases at a rate of 0.007 N/mm^2 per degree. The thermal properties are conductivity of 242.0 N/s°C and specific heat of 2.4255 Nmm/g°C.

The block is treated as an elastic material with a Young's modulus of 100,000 N/mm^2, a Poisson's ratio of 0.33 and a mass density of 1 g/mm^3. The thermal properties are conductivity of 19.0 N/s°C and specific heat of 3.77 Nmm/g°C.

Distributed Flux

This distributed flux block is used to indicate that internal heat is generated due to plastic deformation.

Convert

The option is used to give the conversion factor between the mechanical energy and the thermal energy.

The internal volumetric flux per unit volume becomes:

$$\phi = cw^p$$

where w^p is the plastic strain energy density.

Contact

This option declares that there are two bodies with adhesive friction between them. The program calculates both the contact tolerance and the sticking tolerance.

The first body is deformable, and is made of the elements of the ring. There is no need to specify any motion. The ring's free surfaces have convection heat transfer defined by a film coefficient of 0.01, and a sink temperature of 20°C. The second body is also deformable, made out of the elements of the block. A reference point and an axial velocity are given, although they are not used in the calculations; this was done as a reminder of what the imposed boundary conditions are simulating. A friction factor of 1.0 defines the interface friction conditions, based on the cohesive model. The block's free surfaces have convection heat transfer defined by a film coefficient of 0.01 N/s-mm°C, and a sink temperature of 20°C. The contact surfaces have a thermal barrier defined by a film coefficient of 35.

This ordering of the two bodies results in imposing the constraint that the nodes of the ring do not penetrate the surface of the block. Friction and thermal barrier at the interface use data taken from the body defining the block.

Load Control

This problem is performed with a fixed time step and fixed increment size. It is specified with a time step of 0.0003 seconds, with a total of 0.03 seconds requested. Each increment imposes a displacement of 0.045mm to the nodes of the block in the plane opposed to the contact surface. This displacement increment is declared in DISP CHANGE and not in the original boundary conditions because the CONTACT option always bypasses increment zero.

In a coupled analysis, if an adaptive time stepping is required, the AUTO TIME option should be invoked. This option is demonstrated in the second analysis. Using AUTO TIME, it is requested that a maximum of 100 increments be used. The analysis used only 26 increments as there are very few changes in the contact surface.

Results

Figure E 8.13-2 shows the deformed body at the end of 100 increments compounding to 50% reduction in height of the ring. Due to the high friction, the ring folds several times into the block on both sides, and there is an increase of the outer diameter as well as a decrease of the inner diameter. It can be seen that the amount of interface sliding is very small, also due to the high friction. Elastic deformations on the block are not visible, therefore it looks like the block had a rigid body translation.

Figure E 8.13-3 shows equivalent plastic strain contours produced on the ring. They range from small amounts in the middle of the contact area (neutral zone) and in the free surface, to very large amounts at the corners where folding took place, and in the center of the middle plane.

In Figure E 8.13-4, the equivalent von Mises stresses give an idea of the stresses produced in the block, which are higher than in the ring. They increase from low values in the free standing areas towards the center. Local peaks in the friction shearing zones also appear.

The thermal part of the analysis produces the temperatures of Figure E 8.13-5. The total time for the deformation is only 0.03 seconds. Therefore, all the effects are confined to the contact region. Aluminum's high temperature, low flow stress produces no noticeable heating due to plastic deformation. On the ring side, the temperature decreases about 75°C at the interface, while the block heats around 50°C. Steel's lower conductivity produces steeper temperature gradients.

Summary of Options Used

Listed below are the options used in example e8x13.dat:

Parameter Options

COUPLE
ELEMENT
END
FINITE
LARGE DISP
PRINT
SIZING
TITLE
UPDATE

Model Definition Options

CONNECTIVITY
CONTACT
CONTROL
CONVERT
COORDINATE
DIST FLUXES
END OPTION
FIXED DISP
FIXED TEMPERATURE
GEOMETRY
INITIAL TEMPERATURE
ISOTROPIC
NO PRINT
POST
TEMPERATURE EFFECTS
WORK HARD

Load Incrementation Options

CONTINUE
DISP CHANGE
TRANSIENT

Listed below are the options used in example e8x13b.dat:

Parameter Options

COUPLE
ELEMENT
END
FINITE
LARGE DISP
PRINT
SIZING
TITLE
UPDATE

Model Definition Options

CONNECTIVITY
CONTACT
CONTROL
CONVERT
COORDINATE
DIST FLUXES
END OPTION
FIXED DISP
FIXED TEMPERATURE
GEOMETRY
INITIAL TEMPERATURE
ISOTROPIC
NO PRINT
POST
TEMPERATURE EFFECTS
WORK HARD

Listed below are the options used in example e8x13c.dat:

Parameter Options

ALIAS
COUPLE
ELEMENT
END
FINITE
LARGE DISP
PRINT
SIZING
TITLE
UPDATE

Model Definition Options

CONNECTIVITY
CONTACT
CONTROL
CONVERT
COORDINATE
DIST FLUXES
END OPTION
FIXED DISP

FIXED TEMPERATURE
GEOMETRY
INITIAL TEMPERATURE
ISOTROPIC
NO PRINT
POST
TEMPERATURE EFFECTS
WORK HARD

Load Incrementation Options

CONTINUE
DISP CHANGE
TRANSIENT

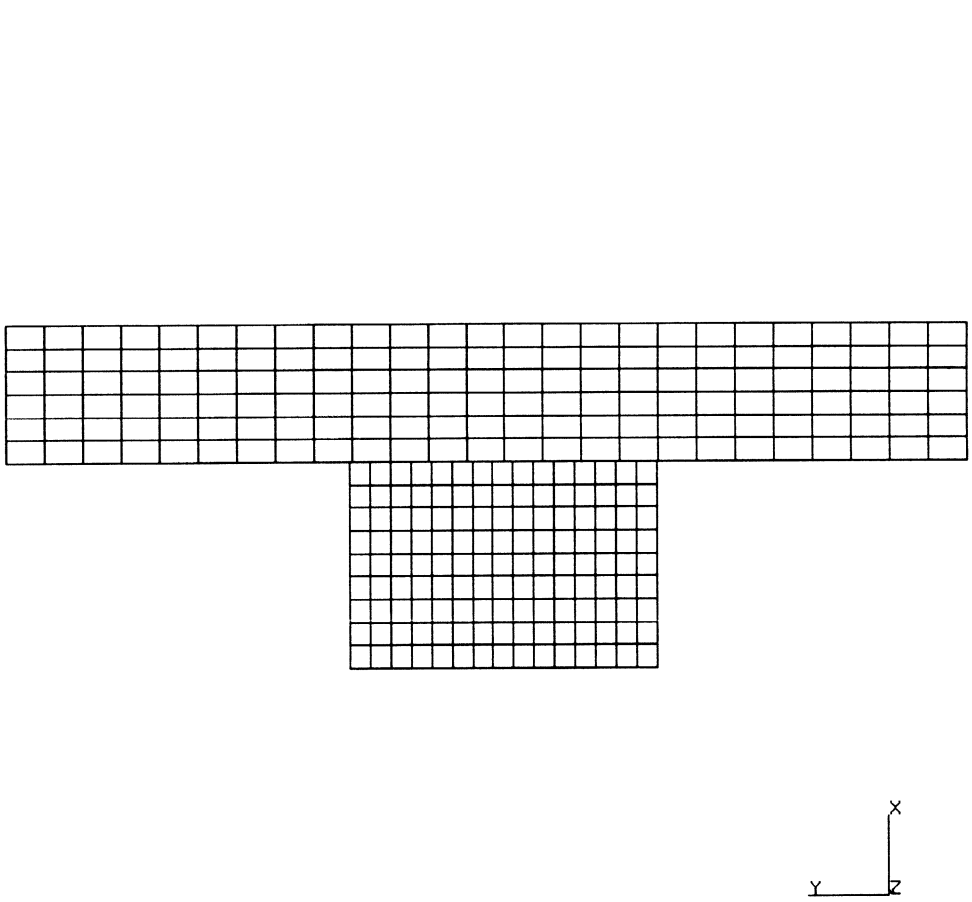

Figure E 8.13-1 Original Mesh

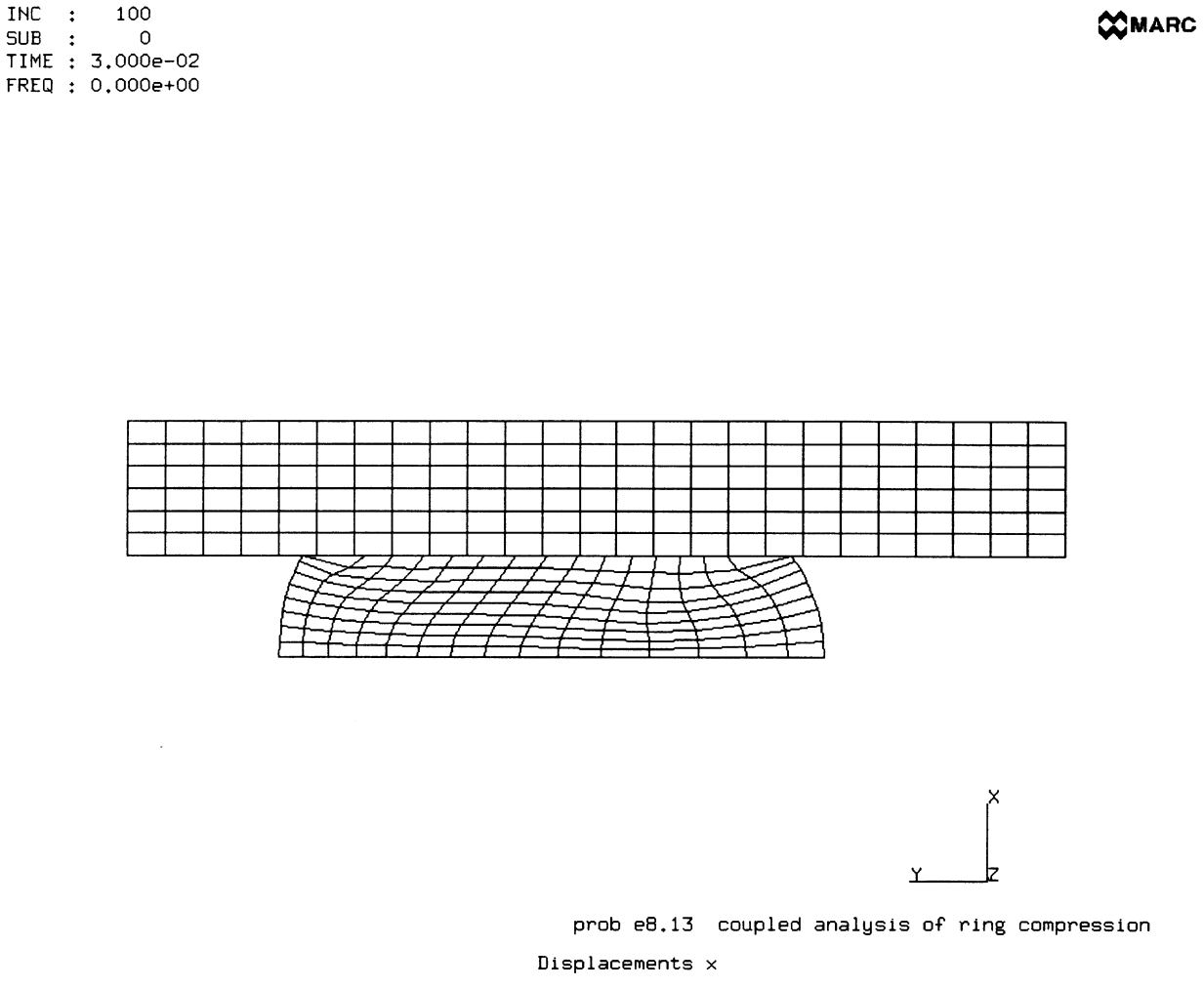

Figure E 8.13-2 Deformed Mesh (50% Height Reduction)

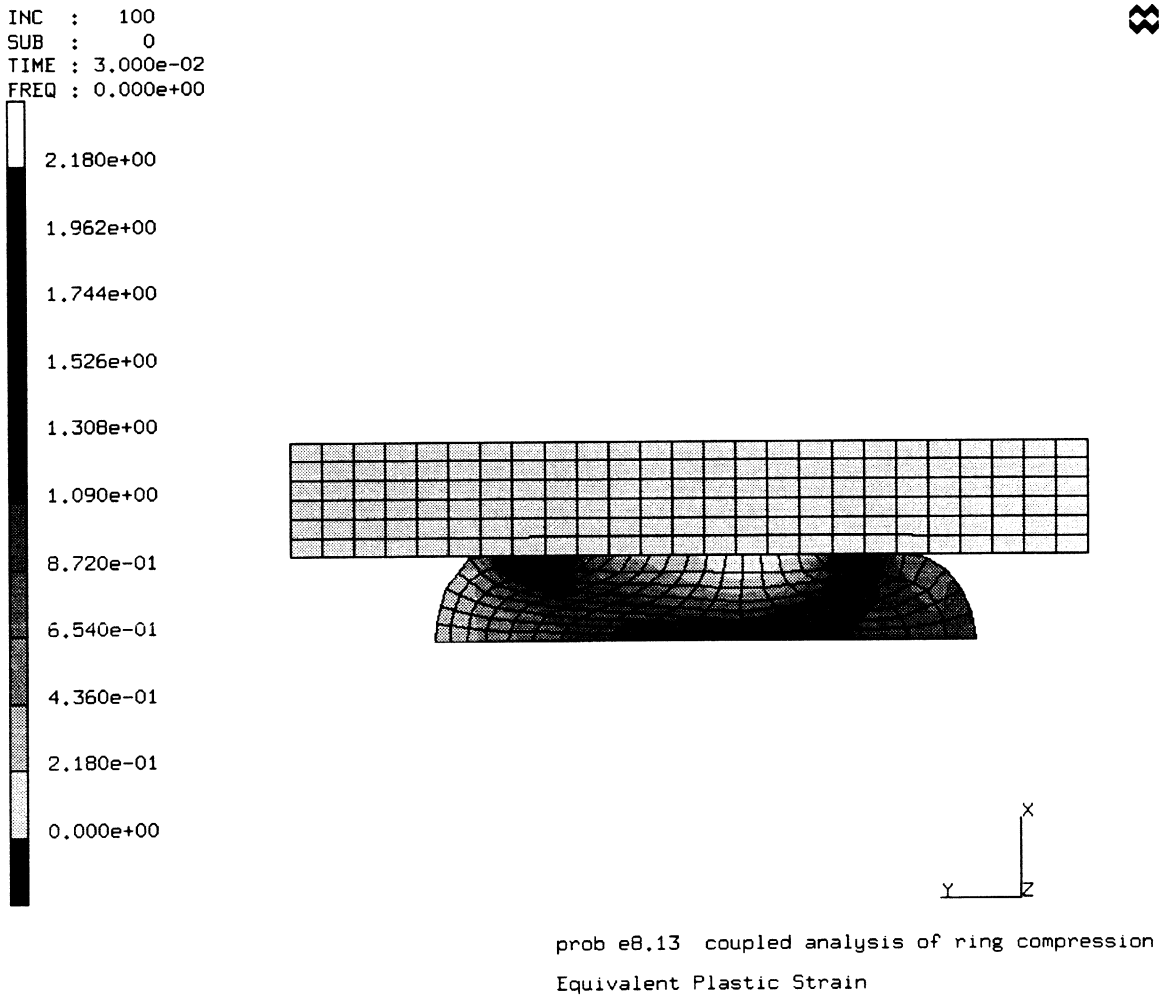

Figure E 8.13-3 Equivalent Plastic Strain

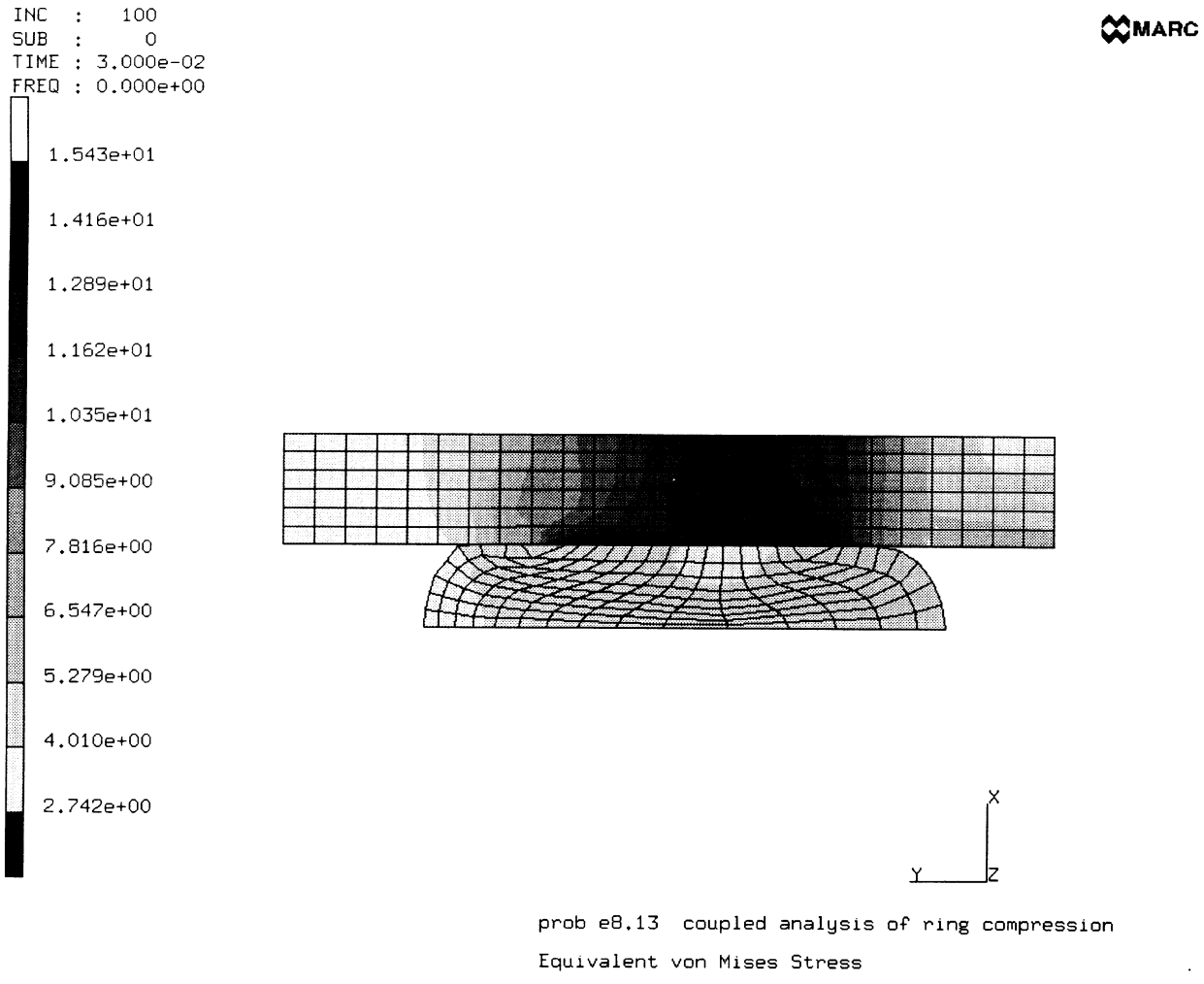

Figure E 8.13-4 Equivalent von Mises Tensile Stress

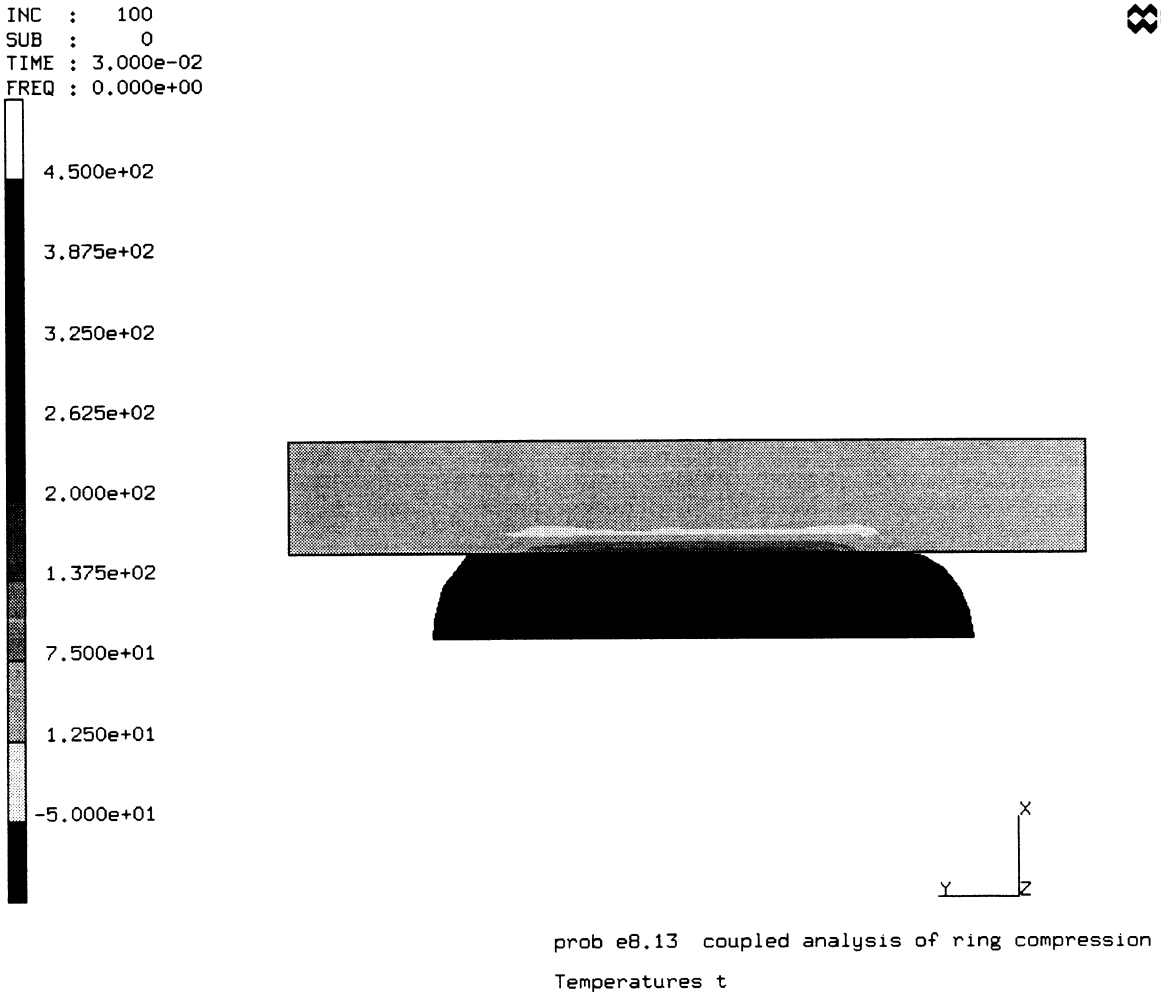

Figure E 8.13-5 Total Nodal Temperature

E 8.14 3D Contact With Various Rigid Surface Definitions

This problem demonstrates the program's ability to perform contact analysis between a deformable body and a rigid die described through various surface definitions.

Parameters

The UPDATE, FINITE and LARGE DISP options are included in the parameter section to indicate that this is a finite deformation analysis. The PRINT,5 option requests additional information in the output regarding nodes acquiring or losing contact.

Geometry

A "1" is placed in the second data field to indicate that the constant dilatation formulation is used. This is particularly useful for analysis of approximately incompressible materials and for structures in the fully plastic range.

Boundary Conditions

To prevent rigid body motions, several nodes are restrained from displacing in the global X,Y,Z directions. These constraints are given through the FIXED DISP option.

POST/PRINT Control

It is requested that the E_{xx} strain (POST code 1) be written onto a formatted POST file. The NO PRINT option limits the amount of printed output to a minimum.

Control

A maximum of two hundred increments is allowed, with no more than 20 recycles per increment. Displacement control is used, with a relative error of 10%. However, keep in mind that control parameters under the CONTACT option set will generally govern the convergence of the problem.

Material Properties

The material for all elements is treated as an elastic-perfectly plastic material, with Young's modulus of 1.75E+07 psi, Poisson's ratio of .3, and an initial yield stress of 35,000 psi.

Contact

This option declares that there are two bodies in contact with no friction between them. The distance tolerance is specified as 0.005 inches. The reaction and velocity tolerances will be computed by the program. A die velocity of -0.3 inches/sec in the global Z-direction constitutes the driving motion for this problem.

Load Control

This problem is loaded by the application of number of increments specified in the AUTO LOAD option of the prescribed die velocities in the CONTACT option. The load increment will be applied once.

Die Surface Definitions

The only difference between problems e8x14a, b, c, d, e is the type of surface defined for the rigid die. In data set 14a, it is a 3D ruled surface with straight line generators. In 14b, it is again a ruled surface with circular arc generators. In 14c, it is a surface of revolution. In 14d, it is a 4-node patch. Finally, in 14e, a 3D poly-surface defines the rigid die.

Results

Figure E 8.14-2 shows the deformed body at the end of increment one with the deformation at the same scale as the coordinates.

Summary of Options Used

Listed below are the options used in example e8x14a.dat:

Parameter Options

ELEMENT
END
FINITE
LARGE DISP
PRINT
SIZING
TITLE
UPDATE

Model Definition Options

CONNECTIVITY
CONTACT
CONTROL
COORDINATE
END OPTION
FIXED DISP
GEOMETRY
ISOTROPIC
NO PRINT
POST

Load Incrementation Options

AUTO LOAD
CONTINUE
TIME STEP

Listed below are the options used in example e8x14b.dat:

Parameter Options

ELEMENT
END
FINITE
LARGE DISP
PRINT
SIZING
TITLE
UPDATE

Model Definition Options

CONNECTIVITY
CONTACT
CONTROL
COORDINATE
END OPTION
FIXED DISP
GEOMETRY
ISOTROPIC
NO PRINT
POST

Load Incrementation Options

AUTO LOAD
CONTINUE
TIME STEP

Listed below are the options used in example e8x14c.dat:

Parameter Options

ELEMENT
END
FINITE
LARGE DISP
PRINT
SIZING
TITLE
UPDATE

Model Definition Options

CONNECTIVITY
CONTACT
CONTROL
COORDINATE
END OPTION
FIXED DISP
GEOMETRY
ISOTROPIC
NO PRINT
POST

Load Incrementation Options

AUTO LOAD
CONTINUE
TIME STEP

Listed below are the options used in example e8x14d.dat:

Parameter Options

ELEMENT
END
FINITE
LARGE DISP
PRINT
SIZING
TITLE
UPDATE

Model Definition Options

CONNECTIVITY
CONTACT
CONTROL
COORDINATE
END OPTION
FIXED DISP
GEOMETRY
ISOTROPIC
NO PRINT
POST

Load Incrementation Options

AUTO LOAD
CONTINUE
TIME STEP

Listed below are the options used in example e8x14e.dat:

Parameter Options

ELEMENT
END
FINITE
LARGE DISP
PRINT
SIZING
TITLE
UPDATE

Model Definition Options

CONNECTIVITY
CONTACT
CONTROL
COORDINATE
END OPTION
FIXED DISP
GEOMETRY
ISOTROPIC
NO PRINT
POST

Load Incrementation Options

AUTO LOAD
CONTINUE
TIME STEP

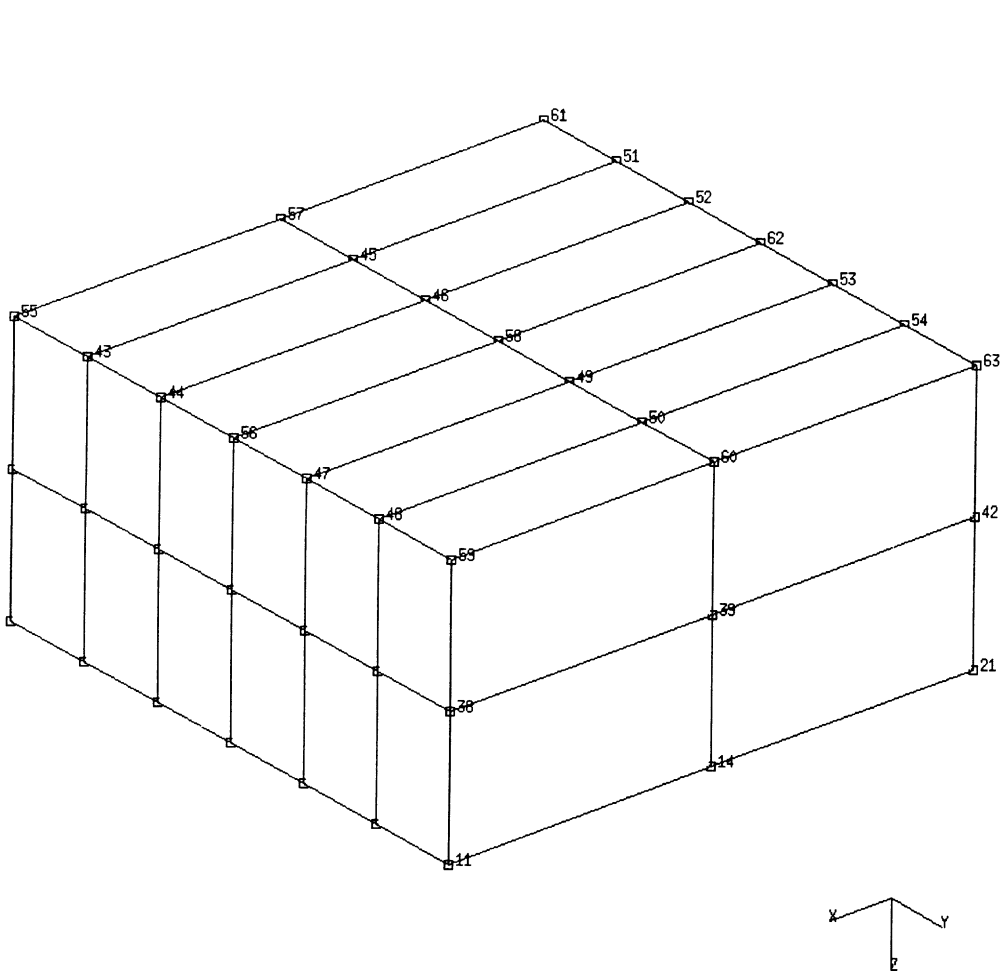

Figure E 8.14-1 Undeformed Block

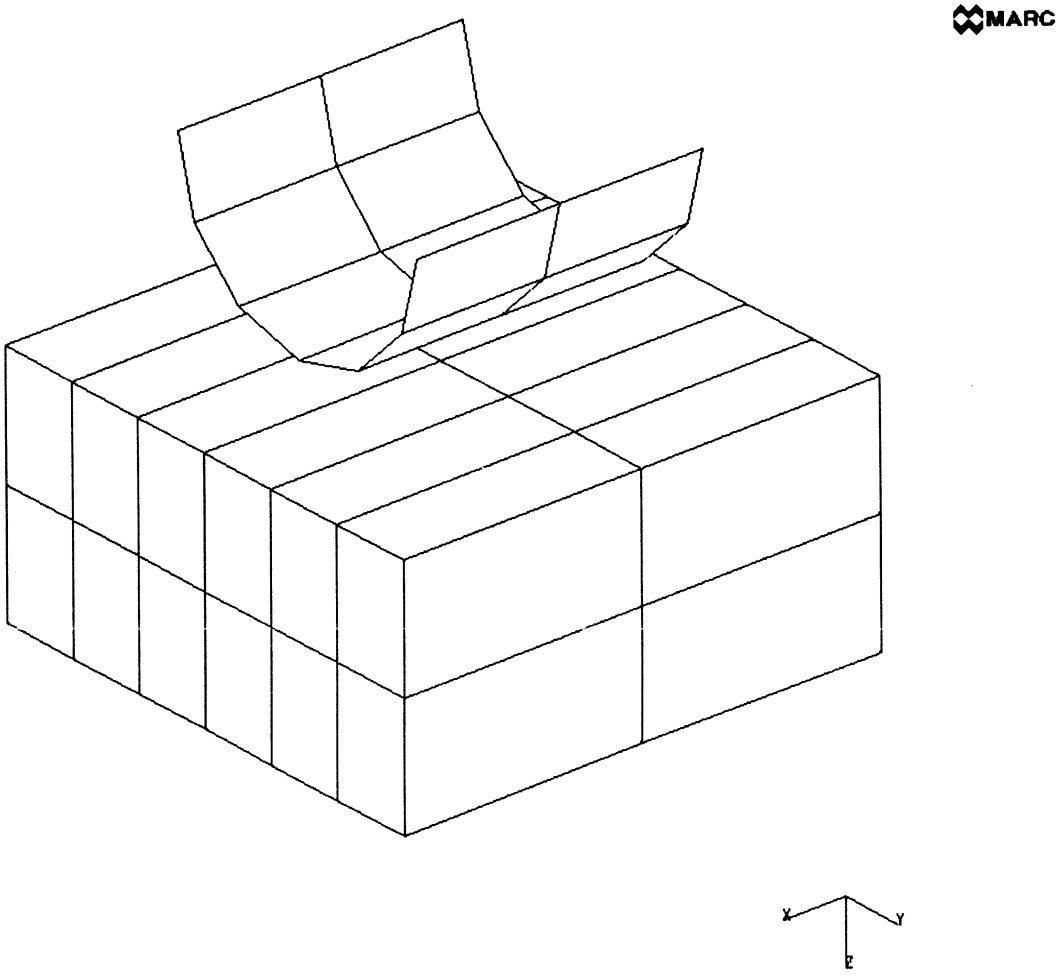

Figure E 8.14-2 Block and Indentor

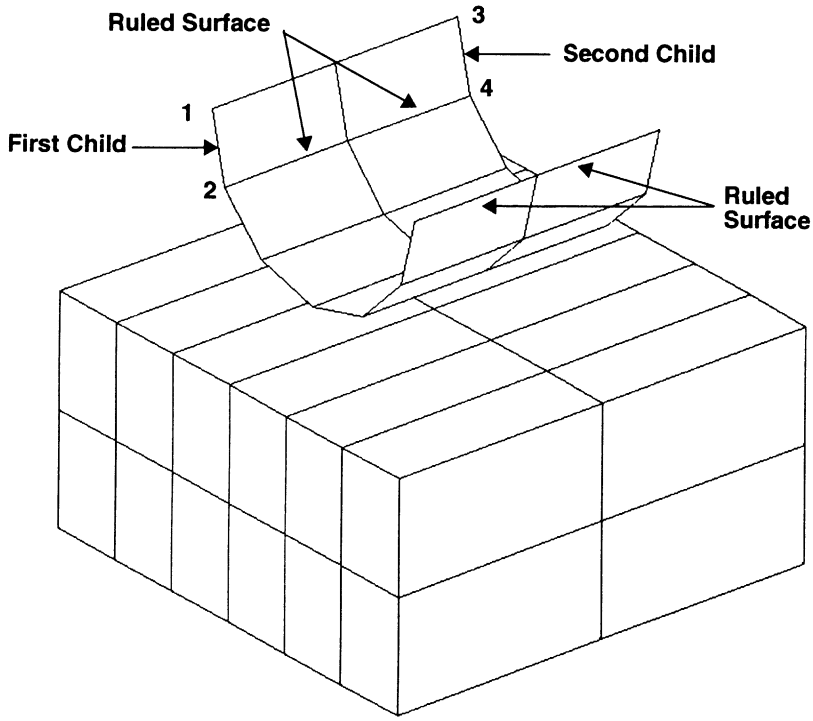

(a) Straight Line Generator

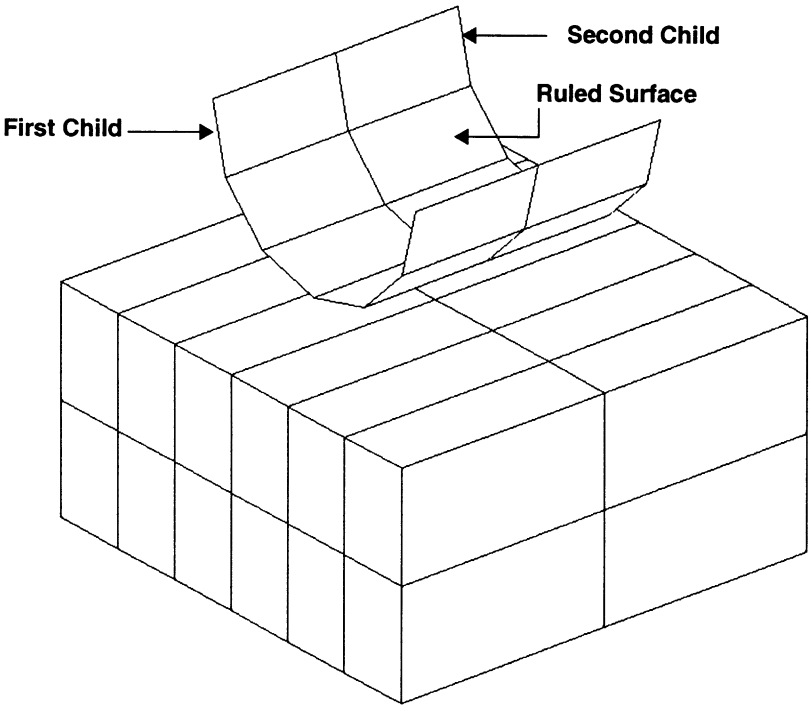

(b) Circular Arc Generator

Figure E 8.14-3 Ruled Surface

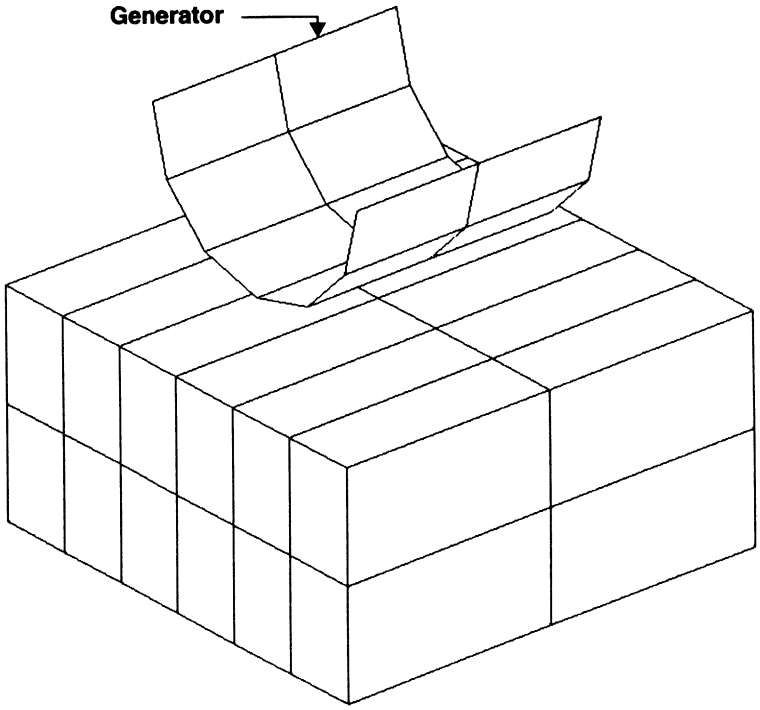

(c) Surface of Revolution

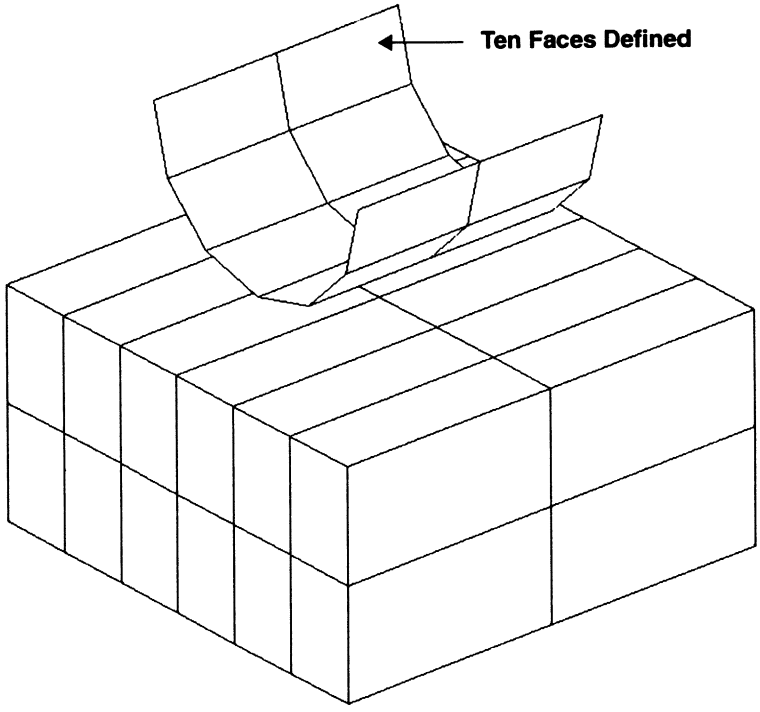

(d) Four Node Patches

Figure E 8.14-3 Ruled Surface (Continued)

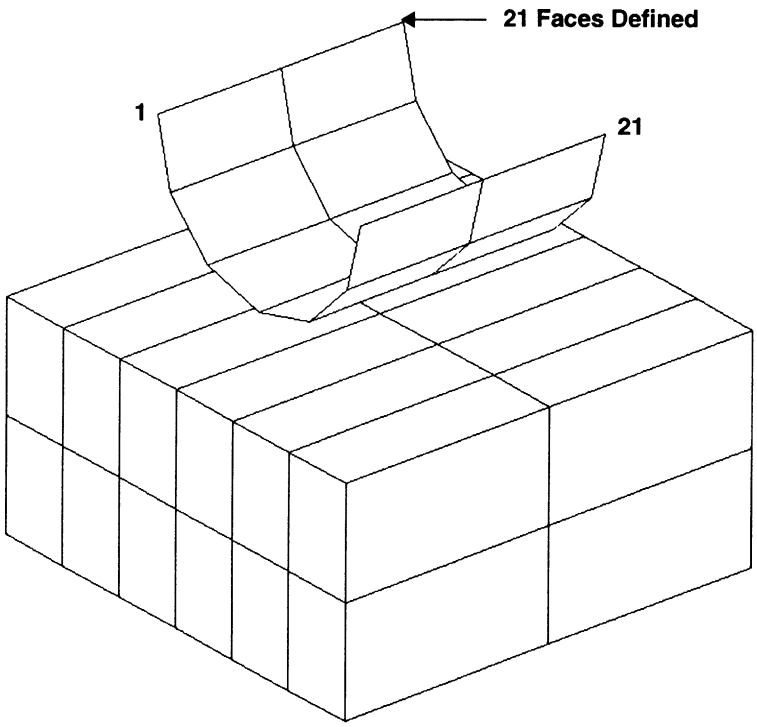

(d) Poly Surface

Figure E 8.14-3 Ruled Surface (Continued)

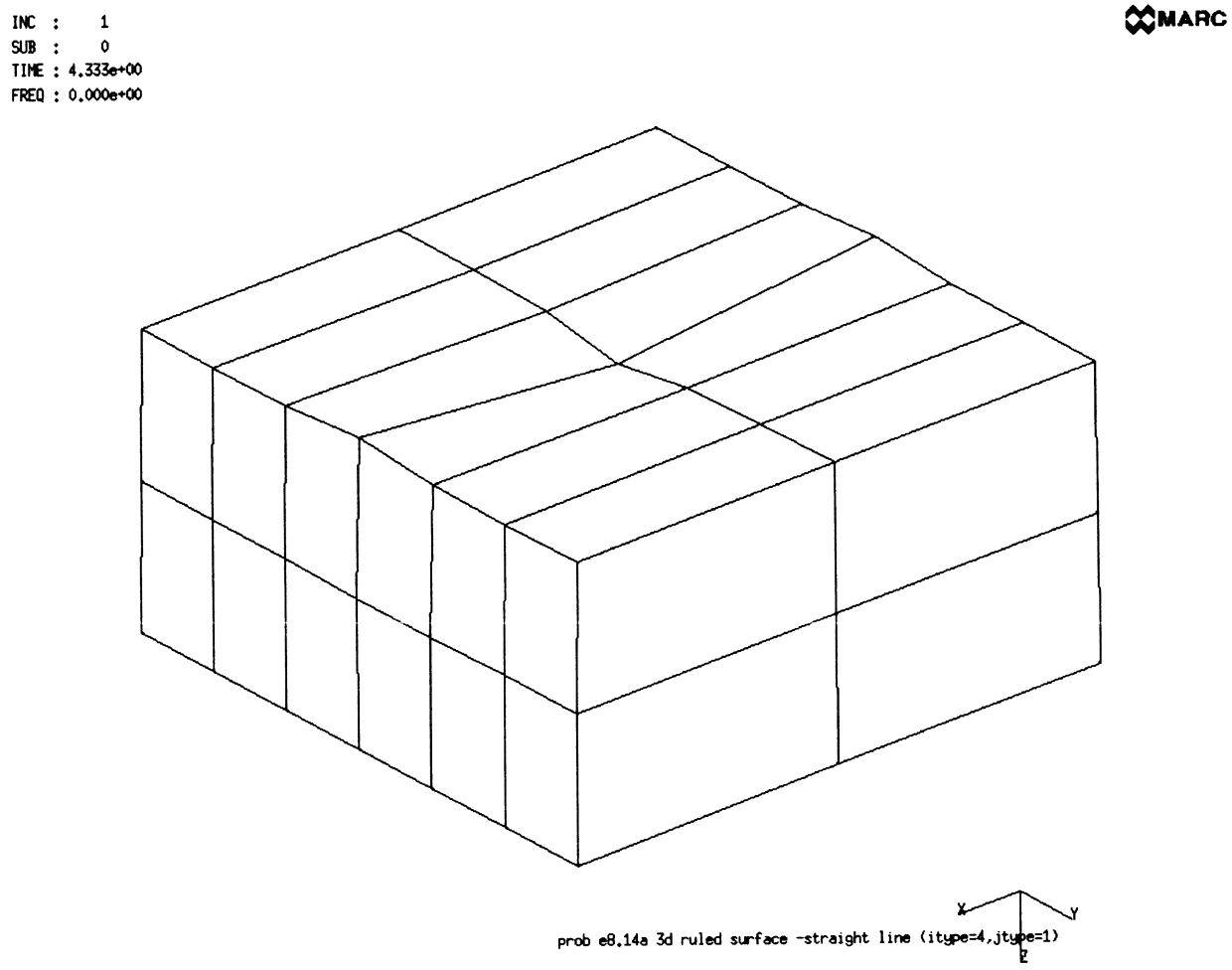

Figure E 8.14-4 Deformed Block

E 8.15 Double-Sided Contact

This problem demonstrates the program's ability to perform multibody contact, incorporating automated double-sided contact with friction between the contact surfaces for linear and parabolic elements. It is not necessary to assign any body as a master or slave.

Parameters

The UPDATE, FINITE and LARGE DISP options are included in the parameter section to indicate that this is a finite deformation analysis. The PRINT,5 option requests additional information in the output regarding nodes acquiring or losing contact.

Elements

Element types 11 and 27 are plane strain quadrilaterals with 4 and 8 nodes respectively.

Mesh Definition

Mentat was used to determine the CONNECTIVITY and COORDINATES of the mesh. The mesh is shown (with the units in inches) in Figure E 8.15-1. In a contact analysis, double sided contact is automatically checked during this deformation.

Geometry

A "1" is placed in the second data field to indicate that the constant dilatation formulation is used. This is particularly useful for analysis of approximately incompressible materials and for structures in the fully plastic range. The 1.0 placed in the first data filed indicates the thickness of 1 inch.

Boundary Conditions

The nodes on the top surface (y = 3) are moved uniformly downward. The left (x = 0) and bottom (y = 0) side are constrained.

Material Properties

The material for all elements is treated as an elastic-plastic material, with Young's modulus of 31.75E+06 psi, Poisson's ratio of 0.268, a mass density of 7.4E-04 lbf-sec^2/in^4, a coefficient of thermal expansion of 5.13E-06 in/(in-deg F), corresponding reference temperature of 70°F, and an initial yield stress of 80,730 psi. The material work-hardens from the initial yield stress to a final yield stress of 162,747 psi at a strain of 1.0 in the WORK HARD DATA block.

Contact

This option declares that there are two bodies in contact with adhesive friction between them. The relative ship velocity is defined as 0.01 in/sec. The contact tolerance distance is 0.01 inches. The coefficient of friction associated with each body is 0.7. The reaction tolerance will be computed by the program.

The CONTACT TABLE is used to indicate that body 1 will potentially come in contact with body 2. As there are only two bodies, this would be the default anyway. Also the CONTACT NODE option is used to only check contact for the corner nodes for the parabolic element, type 27.

Load Control

This problem is loaded by the repeated application of the load increment created by the prescribed boundary conditions in the AUTO LOAD option. The load increment will be applied 20 times. The TIME STEP option allows the user to enter the time variable for static analysis. All contact analyses are time driven and require the definition of a time step. A formatted POST tape containing the equivalent plastic strain, the first two stress components, von Mises equivalent stress, and the mean normal stress. The NO PRINT option limits the amount of printed output to a minimum. Displacement control is used, with a relative error of 20%. The RESTART LAST option is used to save the last increment of data if a later restart is required.

Results

Figure E 8.15-1 shows the original mesh with the elements labeled of double-sided contact problem for both element types. Figure E 8.15-2 and Figure E 8.15-3 respectively show the nodal labels for element types 11 and 27. Figure E 8.15-4, Figure E 8.15-5, and Figure E 8.15-6 show the deformed body at the end of 10, 20 and 30 increments with the deformation at the same scale as the coordinates. Figure E 8.15-8, Figure E 8.15-9, and Figure E 8.15-10 show the deformed body at the end of 10, 20 and 30 increments for element type 27. Due to the high level of friction, significant transverse deformation is shown along the contact surfaces. Figure E 8.15-7 and Figure E 8.15-11 show the equivalent plastic strain at the end of increment 30. The peak values of equivalent plastic strain is 137% and 151% for element types 11 and 27, respectively. The additional degrees of freedom in the model using element type 27 makes the structure more flexible. The larger plastic strain found for the higher degrees of freedom model is on the high side of convergence tolerance.

A user written subroutine, IMPD, is used in conjunction with the UDUMP model definition option to sum the nodal loads across the y = 3 (top) surface and print the nodal load and displacement for each increment into the output file. This information is plotted and shown in Figure E 8.15-12 for both element types. The overall force-displacement behavior of the two element types is in good agreement with all differences occurring in the early portion of the contact.

Summary of Options Used

Listed below are the options used in example e8x15.dat:

Parameter Options

ELEMENT
END
FINITE
LARGE DISP
PRINT
SIZING
TITLE
UPDATE

Model Definition Options

CONNECTIVITY
CONTACT
CONTACT TABLE
CONTROL
COORDINATE
DEFINE
END OPTION
FIXED DISP
GEOMETRY
ISOTROPIC
NO PRINT
POST
RESTART LAST
WORK HARD

Load Incrementation Options

AUTO LOAD
CONTINUE
TIME STEP

Listed below are the options used in example e8x15b.dat:

Parameter Options

ELEMENT
END
FINITE
LARGE DISP
PRINT
SETNAME
SIZING
TITLE
UPDATE

Model Definition Options

CONNECTIVITY
CONTACT
CONTACT NODE
CONTACT TABLE
CONTROL
COORDINATE
DEFINE
END OPTION
FIXED DISP
GEOMETRY
ISOTROPIC
NO PRINT
OPTIMIZE
POST
RESTART LAST
WORK HARD

Load Incrementation Options

AUTO LOAD
CONTINUE
TIME STEP

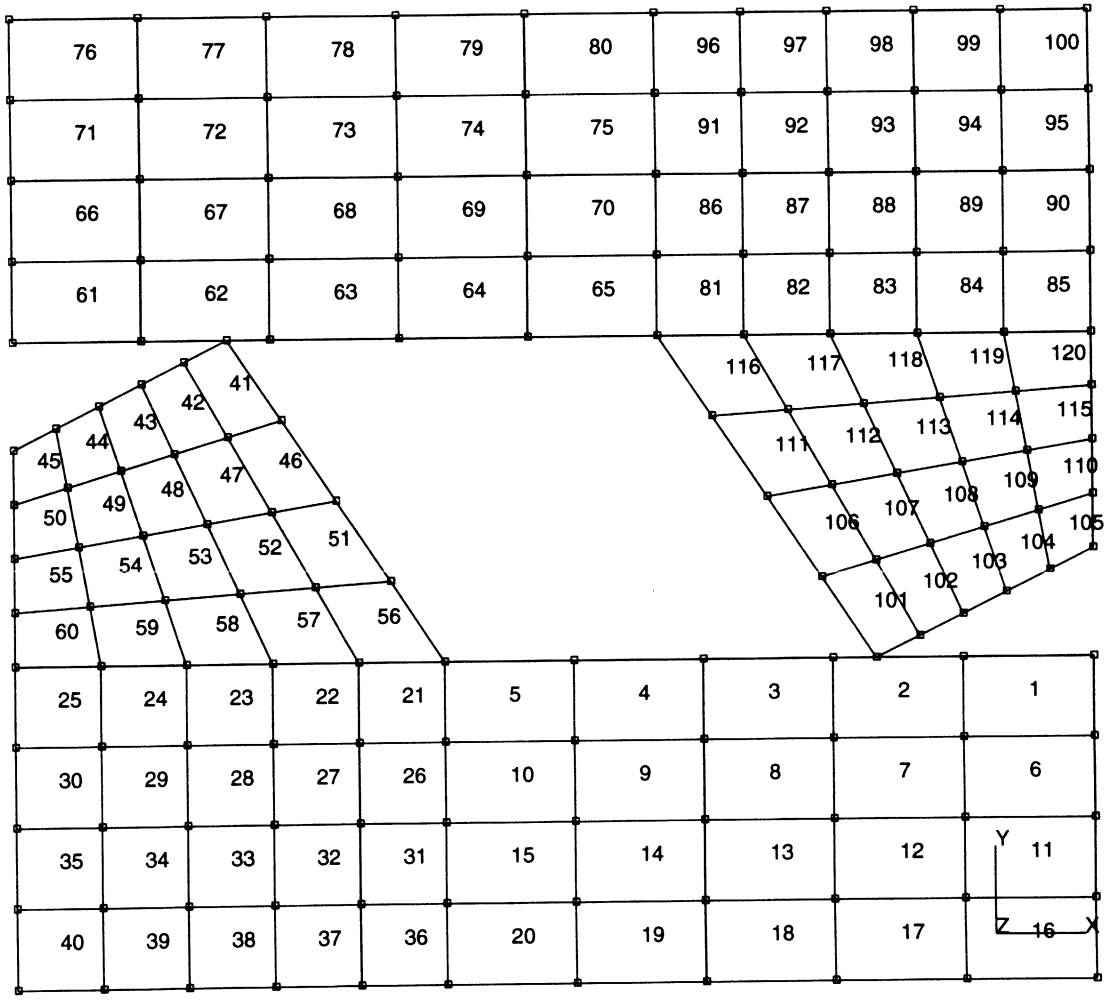

Figure E 8.15-1 Mesh

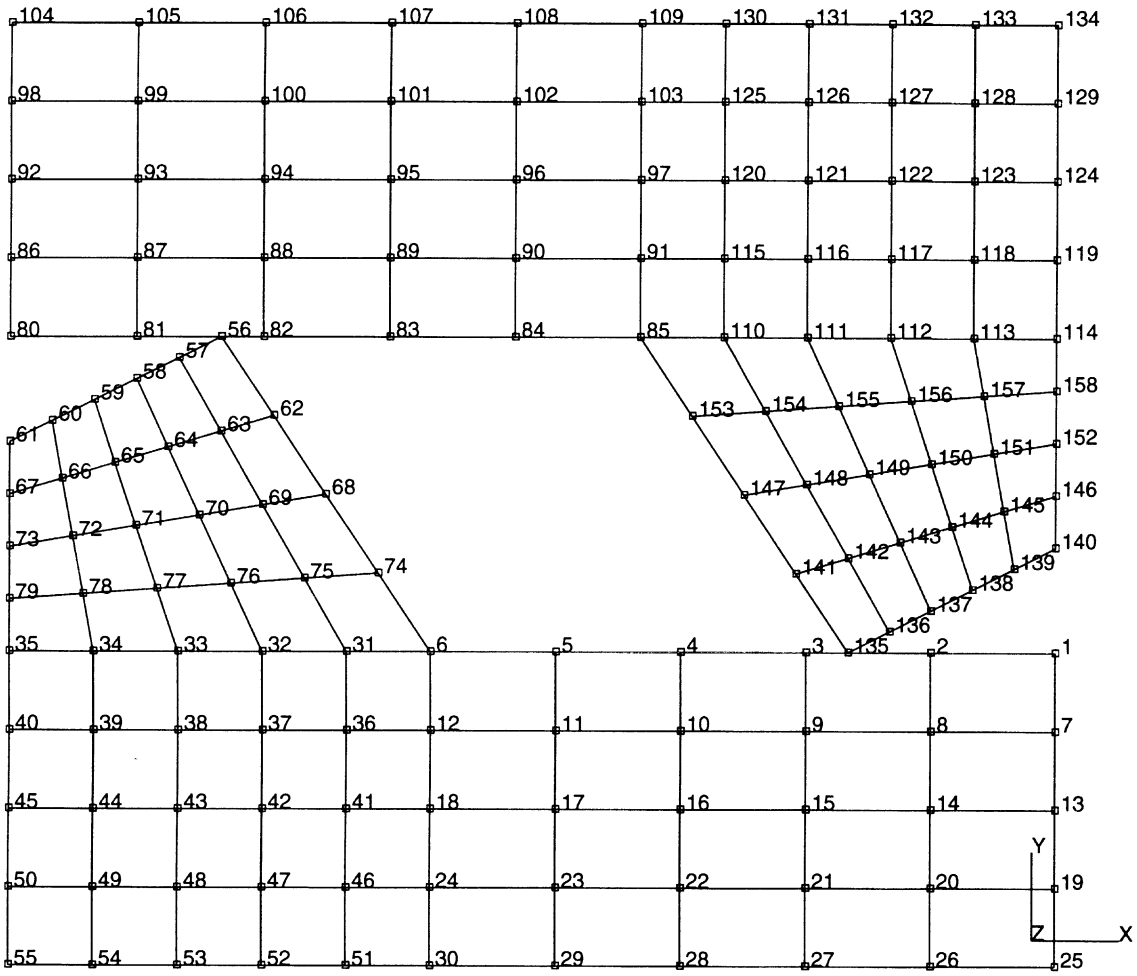

Figure E 8.15-2 Nodal Configuration, Element Type 11

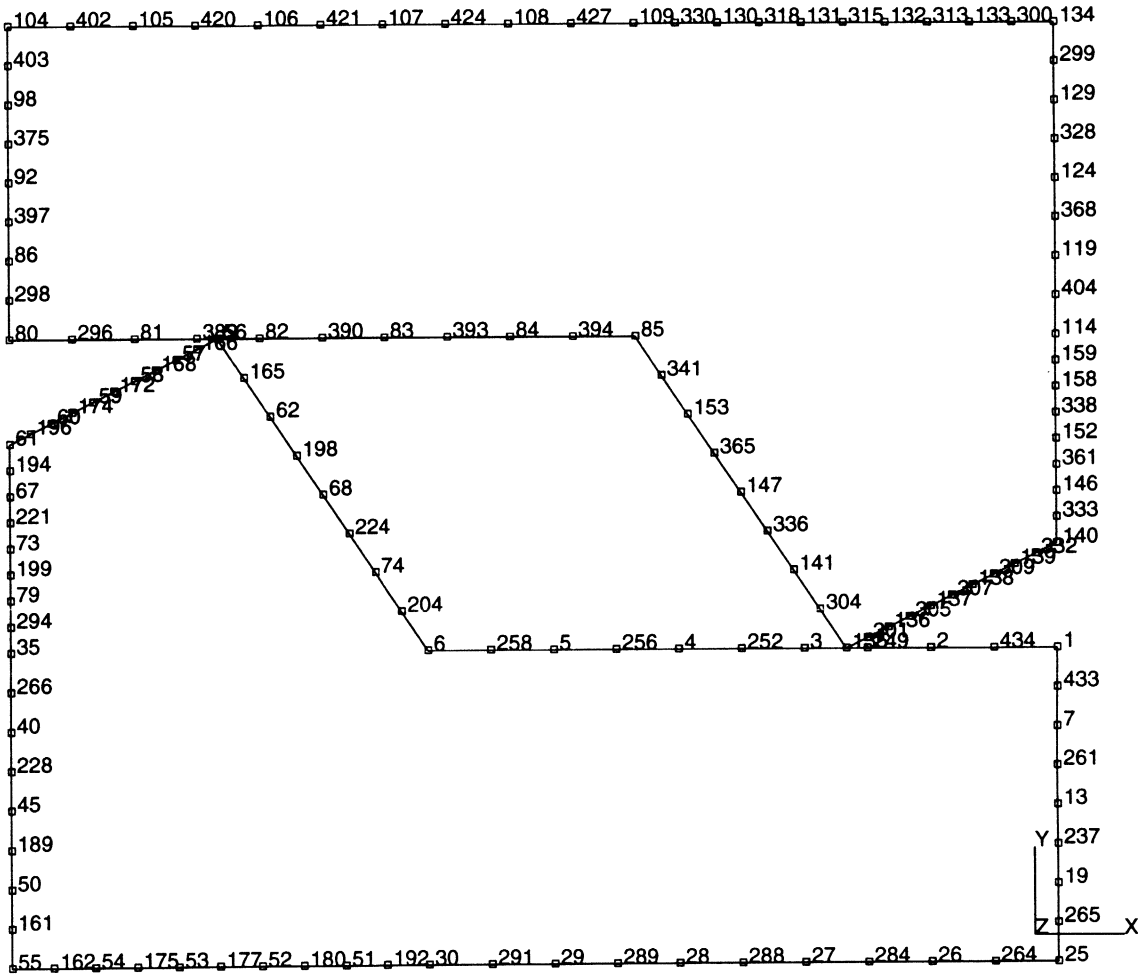

Figure E 8.15-3 Nodal Configuration, Element Type 27

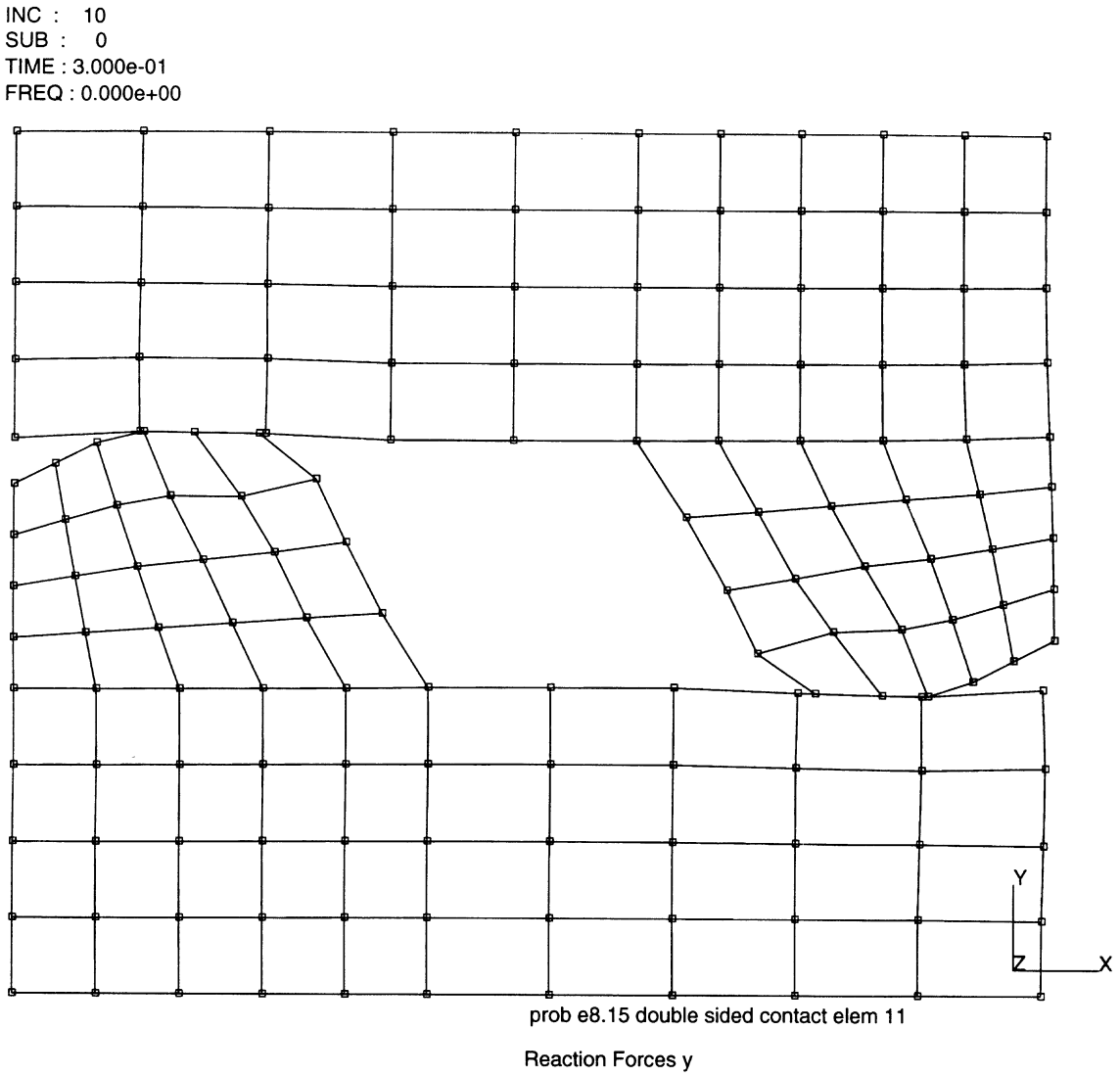

Figure E 8.15-4 Nodal Displacements at Increment 10, Element Type 11

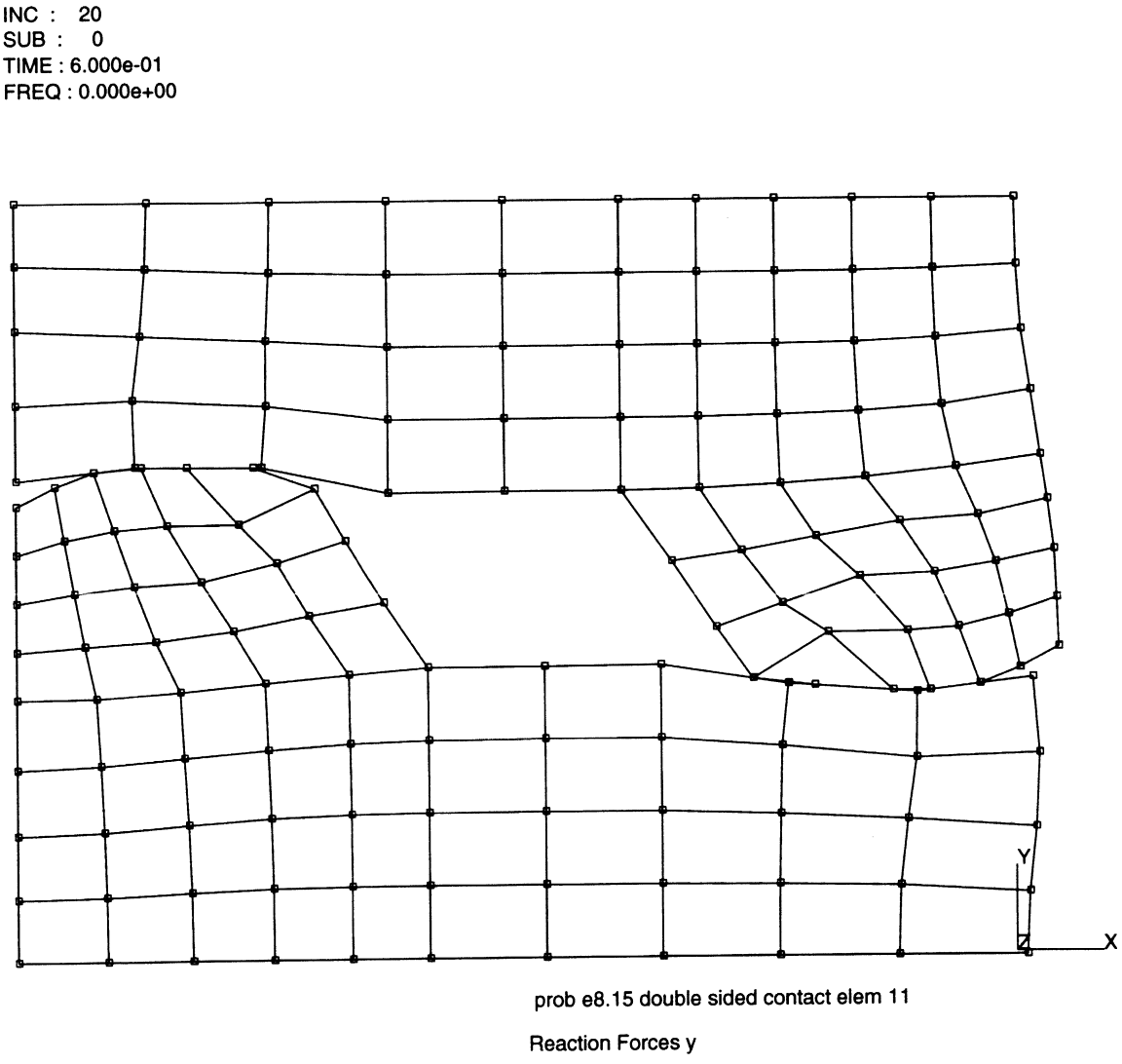

Figure E 8.15-5 Nodal Displacements at Increment 20, Element Type 11

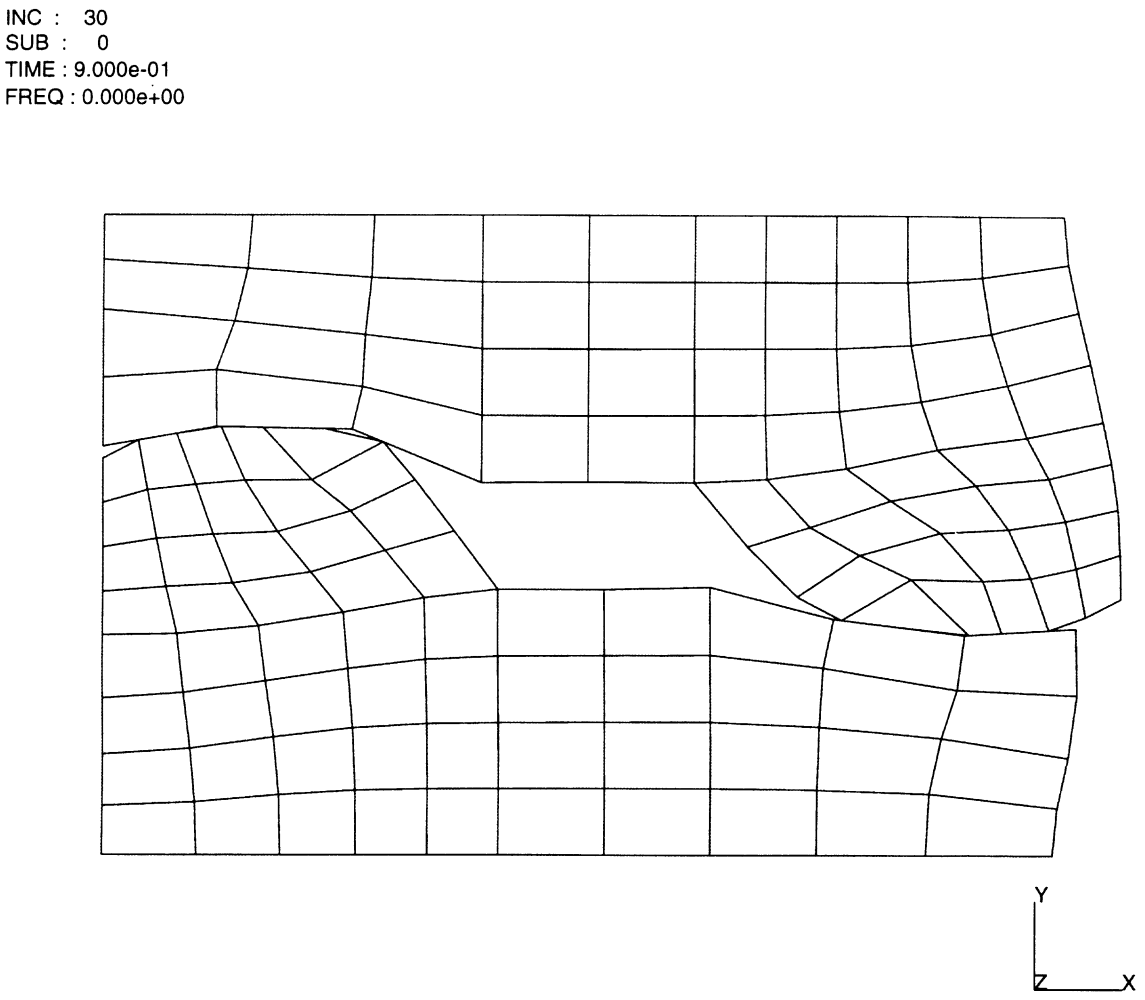

Figure E 8.15-6 Nodal Displacements at Increment 30, Element Type 11

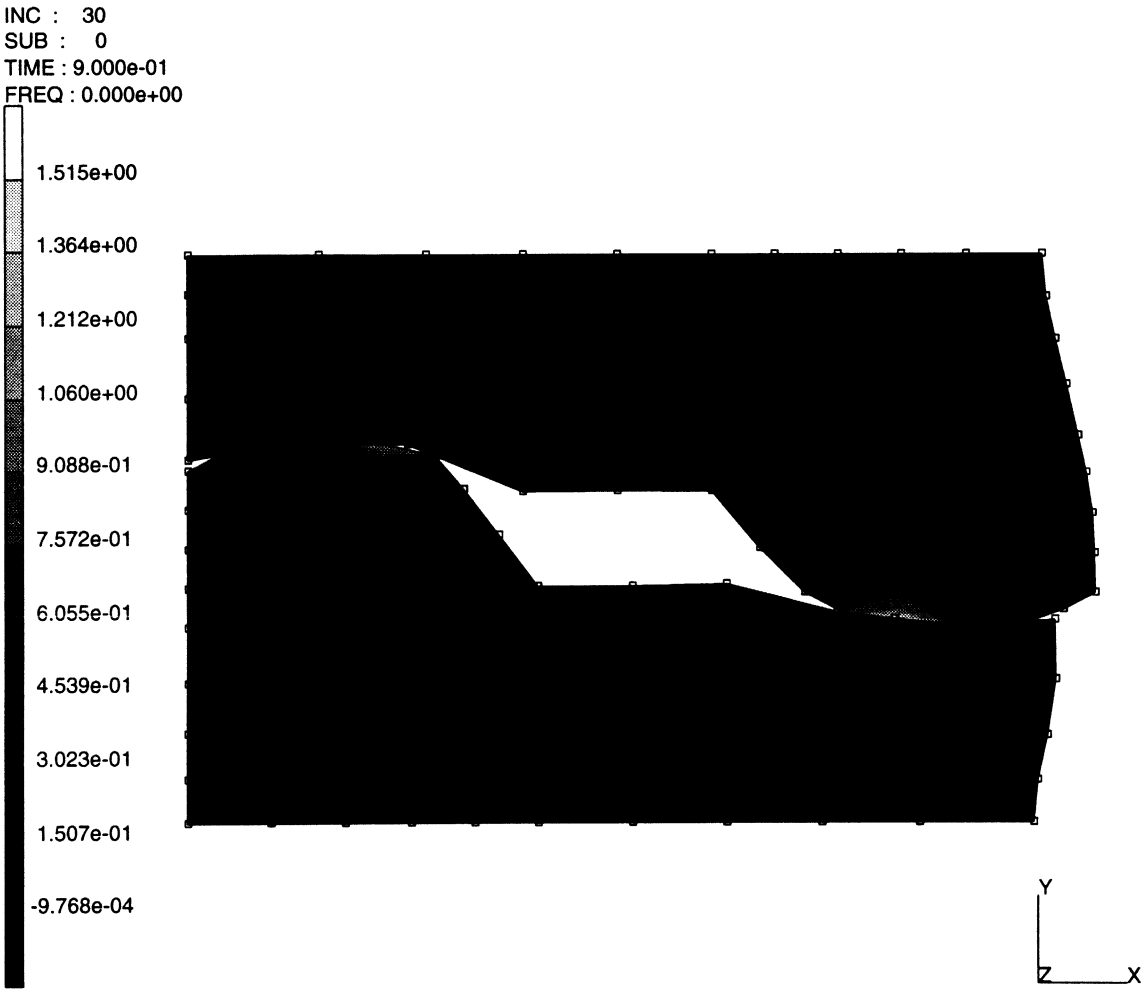

Figure E 8.15-7 Equivalent Plastic Strain at Increment 30, Element Type 11

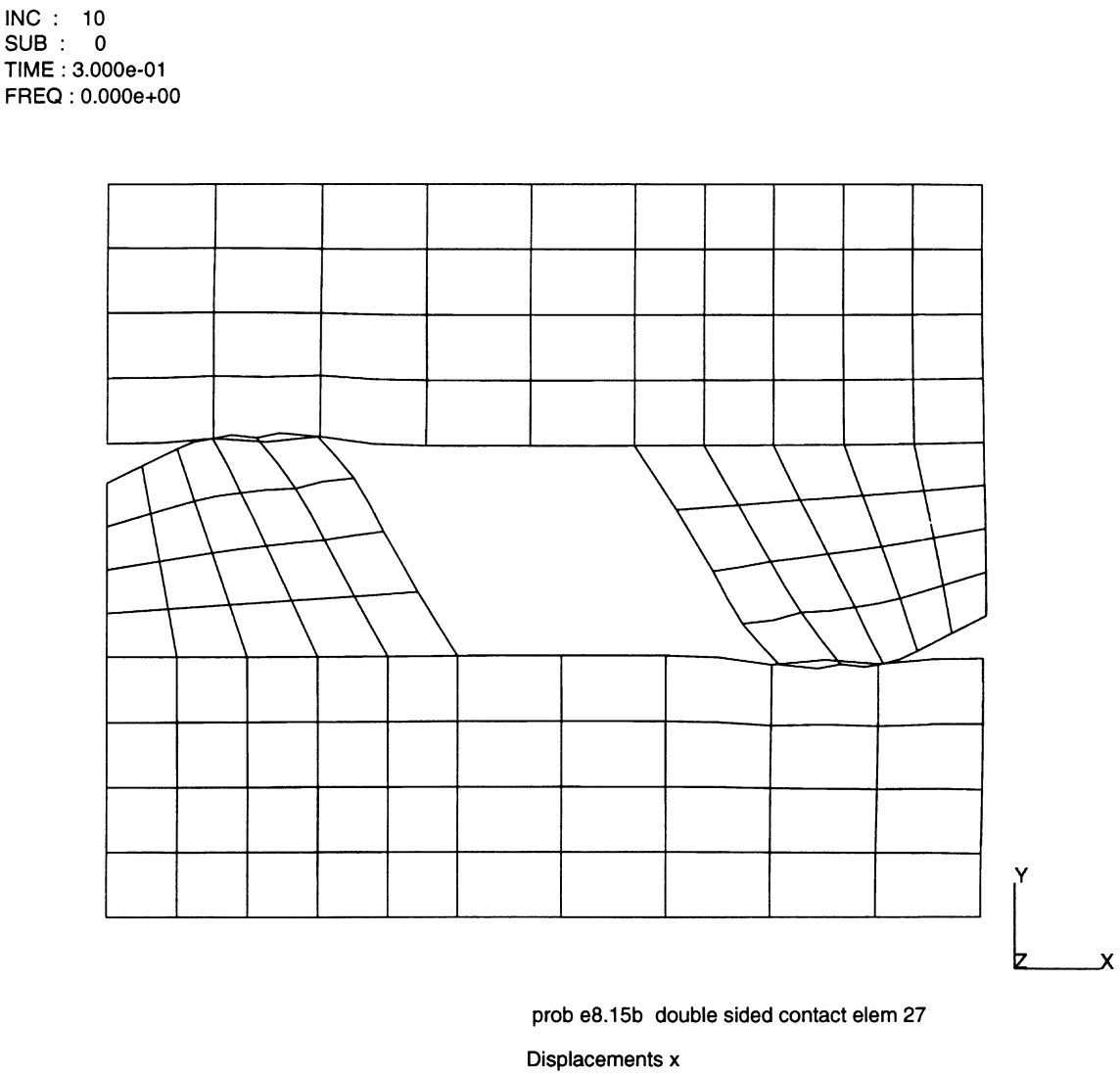

Figure E 8.15-8 Nodal Displacements at Increment 10, Element Type 27

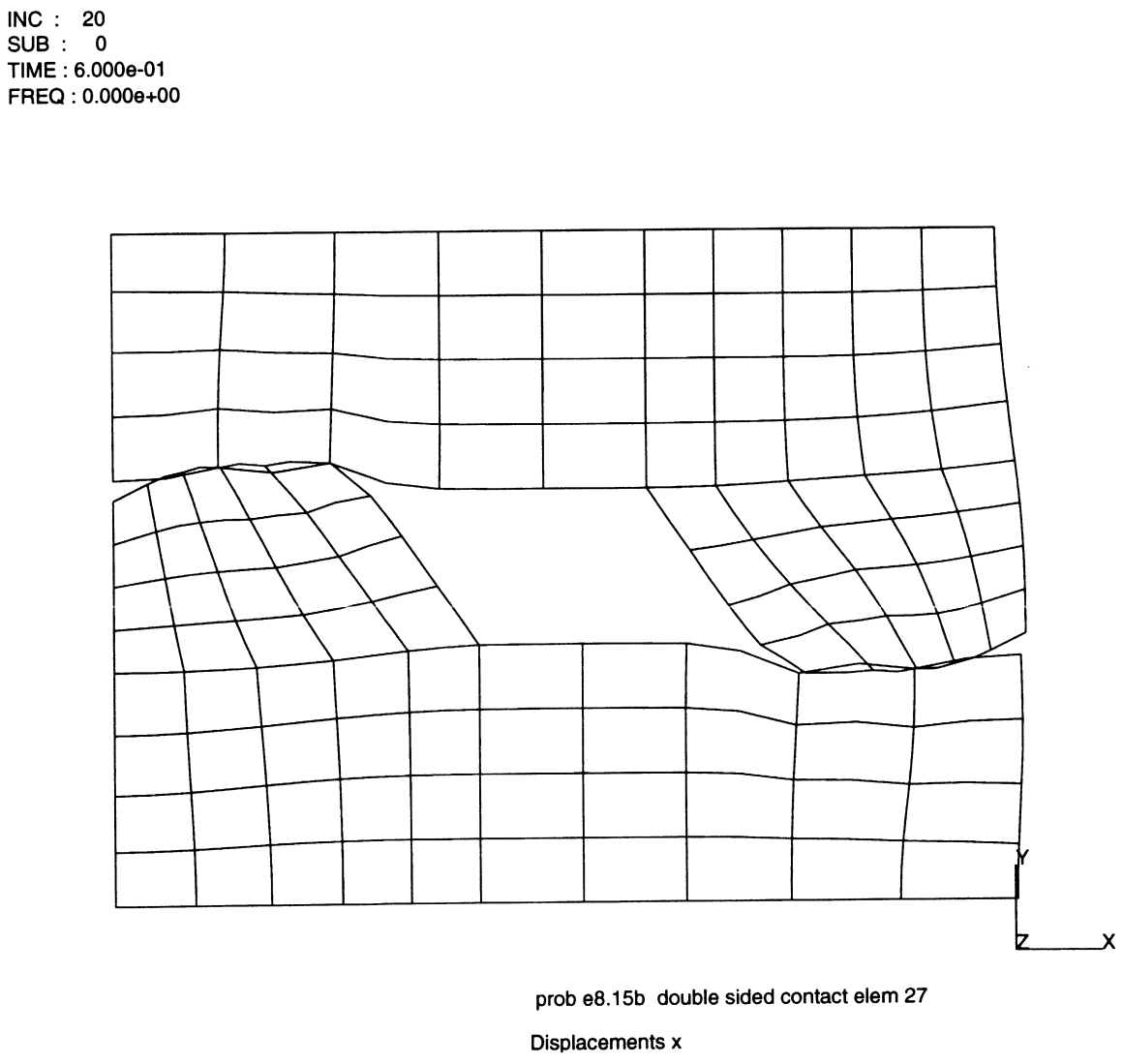

Figure E 8.15-9 Nodal Displacements at Increment 20, Element Type 27

INC : 30
SUB : 0
TIME : 9.000e-01
FREQ : 0.000e+00

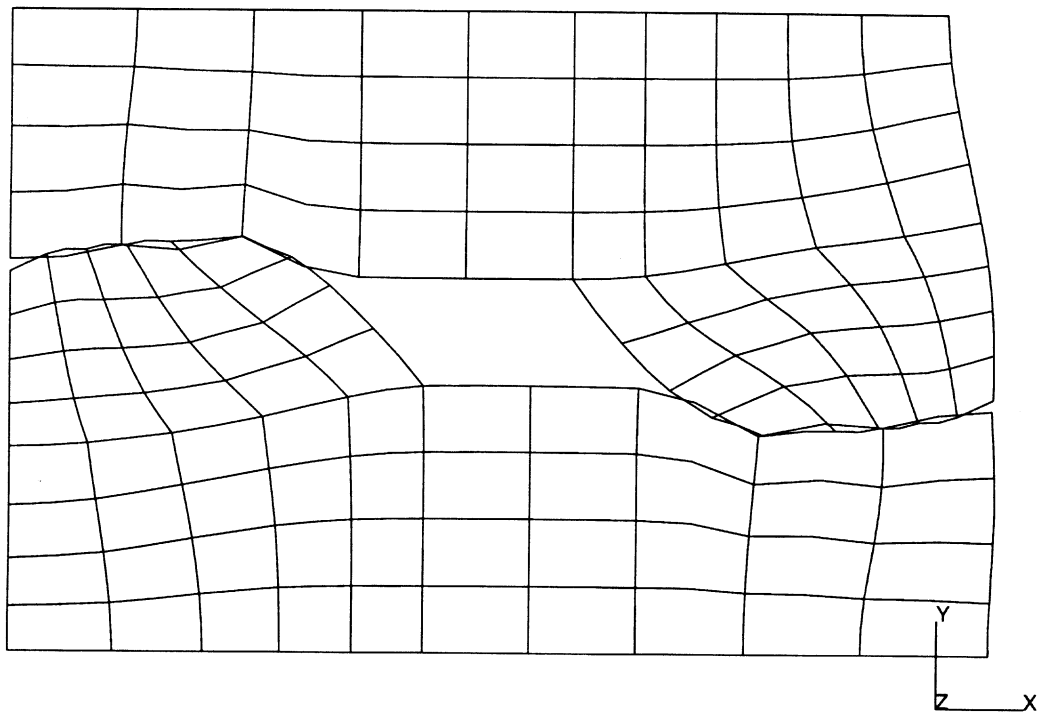

prob e8.15b double sided contact elem 27

Displacements x

Figure E 8.15-10 Nodal Displacements at Increment 30, Element Type 27

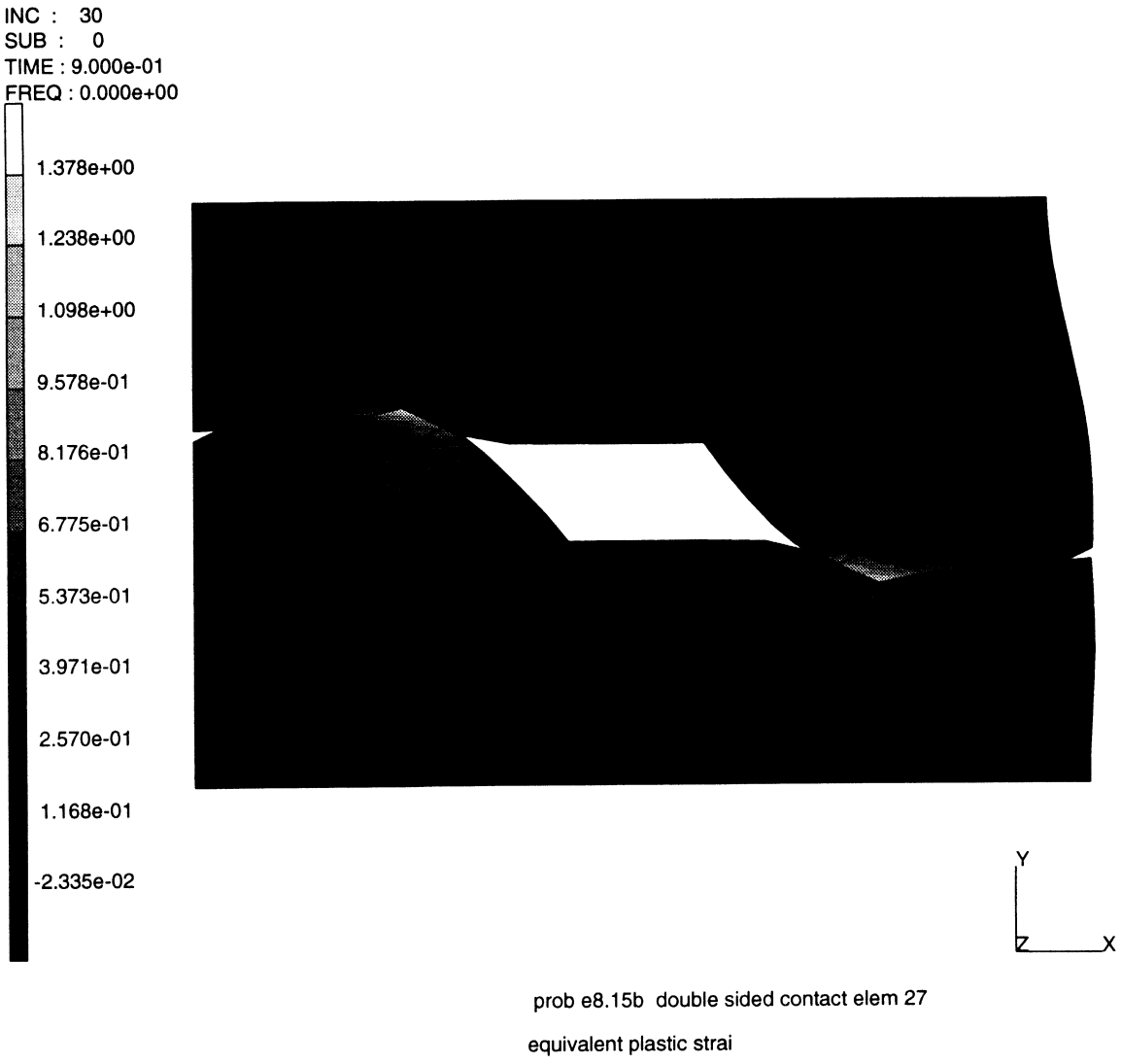

Figure E 8.15-11 Equivalent Plastic Strain at Increment 30, Element Type 27

Disp (x-1e+0)	Load (x-1e+5)		Disp (x-1e+0)	Load (x-1e+5)	
	Type 11	Type 27		Type 11	Type 27
0.00000E+00	0.00000E+00	0.00000E+00	4.50000E-01	5.73937E+00	5.76850E+00
3.00000E-02	1.49358E+00	9.65015E-01	4.80000E-01	5.82146E+00	5.92706E+00
6.00000E-02	1.36351E+00	1.34468E+00	5.10000E-01	5.88858E+00	6.02711E+00
9.00000E-02	1.40418E+00	1.61070E+00	5.40000E-01	5.95362E+00	6.11778E+00
1.20000E-01	3.59213E+00	2.52490E+00	5.70000E-01	6.01384E+00	6.20322E+00
1.50000E-01	3.26189E+00	3.02085E+00	6.00000E-01	6.28412E+00	6.28309E+00
1.80000E-01	3.31538E+00	3.35550E+00	6.30000E-01	6.35279E+00	6.35828E+00
2.10000E-01	3.52452E+00	3.70196E+00	6.60000E-01	6.39055E+00	6.42653E+00
2.40000E-01	4.55123E+00	4.33235E+00	6.90000E-01	6.43786E+00	6.52579E+00
2.70000E-01	4.74629E+00	4.63125E+00	7.20000E-01	6.56095E+00	6.55766E+00
3.00000E-01	4.89159E+00	4.88421E+00	7.50000E-01	6.72437E+00	6.52325E+00
3.30000E-01	5.03333E+00	5.07415E+00	7.80000E-01	6.77405E+00	6.70139E+00
3.60000E-01	5.16167E+00	5.23750E+00	8.10000E-01	6.70833E+00	6.79742E+00
3.90000E-01	5.39677E+00	5.41752E+00	8.40000E-01	6.89754E+00	7.02602E+00
4.20000E-01	5.51851E+00	5.60917E+00	8.70000E-01	6.97591E+00	7.14885E+00
			9.00000E-01	7.01286E+00	7.24298E+00

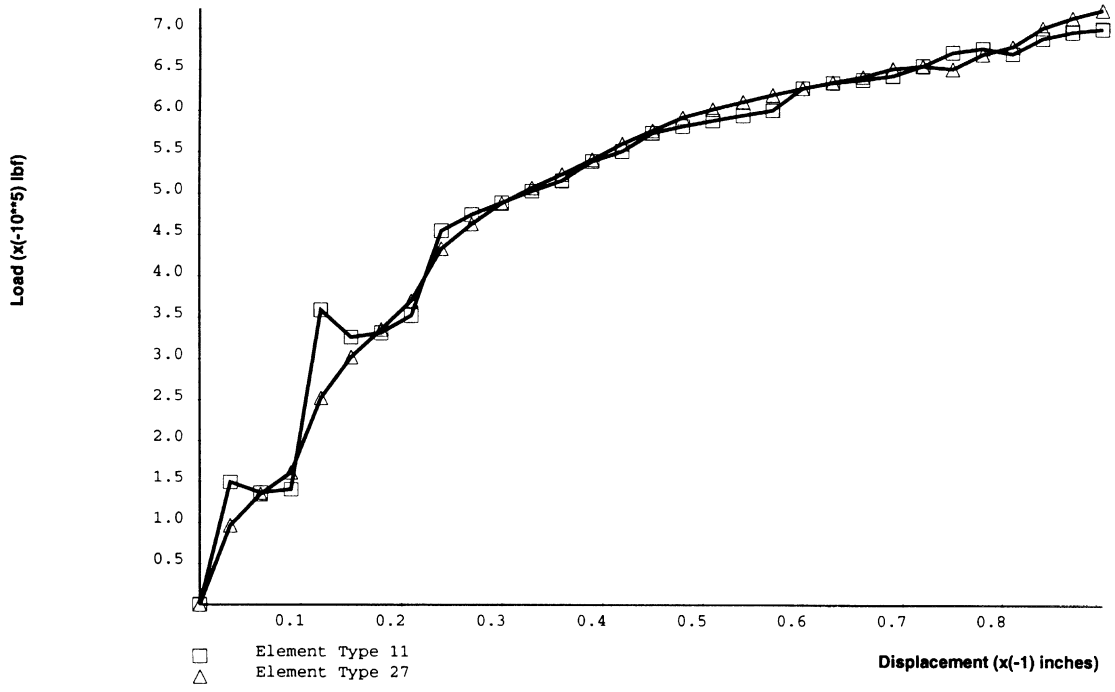

Figure E 8.15-12 Load History for Both Element Types

E 8.16 Demonstration Of Springback

A metal part is formed and the springback is examined.

Model

The original part is shown in Figure E 8.16-1 and is composed of 197 elements type 11 plane strain quadrilaterals. A rigid cylinder is used to deform the part.

Parameters

The LARGE DISP, FINITE and UPDATE options are included because it is anticipated that large plastic strains will occur. The PRINT, 5 option results in additional output regarding contact.

Geometry

The "1" in the second field invokes the constant dilatation option. This gives improved behavior for nearly incompressible behavior that occurs during plastic deformation. The "1" in the third field invokes the assumed strain formulation for element type 11. This gives improved behavior in bending which will be the dominant mechanism in this problem.

Boundary Conditions

The left side is constrained in the first degree of freedom. A spring is used to constrain the motion in the y-degree of freedom, so there will not be any rigid body modes.

Material Properties

The part is made of aluminum with a Young's modulus of 10.6E+6 psi^2. The material strain hardens such that at 5.8% strain the flow stress will be 50,355 psi. It is important that the first stress in the WORK HARD DATA be the same as given through the PROPERTY option.

Contact

Two contact bodies are defined. The first is the deformable body, consisting of 147 elements. The second body is the rigid pin, defined as 4 circular arcs. Each arc is subdivided into ten segments. The circular pin has a velocity of 0.2 in/sec.

Control

The full Newton-Raphson procedure is used in this analysis. Displacement control is requested with a tolerance of 2%. The Cuthill-McKee method is used to minimize the bandwidth. The POST tape frequency is specified through the POST and POST INCREM options. The post tape will be written at increments 0 (default), 18, and 19.

The AUTO LOAD and TIME STEP options are used to request 18 increments each with a time step of 0.1 second. At this point, the pin is removed from the model.

This is done in one step by using the RELEASE option and the MOTION CHANGE options. The RELEASE option is used to ensure that all of the nodes separate from body 2, the rigid pin. The MOTION CHANGE option is used to move the pin away from the body, so that it will not make any further contact.

Results

The deformed shape at increment 18 is shown in Figure E 8.16-2. The stresses at this point are shown in Figure E 8.16-3. After release of the pin, there is a slight amount of spring back. Recall that the elastic strain is, at the most, 5.4 E4/10.6 = 0.5% which will limit the amount of springback.

Summary of Options Used

Listed below are the options used in example e8x16.dat:

Parameter Options

ELEMENT
END
FINITE
LARGE DISP
PRINT
SIZING
TITLE
UPDATE

Model Definition Options

CONNECTIVITY
CONTACT
CONTROL
COORDINATES
END OPTION
FIXED DISP
GEOMETRY
ISOTROPIC
OPTIMIZE
POST
PRINT CHOICE
WORK HARD

Load Incrementation Options

AUTO LOAD
CONTINUE
POST INCREMENT
RELEASE
TIME STEP

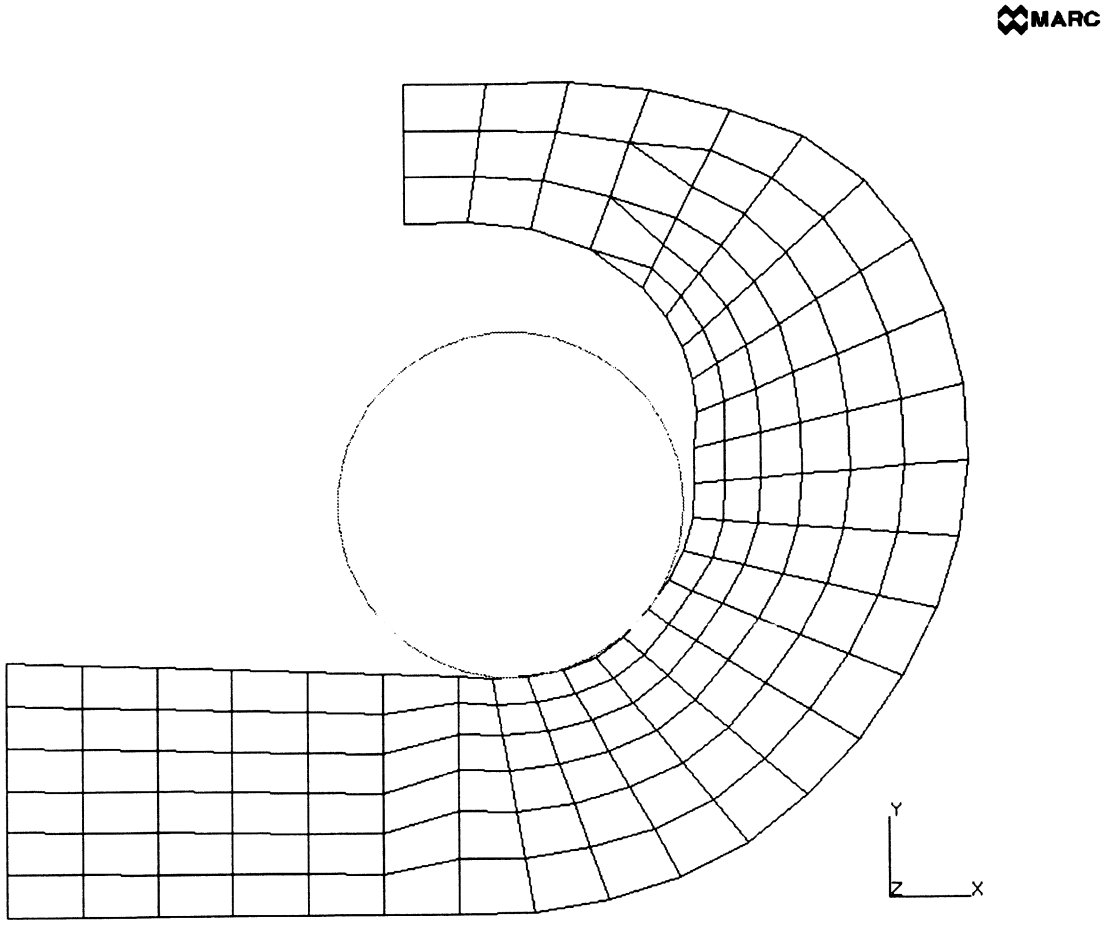

Figure E 8.16-1 Original Configuration

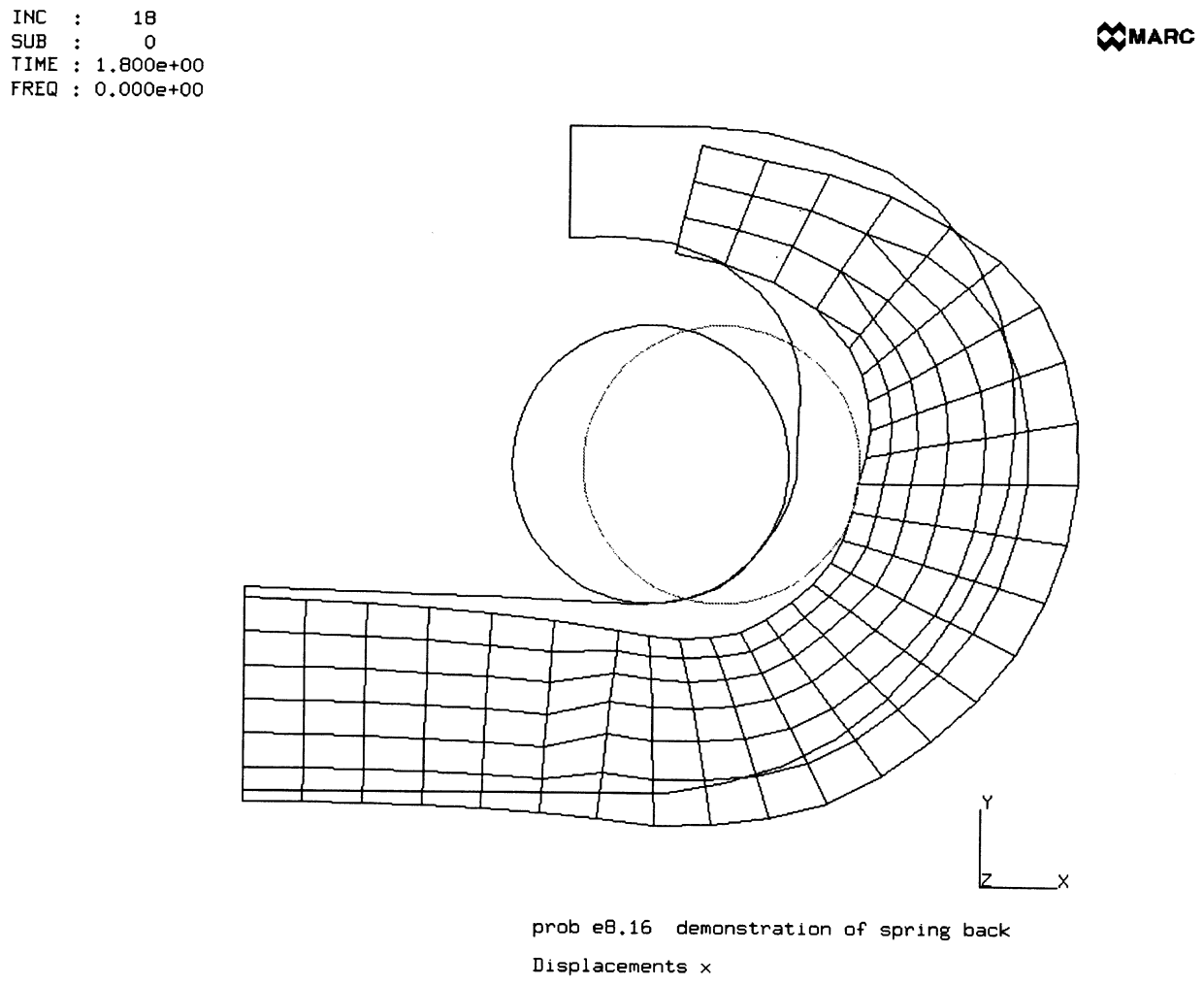

Figure E 8.16-2 Deformed Mesh

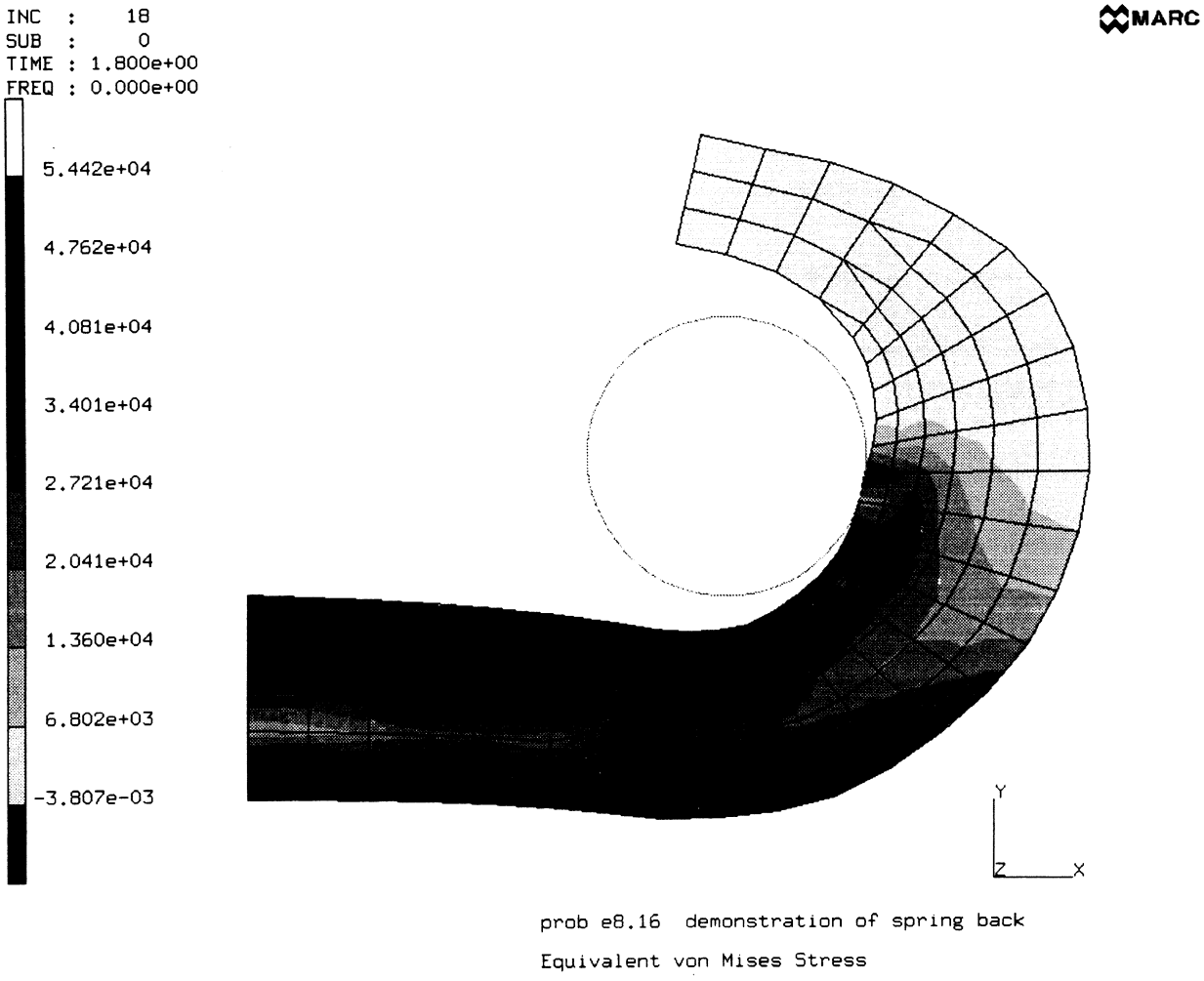

Figure E 8.16-3 Equivalent Stress

E 8.17 3D Extrusion Analysis With Coulomb Friction

This problem demonstrates the program's ability to perform metal extrusion analysis using the CONTACT option. The analysis is complicated by the multiple intersecting contact surfaces.

Parameters

The UPDATE, FINITE and LARGE DISP options are included in the parameter section to indicate this is a finite deformation analysis. The PRINT,8 option requests the output of additional information concerning contact. The REZONE parameter option is included to allow the potential for future mesh rezoning to compensate for gross distortions in the original mesh.

Geometry

Element type 7, the eight-node brick element, is used in this analysis. A "1" is placed in the second data field (EGEOM2) to indicate that the constant dilatation formulation is used. This is done in recognition of the fact that metal extrusion results in large plastic deformations which are nearly incompressible.

Boundary Conditions

Appropriate nodal constraints are applied in the global X, Y directions to impose symmetry. The billet is extruded by having a constant velocity imposed.

POST/RESTART

The following variables are written to a formatted POST tape at every 35 increments:

7 } Equivalent plastic strain 17 } Equivalent von Mises stress

The last converged increment is written to a restart tape.

Control

A maximum of 200 increments are to be carried out, with no more than 20 recycles per increment. Displacement control is used, with a relative error of 10%.

Material Properties

The material for all elements is treated as an elastic-perfectly plastic material, with Young's modulus of 1.75E+07 psi, Poisson's ratio of 0.3, and an initial yield stress of 35,000 psi.

Contact

This option declares that there are three bodies in contact with Coulomb friction between them. In particular, the friction coefficient associated with each rigid die is 0.1. The relative slip velocity is 0.01 inch/second. The contact tolerance distance is 0.01 inches.

The three contact bodies are defined as follows:

Body 1: The deformable body consisting of 16 brick elements. Note that the velocity cannot be entered for a deformable body.

Body 2: A single plane is used to represent the ram and is given a velocity of -0.3 in/sec.

Body 3: Six planes are used to define the die.

Load Control

This problem is loaded by the repeated application of the prescribed die velocities with the AUTO LOAD option. The load increment will be applied 70 times. The TIME STEP option allows the user to enter the time variable for static analysis should time dependent constitutive relations be used.

Results

Figure E 8.17-1 show the geometry configuration for the extrusion analysis. Figure E 8.17-2 and Figure E 8.17-3 shows the deformed body at the end of 35 increments with the deformation at the same scale as the coordinates. Due to the high level of friction, significant transverse deformation is shown along the contact surfaces.

Figure E 8.17-4 and Figure E 8.17-5 show the deformed body at the end of 70 increments.

Figure E 8.17-6 shows the equivalent plastic strain contours on the deformed structure at increment 70 with the largest strain level at 0.705.

Figure E 8.17-7 shows the equivalent von Mises stress contours on the deformed structure at increment 70 with peak values at 37,820 psi.

Summary of Options Used

Listed below are the options used in example e8x17.dat:

Parameter Options

ELEMENT
END
FINITE
LARGE DISP
PRINT
REZONE
SIZING
TITLE
UPDATE

Model Definition Options

CONNECTIVITY
CONTACT
CONTROL
COORDINATE
END OPTION
FIXED DISP
GEOMETRY
ISOTROPIC

POST
PRINT CHOICE
RESTART LAST

Load Incrementation Options

AUTO LOAD
CONTINUE
TIME STEP

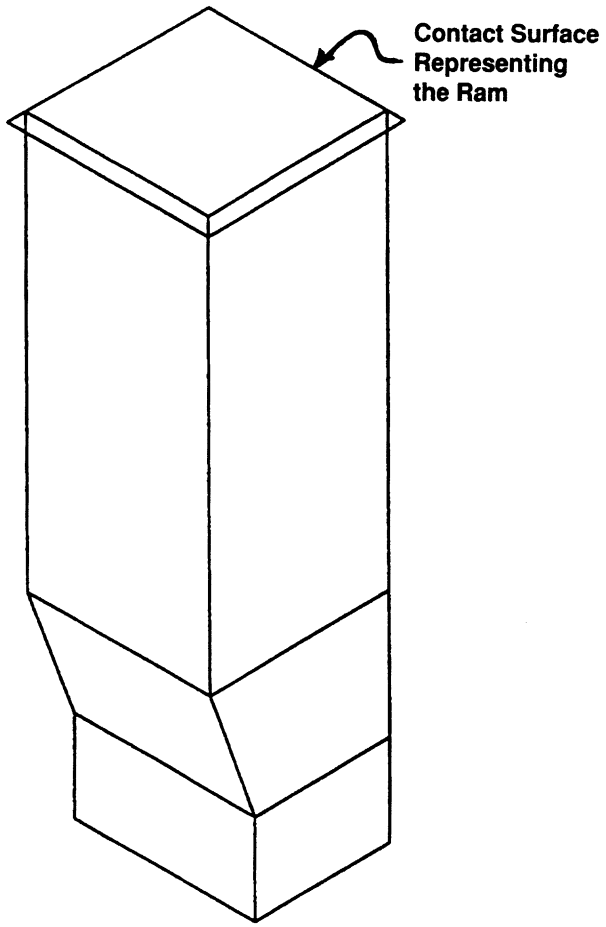

Figure E 8.17-1 Rigid Surfaces Defining Extrusion Die

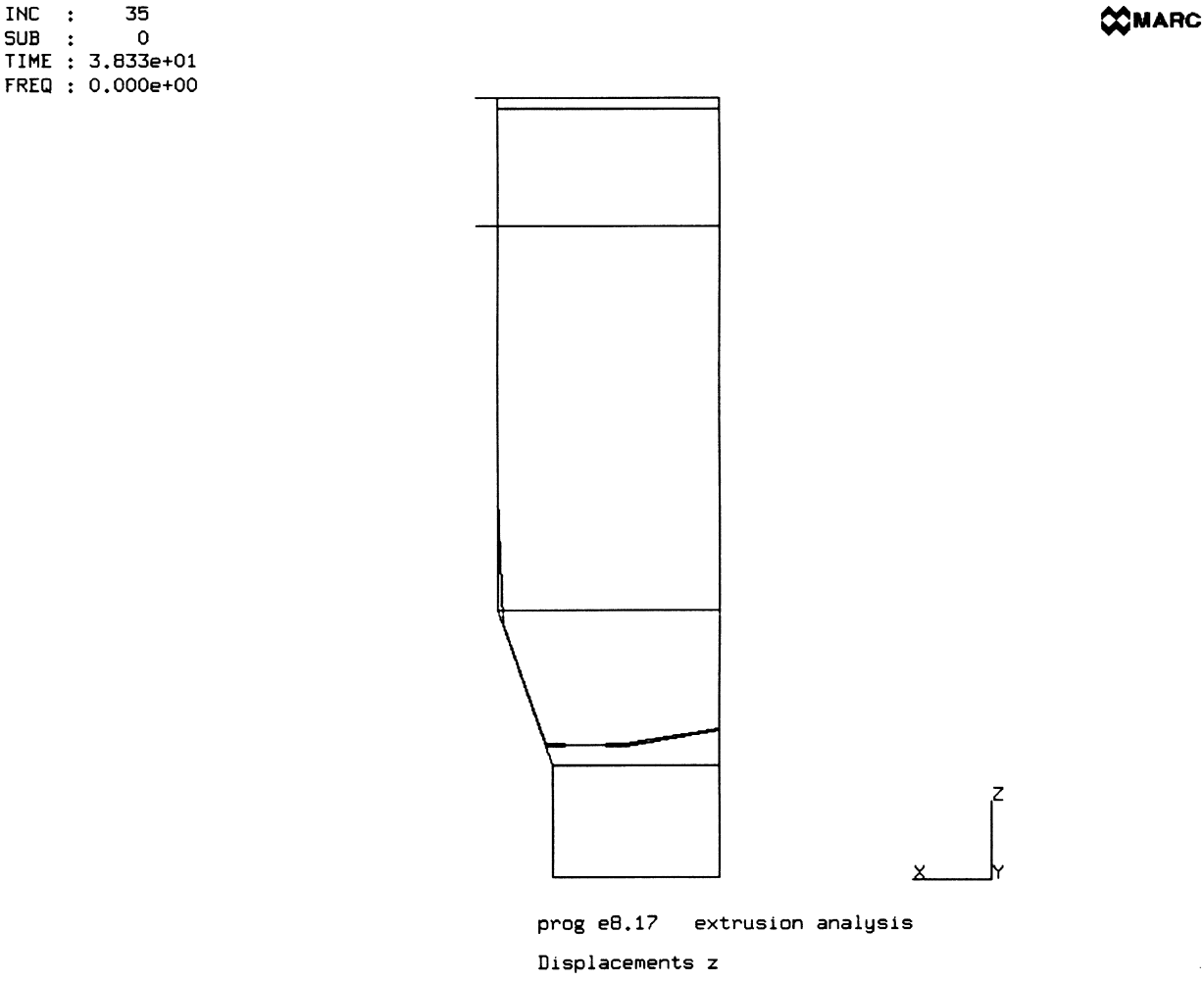

Figure E 8.17-2 Deformed Mesh, Increment 35

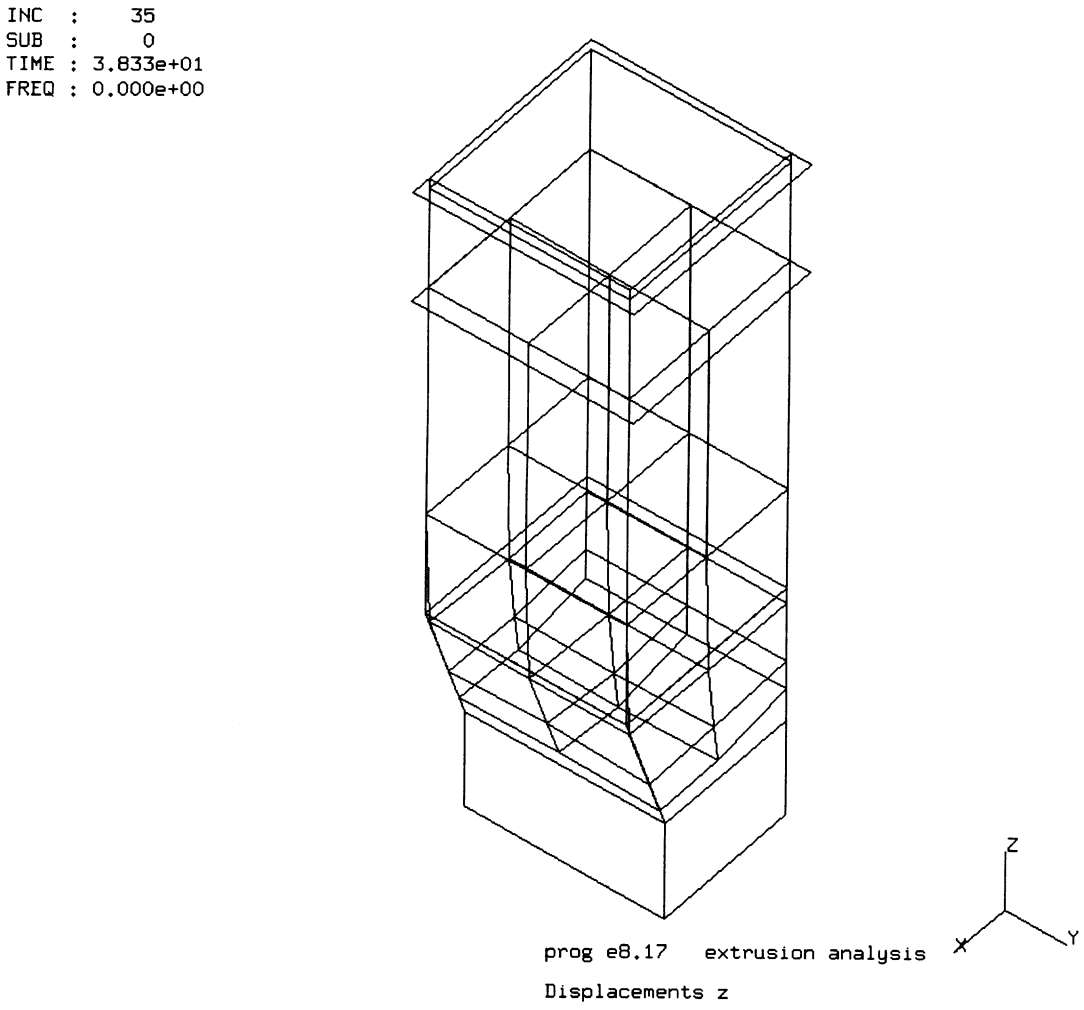

Figure E 8.17-3 Deformed Mesh, Increment 35

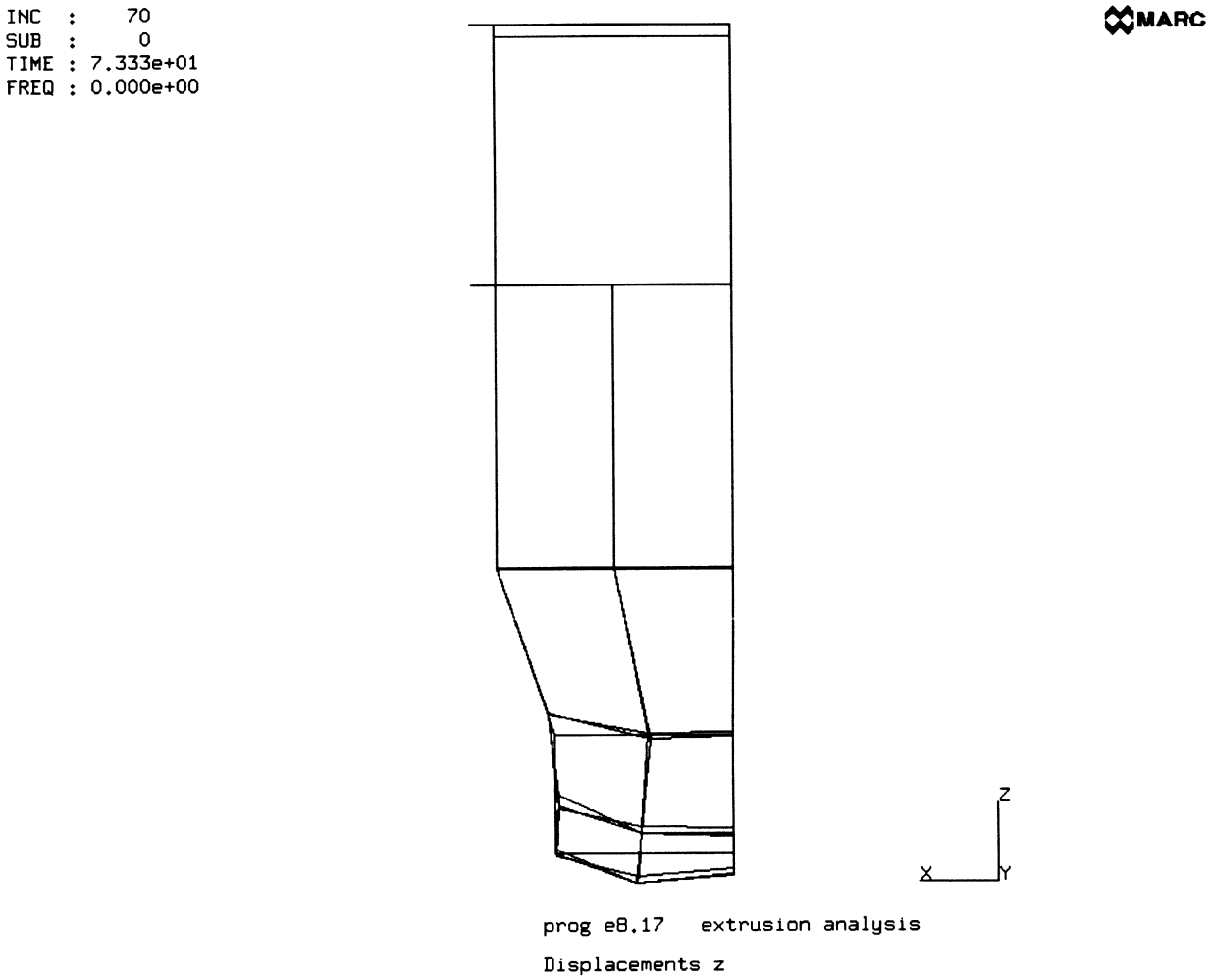

Figure E 8.17-4 Deformed Mesh, Increment 70

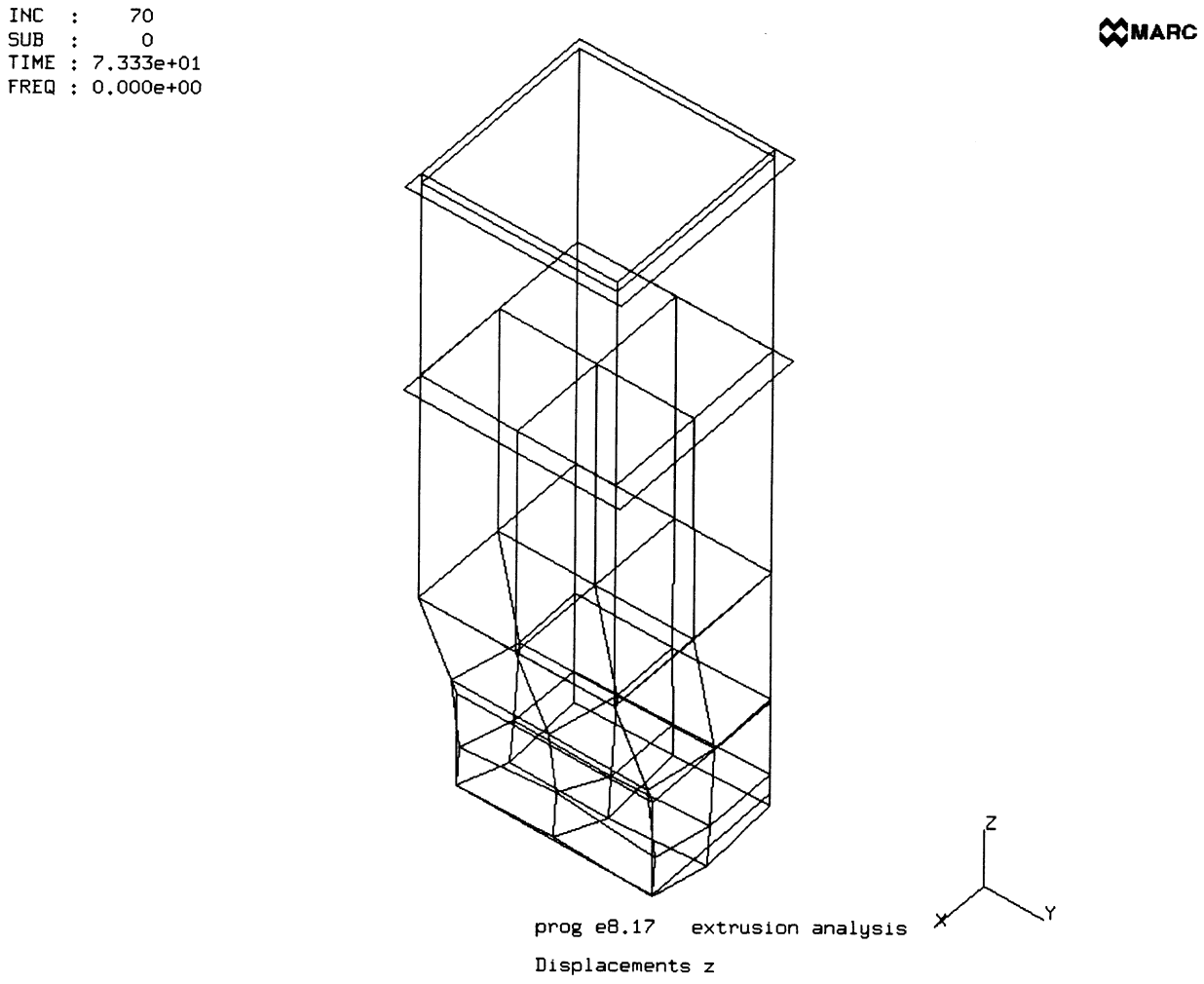

Figure E 8.17-5 Deformed Mesh, Increment 70

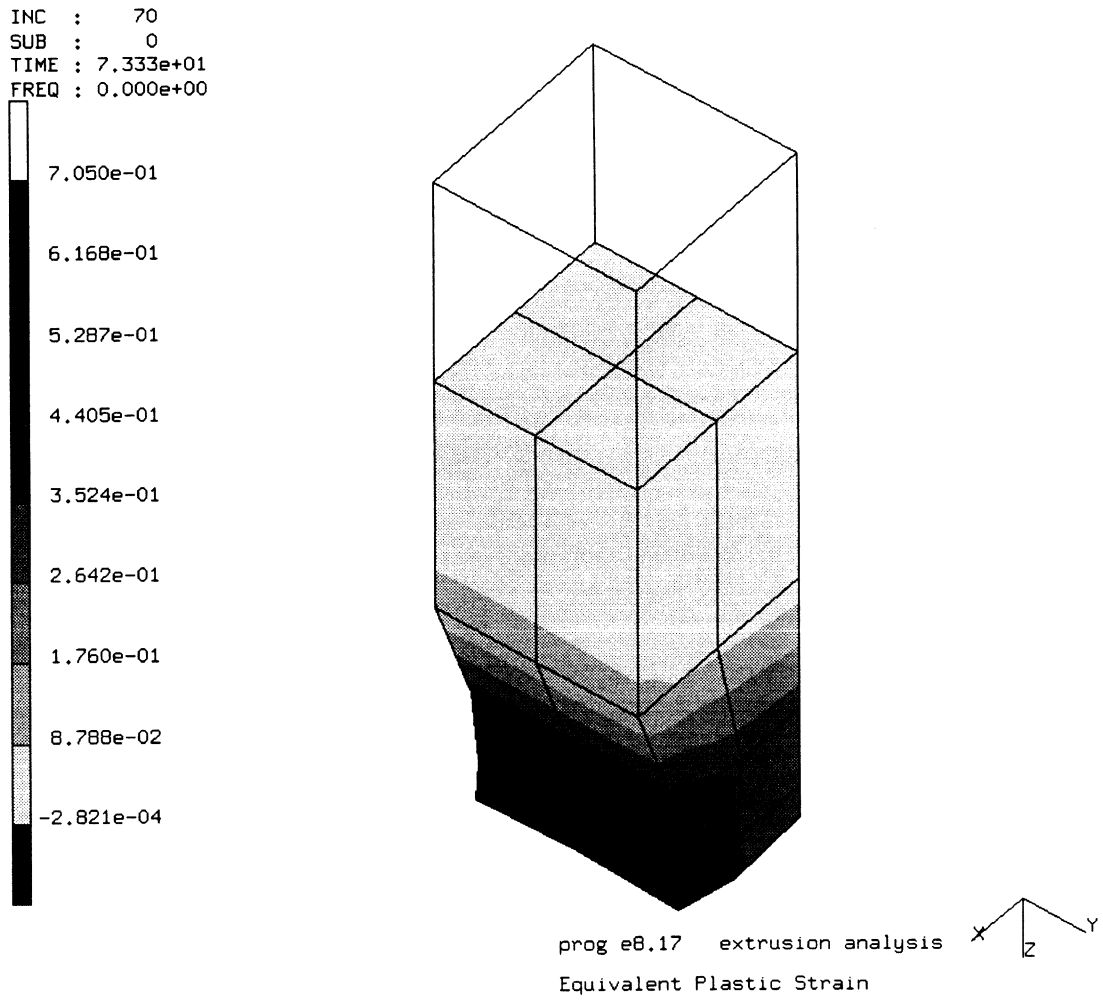

Figure E 8.17-6 Equivalent Plastic Strain, Increment 70

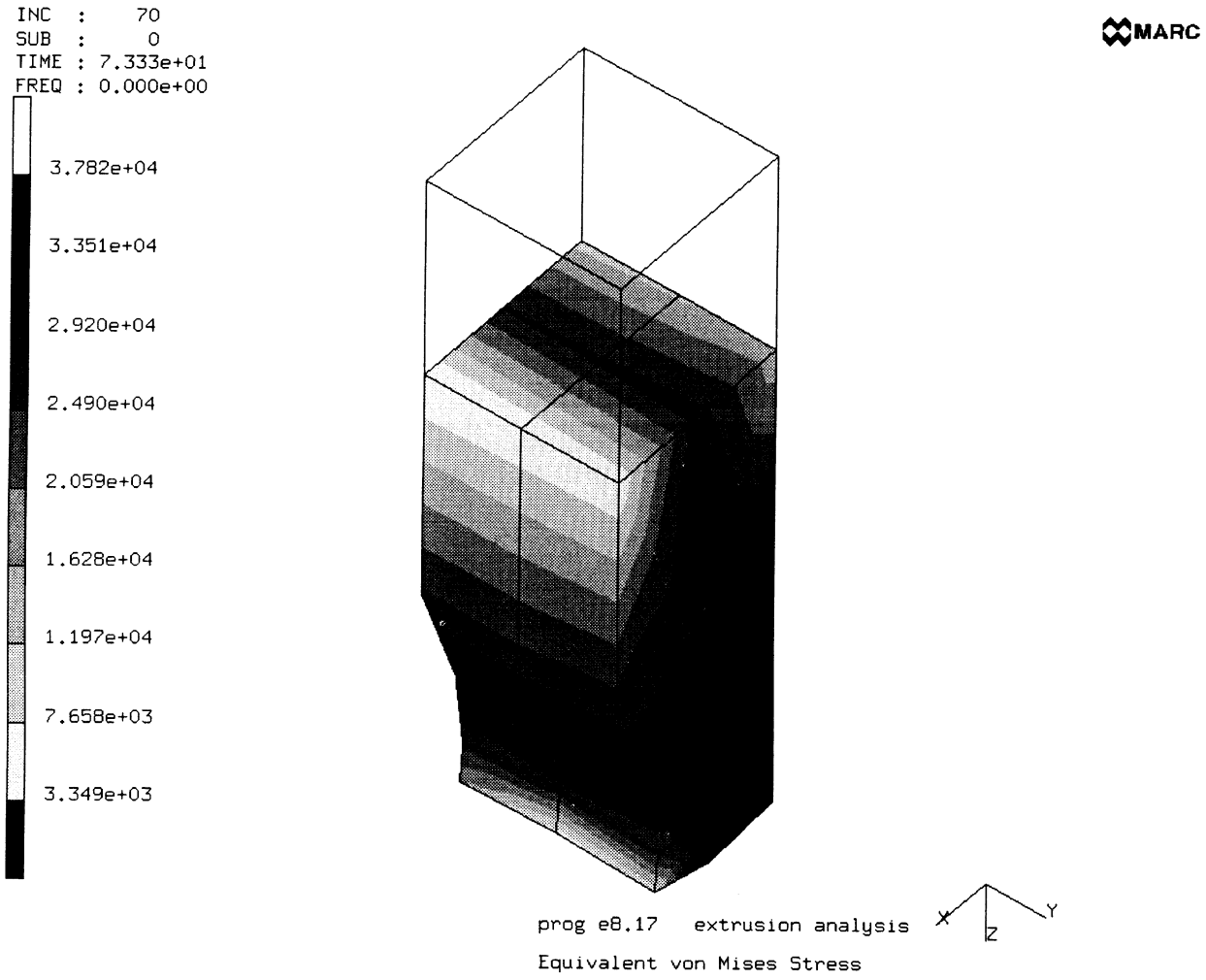

Figure E 8.17-7 Equivalent Stress, Increment 70

E 8.18 3D Forming Of A Circular Blank Using Shell Elements And Coulomb Friction

This problem demonstrates the program's ability to perform stretchforming by a spherical punch using the CONTACT option and shell elements.

Parameters

The UPDATE, FINITE and LARGE DISP options are included in the parameter section to indicate this is a finite deformation analysis. The PRINT,8 option requests the output of incremental displacements. Element type 75, the four-node thick shell element, is used in this anlysis. Seven layers are used through the thickness of the shell.

Geometry

A shell thickness of one cm is specified through the GEOMETRY option in the first field (EGEOM1).

Boundary Conditions

The first boundary condition is used to model the binding in the stretch forming process. The second and third boundary conditions are used to represent the symmetry conditions.

POST

The following variables are written to a formatted post tape:

7 } Equivalent plastic strain 17 } Equivalent Von Mises stress
20 } Element thickness

Furthermore, the above three variables are also requested for all shell elements at layer number 4, which is the midsurface.

Control

A full Newton-Raphson iterative procedure is requested, along with the mean normal method approach to solve plasticity equations. Displacement control is used, with a relative error of 5%. Twenty six load steps are prescribed, with a maximum of twenty recycles (iterations) per load step.

Material Properties

The material for all elements is treated as an elastic-plastic material, with Young's modulus of 690,040 lbf/cm^2, Poisson's ratio of 0.3, and an initial yield stress of 80,560 lbf/cm^2. The yield stress is given in the form of a power law and is defined through the WKSLP user subroutine.

Contact

This option declares that there are three bodies in contact with Coulomb friction between them. A coefficient of friction of 0.3 is associated with each rigid die. The first body represents the work piece. The second body is the lower die, defined as three surfaces of revolution. The first and third surfaces of revolution use a straight line as the generator, the second uses a circle as

the generator. The third body is the punch, defined as two surface of revolution. These surfaces are extended from -0.5 to 101.21 degrees. The relative slip velocity is specified as 0.01 cm/sec. The contact tolerance distance is 0.05 cm.

Load Control

This problem is displacement controlled with a velocity of 1 cm/sec. applied in the negative Z direction with the AUTO LOAD option. The load increment will be applied 40 times. The MOTION CHANGE option is illustrated to control the velocity of the rigid surfaces.

Results

Figure E 8.18-2 shows the deformed body at the end of 40 increments with the deformation at the same scale as the coordinates. Due to the high level of friction, significant transverse deformation is shown along the contact surfaces.

Figure E 8.18-3 shows the equivalent plastic strain contours on the deformed structure at increment 40, with the largest strain level at 60%.

Figure E 8.18-4 shows the equivalent von Mises stress contours on the deformed structure at increment 40 with peak values at 527.4 lbf/cm^2.

Summary of Options Used

Listed below are the options used in example e8x18.dat:

Parameter Options

ELEMENT
END
FINITE
LARGE DISP
PRINT
SHELL SECT
SIZING
TITLE
UPDATE

Model Definition Options

CONNECTIVITY
CONTACT
CONTROL
COORDINATE
END OPTION
FIXED DISP
GEOMETRY
ISOTROPIC
POST
PRINT CHOICE
WORK HARD

Load Incrementation Options

AUTO LOAD
CONTINUE
MOTION CHANGE
TIME STEP

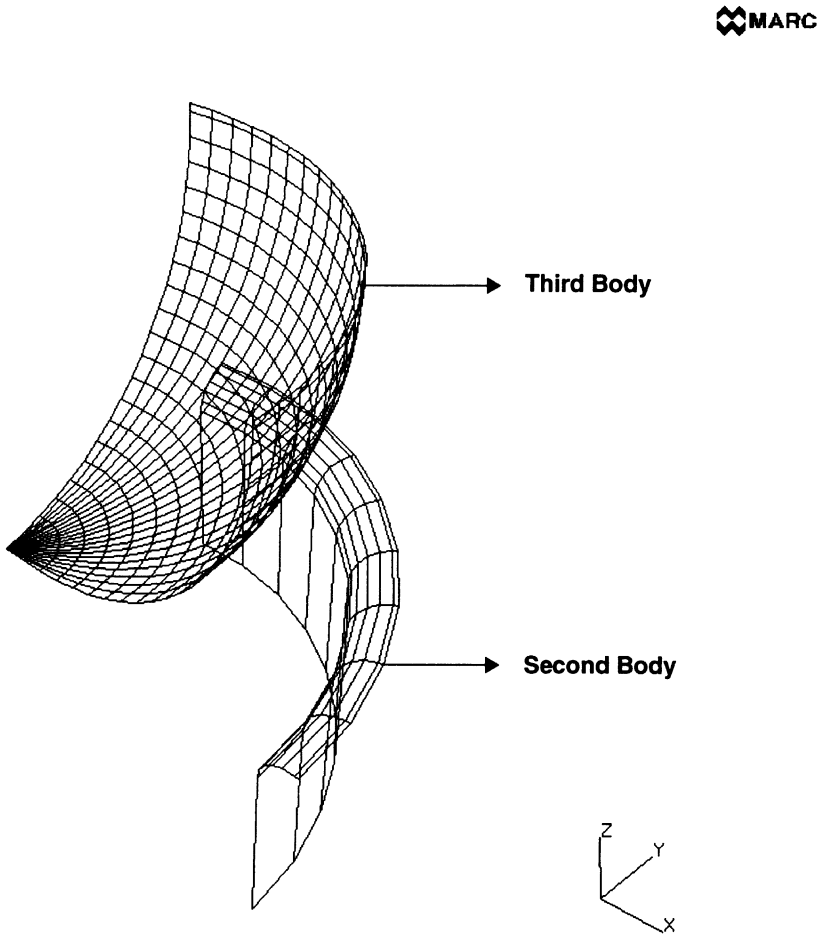

Figure E 8.18-1 Circular Blank Holder and Punch

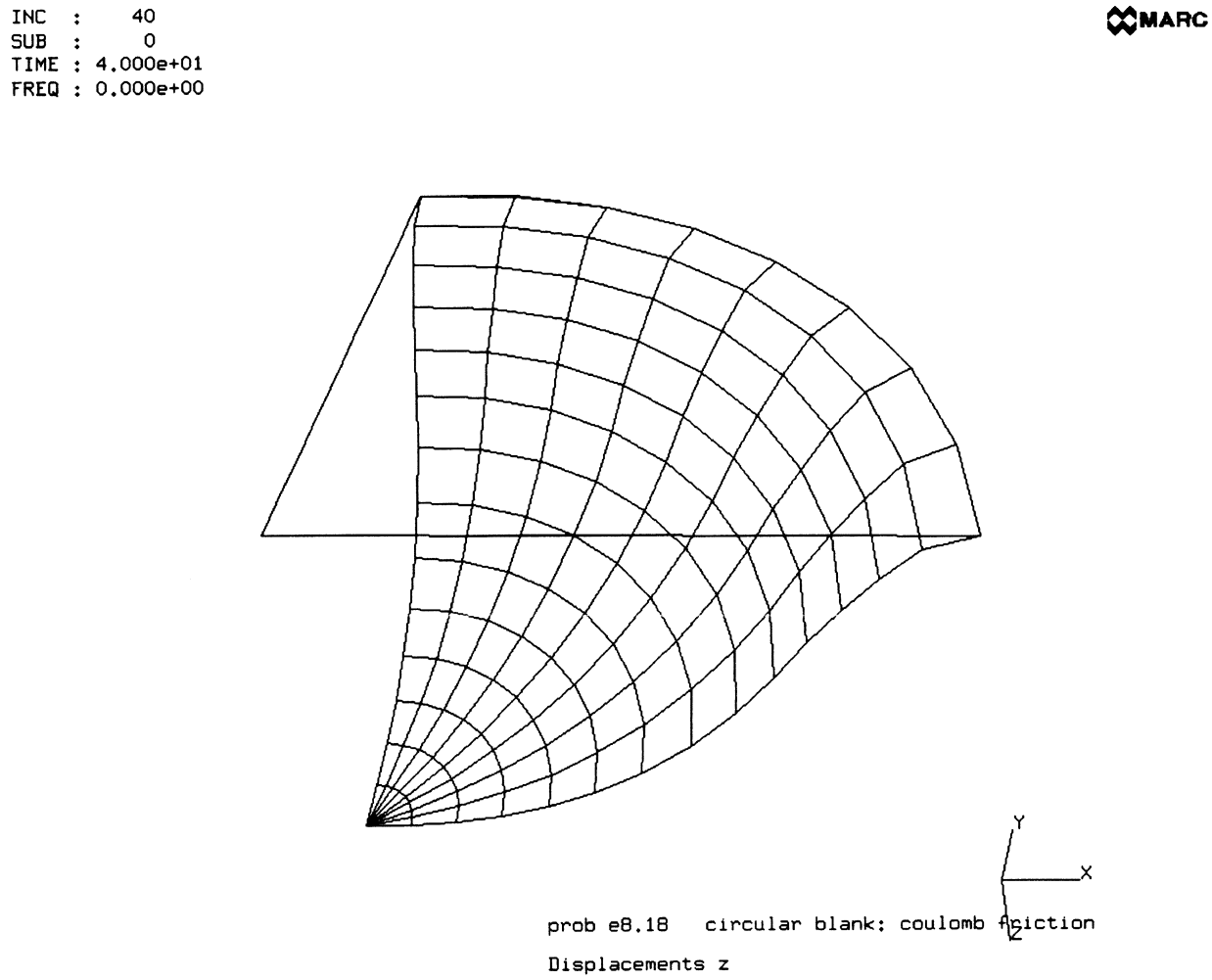

Figure E 8.18-2 Deformed Sheet at Increment 40

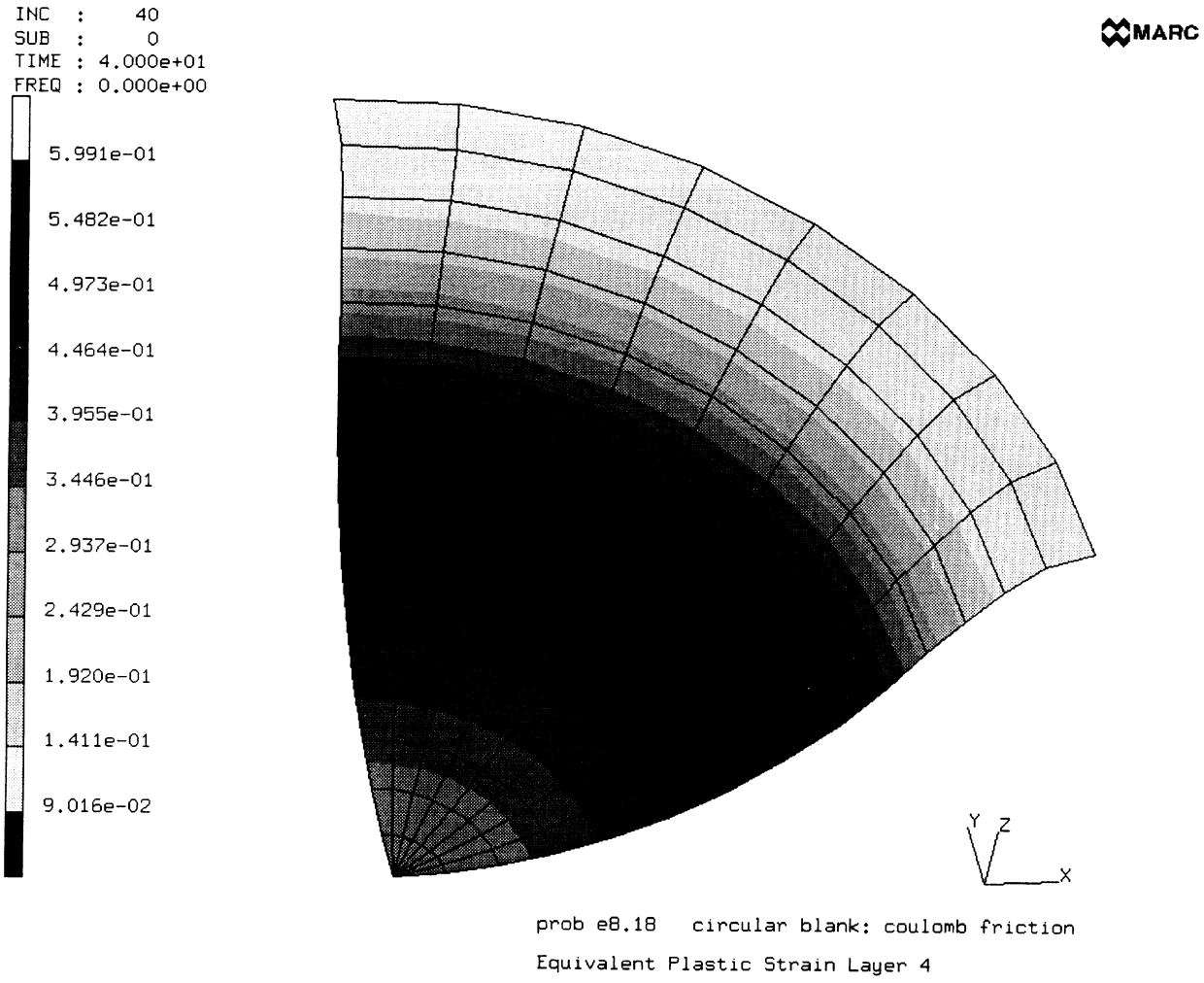

Figure E 8.18-3 Plastic Strain at Increment 40

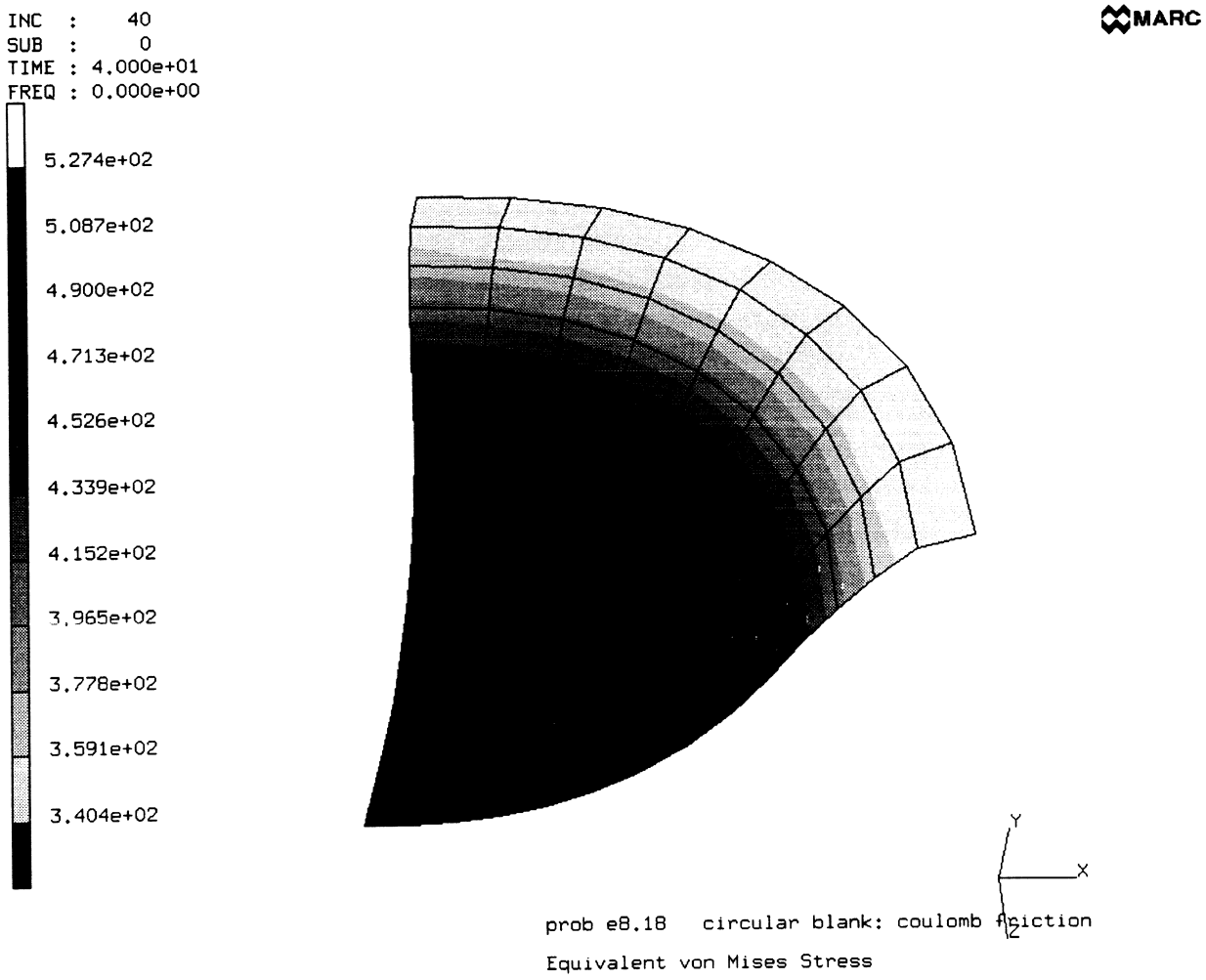

Figure E 8.18-4 Equivalent Stress at Increment 40

E 8.19 3D Indentation And Rolling Without Friction

This problem demonstrates the program's ability to perform metal forming analyses (e.g., rolling) using the CONTACT option. This problem also demonstrates using the iterative solver.

Parameters

The UPDATE, FINITE and LARGE DISP options are included in the parameter section to indicate this is a finite deformation analysis. The PRINT,8 option requests the output of additional information regarding contact.

Geometry

The model consists of 128 brick elements, type 7. A "1" is placed in the second data field (EGEOM2) to indicate that the constant dilatation formulation is used. This is done in recognition of the fact that metal extrusion results in large plastic deformations which are nearly incompressible.

Boundary Conditions

Appropriate nodal constraints are applied in the global X-, Y-directions. Since the geometry and loading are symmetric in the Z-direction, no boundary conditions are applied in that direction. A contact surface is used to represent this symmetry surface.

POST/PRINT Control

The following variables are written to a formatted POST tape:

11	σ_{XX}
12	σ_{YY}
13	σ_{ZZ}
17	Mean normal stress
7	Equivalent total plastic strain.

These variables are written every 12th increment. The PRINT CHOICE option selects element number 1 as the only one which will have printed output (every 12th increment, like the post tape). Such output will be for integration points 1 and 5 only.

Material Properties

The material for all elements is treated as an elastic-plastic material, with Young's modulus of 1.75E+07 psi, Poisson's ratio of 0.3, and an initial yield stress of 35,000 psi.

Contact

The first body is the deformable workpiece; the second is the rigid roller defined using the surface of revolution method. The radius is 10 inches. The third body is the symmetry surface. The contact tolerance distance is specified as 0.02 inches.

Load Control/Restart

This problem is loaded by calling the MOTION subroutine where die velocities are computed as a function of time (or increment number). In the first 25 increments, the rigid roll is pushed into the workpiece with a velocity of 0.25 in/sec. The total indentation is 6.25 inches. In increment 26, no motion is prescribed. In the remaining increments, the roll is given an angular velocity of 0.05 radians/sec. and a forward motion of 5 in/sec.

A restart tape will be written at the end of increment 26.

Because large incremental changes of motion may occur, many recycles may be required. The CONTROL option allows for a maximum of 20 recycles and specifies the displacement tolerance checking be performed with a tolerance of 10%.

Solver

In three dimensional continuum problems, it is often beneficial to use an iterative solver because of the large bandwidth. To invoke the iterative solver, one needs to use the SOLVER option. Additionally, one must set a tolerance on the error associated with this method. To use the Element-By-Element (EBE) iterative solver, add the following into the model definition section:

```
SOLVER
1,,,
,,,,,
1.0E-05,1.0E-05,,
```

If no solver option is selected, the direct matrix solver is used.

Results

Figure E 8.19-1 shows the geometry configuration for this problem. The cylindrical rigid surface will be pushed into the deformable block that is resting on the flat rigid surface.

Figure E 8.19-2, Figure E 8.19-3, and Figure E 8.19-4 show the deformed workpiece in increments 12, 24, and 36.

Figure E 8.19-5 and Figure E 8.19-6 show the equivalent total plastic strain contours on the deformed structure at increment 36 for the direct and iterative solver, respectively. Observe that the maximum plastic strain is between 132% and 131% for the direct and iterative solver, respectively. Because of many nodes coming into contact requiring many assemblies, the overall time of the iterative and direct solvers are about the same.

Summary of Options Used

Listed below are the options used in example e8x19.dat:

Parameter Options

ELEMENT
END
FINITE
LARGE DISP
PRINT
SIZING
TITLE
UPDATE

Model Definition Options

CONNECTIVITY
CONTACT
CONTROL
COORDINATE
END OPTION
FIXED DISP
GEOMETRY
ISOTROPIC
POST
PRINT CHOICE
UDUMP
UMOTION

Load Incrementation Options

AUTO LOAD
CONTINUE
TIME STEP

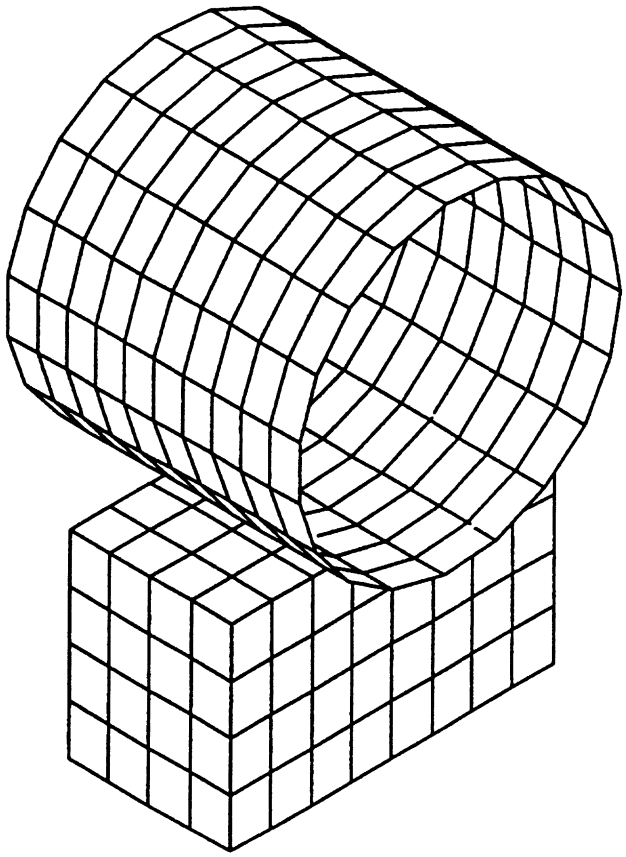

Figure E 8.19-1 Geometry Configuration

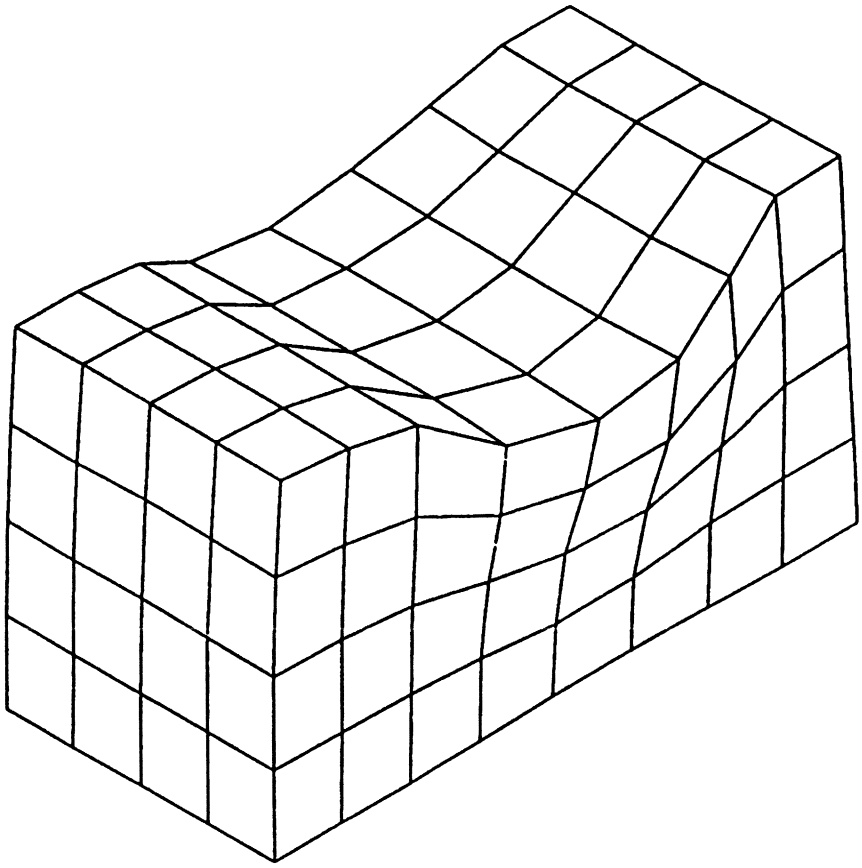

Figure E 8.19-2 Deformed Mesh at Increment 12

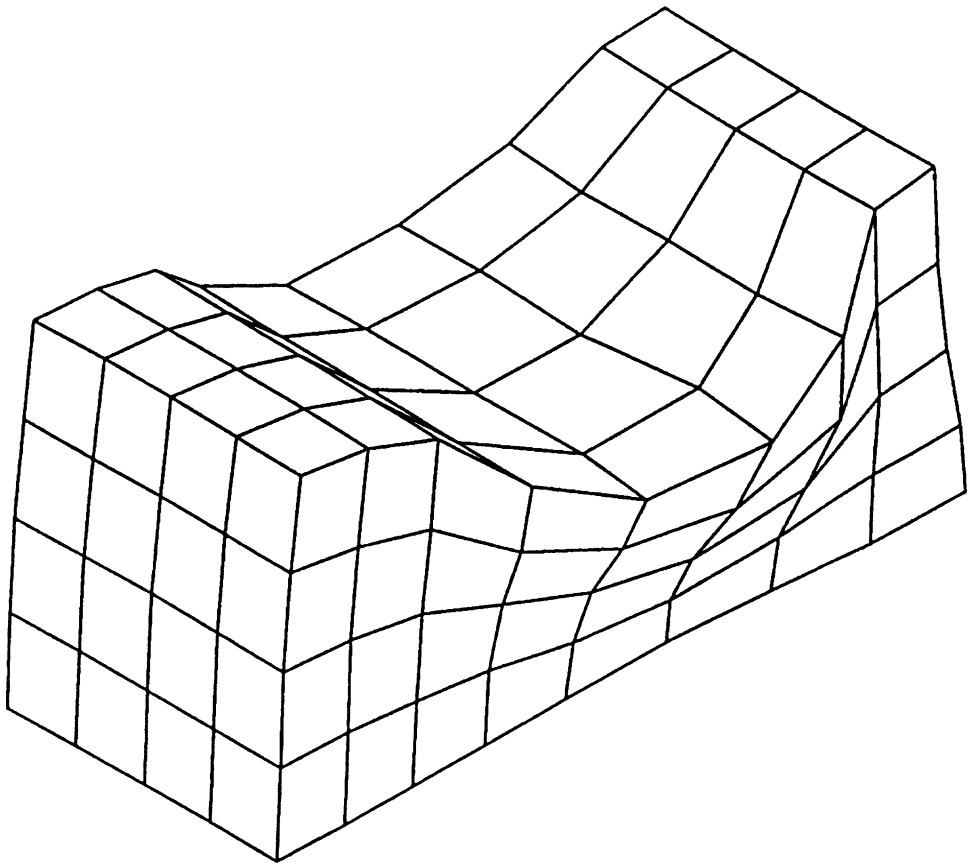

Figure E 8.19-3 Deformed Mesh at Increment 24

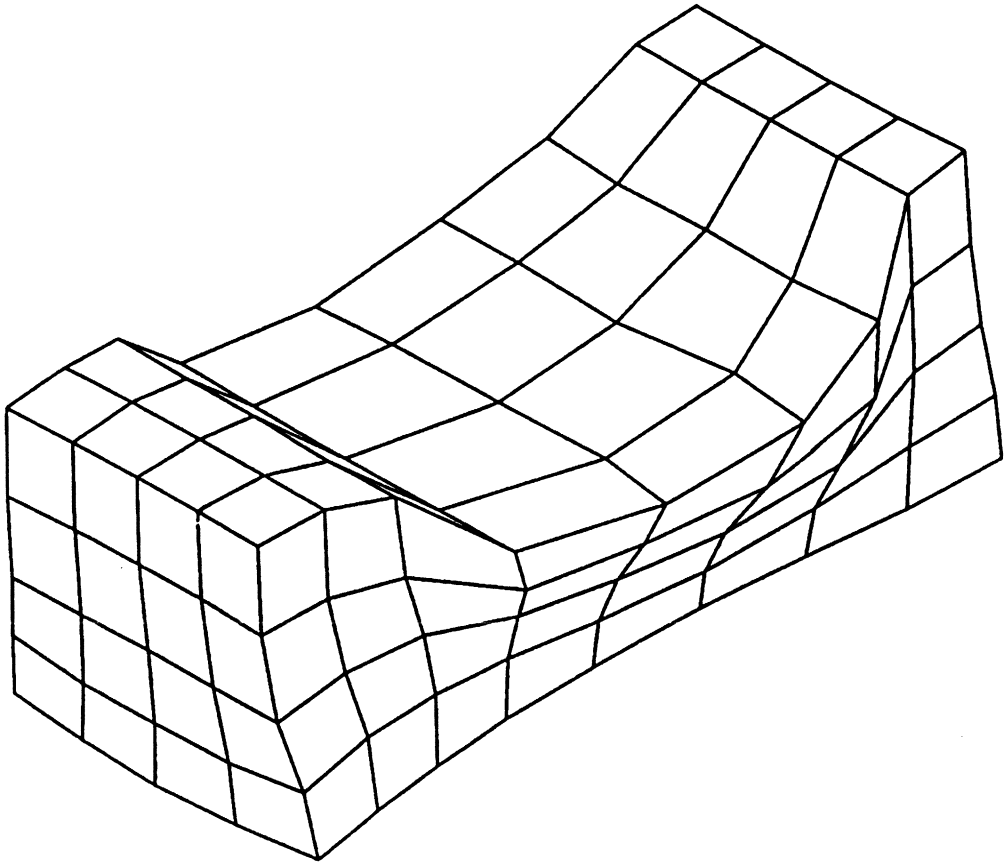

Figure E 8.19-4 Deformed Mesh at Increment 36

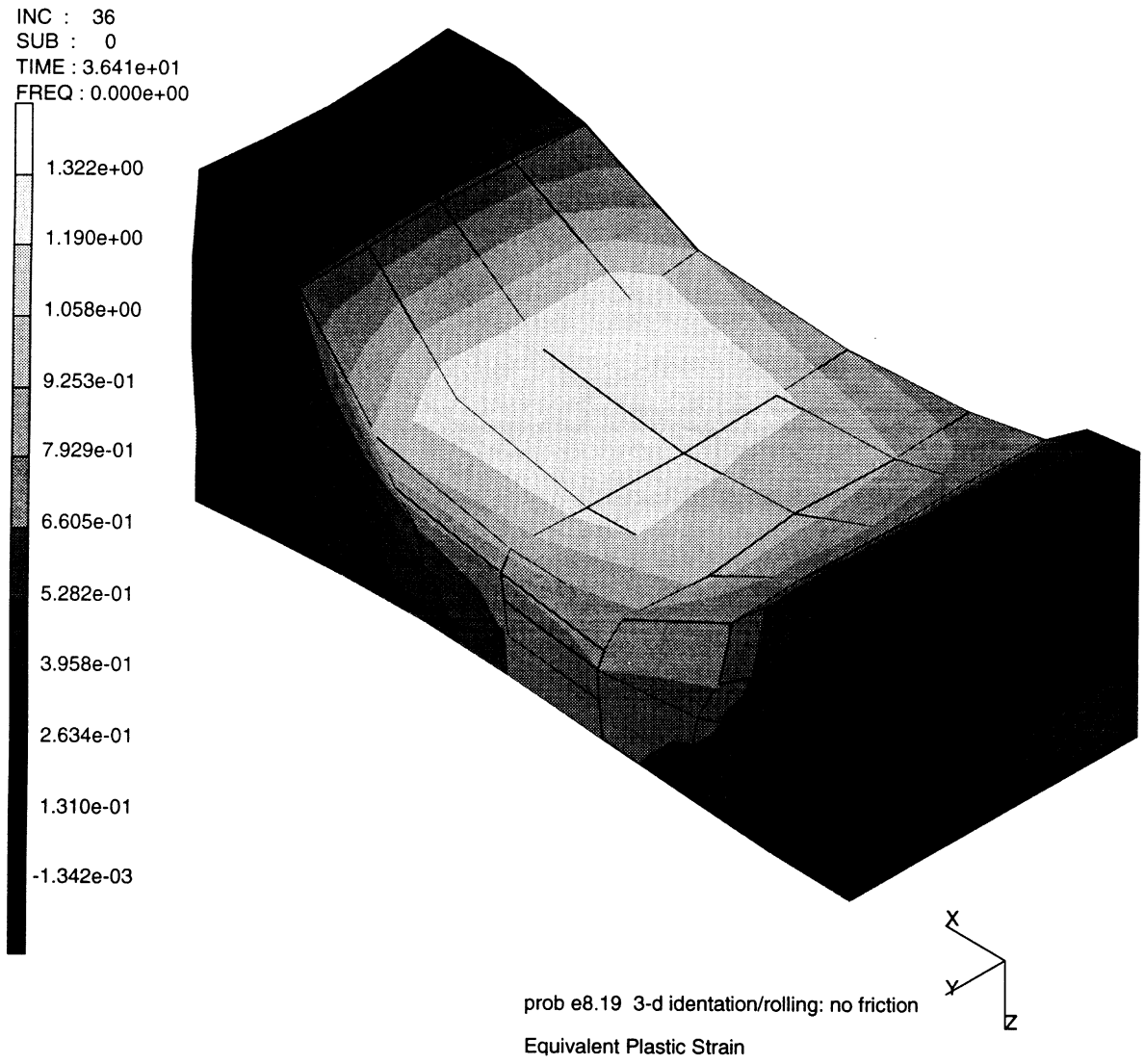

Figure E 8.19-5 Equivalent Total Plastic Strain at Increment 36 (Direct Solver)

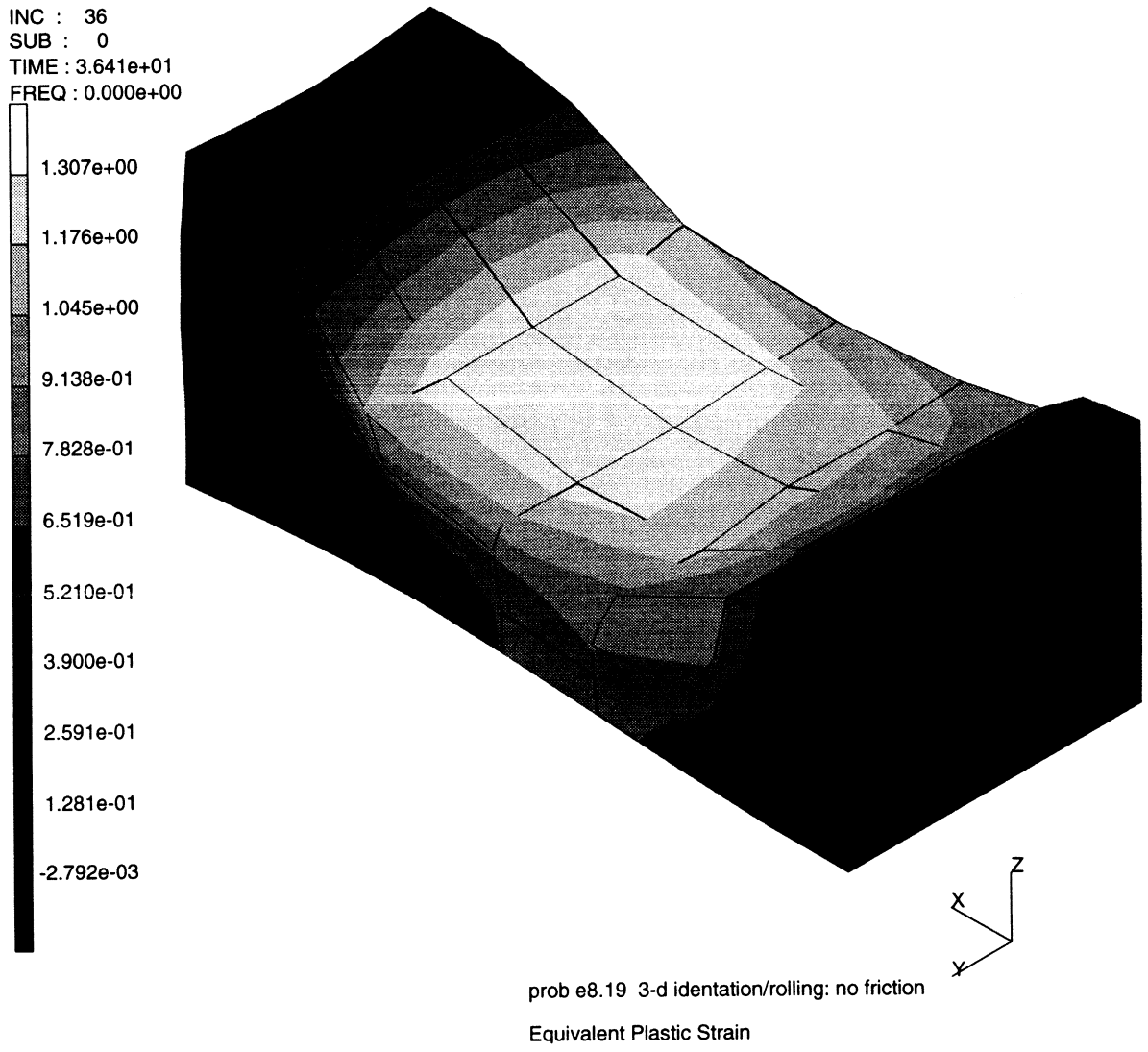

Figure E 8.19-6 Equivalent Total Plastic Strain at Increment 36 (Iterative Solver)

E 8.20 2D Electrostatic Analysis Of A Circular Region

This problem analyses a point charge in a circular region to demonstrate MARC's electrostatic analysis capability using a 2D element formulation. The electrostatic problem is governed by Poisson's equation for scalar potential, valid for heat transfer and electrostatic analyses among others. Using this duality, heat transfer elements (type 39) are used but all input and output is seen in terms of an electrical problem.

Parameters

The ELECTRO parameter is included to indicate an electrostatic analysis.

Mesh Definition

Half of the circle is modeled due to symmetry. The mesh has 100 elements and 111 nodes. Figure E 8.20-1 shows the nodes, and Figure E 8.20-2 shows the element configuration.

Boundary Conditions

A potential of zero volts is specified along the outer radius which is nodes 11 to 111 by 10 through the FIXED POTENTIAL option.

Material Properties

The permittivity of the medium is specified at 1.0 farad/cm in the ISOTRPOIC option.

Electrostatic Charge

A point charge of 1.0 coulomb is applied at node 1 through the POINT CHARGE option.

POST

The following variables are requested to be written to both binary and formatted post tapes:

130 } Scalar potential 131,132 } Components of electric field vector
134,135 } Components of electric displacement vector

Control

The STEADY STATE option is used to initiate the analysis.

Results

Figure E 8.20-3 shows the scalar potential (POST code 130). Figure E 8.20-4 and E8.20-5 show the first and second components of displacement the electric field (POST codes 131,132). Figures E8.20-6 and E8.20-7 show the first and second components of electric displacements (POST codes 134,135).

Summary of Options Used

Listed below are the options used in example e8x20.dat:

Parameter Options

ELECTROSTATIC
ELEMENT
END
SIZING
TITLE

Model Definition Options

CONNECTIVITY
COORDINATE
END OPTION
FIXED POTENTIAL
ISOTROPIC
POINT CHARGE
POST

Load Incrementation Options

CONTINUE
STEADY STATE

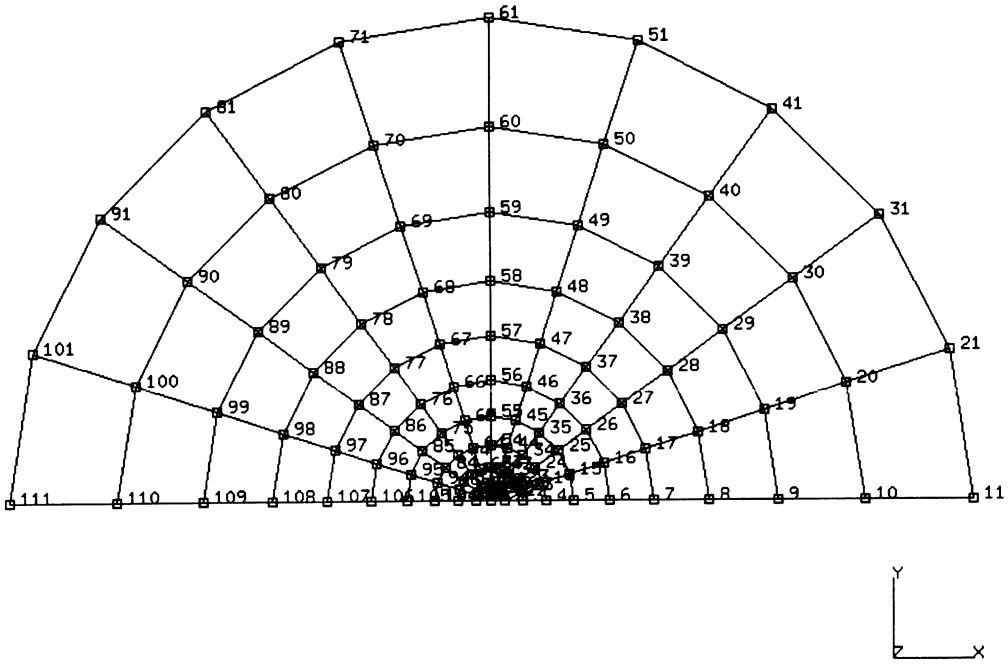

Figure E 8.20-1 Node Numbers in Circular Region

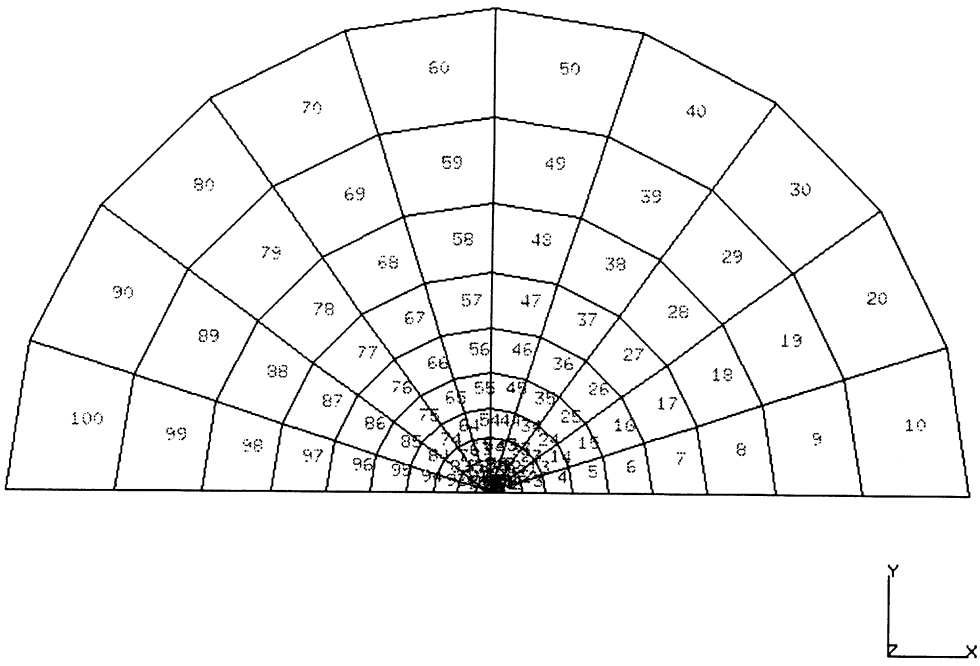

Figure E 8.20-2 Element Numbers in Circular Region

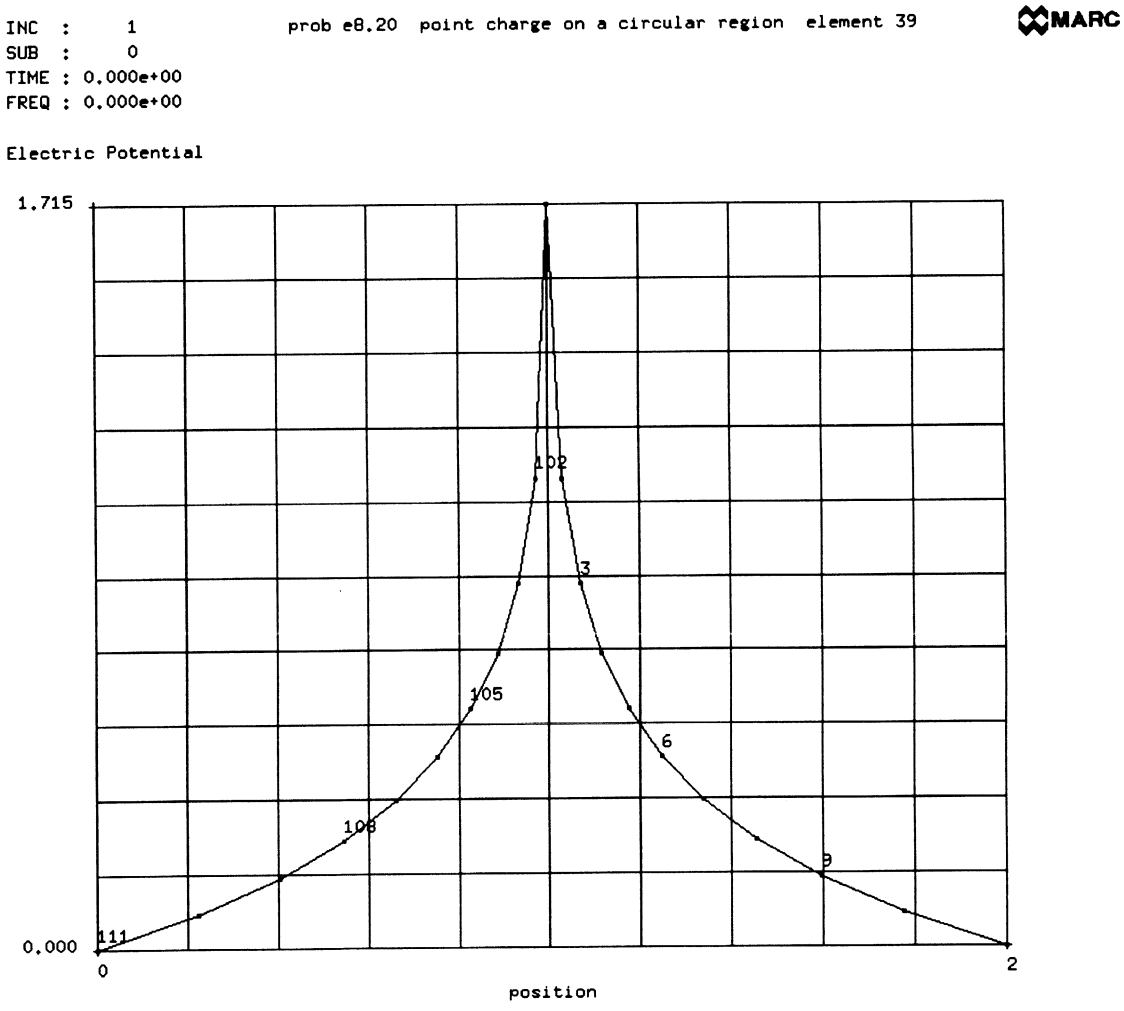

Figure E 8.20-3 Electric Potential Along Diameter

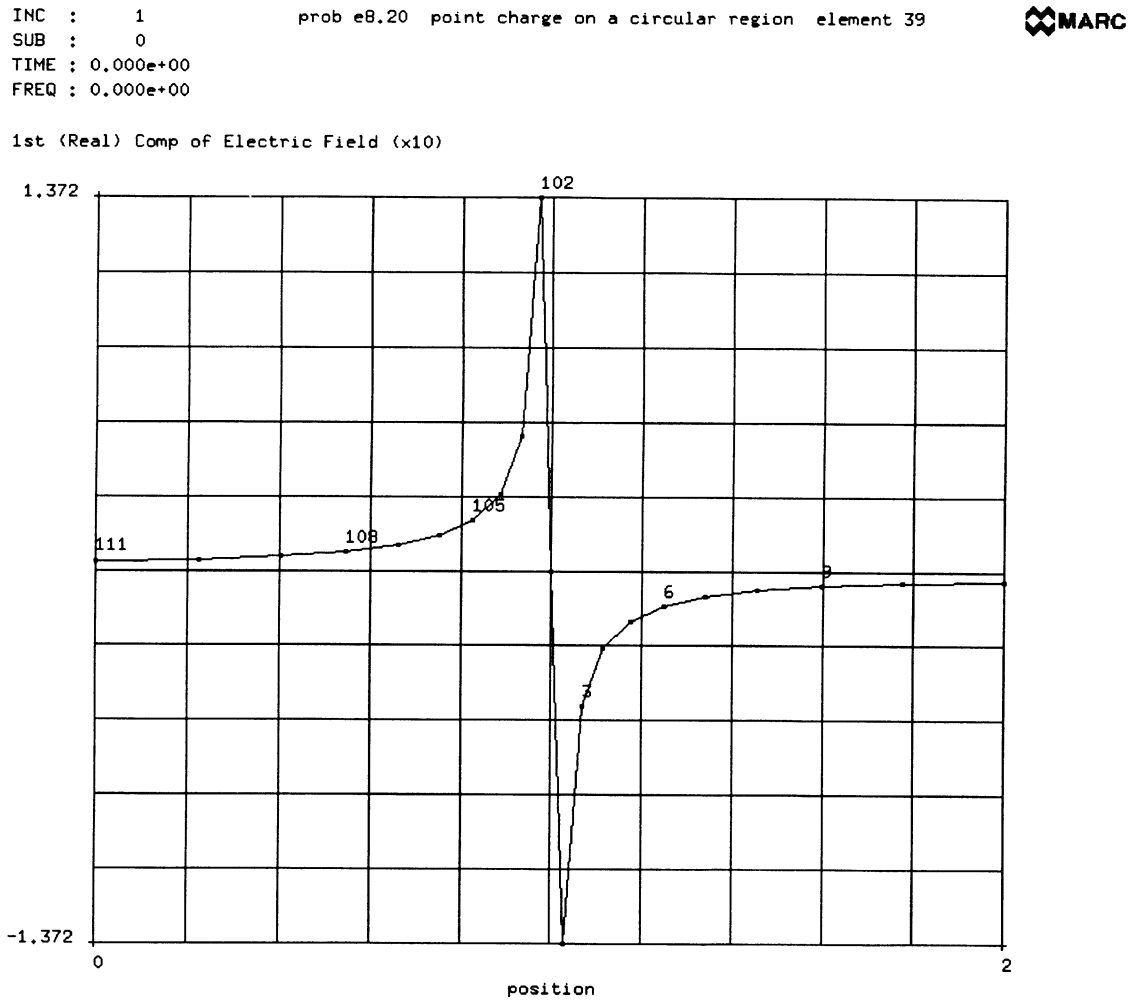

Figure E 8.20-4 First Component of Electric Field

E 8.21 3D Electrostatic Analysis Of A Circular Region

This problem analyses a point charge in a circular region to demonstrate MARC's electrostatic analysis capability using a 3D element formulation. The electrostatic problem is governed by Poisson's equation for scalar potential, valid for heat transfer and electrostatic analyses among others. Using this duality, eight-noded heat transfer elements (type 43) are used but all input and output is seen in terms of an electrical problem.

Parameters

The ELECTRO parameter is included to indicate an electrostatic analysis.

Mesh Definition

One half of the region is modeled due to symmetry. The model has 100 brick elements and 222 nodes. Figure E 8.21-1 shows the mesh nodal points, and Figure E 8.21-2 shows the element configuration.

Boundary Conditions

A potential of zero volts is specified along the outside radius at nodes 201 to 222.

Material Properties

The permittivity of the medium is specified at 1.0 farad/cm for all elements.

Electrostatic Charge

A point charge of 0.1 coulomb is applied at nodes 1 and 2.

POST

The following codes are requested to be output to both binary and formatted post tapes:

130 } Scalar potential 131-133 } Components of the electric field vector
134-136 } Components of the electric displacement vector

Control

The STEADY STATE option is used to initiate the analysis.

Results

Figure E 8.21-3 shows the scalar potential (POST code 130). As anticipated, the calculated potential is of the same magnitude as the two-dimensional problem E 8.20.

Summary of Options Used

Listed below are the options used in example e8x21.dat:

Parameter Options

ELECTROSTATIC
ELEMENT
END
SIZING
TITLE

Model Definition Options

CONNECTIVITY
COORDINATE
END OPTION
FIXED POTENTIAL
ISOTROPIC
POINT CHARGE
POST

Load Incrementation Options

CONTINUE
STEADY STATE

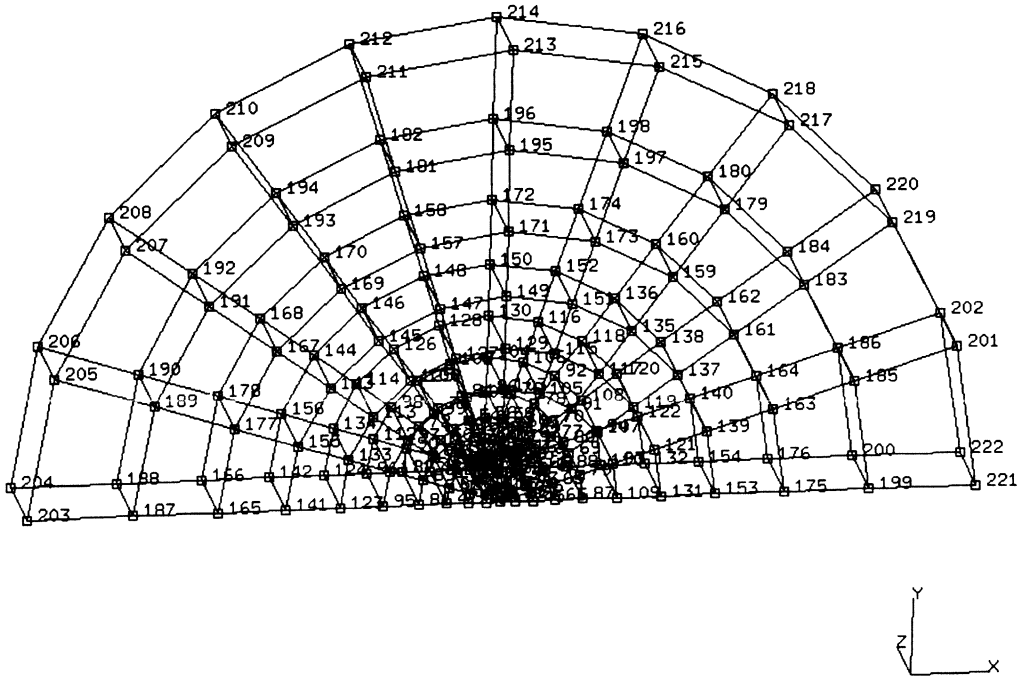

Figure E 8.21-1 Node Numbers in Mesh

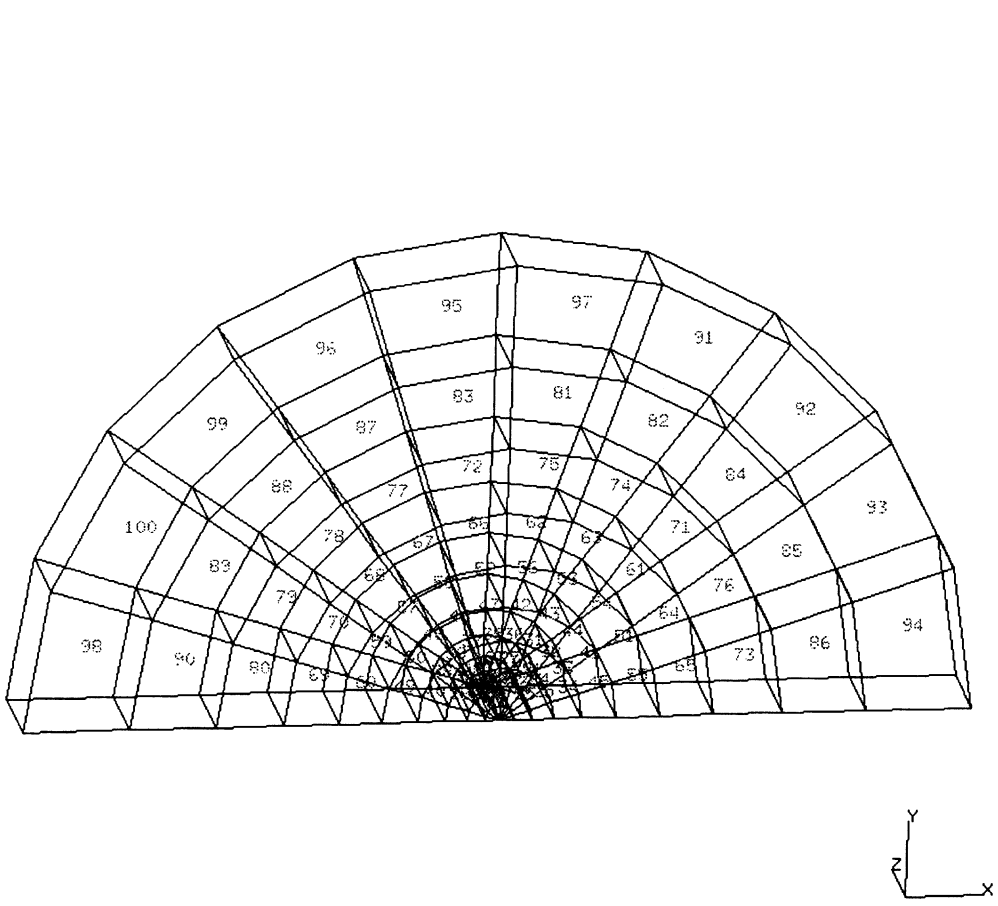

Figure E 8.21-2 Element Numbers in Mesh

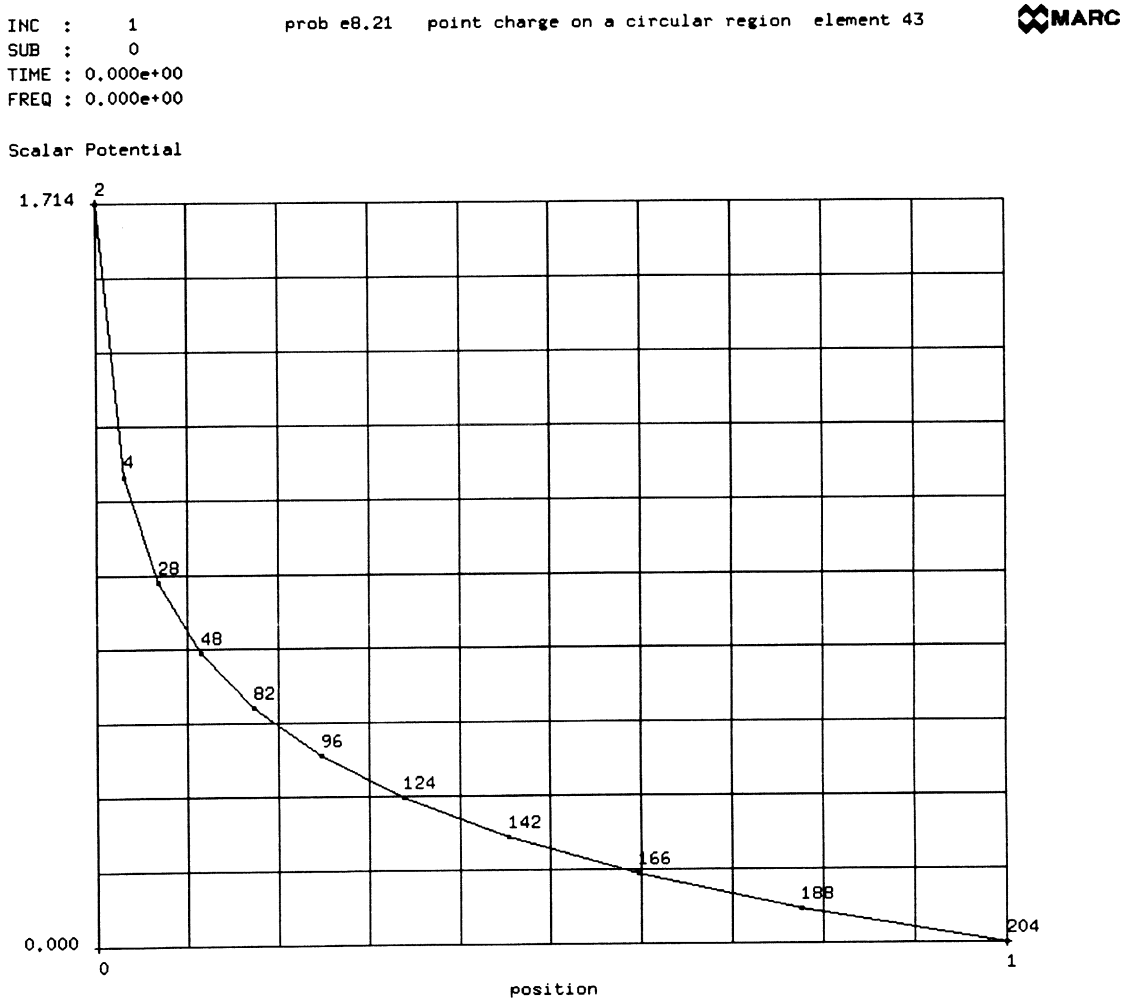

Figure E 8.21-3 Scalar Potential Through Radius

E 8.22 2D Magnetostatic Analysis Of A Circular Region

This problem shows MARC's magnetostatic analysis capability using a 2D element formulation. The two-dimensional magnetostatic problem is governed by Poisson's equation for scalar potential, valid for heat transfer, magnetostatic and electrostatic analyses among others. When using this duality, eight-noded heat transfer elements (type 39) are used, but all input and output is seen in terms of an electrical problem.

Parameters

The MAGNET parameter is included to indicate a magnetostatic analysis.

Mesh Definition

Half of the circular region is modeled due to symmetry. The mesh has 100 elements and 111 nodes. Figure E 8.22-1 shows the nodal configuration of the mesh and Figure E 8.22-2 shows the element configuration.

Boundary Conditions

A potential of zero volts is specified on the outside radius which is at nodes 11 to 111 by 10.

Material Properties

The magnetic permeability of the medium is specified at 1.0 henry/cm for all elements.

Current

A point current of 1.0 amps is applied at node 1 through the POINT CURRENT option.

POST

The following variables are requested to be written to both a binary and a formatted POST tape:

140 } Scalar potential 141,142 } Components of magnetic flux
144,145 } Components of magnetic density

Results

Figure E 8.22-3 shows the scalar potential (POST code 140). Figure E 8.22-4 shows the vector plot of the magnetic flux.

Summary of Options Used

Listed below are the options used in example e8x22.dat:

Parameter Options

ELEMENT
END
MAGNETOSTATIC
SIZING
TITLE

Model Definition Options

CONNECTIVITY
COORDINATE
END OPTION
FIXED POTENTIAL
ISOTROPIC
POINT CURRENT
POST

Load Incrementation Options

CONTINUE
STEADY STATE

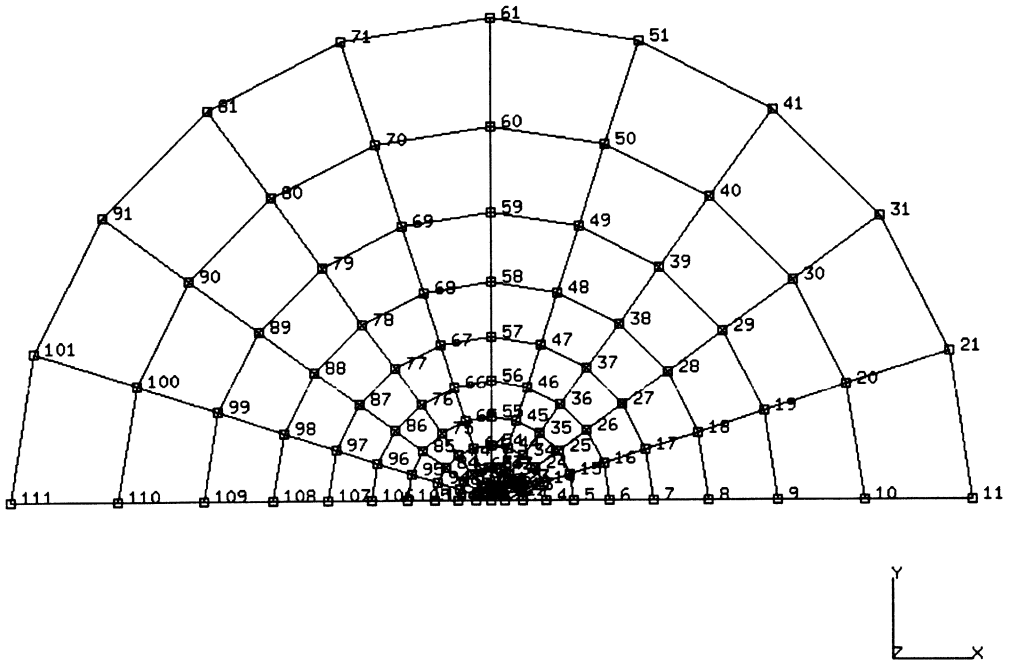

Figure E 8.22-1 Node Numbers in Circular Region

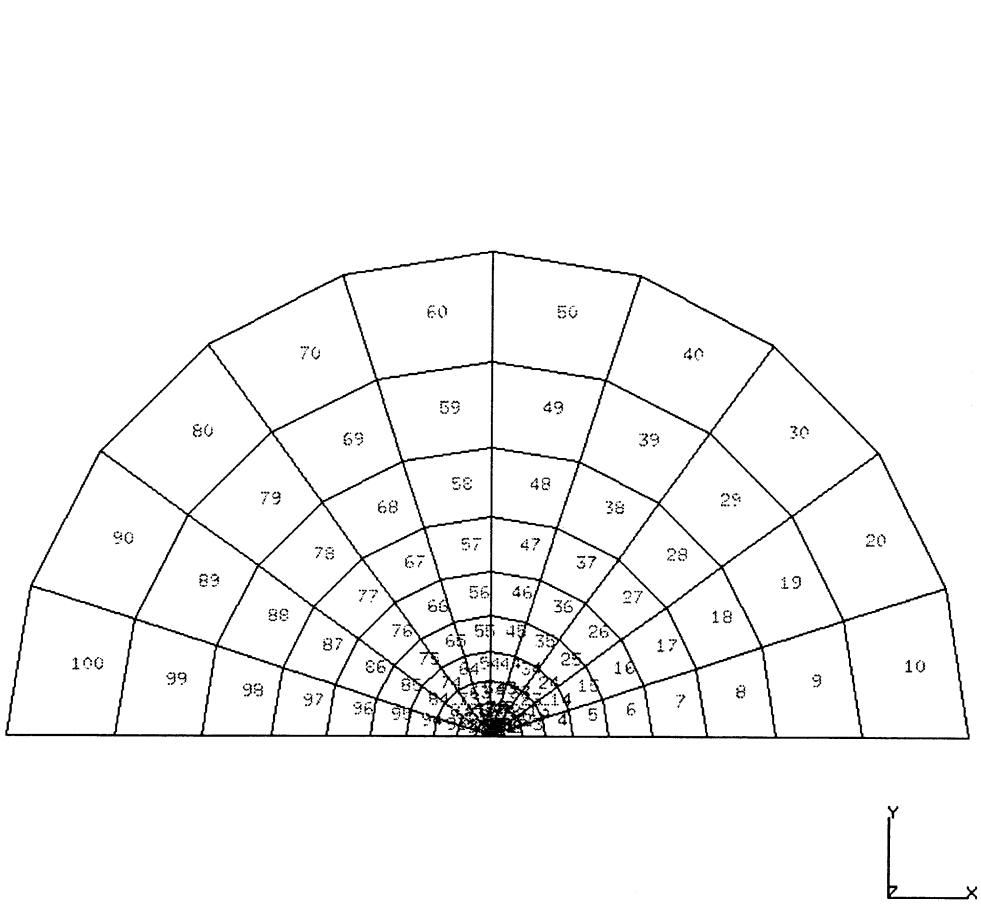

Figure E 8.22-2 Element Numbers in Circular Region

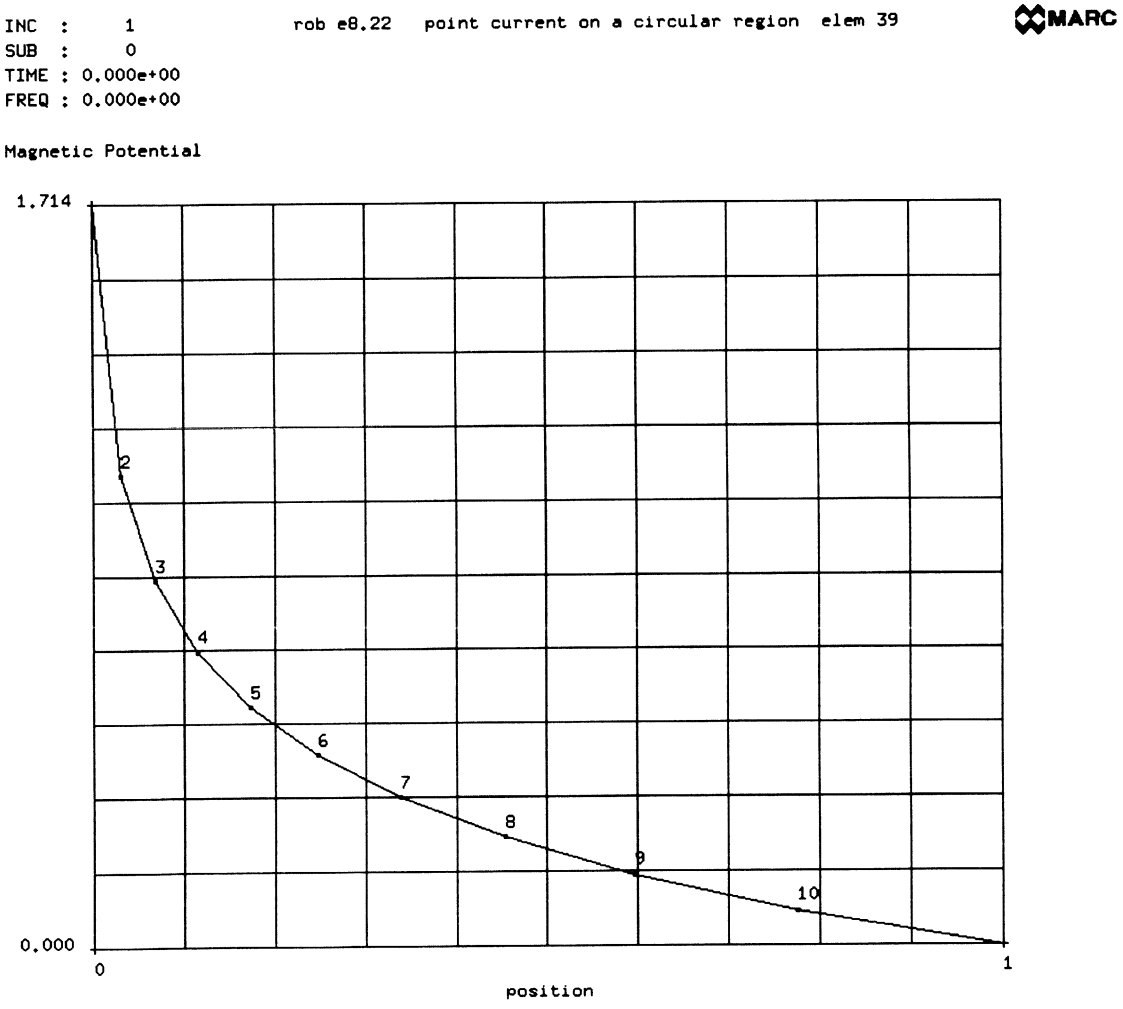

Figure E 8.22-3 Magnetic Scalar Potential Along Radial Line

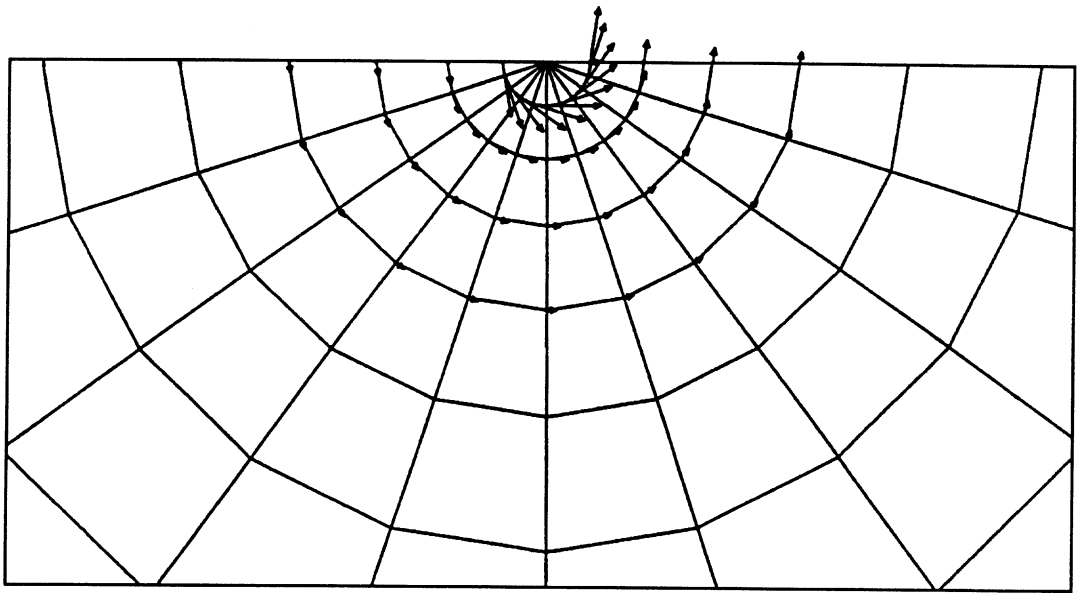

Figure E 8.22-4 Magnetic Flux Distribution

E 8.23 3D Magnetostatic Analysis Of A Coil

This problem shows magnetostatic analysis capability using a 3D element formulation in the MARC program. Since the potential to be solved is a new vector potential, the normal "heat transfer" approach cannot be used. Instead, an eight-noded magnetostatic element (type 109) is used for this analysis.

Parameters

The MAGNETO parameter is included to indicate a magnetostatic analysis.

Mesh Definition

One quarter of the coil is modeled using element type 109. The outside radius is 2.405 cm. Figure E 8.23-1 shows the mesh and applied current.

Boundary Conditions

Along the y = 0 edge $A_1 = 0$. Along the x = 0 edge $A_2 = 0$. Along the outside radius $A_1 = A_2 = 0$. $A_3 = 0$ everywhere to simulate a two dimensional problem.

Material Properties

The magnetic permeability of all elements is set to 1000.0 henry/cm.

Currents

A current running in the circumferential direction at a radius of 1 cm is applied. The point currents ranging in value from -0.951 amps to +0.951 amps are applied at nodes 111 to 120.

POST

The following variables are written to both a binary and a formatted POST tape:

141-143 } Components of magnetic flux
144-146 } Components of magnetic intensity

Results

The third component of the magnetic flux is shown as a function of the radius in Figure E 8.23-2. One can observe that a steep gradient occurs about the ring of nodes to which the current is applied. In addition, the total magnetization is zero, as:

$$\pi r_c^2 (338.5) + \pi(r_o^2 - r_c^2) (-42.32) = 2.7$$

where $r_c = 1$, and $r_o = 3$.

The vector potential A is shown in Figure E 8.23-3.

Summary of Options Used

Listed below are the options used in example e8x23.dat:

Parameter Options

ELEMENT
END
MAGNETOSTATIC
SIZING
TITLE

Model Definition Options

CONNECTIVITY
COORDINATE
END OPTION
FIXED POTENTIAL
ISOTROPIC
POINT CURRENT
POST

Load Incrementation Options

CONTINUE
STEADY STATE

Listed below are the options used in example e8x23b.dat:

Parameter Options

ELEMENT
END
MAGNETOSTATIC
SIZING
TITLE

Model Definition Options

CONNECTIVITY
COORDINATE
DEFINE
END OPTION
FIXED POTENTIAL
ISOTROPIC
POINT CURRENT
POST

Load Incrementation Options

CONTINUE
STEADY STATE

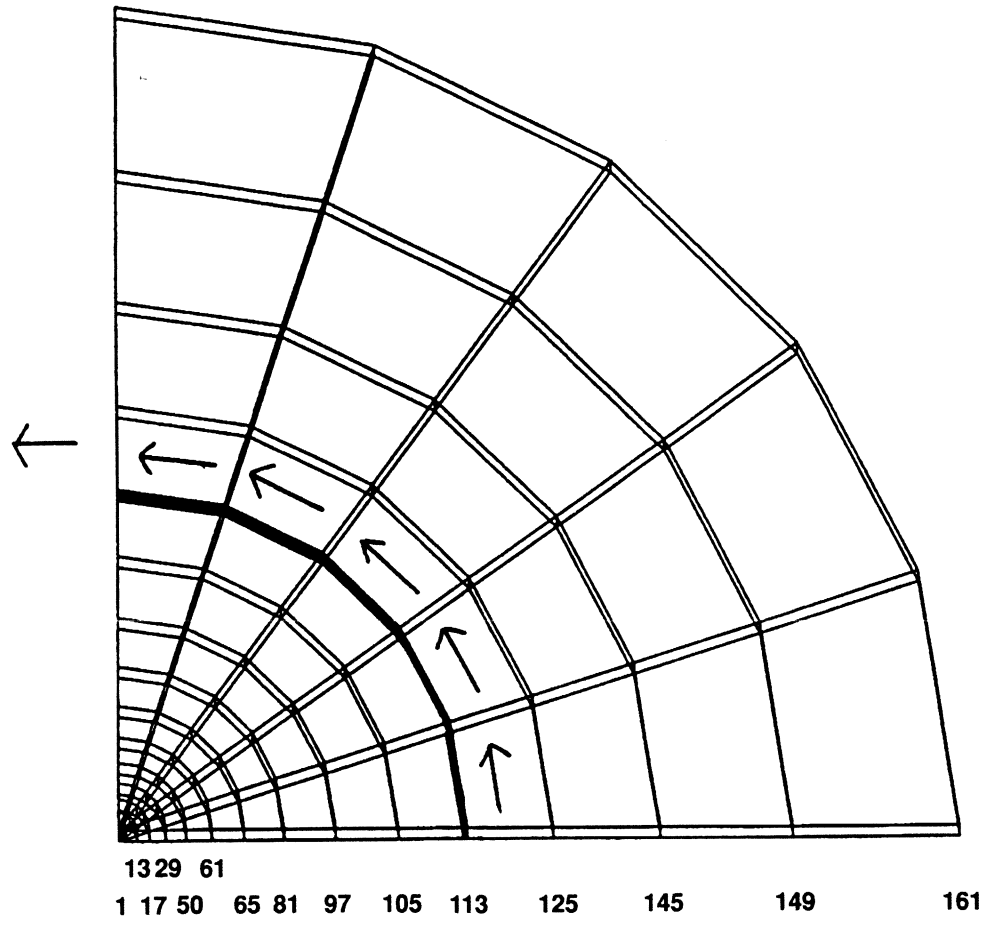

Figure E 8.23-1 Mesh and Applied Current

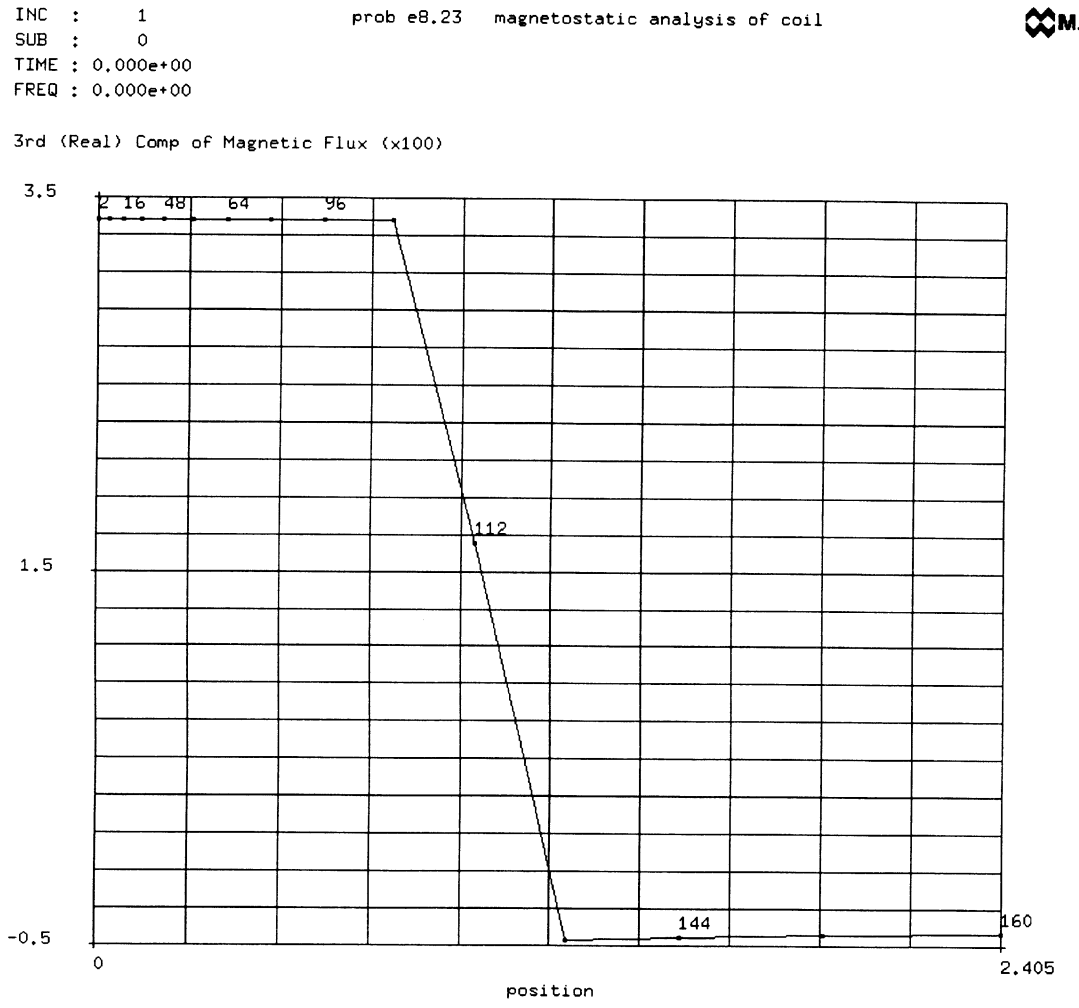

Figure E 8.23-2 Third Component of Magnetic Flux Along Radial Line

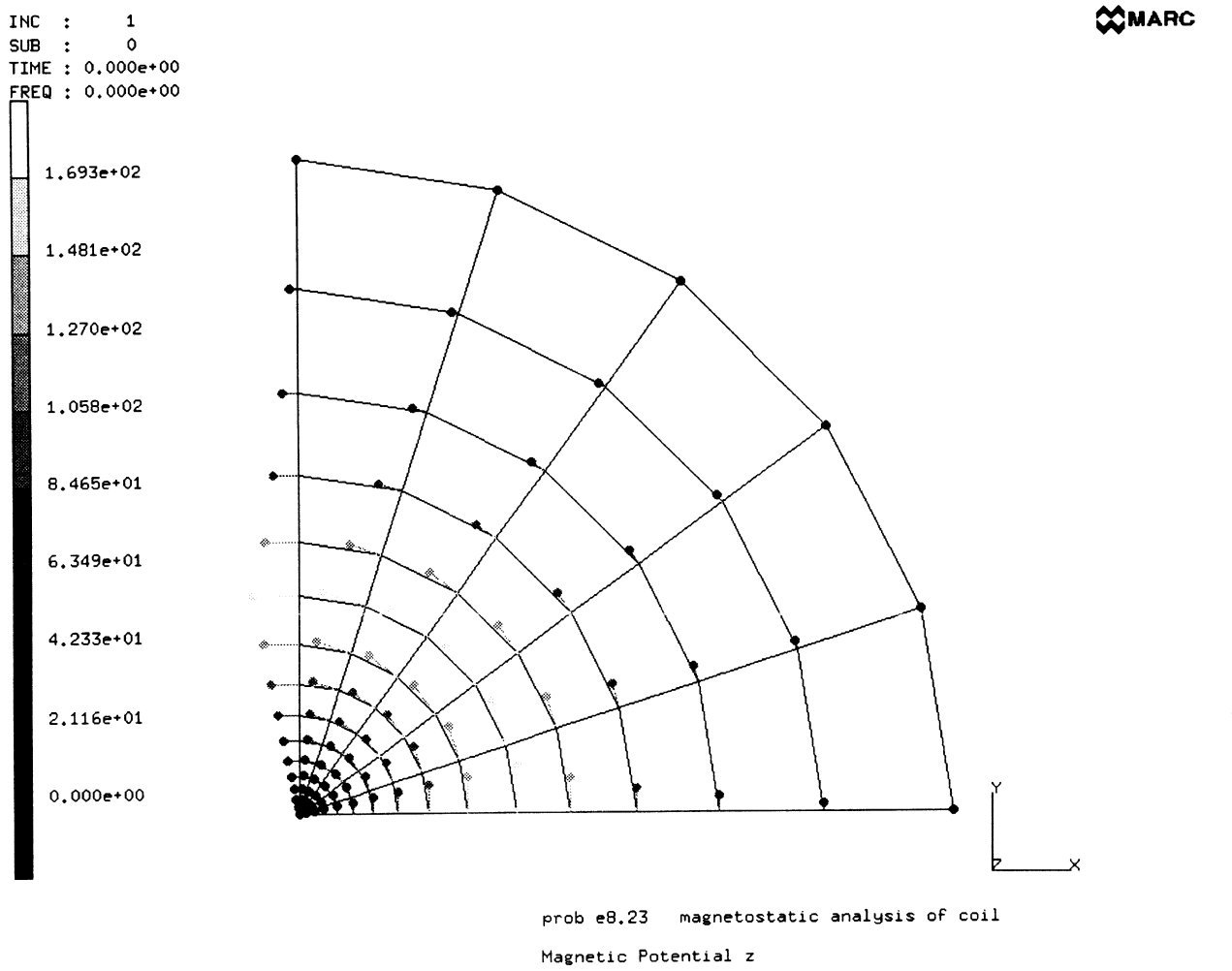

Figure E 8.23-3 Magnetic Potential Vector

E 8.24 2D Nonlinear Magnetostatic Analysis

An infinite wire carries a current through a circular region.

This problem shows MARC's magnetostatic analysis capability using a 2D element formulation together with an orthotropic magnetic permeability that is a function of the magnetic flux density. The latter requires that a nonlinear problem be solved.

Parameters

The MAGNET parameter is included to indicate a magnetostatic analysis.

Mesh Definition

Only a section of the region is modeled due to symmetry. Element type 39, the four-node heat transfer element, is used. Figure E 8.24-1 shows the mesh nodal points, and Figure E 8.24-2 shows the element configuration.

Boundary Conditions

A potential of zero volts is specified at nodes 20 and 21.

Material Properties

Use of the ORTHOTROPIC model option allows the input of the baseline magnetic permeabilities in the principal directions. These are set to 1000.0, 1200.0, and 1400.0 henry/cm in the 1, 2, and 3 directions respectively. These permeabilities are functions of the magnetic flux density, the functionality being described through the B-H RELATION model definition option.

Current

A point current of 1.0 amps is applied at nodes 1.

POST

The following variables are written to a formatted POST tape:

140	}	Scalar magnetic potential
141-142	}	Components of magnetic flux
144-1465	}	Components of magnetic intensity

Results

Figure E 8.24-3 shows the scalar potential (POST code 140) using linear material properties. Figure E 8.24-4 shows the potential when the nonlinear material behavior is represented.

Summary of Options Used

Listed below are the options used in example e8x24a.dat:

Parameter Options

ELEMENT
END
MAGNETOSTATIC
SIZING
TITLE

Model Definition Options

CONNECTIVITY
COORDINATE
END OPTION
FIXED POTENTIAL
ISOTROPIC
POINT CURRENT
POST
PRINT ELEM

Load Incrementation Options

CONTINUE
STEADY STATE

Listed below are the options used in example e8x24b.dat:

Parameter Options

ELEMENT
END
MAGNETOSTATIC
SIZING
TITLE

Model Definition Options

B-H RELATION
CONNECTIVITY
CONTROL
COORDINATE
END OPTION
FIXED POTENTIAL
ISOTROPIC
POINT CURRENT
POST
PRINT ELEM

Load Incrementation Options

CONTINUE
STEADY STATE

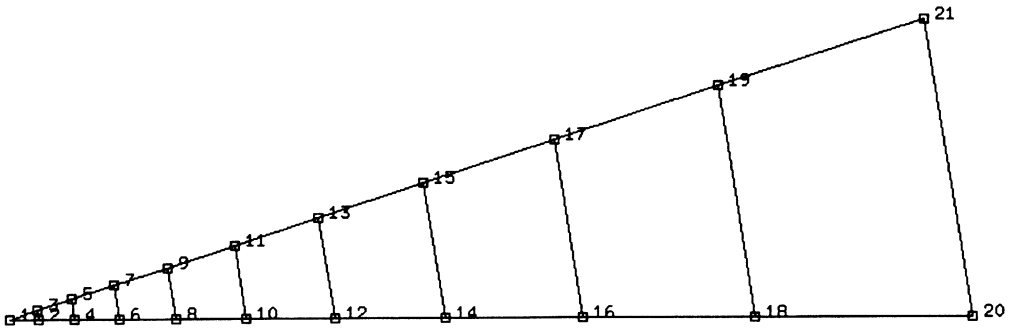

Figure E 8.24-1 Mesh with Node Numbers

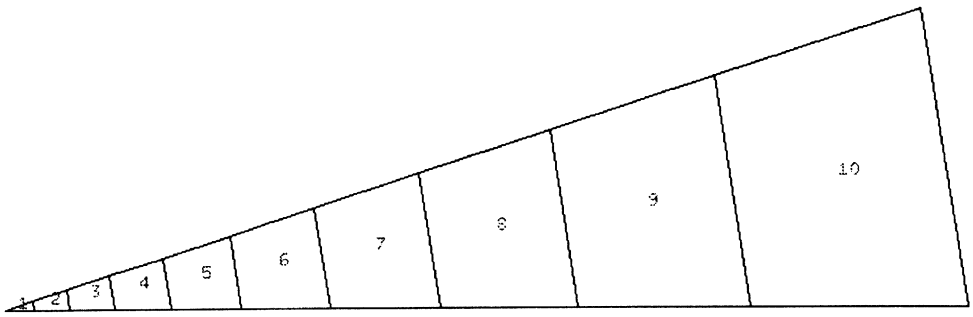

Figure E 8.24-2 Mesh with Element Numbers

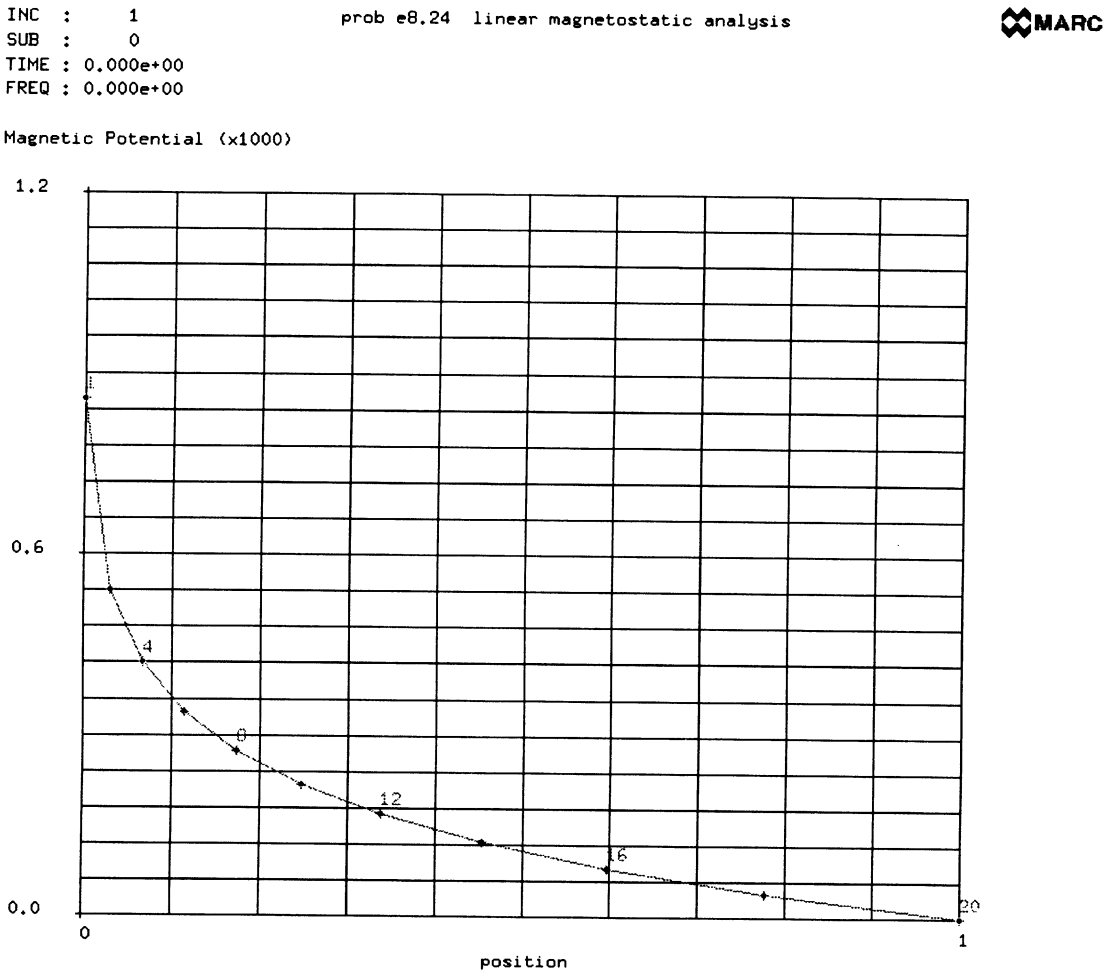

Figure E 8.24-3 Magnetic Scalar Potential Linear Material Behavior

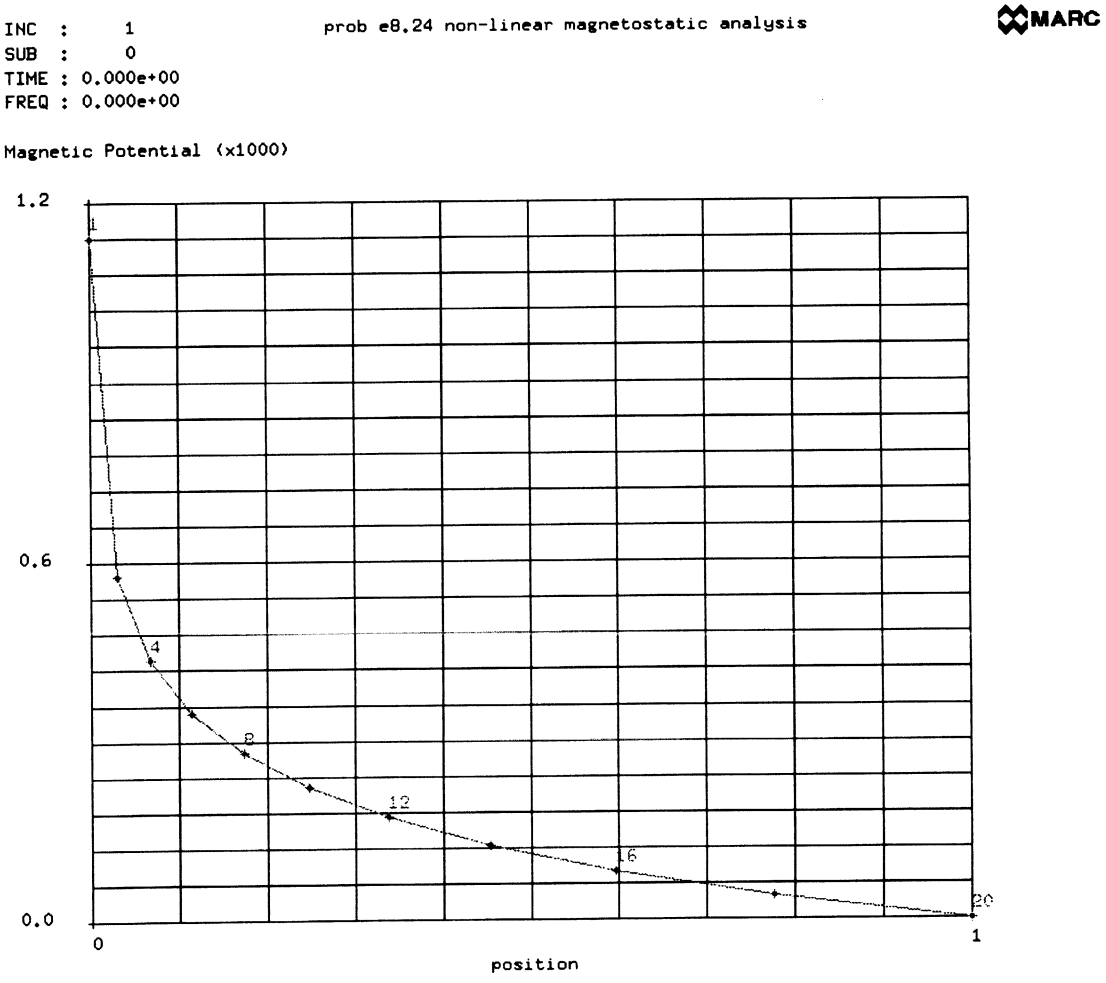

Figure E 8.24-4 Magnetic Scalar Potential Nonlinear Material Behavior

E 8.25 Acoustic Problem: Eigenvalue Analysis Of A Circular Cavity

This problem demonstrates the acoustic analysis capability using a 2-D element formulation in the MARC program. MARC can be used to obtain the pressure distribution in a cavity with rigid reflecting boundaries. A transient analysis is then performed.

Parameters

The ACOUSTIC parameter is included to indicate an acoustic analysis. A maximum of six modes are to be used in the modal superposition. The Lanczos method will be used for eigenvalue analysis, and resulting mode shapes are written onto the POST tape. PRINT 3 is used to force the solution of a non-positive definite stiffness matrix.

Elements/Mesh Definition

The input was originally created with element type 11. Using the ALIAS parameter option, we can easily respecify them as element type 39. Figure E 8.25-1 and Figure E 8.25-2 show the node numbers and the elements in the cavity. The reflecting barrier is modeled by having a free surface. This can be seen in Figure E 8.25-3 showing the double nodes. A refined mesh is used around the edges of the plate.

Boundary Conditions

No boundary conditions are applied. This will result in the first mode being the "rigid body" mode.

Material Properties

A bulk modulus of 139,000 psi and a material density of 1.2 lb/in^3 are specified through the ISOTROPIC model option.

Loading

An acoustic source pulse is applied in increment 1 with a time step of 0.000001. Ten increments are then performed with a time step of 0.001 at node 3. The DYNAMIC CHANGE option is used to define the time step.

Print Control

Print output of mode shapes and nodal reactions is requested through the use of a PRINT NODE option with MODE and REAC subparameters. All relevant element quantities are requested for elements 1 to 20 (at all four integration points) through the use of a PRINT ELEMENT option.

POST Tape

The pressure (POST code 120) and the first two components of the pressure gradient (POST codes 121, 122) are written to a formatted post tape. In addition, by providing a RECOVER option, the first two eigenvectors are also written to this tape.

Results

Figure E 8.25-4 through Figure E 8.25-8 show the eigenmodes in the cavity. The frequencies are as follows:

Mode	Frequency (Hz)
1	0
2	4,110
3	6,150
4	9,430
5	10,300
6	12,470

The pressure distribution in the transient analysis is shown in Figure E 8.25-9 through Figure E 8.25-11. One can observe the pressure pulse propagating through the cavity.

Summary of Options Used

Listed below are the options used in example e8x25.dat:

Parameter Options

ACOUSTIC
ALIAS
ELEMENT
END
PRINT
SIZING
TITLE

Model Definition Options

CONNECTIVITY
COORDINATE
END OPTION
GEOMETRY
ISOTROPIC
POST
PRINT ELEM
PRINT NODE

Load Incrementation Options

CONTINUE
DYNAMIC CHANGE
MODAL SHAPE
POINT SOURCE
RECOVER

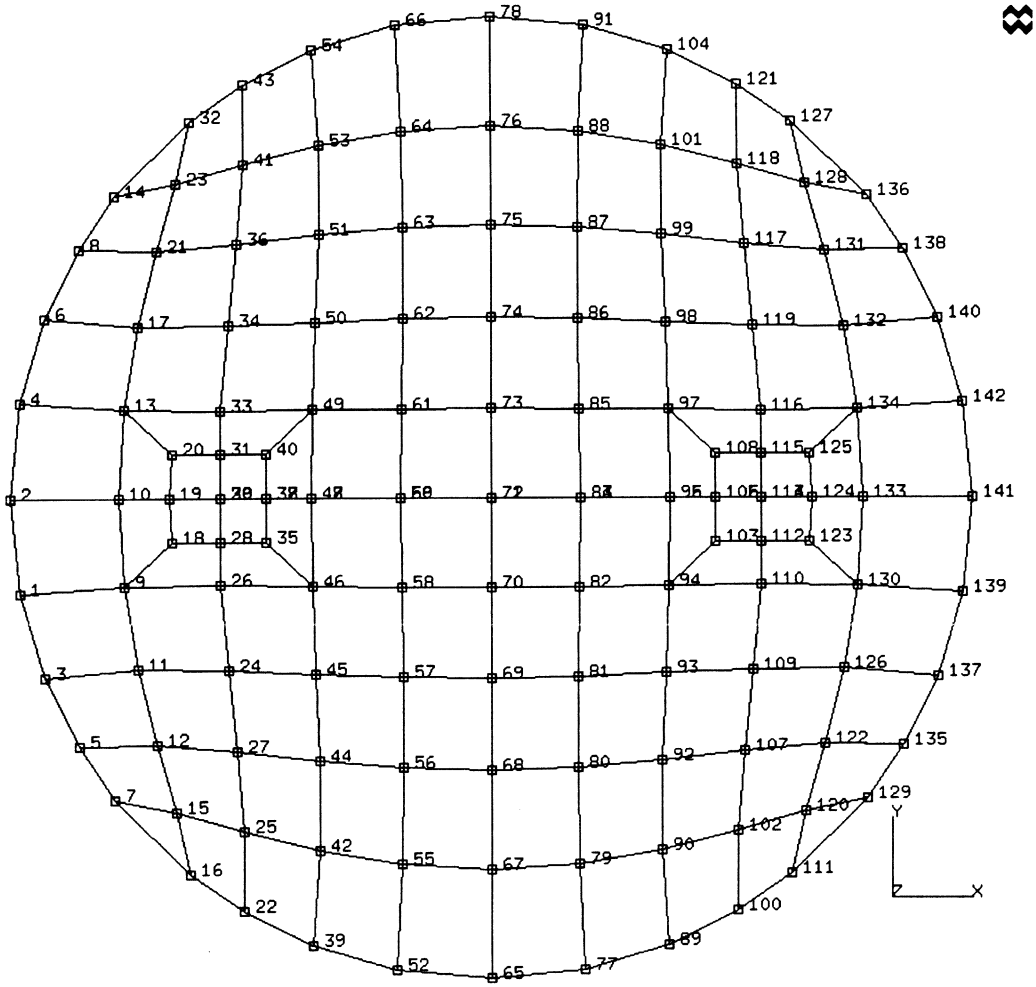

Figure E 8.25-1 Acoustic Cavity Mesh with Node Numbers

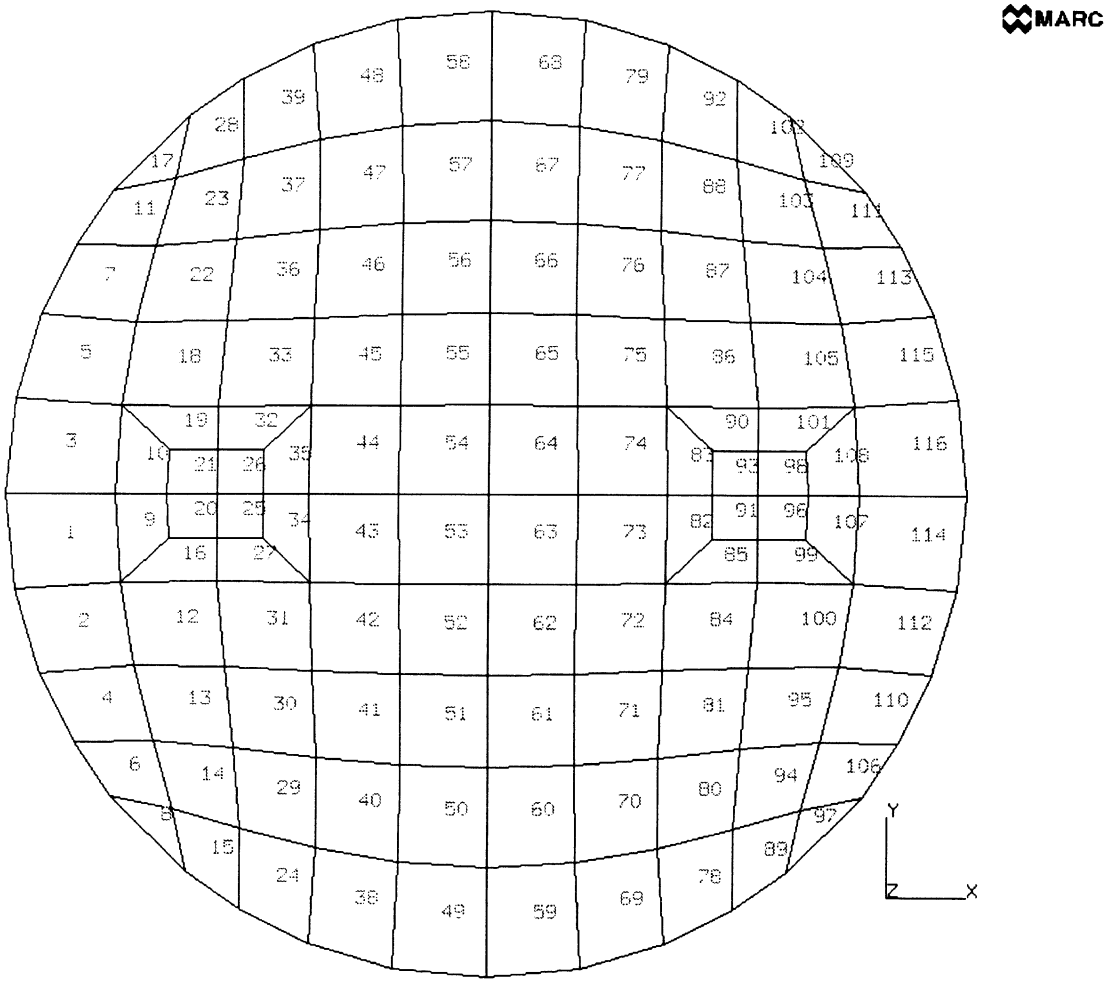

Figure E 8.25-2 Acoustic Cavity Mesh with Element Numbers

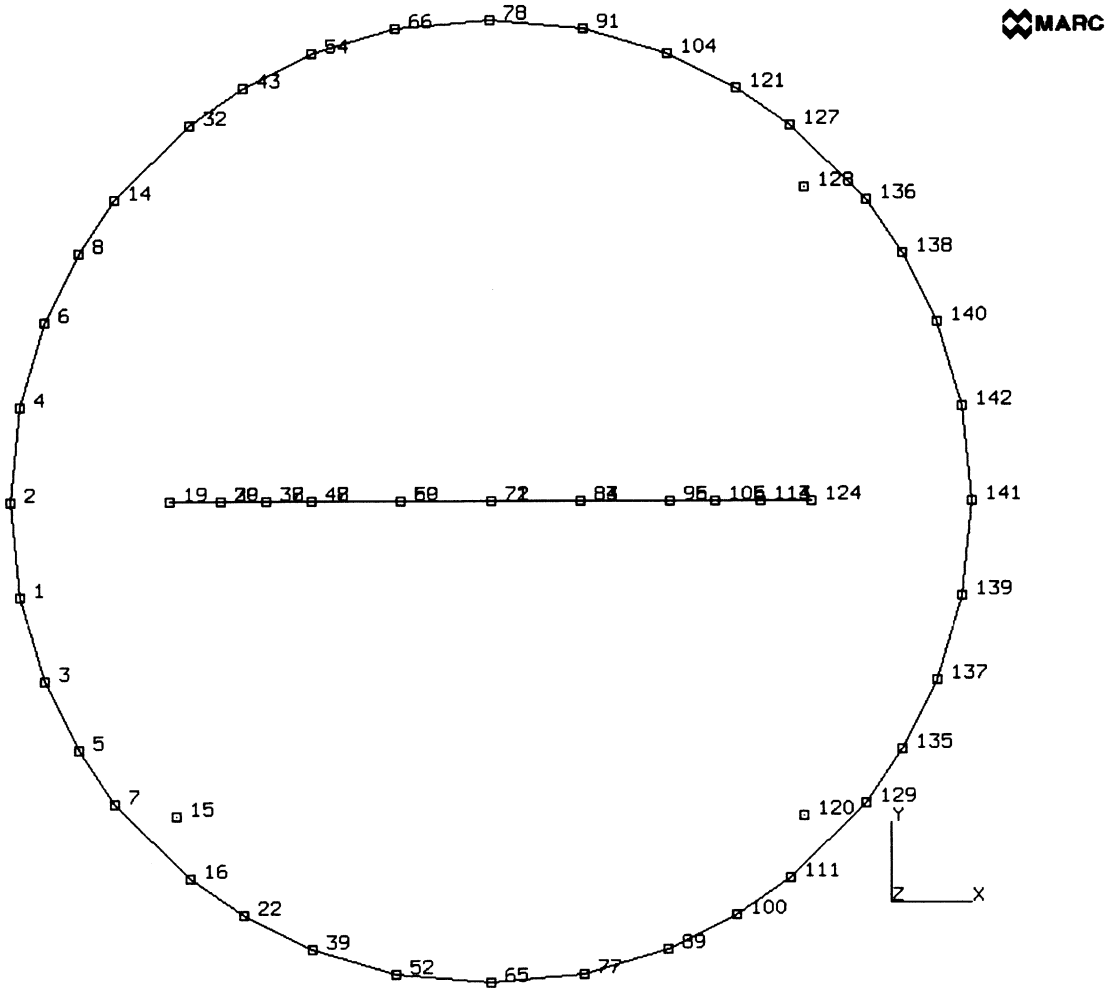

Figure E 8.25-3 Outline Plot Showing Internal Barrier

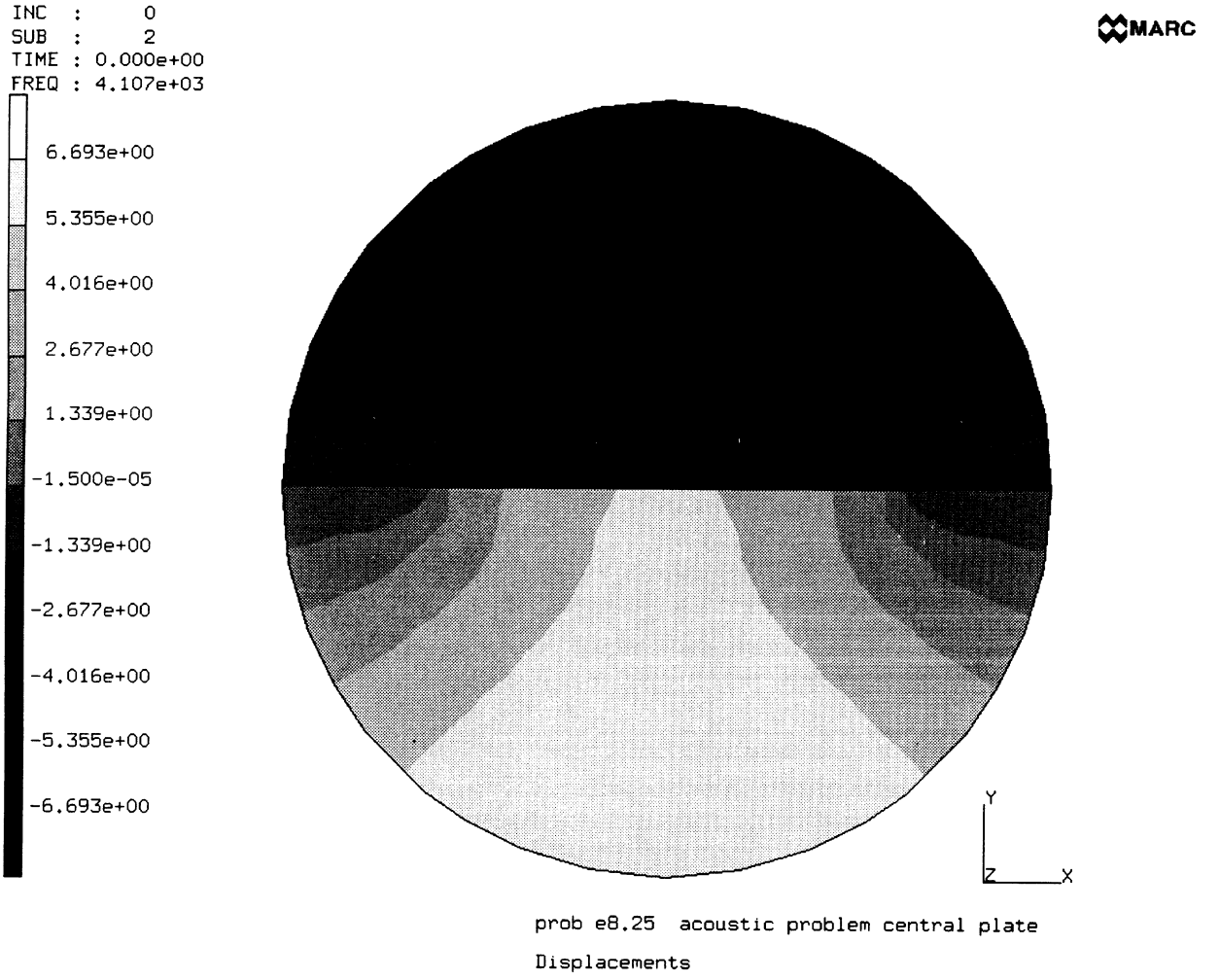

Figure E 8.25-4 Second Mode

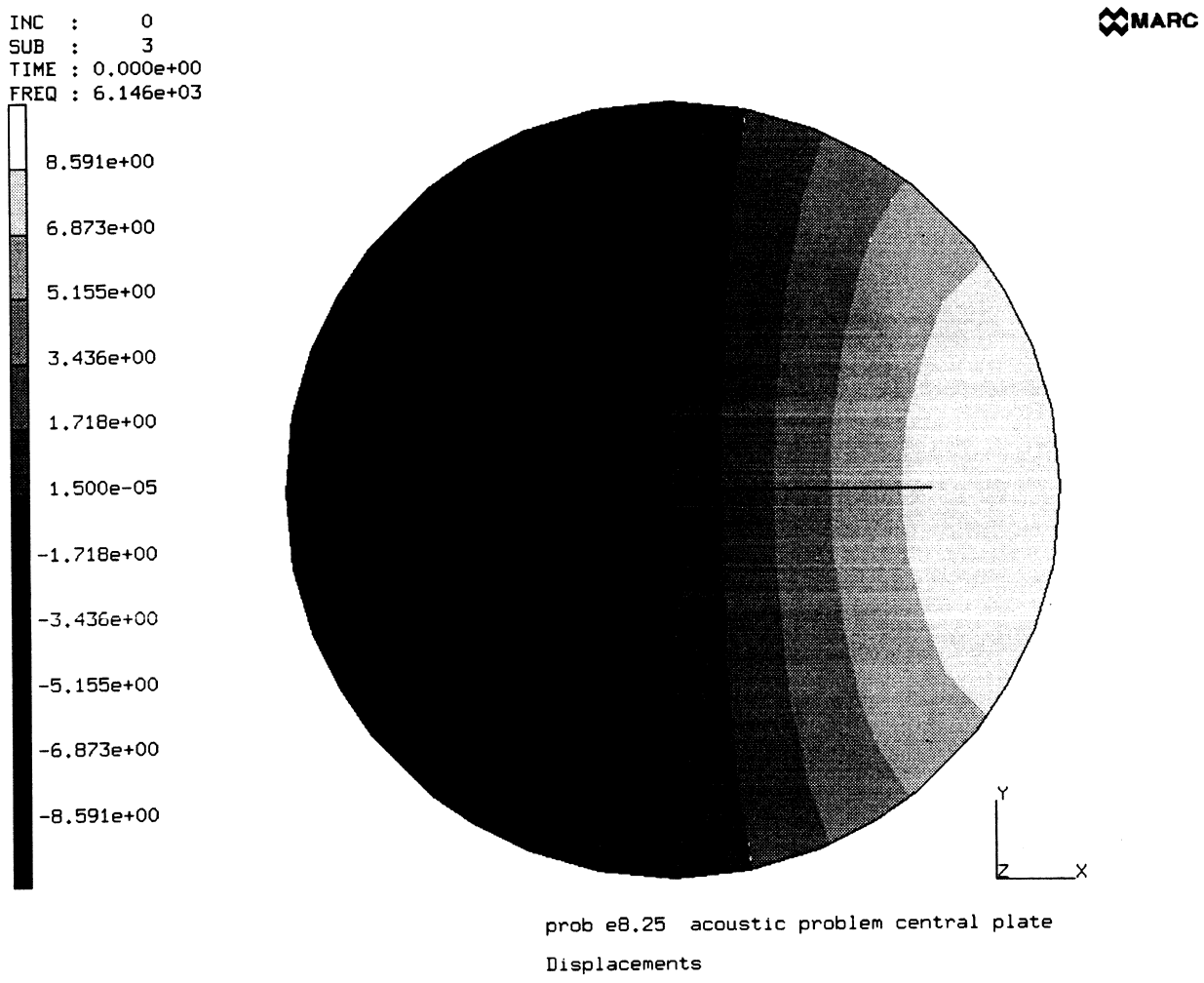

Figure E 8.25-5 Third Mode

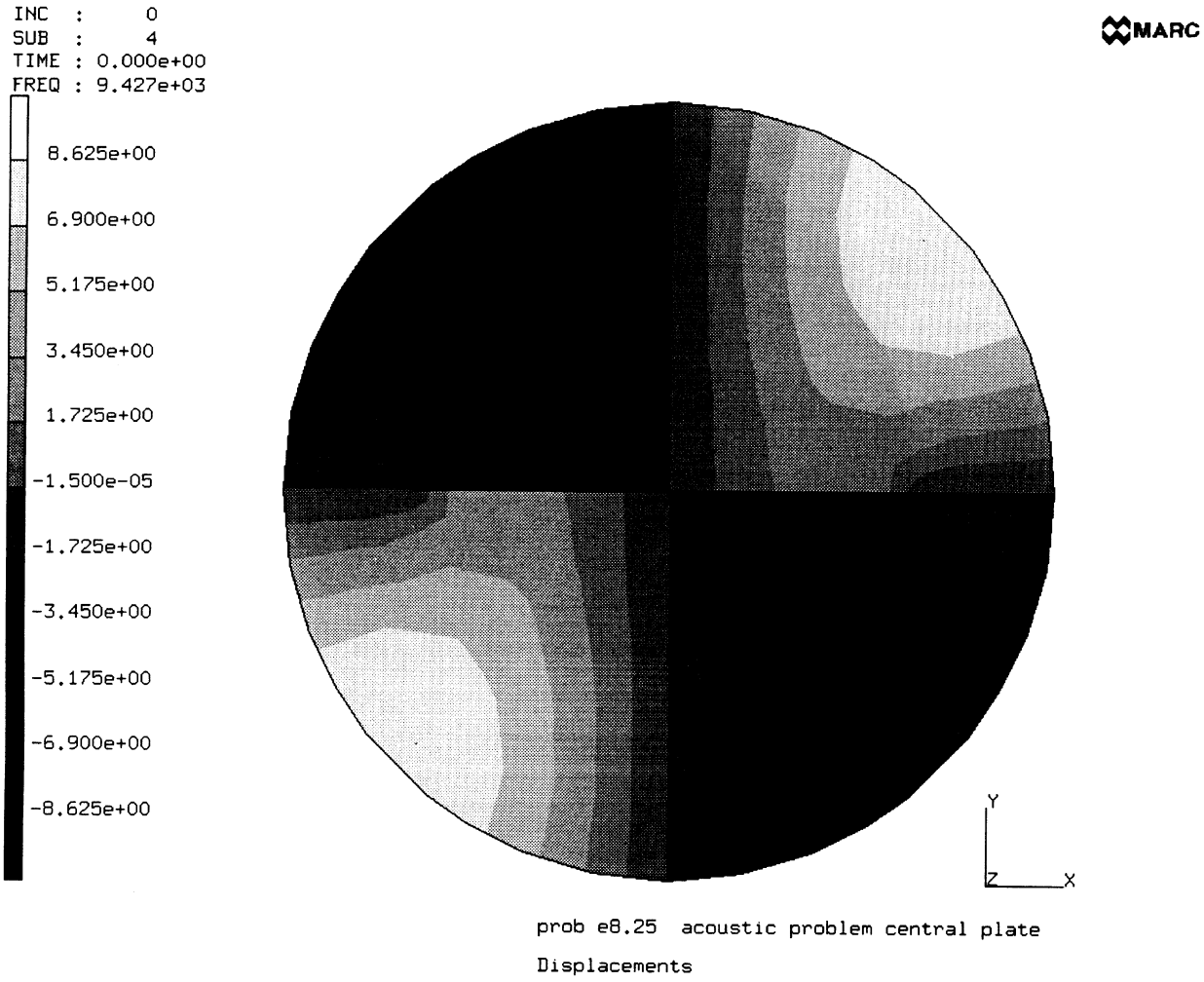

Figure E 8.25-6 Fourth Mode

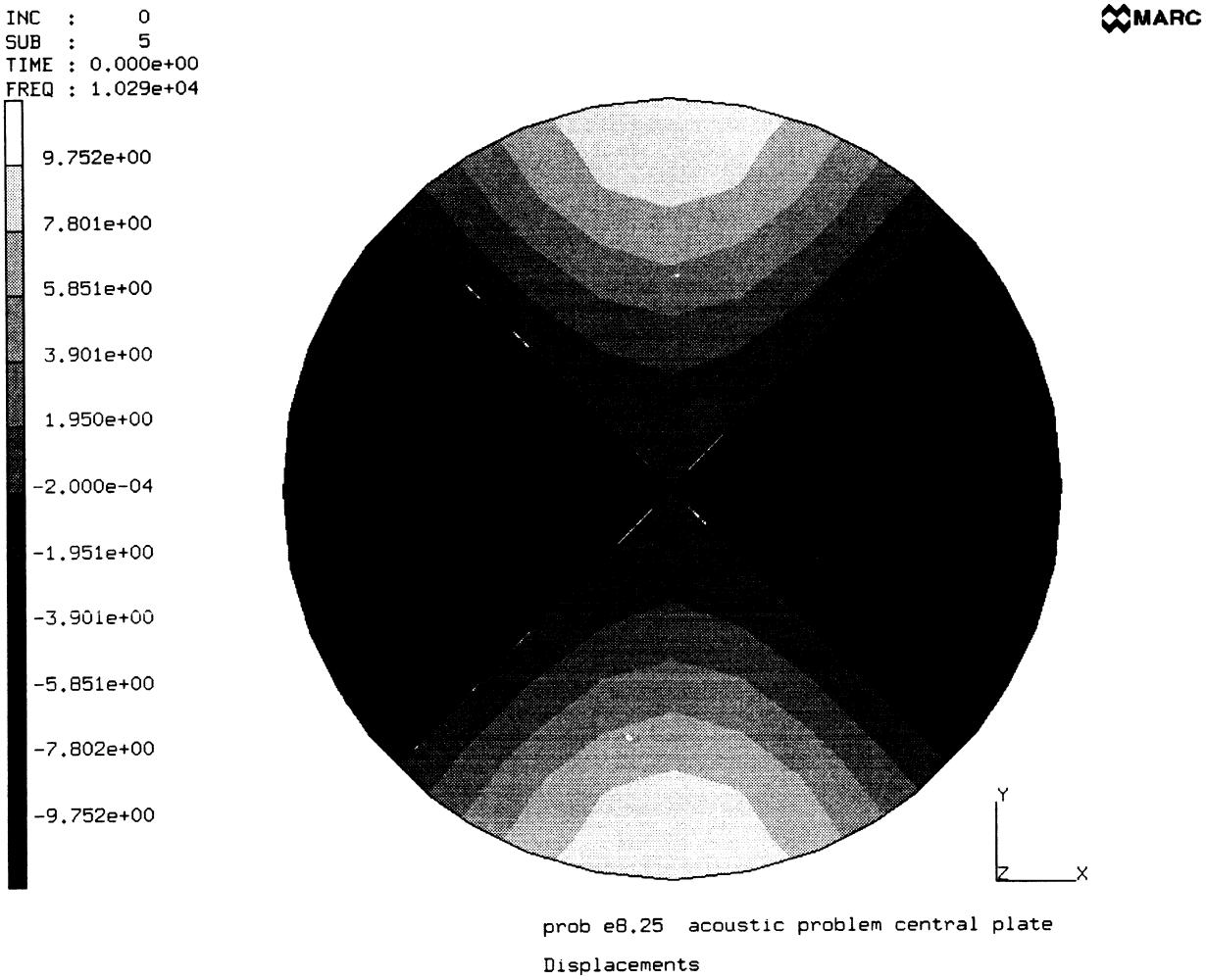

Figure E 8.25-7 Fifth Mode

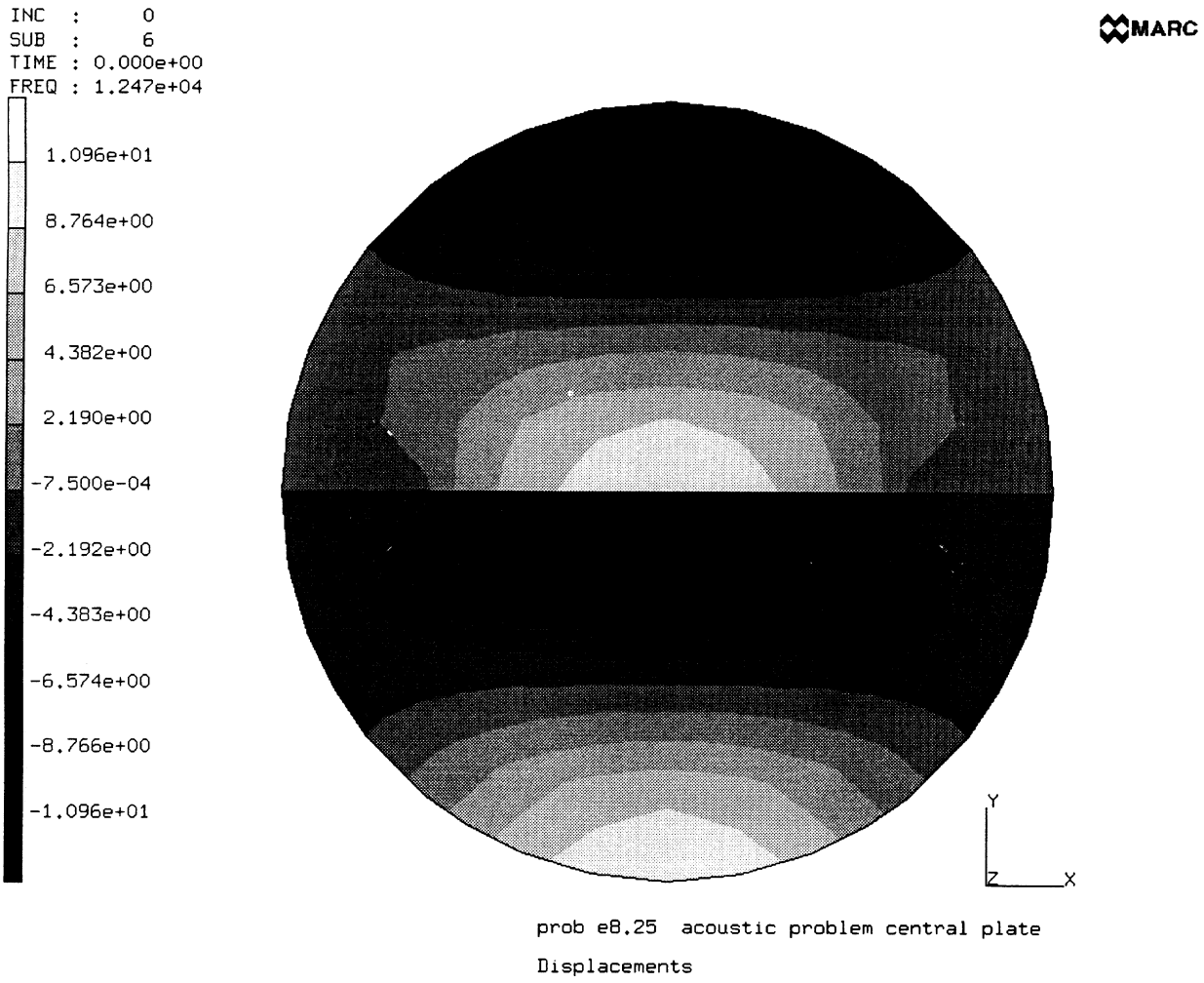

Figure E 8.25-8 Sixth Mode

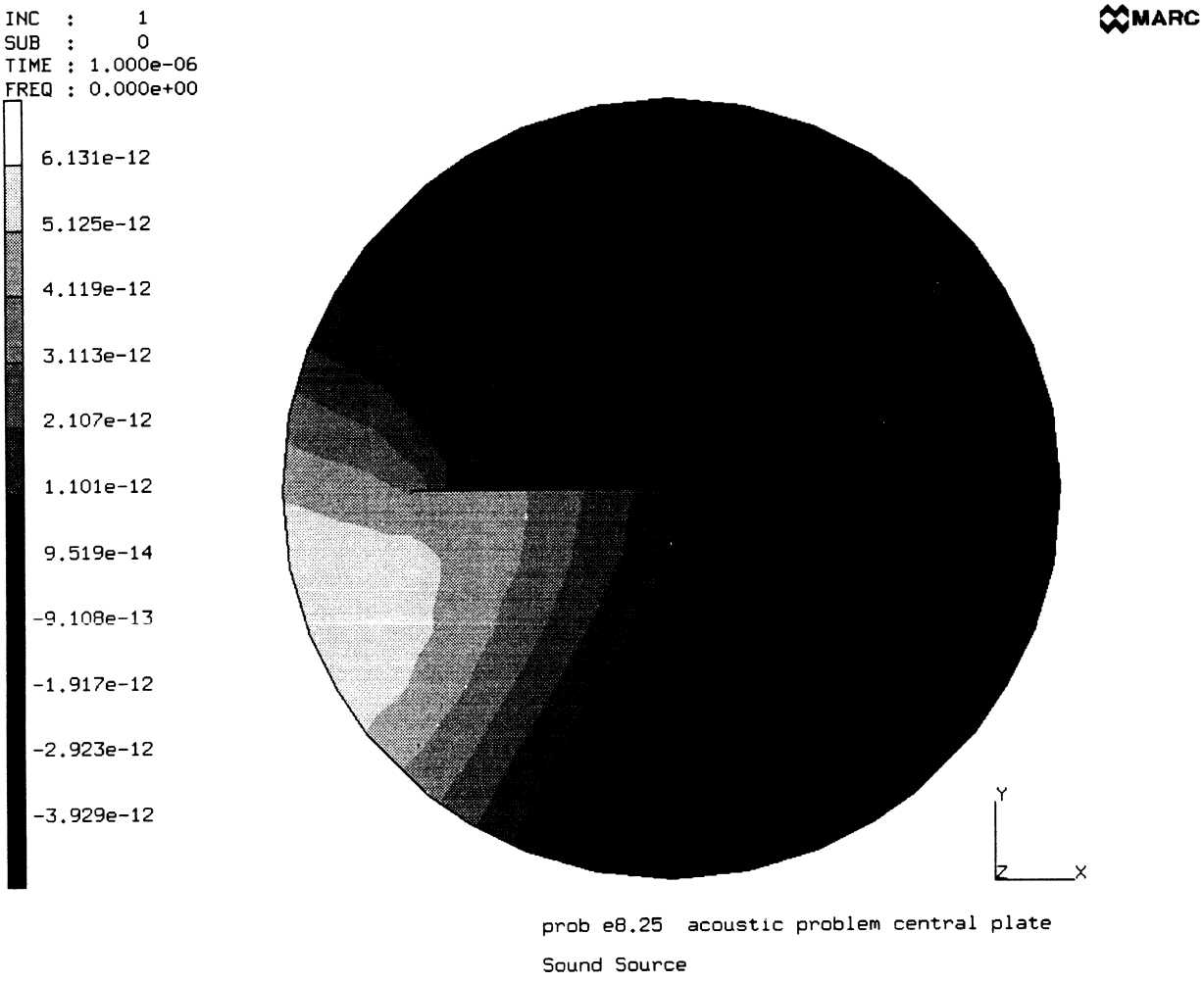

Figure E 8.25-9 Acoustic Pressure at Time = 0.000001

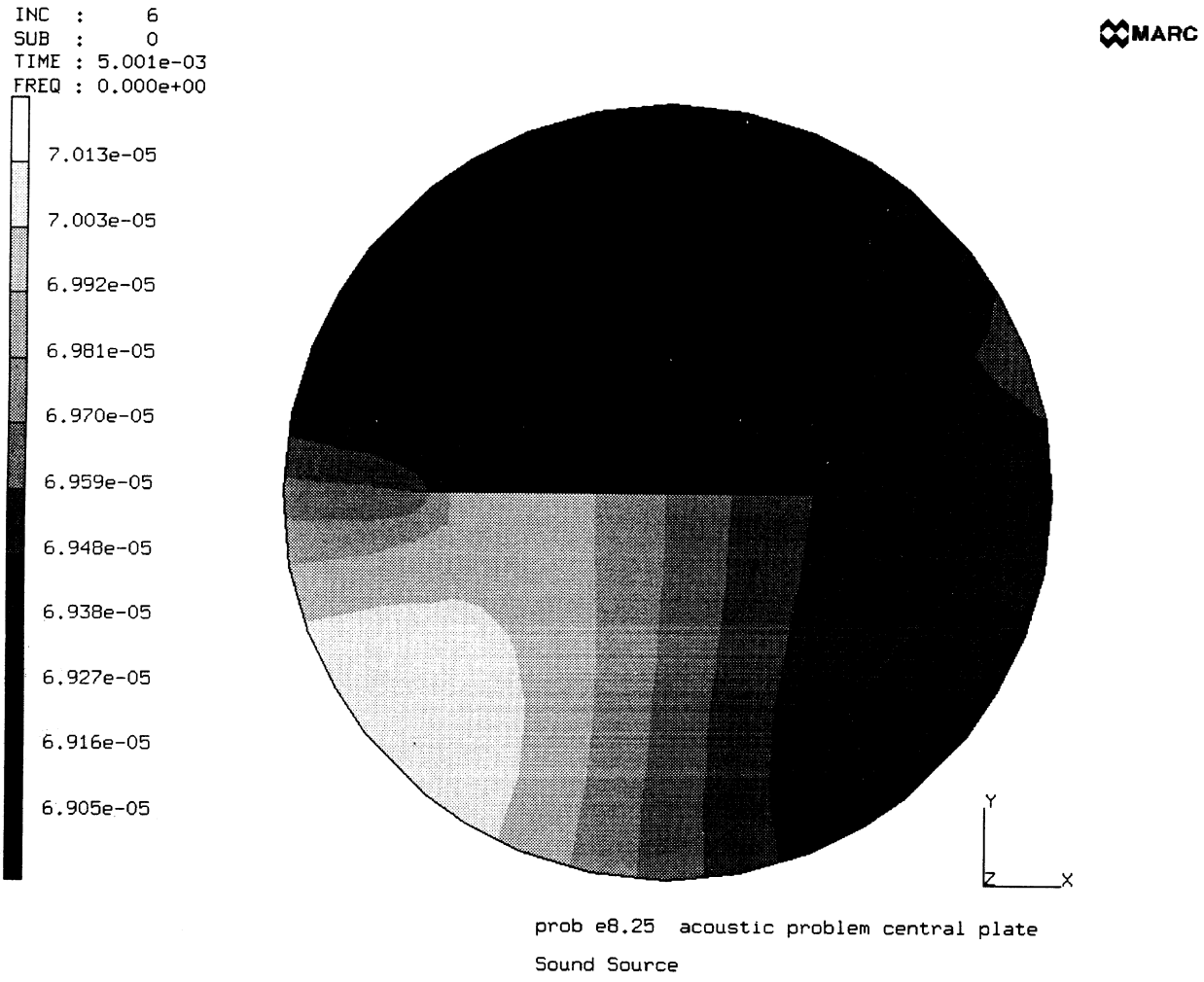

Figure E 8.25-10 Acoustic Pressure at Time = 0.005

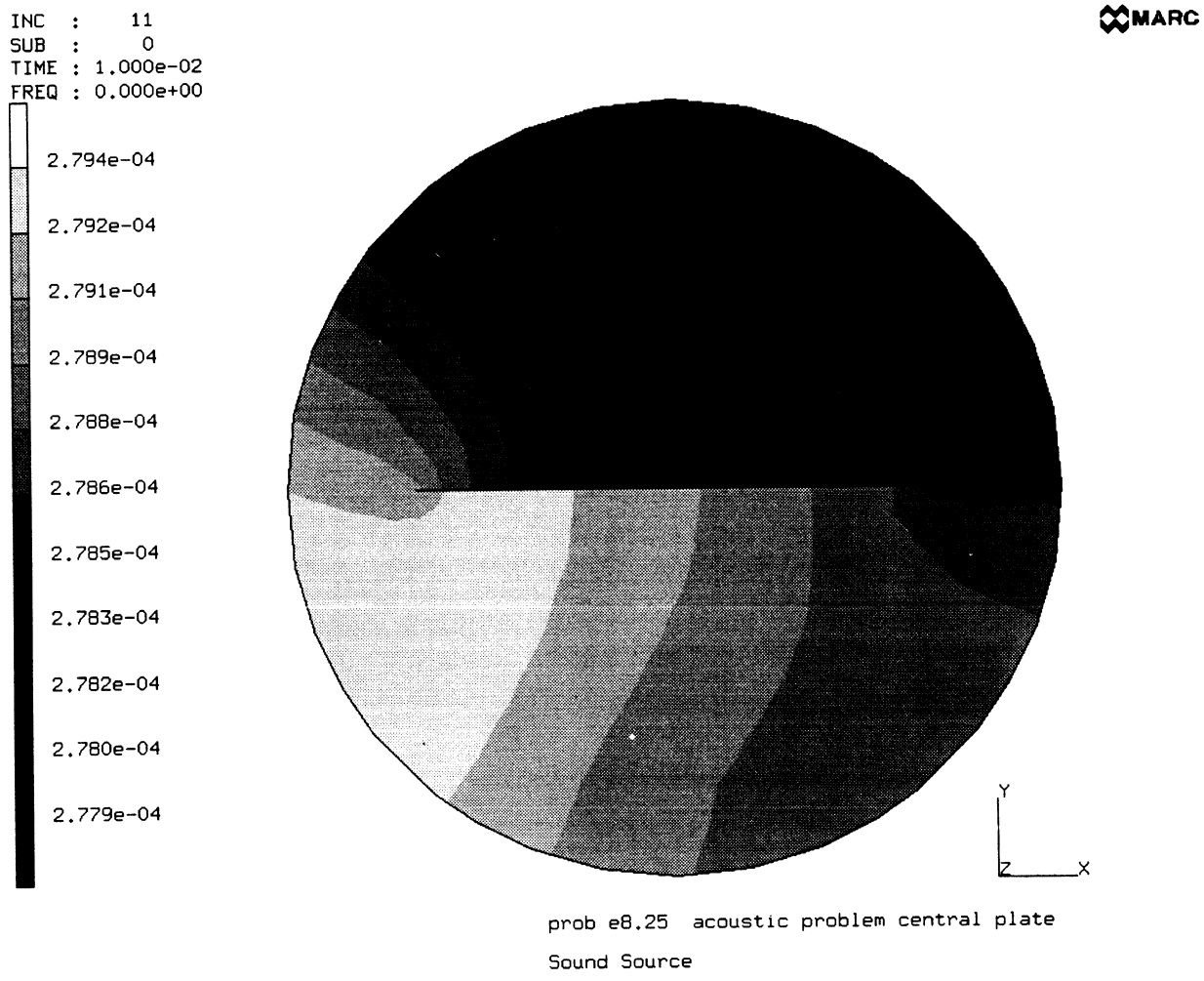

Figure E 8.25-11 Acoustic Pressure at Time = 0.01

E 8.26 Acoustic Problem: Eigenvalue Analysis Of A Rectangular Cavity

This problem shows MARC's acoustic analysis capability using a 2D element formulation. The acoustic pressure distribution in a rectangular cavity is to be calculated.

Parameters

The ACOUSTIC parameter is included to indicate an acoustic analysis. It further indicates that a maximum of 5 modes are to be used for modal superposition, that the eigenvalue problem is to be solved using the Lanczos formulation, and that the mode shapes are to be saved in the post tape. PRINT 3 is used to force the solution of a non-positive definite stiffness matrix, which occurs due to the presence of a zero frequency (constant pressure) mode shape.

Boundary Conditions

A fixed pressure of zero psi is prescribed at nodes 1 and 2. The remaining edges have reflecting boundaries; no boundary conditions are required.

Material Properties

Through use of the ISOTROPIC option, the bulk modulus is given to be 139,000 psi, and the material density of 1.2 lbm/in^3.

Loads

A sinusoidal forcing function is defined using user subroutine FORCDT of magnitude sin (1074t) on the second edge of nodes 21 and 22. Note that FORCDT must apply incremental source quantities and not total source quantities.

Dynamics

A total of five mode shapes are to be extracted using the Lanczos eigensolver. The lowest frequency is specified to be -10 Hz, which ensures the capture of zero frequency modes. The DYNAMIC CHANGE option provides the following parameters that are necessary for the integration of the modal equations of motion:

Time step size = 0.0003 seconds Duration = 0.0091 seconds
Number of time steps = 30

Print Control/POST

Through the PRINT NODE option, it is requested that the both the mode shapes and the reactions/residual forces be output at each node. With a PRINT ELEMENT option, it is requested that all relevant quantities be output at integration points 1 to 4. The following variables are requested to be written to a formatted POST tape:

120} Pressure 121,122 } Components of pressure gradient

Results

Figure E 8.26-1 shows the cavity with the node numbers.

The calculated eigenfrequencies are listed below:

Mode	Frequency (rad/time)
1	5.312 E2
2	1.619 E3
3	2.742 E3
4	3.932 E3
5	5.214 E3

Thus, the exitation frequency ω = 1074 rad/sec is in the range between the first and second mode of exitation.

The propagation of the acoustic wave in shown in Figure E 8.26-2. The pressures are labeled "displacement" in this plot.

Summary of Options Used

Listed below are the options used in example e8x26.dat:

Parameter Options

ACOUSTIC
ELEMENT
END
PRINT
SIZING
TITLE

Model Definition Options

CONNECTIVITY
CONTROL
COORDINATE
DEFINE
END OPTION
FIXED PRESSURE
FORCDT
GEOMETRY
ISOTROPIC
POST
PRINT ELEM
PRINT NODE

Load Incrementation Options

CONTINUE
DYNAMIC CHANGE
MODAL SHAPE

MARC

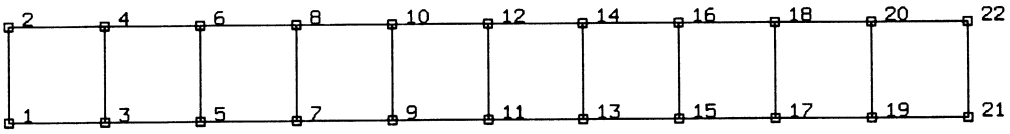

Figure E 8.26-1 Acoustic Cavity Mesh

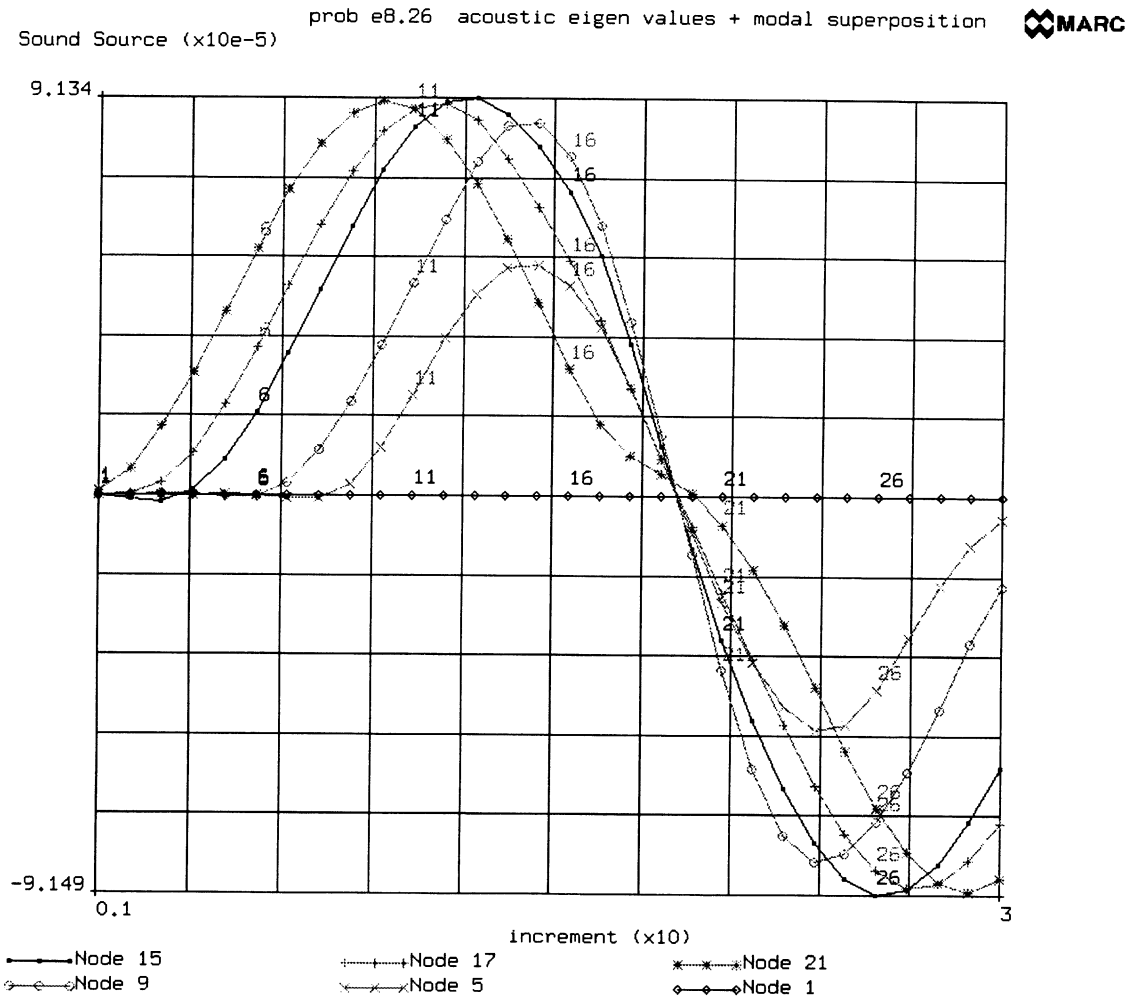

Figure E 8.26-2 Time History of Pressure Pulse

E 8.27 Progressive Failure Of A Plate With A Hole

This problem demonstrates the application of MARC's progressive failure modelling capability applied to a plane stress problem. A plate with a circular hole, made of an orthotropic material, is loaded until selective regions fail.

Parameters

The use of element 26 (8-noded plane stress quadrilateral) is specified through an ELEMENT parameter option.

Mesh Definition

The square plate is 100 mm long. The radius of the hole is 10 mm. Only one-quarter of the plate is modeled due to symmetry. A thickness of 1 mm is provided through the first field in the GEOMETRY card (EGEOM1). Figure E 8.27-1 shows the nodal configuration of the mesh and Figure E 8.27-2 shows the element configuration.

Boundary Conditions

Constraints in the global X-, Y-directions are applied through the use of the FIXED DISP Model Definition option.

Material Properties

Use of the ORTHOTROPIC model option allows the input of directional moduli. The following values are specified:

$E = 14.0 \times 10^9$ N/mm^2 $\quad E = 3.50 \times 10^9$ N/mm^2 $\quad G = 4.2 \times 10^9$ N/mm^2

Poisson's ratio relating strains in the 1-2 directions is 0.4. The orthotropic axes are skewed with respect to the global X,Y by an angle of sixty degrees. To take this into account, an ORIENTATION option group is given defining the material axis base vectors to be a function of the intersection of the element tangent plane and the global ZX plane. The progressive failure option is invoked through the FAIL DATA model option, specifically by entering a "1" in the third field of the third record. Two failure criteria coexist: maximum stress (MX STRESS option) and Hill (HILL). For the both stress criteria, failure is predicated on the following stress levels:

σ_X (tension) = Sigma X (compression) = 250,000,000 N/mm^2

σ_Y (tension) = 500,000 N/mm^2

σ_Y (compression) = 10,000,000 N/mm^2

σ_{XY} = 8,000,000 N/mm^2

Failure will occur when the corresponding interaction equation (see Volume A) reaches or exceeds unity.

Loads

A distributed load of 300,000 N/mm^2 is applied on the 2-6-3 face of elements 13 and 14 during increment zero. Five load steps of 20% of the increment zero load are applied bringing the total distributed load magnitude to 600,000 N/mm^2. This is done through the use of the AUTO LOAD and PROPORTIONAL INC options.

Control

A maximum of ten load steps and 4 recycles per step is allowed through the CONTROL option. Furthermore, convergence is considered to be reached when the maximum residual force divided by the maximum reaction force falls below the value 0.1.

POST Output

A formatted post tape is requested with the following variables:

code 94 Failure index

code 111 Direct stress 11 in preferred 1 direction
code 112 Direct stress 22 in preferred 2 direction
code 113 Shear stress 12

Results

Figure E 8.27-3, Figure E 8.27-4, and Figure E 8.27-5 show the fourth failure index at increments 1, 3 and 5, respectively. The stresses in the preferred directions are shown in Figure E 8.27-6 and Figure E 8.27-7.

Summary of Options Used

Listed below are the options used in example e8x27.dat:

Parameter Options

ELEMENT
END
SIZING
TITLE

Model Definition Options

CONNECTIVITY
CONTROL
COORDINATE
DIST LOADS
END OPTION
FAIL DATA
FIXED DISP
GEOMETRY
ORIENTATION
ORTHOTROPIC
POST
PRINT ELEM

Load Incrementation Options

AUTO LOAD
CONTINUE
PROPORTIONAL INCREMENT

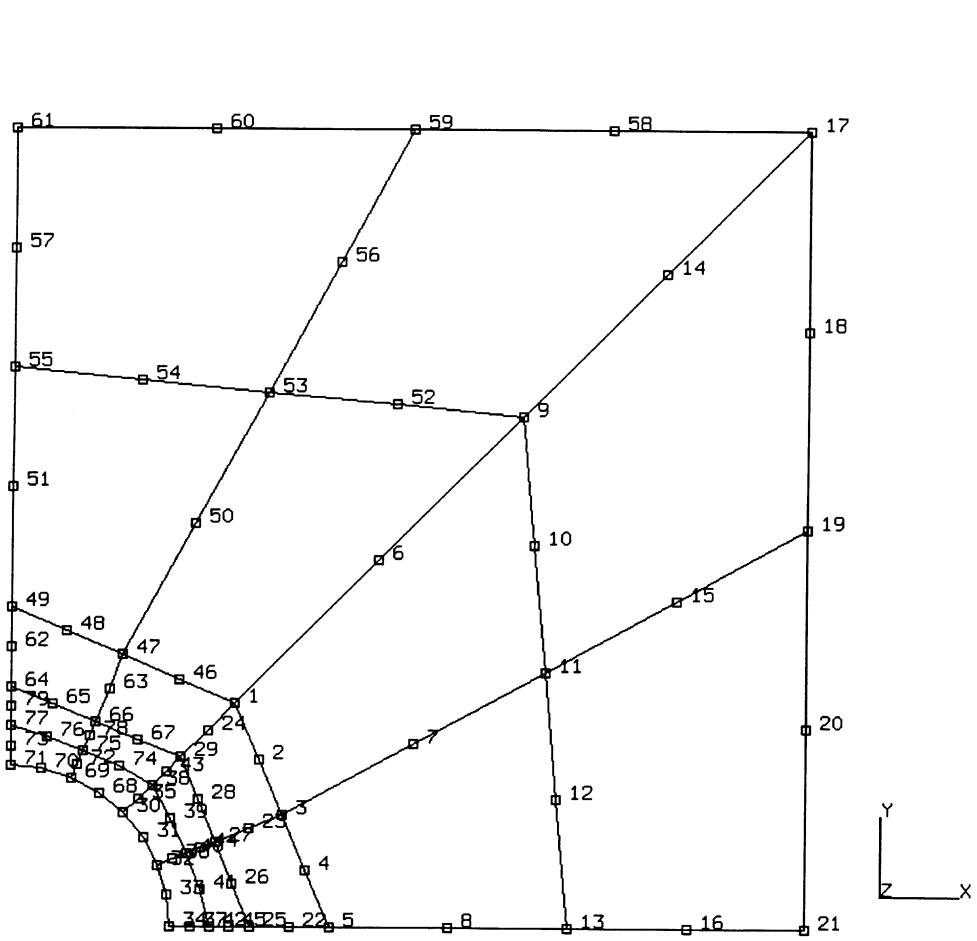

Figure E 8.27-1 Finite Element Mesh – Nodes

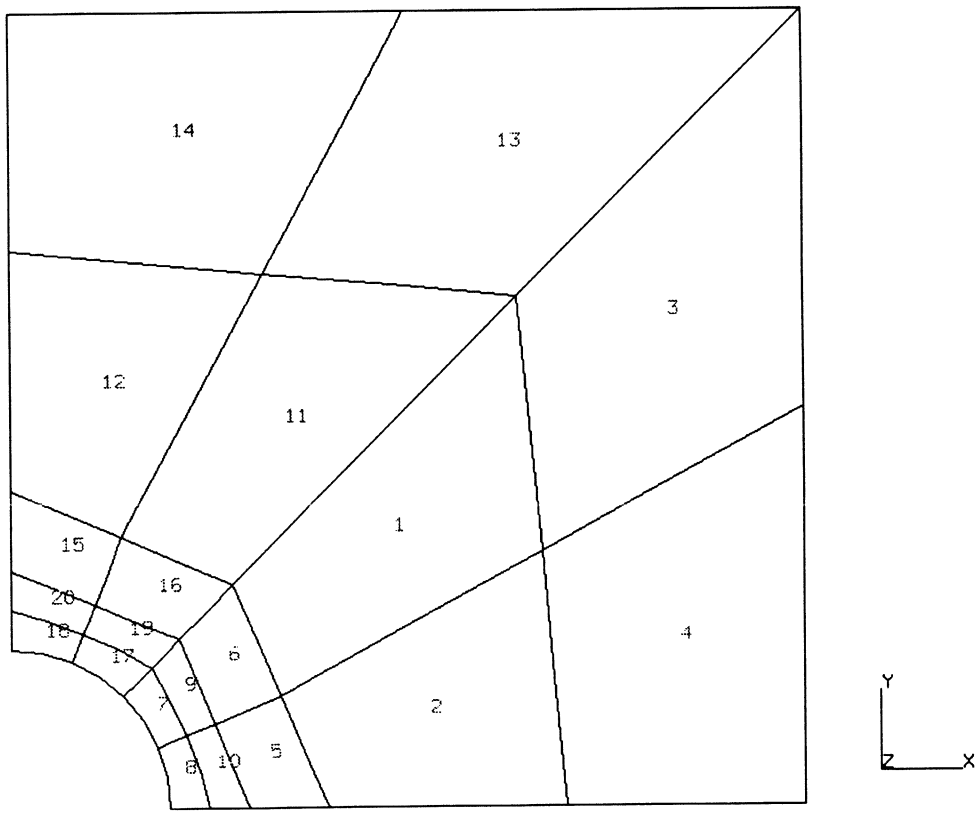

Figure E 8.27-2 Finite Element Mesh – Nodes

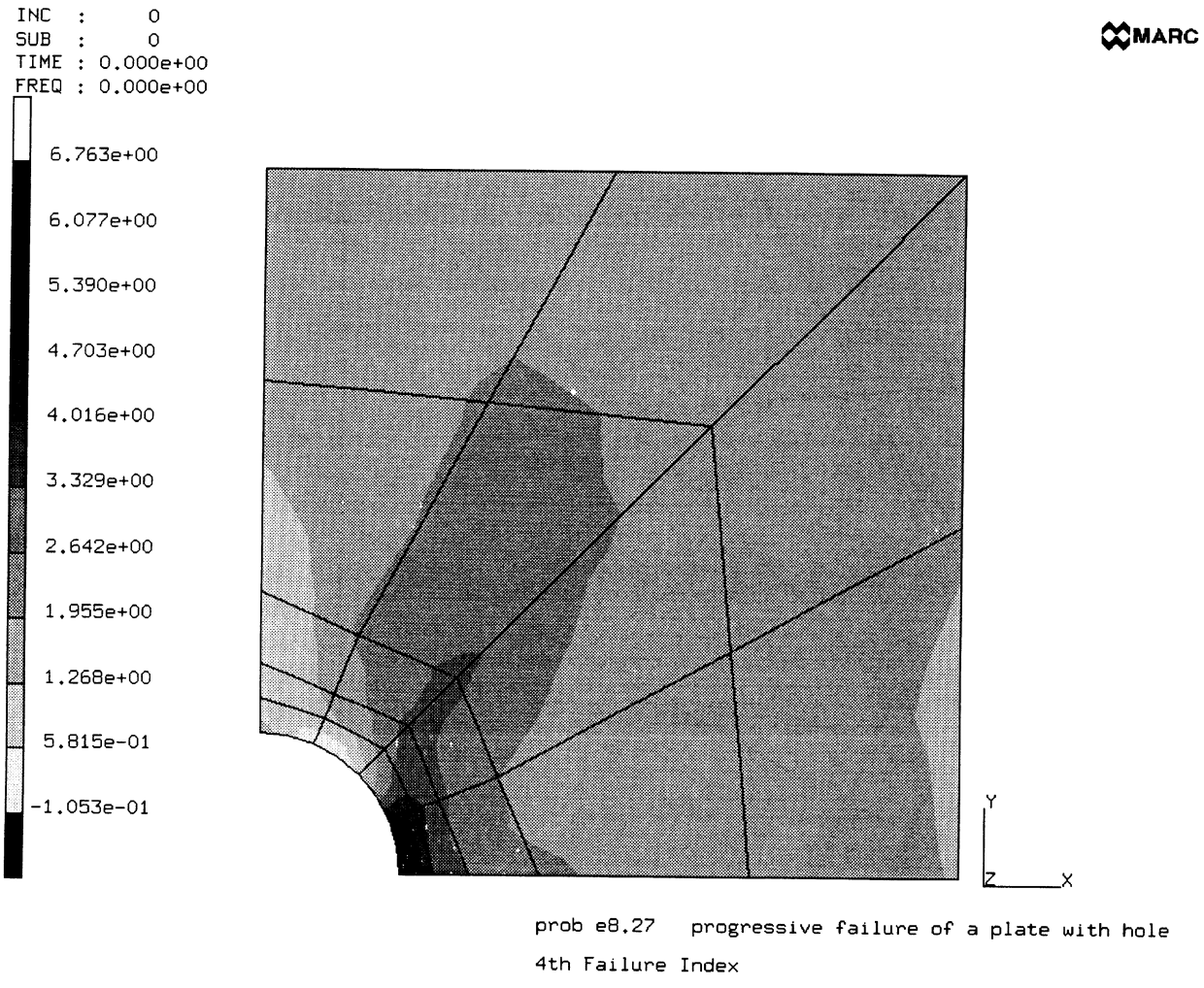

Figure E 8.27-3 Failure Index, Increment 0

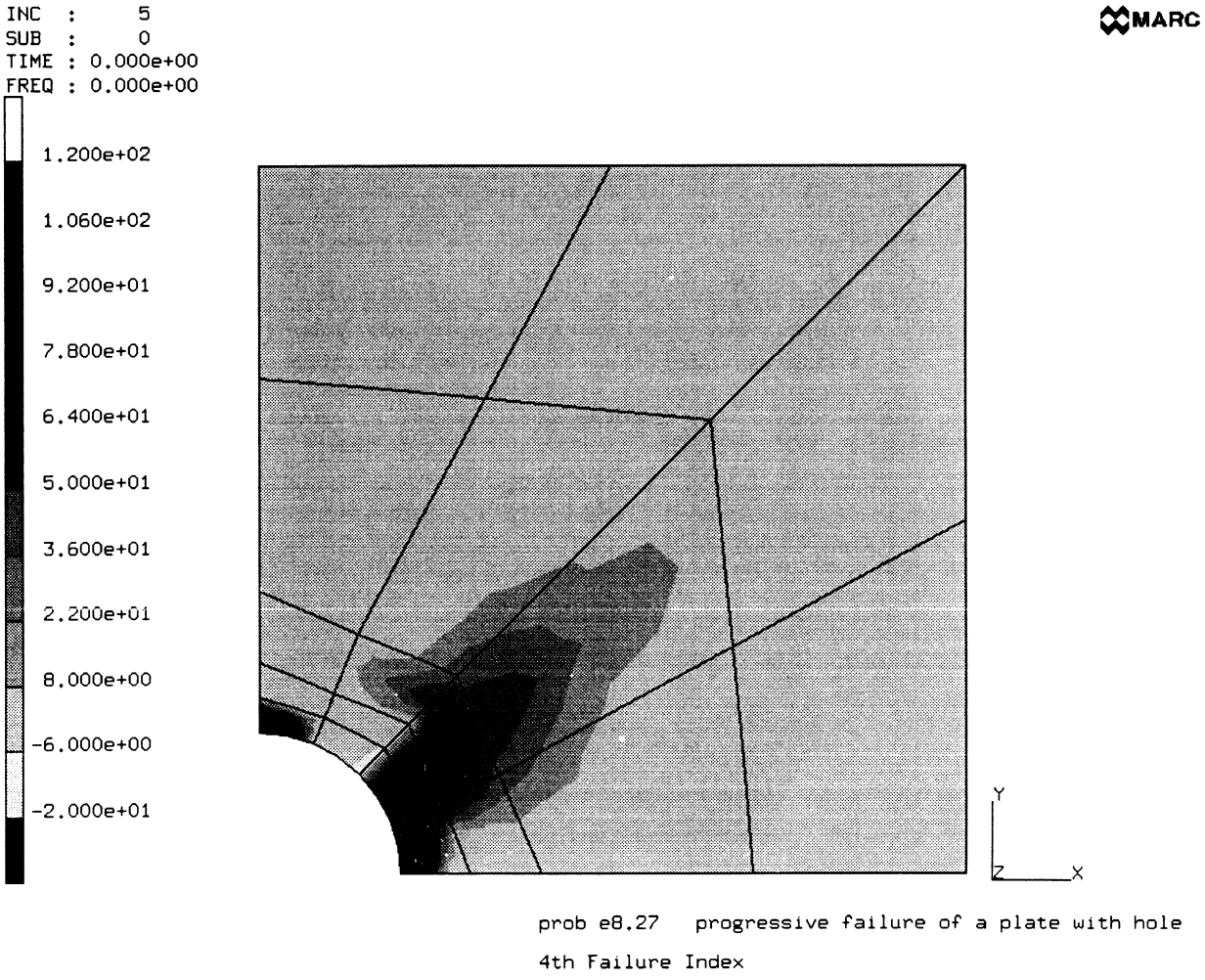

Figure E 8.27-4 Failure Index, Increment 5

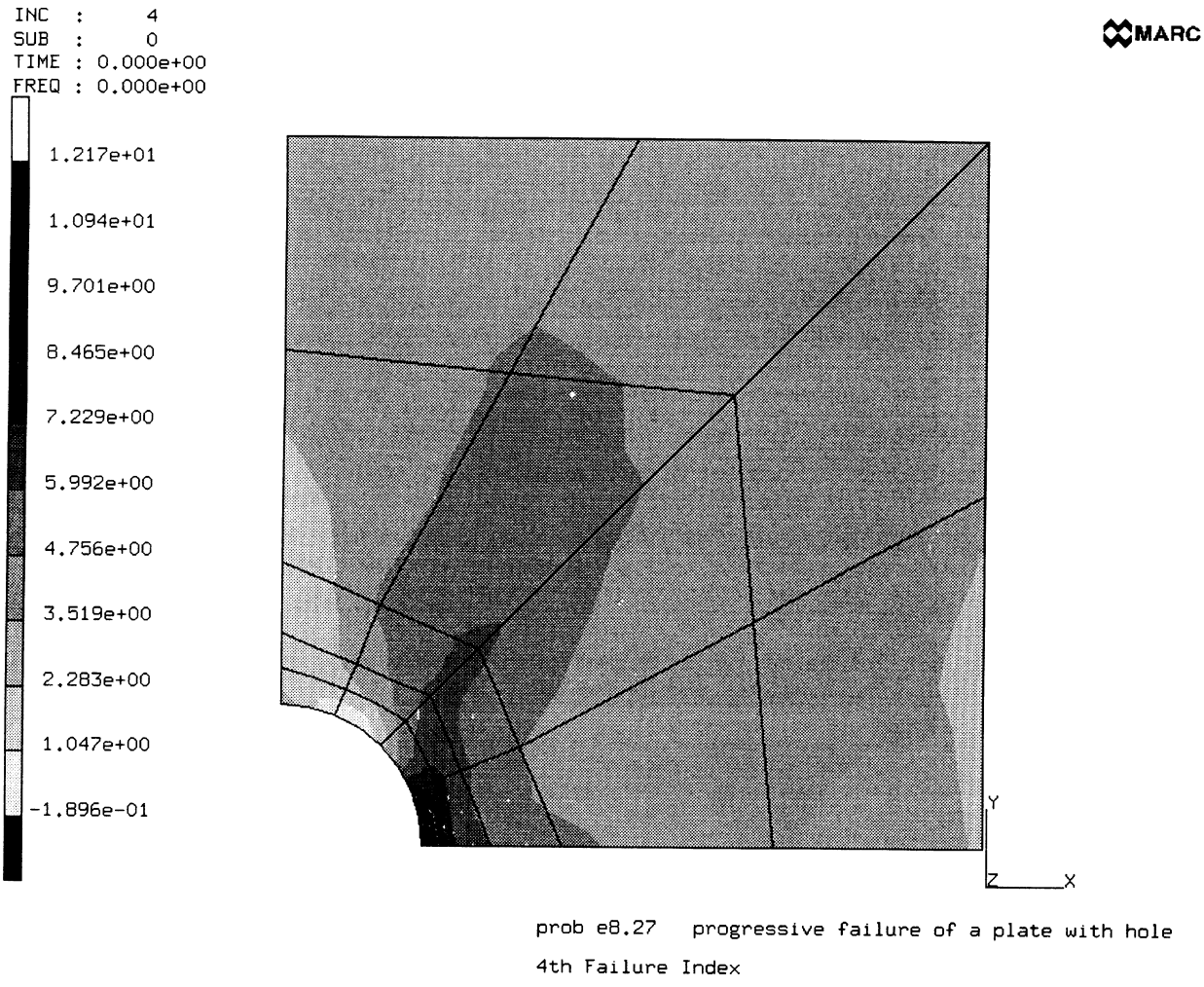

Figure E 8.27-5 Failure Index – No Failure Allowed

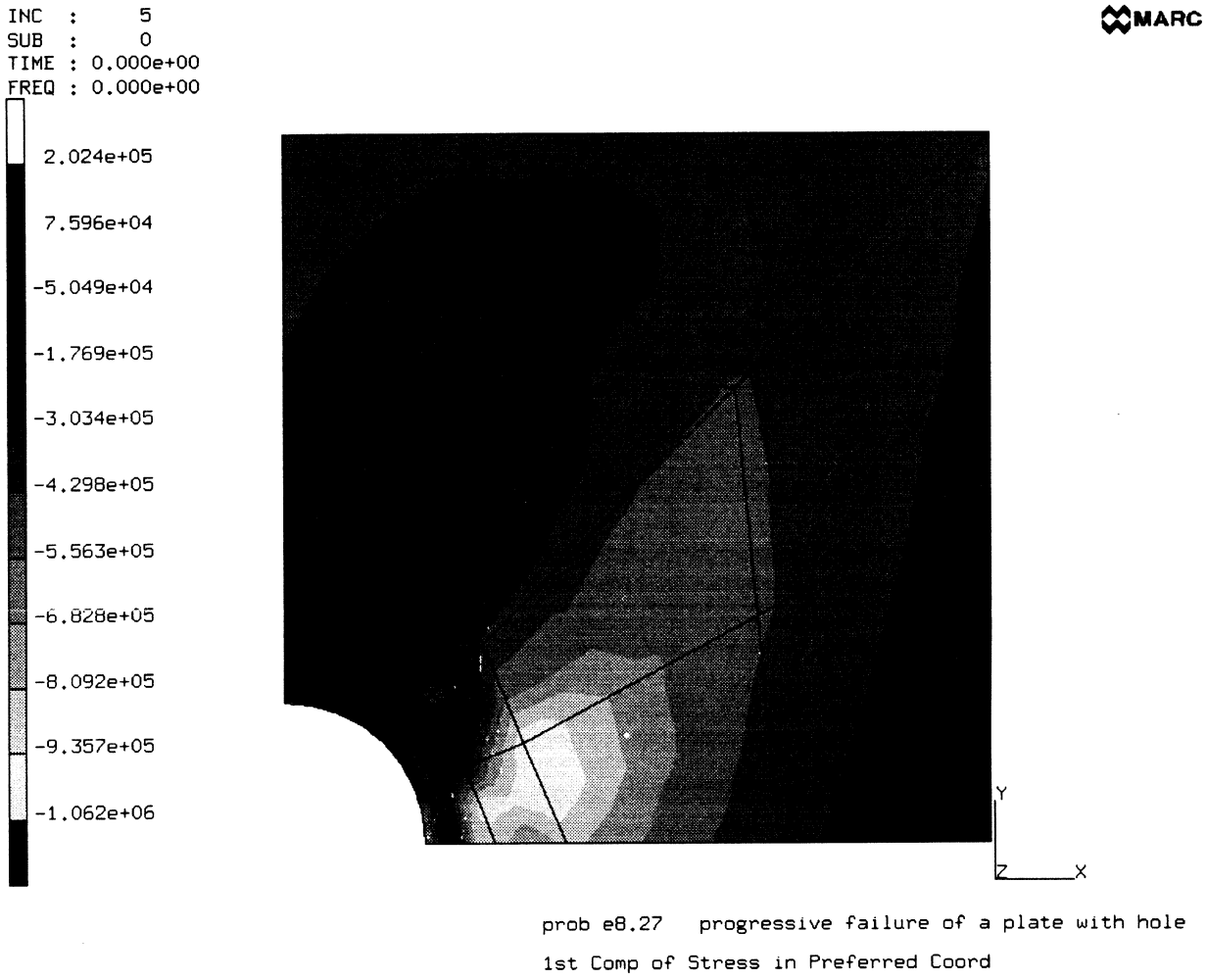

Figure E 8.27-6 First Component of Stress in Preferred Direction

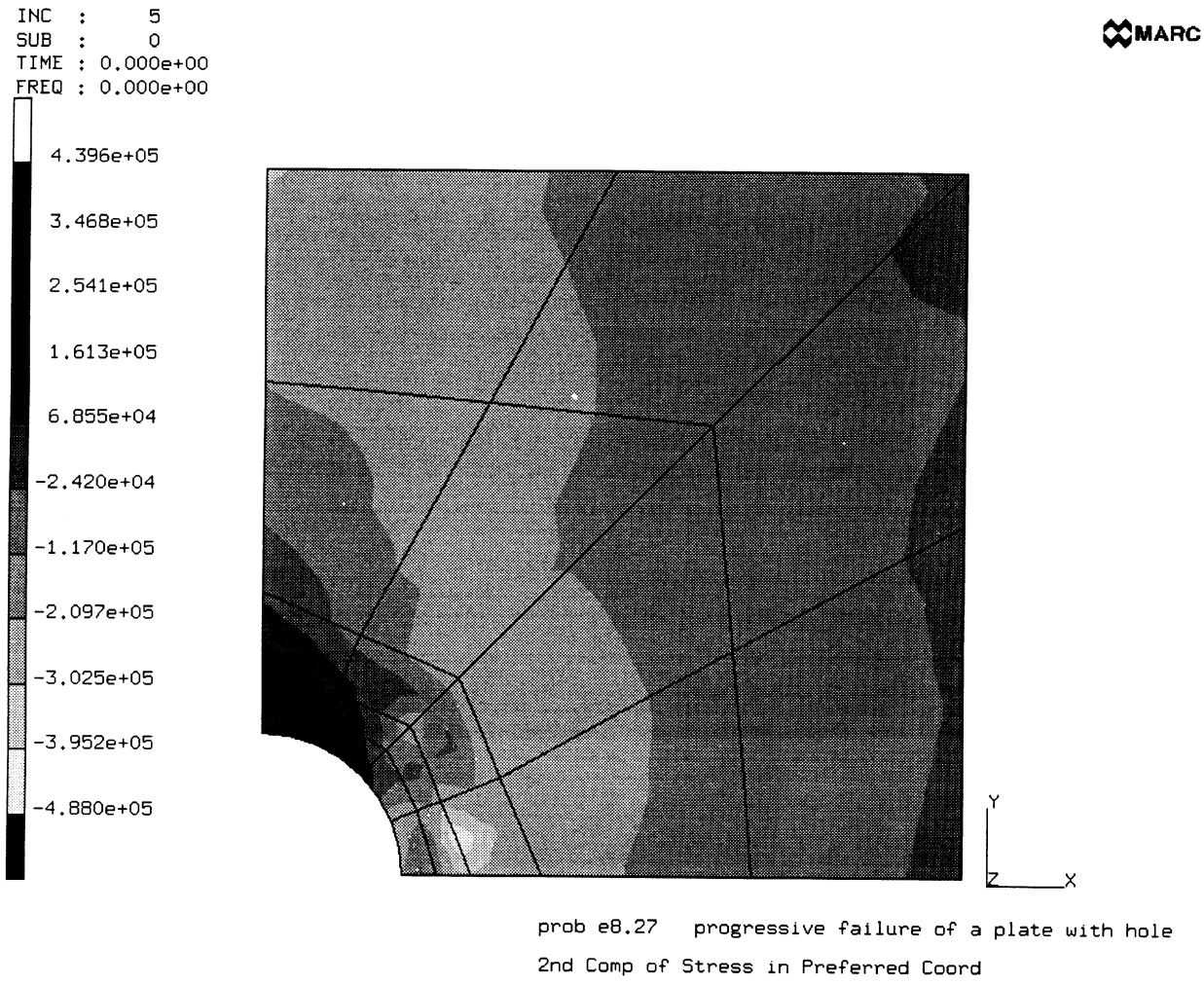

Figure E 8.27-7 Second Component of Stress in the Preferred Direction

E 8.28 Linear Distribution Of Dipoles

The problem presented here is the determination of the two-dimensional electric field generated in a vacuum around two wires with uniform electrostatic charge of opposite signs. The numerical results are compared with the analytic solution.

Parameters

The ELECTRO parameter is included to indicate that an electrostatic analysis is being performed.

Element

Elements type 41 and 103 are used.

Element 41 is a second-order planar isoparametric quadrilateral for "quasi-harmonic" field problems. Element type 103 is a nine-node semi-infinite element. In the first direction, special interpolation functions are used which may represent exponential decay.

Model

The mesh of the plane is shown in Figure E 8.28-1. The outer ring is modeled with semi-infinite elements. The outer radius is 1.5 m.

Material Properties

The permittivity of the medium (vacuum) is 8.8×10^{-12} farad/m.

Point Charge

A linear distribution normal to the plane of 10^{-12} coulomb/m is prescribed with opposite signs at nodes 80 and 81 ($X = 0$, $Y = \pm 0.21621$ m).

Fixed Potential

The potential is prescribed to be zero at the center of the plane.

Control

The STEADY STATE option initiates the analysis. A formatted post tape is created.

Results

A contour plot of the electric potential is shown in Figure E 8.28-2. A vector plot of the electric field is shown in Figure E 8.28-3. An X-Y plot of the potential along the Y-axis is shown in Figure E 8.28-4. Table E 8.28-1 shows a comparison of the MARC results with the analytical solution.

Table E 8.28-1 Comparison of MARC Results

Node	Y (m.)	Potential (Volt)		Error (%)
		MARC	Analytical	
8	0.07254	1.302	1.255	+ 3.7
36	0.14435	2.729	2.900	– 5.9
165	0.29150	3.257	3.432	– 5.1
320	0.48159	1.732	1.739	– 0.4
558	1.0	0.789	0.790	– 0.1

Summary of Options Used

Listed below are the options used in example e8x28.dat:

Parameter Options

ELECTROSTATIC
ELEMENT
END
SIZING
TITLE

Model Definition Options

CONNECTIVITY
COORDINATE
DEFINE
END OPTION
FIXED POTENTIAL
ISOTROPIC
POINT CHARGE
POST
PRINT ELEM

Load Incrementation Options

CONTINUE
STEADY STATE

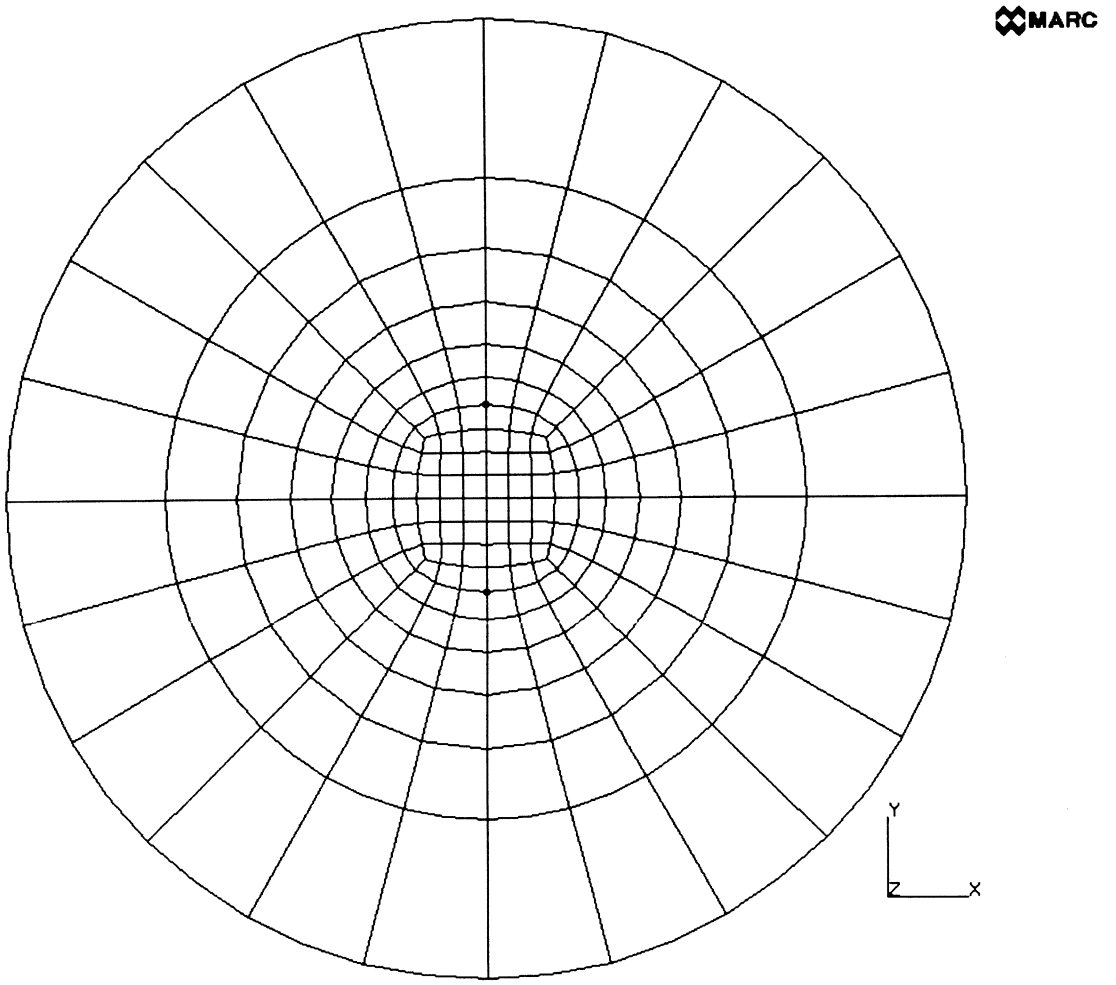

Figure E 8.28-1 Finite Element Mesh with Dipole

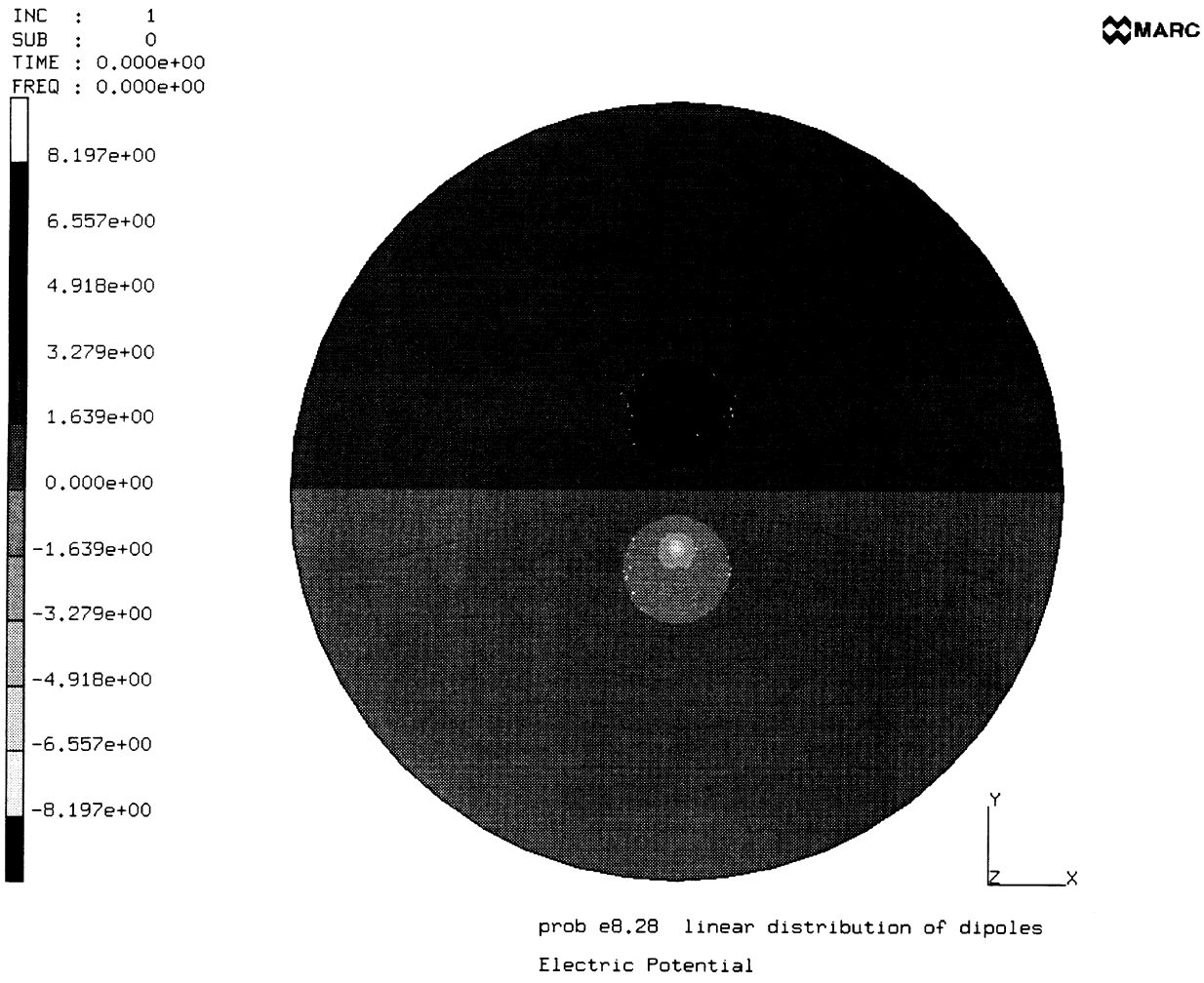

Figure E 8.28-2 Scalar Potential

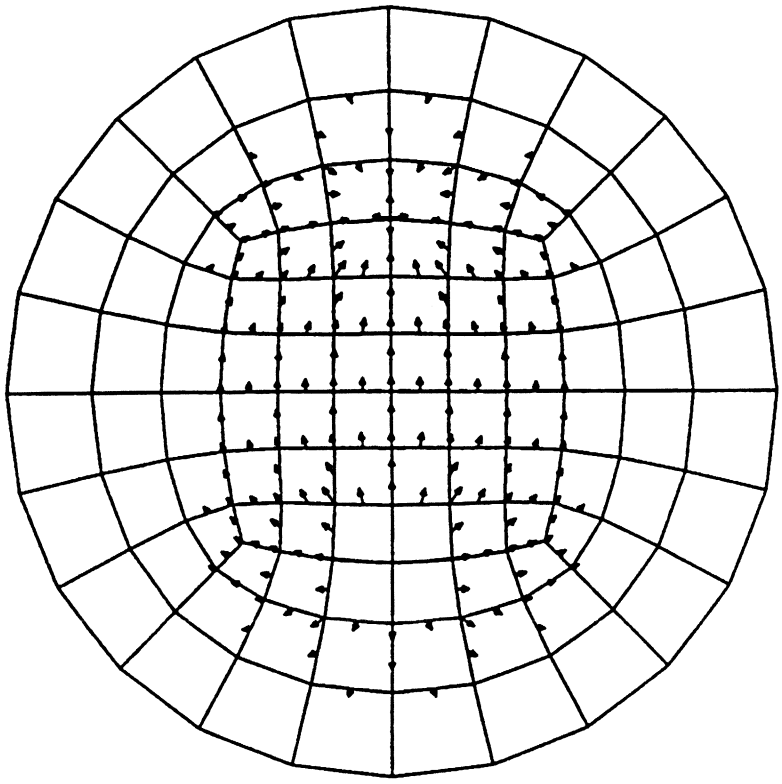

Figure E 8.28-3 Vector Plot of Electric Field

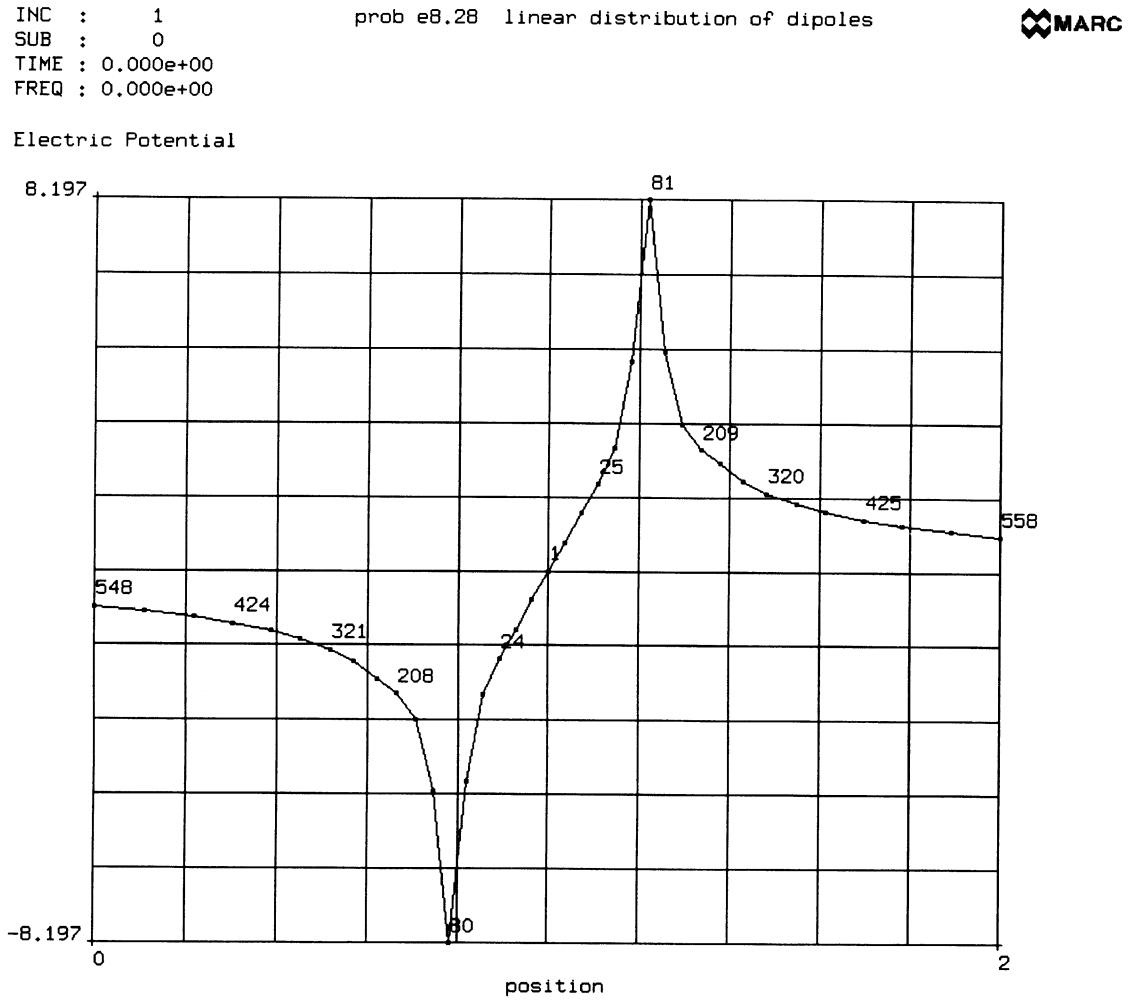

Figure E 8.28-4 Scalar Potential Distribution

E 8.29 Magnetic Field Around Two Wires Carrying Opposite Currents

The problem presented here is the determination of the two-dimensional electric field generated in a vacuum around two wires carrying equal current of opposite signs. The numerical results are compared with the analytical solution.

Parameters

The MAGNETO parameter option is included to indicate that a magnetostatic option is being performed.

Element (Ref. B41.1 and B103.1)

Elements type 41 and 103 are used.

Element 41 is a second-order planar isoparametric quadrilateral for "quasi-harmonic" field problems.

Element 103 is a nine-node planar semi-infinite quadrilateral for "quasi-harmonic" field problems.

Model

The mesh of the plane is shown in Figure E 8.29-1. The outer ring is modeled with semi-infinite elements. The outer radius is 1.5 m.

Material Properties

The magnetic permeability of the medium (vacuum) is 1.26×10^{-6} henry/m.

Point Current

A point current of 10^{-6}amp running normal to the plane is prescribed with opposite signs at nodes 80 and 81 ($X = 0$, $Y = \pm 0.21621$ m).

Fixed Potential

The potential is prescribed to be zero at the center of the plane.

Control

The STEADY STATE option initiates the analysis. A formatted post tape is created.

Results

A contour plot of the scalar potential (only available for 2D magnetostatic) is shown in Figure E 8.29-2. A vector plot of the magnetic flux density is shown in Figure E 8.29-3. An X-Y plot of the potential along the Y-axis is shown in Figure E 8.29-4. Table E 8.29-1 shows a comparison of the MARC results with the analytical solution.

Table E 8.29-1 Comparison of MARC Results

Node	X (m.)	Bx (weber/m^2)		Error (%)
		MARC	Analytical	
1	0.	1.855	1.855	+ 0.0
6	0.072534	1.674	1.667	+ 0.4
34	0.14434	1.288	1.283	+ 0.4
162	0.29149	0.664	0.658	+ 0.9
319	0.48158	0.316	0.311	+ 1.6
547	1.0	0.0832	0.0828	+ 0.5

Summary of Options Used

Listed below are the options used in example e8x29.dat:

Parameter Options

ELEMENT
END
MAGNETOSTATIC
SIZING
TITLE

Model Definition Options

CONNECTIVITY
COORDINATE
DEFINE
END OPTION
FIXED POTENTIAL
ISOTROPIC
POINT CURRENT
POST
PRINT ELEM

Load Incrementation Options

CONTINUE
STEADY STATE

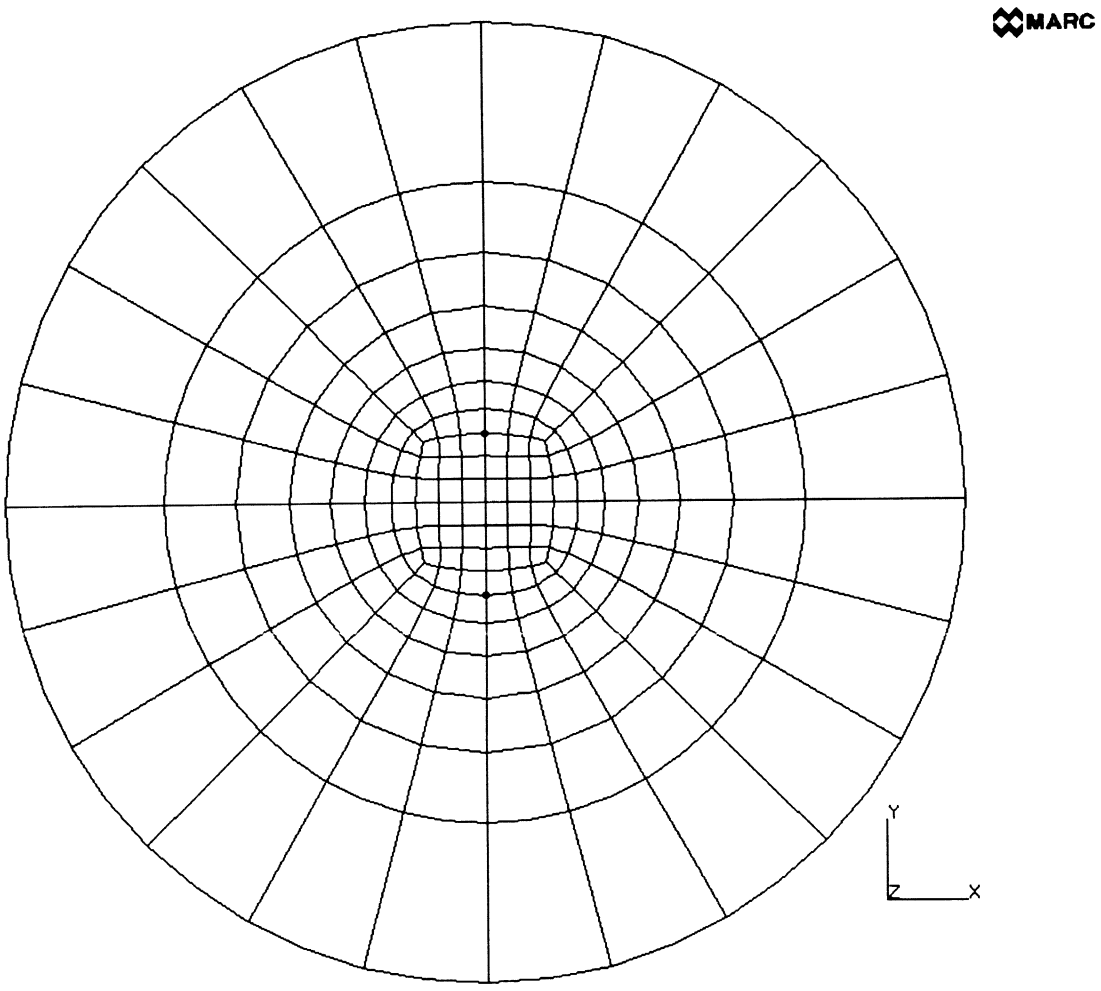

Figure E 8.29-1 Finite Element Mesh and Parallel Wires

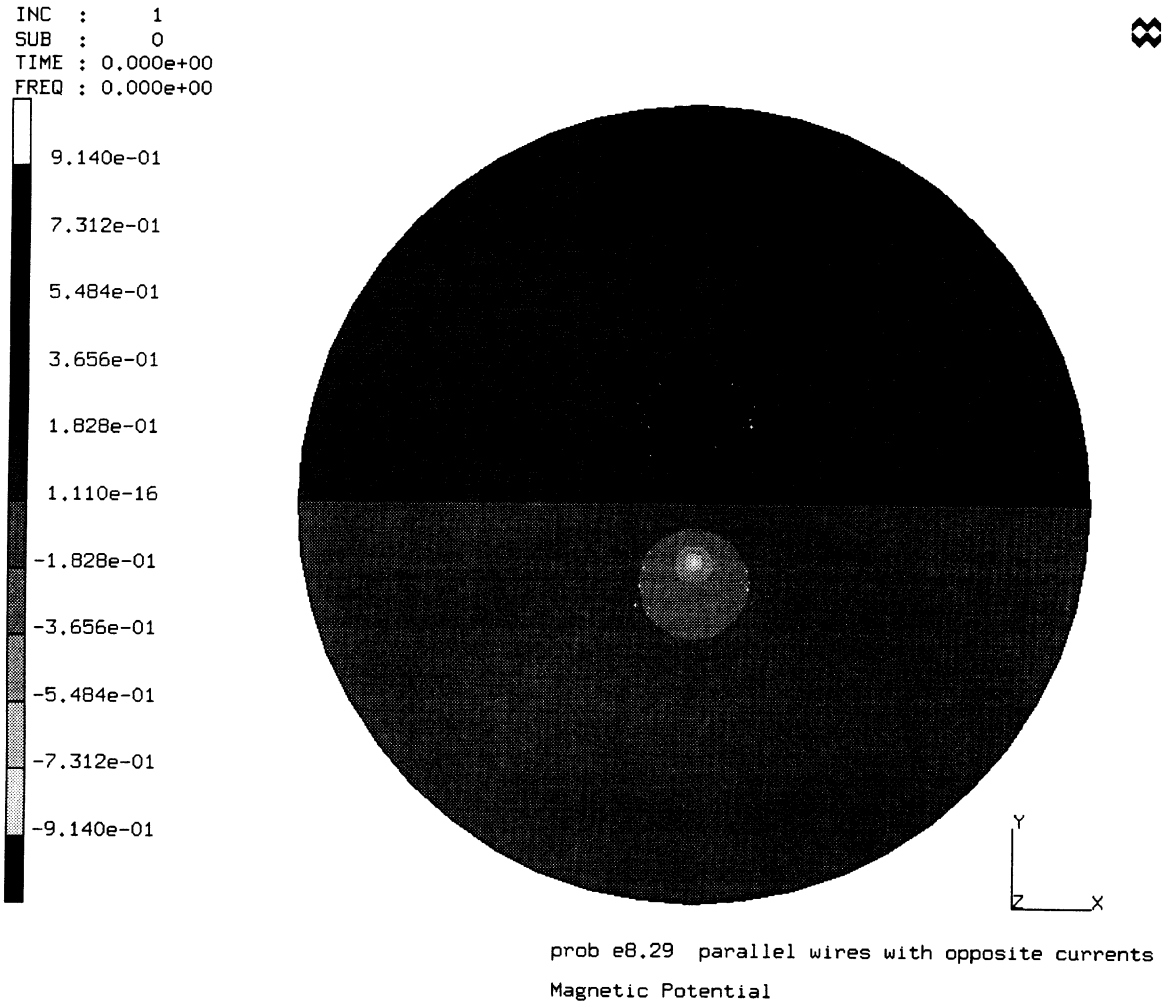

Figure E 8.29-2 Magnetic Scalar Potential

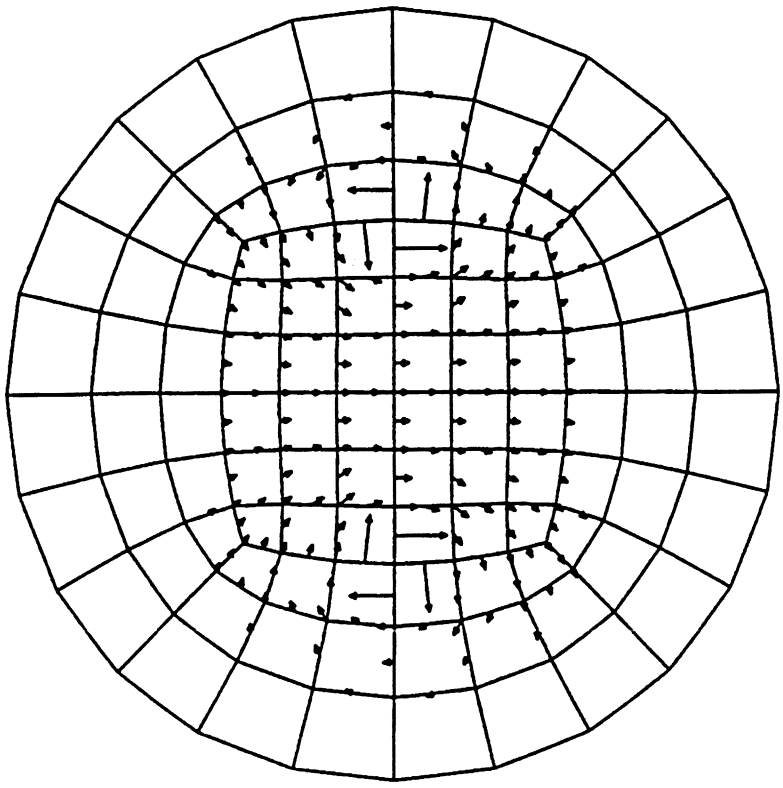

Figure E 8.29-3 Magnetic Flux Density

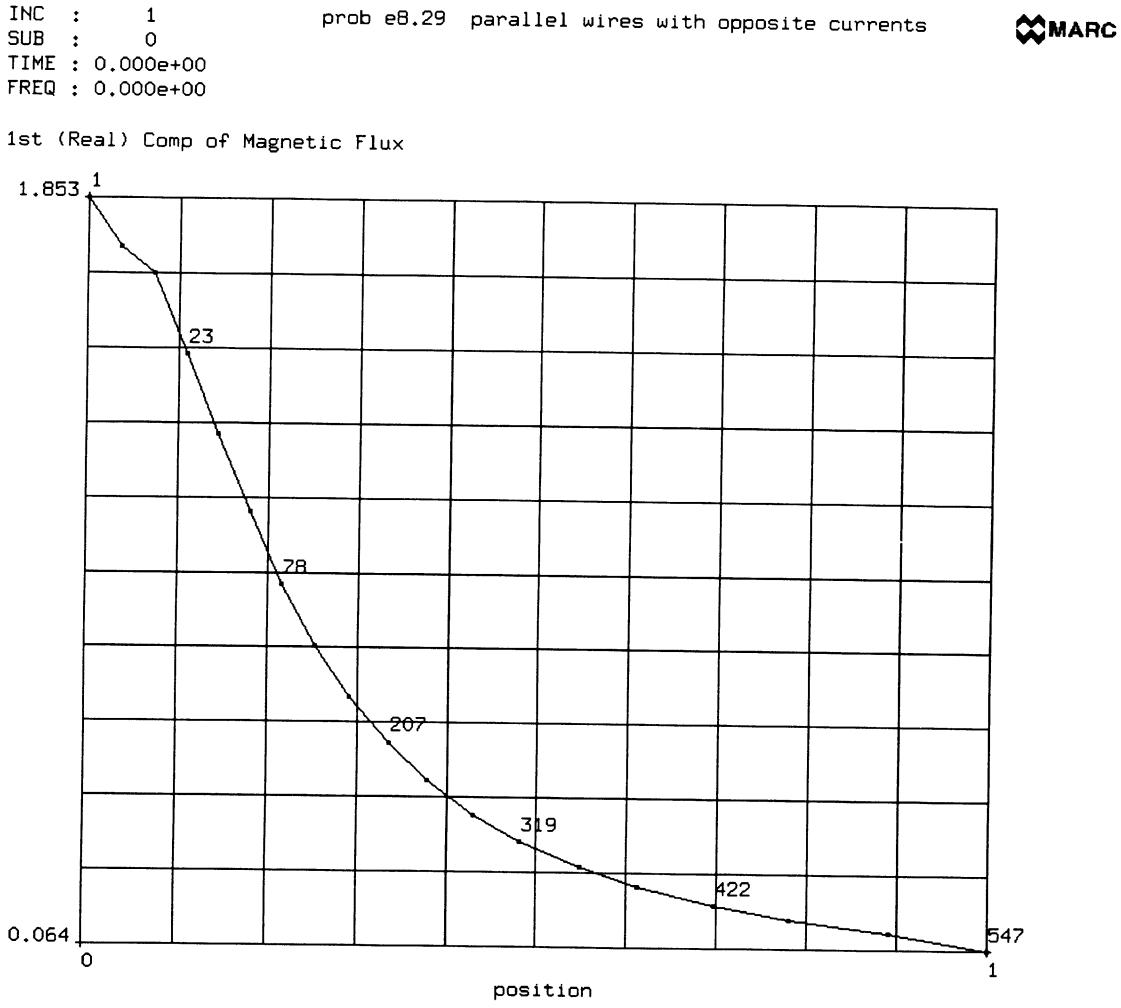

Figure E 8.29-4 Magnetic Flux Distribution

E 8.30 Harmonic Electromagnetic Analysis Of A Wave Guide

This problem demonstrates MARC's capability to perform electromagnetic analysis of a wave guide. The harmonic procedure is utilized in this problem.

Parameters

The EL-MA, 1 parameter option is used to indicate that a harmonic electromagnetic analysis is performed. This always results in a complex formulation. The HARMONIC parameter option is used to give an upper bound to the number of harmonic boundary conditions.

Element

Element 111 is used in this problem. This element is a four-node planar element for electromagnetic analysis. There are four degrees of freedom, the vector magnetic potential A and the scalar electrical potential ϕ.

Model

The model, as shown in Figure E 8.30-1, has a length of 1 m and a width of 0.5m. A wall is placed at 0.5 m which is 0.02 m thick (elements 33 to 36).

Loading

The outside periphery labeled "metal" is held at a fixed magnetic potential of zero. The corner, node 46, is given a fixed electrical potential of zero. A distributed current is applied to element one. The current is applied at a frequency between 200 MHz to 240 MHz in 2 MHz steps.

Material Properties

There are two materials in this analysis: the air and the wall. The material properties are:

	Permeability (henry/m)	Permittivity (farad/m)	Permeability of Air (henry/m)	Conductivity (s/m)
Air	1.2566×10^{-6}	8.854×10^{-12}	1.2566×10^{-6}	1000
Wall	1.2566×10^{-6}	8.854×10^{-12}	1.2566×10^{-6}	1×10^{-8}

Control

As this is a linear analysis, no controls are required.

Results

The third component of the electric field varies in magnitude from 0.989 to 0.831 over the frequency range requested. One may also observe that there is no distribution on the right side of the wall in Figure E 8.30-3. Note that the frequency is input in cycles/time, but Mentat reports the frequency in radians/time.

Table E 8.30-1 Electric Field as a Function of Frequency

Subincrement	ω x MHz	E_3
1	200	9.892
5	210	9.512
10	220	9.076
15	230	8.679
20	240	8.314

Summary of Options Used

Listed below are the options used in example e8x30.dat:

Parameter Options

ELEMENT
EL-MA
END
PRINT
SIZING
TITLE

Model Definition Options

CONNECTIVITY
COORDINATE
DEFINE
END OPTION
FIXED POTENTIAL
ISOTROPIC
OPTIMIZE
POST

Load Incrementation Options

CONTINUE
DIST CURRENT
HARMONIC

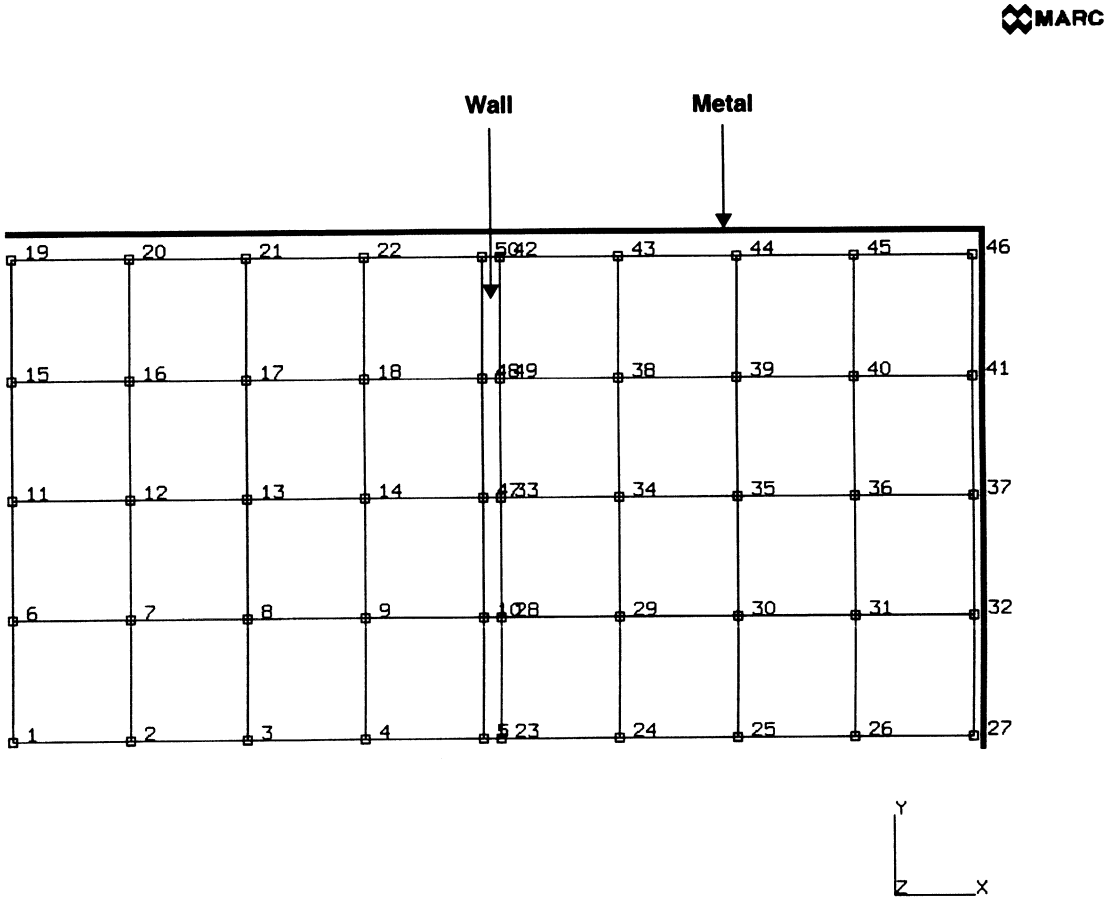

Figure E 8.30-1 Finite Element Mesh with Node Numbers

MARC

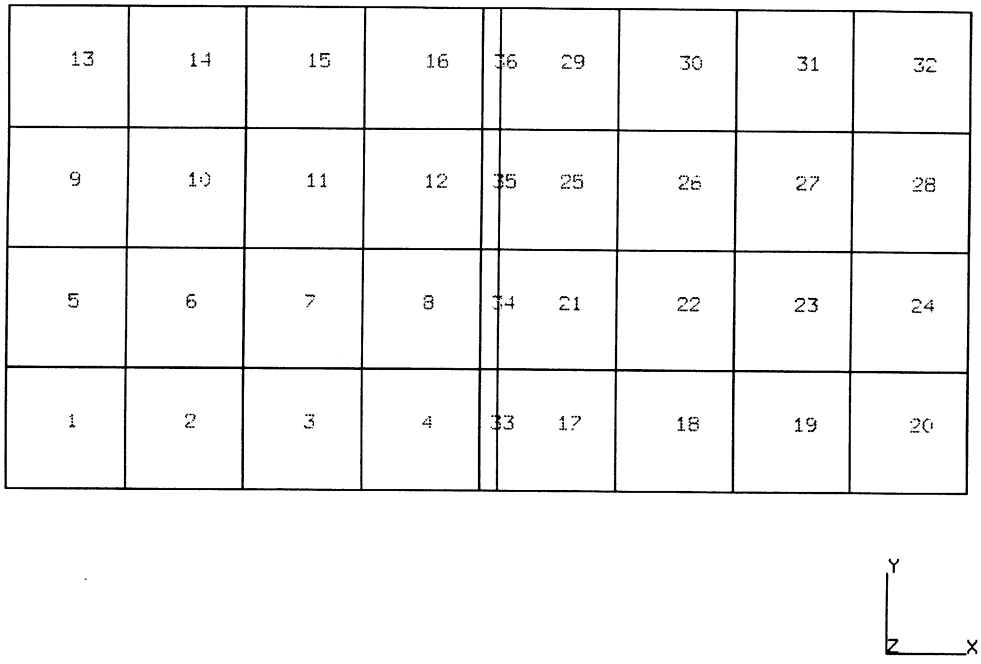

Figure E 8.30-2 Finite Element Mesh with Element Numbers

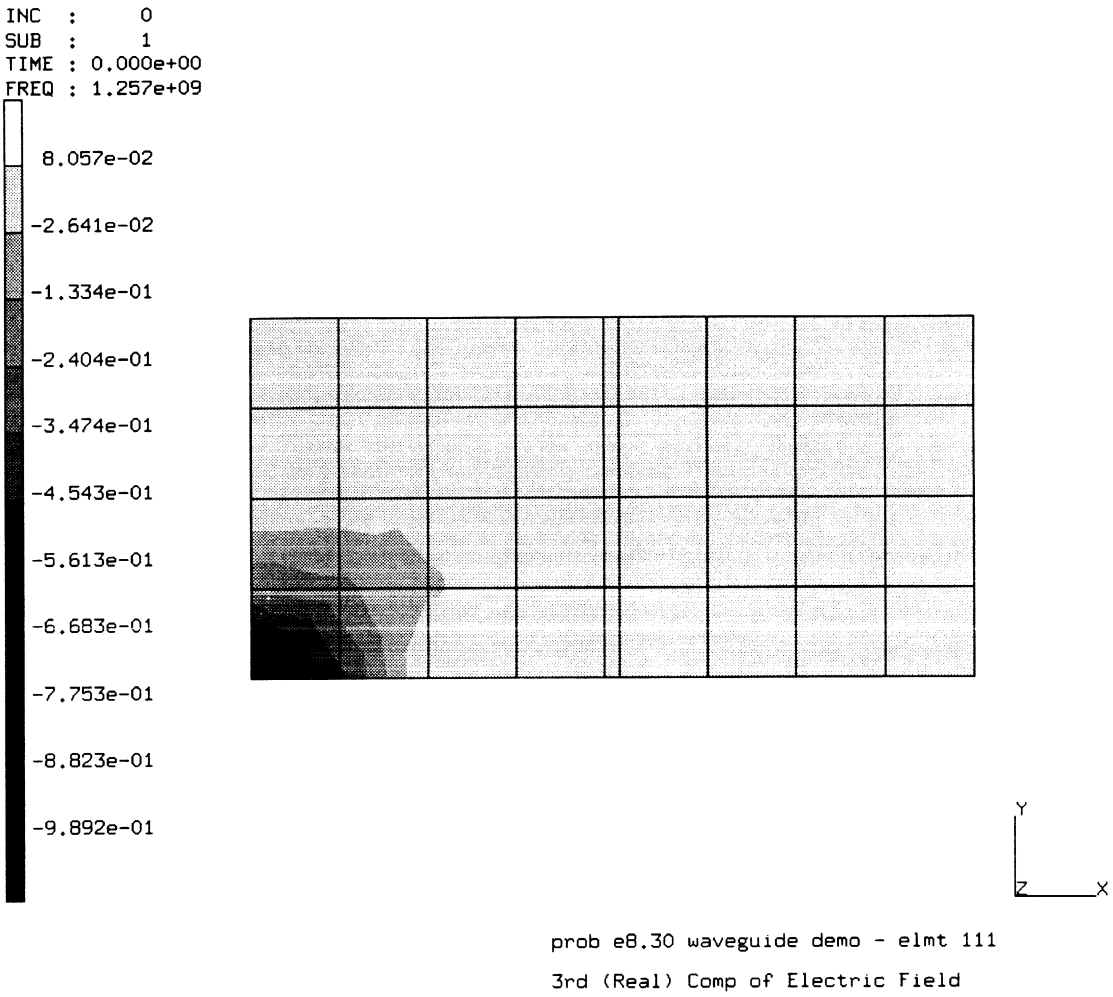

Figure E 8.30-3 Third Component of Electric Field at 20 MHz

E 8.31 Transient Electromagnetic Analysis Around A Conducting Sphere

This example demonstrates the transient electromagnetic analysis around a conducting sphere subjected to a planar pulse.

Parameters

The EL-MA,0 parameter option is used to indicate that a transient electromagnetic analysis is to be performed.

Element

This model consists of 165 element type 112 as shown in Figure E 8.31-1. Element type 112 is a four-node axisymmetric element for electromagnetic analysis. It has four degrees of freedom. The first three represent the magnetic vector potential. The last represents the scalar electrostatic potential. The spherical shell is elements 135–143 and 153. The inner radius is 5 cm and the outer radius is 5.5 cm.

Loading

The vertical symmetry line at z = 0 is constrained such that all components of A are zero. The nodes along z = 15 have $A_z = 0$. The nodes along r = 0 and r = 15 have A_x and A_z prescribed to be zero. The nodes along z = 15 have a ramp charge applied to the second component that varies from 0 to 25 x 10^{-6} coulomb over 25 microseconds. This data is entered using the DYNAMIC CHANGE and the POTENTIAL CHANGE options.

Material Properties

There are two materials in this analysis: the air and the metal sphere. The material properties areas follows:

	Permeability (henry/m)	Permittivity (farad/m)	Permeability of Air (henry/m)	Conductivity (s/m)
Air	1.2566 x 10^{-6}	8.54 x 10^{-12}	1.2566 x 10^{-6}	5 x 10^{8}
Sphere	1.2566 x 10^{-6}	8.54 x 10^{-12}	1.2566 x 10^{-6}	0.0

These are specified through the ISOTROPIC option.

Control

The convergence tolerance requested is 10% on residuals. The POST option is used to save the magnetic flux for post processing. The DYNAMIC CHANGE option is used to specify a time period of 25 microseconds to be performed in 25 increments with a fixed time step of 1 microsecond.

Results

Figure E 8.31-2 and Figure E 8.31-3 show the propagation of the magnetic field with time. The time history of the magnetic field is shown in Figure E 8.31-4. Finally, the current density is shown in Figure E 8.31-5. As expected, most of the current is in the sphere and the magnetic field is virtually zero within the sphere.

Summary of Options Used

Listed below are the options used in example e8x31.dat:

Parameter Options

ELEMENT
EL-MA
END
PRINT
SIZING
TITLE

Model Definition Options

CONNECTIVITY
COORDINATE
CONTROL
DEFINE
END OPTION
FIXED POTENTIAL
FORCDT
ISOTROPIC
OPTIMIZE
POST

Load Incrementation Options

CONTINUE
DYNAMIC CHANGE

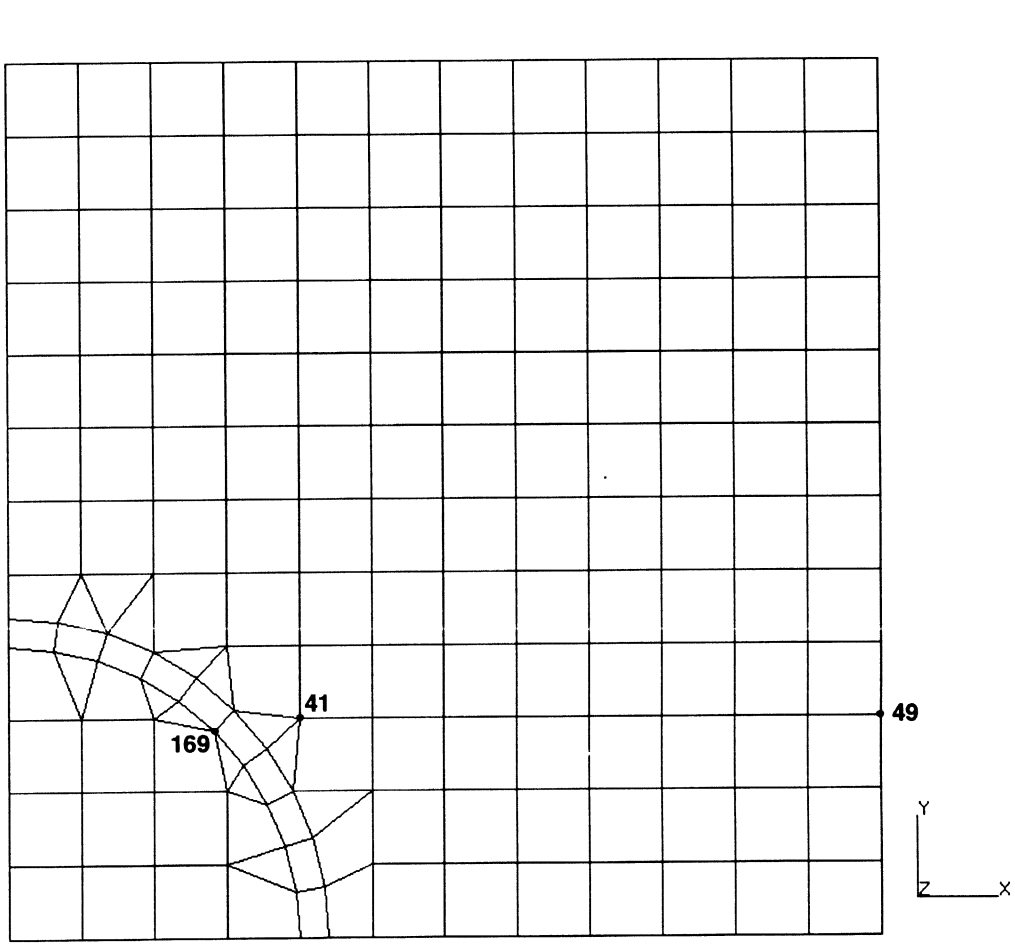

Figure E 8.31-1 Finite Element Mesh

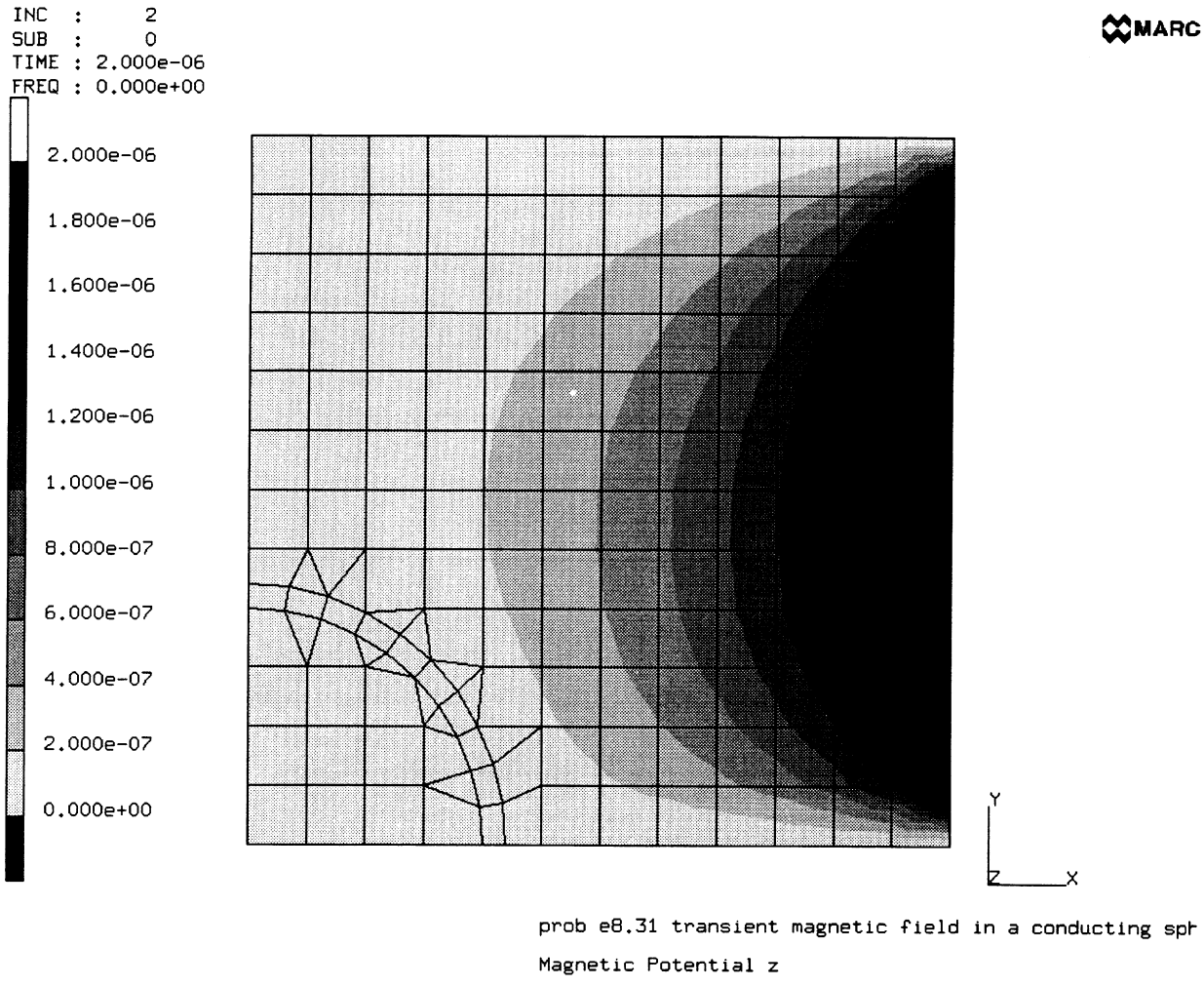

Figure E 8.31-2 Third Component of Magnetic Potential, Time = 2 microseconds

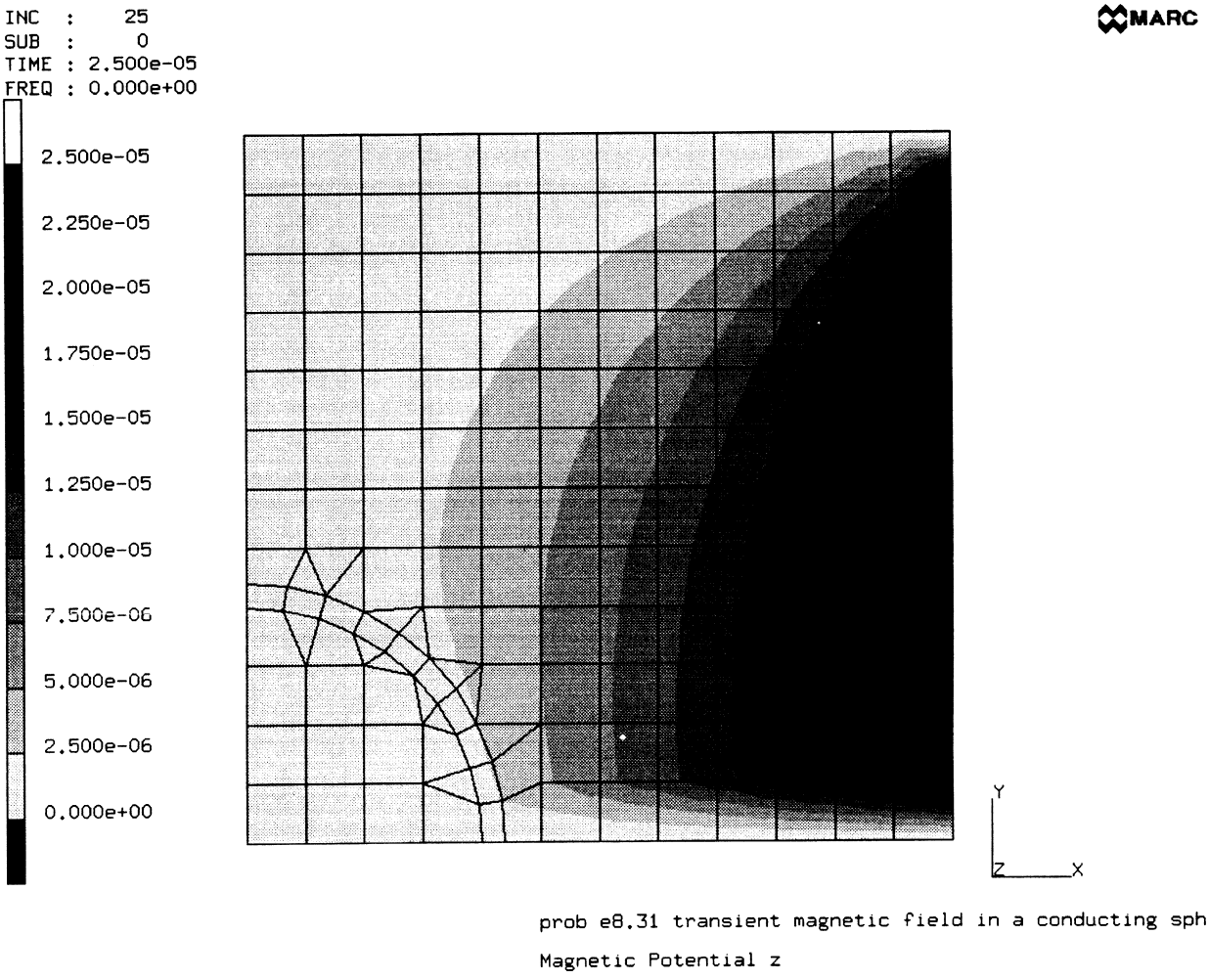

Figure E 8.31-3 Third Component of Magnetic Potential, Time = 25 Microseconds

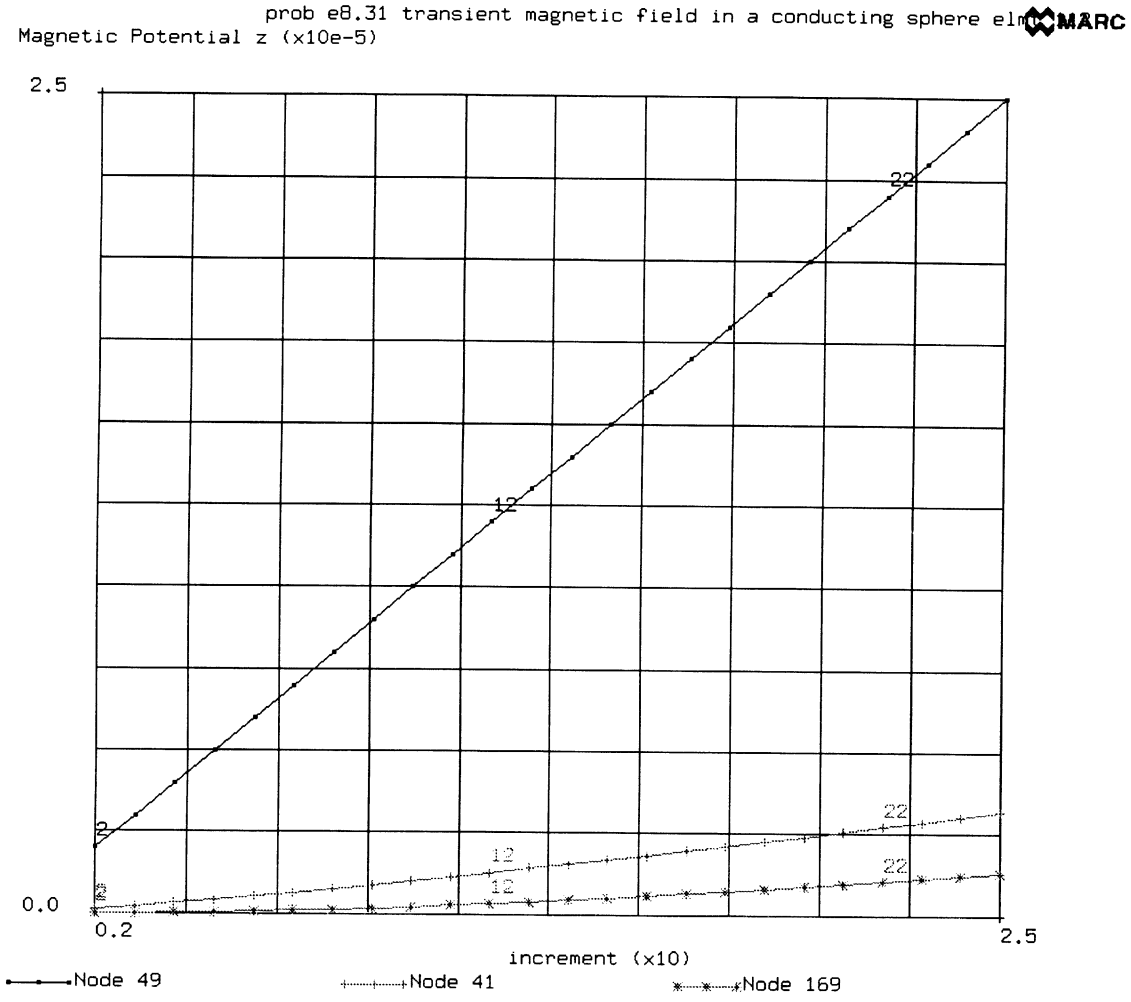

Figure E 8.31-4 Time History of Magnetic Potential

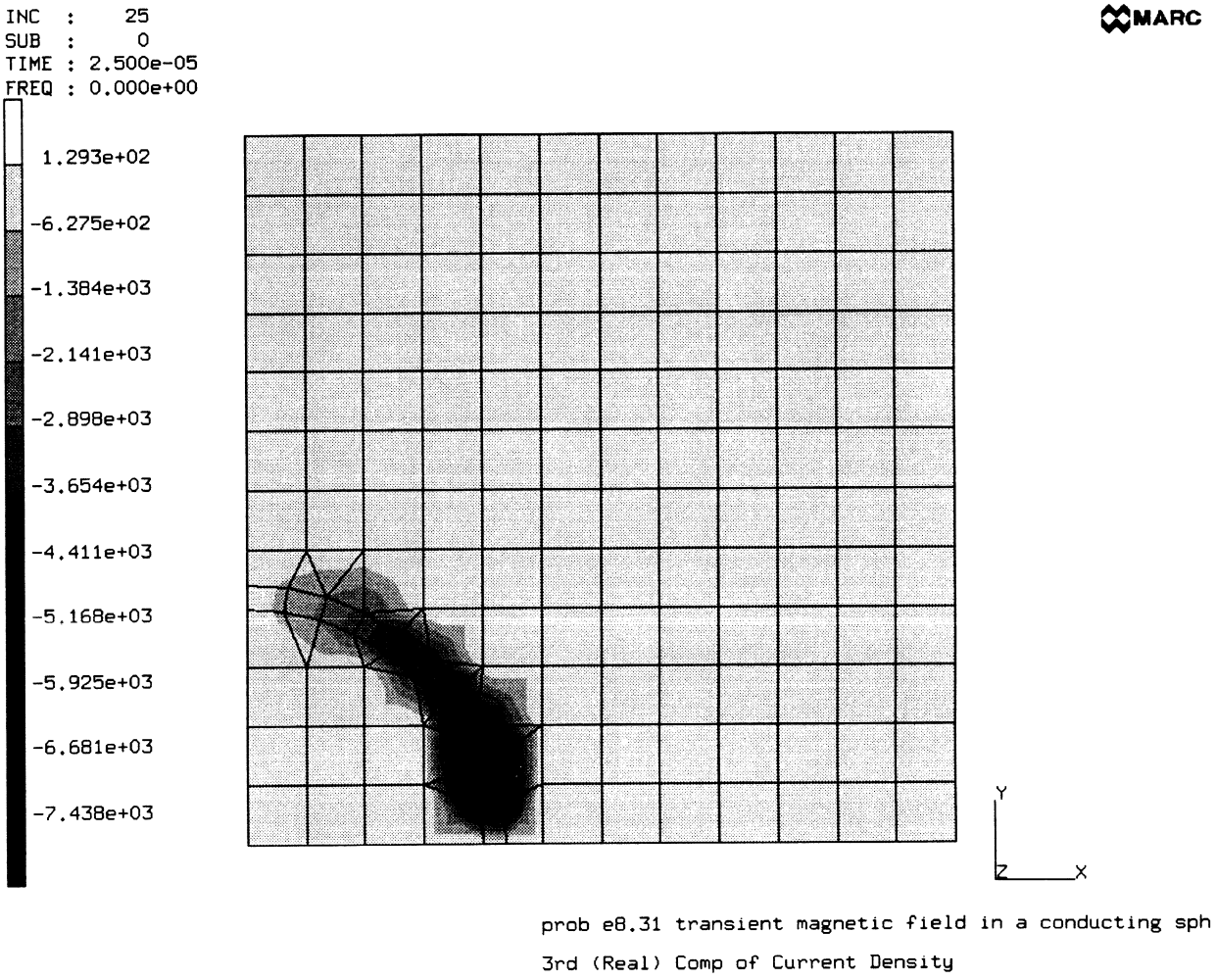

Figure E 8.31-5 Current Density, Time = 25 Microseconds

E 8.32 Cavity Resonator

This problem demonstrates the use of the harmonic electromagnetic capability for a prismatic resonator.

Parameters

The EL-MA,1 parameter option indicates that a harmonic electromagnetic analysis is to be performed. The HARMONIC option gives an upper bound to the number of harmonic boundary conditions.

Element

Element 113, an eight-node electromagnetic brick, is used in this example. The cavity is 0.5 x 0.25 x 1 meter long. The mesh of 12 elements is shown in Figure E 8.32-1.

Loading

Along the surfaces x = 0 and x = 0.5	$A_y = A_z = 0.$
Along the surfaces y = 0 and y = 1.0	$A_x = A_z = 0.$
Along the surfaces z = 0 and z = 0.25	$A_x = A_y = 0.$

A current is placed on element 1. This is applied for a frequency range of 200 MHz to 250 MHz.

Material Properties

The material properties of the air in the cavity is permeability = 1.2566 x 10^{-6} henry/m, permeability = 8.854 x 10^{-12} farad/m, and conductivity = 1 x 10^{-4} s/m.

Control

The POST option is used to save the electric field and magnetic flux (both real and imaginary components). As this is a linear problem, no additional controls are necessary. The PRINT option is used to force the solution of the non-positive definite system.

Results

Table E 8.32-1 gives the electric field as a function of frequency. One observes that MARC indicates that the resonance occurs at 230 MHz.

Table E 8.32-1 Electric Field as a Function of Frequency

Frequency (MHz)	$E_x \times 10^2$	$E_y \times 10^2$	$E_z \times 10^2$
200	-4.57	-3.42	-9.13
202	-4.38	-3.28	-8.76
204	2.43	1.82	4.87
206	5.45	4.09	10.90
208	-1.56	-1.17	-3.12
210	-14.52	-10.89	-2.90
212	-1.35	-1.02	-2.71
214	2.75	2.07	5.51
216	-5.14	-3.86	-10.29
218	-16.05	-12.04	-32.11
220	2.39	1.80	4.77
222	-0.32	-0.24	-0.60
224	-5.07	-3.80	-10.14
226	0.69	0.51	1.37
228	4.32	3.24	8.64
230	56.29	42.22	112.60
232	5.24	3.93	10.48
234	-0.82	0.61	-1.63
236	-16.15	-12.11	-32.30
238	-1.96	-1.47	-3.93
240	0.89	0.67	1.79
242	-1.15	0.86	-2.30
244	0.02	0.02	0.05
246	1.95	1.46	3.90
248	-4.14	-3.10	-8.27

Summary of Options Used

Listed below are the options used in example e8x32.dat:

Parameter Options

ELEMENT
EL-MA
END
HARMONIC
PRINT,3
SIZING
TITLE

Model Definition Options

CONNECTIVITY
COORDINATE
DEFINE
END OPTION
FIXED POTENTIAL
ISOTROPIC
OPTIMIZE
POST

Load Incrementation Options

CONTINUE
DIST CURRENT
HARMONIC

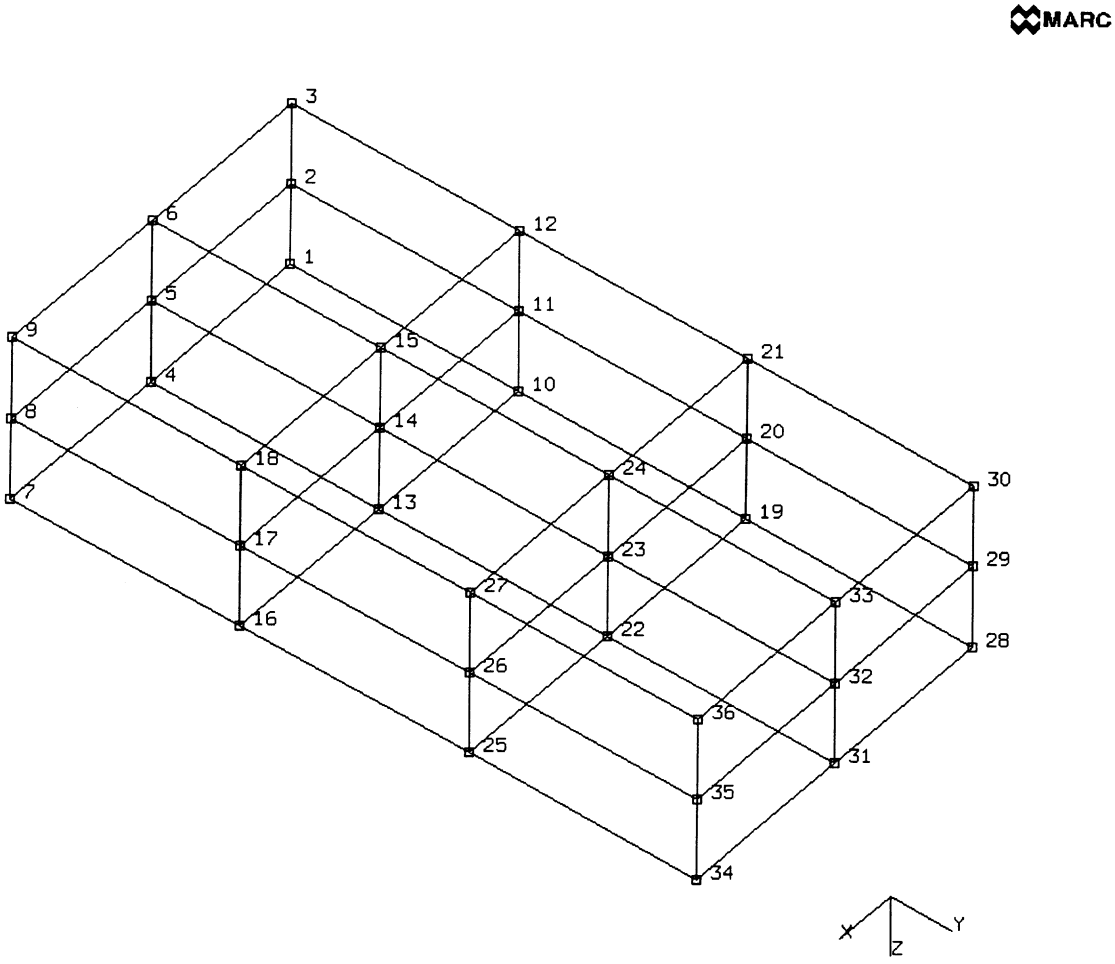

Figure E 8.32-1 Finite Element Mesh of Resonator

E 8.33 Electromagnetic Analysis Of An Infinite Wire

In this example, the harmonic and transient electromagnetic capabilities will be used to predict the steady state magnetic field distribution due to a wire. This is the same problem as E 8.20 where the MAGNETOSTATIC procedure was used.

Parameters

The EL-MA parameter option indicates that an electromagnetic analysis is being performed. The "0" option indicates a transient analysis while a "1" indicates a harmonic analysis.

Element

Element type 111, a four node planar electromagnetic element, is chosen. This element has the vector potential A and the scalar potential ϕ as its degrees of freedom.

Only a sector of a circular region is modeled as shown in Figure E 8.33-1. The outer radius is 1 cm.

Loading

In both analyses, the magnetic potential and scalar at the outside radius is prescribed to be zero. A harmonic point charge of 0.05 amps is applied at node 1 at a frequency of 1×10^{-6} Hz in the harmonic analysis. In the transient analysis, a point charge of 0.05 amps is applied at node 1 during the first step of 0.01 seconds. This is then held constant for ten steps of 1×10^{6} second each. The load is applied using the POINT CURRENT-CHARGE option.

Material Properties

The magnetic permeability of 1000 henry/cm is entered through the ISOTROPIC option.

Results

When using the harmonic procedure, the z component of the magnetic potential is shown in Figure E 8.33-2. It is virtually identical to Figure E 8.20-3. When using the transient procedure, the solution oscillates about the correct solution. This is shown in Figure E 8.33-3.

Summary of Options Used

Listed below are the options used in example e8x33a.dat:

Parameter Options

ELEMENT
EL-MA
END
HARMONIC
SIZING
TITLE

Model Definition Options

CONNECTIVITY
COORDINATE
END OPTION
FIXED POTENTIAL
ISOTROPIC
POST
PRINT ELEMENT

Load Incrementation Options

CONTINUE
HARMONIC
POINT CURRENT-CHARGE

Listed below are the options used in example e8x33b.dat:

Parameter Options

ELEMENT
END
PRINT
SIZING
TITLE

Model Definition Options

CONNECTIVITY
CONTROL
COORDINATE
END OPTION
FIXED POTENTIAL
ISOTROPIC
POST
PRINT ELEMENT

Load Incrementation Options

CONTINUE
DYNAMIC CHANGE
POINT CURRENT-CHARGE

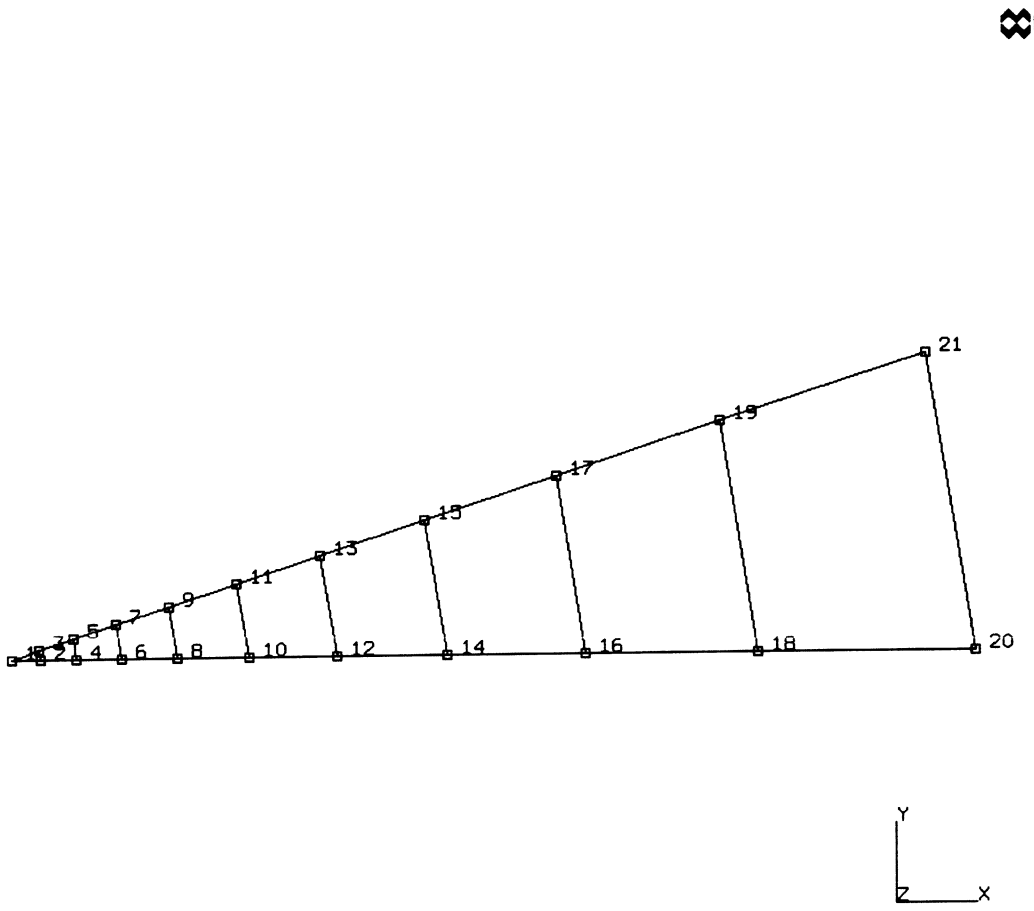

Figure E 8.33-1 Sector of Circular Region

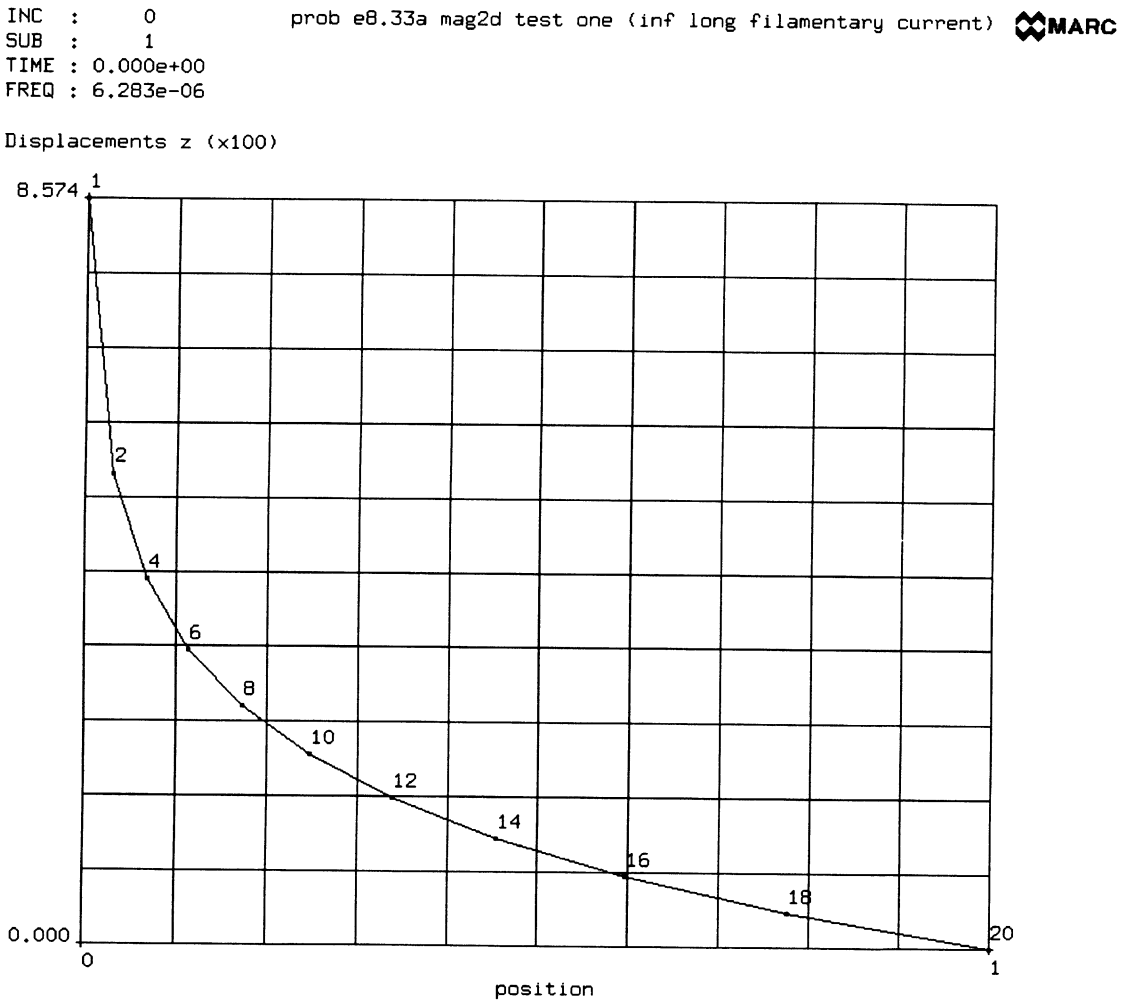

Figure E 8.33-2 Third Component of Magnetic Potential Using Harmonic Procedure

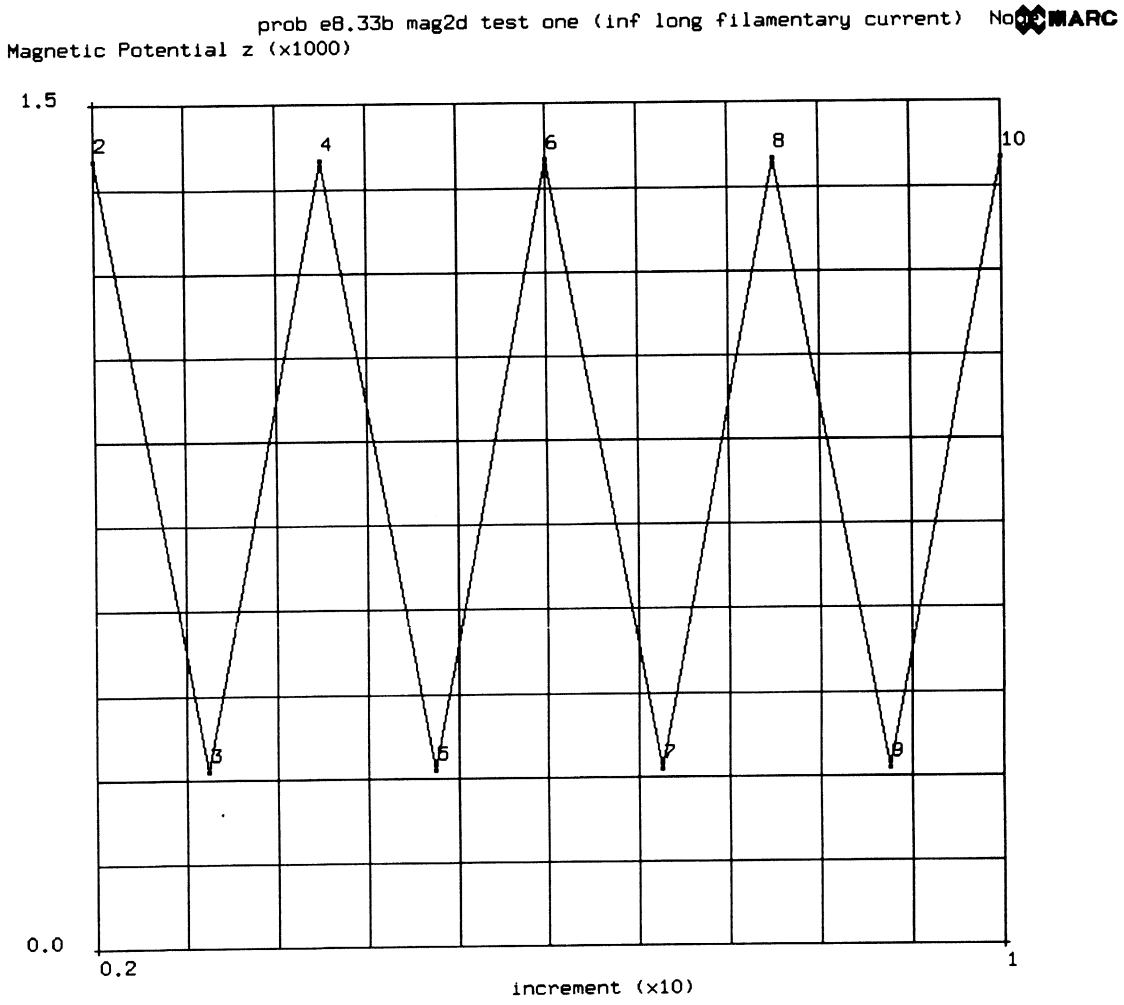

Figure E 8.33-3 Time HIstory of Magnetic Potential of Node 1, Transient Procedure

E 8.34 Triaxial Test On Normally Consolidated Weald Clay

This problem demonstrates the uncoupled pore plasticity analysis of a homogeneous specimen. A drained triaxial test on a normally consolidated clay is simulated.

Parameters

The PORE, 0, 1 parameter option indicates that a stress analysis is to be performed, but the fluid pore pressure will not be calculated. The ISTRESS parameter indicates that an initial stress will be defined as is usually the case in soil analysis. The UPDATE parameter indicates that the analysis is to perform the calculation using the current (deformed) geometric configuration. As the Cam-Clay soil model involves volumetric plastic behavior, a different procedure is used as compared to metal plasticity.

Model

A single axisymmetric element, type 28, is used in the analysis. The specimen is 4 inches long and has a radius of 0.75 inch as shown in Figure E 8.34-1.

Material Properties

The Cam-Clay model is invoked using the SOIL model definition option. The material data is:

$E = 100$ psi	Young's modulus
$\upsilon = 0.4$	Poisson's ratio
$\sigma_y = 200$ psi	Yield stress
$K_{Fluid} = 100$ psi	Bulk modulus of fluid
$\upsilon = 0.3982$	Dynamic viscosity of fluid
$= 0.0$	Permeability of soil
$\lambda = 0.88$	Virgin compression ratio
$\kappa = 0.031$	Recompression ratio
$M_{cs} = 0.882$	Slope of critical state line

In the Cam-Clay model, the Young's modulus and the Poisson's ratio are not actually used.

The initial void density, $e_0 = 0.7977$, is entered through the INITIAL VOID option. It is assumed to be homogeneous over all nine integration points.

Loading

The initial confining pressure is 30 psi. This is entered in two places. First, the INITIAL PC option is used to define the initial preconsolidation pressure to be 30 psi. The INIT STRESS is then used to enter the value of the initial stress to be -30 psi (remember that compressive stresses are negative).

In increment 0, no deformation occurs.

In increment 1, a pressure of 30 psi is applied on the outside radius and the right side. This is to ensure that equilibrium exists.

This is followed by an axial compression of 0.004 inch per increment for 200 increments. The total axial compression is then 0.8 or an engineering axial strain of about 20%. The time step is two seconds per increment.

Results

The time history of the axial stress is shown in Figure E 8.34-2. The time history of the void ratio is shown in Figure E 8.34-3. We can observe that the void ratio decreases from the original value of 0.7977 to 0.7202. The preconsolidation pressure history is shown in Figure E 8.34-4. The value increases from 30 psi to 87.78 psi.

Summary of Options Used

Listed below are the options used in example e8x34.dat:

Parameter Options

ELEMENT
END
ISTRESS
PORE
SIZING
TITLE
UPDATE

Model Definition Options

CONNECTIVITY
CONTROL
COORDINATES
DIST LOADS
END OPTION
FIXED DISP
INIT STRESS
INITIAL PC
INITIAL VOID
POST
SOIL

Load Incrementation Options

AUTO LOAD
CONTINUE
DISP CHANGE
DIST LOADS
TIME STEP

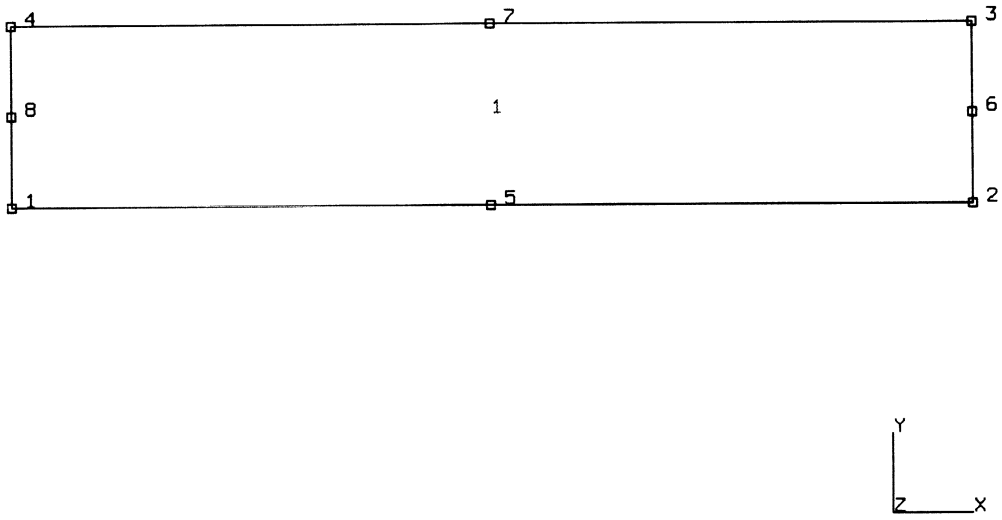

Figure E 8.34-1 One-Element Model

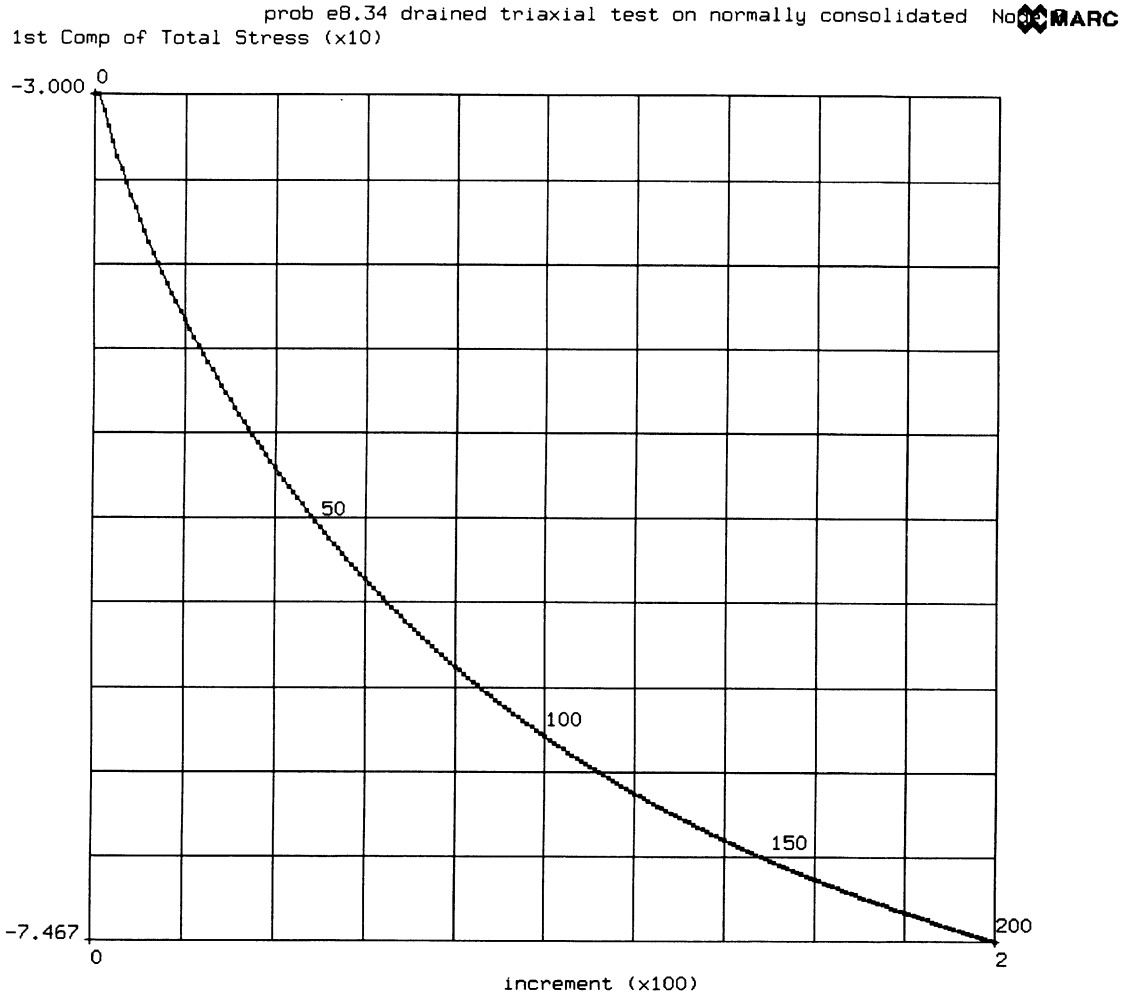

Figure E 8.34-2 Time History of Axial Stress

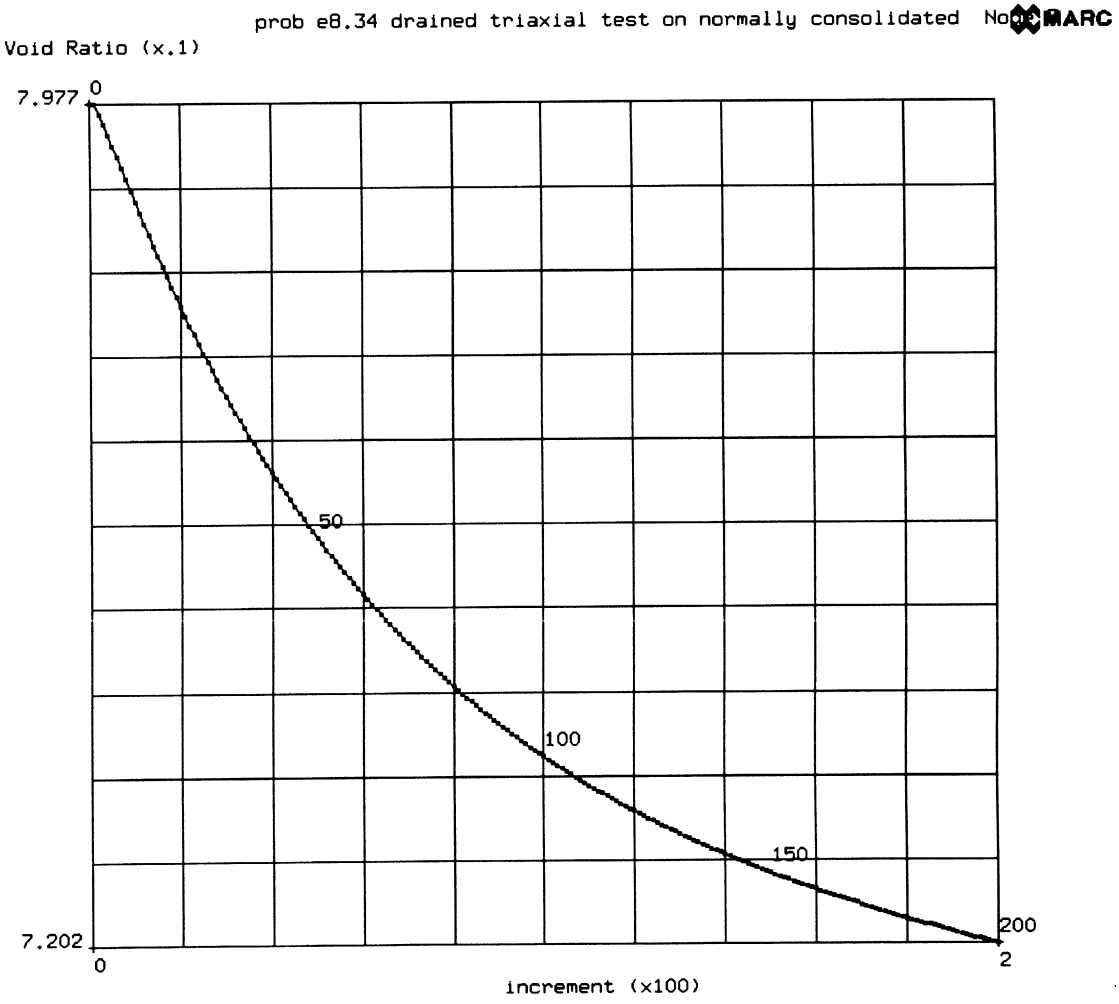

Figure E 8.34-3 Time History of Void Ratio

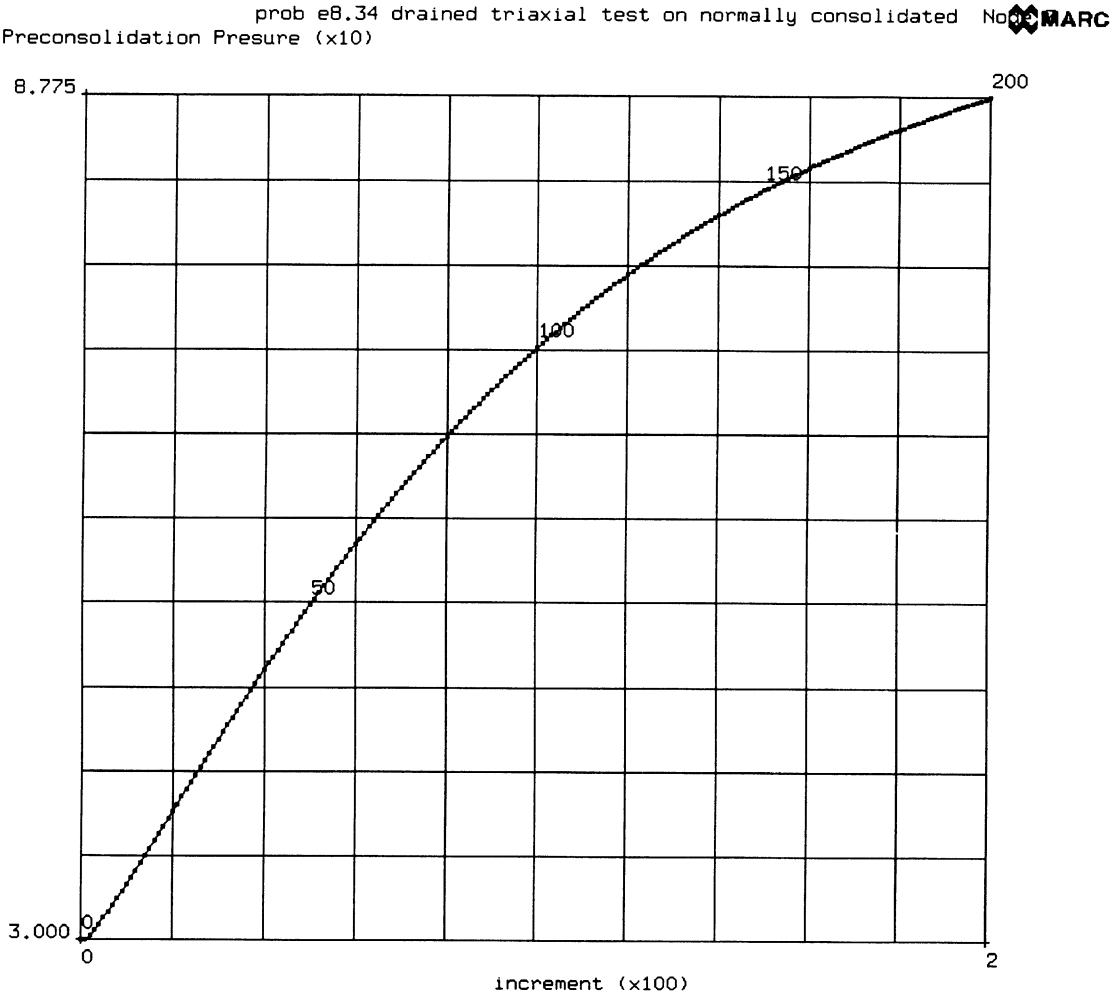

Figure E 8.34-4 Time History of Preconsolidation Pressure

E 8.35 Soil Analysis Of An Embankment

This problem demonstrates the use of MARC for a coupled pore pressure soil analysis. The I-95 embankment across the tidal marshes of Saugus, just north of Boston, is modeled under the conditions of plane strain. The original description was given by Wroth.

Parameters

The PORE, 2, 1 parameter option indicates that a fully coupled pore pressure calculation is to be performed. The ISTRESS parameter indicates that an initial stress will be applied in increment 0.

Model

Element type 32 is used in this analysis. This element is a Herrmann element which is normally used for incompressible material. When used in a pore pressure calculation, the fourth degree of freedom at the corner nodes is no longer the Lagrange multiplier, but instead the fluid pore pressure. The model consists of 126 elements and 427 nodes. The model consists of eight groups of elements that will be used to define the different preconsolidation pressures. Three groups will be used to define the material properties. These groups are shown in Figure E 8.35-1.

Material Properties

The material properties are grouped into the fill, silt, and all of the rest (bbc). The properties are as follows:

	bbc	Silt	Fill
E (psi)	2.5×10^6	2.5×10^6	2.5×10^6
υ	0.4	0.4	0.4
ρ	0.000054	10.0	10.0
σ_y	0	0	0
K_{Fluid}	100	100	100
Dynamic viscosity of fluid – υ	0.1	0.1	0.1
Permeability	1	1	1
Virgin compression ratio – λ	0.147	0.147	0.147
Recompression ratio – κ	0.060	0.060	0.060
Slope of critical state line – M	1.05	1.05	1.05

This data is entered through the SOIL option.

When using the Cam-Clay model, Young's modulus, Poisson's ratio, and yield stress are ignored.

The initial preconsolidation is dependent on the depth. The values entered through the INITIAL PC option are as follows:

Region	Initial Preconsolidation (psi)
Fill	10
Silt	10,000
Layer 1	95
Layer 2	80
Layer 3	71
Layer 4	70
Layer 5	57
Layer 6	50

A small hydrostatic initial stress is entered for all elements as 1 psi. It is entered as a negative value to indicate compression. The Cam-Clay model does not behave well when the hydrostatic stress is zero or positive (tensile).

The initial void ratio is 0.74 for all elements. This is entered through the INITIAL VOID option.

Boundary Conditions

The boundary conditions consist of no motion in the x direction on the right and left side. No motion in the y direction along the bottom surface. And the pore pressure is zero along the top surface. This is shown in Figure E 8.35-2.

In increment 0, only the initial stress is on the structure.

In increment 1, a pressure of 1 psi is placed along the complete top surface (fill). A very small time step of 1×10^{-20} seconds is chosen.

A uniform body force/area is then applied of magnitude 0.6 psi/in^2 per increment for 15 increments or a total of 9 psi/in^2. Each time step is 10000 seconds $\equiv$ 2.78 hours.

This is followed by a distributed load of 0.5 psi/increment on the embankment and a load of 0.25 psi/increment on element 72. In the AUTO LOAD section, 290 increments are requested with each of a time step of 0.4138 seconds. Because the CONTROL option indicates 200 increments, this load sequence will not be completed.

Results

A contour plot of the vertical displacements on the superimposed deformed mesh is shown in Figure E 8.35-3. The stress in the y-direction is given in Figure E 8.35-4. The hydrostatic pressure is shown in Figure E 8.35-5. The void ratio is shown in Figure E 8.35-6. The preconsolidation stress is shown inFigure E 8.35-7. The pore pressure is shown in Figure E 8.35-8.

Summary of Options Used

Listed below are the options used in example e8x34.dat:

Parameter Options

ELEMENT
END
ISTRESS
PORE
SIZING
TITLE

Model Definition Options

CONNECTIVITY
CONTROL
COORDINATES
DEFINE
DIST LOADS
FIXED DISP
INIT STRESS
INITIAL PC
INITIAL VOID
OPTIMIZE
POST
PRINT ELEM
PRINT NODE
RESTART
SOIL
SOLVER

Load Incrementation Options

AUTO LOAD
CONTINUE
CONTROL
DIST LOAD
TIME STEP

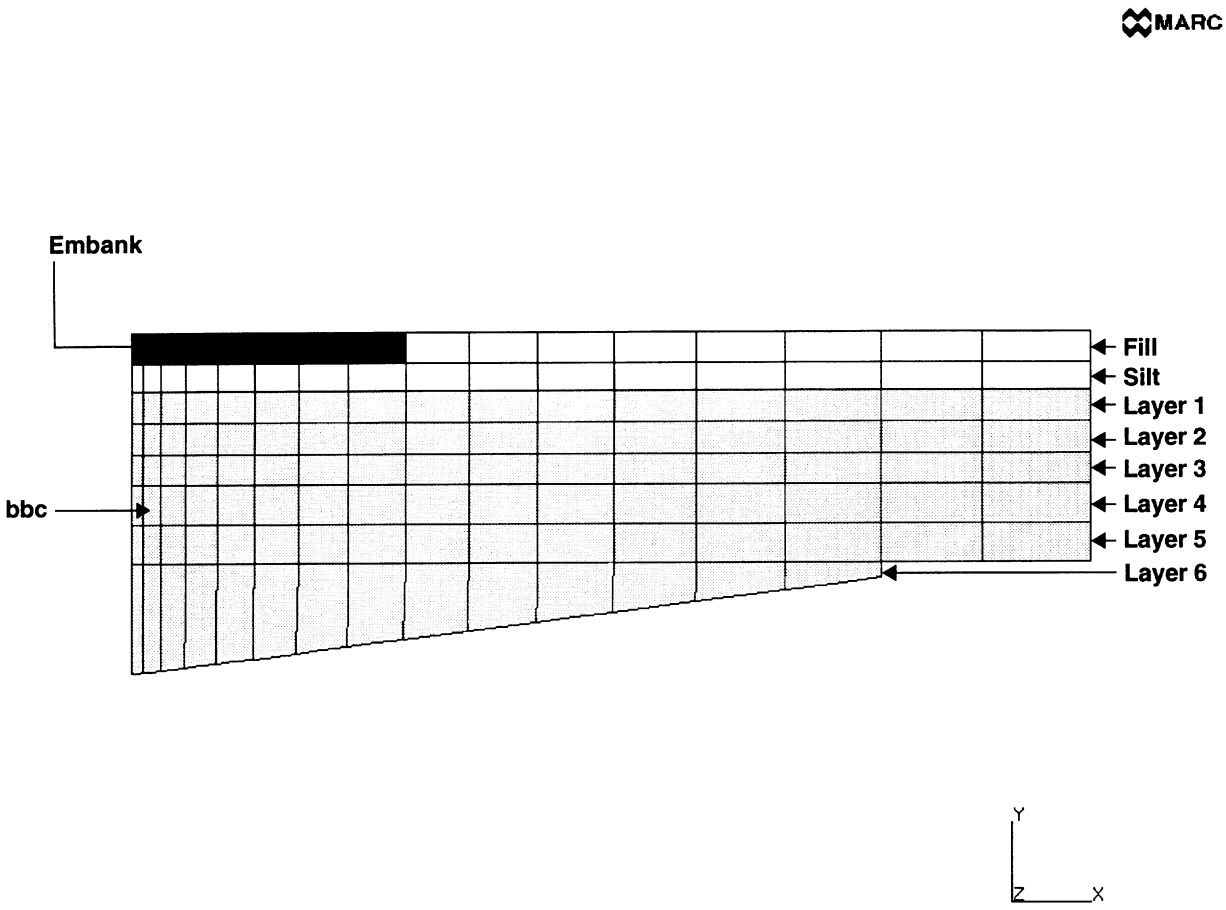

Figure E 8.35-1 Mesh of Embankment with Sets Used for Material Definition and Initial Preconsolidation

MARC

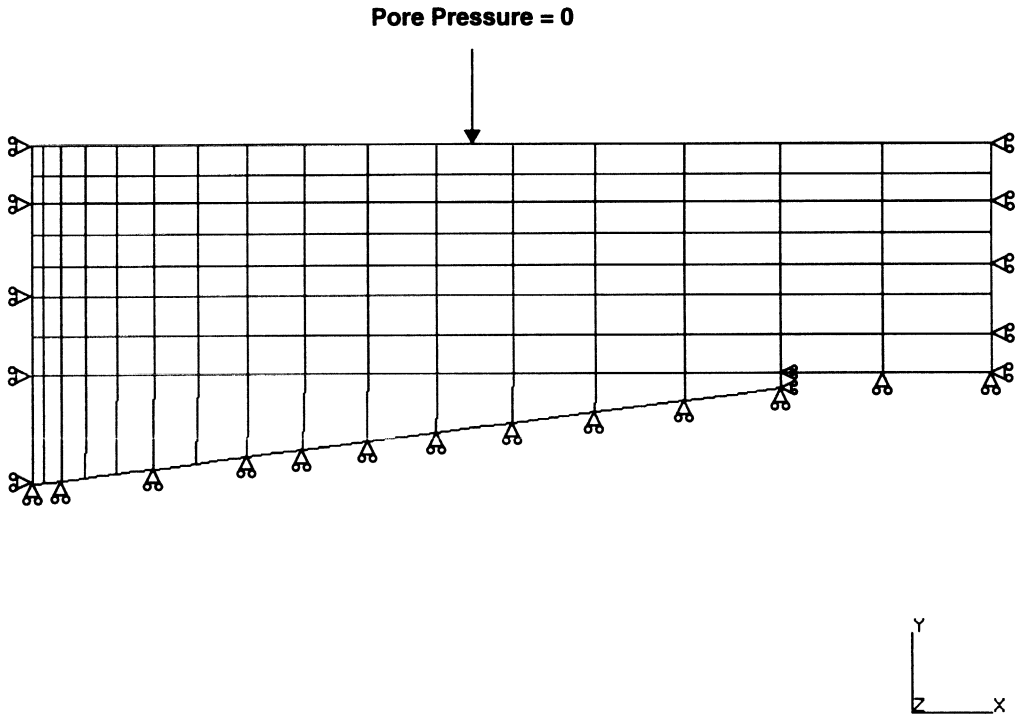

Figure E 8.35-2 Boundary Conditions

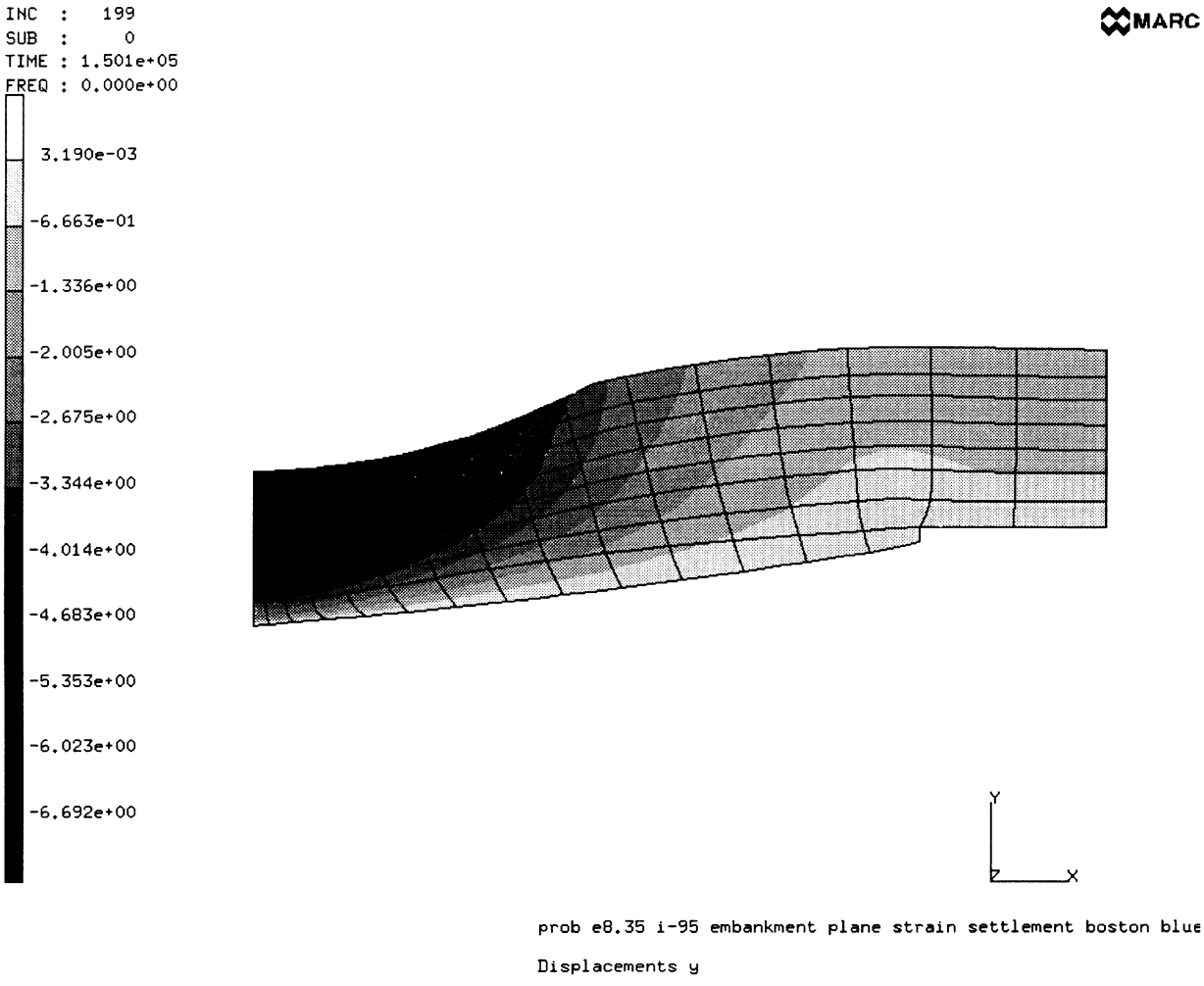

Figure E 8.35-3 Contour of Settlement

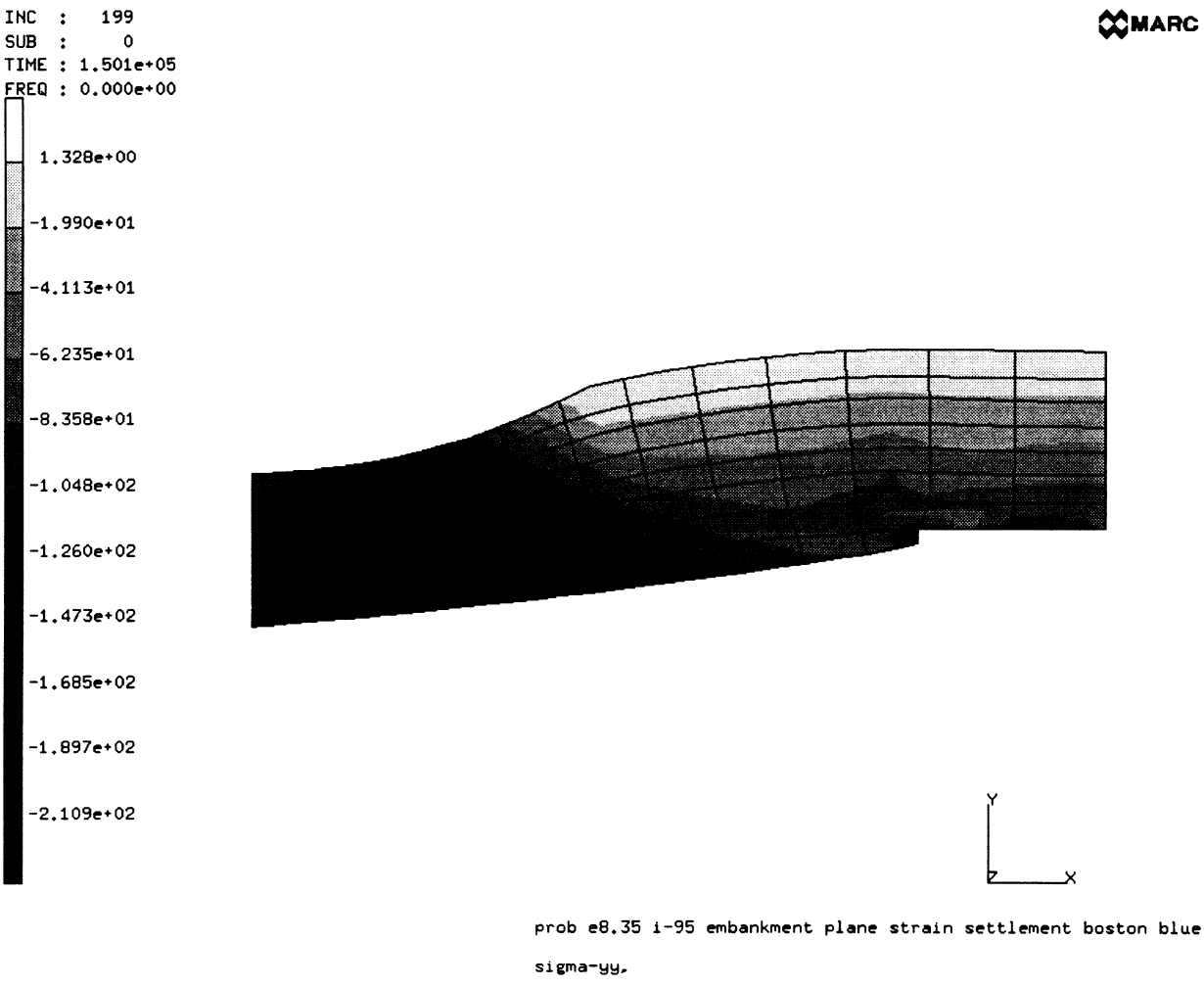

Figure E 8.35-4 Vertical Stresses

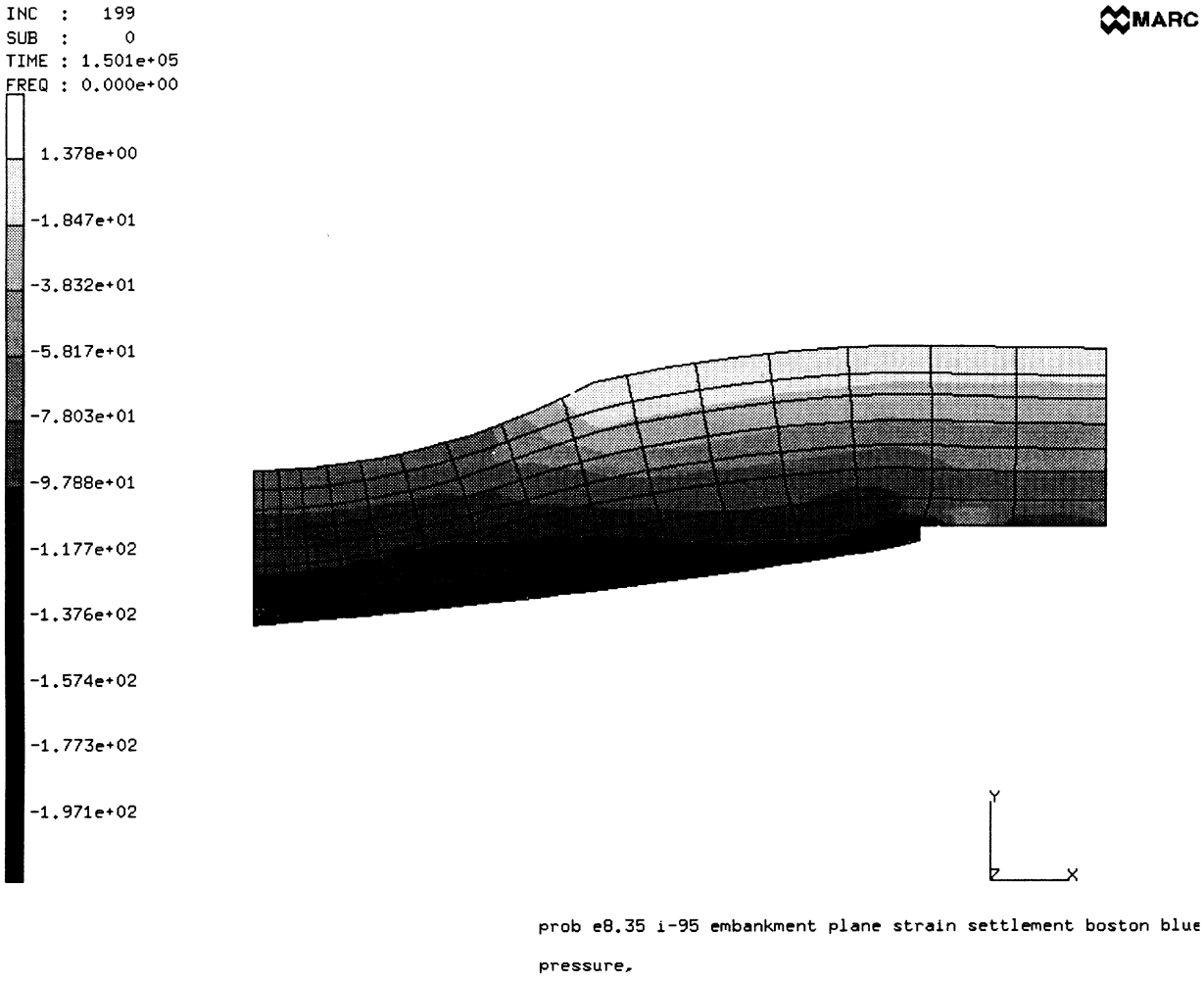

Figure E 8.35-5 Mean Pressure in Soil

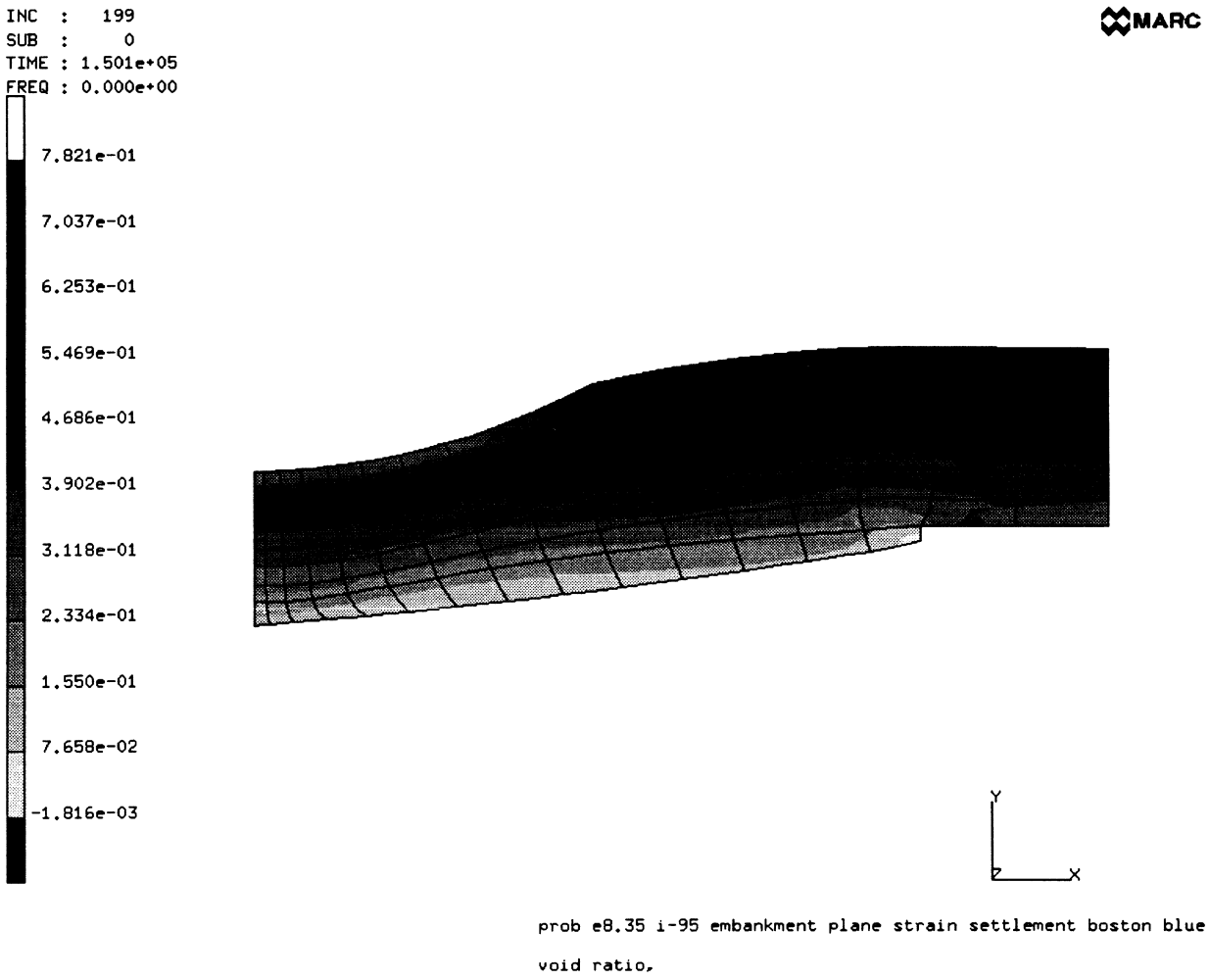

Figure E 8.35-6 Void Ratio

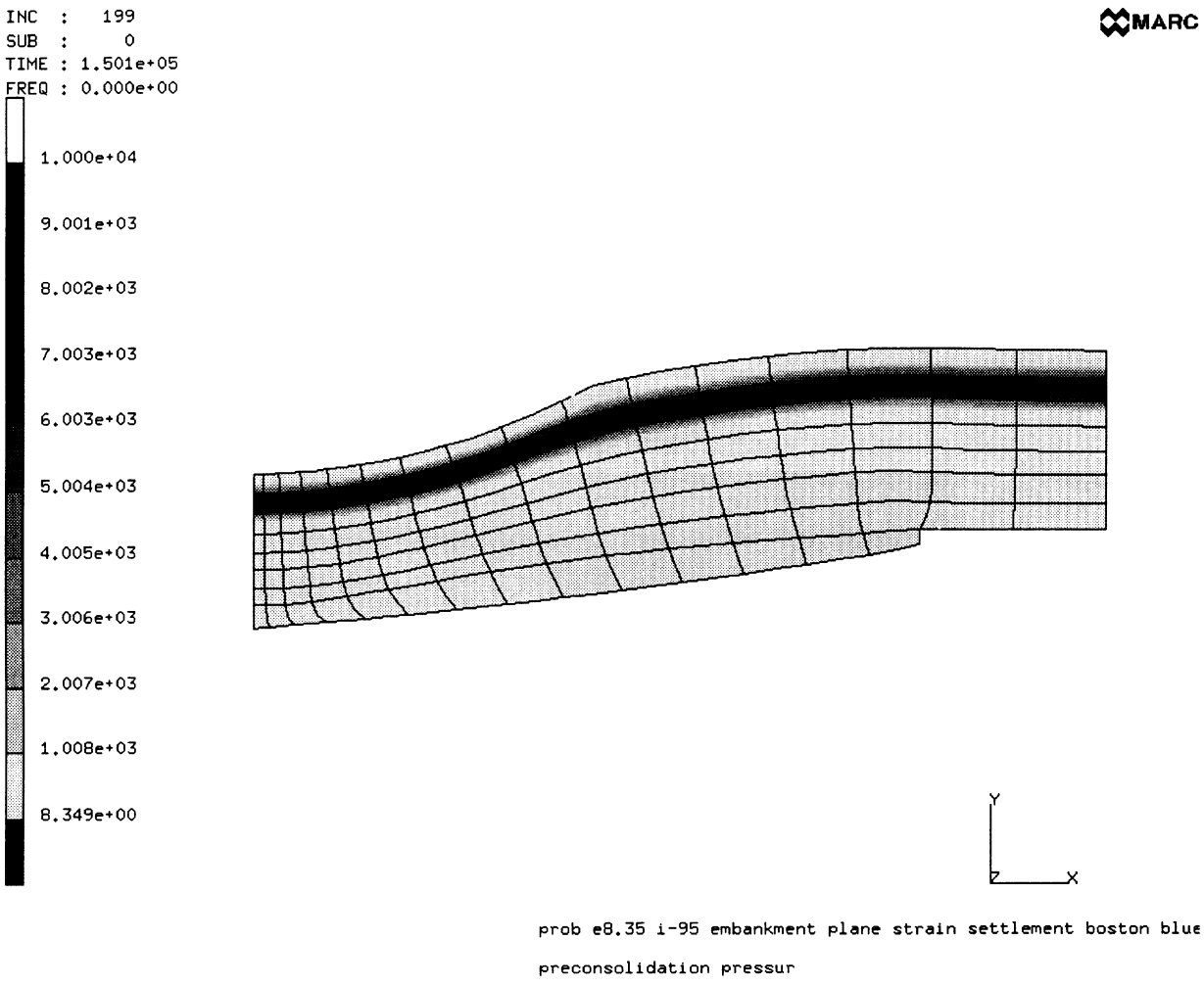

Figure E 8.35-7 Preconsolidation Pressure

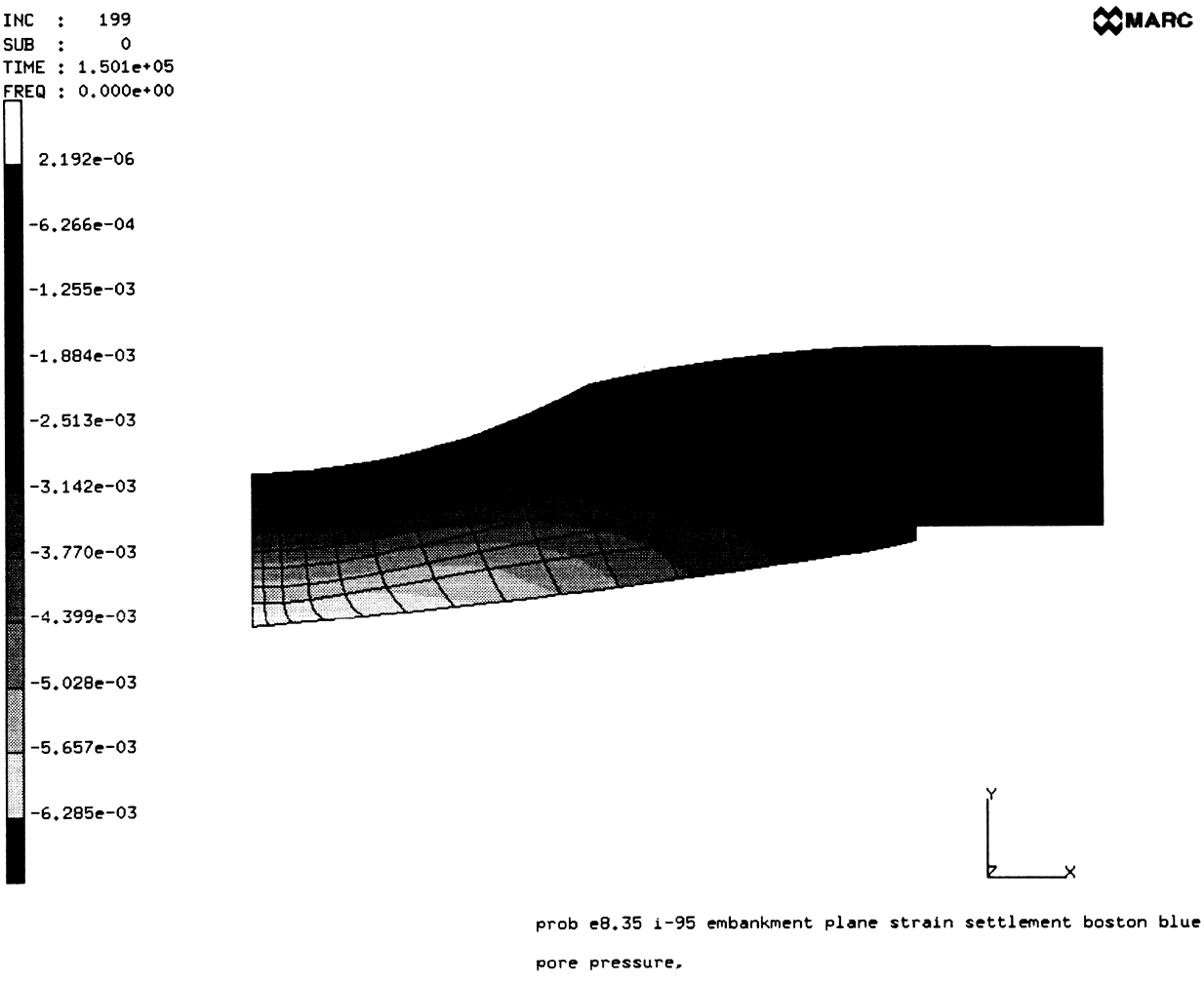

Figure E 8.35-8 Fluid Pore Pressure

E 8.36 Interference Fit Of Two Cylinders

This example demonstrates the interference fit capabilities and the use of symmetry planes in MARC. Two rings have an initial overclosure, and the resultant stress distribution is determined.

Element

Element type 116, a four node axisymmetric element with reduced integration and hourglass control, is used in this analysis. The mesh was originally defined using element type 10. The ALIAS option was used to switch it to type 116.

Loading

The line z = 0 is considered to be a symmetry boundary condition. A rigid surface (body 3) is defined and is given the characteristic of a symmetry plane. This means that the displacement of nodes initially in contact with this plane will be zero, and that the nodes cannot separate from this plane. No other loading or boundary condition is necessary.

The CONTACT option is used to specify that three bodies exist: inner cylinder, outer cylinder and the symmetry plane. There is no friction on any of the surfaces. A closure distance of 0.0001 is initially specified. This will be reset in the CONTACT TABLE option to be 0.0002.

The CONTACT TABLE option then specifies that body 1 and 2 have an interference distance of 0.001. It also specifies that body 1 and 2 are potentially in contact and that 1 and 2 are potentially in contact with 3. Note because of the geometries involved, this is more than a mere potential, but reality. The CONTACT TABLE option is a very powerful way to control the interaction between bodies. In this example, it was positioned in the LOAD INCREMENTATION block. This implies that this data may be changed during the incremental analysis.

Material Properties

The material is a high strength steel with Young's modulus = 30 x 10^6 psi, Poisson's ratio = 0.3, and the yield stress of 50,000 psi.

Control

The CONTROL option specifies that displacement control is being used with a tolerance of 10%. The convergence messages are written to the log file. A restart file and a post file is written for each increment. A single load step is performed with a time step of 0.03. The time step in this problem is totally arbitrary. A PRINT,5 option is included which generates additional messages in the output regarding contact.

Results

By examining the contact forces, one can calculate a total contact force of 44,177 pounds. This is available on the post tape as the "EXTERNAL FORCES" and is given in the output.

Figure E 8.36-2 shows the radial stress and the hoop stress as a function of the radius. Note that nodes 5 and 26 are the corresponding contact nodes between the inner and outer cylinder. One can easily observe that the inner cylinder has gone into compression (hoop stress) while the

external cylinder has gone into tension. Also, observe the antisymmetries of the stress. Note that the radial stress should have gone to zero at nodes 1 and 30. The error is due to the extrapolation procedure employed.

Summary of Options Used

Listed below are the options used in example e8x36.dat:

Parameter Options

ALIAS
ELEMENT
END
PRINT
SIZING
TITLE

Model Definition Options

CONNECTIVITY
CONTACT
CONTROL
DEFINE
END OPTION
ISOTROPIC
POST
RESTART

Load Incrementation Options

AUTO LOAD
CONTACT TABLE
CONTINUE
TIME STEP

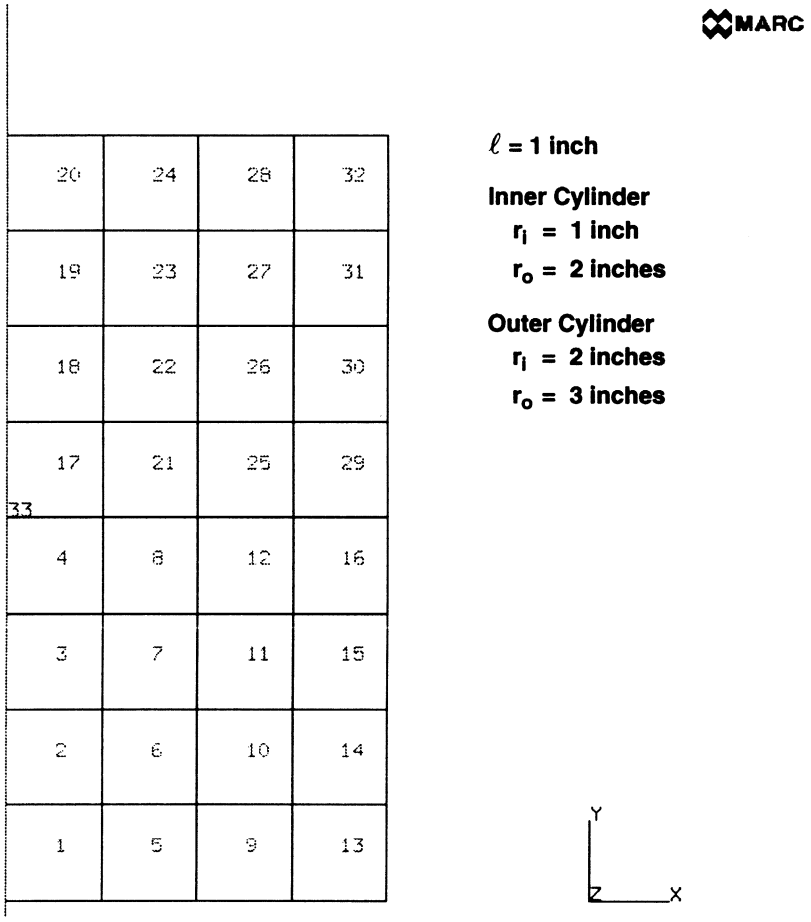

Figure E 8.36-1 Two Cylinders

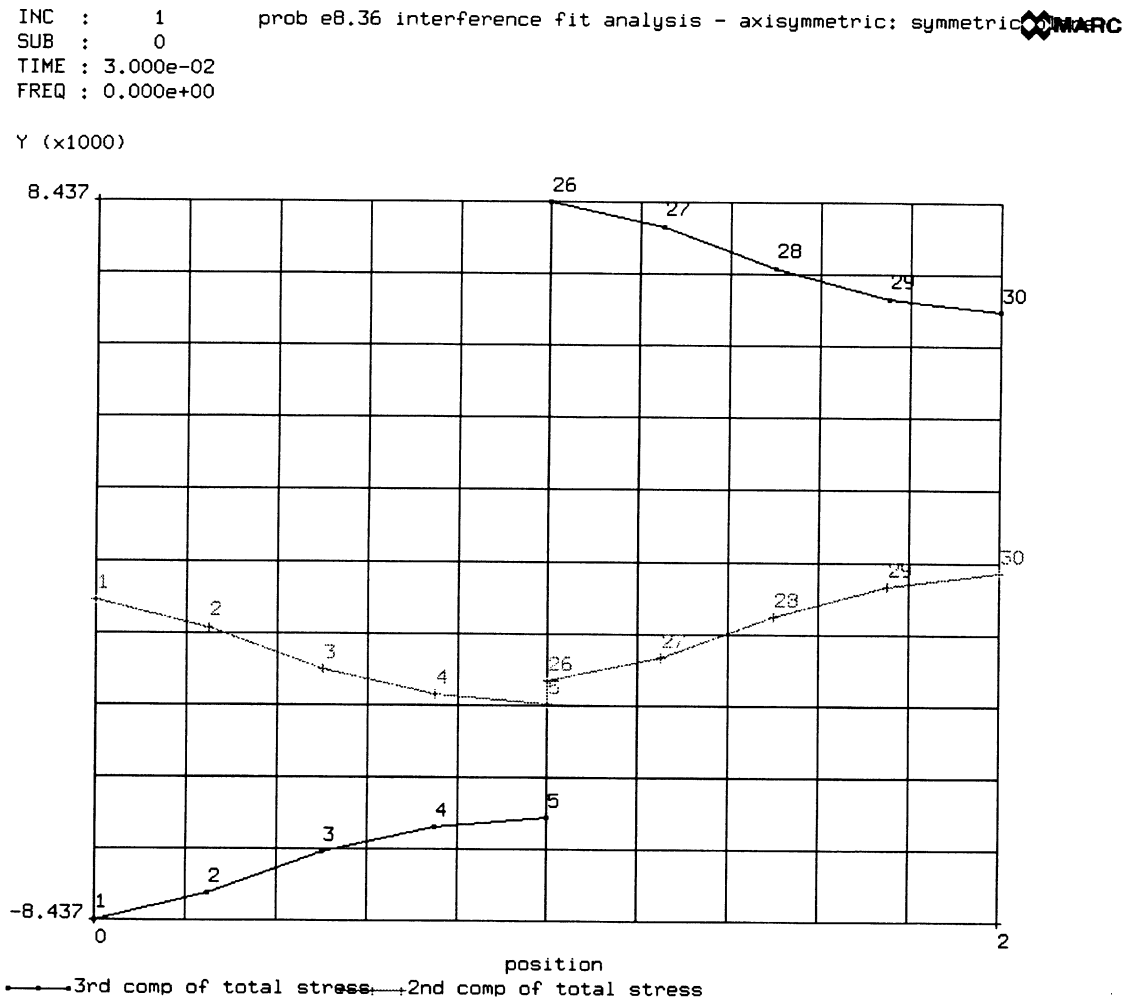

Figure E 8.36-2 Radial and Hoop Stresses Through Radius

E 8.37 Interference Fit Analysis

This example demonstrates the interference fit capabilities in MARC and the use of symmetry planes.

Element

Element type 11, a four node plane strain element, is used in this analysis. The model, as shown in Figure E 8.37-1, consists of a 90° segment of two rings rotated by 45°. Ten elements (9° each) are used in the circumferential direction. The inner cylinder, with r_i = 1 inch and r_0 = 2 inches, has five elements through the radius. The outer cylinder, with r_i = 2 inches and r_o = 3 inches, has six elements. Two symmetry surfaces at 45° and 135° are used. To prevent any rigid body motion, a spring was placed between the two bodies. While this was not necessary in this problem, it is often a good idea.

Loading

The kinematic boundaries are specified using the symmetry surfaces. This problem will be driven by the overclosure fit of 0.01 inch specified through the CONTACT TABLE option.

Material Properties

The material is a high strength steel with a Young's modulus of 30 x 10^6 psi, a Poisson's ratio of 0.3 and a yield stress of 50,000 psi. The material remains elastic in this analysis.

Contact

There are four bodies defined: the inner cylinder, outer cylinder, symmetry surface at $\theta = 135°$, and symmetry surface at $\theta = 45°$.

No friction exists on any surface. Note the flag set on the fourth card series to indicate that surface 3 and 4 are symmetry surfaces. The CONTACT TABLE option is used to indicate which bodies can potentially contact others and to specify the closure distance and the overclosure amount. The overclosure was set to 0.01 inch.

Control

Displacement control was used with a convergence tolerance of 10%. A post file was created using POST and the output was suppressed using NO PRINT. A single increment with a time step of 0.03 second was performed. In this rate independent problem, the time step is arbitrary. The OPTIMIZE option is used to reduce the bandwidth. This is very important in deformable-deformable contact problems.

The PRINT,8 option was used to obtain additional information regarding the contact conditions, such as when a node comes into contact and the displacements relative to rigid surfaces.

Results

The reaction and contact forces are shown in Figure E 8.37-2. One can observe a nice uniform pattern along the contact surfaces. The stresses σ_{xx} and σ_{yy} are shown through the radius at $\theta = 90^{\circ}$. These would be similar to the $\sigma_{\theta\theta}$ and σ_{rr} components, respectively. Note that the stresses are an order of magnitude greater than in E 8.36, but on closer observation, the overclosure distance is also an order of magnitude larger. Note that accuracy could have been improved if the outer elements would have been offset relative to the inner elements by 4.5°. This would have resulted in a more accurate surface normal calculations.

Summary of Options Used

Listed below are the options used in example e8x37.dat:

Parameter Options

ELEMENT
END
PRINT
SIZING
TITLE

Model Definition Options

CONNECTIVITY
CONTACT
CONTROL
COORDINATES
DEFINE
END OPTION
ISOTROPIC
NO PRINT
OPTIMIZE
POST

Load Incrementation Options

AUTO LOAD
CONTACT TABLE
CONTINUE
TIME STEP

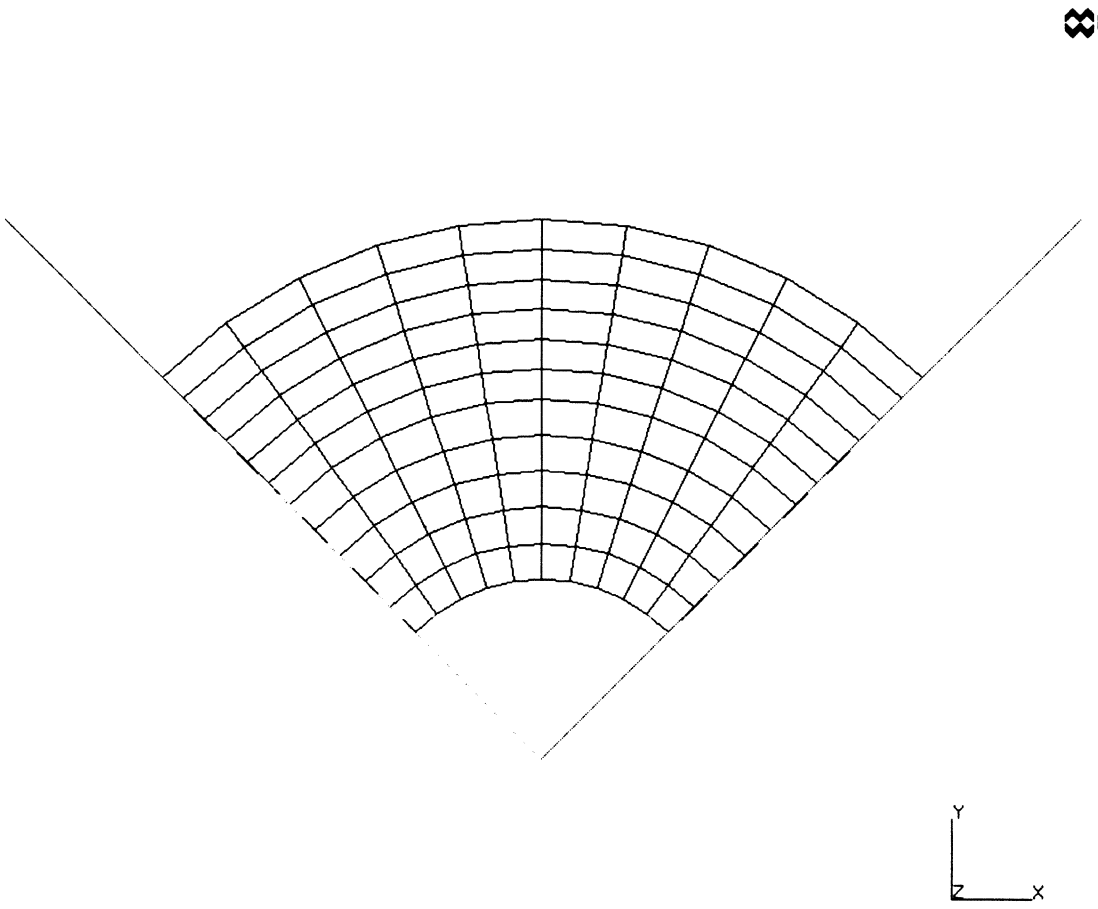

Figure E 8.37-1 Finite Element Mesh with Symmetry Surfaces

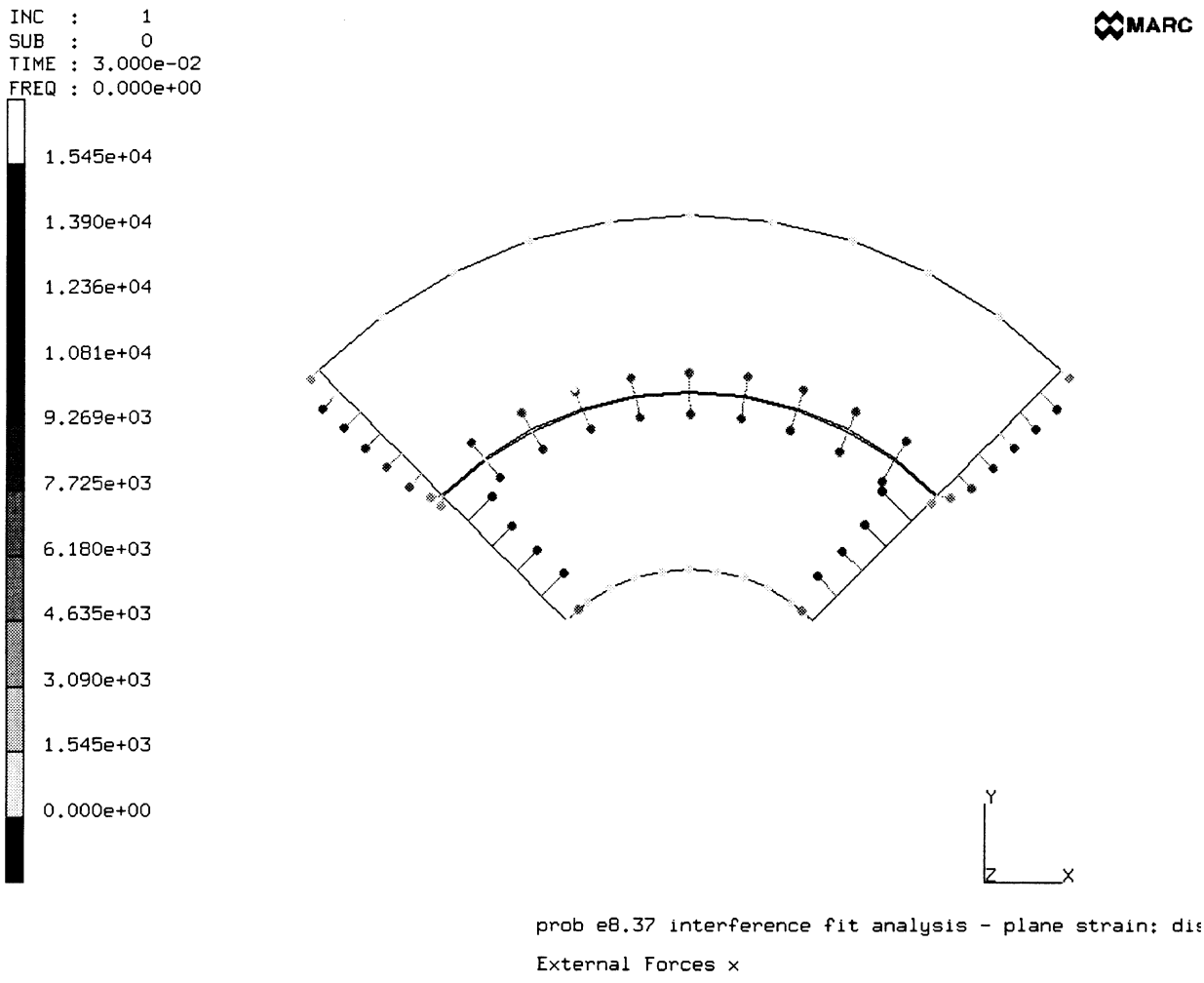

Figure E 8.37-2 Reaction and Contact (Interference) Forces